COGNITIVE 2014

The Sixth International Conference on Advanced Cognitive Technologies and Applications

ISBN: 978-1-61208-340-7

May 25 - 29, 2014

Venice, Italy

COGNITIVE 2014 Editors

Hakim Lounis, UQAM, Canada

Darsana Josyula, Bowie State University; University of Maryland, College Park, USA

COGNITIVE 2014

Foreword

The Sixth International Conference on Advanced Cognitive Technologies and Applications (COGNITIVE 2014), held between May 25-29, 2014 in Venice, Italy, targeted advanced concepts, solutions and applications of artificial intelligence, knowledge processing, agents, as key-players, and autonomy as manifestation of self-organized entities and systems. The advances in applying ontology and semantics concepts, web-oriented agents, ambient intelligence, and coordination between autonomous entities led to different solutions on knowledge discovery, learning, and social solutions.

We take here the opportunity to warmly thank all the members of the COGNITIVE 2014 Technical Program Committee, as well as all of the reviewers. The creation of such a high quality conference program would not have been possible without their involvement. We also kindly thank all the authors who dedicated much of their time and efforts to contribute to COGNITIVE 2014. We truly believe that, thanks to all these efforts, the final conference program consisted of top quality contributions.

Also, this event could not have been a reality without the support of many individuals, organizations, and sponsors. We are grateful to the members of the COGNITIVE 2014 organizing committee for their help in handling the logistics and for their work to make this professional meeting a success.

We hope that COGNITIVE 2014 was a successful international forum for the exchange of ideas and results between academia and industry and for the promotion of progress in the area of advanced cognitive technologies and applications.

We are convinced that the participants found the event useful and communications very open. We hope that Venice, Italy, provided a pleasant environment during the conference and everyone saved some time to enjoy the charm of the city.

COGNITIVE 2014 Chairs:

Hermann Kaindl, TU-Wien, Austria
Sugata Sanyal, Tata Consultancy Services, Mumbai, India
Po-Hsun Cheng (鄭伯壎), National Kaohsiung Normal University, Taiwan
Narayanan Kulathuramaiyer, UNIMAS, Malaysia
Susanne Lajoie, McGill University, Canada
Jose Alfredo F. Costa, Universidade Federal do Rio Grande do Norte (UFRN), Brazil
Terry Bosomaier, Charles Sturt University, Australia
Hakim Lounis, UQAM, Canada
Darsana Josyula, Bowie State University; University of Maryland, College Park, USA
Om Prakash Rishi, University of Kota, India
Qin Xin, Simula Research Laboratory, Norway
Arnau Espinosa, g.tec medical engineering GmbH, Austria
Knud Thomsen, Paul Scherrer Institute, Switzerland

COGNITIVE 2014

Committee

COGNITIVE Advisory Chairs

Hermann Kaindl, TU-Wien, Austria
Sugata Sanyal, Tata Consultancy Services, Mumbai, India
Po-Hsun Cheng (鄭伯壎), National Kaohsiung Normal University, Taiwan
Narayanan Kulathuramaiyer, UNIMAS, Malaysia
Susanne Lajoie, McGill University, Canada
Jose Alfredo F. Costa, Universidade Federal do Rio Grande do Norte (UFRN), Brazil
Terry Bosomaier, Charles Sturt University, Australia
Hakim Lounis, UQAM, Canada
Darsana Josyula, Bowie State University; University of Maryland, College Park, USA
Om Prakash Rishi, University of Kota, India

COGNITIVE Industry/Research Chair

Qin Xin, Simula Research Laboratory, Norway
Arnau Espinosa, g.tec medical engineering GmbH, Austria
Knud Thomsen, Paul Scherrer Institute, Switzerland

COGNITIVE 2014 Technical Program Committee

Siby Abraham, University of Mumbai, India
Witold Abramowicz, Poznan University of Economics, Poland
Thomas Ågotnes, University of Bergen, Norway
Rajendra Akerkar, Western Norway Research Institute, Norway
Zahid Akhtar, University of Cagliari, Italy
Jesús B. Alonso Hernández, Universidad de Las Palmas de Gran Canaria, Spain
Giner Alor Hernández, Instituto Tecnológico de Orizaba - Veracruz, México
Galit Fuhrmann Alpert, eBay Inc. / Interdisciplinary Center (IDC) Herzliya, Israel
Stanislaw Ambroszkiewicz, Institute of Computer Science - Polish Academy of Sciences, Poland
Haitham Bou Ammar, University of Pennsylvania, USA
Alla Anohina-Naumeca, Riga Technical University, Latvia
Ezendu Ariwa, London Metropolitan University, UK
Ilkka Arminen, University of Helsinki, Finland
Rafael E. Banchs, Institute for Infocomm Research, Singapore
Farah Benamara, IRIT - Toulouse, France
Petr Berka, University of Economics - Prague, Czech Republic
Ateet Bhalla, Oriental Institute of Science & Technology - Bhopal, India
Mauro Birattari, IRIDIA, Université Libre de Bruxelles, Belgium
Terry Bossomaier, CRiCS/ Charles Sturt University, Australia
Djamel Bouchaffra, Grambling State University, USA
Daniela Briola, University of Genoa, Italy
Rodrigo Calvo, University of Sao Paulo - São Carlos, Brazil

Copyright Information

For your reference, this is the text governing the copyright release for material published by IARIA.

The copyright release is a transfer of publication rights, which allows IARIA and its partners to drive the dissemination of the published material. This allows IARIA to give articles increased visibility via distribution, inclusion in libraries, and arrangements for submission to indexes.

I, the undersigned, declare that the article is original, and that I represent the authors of this article in the copyright release matters. If this work has been done as work-for-hire, I have obtained all necessary clearances to execute a copyright release. I hereby irrevocably transfer exclusive copyright for this material to IARIA. I give IARIA permission or reproduce the work in any media format such as, but not limited to, print, digital, or electronic. I give IARIA permission to distribute the materials without restriction to any institutions or individuals. I give IARIA permission to submit the work for inclusion in article repositories as IARIA sees fit.

I, the undersigned, declare that to the best of my knowledge, the article is does not contain libelous or otherwise unlawful contents or invading the right of privacy or infringing on a proprietary right.

Following the copyright release, any circulated version of the article must bear the copyright notice and any header and footer information that IARIA applies to the published article.

IARIA grants royalty-free permission to the authors to disseminate the work, under the above provisions, for any academic, commercial, or industrial use. IARIA grants royalty-free permission to any individuals or institutions to make the article available electronically, online, or in print.

IARIA acknowledges that rights to any algorithm, process, procedure, apparatus, or articles of manufacture remain with the authors and their employers.

I, the undersigned, understand that IARIA will not be liable, in contract, tort (including, without limitation, negligence), pre-contract or other representations (other than fraudulent misrepresentations) or otherwise in connection with the publication of my work.

Exception to the above is made for work-for-hire performed while employed by the government. In that case, copyright to the material remains with the said government. The rightful owners (authors and government entity) grant unlimited and unrestricted permission to IARIA, IARIA's contractors, and IARIA's partners to further distribute the work.

Table of Contents

Modeling Interaction in Automated E-Coaching

A Case from Insomnia Therapy

Robbert Jan Beun, Fiemke Griffioen-Both, René Ahn
Information and Computing Sciences
Utrecht University (UU)
Utrecht, The Netherlands
R.J.Beun@uu.nl, F.Griffioen-Both@uu.nl, R.M.C.Ahn@gmail.com

Siska Fitrianie
Interactive Intelligence Group
Technical University Delft (TUD)
Delft, The Netherlands
S.Fitrianie@tudelft.nl

Jaap Lancee
Dep. of Clinical Psychology,
University of Amsterdam (UVA)
Amsterdam, The Netherlands
J.Lancee@uva.nl

***Abstract*—This paper presents the work in progress on the Sleepcare-project. The aim of the project is to enhance the understanding of personalized self-help therapy with the aid of existing (mobile) technology, in particular in the domain of insomnia. For that, an agent-based e-coaching system is being developed in which various persuasion strategies for sustainable behavior change are evaluated. The e-coach is considered as a cooperative partner that combines various interaction modalities (e.g., dialogue, buttons, sensors) and that supports the individual with various exercises for insomnia therapy. Central in the approach is to improve the individual's adherence to these exercises. In this paper, we focus on the basic interaction model of the e-coach and some of its requirements, such as transparency, mutual commitment and adaptation.**

Keywords-cooperative agent; interaction model; e-coaching; cognitive behavioral therapy; insomnia.

I. INTRODUCTION

Personal coaching covers a variety of areas: there are sport coaches, sleep coaches, time-management coaches, and even life coaches in psychology. Personal coaching is regarded as a systematic application of behavioral science to the enhancement of work performance and well-being for individuals that do not have clinically significant mental health issues or abnormal levels of stress [1].

With advancing research in the field of information technology (IT), early attempts are made to replace a human coach with an automated system. In particular, health coaching dialogue systems have been developed on the basis of research methods from persuasive technology and behavior medicine, ranging from the treatment of depression to sleep disorders [2][3][4][5]. Below, we will refer to these automated coaching activities as e-coaching. N.B. Strictly speaking, e-coaching also covers the inclusion of human therapists that communicate by means of IT.

Compared to traditional human-human coaching, (mobile) e-coaching offers important advantages: mobile IT permits the assessment of relevant momentary information and the delivery of fully automated feedback tailored to the individual and the current context; its infrastructure enables the obtainment of objective data from non-obtrusive sensory measurement and integration of these data into the treatment; and its communication platform facilitates information exchange between user groups, i.e., peers, human therapists, and medical institutions. The e-coach can be part of a stepped health-care structure where human care providers take over when problems are detected.

This paper presents the general interaction model of an agent-based e-coaching system for Cognitive Behavior Therapy (CBT). The model is applied in the context of the Sleepcare-project [6], where a mobile e-coach is being developed that mimics the role of a personal coach and that offers a tailored counseling program in the domain of insomnia. In the project, we carefully try to separate coaching and insomnia related knowledge, and aim at experimental validation of persuasive strategies that improve adherence to exercises. Before we discuss the details of the model (Sections III and IV), we first briefly focus on some relevant properties of CBT for Insomnia (CBT-I, Section II).

II. INSOMNIA THERAPY

Insomnia is a sleep disorder with a prevalence of about 10% in the general population [7]. People with insomnia have difficulty initiating and/or maintaining sleep which impairs daytime functioning [8]. Insomnia can have severe consequences (e.g., concentration problems, emotional instability, increased risk of accidents).

Today, it is widely accepted that non-pharmacological treatments, such as CBT-I, produce sustainable positive changes in the condition of insomnia [9]. CBT-I is designed to change dysfunctional beliefs, attitudes and behavior that support sleep-disruptive habits, thoughts and emotions, and offers a variety of exercise types that differ in aim and properties [10]. For instance, relaxation exercises aim at a relaxed body and mind; sleep restriction involves curtailing the time spent in bed to build up a sleep debt during the day; sleep hygiene aims at managing environmental factors and non-sleep related behavior that may be either detrimental or beneficial for sleep. In human-human therapy, the actual intervention is usually preceded by a one- or two-week baseline sleep diary monitoring period, but some exercises, such as relaxation, may be started right from the beginning.

In general, the therapy has a particular time frame, a variety of assignments that may be scheduled in a particular order (allowing overlap), and a periodic evaluation of the assignments. We will return to this in Section IV-C.

 ISBN: 978-1-61208-340-7

One of the major problems in CBT is non-adherence to the therapy [11] and CBT-I is no exception to this. In CBT-I there may be various reasons for non-adherence. Exercises may be too strenuous: people may enthusiastically start the therapy and discover that sizing down the time spent in bed or getting out of bed in the middle of a cold and dark night requires a great deal of effort. In addition, people may have doubts that an exercise contributes to a solution of the problem. Research has been done on improving the treatment efficacy of self-help therapy by the inclusion of persuasive strategies to support adherence to therapy exercises [12][13]. For instance, it was demonstrated that adding feedback to an online treatment for insomnia enhanced both adherence and efficacy [14]. Mimicking the persuasive characteristics of human coaching could be an important factor in the improvement of adherence, but introducing these strategies requires careful analysis of the coaching process.

III. THE COACHING PROCESS

The coaching process can be considered as a series of conversations between two individuals – the coach and the coachee – for the benefit of the coachee in a way that relates to the coachee's learning process [15]. Crucial element is a relation of trust between coach and coachee. Often, therapy related activities are extrinsically motivated (by the coach telling the coachee what to do) and the coachee may not experience immediate intrinsic reward after performing an exercise. Within certain limits, the coach controls the life of the coachee. Therefore, a coach that suggests exercises that are too demanding or that do not manage the coachee's expectations with respect to the required effort or outcome, will likely cause mistrust, frustration and premature withdrawal from the therapy.

A coach should act as a cooperative partner who not only helps to set therapy related goals, but who also offers support to develop a personal treatment plan and uses persuasive strategies to improve adherence to the exercises. To apply this approach, the coaching process should have at least the following elements: a. the coach should be *transparent* about the source of, the importance of and rationale behind exercises; b. the coach and coachee should agree on the investments in the therapy in terms of closing a *contract* (c.f. [16]) and c. the intervention and support should be *adapted* to the individual coachee on the basis of the unique circumstances and characteristics of the coachee [13]. These three elements will form the basis of the interaction scheme presented in Fig. 3 that models the interaction between e-coach and coachee.

IV. BEHAVIOR MODEL OF THE E-COACH

Fig. 1 shows the interaction scheme between the coachee, who interacts through a (mobile) communication device, external sensor devices, a communication medium, such as the internet, and the e-coach system. Sensor devices may deliver, for instance, sleep related and environmental information, such as wake/sleep stage, and light and sound conditions.

The e-coach system consists of various interaction channels, an I/O-Manager that deals with technicalities of the in-

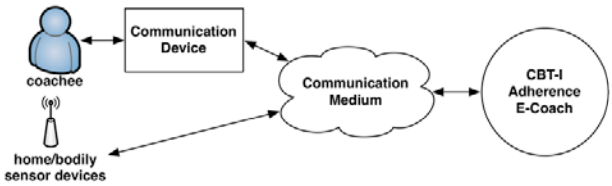

Figure 1. The basic interaction of a CBT-I adherence e-coach

and output, and a supportive agent that communicates with the coachee to initiate and support the coaching process in accordance with the therapy and communication standards.

A. Constraint based dialogue act generation

For the generation of supportive behavior by the e-coach, we propose a constraint-based approach [17]. The basic idea is that the coaching model of a well-formed coaching process needs to conform to a number of constraints. Whenever constraints are violated and detected, they have to be repaired by the e-coach by the generation of a dialogue act.

A constraint describes, for example, that the coachee should adhere to the details of a commitment: doing relaxation exercises twice a day. This constraint is violated when the coachee performs less relaxation exercises and the coach resolves the conflict with a dialogue act, e.g., by explaining the importance of the assignment.

Violations are not necessarily negative, however: if the coachee shows an outstanding performance and the coach did not generate a compliment, this is an undesirable state that has to be repaired. In this respect, the coaching process may be regarded as the maintenance of a balanced state [18]; as long as the coaching model is balanced, nothing happens.

The constraint approach is depicted in Fig. 2. The e-coach detects violations (*constraint checker*) and generates dialogue actions (*dialogue action generator*) on the basis of three types of information: background knowledge about timeless information (e.g., information about sleep disorders, persuasive strategies, constraints), the coaching process (history, plans, therapy schedule), and a repository that reflects information from the coachee's point of view (e.g., feelings, sleep quality, circumstances). Together, they form the *information base* of the coach. The generated dialogues are communicated to the coachee through the *I/O manager* using one of the communication channels. The I/O manager sends new information arising from the interaction with the coachee to the information base (via the *updater*).

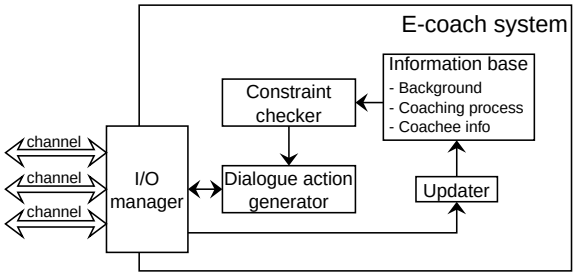

Figure 2. A constraint-based e-coach system.

 ISBN: 978-1-61208-340-7

B. Conversational Behaviour

There are a number of dialogue actions between the coachee and the coach that update the information base (coaching process and repository) of the coach and change the state of the coachee. They can take place through various channels, most of them on a smartphone. Dialogue actions are the basic communicative actions that are the building blocks of more elaborate interaction recipes, such as introductions and evaluations of an exercise.

Both coach and coachee can take the initiative to start the interaction. The partners make working agreements as soon as possible and plan regular briefing sessions where they discuss, negotiate and plan the therapy and the coach process.

In one of the early introduction sessions, the coach introduces the *schedule*, which is essentially a shared agenda that corresponds with an object in the coaching model. All plans and agreements the coach and coachee make are stored into the schedule, where they can be viewed by both partners. In addition, both coach and coachee can initiate a conversation if one of them does not agree anymore with the specifics of a plan or agreement.

C. Interaction model of basic coaching process

The coaching process (introduced in Fig. 3) consists of three phases: an opening phase consisting of a two-way learning process between the coach and coachee, an intervention phase where the actual therapy is conducted and a closure phase during which the therapy can be ended.

The goal of the **opening phase** is twofold: improving transparency through a process of alignment and establishing commitment to the therapy in the form of an agreed contract. Depending on the extent of the process, alignment may refer to various types of information at three different levels [13]: the therapy level (time and effort investments, goals, insomnia-related knowledge), communication level (interface design, gender) and ethical level (privacy, trust, risks). Based on the information exchange, the coach may advise the coachee to withdraw from the therapy, for example on the basis of contra-indications in CBT-I, such as addiction and depression. In that case, the coach may refer the coachee to an experienced human therapist or a general practitioner (*inclusion/exclusion advice*). The coachee however, makes the final decision about whether to continue.

The **intervention phase** consists of different types of exercises, all aiming at support to reach the coachee's goal. The timing of each exercise is entered into the *schedule* in the introduction phase. The coach uses the schedule to initiate communication about a new exercise. Fig. 3 shows four exercises partially overlapping, as an example of a therapy plan.

The **closure phase** starts after all exercises have been performed or when the coachee desires to withdraw from the therapy. In this phase, the coach and coachee may evaluate the progress of the coachee, have a discussion about why the coachee ends the therapy, or make plans for relapse prevention. Discussing the (ending of the) therapy may give important information for future support strategies.

D. Exercise support

Although the exercises can be very different, they follow the same four steps (see Fig. 4). Every exercise starts with an introduction to the exercise (step A). During step B, the coach explains what is expected of the coachee and they can negotiate about the specifics of the exercise (e.g., frequency and timing of the assignments). When the coach and coachee agree, they establish a commitment by 'signing' a contract. The exercise properties are stored in the schedule, so that the coachee can view and adapt them and the coach can respond to constraint violations (e.g., by sending reminders to the coachee if the task is not executed on time). Step C consists of the coachee performing the exercise based on the schedule agreed upon in the plan & commit process. The final step D is a briefing session evaluating the performance at a scheduled time (committed to in the contract in step B). The coach may use adherence data and will ask the coachee about their

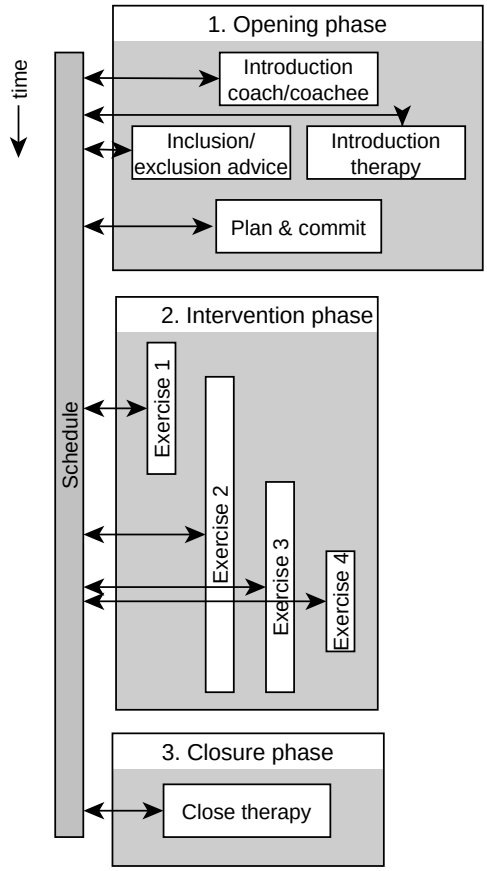

Figure 3. The interaction model of a basic coaching process.

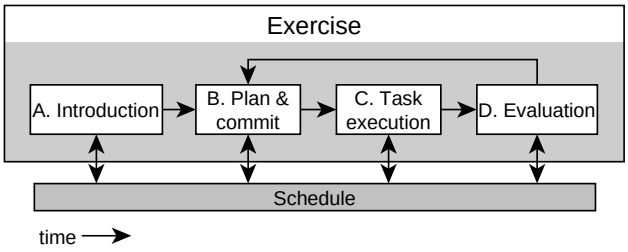

Figure 4. Interaction model of an exercise.

opinion. After evaluation, the exercise either ends, or continues with discussing the plan for the next cycle of the exercise.

V. DISCUSSION

This paper presents a generic constrained based interaction model applied in the domain of automated CBT-I. Since CBT-I is considered as an amalgam of a wide range of individual and communicative activities, it is to be expected that the model pertains to other mobile e-coaching domains as well. Therapy related exercises can be viewed as a particular type of activities that should be scheduled and adhered to by the coachee. Moreover, in all domains, e-coach and coachee should align, build mutual agreement about the investments, and evaluate and adapt exercises and communication to the individual characteristics of the coachee.

To improve exercise adherence, three elements were included that play a crucial role in the communicative behavior of the e-coach: *transparency*, *adaptation* and commitment to *contracts*. These elements can be found in various stages of the therapy. Transparency is implemented in the extensive introduction of the therapy and exercises at various levels; adaptation to personal circumstances or preferences is established in the introduction stage (plan and commit) and the various briefing sessions; the closing of various contracts is implemented in the introduction and intervention phases where the coachee can either commit to an agreed plan or withdraw from the treatment or exercise.

VI. CONCLUSION AND FUTURE WORK

The aim and strength of the Sleepcare project is the genericness of the approach, i.e., developing a system that can be applied to many coaching domains. In addition, developing a mobile phone app allows the coach to support the coachee at any time, not only during therapy hours. The generic nature together with the limitations of smartphone applications (limited resources, small screen, etc.) provide a challenge: the need for designing an efficient system with many functionalities and still compact enough to run on a mobile phone.

Currently in the Sleepcare project, a smartphone app is being developed and tested. The latest version contains a sleep diary tool, a relaxation exercise and is able to send reminders. Three reminder settings are currently being tested in an experiment: no reminders, self-scheduled reminders and opportunity detection reminders.

Future work consists of further development, implementation and empirical validation of the model in the domain of CBT-I. Important questions to be answered are how coaching strategies and sleep related knowledge can be separated to guarantee the generic nature of the coaching model and how the abstract interaction scheme can be transformed into user-friendly and natural interface characteristics.

ACKNOWLEDGMENT

This research is supported by Philips and Technology Foundation STW, Nationaal Initiatief Hersenen en Cognitie NIHC under the Partnership programme Healthy Lifestyle Solutions.

REFERENCES

[1] M.A. Grant, “A personal perspective on professional coaching and the development of coaching psychology”, International Coaching Psychology Review, 1(1), 2006, pp. 12- 22.

[2] T.W. Bickmore, D. Schulman, and C.L. Sidner, “A reusable framework for health counseling dialogue systems based on behavioral medicine ontology”, J. of Biomedical Informatics, 44, 2011, pp. 183-197.

[3] O.A. Blanson Henkemans, P.J.M. van der Boog, J. Lindenberg, C.A.P.G. van der Mast, M.A. Neerincx, and B.J.H.M. Zwetsloot-Schonk, “An online lifestyle diary with a persuasive computer assistant providing feedback on self-management” Technology & Health Care, 17(3), 2009, pp. 253-257.

[4] F. Both, P. Cuijpers, M. Hoogendoorn, and M. Klein, “Towards Fully Automated Psychotherapy for Adults: BAS - Behavioral Activation Scheduling via web and mobile phone”, In: Proc. of the 3d Inter. Conf. on Health Informatics, HEALTHINF'10, 2010, pp. 375-380.

[5] C.A. Espie et al., “A Randomized, Placebo-Controlled Trial of Online Cognitive Behavioral Therapy for Chronic Insomnia Disorder Delivered via an Automated Media-Rich Web Application”, Sleep, 35(6), 2012, pp. 769-781B.

[6] Sleepcare project, http://www.ikgalekkerslapen.nl [accessed 11th April 2014]

[7] M.M. Ohayon,“Epidemiology of insomnia: What we know and what we still need to learn”, Sleep Medicine Reviews, 6(2), 2002, pp. 97-111.

[8] American Psychiatric Association. "Diagnostic and Statistical Manual of Mental Disorders", Fifth Edition. Arlington, VA: American Psychiatric Association, 2013.

[9] C.M. Morin et al., “Psychological and behavioral treatment of insomnia: Update of the recent evidence (1998-2004)”, Sleep 2006, 29, pp. 1398-1414.

[10] C.M. Morin and C.A. Espie, “Insomnia. A clinical Guide to Assessment and Treatment”, New York: Springer; 2003.

[11] T.W. Bickmore, D. Mauer, F. Crespo, and T. Brown, “Persuasion, task interruption and health regimen adherence”. In: de Kort Y. IJsselsteijn W, Midden C, Eggen B, Fogg BJ (eds) Persuasive technology. LNCS volume 4744. Springer, Berlin, 2007, pp 1–11.

[12] C. H. G. Horsch, W. P. Brinkman, R. M. van Eijk, and M. A. Neerincx, “Towards the usage of persuasive strategies in a virtual sleep coach”, Proc. of UKHCI 2012 Workshop on People, Computers and Psychotherapy, 2012.

[13] R. J. Beun, “Persuasive strategies in mobile insomnia therapy: alignment, adaptation, and motivational support”, Personal and Ubiquitous Computing, 17(6), 2013, pp. 1187-1195.

[14] J. Lancee, J. van den Bout, M.J. Sorbi, and A. van Straten, “Motivational support provided via email improves the effectiveness of internet-delivered self-help treatment for insomnia: A randomized trial”, Behaviour Research and Therapy, 2013, 51, pp. 797-8056.

[15] J. Starr, “The coaching manual. The definitive guide to the process, principles and skills of personal coaching”. London: Pearson Prentice Hall Business, 2008.

[16] R. Cialdini, “Influence, Science and Practice”, HarperCollings College, New York, 1993.

[17] R.M.C. Ahn, “Basic Sleep Coach Knowledge Architecture.” Sleepcare Internal Document, 23112013, 2013.

[18] R.J. Beun. "On the generation of coherent dialogue: a computational approach". Pragmatics & Cognition, 9(1), 2001, pp. 37-68.

 ISBN: 978-1-61208-340-7

Towards Agent-based Data Privacy Engineering

Kato Mivule
Computer Science Department,
Bowie State University
Bowie, MD, USA
kmivule@gmail.com

***Abstract* – While a number of agent-based software engineering frameworks have been proposed in the recent years, a few have been suggested specifically for the data privacy procedure. Yet still, one of the challenges in designing agent-based data privacy frameworks is that the very definition of privacy remains ambiguous and a case-by-case approach would have to be adopted. Therefore, as a contribution, we take a look at the literature on agent-based software engineering and present SIED (Specifications, Implementation, Evaluation, Dissemination), a conceptual framework that takes a holistic approach to the data privacy engineering process by looking at the Specifications, Implementation, Evaluation, and finally, Dissemination of the privatized datasets by autonomous intelligent agents.**

Keywords – Data privacy engineering; autonomous agents; statistical disclosure control.

I. INTRODUCTION

In 2009, a privacy-by-design challenge was put forward and described by Cavoukian [1], in which privacy is entrenched and embedded into the engineering requirements of different methodologies and technologies [2]. Moreover, recent revelations by Edward Snowden concerning covert electronic operations by US Government security agencies and the alleged infringement of personal privacy [3], have pushed to the forefront the importance and necessity of privacy by design, and in this case, engineering privacy into the design of software and autonomous multi-agents. Yet still, engineering data privacy remains an ongoing challenge largely due to what considerations the definition of data privacy should encompass [4][5]. Consequently, one of the problems of data privacy engineering, is that the notion of privacy is ambiguous, normally misidentified with data security, thus making it difficult to engineer and implement [4][5][6][7]. To appropriately design and implement data privacy agents, an all-encompassing approach for describing data privacy should entail the legal, technical, and ethical features; as such, providing an understandable logical context for all shareholders in the data privacy process [8]. While efforts have been made to theoretically explain data privacy, human perceptions such as, ambiguousness and evolutions of personal understanding of privacy, remain a crucial influence in the design and implementation of data privacy [9]. As a result, any design and implementation of privacy agents has to imperatively consider what personal information entities see as appropriate for public revelation [5][6][7]. Therefore, to assist in a thorough data privacy requirements elicitation, we employ software engineering concepts outlined by Sommerville (2010), and have been effectively used to capture ambiguous requirements in the software engineering domain [10].

As a contribution, a literature review on agent-based software engineering frameworks is presented; SIED, as conceptual framework for agent-based data privacy engineering, is suggested. Moreover, to aptly deal with the intricacy of data privacy engineering, the abstraction, decomposition, and hierarchical perspectives of dealing with complexity as outlined by Booch (1994) have to be considered [11].

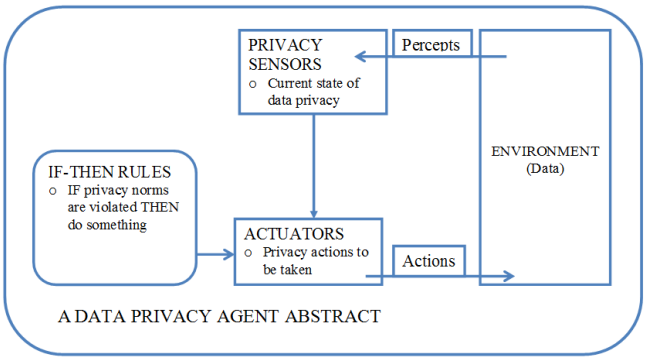

Figure 1. An Abstract of a data privacy agent.

Moreover, our aim in this paper is to give an abstraction and conceptual view (Figure 1) of an agent-based data privacy engineering framework, while keeping the decomposition and hierarchical aspects to future works. At the same time, while SIED is proposed as a framework for agent-based data privacy engineering, the same framework could be generalized for basic non-autonomous data privacy implementations. The rest of the paper is organized as follows. In Section II, a review of literature on related work is given. In Section III, the SIED conceptual framework is explained. In Section IV, a conclusion and future works is given.

II. RELATED WORK

While few works exist on engineering privacy in agents, considerable amount of work has been done in the area of agent-based software engineering; providing principles that could be applied in the data privacy engineering domain. For instance, Wooldridge (1997) [12] noted three essential

 ISBN: 978-1-61208-340-7

considerations when engineering multi-agents, namely, (i) how agents should be specified, (ii) how to turn the specifications into agent implementation, and lastly (iii) how to validate that the newly developed agent meets the original specifications. The Wooldridge (1997) [12] three essential considerations are relevant for the design and engineering of data privacy agents, in that a meticulous elicitation of privacy specifications, in this case requirements, has to be done. Yet still, Wooldridge and Jennings (1999) [13] warned about some of the pitfalls when it comes to agent-based software engineering. Wooldridge and Jennings (1999) [13] noted that one of the common pitfalls, is the tendency to offer generic architectures for intelligent agents, yet such costly one-size-fits-all architectures would rarely work for every agent-based software problem. This observation by Wooldridge and Jennings (1999) [13] is an essential consideration for agent based privacy engineering, as each privacy problem tends to be unique and based on the privacy definition of that particular user [5]. Additionally, Jennings (2000) [14] observed that while agent based software engineering was being used to address real world problems, building such systems remained complex and difficult, due to the interactions between different components that are rigidly defined, and inadequate methods available to represent a systems architecture. The Jennings (2000) [14] study is applicable when it comes to agent based privacy engineering. The very definition of what constitutes privacy, makes building such systems complex and therefore a case-by-case perspective has to be done, especially when communication and data transaction between various autonomous privacy agents is taken into account.

Yet, from a legal perspective on technology, calls for Privacy Enhancing Technologies (PET) were issued as in the case of Borking and Raab (2001) [15], who made an elaborate elucidation of PETs and how data safety systems and legal processing of personal data could be enhanced by such technologies. Among the guidelines noted by Borking and Raab (2001) [15] are (i) reporting of data processing, (ii) transparent data processing, as required data processing, (iii) legitimacy of the data processing, (iv) data quality, (v) rights of parties involved in the data processing, (vi) data traffic across international borders, (vii) processing personal data by a processor, and (viii) protection against loss and unlawful processing of personal data. In the same period of time, Kenny and Borking (2002) [16] defined privacy engineering as a methodical endeavor to embed privacy applicable legal primitives into technological and governance blueprints. Kenny and Borking (2002) [16] proposed DEPRM, a Design Embedded Privacy Risk Management framework, to integrate both privacy engineering and risk management. While Kenny and Borking (2002) [16] did not distinctively define privacy engineering for the purposes of designing autonomous agent systems, their definition of privacy engineering certainly remains relevant and pertinent in designing privacy conscience agents today. Furthermore, Van Blarkom, Borking, and Olk (2003) [17], in their case for PETs in intelligent software agent systems argued that PETs would be helpful in tackling privacy threats caused by intelligent agents that illegally disclose a user's personal information. PETs would also help in dealing with threats caused by external intelligent agents that act on behalf of adversaries via traffic flow monitoring, data mining, and covert attempts to obtain personal information directly from a user. On a remarkable note, the term "privacy engineering" by Kenny and Borking (2002) [16], was being used and appearing in legal literature then, while mainstream software engineering and data privacy domains would begin to pick up this term at a later point. Research on privacy enhancing technologies was ongoing in the legal communities while such efforts were not obvious in the software engineering domain.

On the issue of norms and behaviors in intelligent agents, y López, Luck, and d'Inverno (2004) [18], proposed a normative framework that would instruct agents on how to behave prescriptively, socially, and under peer pressure. y López et.al, noted that autonomous agents while working to satisfy their own goals, still have to comply with social responsibilities [18]. While a number of norms could be considered for agent based software engineering, in this article, we are interested in what privacy norms an autonomous agent could be engineered to observe. For example, not revealing an entity's sensitive information could be considered as a social norm that an autonomous agent would be expected to observe. On agent-based software engineering, Bresciani, Perini, Giorgini, Giunchiglia, and Mylopoulos (2004) [19], proposed Tropos, an agent based software engineering methodology that utilized the very definition of an intelligent agent, its, goals, plans, and environment in software requirements and implementation phases. While Tropos provided a framework for the development of agent-based software, engineering privacy in the design of such agents was not the main focus, a trait in many earlier agent-based software engineering frameworks. Besides, Zambonelli and Omicini (2004) [20] observed and argued at that time, that while agent-based software engineering was experiencing a great amount of research, one of the challenges included how to turn generated agent-based software abstractions into practical tools to solve complex problems. Yet still, to this date, the same challenge remains when it comes to privacy. Given the complex and ambiguous definition of privacy, turning generated agent-based privacy engineered abstracts into real useful tools that could help solve some of the privacy problems, remains a challenge.

On the other hand, Sooyong and Vijayan (2005) [21], proposed using a goal based approach in the problem domain requirements analysis such that each autonomous agent could appropriately get mapped to the system's refined goals. In this paper, we take a similar approach to Sooyong, and Vijayan (2005) [21], by emphasizing the specifications phase of the engineering process to comprehensively map out the environment, goals, and actions of a data privacy agent. Bellifemine, Caire, Poggi, and Rimassa (2008) [22], gave an elaborate overview on JADE, a Java based software framework for developing multi-agent applications. While JADE is still a popular framework utilized to this date, the challenge is how to implement agent based privacy engineering using JADE.

 ISBN: 978-1-61208-340-7

However, Weyns, Parunak, and Shehory (2008) [23] argued that despite the interest in agent based software engineering research, implementation was still a challenge due to disconnect between proposed frameworks in academia and implementation in industry. Weyns et al. (2008) [23] observed that this disconnect between academia research and adoptability in industry was largely due to a poor understanding of industry needs. To address this problem in the privacy domain, we suggest a thorough case-by-case requirements analysis in the specifications phase of an agent development. Cossentino, Gaud, Hilaire, Galland, and Koukam (2009) [24], proposed ASPECS, a framework that utilizes a holonic structural meta-model and offers a step-by-step monitoring, from requirements to implementation, with modeling in each phase of the development cycle. However, Léauté and Faltings (2009) [25], proposed an agent based privacy engineering solution using constraint satisfaction model by mapping out privacy constraints in the domain. In such a scenario, each agent makes decisions that keep with the privacy norm – constraints in this case; for example, by not revealing sensitive information when communicating with other agents [25]. On the subject of meta-modeling, Gascueña, Navarro, and Fernández-Caballero(2011) [26], observed that Model-Driven Engineering (MDE) allowed developers and stakeholders to use abstractions closer to the domain than generalized computing concepts. However, due to the relatively growing research on agent-based data privacy engineering, not many such models exist.

Furthermore, Cavoukian (2011) [27] outlined seven privacy by design principles that included: (i) proactive, not reactive privacy design; preventative not remedial design approach; (ii) engineering privacy as the default; (iii) privacy embedded into design; (iv) full privacy functionality by avoiding needless trade-offs; (v) end-to-end security and life cycle protection privacy design; (vi) visibility and transparency of privacy practices; and finally (vii) respect for user privacy. However, to fully meet the seven privacy by design principles outlined by Cavoukian (2011) [27], we strongly believe that a comprehensive specifications and requirements solicitation and analysis has to be done, especially when it comes to engineering data privacy agents. More recently, Such, Espinosa, and Garcia-Fornes (2012) [28], in their extensive survey on privacy in multi-agent systems, noted that the concern of privacy in multi-agents is still a problem, and has increased due to the robust growth and utilization of the internet for data transaction. Among the privacy violations that autonomous agents engage in, as noted by Such et.al., include, (i) secondary use, such as profiling, (ii) identity theft, (iii) spy agents, (iv) unauthorized access, (v) traffic analysis, and (vi) unauthorized dissemination of data [28]. Such et.al., argued that to combat some of these agent based privacy vices, agent based privacy solutions should be incorporated in the design of information technology systems [28].

Nevertheless, Aggarwal and Singh (2013) [29], presented a mechanism for the reuse of already existing software agents in the development of specific software, by utilizing the abstract description of an agent and reusing such systems in other specific domains. Still, as in the case with Gascueña et.al. (2011) [26], on model-driven engineering and reusing abstractions that are closer to the domain, the Aggarwal and Singh (2013) [29], model of reuse, would not be without challenges in the data privacy domain. Engineering such agents remains difficult and would have to be done on a case by case basis, due to the very subjective definition of what privacy is among various entities. As we noted in Mivule, Josyula, and Turner (2013) [6], the definitions of privacy vary, are fuzzy, indistinguishable, and are largely attached to how humans see privacy and what data they are willing to share or consider private. However, despite such challenges, intelligent autonomous agents offer possibilities when it comes to engineering privacy in agents. For instance, agents could be designed to learn privacy norms after a methodical privacy requirement analysis is done for that specific case.

III. THE SIED FRAMEWORK

The motivation behind the SIED framework is to create a systematic outline that can be followed for the data privacy engineering process. Given any original dataset *X*, a set of data privacy engineering phases should be followed from start to completion in the generation of a privatized dataset *Y*.

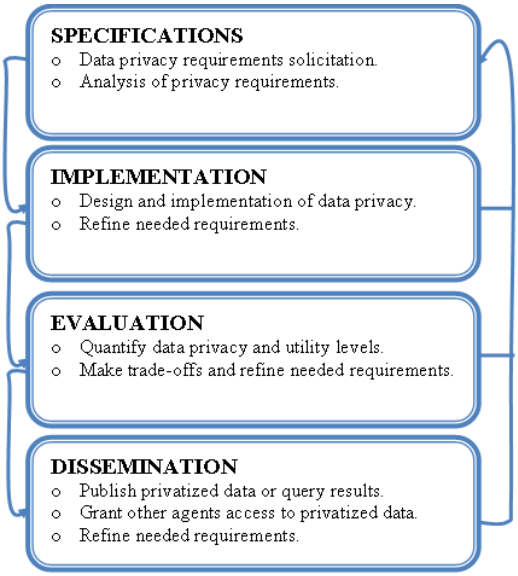

Figure 2. The SIED conceptual framework.

In this article, SIED, as shown in Figure 2, is proposed as a holistic conceptual approach that could be employed for the data privacy engineering process. The four main phases of the SIED data privacy engineering framework are as follows:

A. *Specification phase*

In this phase, data privacy engineers gather data privacy specifications and requirements from the client. In the suggested SIED framework, requirements solicitation and analysis is the most crucial phase of the agent-based data privacy engineering process. While a series of questions could be generated to comprehensively assess the data privacy requirements of a user, we suggest the following

questions as being essential for a holistic agent-based data privacy specifications analysis:

- What are the data privacy legal and policy compliance requirements?
- What is the client description for Personal Identifiable Information (PII), quasi, sensitive, and non-confidential attributes?
- What are the current client data privacy threats or vulnerabilities?
- How far would client data be affected by auxiliary data?
- How is the client planning on dissemination of privatized dataset?
- Will privatized data access be by query access, published categorical data, or tabulated data?
- Will the privatized dataset be in microdata or macrodata form?
- What type of original data from the client is to be handled, continuous or categorical?

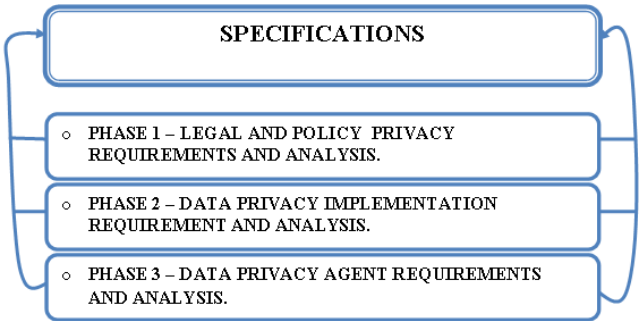

Figure 3. Suggested specification phases.

- What is the variable size for the original data, univariate or multivariate?
- What type of partitioning on the original data will be required, horizontal or vertical partitioning?
- What types of Statistical Disclosure Control (SDC) methods are required by client, non-perturbative, or perturbative?
- What nonfunctional requirements are suggested by the data privacy engineers?
- What is the client expected data privacy needs?
- What is the client expected data utility needs?
- What trade-offs can be accommodated between data privacy and utility needs?

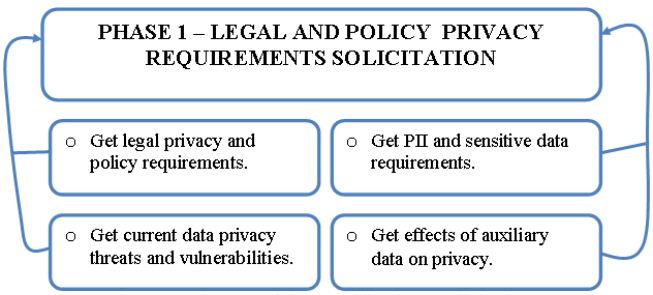

Figure 4. Phase 1 of the specifications solicitation.

While this set of solicitation questions is not exhaustive, the responses generated could be used to construct a set of beliefs and inference rules for the data privacy autonomous agent. In addition, specification is done in three requirements phases, as shown in Figure 3, namely, (i) Legal data privacy requirements solicitation and analysis, (ii) Data privacy application requirements solicitation and analysis, and (iii) Data privacy agent requirements solicitation and analysis.

Phase 1: Legal data privacy requirements solicitation and analysis: In the first phase of specification analysis, a review of issues pertaining to legal privacy and policy compliance is done, as illustrated in Figure 4:

- Solicitation and analysis of legal privacy and policy compliance requirements is done.
- Assessment of user description of what constitutes PII, quasi, sensitive, and non-confidential attributes is carried out.
- Assessment of current client data privacy threats or vulnerabilities is done.
- Assessment of how user data privacy would be affected by auxiliary data, such as, posts on social media is carried out.
- Assessment of privacy threats and vulnerabilities, including effects of auxiliary data, is done in Phase 1.

Requirements solicitation and analysis generated from this phase will later be used in creating a beliefs set and IF-THEN rules for the autonomous privacy agent.

Phase 2: Data privacy application requirements solicitation and analysis: In the second phase of the specification analysis, a review of issues pertaining to how data privacy will be implemented by the autonomous privacy agent is done, as shown in Figure 5.

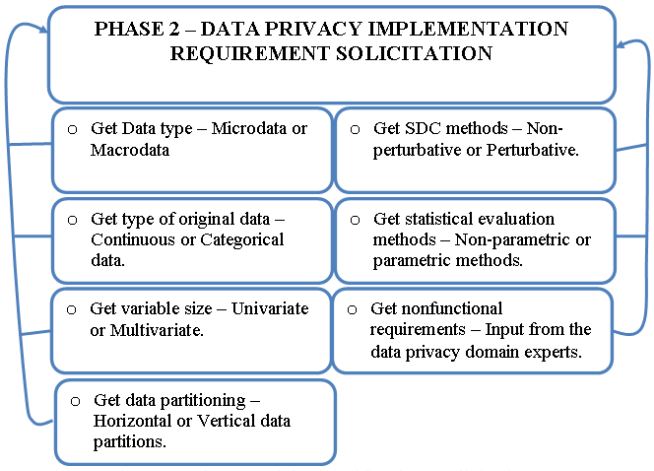

Figure 5. Phase 2 of the specifications solicitation.

The main question asked in this phase is what action the data privacy agent would take in response to a privacy violation. The type and characteristics of the data should be analyzed and included in the specifications. As such, the data privacy agent should be able to do the following:

- Assessment of the data type – microdata or macrodata form.

- Assessment of the type of original data from the client to be handled – continuous or categorical.
- Assessment of the variable size for the original data – univariate or multivariate.
- Assessment of the partitioning on the original data – horizontal or vertical partitioning.
- Assessment of SDC methods required – non-perturbative or perturbative.
- Assessment of evaluation requirements – non-parametric or parametric methods.
- Assessment of the nonfunctional requirements from the data privacy engineers.

Non-functional requirements, as noted by Summerville (2010), are requirements not suggested by the client but suggested by an expert in the field who might see other necessary needs that a non-expert might not see; in this case, the expert is the data privacy engineer [10].

Phase 3: Data privacy agent requirements solicitation and analysis: The requirements solicitation and analysis done in the Phase 1 and Phase 2 is utilized to generate specifications for the data privacy agent. Following Wooldridge's (1997) [12] articulation on the characteristics of an agent, it is at this point that subsequent features of a detailed agent-based data privacy requirements is done as outlined in Figure 6.

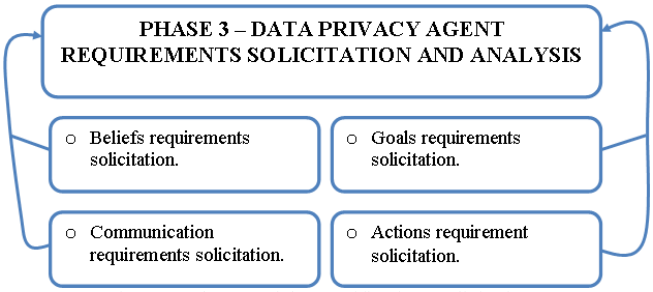

Figure 6. Phase 3 of the specifications solicitation.

- *Beliefs requirements solicitation*: Beliefs could include information about the environment concerning privacy, and the inference rules that need to be generated. Generated belief requirements could then be transformed into privacy centric IF-THEN statements and rules [30].
- *Communication requirements solicitation*: At this point, it would be important to know what privacy specifications and rules the agent should follow when communicating with other agents. This could include what privacy information is shared, when and how, with other agents.
- *Goals requirements solicitation*: In this solicitation phase, the overall goal of the agent should be stipulated. In the case of privacy, the aim of the agent is to ensure confidentiality of data by following a set of beliefs and inference rules.
- *Actions requirement solicitation*: Some of the questions that could be asked in this phase could include, what action should an agent do when PII is detected in a data set? In this case, the agent could decide to suppress, generalize, or perturb such sensitive information based on the inference rules.

B. Implementation phase

In this stage, design, application, and implementation of the appropriate specifications for the data privacy agent is done. Specifications are then used to build both the belief and action set of the data privacy agent. Appropriate data privacy algorithms for the appropriate data types are selected as part of the belief system for the data privacy agent. The implementation phase takes the specification analysis recommendations for implementation and executing the data privacy process. Various data privacy algorithms are chosen based on the specifications and requirement analysis and added to the agent belief set and action plan, as shown in Figure 3. A detailed description of the data privacy algorithms, statistical disclosure control methods, data characteristics, statistical analysis methods, and data partition methods, is given by Mivule and Turner (2013) [31]. The goal of the implementation phase, is to have the appropriate data privacy belief set generated from the requirements solicitation, that the agent could appropriately use to apply data privacy. Some of following set of IF-THEN statements and rules, generated and recommended from the user requirements, could be used as a set of beliefs for the data privacy agent, as highlighted in Figure 7:

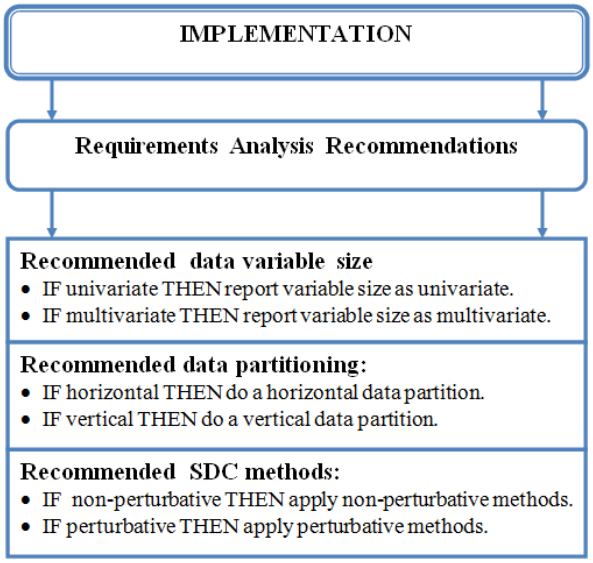

Figure 7. The SIED Implementation phase.

- *Detecting the data variable by agent*:
  - IF univariate THEN report variable size is univariate. IF multivariate THEN report variable size is multivariate [31].
- *Data partitioning by agent based on user requirements*:
  - IF horizontal THEN do a horizontal data partition. IF vertical THEN do a vertical data partition [31].
- *Type of SDC methods to be applied by agent*:
  - IF non-perturbative THEN apply the following non-perturbative methods:

Suppression, Generalization, k-anonymity, l-Diversity, among others [31].
    - IF perturbative THEN apply the following perturbative methods based on the dissemination method: Noise Addition, Multiplicative noise, Logarithmic multiplicative noise, Differential data privacy, Data swapping, and Synthetic datasets [31].
- *Statistical analysis to be applied on data by agent*:
    - IF numerical data THEN apply parametric methods. IF categorical THEN apply non-parametric methods.
- *Data dissemination by agent*:
    - IF privatized query results are requested THEN apply Differential Privacy. IF Privatized published micro and macro data are requested THEN apply Noise Addition [31].

C. Evaluation phase

In this phase, as shown in Figure 8, statistical evaluation of both original and privatized data is done by the data privacy agent. The goal of the agent at this stage would be to test if acceptable levels of both data privacy and utility are met, based on user requirements for a particular data set. Some of the evaluation questions that could be raised in this phase include:

- What are the expected client data privacy needs? What is the expected client data utility needs?
- What trade-offs can be accommodated between data privacy and utility needs?
- Answers to these questions would help formulate the evaluation belief set of the data privacy agent.

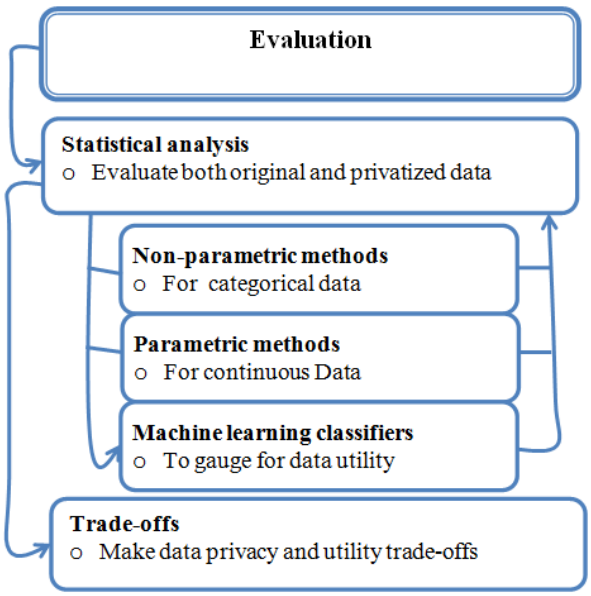

Figure 8. The SIED Evaluation phase.

Moreover, the data privacy agent would take into consideration the type of original data being handled. If the data type is numerical (continuous) then the agent would apply parametric statistical methods in evaluation, such as, mean squared error and entropy. If the data is categorical, the agent would apply non-parametric methods such as frequency count analysis. Because finding an optimal balance between privacy and utility needs is intricate [32], trade-offs are a necessity and made by the agent in this phase. It is in this phase that metrics used to measure data utility are implemented by the agent. Such metrics could include the mean, entropy; mean squared error, and classification error. The data privacy agent would measure the statistical traits of both the original and privatized data and find the difference. If the difference, say between the mean values of both the original and privatized data is higher than a set threshold (set by user or derived from the requirements solicitation), then data utility is low but privacy is high. The goal would be to find an optimal balance.

Furthermore, trade-offs are decided at this point in the evaluation phase. In addition, data privacy and utility expectations of the client are taken into consideration. Therefore, a data privacy agent would need to know at what point to autonomously make such trade-offs. While this is a difficult problem and would be one of the most challenging for the data privacy agent to make, a methodical specification analysis would help generate the appropriate belief sets and inference rules needed for the agent to take action. A number of evaluations could be considered in this phase:

- Assessment of the client expected data utility needs.
- Assessment of data privacy and utility trade-offs.
- Assessment of how privatized data would be disseminated.

For this particular data privacy engineering framework, we envision evaluation using machine learning classification as a gauge, as outlined in Mivule and Turner (2013) [7]. Basically, in the initial phase, the data privacy agent would apply privacy on data and pass the results through a machine learning classifier. The classification accuracy would be measured, with higher accuracy indicating better data utility but perhaps lower privacy. If the classification accuracy meets a set threshold, then the agent would proceed to publish the results, otherwise, the data privacy agent would adjust the parameters in the data privacy algorithm and then re-classify the data. The agent would repeat this process until the threshold criteria is attained.

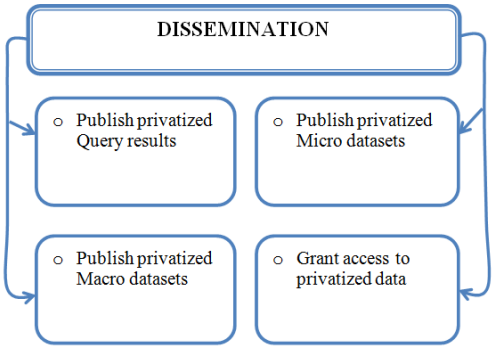

Figure 9. The SIED Dissemination phase.

 ISBN: 978-1-61208-340-7

D. Dissemination phase

The last phase of the SIED framework is concerned mainly with how the data privacy agent disseminates privatized data, as shown in Figure 9. Publication of the privatized data set would largely depend on user requirements. For instance if the user requires that query results to be privatized, differential privacy could be applied in the initial stages on the original data and the disseminated results would be privatized query results. On the other hand the user might require publication of micro and macro tabulated results. However, the requirements might be that the agent communicates privatized results to other agents for further processing. Therefore, agent dissemination of privatized data would largely depend on the user requirements.

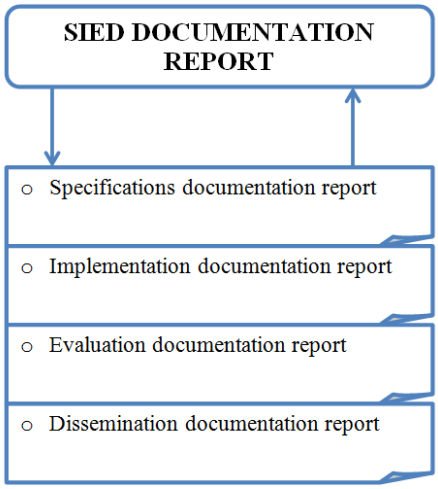

Figure 10. The SIED documentation outline.

As illustrated in Figure 10, documentation is done at every phase of the SIED data privacy engineering process, resulting in a final complete documentation report on the data privacy engineering process for that particular data set.

IV. CONCLUSION AND FUTURE WORK

We have presented an abstract view of SIED, an agent-based data privacy engineering framework that could be employed for a systematic data privacy design and implementation. We believe that this a contribution to the privacy-by-design challenge. In addition, we presented a literature review of related work on agent-based software engineering and the influence of such work on data privacy engineering. While SIED is proposed as a framework for agent-based data privacy engineering, it could be generalized for other non-agent-based data privacy processing as well. The subject of data privacy remains a challenge and more research, design, implementation, and metrics is needed to accommodate the ambiguous and fuzzy privacy requirements of individuals and entities. We believe that intelligent agent-based architectures offer optimism for data privacy solutions. For future works, we plan on expanding this study to take a decomposition approach in dealing with the complexity of agent-based data privacy engineering.

REFERENCES

[1] A. Cavoukian, Privacy by Design… Take the Challenge. Information & Privacy Commissioner of Ontario, 2009.
[2] A. Cavoukian, S. Taylor, and M. Abrams, “Privacy by Design: Essential for Organisational Accountability and Strong Business Practices.,” Identity Inf. Soc., vol. 3, no. 2, 2010, pp. 405–413.
[3] V. G. Cerf, “Freedom and the social contract,” Commun. ACM, vol. 56, no. 9, 2013, pp. 7.
[4] S. Spiekermann, “The challenges of privacy by design,” Commun. ACM, vol. 55, no. 7, Jul. 2012, pp. 38.
[5] V. Katos, F. Stowell, and P. Bednar, “Surveillance , Privacy and the Law of Requisite Variety,” 2011, pp. 123–139.
[6] K. Mivule, D. Josyula, and C. Turner, “An Overview of Data Privacy in Multi-Agent Learning Systems,” in The Fifth International Conference on Advanced Cognitive Technologies and Applications, 2013, no. c, pp. 14–20.
[7] K. Mivule and C. Turner, “A Comparative Analysis of Data Privacy and Utility Parameter Adjustment, Using Machine Learning Classification as a Gauge,” Procedia Comput. Sci., vol. 20, 2013, pp. 414–419.
[8] R. Dayarathna, “Taxonomy for Information Privacy Metrics,” J. Int. Commer. Law Technol., vol. 6, no. 4, 2011, pp. 194–206.
[9] G. J. Matthews and O. Harel, “Data confidentiality: A review of methods for statistical disclosure limitation and methods for assessing privacy,” Stat. Surv., vol. 5, 2011, pp. 1–29.
[10] I. Sommerville, Software Engineering, 9th ed. Addison-Wesley, 2010, pp. 27–50.
[11] G. Booch, Object Oriented Analysis & Design with Application. Santa Clara, CA: Addison-Wesley, 1994, pp. 14–20.
[12] M. Wooldridge, “Agent-based software engineering,” IEE Proc. - Softw. Eng., vol. 144, no. 1, 1997, pp. 26.
[13] M. J. Wooldridge and N. R. Jennings, “Software engineering with agents: Pitfalls and pratfalls.,” IEEE Internet Comput., vol. 3, no. Jun, 1999, pp. 20–27.
[14] N. R. Jennings, “On agent-based software engineering,” Artif. Intell., vol. Volume 117, no. 2, 2000, pp. 277–296.
[15] J. J. Borking and C. Raab, “Laws, PETs and other technologies for privacy protection.,” J. Information, Law Technol., vol. 1, 2001, pp. 1–14.
[16] S. Kenny and J. Borking, “The Value of Privacy Engineering,” J. Information, Law Technol., vol. 2., no. 1, 2002.
[17] G. W. Van Blarkom, J. J. Borking, and J. G. E. Olk, Handbook of privacy and privacy-enhancing technologies. The Hague: College Bescherming Persoonsgegevens, 2003, pp. 1–4.
[18] F. L. y López, M. Luck, and M. D’Inverno, “A Normative Framework for Agent-Based Systems,” Comput. Math. Organ. Theory, vol. 12, no. 2–3, 2004, pp. 227–250.
[19] P. Bresciani, A. Perini, P. Giorgini, F. Giunchiglia, and J. Mylopoulos, “Tropos: An agent-oriented software development methodology.,” Auton. Agent. Multi. Agent. Syst., vol. 8, no. 3, 2004, pp. 203–236.
[20] F. Zambonelli and A. Omicini, “Challenges and research directions in agent-oriented software engineering,” Auton. Agent. Multi. Agent. Syst., vol. 9, no. 3, pp. 253–283.
[21] S. Park and V. Sugumaran, “Designing multi-agent systems: a framework and application,” Expert Syst. Appl., vol. 28, no. 2, Feb. 2005, pp. 259–271.
[22] F. Bellifemine, G. Caire, A. Poggi, and G. Rimassa, “JADE: A software framework for developing multi-agent applications. Lessons learned,” Inf. Softw. Technol., vol. 50, no. 1–2, Jan. 2008, pp. 10–21.
[23] D. Weyns, H. V. D. Parunak, and O. Shehory, “The Future of Software Engineering and Multi-Agent Systems,” Int. J. Agent-Oriented Softw. Eng., vol. 3, no. 4, 2008, pp. 1–8.
[24] M. Cossentino, N. Gaud, V. Hilaire, S. Galland, and A. Koukam, “ASPECS: an agent-oriented software process for engineering complex systems,” Auton. Agent. Multi. Agent. Syst., vol. 20, no. 2, Jun. 2009, pp. 260–304.
[25] T. Leaute and B. Faltings, “Privacy-Preserving Multi-agent Constraint Satisfaction,” in 2009 International Conference on Computational Science and Engineering, 2009, pp. 17–25.
[26] J. M. Gascueña, E. Navarro, and A. Fernández-Caballero, “Model-driven engineering techniques for the development of multi-agent systems,” Eng. Appl. Artif. Intell., vol. 25, no. 1, 2012, pp. 159–173, Feb.

 ISBN: 978-1-61208-340-7

[27] A. Cavoukian, Privacy by Design The 7 Foundational Principles Implementation and Mapping of Fair Information Practices. Office of the Information and Privacy Commissioner (2011), 2011.
[28] J. M. Such, A. Espinosa, and A. Garcia-Fornes, “A survey of privacy in multi-agent systems,” Knowl. Eng. Rev., 2012, pp. 1–31.
[29] D. Aggarwal and A. Singh, “Software Agent Reusability Mechanism at Application Level,” Glob. J. Comput. Sci. Technol., vol. 13, no. 3, 2013, pp. 8–12.
[30] H. Hayashi, S. Tokura, F. Ozaki, and M. Doi, “Background sensing control for planning agents working in the real world.,” in Agent and Multi-Agent Systems: Technologies and Applications, 2008, pp. 11–20.
[31] K. Mivule and C. Turner, “A Review of Privacy Essentials for Confidential Mobile Data Transactions,” Int. J. Comput. Sci. Mob. Comput. ICMIC13,, no. December, 2013, pp. 36–43.
[32] A. Krause and E. Horvitz, “A Utility-Theoretic Approach to Privacy in Online Services,” J. Artif. Intell. Res., vol. 39, 2010, pp. 633–662.

 ISBN: 978-1-61208-340-7

Improving Skills Management using Objectives within a Multi-Agent System

Olivier Chator
Conseil Général de la Gironde
IMS Laboratory, CNRS, IPB
Bordeaux, France
o.chator@cg33.fr

Jean-Marc Salotti
IMS Laboratory, CNRS, IPB
Bordeaux, France
jean-marc.salotti@ensc.fr

***Abstract*—Whatever the professional sector of activity, achievements are the results of dedicated processes and skill usage. If a project is successful, the knowledge and know-how that have been used have to be capitalized for a possible use in other projects. However, this is a dynamic process. Skills are always evolving. The issue is how to improve the management of skills to make them more efficient over time. A new approach is proposed to address this problem. It is based on the management of objectives through a multi agent learning system where skills are represented as agents. Being autonomous entities, and having their own learning abilities, skills will enforce project efficiency, capitalizing on past iterations. The key point of our approach is the appropriate exploitation of past objectives to help the user identifying the required skills for the new project.**

Keywords-Multi-agent systems; objectives; skills; governance

I. INTRODUCTION

Whatever the goal is (e.g., improve the energy balance of a house by installing photovoltaic panels on the roof or win a rugby match next Sunday), the problem is always stated as doing something to achieve something. Then, the project comes into place. Goals and objectives are statements that describe what the project will accomplish. Each project is defined (structured) by a set of resources and processes according to a specific schedule. The processes are based on a set of required skills. Importantly, the definition of the project may evolve according to the environmental conditions, the past experiences, meaning that the list of skills required to reach the goal may not always be the same. Let us consider the goal of "building a house". Even if the process is almost the same, different construction materials (like cinderblocks or bricks) may be used. This implies different skills for each building project. Considering past experience in the domain, a dynamic dimension is observed for each project over time.

Then, the point is how to improve the management of skills to make them more efficient, throughout projects, and over time. If a user wants to address a new goal, how to define the project and what are the skills needed to implement it? How to get benefits from past projects? In order to solve the problem, it is suggested to work on the goals and skills of past projects using a learning multi-agent system [1] [2] [3], where skills are autonomous agents [4].

Our proposal is based on a "Skill sharing" multi-agent system (MAS). It has already been presented in a previous paper [4] and implements learning abilities that are close to "Case Based Reasoning" mechanisms [13]. In this new paper, Section II starts with a short reminder of the MAS. A new method is then proposed to help the user defining a new project based on previous objectives, objective domains and skills used to implement past projects. The first results are shown in Section III. Section IV concludes this document.

II. MODEL

A. The issue

Let us present one of the missions of "Conseil Général de la Gironde" (CG33). As a local authority, CG33 defines policies and practices for the Sustainable Development (SD) of the "département" (a territorial division lower than regions). In Gironde, 61 of the local authorities are part of an "SD Network". When looking for feedbacks about SD projects, each Network Member (NM) uses an information system, where they share experience and skills [4]. When defining an (potentially new) SD project, each NM needs to identify the skills needed to make his project a success. It is also interesting to get benefits from past experience on similar projects to build the new one. Let us illustrate with the objective: "*I want to put photovoltaic panels on the roof of my house*". I have to find the skills required for this new project. At time T, taking into account my needs and experience of past projects, there are two options:

- I find a past project that reflects exactly what I want to do. Thus, what I need is to find a way to retrieve all the skills of this project, and proceed to my new project creation using this list.
- I find a past project, but it is not exactly what I want to do. Thus, what I need is to retrieve a subset of the skills of this project, and proceed to my new project creation using this restricted list.

The two points above are efficient if the user finds projects that already required all or part of the skills required to implement the new one. However, this is not always the case. Skills may be scattered throughout various projects. Thus, the point is to find a way to answer to a limited expression of needs at specification level. For example, consider we have already in the system the two past projects: "wind turbine implementation" and "hydraulic micro power implementation". They both belong to the same "domain": "new means of energy production". If the user wants to build a new project, in the same domain (e.g., the implementation

 ISBN: 978-1-61208-340-7

of solar panels), an interesting idea is to look for skills used in all the past projects of this domain. Thus, the system will suggest integrating the skills that were fluently used across all projects in the domain. It is possible to generalize this example. Each professional sector of activity has procedures and processes, each of them used to reach specific goals or objectives. Each objective may be declined throughout concrete projects, themselves composed by skills. Generally speaking, it may be difficult to make processes evolve according to environmental constraints. When successful, the knowledge and know-how that have been used should be capitalized for a possible use in further projects. Finally, an important issue is to find a way to improve the management of skills to make projects more efficient over time. To do this, it is possible to build new projects, working on past projects or objective domains. The goal of this work is thus to dynamically improve new projects definitions and to identify the skills needed to make them a success.

B. Working with objectives: theoretical proposal

1) Main concepts

Let us consider an example to illustrate the use of "objective" in our MAS: "*To make energy savings, I want to put a better insulation into the walls of my flat*". This example drives us to the definition of five concepts further used in this paper.

a) Environment

An environment is viewed as a professional sector of activity. In our example, "*sustainable building sector*" is the environment in which the user request occurs. This is the highest level of abstraction and it is related to the professional sector of activity.

b) Objective domain

An objective domain is a group of objectives, concerned by the same thematic of activity. In our example, "*thermal insulation improvement*" is the objective domain in which the user request occurs. Another domain could be "*air tightness improvement*". The idea is to position objectives into one or several objective domains.

c) Objective

An objective is a simple textual description of a goal to reach (the term "goal" would have been more appropriate, but "objective" was chosen from the start for convenient reasons and links with the French language). In our example, the objective is to "*put a better insulation into the walls*". This objective is part of the "*thermal insulation improvement domain*". Considering this simple question from the user, no constraint about materials or skills used to reach the goal is expressed. Another objective could be "*improve air tightness in my flat*". In our implementation, an *Objective* agent is available. To transpose an objective in "real life", it is mandatory to firstly define first a project.

d) Projects

A project is defined by an objective, a start date, an end date, resources (like human actors) and processes to schedule the list of skills to use. In our example, a project defined by the "*integration of glass wool into walls*" is proposed. It will start next week, will stop in 15 days, and requires several skills. Finally, the project is implemented and evaluated at the end using the Elementary Competencies (ECs) of each skill.

e) Skills

As already mentioned in [4], the skill is the ability to exploit some knowledge and know-hows in order to solve a class of problems. It is different from a competency, which is generally accepted as a set of behaviors or actions that have to be successfully implemented within a particular context [8]. Skills are used into projects to reach the goal (the objective).

2) Objectives' type

For a user, the problem is to reach a goal. It is usually defined by a simple assertion like "*I want to do something*". In order to reach the goal, the user will define in our system a new project. He does not often have the knowing of all skills that have to be used into the project. As it is difficult to give a unique answer, depending on the user request at time T, two approaches are proposed to build new projects. The first one is based on completed projects and their objective. The second consists of building the new project using only concerns about the objective's domain, and eventually the environment. This case occurs when the user wants to do actions in a particular domain of activity, but does not exactly know what to do.

C. Skill Agents

1) Integrating feedbacks from experience

As described in a previous work [4], at CG33 and in "real life", numerous SD projects have been realized. To improve future SD projects efficiency, feedbacks show that it is important to enhance human cooperation, and that each actor has only a partial knowledge of the capabilities of the other. An information system, accessible by all actors, offers to each of them a better view of their various expertise areas. Even if the final goal is to know who is able to do something, defining the need as precisely as possible is the key Thus, the proposed information system is centered on skills and not on actors [8]. Furthermore, as skills always evolve, and it is often difficult to explicit them, the proposal is to use a multi-agent system with skill agents. Each of these agents considers human actors as resources, tries to determine its elementary skills over time (self definition), and aims to be involved in SD projects. Generalizing, the challenge is to allow each stakeholder of a project to share and learn more about the expertise and know-how of the others. A traditional approach is to consider direct links between actors and skills, in a "static point of view". Here, the central role of skills, and not of actors, is explicit. Thus, at CG33, an online collaborative skills sharing tool has been elaborated.

 ISBN: 978-1-61208-340-7

2) Definition

It is assumed that a skill is unique and can be implemented as an agent in a multi-agent system. A skill agent is cognitive, non-conversational and non-dialogic [1] [7]. It has resources (a list of physical actors) and its own life cycle. For the sake of simplicity, it has been assumed that a skill is a sum of ECs [8] within projects. Each EC is evaluated after realization and contributes to the learning abilities. Doing so, defining the "embodiment" [5][6] of skill agents, an EC is part of the global skill definition. The skill agent environment is defined by indirect (through another technical agent called *WebRequester*) interactions with the users. It has:

- *Perception*: It listens to information broadcasted by other agents or environmental evolutions, e.g., a new project starts.
- *Internal attributes*: It is defined by a list of elementary competencies, a creation date, a domain(s) of activity, and a specific "*age*".
- *Action*: It updates its behavioral rules and the weight of elementary competencies that define it.

3) Learning mechanisms

The main concerns of the learning mechanism, for a skill agent, are actors' selection (identifying a human person for the embodiment [5][6] of the skill), links establishment with other skill agents, and improving skills management using objectives. The link establishment decision is based on similarity studies, like common involvement into projects over time. Behavioral rules' evolution is a consequence of those learning mechanisms. Skills management improvement concerns will be detailed further.

D. Building new projects from past Projects

Two cases are available to build the new project, duplicating, or customizing existing ones. From our previous example, we will suppose that the user finds the project "*integration glass wool into walls*". One may then:

- Think that it is exactly his objective. Thus, he will duplicate this project and all its skills, without creating a new one, changing only contextual information like the start date for example.
- Think that it is not exactly his objective, but is very close. He decides to create a new project and customizes the list of skills associated to the existing project. A new objective is thus created with a new list of skills built from a subset of the previous one.

Finally, in both cases, a new project instance is generated from the objective. In our implementation, those operations are done throughout our unique *Objective* agent into the MAS. As those actions are based on historical data, no communication with skill agents themselves is needed.

E. Building new projects from an objective domain

Let us assume that a new project has to be built according to the user needs. There is sometimes a limited expression of needs at the specification level and the objective might be met for the first time. The user would probably not know how to address the problem and how to exploit past projects. There is nevertheless a solution to help the user. The idea is to determine all the skills involved in past projects in the same objective domain, or eventually in the same environment. In our system, a skill "***wants to be involved***" in the new project according to a degree of involvement in past projects (see further). In contrast to what we have proposed in paragraph D, this method is not limited to an exchange with the *Objective* agent. In cognitive science, effective agents are obtained by the embodiment of mind [5] [6]. If a skill alone has no perception, no motivation and no means to perform an action and change its environment, it is always possible to define them artificially. Several types of motivations have been integrated in skill agents: contribution to new projects, determine the list of elementary competencies that define themselves [4], and determine their relationships with the other skills [4]. Let us develop an example showing the motivation of being involved in new projects. A user defines a project in the "*thermal insulation improvement*" objective domain. No more detail is forwarded to the system. "*Thermal insulation improvement"* is an objective domain and is part of the environment "*sustainable building sector*". The answer of our system is defined by the following process:

- The *Objective agent* receives the user request.
- The *Objective* agent sends (broadcasts) the request to all skill agents within the MAS.
- Each skill agent computes a "*relevance coefficient"* according to the request content, and returns an answer to the Objective agent (see next paragraph).
- The *Objective* agent consolidates all answers from skill agents, and returns the list of candidates to the user

Each skill agent is autonomous and decides if it wants (or not) to contribute to the new project. The key point is the computation of the relevance coefficient. It is the percentage of projects in which the skill has been involved in the past among all projects of the objective domain. If it exceeds a threshold, the skill agent wants to be involved in the new project.

III. IMPLEMENTATION AND RESULTS

A. The MAS architecture

The model has been implemented using the JADE MAS and standard multi-agent tools [4][9][10][11][12] (see Figure 1, where the focus is on exchange of flows). Synthetically, the Web *Requester Servlet*, *Gateway*, and *WebRequester Agent* are java components used for the management of the exchanges between human users and the MAS itself. The *WebRequester Agent* is in charge of the interactions with the human user, forwarding requests to other agents, and sending back their answers. It guarantees (FIPA compliance [11]) that no direct exchange is possible between human users and skill agents. The *Objective* Agent, according to Ferber's classification, is reactive [1]. When a

 ISBN: 978-1-61208-340-7

new project creation request is received from the user, through the technical agent *WebRequester*, this agent retrieves "existing projects" or sends broadcasts to all skill agents. At CG33, 110 skill agents are active and running into the JADE MAS [4].

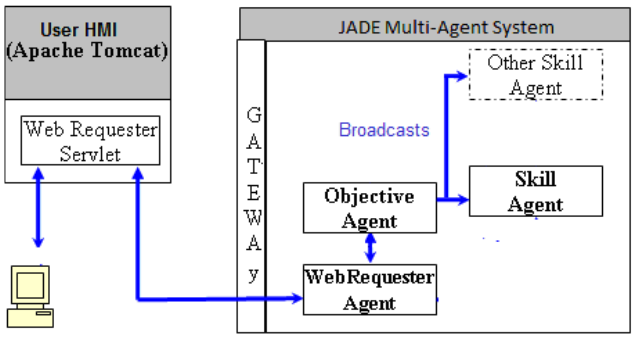

Figure 1. The MAS – Focus on broadcasts

B. Results

1) Real context

As already seen, in Gironde, there are 61 "SD Network" members. They share their experiences and skills through the collaborative "*Sustainable development Skill Sharing System*" application. Skills have been classified into a preliminary list of 9 objective domains: political wishes, sensitization, diagnostic, prospective, developing the strategy, elaborating the action plan, implementation of the action plan, evaluation, and continuous improvement. This application started to be used by the beginning of the year 2013. The first skills concern the management of SD projects. Thus, the results presented below are expressed in this context.

2) Case 1: new projects from past Objectives

The user request, through the *WebRequesterAgent*, is transmitted to the *Objective* agent (see figure 2).

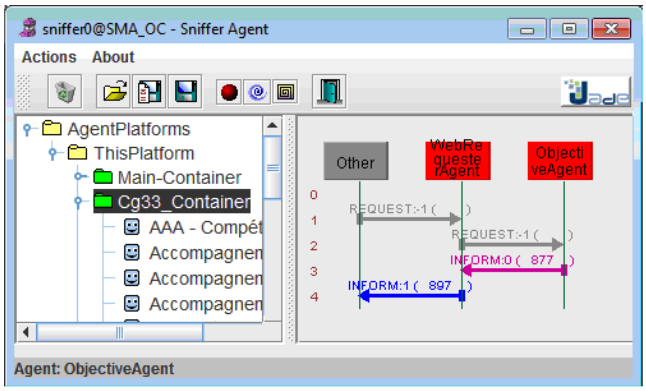

Figure 2. Case 1 - Exchanges between agents into the JADE MAS

Figure 2 is a screen copy of the JADE MAS Sniffer tool that monitors message exchanges among agents. The left part shows the MAS Agent tree where an agent is part of a container, a container belongs to a platform (*ThisPlatform*) and a platform is included in all agent platforms (*AgentPlatForms*). The right part shows three "boxes":

- *Other*: reflects other agents within the MAS, or in this case, the JADE gateway that manages exchanges with the external users
- *ObjectiveAgent*: see next paragraph for details.

The arrows (1 to 4) show the message exchanges, with their type (REQUEST or INFORM for the answer), and their directions (from sender to receiver).

The *ObjectiveAgent* ensures the treatments, based onto historical data, to retrieve projects instances and related skills. At the end, it processes the answer by means of an XML flow (see Table 1 of this flow).

TABLE I. LIST OF THE XML FIELDS INTO THE ANSWER FLOW

XML Tag	Comment
answers	Main tag encapsulating the answers
answer	Main tag for each answer, 1 for each project
newObjective	Boolean value indicating that the project is new. Value always false here because the project is over and taken into the historical
objective	Main tag for the past project
code	The past project code within the projects database table
description	The past project textual description within the projects database table
startDate	The past project start date
endDate	The past project end date
skills	Main tag encapsulating the skills list
skill	Main tag, 1 per skill
code	The current skill code within the skills database table
description	The current skill textual description within the database table

At the front-office user level, a list of projects and skills is proposed. The new user project is then generated according to one of the 2 identified methods: duplicate, or customize.

3) Case 2: new projects from objective domain

The user request is sent to the *ObjectiveAgent* that does a broadcast to all skill agents, consolidates their answer. At the end, the answer is also returned to the user as an XML flow (see Case 1 for details). Please note that a level of "genericity" for the broadcasting mechanisms is introduced (see figure 3).

 ISBN: 978-1-61208-340-7

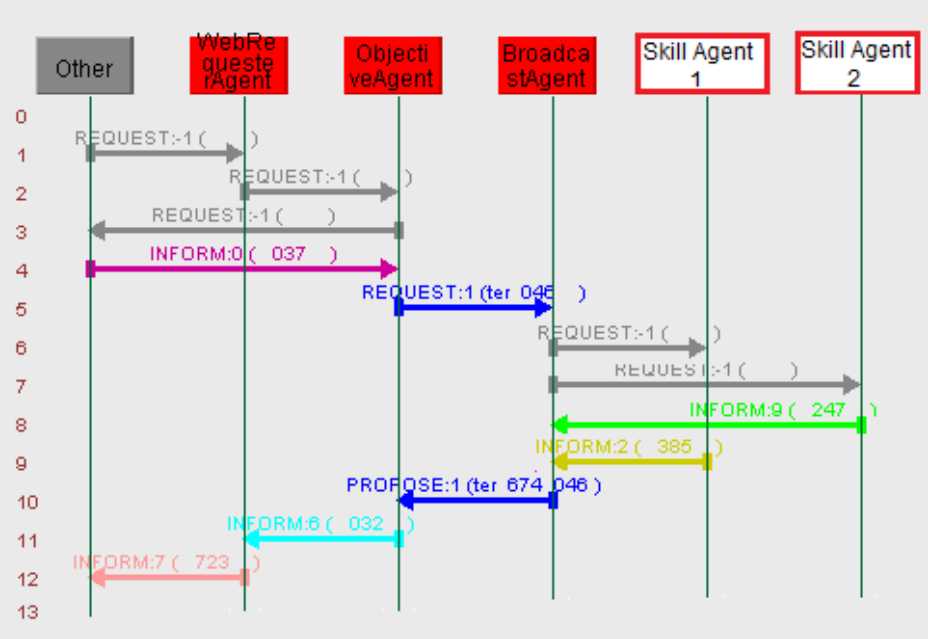

Figure 3. Case 2 - Exchanges between agents into the JADE MAS. See text.

Figure 3 is also a screen copy of the JADE MAS Sniffer tool. Only the right part of the window is shown to improve the visibility. The first three "boxes" are identical as those described for figure 2. Please note that *BroadcastAgent* is a technical agent. It receives a message from an original sender, broadcasts it to all agents, and consolidates all answers into a single one. The global answer, an XML flow, is then sent back to the original sender. *All other boxes on the right* are all skill agents within the MAS. The screen copy above shows only two skill agents.

For illustration, let us reuse the example where the objective domain is "*new means of energy production*". A project for a "*wind turbine implementation*" has 5 phases:

1. *Project management / implementation*
2. *Definition of power requirements*
3. *Selection of the best technology of wind turbine among models and worldwide suppliers*
4. *Logistic definition (transportation organization)*
5. *Wind turbine installation*

A second project, entitled "*hydraulic micro power implementation*", shares 3 (over 5) common phases with the first project, and has 5 *specific ones*:

1. *Project management / implementation*
2. *Definition of power requirements*
3. *Selection of the best technology of hydraulic micro power among models and worldwide suppliers*
4. *Logistic definition (transportation organization)*
5. *Hydraulic micro power installation*
6. *Technology transfer of appropriate designs to developing country manufacturers*
7. *Project formulation and appraisal for national and international aid agencies*
8. *Training on small-hydro technology and economics*

A third one, entitled: "*installation of a biodiesel generation system to power up a highway construction site*". Let us assume the project also shares the 3 common phases, and has *4 specific ones*:

1. *Identify the best site*
2. *Environmental benefits evaluations*
3. *Project management / implementation*
4. *Definition of power requirements*
5. *Selection of the best technology of biodiesel generation system among models and worldwide suppliers*
6. *Logistic definition (transportation organization)*
7. *Biodiesel generation system installation*

Considering these phases as skills (of course at a high level of abstraction), let us introduce into the system a new user request where the new project is "*solar panels implementation*". This project also belongs to the objective domain "*new means of energy production*". The requested minimum value for the relevance coefficient is 75%. Thus, according to our algorithm:

- The *ObjectiveAgent* send (broadcasts) the user request to all the skill agents within the MAS (here 3 common + 5 specifics according to the second and third project phases)
- Each skill agent computes its dedicated relevance coefficient. If this computed value is greater than the requested one, that means the skill agent "wants" to

 ISBN: 978-1-61208-340-7

contribute to the new objective, and the boolean value "*true*" is returned to the *ObjectiveAgent*

- The *ObjectiveAgent* consolidates the results where the answer is "*true*". Finally, it returns to the user the list of the skills as an XML flow:
  a - Project management / implementation
  b - Definition of power requirements
  c - Logistic definition (transportation organization)
- Through the front-office interface, the user then validates (partially or totally) the skills list to build its new project. This validation is stored into memory.

C. Discussion

The proposed information system proposes solutions to the problems of each SD Network Member at CG33, who needs to identify the required skills to make his project successful. Whatever the activity sector, project management is usually carried out through software applications, where tasks are defined and described in a static way. The definition of a new project requires the identification of human actor(s) for each of them. Two problems may be encountered:

- The first problem occurs when an evolution of the processes is considered. A traditional approach is to statically update the list of tasks for the project. Setting renewals have to be done by administrators, or advanced users, into the project management tool itself. This update is often generating costs, because in some cases an external help (e.g., of the software editor) is required. This way, there is a lack of efficiency, inducing at least a waste of time, and sometimes substantial costs overruns.
- Another problem is the management of the dynamic nature of projects according to the evolving needs of users. As a project reflects the user needs at a given date, there can be as many projects as user needs expressions within the system. The global skill sharing system presented in this paper is a collaborative and adaptive tool. The new projects are built "on the fly", from the real user needs. Thus, the list of new skills is built from those available in past projects and reflects the user needs at the time of the request. As the number of projects grows in our collaborative system, the global list of skills and the objective domains evolve and may converge. At a global level, our system learns from the requests of the users and reflects the evolution of activity over time. The observation of those evolutions will drive the management of the company to put the focus or to drop certain skills. Our proposal provides, therefore, an interesting solution to the problem of skills management, using objectives, at the project and organization levels.

IV. CONCLUSION AND FUTURE WORK

Over time, more and more objectives will be concretized through projects, and more and more information will be available to help the user. This work suggests interesting perspectives. From a professional point of view, concerning the problem of skills management, the analysis of skills applications through projects provides a wealth of information. After a period of running, managers and human resources management services will be able to identify the key skills, the cross-domain skills, the evolution of "sensibility" of each skill into the professional sector processes, and all of this over time. This work may introduce real benefits in human resources management to anticipate future evolutions of needs in terms of collaborators profiles.

In our proposal, the adaptation over time is made possible by the computation of a relevance coefficient value. This value is stored into the memory of each skill agent. One of the future directions of works is to implement complementary learning mechanisms to optimize the computation of this value over time.

REFERENCES

[1] J. Ferber, "Multi-Agent Systems. An Introduction to Distributed Artificial Intelligence", Addison Wesley, London, UK, 1999.

[2] N. R. Jennings, M. Wooldridge, and K. Sycara, "A roadmap of agent research and development. Int Journal of Autonomous Agents and Multi-Agent Systems", Kluwer Academic Publishers, Boston (USA), 1998, pp. 7-38.

[3] L. Shapiro, "Embodied Cognition", in Oxford Handbook of Philosophy and Cognitive Science, E. Margolis, R. Samuels, and S. Stich (eds.), Oxford University Press, 2010

[4] O. Chator, J. M. Salotti, and P. A. Favier, "Multi-agent System for Skills Sharing in Sustainable Development Projects", proceedings of COGNITIVE 2013, the 5th International Conference on Advanced Cognitive Technologies and Applications, IARIA Conference, Valencia, May 27-June 1, 2013, pp. 21-26,

[5] F. Varela, E. Thompson, and E. Rosch, "The Embodied Mind: Cognitive Science and Human Experience", MIT Press, 1991.

[6] L. Shapiro, "Embodied Cognition", in Oxford Handbook of Philosophy and Cognitive Science, E. Margolis, R. Samuels, and S. Stich (eds.), Oxford University Press, 2010

[7] G. Weiss, "Multiagent Systems, a Modern Approach to Distributed Artificial Intelligence", MIT Press, 2013.

[8] M. Mulder, T. Weigel, and K. Collins, "The concept of competence in the development of vocational education and training in selected EU member states: a critical analysis", Journal of Vocational Education and Training , vol. 59, 2007, pp. 67-88.

[9] G. Rocher, "The Definitive Guide to Grails", Apress, New York, USA, 2006.

[10] S. Goderis, "On the separation of user interface concerns: A Programmer's Perspective on the Modularisation of User Interface Code", Ph.D. thesis, VrijeUniversiteit Brussels, Belgium, 2007.

[11] FIPA, "Foundation for Intelligent Physical Agents - Abstract Architecture Specification (Standard Version)", publication des Technical Committee de la FIPA, Geneva, Switzerland, 2002.

[12] F. Bellifemine, A. Poggi, and G. Rimassa, "JADE – A FIPA-compliant agent framework", 4th International Conference on Practical Application of Intelligent Agents and Multi-Agent Technology (PAAM-99), London (UK), 1999, pp. 97-108.

[13] J. L. Kolodner, "Case-Based Reasoning", Morgan Kaufmann Publishers, San Mateo, USA, 1993

 ISBN: 978-1-61208-340-7

Discriminative Learning of Relevant Percepts for a Bayesian Autonomous Driver Model

Mark Eilers
Human Centered Design
OFFIS Institute for Information Technology
Oldenburg, Germany
e-mail: mark.eilers@offis.de

Claus Möbus
Learning and Cognitive Systems
Carl-von-Ossietzky University
Oldenburg, Germany
e-mail: claus.moebus@uni-oldenburg.de

***Abstract*—Models of the human driving behavior are essential for the rapid prototyping of assistance systems. Based on psychological studies, various percepts and measures have been proposed for the lateral and longitudinal control in driver models without demonstrating the generalizability of results to natural settings. In this paper, we present the learning of a probabilistic driver model. It represents and mimics the lateral and longitudinal human driving behavior on virtual highways by performing situation-adequate lane-following, car-following, and lane changing behavior. Because there is considerable uncertainty about the relevant percepts in natural driving behavior, we select hypothetically relevant percepts from the variety of possibilities based on their statistical relevance. This is a new approach to generate hypothesis about the relevant percepts and situation-awareness of drivers in dynamic traffic scenes. The percepts are revealed in a structure-learning procedure using a discriminative scoring criterion based on the Bayesian Information Criterion. Discriminative learning maximizes the conditional likelihood of probabilistic models, whereas the traditional generative learning maximizes the unconditional likelihood. This way, it attempts to find the structure with the best performance for the intended use, which in our application is the best prediction of driving actions given the available percepts.**

Keywords–Probabilistic Driver Models; Bayesian Autonomous Driver Models; Machine-Learning; Structure-Learning; Discriminative Learning.

I. INTRODUCTION

The Human Centered Design of intelligent transport systems requires computational models of human behavior and cognition. Particularly models of the human driving behavior (i.e., driver models) are essential for the rapid prototyping of error-compensating assistance systems [1]. Various authors proposed control-theoretic models (e.g., [2]), closely related perception-action models (e.g., [3][4]), and production-system models implemented in cognitive architectures (e.g., [5]). Due to the variability of human cognition and behavior, the irreducible lack of knowledge about underlying cognitive mechanisms, and the irreducible incompleteness of knowledge about the environment [6], we conceptualize, estimate, and implement models of human drivers as probabilistic models: Bayesian Autonomous Driver (BAD) models.

In earlier research [7], we developed a BAD model with Dynamic Bayesian Networks (DBNs), based on the assumption that a single DBN representing a single skill is sufficient for lateral and longitudinal control. Later, we realized that for modeling the complex competence of human drivers, a skill hierarchy (e.g., Figure 1) is necessary. We developed a hierarchical modular probabilistic architecture that allows to construct driver models by decomposing complex behaviors into pure behaviors and vice versa: Bayesian Autonomous Driver Mixture-of-Behaviors (BAD MoB) models [8][9][10].

Based on psychological studies (e.g., [11][12][13] [14][15]), various percepts and measures have been recommended for the lateral and longitudinal control in driver models. These proposals are partly contradictory and often depend on special experimental settings, like straight roads, winding roads, low speed, and/or the absence of other traffic participants. Other and more natural scenarios may provide and require different perceptual cues that are not yet fully understood or formalized. A general computational vision theory of driving behavior is still pending.

Because there remains considerable uncertainty about the relevant percepts in natural driving behavior, we propose the use of structure-learning procedures to select hypothetically relevant percepts from the variety of possibilities based on their statistical relevance. We used the proposed procedure to learn the relevant percepts for a BAD MoB model that represents and mimics the lateral and longitudinal human driving behavior on virtual two-lane highways according to the skill hierachy shown in Figure 1. We assume that the overall complex driving behavior can be decomposed into the simpler behaviors lane-following, car-following, performing lane changes to the left and lane changes to the right.

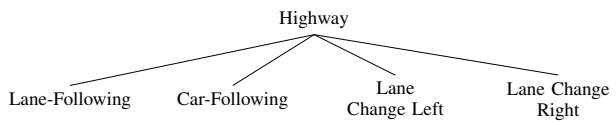

Figure 1. Skill hierarchy representing the human driving behavior on virtual two-lane highways.

 ISBN: 978-1-61208-340-7

The paper is organized as follows. In the following section we give a brief overview of percepts and measures that have been recommended in the literature for modeling the lateral and longitudinal human control behavior. Section III introduces the fundamentals of BAD MoB models. In Section IV, we describe a structure-learning procedure for selecting the pertinent percepts from a universe of hypothetically available percepts, using a discriminative version of the Bayesian Information Criterion. In Section V, we present a resulting BAD MoB model that mimics the human driving behavior on virtual highways and discuss the meaningfulness of the learned percepts with respect to the literature. Finally, we conclude with Section VI.

II. A UNIVERSE OF PERCEPTS

For the most part, the literature considers three types of percepts as important for lateral control: *bearing angles* [13][14][3][16], *splay angles* [13][14][17], and the *optic flow* [13][14][17] (Figure 2).

Bearing angles are defined as the angles between the driver's heading (the driver's body axis, assuming that he is belted in) and the direction to specific reference points in the driver's field of view (Figure 2a) [14]. If available, obvious choices for such reference points are the lane edges. When aligned with the course of the road, a conceivable strategy for lane-keeping on a straight path is to keep the bearing angle to a reference point on the left lane edge and the bearing angle to a reference point on the right lane edge constant [14].

Bearing angles to single reference points that drivers tend to *visually target* are also known as *visual direction angles* [13]. Notable proposed examples for such targeted reference points are points on the future path of the driver, the centerline, lead-cars, and for curved roadways, the tangent point [3][18][19].

Splay angles are defined as the optical projections of lane edges or the centerline around a reference point on the driver's retina relative to a vertical line in the driver's field of view, e.g., the heading [14] (Figure 2b). Similar to bearing angles, when aligned with the course of the road, a valid strategy for lane-keeping would be to keep the splay angle to the left lane edge and the splay angle to the right lane edge constant.

The optic flow denotes the global image motion of the environment projected on the retina when one moves in the world [14][16]. Similar to bearing and splay angles, we can define flow angles as the angles between the driver's heading and the direction of the optic flow of reference points in the driver's field of view (Figure 2c). A simple strategy for lane-keeping using the optic flow would be to align the focus of expansion (specified by the intersection of two flow angles) with the intended target direction.

For longitudinal control, the literature mainly discusses the time-to-contact/collision (TTC) [13][20][21] and the time-headway (THW) [21][22]. The TTC of a vehicle A with a speed v_A, following a vehicle B with a speed v_B, in a distance d, is defined as TTC $= d/(v_A - v_B)$ and denotes the remaining time until A reaches B. As a special case of the TTC, the THW denotes the remaining time until A will reach the current position of B and is defined as THW $= d/v_A$.

III. BAYESIAN AUTONOMOUS DRIVER MIXTURE-OF-BEHAVIOR MODELS

Throughout this paper, we will be concerned with probability distributions over sets of discrete random variables. Variables and set of variables will be denoted by capital letters, while specific values taken by those (sets of) variables will be denoted by lowercase letters. For time series, we assume that the timeline is discretized into time-slices with a constant granularity of 50ms. We will index these time-slices by non-negative integers and will use X_i^t to represent the instantiation of a variable X_i at time t. A sequence $X_i^j, X_i^{j+1}, \ldots, X_i^k$ will be denoted by $X_i^{j:k}$ and we will use the notation $x_i^{j:k}$ for an assignment of values to such sequences.

A Bayesian Network (BN) is an annotated directed acyclic graph (DAG) that encodes a joint probability over a set of variables $X = \{X_1, \ldots, X_n\}$ [23]. Formally, a Bayesian Network B is defined as a pair $B = \{G, \theta\}$. The component G is a DAG, whose vertices correspond to the random variables $X_1, \ldots, X_n$, and whose arcs define the (in)dependencies between these variables, in that each variable X_i is independent of its non-descendants given its (possibly empty) set of parents $Pa(X_i)$ in G. The component θ represents a set of parameters that quantifies the probabilities of the network. We assume that θ contains a parameter $\theta_{x|pa(X)} = P(x|pa(X))$ for each possible value $x \in X$ and $pa(X) \in Pa(X)$. Given G and θ, a Bayesian network B defines a unique joint probability distribution (JPD) over X as:

$$P_B(X) = \prod_{i=1}^{n} P(X_i|Pa(X_i)). \quad (1)$$

DBNs extend BNs to model the stochastic evolution of a set of variables $X = \{X_1, \ldots, X_n\}$ over time [24]. A DBN D is defined as a pair $D = \left(B^1, B^{\rightarrow}\right)$, where $B^1 = \left(G^1, \theta^1\right)$ is a BN that defines the probability distribution $P\left(X^1\right)$ and, under the assumption of first-order Markov and stationary processes, $B^{\rightarrow} = (G^{\rightarrow}, \theta^{\rightarrow})$ is a two-slice Bayesian network (2TBN) that defines the CPD $P\left(X^t|X^{t-1}\right)$ for all t. The nodes in the first slice of the 2TBN do not have any parameters associated with them, but each node in the second slice of the 2TBN has an associated CPD which defines $P(X_i^t|Pa(X_i^t))$, where a parent $X_j \in Pa(X_i^t)$ can either be in time-slice t or $t-1$. The JPD over any number of T time-slices is then given by:

$$P_D(X^{1:T}) = \prod_{t=1}^{T} \prod_{i=1}^{n} P\left(X_i^t|Pa\left(X_i^t\right)\right). \quad (2)$$

A. Definition of BAD MoB models

In essence, a BAD MoB model is a combination of several DBNs, whose functional interaction allow the generation of context dependent driving behavior by sequencing and mixing simpler behaviors according to a skill hierarchy [9][10] (e.g., Figure 1).

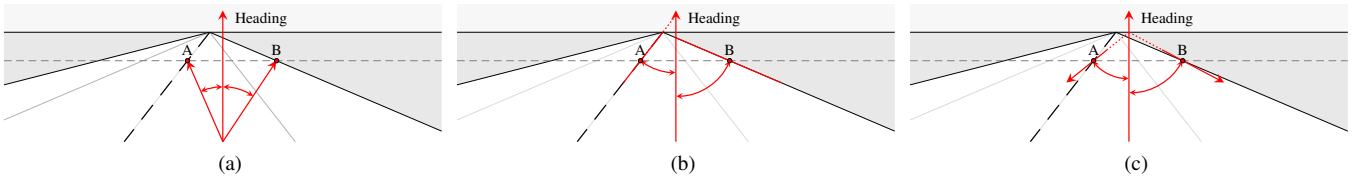

Figure 2. Illustration of bearing angles (a), splay angles (b) and flow angles (c).

Let A denote a set of discrete random variables representing the lateral and longitudinal control actions of a driver. In this paper, we assume the use of steering wheel angles for lateral control and the position of a combined acceleration and braking pedal for longitudinal control. $P = \{P_1, \ldots, P_m\}$ denotes a set of discrete random variables representing hypothetical percepts that could be available to the driver due to foveal and ambient vision [25]. Given a skill hierarchy, decomposing a complex behavior in a number of n simple behaviors, B denotes a discrete random variable with n values for the n simple behaviors.

We assume, that the sensor-motor schema of each of the n simple behaviors in the skill hierarchy can be modeled by a distinct DBN π_i that defines a JPD $P_{\pi_i}\left(A^{1:T}, P^{1:T}\right)$. Due to their purpose, we refer to these models as *action-models*. In addition, we assume that the appropriateness of the simple behaviors in a given situation can be modeled by a DBN π_B that defines a JPD $P_{\pi_B}\left(B^{1:T}, P^{1:T}\right)$, which we refer to as a *behavior-classification-model*.

A BAD MoB model π is then defined as a DBN that combines both action- and behavior-classification-models, using a technique called *behavior-combination* [26]. The combination is achieved by specifying the CPDs of π as queries to be inferred by the action- and behavior-classification-models. Under the assumption of first-order Markov and stationary processes, the JPD of π for any number of T time slices is defined as:

$$P_\pi\left(A^{1:T}, B^{1:T}, P^{1:T}\right) = \prod_{t=1}^{T} P\left(P^t\right) P\left(B^t|B^{t-1}, P^t\right) P\left(A^t|A^{t-1}, P^t, B^t\right). \quad (3)$$

The CPD $P\left(B^t|B^{t-1}, P^t\right)$ represents the appropriateness of each simple behavior in the given situation and is defined as a query $P_{\pi_B}\left(B^t|B^{t-1}, P^t\right)$ to be inferred by the behavior-classification-model π_B. Each CPD $P\left(A^t|A^{t-1}, P^t, B^t = i\right)$ represents the motor-output of a specific behavior in a given situation and is defined as a query $P_{\pi_i}\left(A^t|A^{t-1}, P^t\right)$ to be inferred by the action-model π_i that realizes the sensor-motor-schema of the corresponding behavior. We would like to emphasize that the structure of π itself is predefined and fixed. In contrast, the structures of action- and the behavior-classification-models will be obtained via structure-learning procedures.

B. Definition of component-models

Action- and behavior-classification-models are defined in the same manner, and we will therefore simply refer to them as *component-models*. Each component-model π_c is a distinct DBN that defines a joint distribution $P_{\pi_c}\left(X^{1:T}, P^{1:T}\right)$ and will be used to infer the query $P_{\pi_c}\left(X^t|X^{t-1}, P^t\right)$ (where $X = A$ in the case of action-models and $X = B$ in the case of behavior-classification-models).

We model component-models in the fashion of state-observation models [23], in that they consist of a *transition model* $P\left(X^t|X^{t-1}\right)$ and an *observation model* $P\left(P^t|X^t\right)$. We rely on the assumption that not all of the available percepts P are necessarily relevant for the realization or classification of driving behaviors. Accordingly, we can separate P into two mutually exclusive sets $P_R \subseteq P$ and $P_I \subseteq P$, where P_R consists of the relevant percepts and P_I consists of the irrelevant percepts.

This allows us to decompose $P\left(P^t|X^t\right)$ to $P\left(P_R^t|X^t\right) P\left(P_I^t\right)$. For $P\left(P_R^t|X^t\right)$, we assume that the percepts are conditionally independent given X^t: $P\left(P_R^t|X^t\right) = \prod_{P_i \in P_R} P\left(P_i^t|X^t\right)$. As the irrelevant percepts P_I have no influence on the estimation of X, we can replace the CPD $P\left(P_I^t\right)$ by $\prod_{P_j \in P_I} P\left(P_j^t\right)$.

A schematic graph-structure of component-models is shown in Figure 3. The JPD over all variables for any number of T time-slices is then given by:

$$P_\pi(X^{1:T}, P^{1:T}) = \prod_{t=1}^{T} \left[P\left(X^t|X^{t-1}\right) \prod_{P_i \in P_R} P\left(P_i^t|X^t\right) \prod_{P_j \in P_I} P\left(P_j^t\right) \right]. \quad (4)$$

The query $P_{\pi_c}(X^t|X^{t-1}, P^t)$ needed for the specification of the BAD MoB model can be inferred by:

$$P_{\pi_c}(X^t|X^{t-1}, P^t) = \frac{P\left(X^t|X^{t-1}\right) \prod_{P_i \in P_R} P\left(P_i^t|X^t\right)}{\sum_{x^t \in X^t} P\left(x^t|X^{t-1}\right) \prod_{P_i \in P_R} P\left(P_i^t|x^t\right)}. \quad (5)$$

As each component-model is a distinct DBN, each may use a different set of relevant percepts. The problem is to decide, which of the available percepts $P_i \in P$ are relevant and which are irrelevant. Due to the considerable uncertainty about the relevant percepts for realization and classification of natural driving behaviors, we use machine-learning methods to learn the graph structure of component-models and obtain the statistically relevant percepts in natural driving behaviors from the variety of proposed percepts.

 ISBN: 978-1-61208-340-7

IV. LEARNING BAD MOB MODELS

We derive the structures of component-models by a machine-learning method, based on the score and search paradigm, where a search in the space of possible graph structures is guided by a scoring function that evaluates the degree of fitness between the model and a set of experimental data. From a Bayesian perspective such a scoring criterion can be defined as $P(G_\pi|\delta)$, the probability of a graph structure G_π of a model π given a dataset δ [23]. Using the Bayes' rule, $P(G_\pi|\delta)$ is given by:

$$P(G_\pi|\delta) = P(\delta|G_\pi)\,P(G_\pi)\,/P(\delta)\,, \tag{6}$$

where $P(\delta|G_\pi)$ is the likelihood of the data given the graph structure, $P(G_\pi)$ is a prior over possible graph structures, and $P(\delta)$ is a constant that does not depend on the actual graph structure and can therefore be neglected [23]. The likelihood of the data given a graph structure can be computed by integrating over all possible parameters θ_π of π [23][24]:

$$P(\delta|G_\pi) = \int P(\delta|G_\pi,\theta_\pi)\,P(\theta_\pi|G_\pi)\,d\theta_\pi, \tag{7}$$

where $P(\delta|G_\pi,\theta_\pi)$ is the likelihood of the data given π and $P(\theta_\pi|G_\pi)$ is a prior distribution over the possible parameter values for a graph structure G_π. A common approach for evaluating the integral, is to use an approximation derived from the asymptotic behavior of (7) for infinite datasets, which results in a scoring criterion known as the *Bayesian Information Criterion* (BIC) [23][24][27][28].

Although their structure is fixed, we derive our structure-learning approach for component-models from the hypothetically learning of BAD MoB models. Let δ denote a *complete* database consisting of n samples $\delta^i = (a^i, b^i, p^i)$, $\hat{\theta}_\pi$ denote the maximum likelihood estimator, and $\mathrm{Dim}[\pi]$ denote the number of independent parameters, the BIC score for a BAD MoB model π is defined as:

$$\mathrm{BIC}(G_\pi : \delta) \;=\; \log P\left(\delta|G_\pi,\hat{\theta}_\pi\right) - \frac{\mathrm{Dim}[\pi]}{2}\log n. \tag{8}$$

For a BAD MoB model π, the log-likelihood $\log P(\delta|G_\pi,\hat{\theta}_\pi)$ is given by $\log P_\pi(a^{1:n},b^{1:n},p^{1:n} : \hat{\theta}_\pi)$ (in the following we will drop $\hat{\theta}_\pi$ for clarity). Using (3) this can be rewritten as a sum of terms:

$$\log P_\pi\left(a^{1:n},b^{1:n},p^{1:n}\right) = \sum_{i=1}^{n}\log P\left(b^i|b^{i-1},p^i\right) + \sum_{j=1}^{n}\log P\left(a^j|a^{j-1},b^j,p^j\right) + \sum_{k=1}^{n}\log P\left(k^i\right). \tag{9}$$

As the structure of a BAD MoB model is predefined, its score only depends on the structure of its component-models and their consequential ability to infer their corresponding queries. This translates the task of learning a BAD MoB model into the task of learning the graph structure for each component-model individually. Consequently, using (9), we can decompose (8) in order to define a scoring criterion for component-models.

A. Discriminative learning of component-models

Let δ_c denote a subset of δ consisting of only the n_c samples $\delta^i = (x^i, x^{i-1}, p^i)$ related with a component-model π_c, the portion of the BIC score for π_c would be given by:

$$\sum_{i=1}^{n_c}\log P_{\pi_c}\left(x^i|x^{i-1},p^i\right) - \frac{\mathrm{Dim}[\pi_c]}{2}\cdot\log n. \tag{10}$$

In contrast to maximizing the unconditional log-likelihood in (8), we now aim to maximize a conditional log-likelihood $\mathrm{CL}\left(\hat{\theta}_{\pi_c} : \delta_c\right) = \sum_{i=1}^{n_c}\log P_{\pi_c}\left(x^i|x^{i-1},p^i\right)$. Learning in order to maximize a conditional (log-)likelihood is known in the literature as *discriminative* learning [23][28][29][30][31]. Accordingly we will refer to the scoring criterion for component-models as a *Discriminative BIC* (DBIC).

For discriminative learning based on the BIC, it has been recognized that its penalty term tends to have a too high impact on the score, resulting in too simple model structures [29][30]. As a consequence, [30] propose to adjust the penalty by multiplying it by a parameter $\beta < 1$, they proposed as $\beta = 1/10$. Following this, the DBIC for a component-model is then defined as:

$$\mathrm{DBIC}(G_{\pi_c} : \delta_c) = \mathrm{CL}\left(\hat{\theta}_{\pi_c} : \delta_c\right) - \beta\frac{\mathrm{Dim}[\pi_c]}{2}\cdot\log n. \tag{11}$$

B. Learning Procedure

For each component-model, the goal of the learning procedure is to find the graph structure from the space of possible graph structures that maximizes the DBIC. Even given the severe structural constraints of component-models (cf. Section III-B), there exist 2^m possible graph structures for a number of m available percepts. As it is not feasible to evaluate all these possibilities, we rely on heuristic methods to find a good but not necessarily optimal solution.

By now, we use a common *greedy hill-climbing* search procedure [23]. We start with an initial "blind" model that does not utilize any percepts (hence with the observation model $P(P^t|X^t) = \prod_{i=1}^{m}P(P_i^t)$) and compute its DBIC. For each available percept $P_j \in P$, we then construct a model in which we utilize P_j by adding an edge in

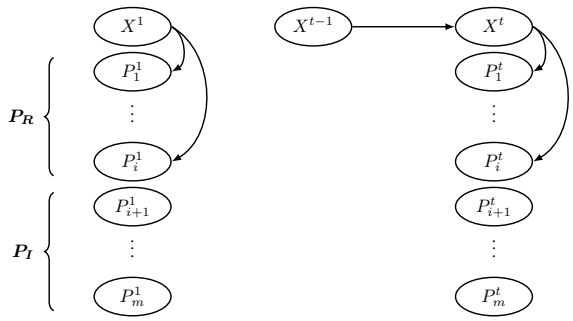

Figure 3. Schematic structure of action- and behavior-classification-models, defined by a BN and a 2TBN.

the graph from X^t to P_j^t (therefore replacing $P\left(P_j^t\right)$ in the observation model with $P\left(P_j^t|X^t\right)$) and compute its DBIC score. Intuitively, a percept P_k^t leading to the highest improvement of the DBIC when utilized can be seen as the most pertinent percept of the given possibilities and will be permanently added to the initial model. The process is then repeated until no further added percept improves the DBIC. Eventually, this learning procedure selects a minimal set of relevant percepts.

V. A BAD MOB MODEL REPRESENTING THE HUMAN DRIVING BEHAVIOR ON VIRTUAL HIGHWAYS

We used the described method to learn the relevant percepts for a BAD MoB model based on the skill hierarchy shown in Figure 1, representing the lateral and longitudinal human driving behavior on virtual highways. For this, we selected approx. 800 percepts that hypothetically could be relevant for the human lateral and longitudinal driving behavior.

Primarily, we selected bearing, splay, and flow angles (c.f. Figure 2), utilizing a variety of possible reference points. Reference points were placed in different fixed $(25m, 50m, \ldots, 250m)$ and time-dependent $(i \cdot speed,\ i = \{1s, 2s, \ldots, 10s\})$ distances, both relative to the driver's current lane (on the lane edge or centerline left to the driver, on the middle of the driver's lane, and on the lane edge or centerline right to the driver) and absolute (on the left lane edge, the middle of the fast lane, the centerline, the middle of the slow lane, and the right lane edge). As additional reference points only applicable for bearing angles, we selected the far point, as proposed by [3] (placed on the tangent point if available and on the vanishing point otherwise), and traffic participants in the vicinity of the driver (the nearest cars in front and behind the driver on the two lanes of the highway).

To enable the possible use of strategies that utilize two angles resp. reference points simultaneously (cf. Section II), we considered percepts that represent the differences between bearing, splay, and flow angles of the reference points on the left and right lane edges or one of these lane edges and the centerline.

From the percepts obtainable from traffic participants in the vicinity of the driver, we selected distances, speed differences to the driver, TTCs, and THWs of the nearest cars in front and behind the driver on the two lanes of the highway.

As further percepts that obviously could have an effect, esp. on longitudinal control, we included the driver's speed v_{ego}, the prescribed speed limit v_{limit}, and the combination of both, which we will refer to as the speed potential, representing the allowed speed gain (resp. prescribed speed reduction) defined as $v_{\text{pot}} = v_{\text{limit}} - v_{\text{ego}}$.

A. Experimental Data

The database needed for the learning procedure was obtained in a simulator study using a fixed based driving simulator that comprises a mockup of the driver's cab of a real car, positioned amidst three projection surfaces for a simulated 3D-environment, providing a realistic field of view of 170° (Figure 4).

The study was conducted with eight participants (four male, four female) between the age of 24 and 30 and with normal or corrected-to-normal vision. The scenario comprised approximately 37 km of a four-lane highway based on a section of the German highway A1, with two lanes in each direction and moderate traffic, generated by a number of non-controlled automated vehicles traveling at varying desired speeds and able to pass other vehicles (including the driver's car).

The experimental procedure consisted of three phases. In the first phase, each participant was introduced to the simulator and performed a training session. In the second phase, the participants drove one trial without other traffic. They were instructed to obey the shown speed-limits (100-130 km/h) and perform lane changes when being asked by the instructor. In the third phase, the participants drove two trials with other traffic. They were instructed to obey the German traffic rules. For the second trial with other traffic, left-hand curvatures were inverted to right-hand curvatures and vice versa. A single participant (participant 1, male) attended two times and in each case performed an additional third trial with other traffic.

During the trials, with a frequency of 60 Hz, we recorded the values of all defined percepts, the steering wheel angle, and the position of a combined acceleration-braking pedal. This led to an experimental database of approx. 1900000 data samples $\delta^i = (a^i, p^i)$ comprising a total time of approx. 525 minutes. In order to define the missing behavior values, we manually completed each sample δ^i with the shown behavior b^i according to the skill hierarchy (Figure 1).

B. Results and Discussion

By now, we used the experimental data of participant 1 (male, approx. 550000 data samples) to learn a BAD MoB model representing an individual driver. In total, twelve percepts were selected during the learning procedure (Table I). In the following, we will attempt to discuss their meaningfulness with respect to the literature.

1) Lane-Following: A single percept was learned as relevant for lateral control, representing the bearing angle

Figure 4. Fixed based driving simulator.

TABLE I. PERTINENT PERCEPTS FOR ACTION-MODELS REPRESENTING THE BEHAVIORS FOR LANE-FOLLOWING, CAR-FOLLOWING, LANE CHANGES TO THE LEFT, AND LANE CHANGES TO THE RIGHT.

Behavior	Relevant Percepts for Lateral Control	Relevant Percepts for Longitudinal Control
Lane-following	1. Bearing angle between the heading and a reference point on the middle of the driver's lane in a distance of $v_{\text{ego}} \cdot 5s$	1. Speed potential
Car-following	1. Flow angle between heading and the optic flow direction of a reference point on the centerline in a distance of $v_{\text{ego}} \cdot 3s$	1. TTC to the lead-car (bumper-to-bumper distance, allowing positive and negative values)
Lane changes to the left	1. Bearing angle between the heading and a reference point on the middle of the right lane in a distance of 100m	1. TTC to the lead-car on the fast lane (bumper-to-bumper distance, only positive values)
	2. Bearing angle between the heading and a reference point on the left lane edge in a distance of $v_{\text{ego}} \cdot 2s$	
Lane changes to the right	1. Flow angle between the heading and the optic flow direction of a reference point on the middle of the right lane in a distance of 75m	1. TTC to the lead-car on the fast lane (bumper-to-bumper, only positive values)
	2. Bearing angle between the heading and a reference point on the right lane edge in a distance of $v_{\text{ego}} \cdot 3s$	
	3. TTC to the lead-car on the fast lane (bumper-to-bumper distance, allowing positive and negative values)	
	4. TTC from the car behind on the slow lane (Euclidean distance, only positive values)	

between the driver's heading and a reference point on the middle of the driver's lane in a distance of $v_{\text{ego}} \cdot 5s$. Under the assumption that the middle of the lane can be seen as an approximation of the future path of the driver, this percept is consistent with the proposals of [13] for roads with gentle curvatures, and findings of [19] and [32], who report that drivers often fixate the center of the road resp. the future path. In contrast, the far point, as proposed by [3] for lane-following, was only the 114^{th} highest-rated percept.

The single relevant percept selected for the longitudinal control represents the speed potential. This seems reasonable, as it should be sufficient for a driver to keep an intended target speed as implied by the current speed limit. However, as German traffic rules prohibits to overtake on the right, we expected a second percept, associated with the lead-car on the lane left to the driver. Indeed, the percept that would have been selected as the second relevant percept (but was rejected due to the increasing penalty) represents the distance to the lead-car on the fast lane.

2) Car-Following: The single percept learned for the lateral control in car-following represents the angle between the driver's heading and the optic flow direction of a reference point on the centerline in a distance of $v_{\text{ego}} \cdot 3s$. This is in contrast to [33], who found that drivers tend to primarily fixate the lead-car during car-following. Based on these findings, [3] concluded that in the presence of a lead-car, the lead-car would act as the primary reference point and consequently proposed the angle between the heading and the lead-car as the most relevant percept for lateral control during car-following. Maybe surprisingly, this angle was only the 353^{th} best-rated percept.

However, the single relevant percept for longitudinal control in car-following represents the TTC to the lead-car. This is consistent with the proposals of [20] and [21] and would imply that the driver indeed primarily focuses the lead-car. Our model would therefore imply that during car-following, the driver primarily depends on ambient vision for lateral control, while using the foveal vision for longitudinal control.

3) Lane Changes: For the lateral control during lane changes to the left, two percept were selected. They represent the bearing angle to the middle of the right lane in a distance of 100m and the bearing angle to the left lane edge in a distance of $v_{\text{ego}} \cdot 2s$. These percepts are consistent with findings of [34], who report that during lane changes to the left lane, drivers direct their gazes primarily and almost equally to the left and the right lane.

In contrast, during lane changes to the right, drivers direct the majority of their gazes to the right lane, while dividing the rest of their gazes equally between the left lane and the mirror [34]. As shown in Table I, the selected percepts are indeed consistent with these findings. The two most relevant percepts represent the angle between the heading and the optic flow direction of a reference point on the middle of the right lane and the bearing angle between the heading and a reference point on the right lane edge. The third percept represents the TTC to the lead-car on the fast lane, which implies a certain attention to the left lane. The last percept represents the TTC to the car behind on the slow lane, which implies a certain attention to the mirror.

Concerning the longitudinal control, for both lane changes to the left and to the right, the single selected percept represents the TTC to the lead-car on the fast lane. This may be explained by a rare and unpredictable tendency of non-controlled traffic participants to surprisingly and recklessly change lanes, which enforced the participant to perform all-out brakings during lane changes. However, this also gives us a hint to explore the use of separated skill hierarchies for lateral and longitudinal control in our future research.

VI. CONCLUSION

We presented the learning of a hierarchical and modular probabilistic driver model that represent and mimics the lateral and longitudinal human driving behavior on virtual highways. Its relevant percepts were selected in a discriminative structure-learning procedure from a set of hypothetical percepts proposed in literature. The performance of the learned BAD MoB model is very promising (videos available at

 ISBN: 978-1-61208-340-7

http://www.lks.uni-oldenburg.de/46350.html). The selected percepts are sufficient for the modeling and simulation of the lateral and longitudinal human driving behavior on virtual highways, including situation-adequate lane-following, car-following, and lane changing behavior. The selected percepts seem reasonable and for the most part consistent with findings reported in psychological studies. This indicates that the proposed method can be used to generate hypothesis about the relevant percepts and situation-awareness of drivers in dynamic traffic scenes to be validated by experiments with human drivers.

In our future work, we will expand our selection of hypothetical percepts and will explore the use of different and separated skill hierarchies for lateral and longitudinal control.

ACKNOWLEDGMENT

This work has been supported by the projects IMoST2 (Integrated Modeling for Safe Transportation II), sponsored by the Government of Lower Saxony, Germany under contracts ZN2245, ZN2253, ZN2366, and the project HoliDes (Holistic Human Factors and System Design of Adaptive Cooperative Human-Machine Systems), funded by the ARTEMIS Joint Undertaking Grant agreement no.: 332933.

REFERENCES

[1] C. Cacciabue, Ed., Modelling Driver Behaviour in Automotive Environments: Critical Issues in Driver Interactions with Intelligent Transport Systems. Springer, 2007.

[2] T. Jürgensohn, Modelling Driver Behaviour in Automotive Environments. Springer, 2007, ch. Control Theroy Models of the Driver, pp. 277–292.

[3] D. Salvucci and R. Gray, "A two-point visual control model of steering," Perception, vol. 33, 2004, pp. 1233–1248.

[4] R. Wilkie and J. Wann, "Controlling steering and judging heading: Retinal flow, visual direction and extra-retinal information," Journal of Experimental Psychology: Human Perception and Performance, vol. 29, 2003, pp. 363–378.

[5] D. Salvucci, Integrated Models of Cognitive Systems. New York: Oxford University Press, 2007, ch. Integrated Models of Driving Behavior, pp. 356–367.

[6] P. Bessière, C. Laugier, and R. Siegwart, Eds., Probabilistic Reasoning and Decision Making in Sensory-Motor Systems. Berlin: Springer, 2008.

[7] C. Möbus and M. Eilers, "Further steps towards driver modelling according to the Bayesian programming approach," in Digital Human Modeling, ser. LNCS (LNAI). San Diego: Springer, 2009, pp. 413–422.

[8] C. Möbus and M. Eilers, "Mixture of behaviors and levels-of-expertise in a Bayesian autonomous driver model," in Advances in Applied Digital Human Modeling, V. Duffy, Ed. Boca Raton: CRC Press, Taylor & Francis Group, 2010, pp. 425–435.

[9] M. Eilers and C. Möbus, "Learning of a Bayesian autonomous driver mixture-of-behaviors (bad-mob) model," in Advances in Applied Digital Human Modeling, V. Duffy, Ed. Boca Raton: CRC Press, Taylor & Francis Group, 2010, pp. 436–445.

[10] M. Eilers and C. Möbus, "Learning the relevant percepts o modular hierarchical Bayesian driver models using a Bayesian information criterion," in Digital Human Modelling, ser. LCNS 6777, V. Duffy, Ed. Heidelberg: Springer, 2011, pp. 463–472.

[11] M. Chattington, M. Wilson, D. Ashford, and D. Marple-Horvat, "Eye-steerig coordination in natural driving," Experimental Brain Research, vol. 180, 2007, pp. 1–14.

[12] M. Land, Vision and Action. Cambridge: Cambridge University Press, 1998, ch. The Visual Control of Steering, pp. 163–180.

[13] M. Land and B. Tatler, Looking and Acting: Vision and eye movements in natural behavior. Oxford: Oxford University Press, 2009.

[14] L. Li and J. Chen, "Relative contribution of optic flow, bearing, and splay angle information to lane keeping," Journal of Vision, vol. 10, 2010, pp. 1–14.

[15] R. Wilkie, D. Poulter, and J. Wann, "Where you look when you learn to steer," Journal of Vision, vol. 4, no. 8, 2004, doi:10.1167/4.8.1.

[16] J. Wann and R. Wilkie, Optical flow and beyond. Norwell, MA, USA: Kluwer Academic Publishers, 2004, ch. How do we control high speed steering?, pp. 401–419.

[17] A. Chatziastros, G. Wallis, and H. Bülthoff, "The use of optical flow and splay angle in steering a central path," Max Planck Institute for Biological Cybernetics, Tübingen, Germany, Tech. Rep. 71, October 1999.

[18] M. Land and D. Lee, "Where we look when we steer," Nature, vol. 369, 1994, pp. 742–744.

[19] O. Lappi, E. Lehtonen, J. Pekkanen, and T. Itkonen, "Beyond the tangent point: Gaze targets in naturalistic driving," Journal of Vision, vol. 13, 2013, pp. 1–18.

[20] D. Lee, "A theory of visual control of braking based on information about time to collision," Perception, vol. 5, 1976, pp. 437–459.

[21] W. van Winsum, "The human element in car following models," Tranportation Research Part F, vol. 2, 1999, pp. 207–211.

[22] M. Gouy, C. Diels, N. Reed, A. Stevens, and G. Burnett, "Preferred or adopted time headway? A driving simulator study," in Proceedings of the International Conference on Ergonomnics & Human Factors, M. Anderson, Ed., 2013, pp. 153–159.

[23] D. Koller and N. Friedman, Probabilistic Graphical Models: Principles and Techniques. MIT Press, 2009.

[24] N. Friedman, K. Murphy, and S. Russell, "Learning the structure of dynamic probabilistic networks," in Proceedings of the 14th conference on Uncertainty in artificial intelligence, 1998, pp. 139–147.

[25] W. Horrey, C. Wickens, and K. Consalus, "Modeling driver's visual attention allocation while interacting with in-vehicle technologies," Journal of Experimental Psychology, vol. 12, no. 2, 2006, pp. 67–78.

[26] P. Bessière et al., "Survey: Probabilistic methodolgy and techniques for artefact conception and development," INRIA - Institut National de Recherce en Informatique et en Automatique, Tech. Rep., 2003.

[27] G. Schwarz, "Estimating the dimension of a model," Ann. Stat., vol. 6, 1978, pp. 461–464.

[28] K. Murphy, Machine Learning: A Probabilistic Perspective. The MIT Press, 2012.

[29] Y. Guo and R. Greiner, "Discriminative model selection for belief net structures," in Proceedings of the 20th National Conference on Artificial Intelligence, 2005, pp. 770–776.

[30] S. Natarajan, W.-K. Wong, and P. Tadepalli, "Structure refinement in first order conditional influence language," in Proceedings of the Workshop on Open Problems in Statistical Relational Learning (SRL), 2006, 8 pages.

[31] G. Santafe, J. Lozano, and P. Larranaga, "Discriminative vs. generative learning of Bayesian network classifiers," in ECSQARU 2007, ser. LNAI 4724, K. Mellouli, Ed. Berlin, Heidelberg: Springer, 2007, pp. 453–464.

[32] R. Wilkie and J. Wann, "Eye-movements aid the control of locomotion," Journal of Vision, vol. 3, no. 11, 2003, pp. 677–684.

[33] D. Salvucci, E. Boer, and A. Liu, "Toward an integrated model of driver behavior in a cognitive architecture," Transportation Research Record, vol. 1779, 2001, pp. 9–16.

[34] D. Salvucci and A. Liu, "The time course of a lane change: Driver control and eye-movement behavior," Tranportation Research Part F, vol. 5, 2002, pp. 123–132.

 ISBN: 978-1-61208-340-7

Modelling Spatial Understanding: Using Knowledge Representation to Enable Spatial Awareness in a Robotics Platform

Martin Lochner, Charlotte Sennersten, Ahsan Morshed, and Craig Lindley
CSIRO Computational Informatics (CCI) Autonomous Systems (AS)
Commonwealth Scientific and Industrial Research Organization (CSIRO)
Hobart, Tasmania, Australia
Contact: martin.lochner@csiro.au, charlotte.sennersten@csiro.au,
ahsan.morshed@csiro.au, craig.lindley@csiro.au

***Abstract*—Robotics in the 21st century will progress from scripted interactions with the physical world, where human programming input is the bottleneck in the robot's ability to sense, think and act, to a point where the robotic system is able to autonomously generate adaptive representations of its surroundings, and further, to implement decisions regarding this environment. A key factor in this development will be the ability of the robotic platform to understand its physical space. In this paper, we describe a rationale and framework for developing spatial understanding in a robotics platform, using knowledge representation in the form of a hybrid spatial-ontological model of the physical world. While such a system may be implemented with classical ontologies, we discuss the advantages of non-hierarchical modes of knowledge representation, including a conceptual link between information processing ontologies and contemporary cognitive models.**

Keywords-Human Robot Interaction; Autonomous Navigation; Knowledge Representation; Spatial Ontology

I. INTRODUCTION

The process of transitioning away from hard-coded robotics applications, which carry out highly pre-determined actions such as the traditional manufacturing robot, is already well underway. With notions such as cloud robotics [1] entering the *zeitgeist*, and highly publicized events such as the DARPA Robotics Challenge (Dec 19-21 2013, Miami FL) bringing public attention to these advances, it is foreseeable that robots will be entering the mainstream realm of human activity – more than in fringe applications (robotic vacuum cleaner; children's toys), but in key areas such as caring for the aged [2], operating vehicles [3], disaster management [4], and undertaking autonomous scientific investigation [5].

The hurdles that must be overcome in reaching these goals, however, are neither few nor small. This can be plainly seen, for example in the aforementioned 2013 Robotics Challenge, in which simple spatial tasks that are routine for a human being (open a door, climb a ladder) are still critically difficult for even the most advanced and highly funded robotics projects. While the state-of-the-art is impressive, it is evident that physical robotics hardware is far in advance of the control systems that are in place to guide the robot. The challenge is, thus, to develop systems whereby a robot can perceive a physical space and understand its position in that space, the components that exist within the space, and how it can or *should* interact with these components in order to achieve implicit or explicit goals. This is furthermore impacted by the requirement that robotic systems be able operate in outdoor environments where distributed connections may not be available; however, describing the development of long-range data networks for robotic communication is beyond the scope of this paper.

While there are a number of ways that the problem of providing a robot with a spatial understanding can be approached (e.g., neuro-fuzzy reasoning [6], dynamic spatial relations via natural language [7]) it is our proposition that leveraging the current advancements in knowledge representation via ontologies [8][9], in combination with an understanding of human spatial-cognitive processing [10][11], and enabled by real-time scene modeling [12] will provide a powerful and accessible methodology for enabling spatial understanding and interaction in a mobile robotics platform. As argued by Sennersten et al. [13], the advantage of using cloud-based repositories of perceptual data annotated with ontology and metadata information is to take advantage of humanly-tagged examples of sense data (e.g., images) to overcome the symbol grounding problem. Symbol grounding refers to the need for symbolic structures to have valid associations with the things in the world that they refer to. Achieving symbol grounding is an ongoing challenge for robotics and other intelligent systems (see, for example, Brooks, 1999 [14]). Using cloud-based annotations attached to sensory exemplars takes advantage of the human ability to ground symbols, obviating the need for robots to achieve this independently of human symbolic expressions.

This paper provides a conceptual overview of how spatial understanding can be developed in a robotics platform. We discuss traditional knowledge representation (classical information processing ontologies), describe the development and use of "cognitive" ontologies, and how this may be transitioned into the development of a physical-spatial ontology, including a possible system of

 ISBN: 978-1-61208-340-7

comprehension for spatial position. Finally, we discuss the notion that truly non-hierarchical systems such as complex chemical structure, and such as the human cortex, may require the development of systems of knowledge representation that transcend the structural limits of today's systems.

II. KNOWLEDGE REPRESENTATION

The development of specific nomological hierarchies for concept representation is currently taking place across many fields of academic endeavor (e.g., genetics, medicine, neuroscience, biology, chemistry, physics). Under the guise of the philosophical concept of an *Ontology*, such applications seek to outline the knowledge which exists within a domain at three levels of representation: Classes, Properties, and Relationships. These nomological hierarchies provide a way of describing the precise relationship that terms in a given domain have to one another. As an information processing construct, the definition of an ontology is refined as an "explicit formal specification of the terms in the domain and relations among them", or more concisely, "a specification of a conceptualization" [15].

A system that operates with such knowledge representation within its core functionality may be considered to be 'knowledge-based'. A knowledge-based system is a computer program that stores knowledge about a given domain (also known as an "expert system", when the knowledge is considered to be from a highly specialized domain). However, an ontology does not intrinsically represent the kinds of truth-functional mappings or procedures captured by rules in more complete knowledge bases. Hence, an ontology provides classifications and the ability to infer associations via subclass/superclass relationships. More complex forms of reasoning required for most forms of useful cognitive task performance require task-oriented rules. As such, the domain knowledge in a knowledge base includes ontology representations, while most task-oriented reasoning is achieved by the use of rules that refer to ontological constructs in the form of domains within rule tuples.

The system attempts to mimic the reasoning of a human specialist by conducting reasoning across rules and in reference to a database of atomic facts. Matching sense data against metadata/ontology-annotated sense data on the web can provide a method of automatically mapping a current sensed situation to the annotations of past situations stored in the cloud. This allows the system to retrieve representations of the situation in an atomic form, as statements formulated using the symbolic forms of annotations which are retrieved by matching against associated sense data. Ontologies hold the potential, therefore, to provide the constructs for symbolic atomic fact expressions that rule-sets can then process for automated cognitive task performance.

A. Cognitive Ontologies

An increasing number of ontologies are available on-line that can potentially support this symbolic structure generation process. Knowledge representation via ontological structure has been applied to the field of cognitive science, both in relation to terminology used within the domain (e.g., DOLCE - Descriptive Ontology for Linguistic and Cognitive Engineering [16][17]) and for concepts relevant to empirical testing paradigms (e.g., CogPo [18]). Indeed, several cognitive ontologies have been developed in the recent years, including DOLCE, WordNet [19], CYC [20], and CogPo.

WordNet is an online lexical knowledgebase system, whose design is inspired by current psycholinguistic theories of human lexical memory, where each cognitive artifact can be semantically classified into English nouns, verbs, and adjectives, with different meanings and relationships in real-world scenarios. DOLCE is developed by Nicola Guarino and his associates at the Laboratory for Applied Ontology (LOA) [21]. It captures the ontological categories underlying natural language and human common sense. DOLCE, however, does not commit to a particularly abstract level of concepts that relate to the world (like imaginary thoughts); rather, the categories it introduces are thought of as cognitive artifacts, which are ultimately dependent on human perception, cultural imprints and social conventions.

The Cyc project goal is to build a larger common-sense background knowledgebase which is intended to support unforseen future knowledge representation and reasoning tasks. The Cyc knowledgebase contains 2.2 million assertions (fact and rules) describing more than 250,000 terms, including nearly 15,000 predicates.

Finally, the Cognitive Paradigm Ontology (CogPo) is developed based on two well-known databases, namely, the Functional Imaging Biomedical Informatics Research Network (FBIRN) Human Imaging Data base [22] and the BrainMap database [23]. The CogPo Ontology has categorized each paradigm in terms of **(**1) the stimulus presented to the subjects, (2) the requested instructions, and (3) the returned response. All paradigms are essentially comprised of these three orthogonal components, and formalizing an ontology around them is a clear and direct approach to describing paradigms. This well-formed standard ontology guides cognitive experiments in formalizing the cognitive knowledge.

While these ontologies are of great value to the community of researchers, and while the knowledge-based mapping of concepts within particular domains may enable robotic systems to rapidly access the linguistic identity of physical objects and their relations within the domain, they do not provide a means whereby the robot may become spatially aware. To achieve this goal, we will need to provide the robot with the ability to identify the spatial characteristics particular to an identified object, and the

 ISBN: 978-1-61208-340-7

physical relations between these objects and the surrounding environment. A robot requires an internal representation of three-dimensional space. It could access two dimensional images on the web, by content-matching those images with contents of its own visual system. The matching process, and especially the ongoing three dimensional interpretation of the images, could be greatly aided if the ontology/metadata associated with images includes representation of the three dimensional context of image capture. The "ontological" schema of knowledge representation for images may provide this means if it is extended to include three dimensional spatial annotations.

III. REPRESENTING RELATIONSHIPS IN THREE DIMENSIONS: SPATIAL ONTOLOGIES

We propose here that this same methodology for specifying semantic relationships between concepts (the ontological structure of knowledge representation, i.e., Classes, Properties, and Relationships) may also be useful in specifying spatial relationships between physical objects. While a traditional ontology will hierarchically represent a concept and its relation to other concepts in a domain, a spatial ontology (e.g., Figure 1) will represent an object, (class), its spatial properties including a detailed 3d representation in a language such as the X3D XML-based file format, and its positional relation (x,y,z) to other objects existing within the scene by using the datatype properties.

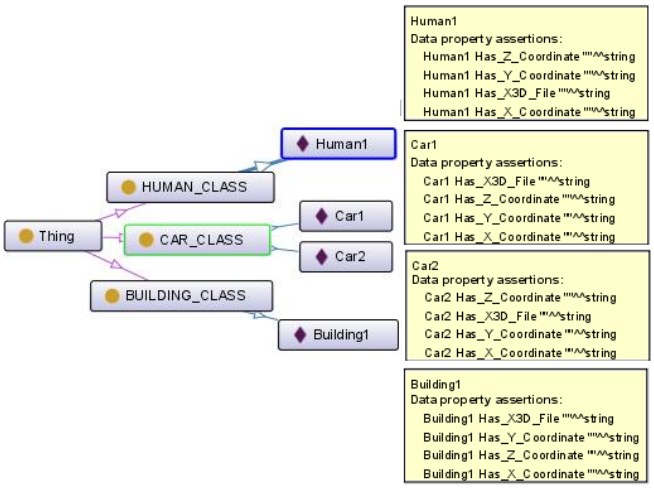

Figure 1. Example of a simple spatial ontology
(Note that the relations between objects are represented via "Data Properties" here.)

An entity (the "*individual*") in a prototypical ontology is comparable to an entity in a spatial ontology, being an object in the physical world. *Class* indicates the category into which the individual falls, for example "person", or "boat". *Attributes* traditionally describe the *individual* – features, properties, or characteristics of the object: a person has arms; a boat has a hull. In a spatial ontology this information will be appended with configural information regarding the object, for example the parent-child node relationship of a human body, including torso, appendages, etc. The *relation* between individuals is where the power of the traditional ontology arises, by specifying the precise ways in which different individuals relate to one another (e.g., "a catamaran is a subclass of boat"). Once again, in a spatial ontology the *relation* will be a precise indicator (a reference, or an 'object index') of the relative positionality of items in the physical space, as described in the following section. By thus, leveraging the existing functionality of ontological representation, augmented with relevant and necessary spatial referencing information, we may develop a knowledge-based system that enables a level of spatial awareness in a robotic platform.

A. A system of comprehension for spatial position

Following the above discussion about relationships in 3D space, we look into how coordinate systems can be synchronized. The physical scale requirement that a robot needs to have can be measured by the accuracy the robot needs to operate in via its navigation system. An autonomous robot must be able to determine its position in order to be able to navigate and interact with its environment correctly (e.g., Dixon and Henlich, 1997 [25]). When the *Class* of "robot" navigates from A to B it is a basic motion, which is similar to the movement of an in-game character via a default keyboard set-up where the key "W" moves the character forward, turning left using key "A", turning right using key "D" and go backwards using key "Z". The 3D digital world uses the X, Y, Z coordinate system called the Cartesian Coordinate Method (CCM) and is expressed in meters (m). To measure distance between two spherical points; X^1, Y^1, Z^1 and X^2, Y^2, Z^2 we take the Euclidean distance using a Cartesian version of Pythagoras' Theorem (1). The distance is the sum of their individual point differences in square.

$$\sqrt{(x_2 - x_1)^2 + (y_2 - y_1)^2 + (z_2 - z_1)^2} \quad (1)$$

To determine a position in the physical world and navigate the robot in map-referenced terms to a desired destination point from A to B, Dixon and Henlich use what they call 1) *Global Navigation*. The positioning accuracy with a standard consumer Geographical Positioning System (GPS) is accurate within a range of 8 feet which is approximately 284 centimeters. This does not give high fidelity position accuracy. As such, when the robot has to operate in a typical indoor manufacturing environment, it needs detailed position support in order to create 3D reference points within the space. What Dixon and Henlich call 2) *Local Navigation*, is to determine one's own position relative to the objects (stationary or moving) in the environment, and to interact with them correctly. If we think

 ISBN: 978-1-61208-340-7

of Human Robot Interaction (HRI) and the robot arm and its gripper(s) (hand/s), the gripper(s) must via eye(s) be able to recognize the object it will manipulate and how it shall be manipulated. The spatial centre points for individual objects are of importance, as well as group of objects and the robot's own centre point in relation to actual manipulation centre point for gripper. From a spatial ontology point of view, the centre points have to be able to change dynamically depending on interaction purpose.

For example, the Puma robot arm series has three different arms with slightly different sophistication and these are Puma 200, Puma 500, and the Puma 700 Series. These robot arms execute 3) *Personal Navigation* [D&H] which make the arm aware of the positioning of the various parts, its own positioning, and also in relation to each other and in handling objects. The Puma 200 Series has been used for absolute positioning accuracy for CT guided stereotactic brain surgery [26]. The Puma 200 robot has a relative accuracy of 0.05 mm. There are already 3D Spatial Vision Systems for robots out on the market which are driven via several cameras. This creates a local world solution for 3D vision robot guidance where the software first make the user calibrate the cameras and the robot and then loading standard CAD files of parts the system shall track.

IV. BEYOND ONTOLOGIES – COMPLEX RELATIONSHIPS, AND ALTERNATIVES TO HEIRARCHICAL DATA REPRESENTATION

As we move from relatively canonical data sets for which the information processing ontology was designed (i.e., semantic relations within a particular knowledge base) to more complex relationships (such as ad-hoc physical relations) in which the hierarchical order is not nearly so explicit, or potentially non-existent, will the classical ontology suffice? Or alternately, will something more adaptive need to take its place? Because relationships in the physical world are multifaceted and multidirectional, it is useful to have a schema which can represent this interconnectedness. The key strength of an ontology is that it provides a concrete nomological environment from which to operate within the chosen domain. Table 1 summarizes the traditional information processing ontology.

TABLE 1: TRADITIONAL ONTOLOGY CHARACTERISTICS

- allows a common understanding of the structure of information
- enables reuse of domain knowledge
- makes domain assumptions explicit
- separates domain knowledge from operational knowledge
- defines a common vocabulary for researchers
- provides machine readable definitions of basic concepts and the relationships among them

However, there are instances (albeit few as of this writing) in which it is being recognized that the intrinsic limitations of the "ontology" such it is commonly understood in 2014, (e.g., OWL-based [Web Ontology Language]) are sufficient as to demand a modification whereby the innate complexities of a real-world phenomenon may be modeled. That is: complex, potentially non-hierarchical relationships.

For example, it has been noted in the field of chemical molecular informatics that while ontologies are able to represent tree-like structures, they are unable to represent cyclical or polycyclical structures [27]. Similarly, the difficulty in building classifications of nano-particles has led some researchers to begin to look into taxonomies based on "physical / chemical / clinical / toxic / spatial" characteristics of an object, supplemented by structural information, in order to account for shapes, forms and volumes [28]. Other examples of representing complex structural relations which stretch the boundaries of ontological representation include using Description Graph Logic Programs (DGLP) to represent objects with arbitrarily connected parts [29], and a hybrid formalism whereby the authors propose a "combination of monadic second order logic and ordinary OWL", where the two representations are bridged using a "heterogeneous logical connection framework" [30].

It is evident that the potential applications of a formalism such as the ontological method of information representation far outreach the initial conceptualizations of the language. While it may be possible to model 3 dimensional spatial information within the constraints of a hierarchical ontology, it is also to be considered that this notion, as well as applications such as those described above, may require the development of progressive, flexible alternatives, which capture the strengths of the ontology (i.e., the points from Table 1), while managing to represent arbitrary or non-hierarchical relationships.

A. Cognitive Models and Ontologies

One information system where a non-hierarchical organization may be necessary, when attempting to map the internal structural relations, is the human brain. For more than half a century, researchers across many fields (e.g., Cognitive Psychology, Neuroscience, Cognitive Science) have been using models to posit and test hypothetical interpretations of how the human brain is structured. These range from the very simple (e.g., Baddely's working memory model, [31]) to complex neurological models (e.g., [32]), though no current model has even begun to approach the actual complexity of the human brain. On a neuronal level, and certainly even on a functional level such as between brain regions, this is a non-hierarchical system.

It is remarkable that at a superficial level, the development of ontologies draws a strong parallel with some theoretical interpretations of how the human cognitive system might be structured (see Table 2). This relation is further discussed in Sennersten et al. [13].

 ISBN: 978-1-61208-340-7

TABLE 2: COMPARISON OF CLASSIC ONTOLOGY, OAR, AND ACT-R MODELS

OAR Model	Ontology Components	ACT-R ACT-R/E
Object(s) Attribute(s) Relation(s)	Class Properties Relationship(s)	ChunkType Chunk Slot(s) Function(s)

In OAR (Object, Attribute, Relation) Wong [10] develops a model which most certainly shares conceptual roots with ontological knowledge representation. Likewise, parallels may be drawn with Anderson's ACT-R model [11] and Trafton's "embodied" version [32] ACT-R/E. In each model, *Objects* in the real world possess characteristics (i.e., *attributes*, or *properties*) and also *relations* with one another. If we can augment these heretofore largely semantic components with a functional representation of three dimensional space (e.g., at the 3 levels *Global*, *Local*, and *Personal*), we may have the fundaments of a system of Spatial Understanding for a robotic platform.

V. SUMMARY

One of the few certainties regarding the immediate future is that robotic control technology will advance from systems which are coded for specific applications, to systems which are designed with an innate adaptability to unexpected environmental situations. This will require new methods of providing on-the-fly relational information to the robot, in order for it to gain an understanding of both its spatial position, and the position of other objects in the vicinity, their characteristics, and the ways in which it can relate to them. A reworking of the traditional OWL-based ontology, with an eye for 3-dimensional spatial relations on 1) Global, 2) Local, and 3) Personal levels of specificity may be sufficient to this end.

It is also noted that as data sets become more complex, and especially as we begin to consider that most complex of biological control systems, the human cognitive system, it may very well become necessary to develop hybrid ontological-type systems of knowledge representation which 1) encompass the full realm of advantages provided by the use of specific nomologial hierarchies, and 2) enable the encoding of arbitrary or non-hierarchical relationships. The development knowledge-based systems that can account for abstract, non-hierarchical relations could potentially facilitate the next generation of spatially aware robotics applications.

REFERENCES

[1] J. Kuffner, "Cloud Enabled Robots," Presentation, IEEE Humanoids conference, Nashville, Tenn. 2010. http://www.scribd.com/doc/47486324/Cloud-Enabled-Robots [retrieved: March, 2014]

[2] R. Khosla, M. Chu, R. Kachouie, K. Yamada, and T. Yamaguchi. "Embodying Care in Matilda: An Affective Communication Robot for the Elderly in Australia." In Proceedings of the 2nd ACM SIGHIT International Health Informatics Symposium, pp. 295–304, 2012. http://dl.acm.org/citation.cfm?id=2110398. [retrieved: March, 2014]

[3] J. M. Lutin, A. L Kornhauser, and E. Lerner-Lam. "The Revolutionary Development of Self-Driving Vehicles and Implications for the Transportation Engineering Profession." Institute of Transportation Engineers, ITE Journal, vol. 83(7), July 2013, pp. 28.

[4] L. M. Hiatt, S. S. Khemlani, and J. G. Trafton, "An Explanatory Reasoning Framework for Embodied Agents," Biologically Inspired Cognitive Architectures, vol. 1, July 2012, pp. 23–31, doi:10.1016/j.bica.2012.03.001.

[5] A. Elfes, J. L. Hall, E. A. Kulczycki, D. S. Clouse, A. C. Morfopoulos, J. F. Montgomery, J. M. Cameron, A. Ansar, and R. J. Machuzak, "An Autonomy Architecture for Aerobot Exploration of the Saturnian Moon Titan," IEEE Aerospace and Electronic Systems Magazine, vol. 23(7), July 2008, pp. 1-9.

[6] K. K. Tahboub and S. N. Al-Din Munaf, "A Neuro-Fuzzy Reasoning System for Mobile Robot Navigation," JJMIE vol. 3(1), March 2009, pp. 77-88. http://pdf.aminer.org/000/361/105/a_neuro_fuzzy_approach_to_autonomous_navigation_for_mobile_robots.pdf. [retrieved: March, 2014]

[7] J. Fasola and M. Matarić, "Using Spatial Language to Guide and Instruct Robots in Household Environments," Refereed Workshop, AAAI Fall Symposium: Robots Learning Interactively from Human Teachers, Arlington, VA, Nov 2012. http://www.aaai.org/ocs/index.php/FSS/FSS12/paper/viewFile/5582/5880. [retrieved: March, 2014]

[8] C. Hudelot, J. Atif, and I. Bloch, "Fuzzy Spatial Relation Ontology for Image Interpretation," Fuzzy Sets and Systems, vol. 159(15), August 2008, pp. 1929–1951. doi:10.1016/j.fss.2008.02.011.

[9] G. Fu, C. B. Jones, and A. I. Abdelmoty, "Ontology-Based Spatial Query Expansion in Information Retrieval," On the Move to Meaningful Internet Systems 2005: CoopIS, DOA, and ODBASE, Springer, 2005, pp. 1466–1482. http://link.springer.com/chapter/10.1007/11575801_33. [retrieved: March, 2014]

 ISBN: 978-1-61208-340-7

[10] Y. Wang, "The OAR model for knowledge representation," Proc. The 2006 IEEE Canadian Conference on Electrical and Computer Engineering (CCECE'06), Ottawa, Canada, May 2006, pp. 1692-1699.

[11] J. R. Anderson, "ACT," American Psychological Association, vol. 51(4), 1995, pp. 355-365.

[12] M. Bosse, R. Zlot, and P. Flick, "Zebedee: Design of a Spring-Mounted 3-D Range Sensor with Application to Mobile Mapping," IEEE Transactions on Robotics, vol. 28(5), October 2012, pp. 1104–1119. doi:10.1109/TRO.2012.2200990.

[13] C. Sennersten, A. Morshed, M. Lochner, and C. Lindley, "Towards a cloud-based architecture for 3D object comprehension in cognitive robotics", The 6th International Conference on Advanced Cognitive Technologies and Applications, 25-29th of May 2014, Venice, Italy (Submitted).

[14] R. A. Brooks, "Cambrian Intelligence." Massachusetts, MIT Press, 1999.

[15] T. R. Gruber, "A Translation Approach to Portable Ontology Specifications," Knowledge Acquisition, vol. 5(2), 1993, pp. 199–220.

[16] C. Masolo, S. Borgo, A. Gangemi, N. Guarino, A. Oltramari, and Schneider, L, "Dolce: a descriptive ontology for linguistic and cognitive engineering, " WonderWeb Project, Deliverable D17, vol. 2(1), 2003.

[17] C. Masolo, S. Borgo, A. Stefano, A. Gangemi, N. Guarino, A. Oltramari and L. Schneider. "The WonderWeb Library of Foundational Ontologies." IST Project 2001 - 33052 WonderWeb: Intermediate Report, May 2003.

[18] J. A. Turner and A. R. Laird, The cognitive paradigm ontology: design and application. Neuroinformatics, vol. 10(1), 2012, pp. 57-66.

[19] G. A. Miller, R. Beckwith, C. Fellbaum, D. Gross, and K. J. Miller, "Introduction to wordnet: An on-line lexical database". International journal of lexicography, vol. 3(4), 1990, pp. 235-244.

[20] C. Matuszek, J. Cabral, M. J. Witbrock, and J. DeOliveira, "An Introduction to the Syntax and Content of Cyc," AAAI Spring Symposium: Formalizing and Compiling Background Knowledge and Its Applications to Knowledge Representation and Question Answering, March 2006, pp. 44-49.

[21] Laboratory for Applied Ontology (LOA) (ISTC-CNR) http://www.loa.istc.cnr.it/ [retrieved: March, 2014].

[22] D. B. Keator, J. S. Grethe, D. Marcus, B. Ozyurt, S. Gadde, S. Murphy, and P. Papadopoulos , "A national human neuroimaging collaboratory enabled by the Biomedical Informatics Research Network (BIRN)", Information Technology in Biomedicine, IEEE Transactions on, vol. 12(2), 2008, pp. 162-172.

[23] A. R. Laird, J. J. Lancaster, and P. T. Fox, "Brainmap," Neuroinformatics, vol. 3(1), 2005, pp. 65-77.

[24] Y. Kwoh, J. Huo, E. Jonckheere, and S. Hayati, "A Robot with Improved Absolute Positioning Accuracy for CT Guided Stereotactic Brain Surgery", IEEE Transactions on Biomedical Engineering, Feb 1988, vol. 35(2), pp. 153-160.

[25] J. Dixon and O. Henlich, "Mobile Robot Navigation", Final Report, Information Systems Engineering, Imperial College, UK, 1997.

[26] D. Martin, C. Fowlkes, D. Tal, and J. Malik, "A database of human segmented natural images and its application to evaluating segmentation algorithms and measuring ecological statistics," Computer Vision 2001 (ICCV 2001), Proceedings, Eighth IEEE International Conference on, vol. 2, pp. 416-423, 2001.

[27] J. Hastings, C. Batchelor, and M. Okada, "Shape Perception in Chemistry," Proceedings of the Second Interdisciplinary Workshop The Shape of Things (SHAPES 2013), Rio de Janeiro, Brazil, April 3-4, 2013, pp. 83-94. http://ceur-ws.org/Vol-1007/paper6.pdf. [retrieved: March, 2014].

[28] V. Maojo, M. Fritts, F. Martin-Sanchez, D. De la Iglesia, R. E. Cachau, M. Garcia-Remesal, and J. Crespo. "Nanoinformatics: Developing New Computing Applications for Nanomedicine." Computing, vol. 94(6), March 7, 2012, pp. 521–539, doi:10.1007/s00607-012-0191-2.

[29] D. Magka, B. Motik, and I. Horrocks, "Modelling structured domains using description graphs and logic programming," Lecture Notes in Computer Science, vol. 7295, 2012, pp. 330-344, Department of Computer Science, University of Oxford, 2011.

[30] O. Kutz, J. Hastings, and T. Mossakowski. "Modelling Highly Symmetrical Molecules: Linking Ontologies and Graphs Artificial Intelligence: Methodology, Systems, and Applications," Lecture Notes in Computer Science, vol. 7557, chap. 11, pp. 103–111, Springer Berlin / Heidelberg, Berlin, Heidelberg, 2012.

[31] A. D. Baddeley and G. Hitch, "Working memory," In The psychology of learning and motivation: Advances in research and theory, vol. 8, G.H. Bower, Ed. New York: Academic Press, 1974, pp. 47–89.

[32] M. Riesenhuber and T. Poggio, "Hierarchical models of object recognition in cortex," Nature Neuroscience, vol. 2(11), November 1999, pp. 1019–1025.

[33] G. Trafton, L. Hiatt, A. Harrison, F. Tanborello, S. Khemlani, and A. Schultz, "ACT-R/E: An Embodied Cognitive Architecture for Human-Robot Interaction," Journal of Human-Robot Interaction, vol. 2(1), March 2013, pp. 30–55. doi:10.5898/JHRI.2.1.Trafton.

 ISBN: 978-1-61208-340-7

Consensus Making Algorithms based on Invariants Perception for Cognitive Sharing in Multi-Robot

Shodai Tomita and Kosuke Sekiyama
Department of Micro-Nano
Systems Engineering, Nagoya University
Furo-cho, Chikusa-ku, Nagoya, Japan
Email: {tomita, sekiyama}@robo.mein.nagoya-u.ac.jp

Toshio Fukuda
Faculty of Science and Engeneering, Meijo University
1-501 Shiogamaguchi, Tenpaku-ku, Nagoya, Japan
Email: tofukuda@meijo-u.ac.jp

***Abstract*—Visual recognition in multi-robot systems is afflicted with a peculiar problem that observations from different viewpoints present different perspectives. Moreover, a representation of the same target object is highly affected by the viewpoint or environmental condition. Hence, realizing cognitive sharing of the object among robots in an unconstructed environment has become challenging. To cope with this issue, we have proposed a Hierarchical Invariants Perception Model (HIPM) in which multiple representations; color, shape, geometric relation, are dynamically evaluated and selected by the robot. In this paper, we propose consensus-making algorithms to acquire viewpoint-invariant representations. Experimental results show the ability of cognitive sharing significantly improved by the proposed method.**

Keywords–cognitive sharing; multi-robot; consensus making

I. INTRODUCTION

Cognitive sharing of an object is a primary issue in multi-robot task execution, where robots with different perspective are expected to cooperate in our daily unstructured environment. As robots engage in more varied and difficult tasks, they will become a ubiquitous part of our daily life in the future [1]. Researchers generally agree that multi-robot systems of inherently distributed character may behave more robustly and effectively and accomplish cooperative tasks that are not possible for single robot systems [2].

However, cognitive sharing methods in conventional works are generally difficult to be applied to unstructured environment. The conventional cognitive sharing has been based on the premise that the target is attached by an artificial marker such as RFID [3] and QR code [4], and that the target is a single-colored sphere [5].

We deem that visual information is suitable for the cognitive sharing in unstructured environment. One of the main issues in the cognitive sharing is to avoid misrecognition of the target object. Since visual information gives many kinds of representations of an object, we deem that, by using a combination of the representations, robots can verify whether or not they observe the same object. Although the cognitive sharing may be realized by sharing a global position of the target, localization errors by robots will make difficult cognitive sharing based on positional information. The position of the target in a global coordinate with errors only enables robots to share a region of interest (ROI).

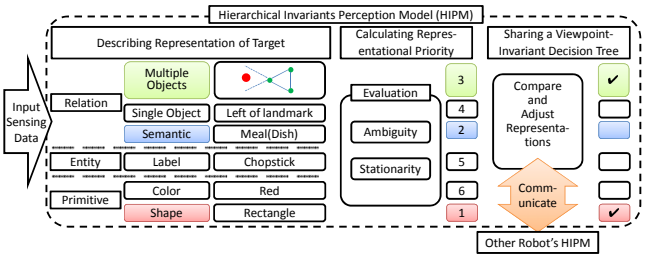

Figure 1. Hierachical Invariants Perception Model

However, visual recognition in multi-robot systems has a peculiar problem that representations are highly affected by the robot's viewpoint and environmental condition. Since observations from different viewpoints present different representations, all representations cannot be shared. Also, unstructured environments abound with unavoidable disturbances, such as illumination changes, object occlusion and sensor faults, that would disturb cognitive sharing and even object recognition.

To cope with these issues, we have proposed a Hierarchical Invariants Perception Model (HIPM) [6] which deals with the cognitive sharing and object tracking simultaneously (Figure 1). A robot describes different classes of representation from sensing data (Describing Representations of Target), and evaluates the *ambiguity*, which estimates the risk of recognition failures for the target in the ROI, and *stationarity* which indicates the steadiness of the ambiguity over time. The robot selects a unique and stable representation based on ambiguity and stationarity (Calculating Representational Priority). Then the robot combines the representations and constructs a decision tree. By comparing and adjusting the representations in the decision tree through communication, robots reach a consensus (i.e., what representations can be shared). Finally, when the robots share the same decision tree, the target is identified (Sharing Viewpoint-Invariant Decision Tree).

In this paper, we extend the HIPM in that a definition of a relation representation and sharing a viewpoint-invariant decision tree are formulated, and experimentally illustrated. Although we have proposed the technique of autonomous landmark generation [7], in which some peripheral objects near the target are selected as landmarks in real time to relate the target to the surroundings, problems resulting from differet viewpoints are not considered and a geometric relation among the target and multiple-landmark has not been used.

 ISBN: 978-1-61208-340-7

This paper is organized as follows. The System overview is described in Section II. Visual representations; *primitive representation* and geometric relation-based representation are presented in Section III. The method of identify the target and consensus-making algorithms are elaborated in Section IV. Experimental results are described in Section V. Finally, the conclusions are discussed in Section VI.

II. SYSTEM OVERVIEW

The purpose of the proposed approach is to share one target object in unstructured environment between two robots: robot A, which recognizes the target, and robot B, which does not know any information on the target. Several assumptions are made as follows.

(a) Environment: Some objects in the environment are similar to the target. The objects do not move. An appearance of the objects may change as a result of a change in viewpoint. An occlusion of the objects may occur.

(b) Robots: The robots can localize themselves though the localization has errors and are equipped with a RGBD sensor.

The proposed approach based on the HIPM has the two features:

- **Describing representations of the target** (in Section III) Robot A describes representations of the target from a RGBD image. In this paper, color, shape and geometric relation-based representation (GRR) are employed.
- **Sharing viewpoint-invariant decision tree** (in Section IV) Robot A constructs a decision tree, which is a suitable combination of the representations for identifying the target from the viewpoint of robot A. Robot B receives the decision tree and decides which representations are viewpoint-invariant. If robot B concludes the received decision tree includes non viewpoint-invariant representations, robot A sends a new decision tree. Through this process, robots share a viewpoint-invariant decision tree gradually.

Calculating representational priority is addressed in [7]. Since we do not assume drastic illumination changes, this component is not discussed in this paper.

III. DESCRIBING REPRESENTATIONS OF TARGET

A. Primitive Representation

We employ color and shape features as the basic representations to recognize an object, which are referred to as *primitive representation* in this paper. In visual recognition, image features (e.g., color [8], shape [9], and feature point [10]) have been used to recognize an object. Although feature points may be salient and therefore suitable for object recognition, they are susceptible to viewpoint changes. However, color and shape features tend to be robust against viewpoint changes.

Because the robots have different viewpoint, the primitive representation should be invariant with respect to scale and illumination changes in the visual recognition. A hue histogram is known to be an invariant representation with respect to scale, illumination direction, and angle changes [11]. In this paper, the histogram similarity function is expressed by histogram intersection [12]. Histogram intersection is computationally efficient and robust against partial occlusion and resolution changes. The histogram axis is divided into 32 sections for computational efficiency and recognition accuracy. The similarity of color representation S_c is calculated from

$$S_c(H^a, H^b) = \sum_{i=1}^{32} min(H^a(i), H^b(i)), \quad (1)$$

where H^a and H^b represent the hue histogram of object O_a and O_b respectively, and $H(i)$ represents the value of i-th histogram's bin.

Also, hu moments of a contour is used as a shape representation in this paper. Hu moments are invariant with respect to scale changes and rotation. By following the definition in [14], the similarity between two moments can be calculated

$$S_s(h^a, h^b) = \sum_{i=1}^{7} \left| \frac{m^a(i) - m^b(i)}{m^a(i)} \right|, \quad (2)$$

where,

$$m(i) = sign(h(i)) \cdot log|h(i)|,$$

h^a and h^b represent hu moments of object O_a and O_b respectively, and $h(i)$ represents the value of i-th hu momemts.

B. Object Segmentation

To describe the primitive representation of each object, the input image has to be divided into objects and the other areas, and the boundaries have to be contours of objects. In general, a computationally efficient segmentation method is required because the robots are supposed to move around. In this paper, we employ a segmentation method based on the depth information obtained using an RGBD sensor [15]. RGBD sensors (Kinect or Xtion) can output sensing data at a frame rate of 30 Hz and this method can extract accurate contours by using the depth information. Fortunately, because the depth information can be captured under any ambient light conditions, the shape representation is invariant against arbitrary illumination changes.

C. Similar Primitive Representation from Different Viewpoints

In general, a primitive representation will be highly affected by changes in viewpoint. However, empirically, a similarity of primitive representation between the same object from different viewpoints lies within a certain range.

Assume a color representation H^a and shape representation h^a of an object O_a are sent from robot A. When a color representation H^b of object O_b, which is perceived by robot B, satisfies

$$S_c(H^a, H^b) \geq 0.7, \quad (3)$$

we define O_b has a similar color representation to H^a. Also, when a shape representation h^b of O_b satisfies

$$S_s(h^a, h^b) \leq 0.3. \quad (4)$$

we define O_b has a similar shape representation to h^a.

 ISBN: 978-1-61208-340-7

If robot B perceives only one similar color (shape) representation to H^a (h^a) after sharing a ROI, define H^a (h^a) as viewpoint-invariant representation. If H^a or h^a is viewpoint-invariant, O_a and O_b may be the same object.

D. Geometric Relation-Based Representation

In this paper, as the relation representation, we use geometric relation between the target and sharable surroundings. Use of geometric relation offers two advantages: 1. the error for the relative positions of objects is comparably smaller than the error of global position and 2. the information is independent of robot localization and odometry. Therefore, this relation is viewpoint-invariant.

Two processes are needed to form a GRR as follows.

1) Select candidate objects of GRR components that have a salient primitive representation.
2) Describe the geometric relation among the target and the components of GRR based on a distance information.

An object which has no similar representation from robot A's viewpoint is likely to be identified uniquely. Therefore, such objects are suitable for candidates of GRR components.

Three objects of the same kind of primitive representation (e.g., three objects which have unique color representations) are selected from the candidates, and a triangle is formed. The reason why the same kind of primitive representation should be selected is that color and shape representations are invariant with respect to different disturbances (e.g., color representation is invariant to partial occlusion and shape representation is invariant to changes in lightning conditions). The reason why a triangle is chosen is that it is the minimum unit needed to divide a flat space into a closed area and other geometric shapes can be represented by a combination of triangles.

A GRR divides the recognition area into 7 areas $A_a (a \in \{1,2,...7\})$. The decomposed area A_a is represented by the triple set of + and - sign as shown in Figure2. The decomposed area where the target belongs is denoted by A_t. Assuming l candidates for the GRR components, the number of constructed GRR m is ${}_lC_3$. A GRR is regarded as viewpoint-invariant when all GRR components are viewpoint-invariant.

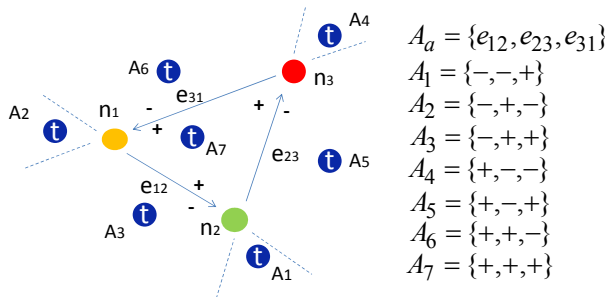

Figure 2. Representation of Target Position. The components of a GRR are denoted by n_1, n_2, n_3 and connected in the counterclockwise direction. A link vector (e_{12}, e_{23}, e_{31}) which connects to the components will decompose the recognition area into two domains. The left-side of the link vector where each vector is linked counterclockwise is denoted as the positive sign (+) and the right-side of each vector is denoted as the negative sign (-).

IV. SHARING VIEWPOINT-INVARIANT DECISION TREE

A. Construction of the Decision Tree

We use a binary decision tree that consists of combined representations to identify the target because it is very rare when the target object can be uniquely identified by means of a single representation. Such a limited case is the following:

(i) When a primitive representation is employed, no similar representation is found closely to the target object.
(ii) When a GRR is employed, only the target object is included in the decomposed area A_t of the GRR.

In order to construct the decision tree, we employ the branch and bound algorithm. In the cognitive sharing, since the data of the target class is only one, conventional methods (e.g., C4.5 and CART) cannot be used because these methods require adequate data to select an effective node.

The branch and bound algorithm has the advantage of constructing a decision tree that can minimize the required number of nodes. Redundant information may increase searching time because not all representations can be shared owing to appearance changes and occlusion. The solution to the problem resulting from viewpoint changes is discussed in Sec. IV-B.

The branch and bound algorithm is given as follows: Assume a set of n objects $O = \{O_1, O_2, \cdots, O_n\}$, which is perceived by robot A. An object $O_i (\in O)$ is described by color representation i.e., hue histogram H^i, shape representation i.e., hu moments h^i and m GRRs $g^i_j (j \in M = \{1,2,...,m\})$. From robot A's viewpoint, candidates of the target object $O_t (\in O)$ can be reduced by using the target's representations H^t, h^t, g^t_j according to

$$R_j = \{O_i \in O | O_i \in A^j_t\} \ (j \in M), \quad (5)$$
$$R_{m+1} = \{O_i \in O | S_c(H^t, H^i) \geq 0.7\}, \quad (6)$$
$$R_{m+2} = \{O_i \in O | S_s(h^t, h^i) \leq 0.3\}. \quad (7)$$

Here R_j, R_{m+1}, and R_{m+2} represent a set of candidates reduced by using similarity criteria g^t_j, h^t, and H^t respectively.

(i) Objective Function and Constraint Condition
Let us denote a collection of the target's candidate sets by $R = \{R_1, R_2, ..., R_m, R_{m+1}, R_{m+2}\}$. The goal is to find a combination of the target's representations that can narrow candidate objects of the target down to one such that the number of tree nodes is minimized. The objective function and constraint condition are defined as follows:

$$\text{minimize} \quad |X| = |\cap_{R_k \in R'} R_k|, \ (R' \subset R), \quad (8)$$
$$\text{subject to} \quad |X| \geq 1, \ |R'| \leq 3, \quad (9)$$

where $|\cdot|$ represents the cardinality of a set. If $R' = \{R_1, R_{m+1}\}$, 1st GRR g^t_1 and color representation H^t are employed as nodes of a decision tree. In order to reduce redundant information, the number of nodes $|R'|$ is limited to 3.

(ii) Branching
Subproblem P_i (breadth first search)
Minimize $|X|$ subject to $|R'| = i \ (i \in \{1,2,3\})$

(iii) Bounding
Prune if $|X| \leq z$. z is the minimum upper bound seen among subproblems examined so far.
Finish if $|X| = 1$.

B. Comparing and Adjusting Representations

As mentioned in Sec. IV-A, a decision tree sent by robot A can include representations which cannot be shared between the robots resulting from different viewpoints. In this section, we discuss how two robots perceive viewpoint-invariant representations and share a viewpoint-invariant decision tree through communication. Figure 3 shows a state transition diagram of robot A and robot B. The consensus-making algorithms are composed of four functional parts; ROI sharing, searching, invariants perception, and decision tree adjustment. We explain how robot B changes its state mainly because robot A changes its state according to robot B's request.

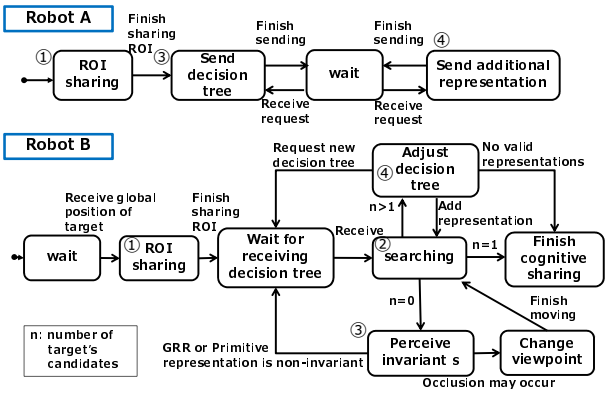

Figure 3. State Transition Diagram of Robot A and B

1) Sharing ROI (Figure 3-①)*:* To verify whether or not a representation is viewpoint-invariant, a ROI has to be shared. Without sharing the ROI, robots cannot determine the cause of the misrecognition by searching another region or a non-viewpoint-invariant representation.

In this paper, since we assume robots can localize themselves and get depth information from RGBD sensor, robots can calculate a global position of objects. We define a region around a global position of the target as a ROI. The robots share the ROI by sharing the global position of the target. However, since the robot localization has errors, cognitive sharing cannot be achieved by only using the positional information.

Robot A sends the global position of the target to robot B. On receiving, robot B moves to a position only a certain distance away from the global position of the target and finish sharing the ROI. In this paper, we define the distance as 1.5m.

2) Searching (Figure 3-②)*:* After sharing ROI, robot A sends a decision tree. On receiving the decision tree, robot B starts searching. Since robot B can calculate a position of objects in robo-centric coordinate, robot B searches while making a map of objects. Considering an area that has been searched, robot B decides where to search. After rotation, robot B perceives objects and updates the map. Robot B compares objects in the map with the received decision tree and moves to a position where objects which has identified representations in the decision tree can be observed.

When all representations in the decision tree are identified and candidates of the target object are found, robot B change the state: change the state to finish cognitive sharing if the number of the candidates is one, change the state to adjust a decision tree if the number of the candidates is more than one. When the number of the candidates is zero or all representations in the decision tree is not identified, robot B lasts searching. Robot B change the state to invariants perception when finishes searching around the ROI.

3) Invariants Perception (Figure 3-③)*:* Representations which are not identified though robot B finishes searching around the ROI are regarded as non viewpoint-invariant representations. Robot B takes different actions according to a kind of the non-viewpoint-invariant representation.

(i) Primitive representation of the target
Two situations are conceivable: the appearance of the target may change or the occlusion of the target occurs. In order to verify whether the occlusion occurs or not, robot B changes its viewpoint and searches around the ROI again. In this paper, changing viewpoint is achieved by moving a certain distance to a tangential direction of a circle whose center is the received global position of the target and the distance is defined as 0.8[m] empirically. If the primitive representation cannot be identified even after changing viewpoint, robot B requires robot A to send a new decision tree which does not include the primitive representation because its description is likely to be varied.

(ii) GRR
When not all components of a GRR in the received decision tree are identified, robot B requires robot A to send a new decision tree which does not include the unidentifiable components of the GRR. When the GRR is shared but the number of candidates narrowed down by using the GRR is zero, robot B changes its viewpoint and begins searching again because an occlusion of the target objects may occurs. If the candidates are not found after changing viewpoint, the GRR is regarded as non-viewpoint invariant. Then, robot B requires robot A to send a new decision tree.

4) Decision Tree Adjustment(Figure 3-④)*:* Even though the robots successfully share viewpoint-invariant representations, robot B sometimes may fail to identify the target when the primitive representation is not viewpoint-invariant. For example, this would occur when an object out of robot A's view exists in A_t of the GRR or when the objects near the target in A_t change their appearance.

In these situations, robot B has to determine what information is needed autonomously. Robot B calculates the similarity of primitive representations among the candidates as reduced by using the received decision tree. If the primitive representations of the candidates are not similar, robot B requests the primitive representation. Then, robot B adds the primitive representation to the decision tree and tries to identify the target. Robot B also requests another decision tree if the number of candidates cannot be reduced by using only the primitive representation. Robot B will finish searching when

 ISBN: 978-1-61208-340-7

the number of candidates is reduced to one or when the number of candidates obtained by using the decision tree is the same between the robots.

V. EXPERIMENT

A. Experimental Conditions

This experiment demonstrates that the proposed approach has robustness against following problems:

- Robot B mistakes the target for a similar object.
- Not all representations can be shared because an occlusion and appearance change may occur resulting from different viewpoints.

The experiment environment is shown in Figure 4. Each robot (robot A: amigobot; robot B: Pioneer 3-AT) is equipped with a Xtion Pro Live and a communication module (OKI UDv4). The initial position and pose of a robot (x, y, θ) are defined by adding random noise w_1, w_2, w_3 with a Gaussian distribution having standard deviation 0.3 to true value $(x_{true}, y_{true}, \theta_{true})$.

$$(x, y, \theta) = (x_{true} + w_1, y_{true} + w_2, \theta_{true} + w_3). \quad (10)$$

The robots localize themselves using odemetry. Robot A recognizes the target in the middle left of Figure 4 and robot B does not know *a propri* target information. There exists a similar object to the target in the environment in the middle of Figure 4 labeled as "dummy". We assume that dramatic illumination changes and the movement of objects will not occur during cooperation.

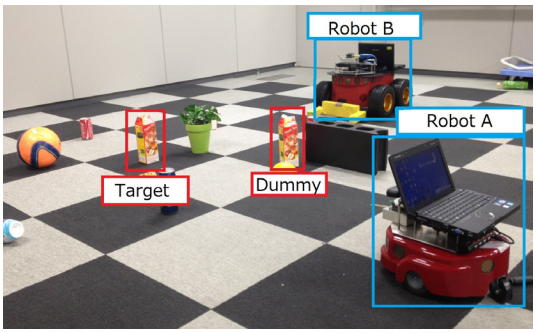

Figure 4. Experiment Environment

B. Experimental Result

Snapshots of the experiment are shown in Figure 5-9. The constructed decision tree is shown in the upper left of each image. Robot's action and communication condition are shown in the above each image. The red bounding box in the image represents the target and the blue bounding boxes represent identified components of the GRR. The objects with white crosses represent non viewpoint-invariant representations.

1) ROI Sharing: By $t = 3[s]$, robot B received the global position of the target and start sharing the ROI. By $t = 8[s]$, Robot B moved 1.5m away from the received global coordinate and finished ROI sharing (Figure 5).

Since the initial position of robots are added random noise, a target position estimated by robot B has an error as shown in Figure 10. Only using positional information of the target, robot B may fail to identify the target because the estimated

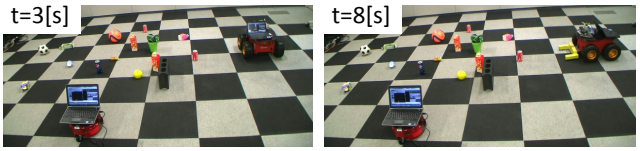

Figure 5. Snapshots of ROI sharing

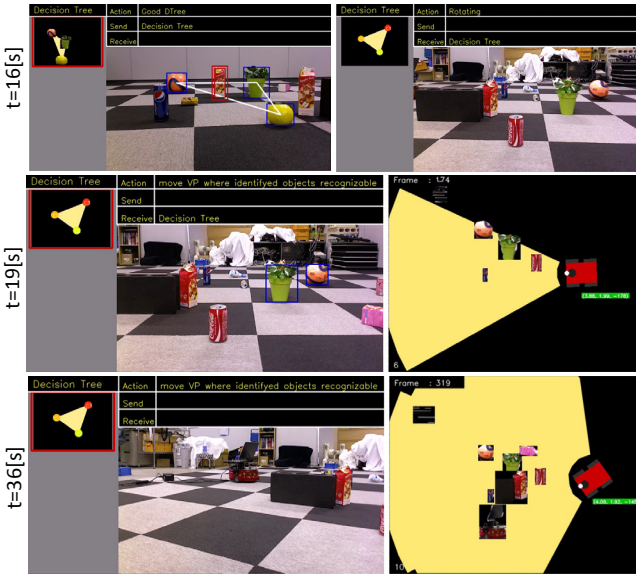

Figure 6. Snapshots of Searching (Top row: robot A's view (left), robot B's view (right). Middle and bottom row: robot B's view (left), a map made by robot B (right).)

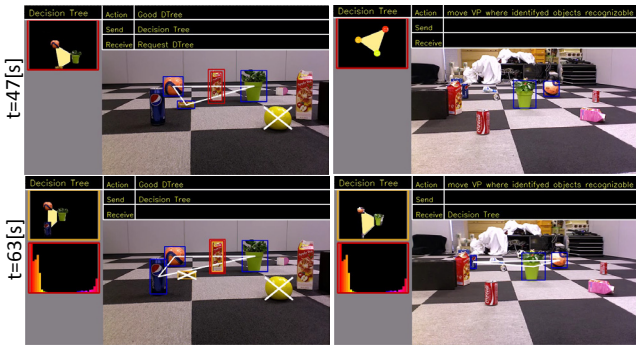

Figure 7. Snapshots of Invariants Perception (Left column: robot A's view. Right column: robot B's view.)

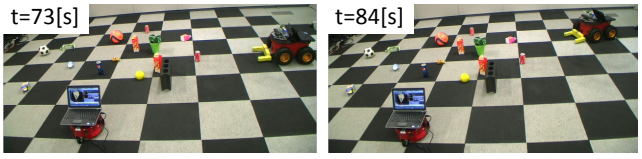

Figure 8. Snapshots of Change Viewpoint

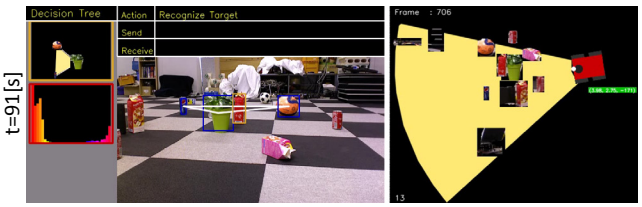

Figure 9. Snapshots of Finish Cognitive Sharing. (Left: Robot B's view, Right: a map made by robot B)

 ISBN: 978-1-61208-340-7

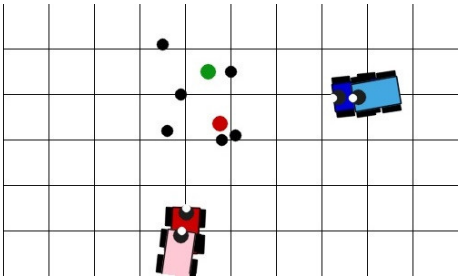

Figure 10. true and estimated position of robots and the target. Red robot: true position of robot A. Pink robot: robot A's position estimated by robot A. Blue robot: true position of robot B. Light Blue robot: robot B's position estimated by robot B. Green circle: true position of the target. Red circle: target position estimated by robot B. Black circles: surroundings near the target (not all). Lines are drawn at intervals of 0.5m.

position is closer to position of surroundings than the true position.

2) Searching: By $t = 16[s]$, robot B received the decision tree from robot A and started searching. By $t = 19[s]$, robot B found two components of the GRR and then continue searching in the ROI to find the rest of components. By $t = 36[s]$, although robot B finished searching in the ROI, robot B did not find the rest of the components. Therefore, robot B changed its state to Invariants Perception. (Figure 6)

3) Invariants Perception: By $t = 40[s]$, robot B regarded the unidentifiable component of the GRR as non-viewpoint-invariant, and required robot A to send a new decision tree which did not include the unidentified component of the GRR. In fact, an occlusion of the component occurred.

By $t = 47[s]$ (Figure 7), robot B received a new decision tree. However, one component of the GRR did not found. Therefore, robot B regarded it as non viewpoint invariant and required the new decision tree. In fact, the appearance of the component changed resulting from different viewpoints.

By $t = 43[s]$ (Figure 7), robot B received the new decision tree and succeeded in identifying the GRR in the decision tree. However, candidates of the target were not found in the decomposed area of the GRR. Robot B considered that the target was occluded, and changed its viewpoint.

By $t = 84[s]$, robot B finished changing its viewpoint by moving 0.8[m] to a tangential direction of a circle whose center is the received global position of the target as shown in Figure 8.

4) Finish Cognitive Sharing: By $t = 91[s]$ (Figure 9), robot B found a candidate of the target in the decomposed area in the new viewpoint. Because the color representation of the candidate corresponded with the color representation of the second tree node, robot B succeeded in sharing the target.

5) Decision Tree adjustment: Another experiment was conducted to demonstrate the necessity of decision tree adjustment as shown in Figure 11. By $t = 95[s]$, the robots shared the decision tree composed of the viewpoint-invariant representations. However, similar color object appeared in the decomposed area owing to an appearance change, so robot B did not make a difference between these candidates. Robot B determined the necessary representation autonomously and requested the

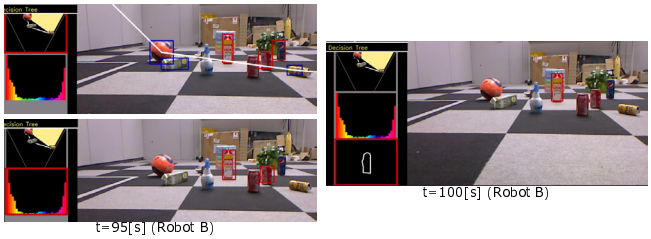

Figure 11. Snapshots of Other Experiment

shape representation in this situation. By $t = 100[s]$, robot B succeeded in cognitive sharing by adding the shape representation to the decision tree.

VI. CONCLUSION AND FUTURE WORK

We proposed cognitive sharing algorithm based on visual information. A decision tree including geometric relation-based representation allows robots to share precise ROI and avoid mistaking the target for a similar object. The Consensus-making algorithms serve to acquire viewpoint-invariant representations.

For future work, an important issue will be adaptation to disturbances. Although we assumed that dramatic illumination changes and the movement of objects would not occur in the experiment, such disturbances occur in unstructured environment. Evaluating ambiguity and stationarity in a HIPM, robots should select robust representations against a certain disturbance.

REFERENCES

[1] B. Gates, "A Robot in Every Home", Scientific American vol.296, pp.58-65, 2007.

[2] T. Arai, E. Pagello and L. E. Parker, "Editorial: Advances in multi-robot systems", IEEE Transaction on Robotics and Automation, vol. 18, no. 5, pp. 655-661, 2002.

[3] K. G. Tan, A. R. Wasif and C.P. Tan, "Objects Tracking Utilizing Square Grid Rfid Reader Antenna Network", Journal of Electromagnetic Waves and Applications, vol. 22 , pp.27-38, 2008.

[4] Y. Xue, G. Tian, R. Li and H. Jiang, "A New Object Search and Recognition Method based on Artificial Object Mark in Complex Indoor Environment", World Congress on Intelligent Control and Automation, pp.6648 - 6653, 2010.

[5] D. Gohring and J. Homann, "Multi Robot Object Tracking and Self Localization Using Visual Percept Relations", Proceedings of IEEE/RSJ International Conference of Intelligent Robots and Systems, pp.31-36. 2006.

[6] T. Umeda, K. Sekiyama and T, Fukuda, "Cooperative Distributed Object Tracking by Multiple Robots Based on Feature Selection", DARS, Springer Berlin Heidelberg, pp.103-114, 2013.

[7] T. Umeda, K. Sekiyama and T. Fukuda, "Vision-Based Object Tracking by Multi-Robots", Journal of Robotics and Mechatronics, vol. 24, No.3, pp.531-539, 2012.

[8] D. Comaniciu, V. Ramesh and P.Meer,"Kernel-Based Object Tracking", IEEE Transactions on Pattern Analysis and Machine Intelligence, vol.25, no.5, pp.564-577, 2003.

[9] M. Isard and A. Blake, "Contour Tracking by Stochastic Propagation of Conditional Density", Proc. Fourth European Conf. Computer Vision, pp.343-356, 1996.

[10] D. G. Lowe, "Object Recognition from Local Scale-Invariant Features," Proc. Seventh IEEE Int'l Conf. Computer Vision, vol. 2, pp.1150-1157, 1999.

[11] T. Gevers and A.W.M. Smeulders, "Color based object recognition," Pattern Recognit., vol. 32, pp.453-465, Mar. 1999.

[12] M.J. Swain and D.H. Ballard, "Color Indexing", International Journal of Computer Vison, vol. 7, No. 1, pp. 11-32, 1991.

[13] B. Gary and A. Kaehler. "Learning OpenCV: Computer vision with the OpenCV library", O'Reilly Media, Incorporated, pp.251-256, 2008.

[14] D. Filliat, E. Battesti, S. Bazeille and G. Duceux, "RGBD object recognition and visual texture classification for indoor semantic mapping.", IEEE International Conference on Technologies for Practical Robot Applications (TePRA), pp.127-132, 2012.

 ISBN: 978-1-61208-340-7

The Role of Expert Judgement in Optimising Preventive Maintenance and System Architecture

Shawulu Hunira Nggada
Department of Computer Science,
Polytechnic of Namibia,
Windhoek, Namibia
e-mail: snggada@polytechnic.edu.na

Yiannis Papadopoulos
Department of Computer Science
University of Hull,
Hull, United Kingdom
e-mail: Y.I.Papadopoulos@hull.ac.uk

***Abstract*-In the current industrial practice, optimisation of maintenance schedules is typically done using expert judgement but not via exhaustive exploration of all possible options for scheduling. Recently, it has been shown that search heuristics such as genetic algorithms can be used in conjunction with stochastic reliability prediction to optimise the maintenance schedules of components in a system. In this paper, we extend this framework to include the optional modelling of informed decisions by experts in terms of the time at which maintenance actions could be performed on components and decisions about which implementations of components should be in the final design. With this method, useful human knowledge and experience can be incorporated in a process that allows extensive exploration of the space of possible options for optimal or near optimal architecture and maintenance scheduling. The approach is demonstrated on a simplified model of fuel system.**

Keywords-maintenance; expert judgement; optimisation; genetic algorithm.

I. INTRODUCTION

Typically, during components inspection, more attention is given to components that have shown signs of poor condition. Such signs may be wear and tear, looseness, stiffness, low or high level of content, etc as it applies to the component in question. In a case where the component is viewed by maintenance personnel as repairable, such component undergoes maintenance actions otherwise replacement is performed. Preventive maintenance promotes carrying out maintenance intervention even before components show sign of poor condition. The time at which such intervention (maintenance actions) is performed is, however, difficult to determine.

Preventive Maintenance (PM) is normally performed periodically which implies a constant maintenance interval. The interval at which maintenance actions are performed on a given component is termed PM time T_p. Hence each component of the system will have a PM time T_{pi}, where i = *1..m*, *m* being the number of components of the system that have been identified for PM. Nggada et al. [1] used probabilistic method to determine the time at which a given component is maintained using the Proportional Age Reduction (PAR) model [2]. This method uses component failure data and ensures that the PM time T_{pi} for the *i-th* component is (i) not too early, incurring unnecessary cost, and (ii) not late when component reliability has significantly dropped. The probabilistic evaluation is proportional to the shortest PM time T of the system. The shortest PM time of the system is chosen such that T is less than the mean time to failure (or mean time between failures as appropriate) of the component that fails most often within the system. Hence each T_{pi} is a multiple of T as shown in Equation 1 [3].

$$T_{pi} = \alpha_i T \quad (1)$$

where: $\alpha_i$is the coefficient of maintenance interval CoMI of the *i-th* component.

The CoMI α_i is an integer value ranging from 1 to $\alpha_{imax}$where $\alpha_{imax}$is obtained from Equation 2 below [1].

$$\alpha_{imax} = \begin{cases} Q\left(\frac{MTTF_i}{T}\right) & ; MTTF_i \leq RT \\ Q\left(\frac{RT}{T}\right) & ; MTTF_i > RT \end{cases} \quad (2)$$

where: Q is the integer quotient of the division;
RT is the system risk time, also referred to as useful life;
$MTTF_i$ is the mean time to failure for the *i-th* component;

However, a scenario may exist where the failure pattern of a given component becomes familiar over a long period of use under same condition. Another scenario that may exist is the lack of failure data which could be used to determine the PM time via probabilistic method. Under either or both scenarios, the use of expert opinion, which is informed by knowledge and experience becomes helpful.

Similarly, at the design stage of a system, each of its constituent components may have several options of its implementation. It is possible to consider all the implementation options of all the components at the system's design stage; giving rise to variants of the system. Nggada et al. [1] demonstrated how such system variants (architectures) could be optimised. The optimised set of the system variants consists of those implementation options that meet system requirements. Similar to the case of component failure, a better implementation option which should be included in the system design may be known to the expert.

 ISBN: 978-1-61208-340-7

The use of a stochastic method and expert opinion in deciding PM time and implementation option of selected components and the overall evaluation of the system model is the focus of this paper. Hence, the reminder of the paper is structured as follows. Section II discusses expert judgement in PM time while Section III discusses expert judgement in implementation option. Section IV discusses the effect of expert judgement on the system and maintenance scheduling optimisation algorithm and process. The modelling and system optimisation process have been implemented in HiP-HOPS, a state-of-the-art tool [11] that is the result of more than fifteen years of research on model-based system dependability analysis and architecture and maintenance optimisation. A case study on maintenance scheduling using this tool is presented in Section V. Evaluations are presented in Section VI, while conclusions are drawn in Section VII.

II. EXPERT JUGDEMENT IN MAINTENANCE TIME

Expert judgement as defined in this paper refers to the elicitation of informed opinions from persons with particular expertise. Expert judgement has been applied in several areas. For instance, expert judgement has been utilised in specifying the number of failures for a component within time interval. The elicitation of such lifetime data from several experts are combined into a consensus distribution which is then updated with failure data. Such combination is done through defined procedures [4]. Another area where expert judgement has been used is reliability prediction in early stages of product development process. Elicitation of expert opinion on lower bound (belief) and upper bound (plausibility) of failure time interval is performed [5]. An increased use of risk assessment in organisations has also increased the role of expert judgement in providing information for safety related decision making. Under such a decision making, expert judgement is required in most of the steps of risk assessment, for instance hazard identification, risk estimation, risk evaluation and analysis options [6].

Under preventive maintenance as used in this paper, expert opinion is used in determining the regular time interval for which a component is to be maintained. In this paper, the time specified by an expert at which a given component is to be maintained is referred to as Expert PM time ($EPMT$). In complying with the expert judgement it is considered appropriate for the PM time of the component to be less or equal to its $EPMT$; $T_{pi} \leq EPMT_i$. The rationale for this is straightforward: so that the likelihood of the component to experiencing unplanned maintenance is minimised. The definition is thus as shown in Equation 3.

$$\left(T_{pi} \leqslant \begin{cases} EPMT_i & ; EPMT_i \leq RT \\ RT & ; ET_i > RT \end{cases}\right) \quad (3)$$

where: $EPMT_i$ is the expert PM time specified for the *i-th* component

In order to follow a similar pattern of evaluation as for components with non-expert specified PM times, the maximum CoMI for the *i-th* component under expert judgement is obtained as shown in Equation 4.

$$\alpha_{iemax} = \begin{cases} Q\left(\frac{EPMT_i}{T}\right) & ; EPMT_i \leq RT \\ Q\left(\frac{RT}{T}\right) & ; EPMT_i > RT \end{cases} \quad (4)$$

where: α_{iemax} is the maximum CoMI of the *i-th* component under expert judgement.

Therefore, the PM time of a component under expert judgement is evaluated similar to Equation 1 shown in Equation 5.

$$T_{pi} = \alpha_{iemax} T \quad (5)$$

III. EXPERT JUDGEMENT IN IMPLEMENTATION OPTION

Assume the following sub-system with two components shown in Fig. 1. X_1 and Y_1 are the implementations of their respective component types X and Y. Fig. 2 shows a variant of Fig. 1 where each component type consists of 3 implementation options.

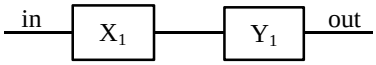

Figure 1. Two components sub-system

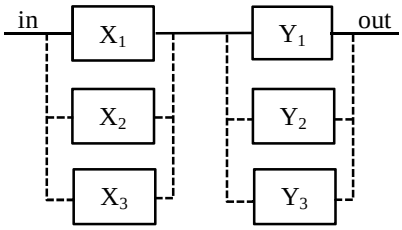

Figure 2. Two sub-system with implementation options

In Fig. 1, X = {X_1} and Y = {Y_1} while in Fig. 2, X = {X_1, X_2, X_3} and Y = {Y_1, Y_2, Y_3}. In Fig. 2 X_1 is the active implementation of component X and similarly Y_1 is the active implementation of component Y. The set of components {X_2, X_3} and {Y_2, Y_3} are the alternative implementations of components X and Y respectively. Fig. 2 implies that the sub-system is a possible combination of any of the implementation options in X and Y. Thus, if the sub-system is represented by S_{sub}, then the potential design models of the sub-system are shown below.

S_{sub} = { {X_1, Y_1}, {X_1, Y_2}, {X_1, Y_3},
{X_2, Y_1}, {X_2, Y_2}, {X_2, Y_3},
{X_3, Y_1}, {X_3, Y_2}, {X_3, Y_3} }

 ISBN: 978-1-61208-340-7

Each of the subsets of potential sub-system design models is referred to as a variant of the sub-system. This scenario also applies to a full system model. At the infancy design stage of a system, as illustrated by Nggada et al. [1], a stochastic process could be used in determining the set of variants which meet design requirements. The engineer could then select one (or more as appropriate) of these variants which will be implemented.

In certain scenarios, the engineer would like to specify which components are to be included in the system model. Such action is an expert opinion that is informed by the engineer's knowledge and, or experience of the system over time. Hence, in addition to stochastically determining the implementation option of a given component type it is also helpful to provide the engineer with an option to specify which of the implementation options should be included in the system model. To achieve this, the engineer would simply select the active implementation of the component while the alternative options are excluded by using a flag.

IV. EFFECT OF EXPERT JUDGEMENT ON OPTIMISATION

An optimisation problem could have single or multi objective, depending on the problem and the approach to optimising the solutions. The work in this paper is multi-objective in nature and maintains a multi-objective approach to optimising the solutions. In general a multi-objective optimisation problem is defined as follows [7][8].

max $\mathbf{F}(x) = \{ f_1(x), f_2(x), f_3(x), .., f_{z-1}(x), f_z(x) \}$
such that:
$x \in \mathbf{X}$
$g_j(x) \leqslant b_j$; $j = 1..k$

where: $f_1, f_2, f_3, .., f_{z-1}, f_z$ are objective functions.
$\mathbf{X}$ is the solution space of all potential solutions.
$x = (x_1, x_2, .., x_{m-1}, x_m)$. In genetic algorithm terminology x is referred to as decision variable vector, while each x_i is referred to as decision variable.
$g_j(x) \leqslant b_j$ is referred to as constraint, where k is the number of constraints imposed on the optimisation.

The left hand side of the constraint; $g_j(x)$ is a real value function, whereas b_j could either be a predefined value or the result of another real value function. $\mathbf{F}(x)$ is referred to as decision vector. The goal of the optimisation problem could be either maximisation (max) or minimisation (min) of the decision vector. The decision vector consists of objective functions as seen in the definition. The objective functions are attributes of the system design and normally include cost and one or more of the following: reliability, availability, safety, weight, etc. The equation $g_j(x) \leqslant b_j$ is known as the inequality constraint. If this is in the form $g_j(x) = b_j$, then it is referred to as equality constraint [8]. When a constraint is present, the optimisation must conform to it. A solution $x \in \mathbf{X}$ which satisfies the constraints is said to be a feasible solution. A collection of all potential feasible solutions defines the feasible region.

Hence, to define the PM optimisation in this paper, the effect of expert judgement will be considered as constraints to the optimisation. The constraints are defined in the next section.

A. Constraints of the optimisation

The constraints guide search algorithm towards the feasible region. When an expert specifies PM time or what implementation option is active and excludes the rest in the optimisation, the size of the feasible region is altered. The size of the feasible region is resizable and without any defined constraint the size is same as the solution space. Firstly, the constraint under PM time is defined followed by component substitution.

B. PM Time Constraints

Constraints guide the selection of individuals within feasible region, where solutions meeting design requirements exit. The constraint of PM time under expert judgement is simply a modification of Equation 3. The time at which maintenance actions are performed when an expert specifies time is the product of the maximum CoMI and the system's shortest PM interval. Thus, the following constraint applies.

$$\left(T_{pi} \leqslant \begin{cases} EPMT_i & ; EPMT_i \leq RT \\ RT & ; EPMT_i > RT \end{cases}\right) \Leftrightarrow \left((expert\_judgement_i = true) \wedge (EPMT_i \geq T)\right) \quad (C1)$$

where: $expert\_judgement_i$ is a Boolean variable that is flagged true for a component that is identified for expert judgement and false otherwise.

When an expert specifies a PM time, Equation 3 ensures that this time is a multiple of T, and if not then converted to such. Additionally constraint $C1$ is enforced if the expert PM time is not less than the system's shortest PM interval. Constraint $C1$ only applies to components that are subjected to expert judgement. Thus for other components the constraint is same as those defined in [10] also shown below.

$$T < \frac{1}{\lambda_H} \quad (C2)$$

$$\alpha_i T \leqslant \frac{1}{\lambda_i} \quad (C3)$$

Where: λ_H is the failure rate of the component that fails most frequently.
λ_i is the failure rate of the *i-th* component.

Constraint $C2$ implies that the shortest PM interval T must be smaller than the mean time to failure (MTTF) of the component that fails most often in the system. The second

constraint defines that for every component *i*, its PM interval must be smaller than its MTTF. These two constraints ensure that maintenance is effective and is not scheduled too late when the reliability of components has dropped too much.

C. Component Substitution Constraint

Component substitution refers to the process of replacing the current active implementation with one of its alternative options. The role of expert judgement under component substitution is to select and to specify the active implementation of the component, and disable such substitution. The constraint used by Nggada et al. [1], which was implemented in HiP-HOPS, could be reused to achieve this, and is as shown below.

$$substitute\_component(i, k_i) \Leftrightarrow \begin{pmatrix} (substitute_i = true) \\ \wedge \\ (k_i > 0) \end{pmatrix} \qquad (C4)$$

Component substitution is performed by a function called $substitute\_component$ and has two parameters. The first is the index *i* of the component under consideration, and then a second index k_i of its current active implementation. The details of the function are contained in Nggada et al. [1]. Constraint $C4$ implies that a component is substituted if and only if the *i-th* component's Boolean parameter $substitute_i$ is flagged *true* and that there exist at least one alternative implementation option. This therefore entails that during component failure annotation in HiP-HOPS the engineer would simply disable substitution for the *i-th* component once an active implementation is selected. Hence for a component which the expert has selected to be fixed throughout the optimisation, the $substitute_i = true$ is replaced with $substitute_i = false$.

D. Defined PM Optimisation

Having defined the optimisation constraints, the optimisation is, therefore, defined as follows.

$min\mathbf{F}(\boldsymbol{\alpha}) = \{ U(\boldsymbol{\alpha}), C(\boldsymbol{\alpha}) \}$

such that: $\boldsymbol{\alpha} \in \mathbf{A}, C1, C2, C3, C4$.

Where: $\boldsymbol{\alpha}$ is a decision variable vector consisting of CoMIs of constituent components of the system.
A is the PM solution space
$C1$, $C3$, $C3$ and $C4$ are the defined constraints.
U and C are the objective functions; unavailability and cost respectively.
The goal of the optimisation is to minimise the objective functions.

V. CASE STUDY

The case study used in Nggada et al. [1] is adopted on which the defined PM optimisation problem is evaluated. The case study is a simplified model of the fuel oil service system (FOSS) which supplies fuel to the main engine of a ship. The FOSS is shown in Fig. 3 and its description is same as in [1]. The system incorporates a service tank which contains stored fuel oil. The booster pump conveys fuel oil to the mixing tank through a filter and flow meter. If the pressure level in the mixing tank exceeds a threshold level, fuel oil is released back into the service tank through a pipe connecting the two. The circulation pump then conveys fuel oil to the main engine through a heater, viscosity meter and a filter. Excess fuel oil not used in the main engine is released to the service tank via the mixing tank.

In order to analyse the model of the fuel oil service system, its constituent components were annotated with HiP-HOPS failure behaviour data. Due to space limitation, a detailed presentation of the annotations is impossible, however the component failure behaviour is simple; each component has a single failure mode which causes omission of outputs while input failures propagate to the outputs of the components.

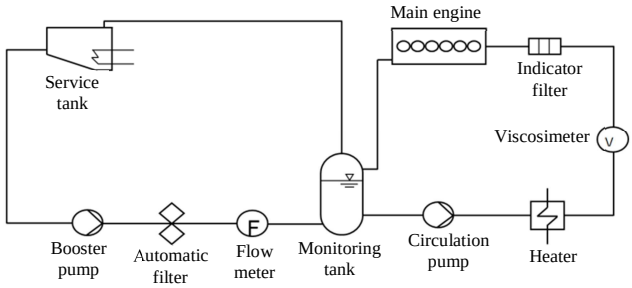

Figure 3. Fuel oil service system (FOSS)

Similarly due to space limitation, short names are also used to represent the actual component names for the FOSS. These short names are as shown in Table I.

TABLE I. COMPONENTS AND THEIR RESPECTIVE SHORT NAMES

Component	**Short Name**
Automatic filter	af
Booster pump	bp
Circulation pump	cp
Flow meter	fm
Heater	ht
Indicator filter	if
Main engine	me
Mixing tank	mt
Service tank	st
Viscosimeter	vm

Table II shows the components that were subjected to expert judgement on PM time. The table also shows the corresponding EPMTs.

TABLE II. COMPONENTS AND EXPERT PM TIMES

Components	Expert PM Time
Main engine	1500
Service tank	1260
Viscosimeter	870

All the components have implementation options; however, those that were subjected to component substitution are shown in Table III.

TABLE III. COMPONENTS, IMPLEMENTATIONS AND SHORT NAMES

Component	Implementations	Short Name
Heater	Heater_1	ht_1
	Heater_2	ht_2
	Heater_3	ht_3
	Heater_4	ht_4
Mixing tank	Mixing_tank_1	mt_1
	Mixing_tank_2	mt_2
	Mixing_tank_3	mt_3
	Mixing_tank_4	mt_4
Flow meter	Flow_meter_1	fm_1
	Flow_meter_2	fm_2
	Flow_meter_3	fm_3
	Flow_meter_4	fm_4
	Flow_meter_5	fm_5

The components which the expert specified as fixed throughout the optimisation are shown in Table IV.

TABLE IV – FIXED COMPONENTS THROUGHOUT THE OPTIMISATION

Component	Short Name
Automatic filter	af
Booster pump	bp
Circulation pump	cp
Indicator filter	if

VI. EVALUATIONS

In order to evaluate the defined PM optimisation on the case study, the evaluation models for the objective functions need to be defined. Similarly the optimisation algorithm that would incorporate the constraints needs to be defined. These definitions are discussed next.

A. Objective Functions Model

The maintenance policy assumed in this paper is perfect preventive maintenance and therefore same evaluation models found in [1] is used. Equation 6 is used to evaluate component reliability where its failure characteristic is assumed to follow the Weibull distribution [1].

$$U_{pc}(t) = 1 - \ exp\left[-n\left(\frac{T_p}{\theta}\right)^{\beta}\right] exp\left[-\left(\frac{t - nT_p}{\theta}\right)^{\beta}\right] \quad (6)$$

$$nT_p \leqslant t \leqslant (n+1)T_p$$

where: U_{pc} is component unavailability under PPM
t is the age of the component
n is the number of PM stages
β is the Weibull shape parameter
θ is the Weibull scale parameter

The system unavailability (U) is evaluated using the Esary-Proschan approximation [12]. The total PM cost of the system is the summation of the individual components' cost as shown in Equation 7.

$$C = \sum_{i}^{m} \left(n_i C_{ppmi} + C_{ci}\right) \quad (7)$$

Where: m is the number of system components
C is the system cost under PPM
C_{ppmi} is the cost of performing PPM for the *i-th* component
C_{ci} is the unit cost of the *i-th* component
n_i is the total number of PM stages for the *i-th* component, n_i is evaluated using Equation 8

The number of PM stages n for each component is evaluated using Equation 8.

$$n = \begin{cases} Q\left(\frac{MTTF}{T_p}\right) & ; \ MTTF \leq RT \\ Q\left(\frac{RT}{T_p}\right) & ; \ MTTF \geq RT \end{cases} \quad (8)$$

Additionally, the following parameter values were assumed.

Weibull shape parameter β = 2
Weibull scale parameter θ = 1500
FOSS shortest PM interval T = 180
Maintenance improvement factor f = 0.875
Maximum optimization generation = 5120

The improvement factor is simply the effectiveness of the maintenance action. The details of which could be found in Nggada et al. [10].

B. Optimisation Algorithm

To optimise the PM schedules of the FOSS, a variant of the Non-dominated Sorting Genetic Algorithm (NSGA) II [13] is developed. It takes into account the defined constraints and objective functions. The mechanics of the adapted algorithm using HiP-HOPS are here discussed. The algorithm first generates a random initial population P of N number of PM individuals, with each individual represented as p. The following steps are then executed:

 ISBN: 978-1-61208-340-7

1. Set population index t = 1.
2. Set front index i = 1.
3. Randomly generate an initial population P_t of N number of PM individuals. This is performed in any of two steps as follows (1) If a given component i qualifies for component substitution, then $\alpha_{i,k_i} = substitute\_component(i, k_i)$, (2) if the component qualifies for expert judgement then $\alpha_{i,k_i} = \alpha_{ie,k_i}$ else $\alpha_{i,k_i} = random(1..\alpha_{imax,k_i})$.
4. $\forall p \in P_t$, configure the variant of the system model with p by using the encoding to set the CoMI of each component and then evaluate the unavailability and cost (objective functions) of the system by calling the automatic fault tree synthesis and analysis functions of HiP-HOPS.
5. $\forall p \in P$, find n_p number of solutions that dominate p, and S_p set of solutions for which p dominates.
6. Add all p with $n_p = 0$ into the set F_i (the i-th front) and assign domination rank R_p = i.
7. For each $p \in F_i$ assign crowding distance to p.
8. Increment front index by 1; i.e. i = i + 1.
9. For each $p \in F_{i-1}$, visit each $q \in S_p$ and decrement n_q by 1, if by doing so, n_q becomes 0 then add q into the set F_i (q belonging to front i, R_q = i).
10. Repeat step 8 to find subsequent fronts.
11. Perform recombination as follows ("a – j" below)
    (a) Set child population $Q_t = \emptyset$.
    (b) Use binary tournament selection to select two parents from population P_t.
    (c) With probability P_c, perform uniform crossover on the selected parents to evolve with a child p.
    (d) With probability P_m, perform mutation in one of the following ways; (1) if the selected locus i corresponds to a component that has been flagged for expert judgement (i.e. $expert\_judgement_i = true$) and $ET_i \geq T$ then exit to step "e" below, else (2) perform normal mutation.
    (e) Add p to Q_t; i.e. $Q_t = Q_t \cup p$.
    (f) If the size of Q_t is not equal to N, then go to step "b".
    (g) $\forall p \in Q_t$, configure the variant of the system model with p. The values of objective functions (unavailability and cost) are also calculated.
    (h) P_t and Q_t are combined into B_t; i.e. $B_t = P_t \cup Q_t$ and B_t is sorted based on non-domination.
    (i) From 2N solutions (combination of P_t and Q_t) in B_t, N best solutions are selected using the crowding calculation and comparison to form P_{t+1}.
    (j) Increment population index by 1; i.e. t = t + 1.
12. If maximum generation is not reached then go to step 4 else terminate giving the set of PM individuals in the first front F_1 as the solution.

C. Results

The Pareto frontier of the optimisation is shown in Fig. 4. A total of 206 optimal PPM schedules were found, with the last found in generation 1722. For the components subjected to substitution Heater_2, Mixing_tank_2 and Flow_meter_3 dominated the optimal solutions. The result indicates that an engineer could choose an optimal design option relative to cost and unavailability requirements. Typically, the optimisation is done manually, which, therefore presents only fewer options.

Table V shows the first and last 5 out of the 206 PPM schedules. It shows that the components Main_engine, Service_tank and Viscosimeter subjected to expert judgement have fixed CoMIs in all the optimal PPM schedules. Similarly none of the alternative options of the components that were not subjected to component substitution appears in the optimal set.

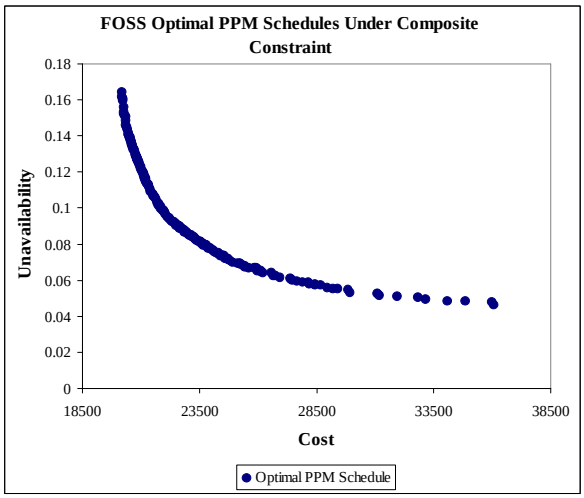

Figure 4. Pareto frontier of FOSS PPM schedules

TABLE V. A SUBSET OF OPTIMAL PPM SCHEDULES; A TABULAR REPRESENTATION

Optimal PPM Schedule	Cost	Unavailability	Generation
af(8) bp(4) cp(6) ft.ft_3(4) ht.ht_2(1) if(3) me(8) mt.mt_2(5) st(7) vm(4)	21866	0.099808	26
af(8) bp(4) cp(6) ft.ft_3(4) ht.ht_2(3) if(3) me(8) mt.mt_2(5) st(7) vm(4)	21746	0.102454	26
af(6) bp(4) cp(6) ft.ft_3(4) ht.ht_2(2) if(3) me(8) mt.mt_2(4) st(7) vm(4)	22217	0.094253	29
af(5) bp(3) cp(6) ft.ft_3(4) ht.ht_2(2) if(3) me(8) mt.mt_2(4) st(7) vm(4)	22678	0.089516	29
af(6) bp(3) cp(6) ft.ft_3(4) ht.ht_2(2) if(3) me(8) mt.mt_2(5) st(7) vm(4)	22237	0.093825	30

 ISBN: 978-1-61208-340-7

af(6) bp(4) cp(6) ft.ft_3(4) ht.ht_2(1) if(3) me(8) mt.mt_2(4) st(7) vm(4)	22307	0.092919	1439
af(1) bp(1) cp(1) ft.ft_3(1) ht.ht_2(1) if(1) me(8) mt.mt_2(2) st(7) vm(4)	34859	0.048226	1453
af(8) bp(4) cp(6) ft.ft_3(4) ht.ht_2(2) if(3) me(8) mt.mt_2(8) st(7) vm(4)	21600	0.105751	1463
af(1) bp(1) cp(1) ft.ft_3(1) ht.ht_2(2) if(1) me(8) mt.mt_2(1) st(7) vm(4)	36001	0.047708	1631
af(8) bp(3) cp(6) ft.ft_3(4) ht.ht_2(2) if(3) me(8) mt.mt_2(5) st(7) vm(4)	21972	0.098662	1722

VII. CONCLUSION AND FUTURE WORK

In the design of engineering systems it is generally helpful to enable systematic and automated exploration of design options using heuristics whilst maintaining the possibility of certain decisions to be taken by informed expert opinion. This paper has illustrated an approach to this in which expert judgement can be integrated in system architecture and maintenance optimisation method where optimisation is driven by dependability and cost. Constraints to represent expert judgement on maintenance time and selection of components were developed and a variant of the NSGA II was adapted within the HiP-HOPS tool to enable the proposed approach. Initial results suggest that the approach is valid and promising. The method is currently being extended to enable more sophisticated ways for incorporating important maintenance constraints related to the geometry and topology of the system.

REFERENCES

[1] S. H. Nggada, Y. I. Papadopoulos, and D. J. Parker, “Combined optimisation of system architecture and maintenance,” 4th IFAC Workshop on Dependable Control of Discrete Systems, 4- 6 September 2013, University of York - UK, IFAC Proceedings Volumes (IFAC-PapersOnline), vol. 4, part 1, pp. 25-30, doi: 10.3182/20130904-3-UK-4041.00026

[2] M. Shafiee, and M. J. Zuo, "Adapting an age-reduction model to extend the useful-life duration," International Conference on Quality, Reliability, Risk, Maintenance, and Safety Engineering (ICQR2MSE), 15-18 June 2012, pp. 1055-1059, doi: 10.1109/ICQR2MSE.2012.6246403

[3] S. H. Nggada, Y. I. Papadopoulos, and D. J. Parker, “Extending HiP-HOPS with capabilities of planning preventative maintenance, in Strategic Advantage of Computing Information Systems in Enterprise Management, M. Sarrafzadeh, Ed, pp. 231-242, ISBN: 978-960-6672-93-4

[4] J. M. van Noortwijk, R. Dekker, R. M. Cooke, and T. A. Mazzuchi, “Expert jugement in maintenance optimization,” IEEE Transactions on Reliability, vol. 41, no. 3, pp. 427-432, 1992

[5] A. Mannhart, A. Bilgic, and B. Bertsche, "Modeling expert judgement for reliability prediction - comparison of methods," Reliability and Maintainability Symposium, RAMS '07, 22-25 January 2007, pp. 1-6, doi: 10.1109/RAMS.2007.328099

[6] T. Rosqvist, “On the use of expert judgement in the qualifcation of risk assessment,” Helsinki University of Technology, PhD Thesis, Finland, 2003.

[7] H. Huang, Z. Tian, and M. J. Zuo, "Intelligent interactive multiobjective optimization method and its application to reliability optimization," IIE Transactions, vol. 37, issue 11, pp. 983-993, 2005

[8] A. Konak, D. W. Coit, and A. E. Smith, "Multi-objective optimization using genetic algorithms: a tutorial," Reliability Engineering and System Safety, vol. 91, issue 9, pp. 992-1007, 2006

[9] M. Gen, and R. Cheng, "Genetic algorithms and engineering design," New York, John Wiley & Sons, 1997

[10] S. H. Nggada, D. J. Parker, and Y. I. Papadopoulos, “Dynamic effect of perfect preventive maintenance on system reliability and cost using HiP-HOPS,” IFAC-MCPL 2010, 5th Conference on Management and Control of Production and Logistics, September 2010, Coimbra – Portugal, IFAC Proceedings Volumes (IFAC-PapersOnline), pp. 204-209, ISSN: 14746670

[11] Y. I. Papadopoulos, and J. A. McDermid, “Hierarchically performed hazard origin and propagation studies,” In: 18th International Conference in Computer Safety, Reliability and Security, Toulouse, France, pp. 139-152, 1999

[12] T. Jin, and D. W. Coit, “Approximating network reliability estimates using linear and quadratic unreliability of minimal cuts,” Reliability Engineering and System Safety, vol. 82, issue 1, pp. 41-48, 2003

[13] K. Deb, A. Pratab, S. Agarwal, and T. Meyarivan, "A Fast and Elitist Multiobjective Genetic Algorithm: NSGA-II," IEEE Transactions on Evolutionary Computation, vol. 6, issue 2, pp. 182-197, 2002

 ISBN: 978-1-61208-340-7

Two Approaches to Implementing Metacognition

Emily Hand*, Darsana Josyula*†, Matthew Paisner*, Elizabeth McNany*, Donald Perlis*, and Michael T. Cox *
*Department of Computer Science
University of Maryland, College Park, College Park, Maryland 20742
†Department of Computer Science
Bowie State University, Bowie, MD 20715
Email: {emhand, darsana, mpaisner, beth, perlis, mcox}@cs.umd.edu

***Abstract*—Metacognition, the ability to monitor and regulate cognition, is important for an agent to adapt to novel situations and fix discrepancies in its knowledge base. In this paper, we discuss two different approaches to implementing metacognition in artificial systems: internally and externally. In the internal approach, metacognition is built into the agent, and thus, is combined with its cognitive reasoning abilities. The same Knowledge Base (KB) is fully shared between the metacognitive and cognitive processes of the artificial system. In the external metacognition approach, only portions of the agent's KB are shared between the agent and the external metacognition. We describe the implementation of external metacognition using our own Metacognitive Loop (MCL2) and internal metacognition using active logic in the context of a dialog agent called Alfred. We discuss how the two systems handle long pauses in dialog and compare the pros and cons of each. Our experiments show that for a system with time-related expectations, it is more efficient to use interleaved metacognition rather than an external metacognition module as the internal metacognition has access to the entire KB of the agent.**

Keywords–Metacognition; Dialog Management.

I. INTRODUCTION

Humans are capable of reasoning about situations and developing expectations about themselves as well as the world around them. They are also able to handle anomalies. Humans can recognize that an expectation has been violated, decide on the best response, and then, implement that response to restore the desired state. Intelligent agents situated in the real world should also have these capabilities. An agent must possess some form of cognitive abilities in order to make decisions. In order to make an agent more intelligent, metacognitive abilities must be added to the system. Metacognition is the ability of an agent to explicitly monitor, evaluate, and improve upon its own internal processes. One approach to providing the agent with the capability to recognize and correct problems is to have the agent maintain some set of expectations about itself and its environment. These expectations would be a part of the metacognition used by the agent in order to properly reason about its situation. There has been some promising work in the fields of Artificial Intelligence and Cognitive Science with metacognition, including [3] and [16].

When faced with anomalies in dialog, humans are able to *note* the anomaly, *assess* the anomaly and determine how to handle it, and finally *guide* a response to resolve the anomaly. This is called the N-A-G cycle [6]. In our previous work, we have found that a N-A-G cycle works quite well in detecting and correcting anomalies in an intelligent agent.

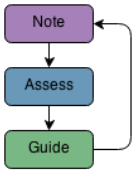

Figure 1. N-A-G Cycle.

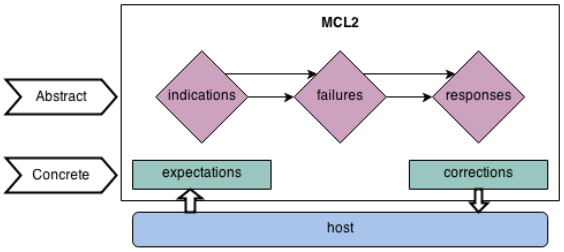

Figure 2. The MCL2 architecture.

We call the algorithm that implements the note-assess-guide-repeat cycle to deal with anomalies as the metacognitive loop (MCL); this basic algorithm is shown in Figure 1. We have developed a domain-independent implementation of MCL, referred to here as MCL2, (Figure 2) which can be used as an external module [5][20]. MCL2 uses three ontologies organized as a Bayes net [5]: *indications* nodes representing different types of expectation violations; *failure* nodes indicating the probable type of problem that is being experienced, and *response* nodes associated with solutions that can be suggested to the host system. Periodically, a system is expected to send its current set of observations to MCL2 using a "monitor" call. If an expectation violation is noted, MCL2 responds with a suggestion of corrective action for the host to implement.

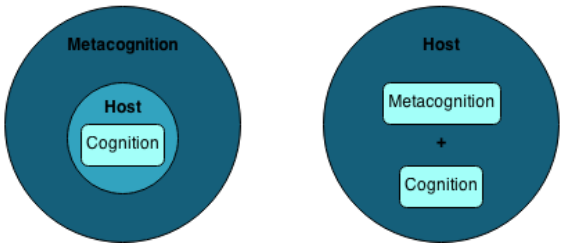

Figure 3. The host system connected to a metacognitive component with only cognitive internal capabilities (left) and the host with full metacognitive and cognitive internal capabilities (right).

 ISBN: 978-1-61208-340-7

In this paper, we will discuss how to incorporate the N-A-G cycle into a cognitive system. Figure 3 shows the two implementations of metacognition. The agent could implement this process internally in conjunction with its regular cognition, allowing it to perform reasoning as well as reasoning about its reasoning. The agent could instead have only cognitive capabilities and be in communication with an external metacognitive module like MCL2. We investigate the two design approaches in detail, and discuss their performance when integrated with a dialog agent Alfred [12][13].

We discuss recent work in dialog agents, as well as metacognition, in Section II. Section III highlights the challenges associated with metacognition in dialog and our agent Alfred. Section IV discusses external metacognition, while Section V describes internal metacognition. Section VI compares the two implementations of metacognition.

II. Related Work

In recent years, there has been a great deal of work in the use of metacognition as a tool for monitoring and regulating cognitive activities including natural language dialog. Monitoring and controlling cognitive activities has been a popular topic, with researchers focusing on explicitly setting time limits for deliberation [10], or limiting the size of current knowledge used for deliberation [18], or both [1][2][17]. Fox and Leake proposed to focus the cognitive activities of an agent by narrowing the knowledge base the agent uses to the subset relevant to the circumstances [9]. They showed that the reduced focus set enables the agent to spend the available deliberation time to produce the optimal action by adapting to the current circumstances. A hybrid approach, where the deliberative process simultaneously produces an immediate action and a strategy, has also been used [8]. Since the action is immediately available, the component of the agent responsible for taking action does not need to wait for the strategy in circumstances that do not permit doing so. This approach implies that the action component is intelligent enough to determine when to wait for a strategy.

McNany et al. [14] discusses metacognition as an integral part of natural language dialog in an artificial agent. The importance of metareasoning has been shown in linguistics. One such example is in [11], where Hymes expresses the idea of communicative competence. This idea was expanded by Canale [7], by detailing four different types of communicative competence. Before the aforementioned work in linguistics, Rieger [19] showed that metareasoning in a natural language dialog can improve deficiencies, and McRoy agreed with this in [15] further stating that in dialog, the ability to handle mistakes is essential. In more recent work on metareasoning in natural language dialog, Anderson and Lee [4] found that a large part of dialog involves metareasoning in order to properly handle misunderstandings, as well as references to previous utterances. Metareasoning and metacognition are a very large part of an intelligent dialog agent.

As metacognition and metareasoning have been identified as essential in an intelligent dialog agent, the next natural question is how to properly integrate these into the agent. Recently, Anderson, Oates, Chong, and Perlis [4] developed a metacognitive system, called MCL, to be used as an external module by an intelligent agent. Continuing with this idea, Schmill et al. [20] extended MCL to use metacognition to reason about and handle anomalies. In our work we extend MCL to handle anomalies in a dialog agent. We adapt MCL to reason about time-related expectations and anomalies and we compare a version of Alfred with internal metacognitive capabilities to Alfred connected with the adapted MCL.

III. Metacognition to Handle Pauses in Dialog

In this paper, we discuss handling expectations and anomalies using metacognition in a dialog system. We believe this to be a good example for testing the two approaches to metacognition because we are dealing with time-related expectations and the work we present here is applicable to any system with time-related expectations, not simply dialog agents. Agents situated in a real-world environment must interact with humans and other agents. These interactions require that the agent has some concept of time, and some expectation for the amount of time certain interactions will require. We discuss these expectations in the context of a dialog agent, but they are generalizeable to any intelligent agent situated in the real world. To motivate our work, let us consider a few examples:

Example 1: Suppose we have two participants in a dialog P_1 and P_2. P_1 says something to P_2 expecting a response. If P_2 leaves the room without responding, a human would understand that something strange was occurring in the conversation. Perhaps P_2 was offended, or simply had to leave. In either case, a human P_1 would recognize the anomaly and not simply sit around waiting for a response. To simulate this behavior, an intelligent dialog agent should have some expectation for the length of conversational pauses associated with a particular user, so that it understands that an anomaly has occurred when P_2 fails to respond in a reasonable time period. Otherwise, it will not understand that there is a problem, and thus, will take no steps to correct it.

Listing 1. Example 1 Dialog in Alfred without Metacognition

```
(t=0) Alfred: "Welcome."
(t=1) ...
...
(t=100) Alfred: "Please tell me what to do now."
(t=101) ...
...
(t=200) Alfred: "Please tell me what to do now."
```

Listing 2. Example 1 Dialog in Alfred with Metacognition

```
(t=0) Alfred: "Welcome."
(t=1) ...
...
(t=100) Alfred: "Are you there?"
(t=101) ...
...
(t=200) Alfred: "Goodbye."
```

Example 2: We have the same dialog participants from Example 1. P_1 says something to P_2 and P_2 is thinking of something to say. While P_2 is thinking, there is a pause in the conversation. Now P_1 does have an expectation of the length of a typical pause, and it notices when the normal pause length has been exceeded. P_1 has an expectation that P_2 will respond within 100 seconds. P_2 is still thinking and 100

 ISBN: 978-1-61208-340-7

seconds pass. P_1 then says "Do you still want to talk?" Now, 101 seconds have passed since P_1 initially started waiting, and P_2 has still not responded. If P_1 does not take into account that it has recently spoken and that P_2 may need more time to respond, then since its expectation has been violated, P_1 would ask again "Do you still want to talk?" This exchange would continue in this way with P_1 continuously asking "Do you still want to talk?" until P_2 responds. An intelligent dialog agent would need to understand that there is a difference between an initial prompt and a prompt issued as a response to an expectation violation. P_1 should understand that when it prompts P_2 that P_2 will need more time to respond.

Listing 3. Example 2 Dialog in Alfred without Metacognition

```
(t=0) Alfred: "Welcome."
(t=1) User: "Send Metroliner to Baltimore."
(t=2) Alfred: "Command sent to domain."
(t=3) Alfred: "Please enter another command."
...
(t=103) Alfred: "Please tell me what to do now."
(t=104) Alfred: "Please tell me what to do now."
(t=105) Alfred: "Please tell me what to do now."
...
```

Listing 4. Example 2 Dialog in Alfred with Metacognition

```
(t=0) Alfred: "Welcome."
(t=1) User: "Send Metroliner to Baltimore."
(t=2) Alfred: "Command sent to domain."
(t=3) Alfred: "Please enter another command."
...
(t=103) Alfred: "Please tell me what to do now."
...
(t=150) User: "Send Northstar to Richmond."
...
```

Example 3: We have the same dialog participants from Example 1. Now, the dialog agent P_1 has an expectation for a typical pause associated with P_2 of 100 seconds. It also understands how to revise its expectations. If P_1 asks P_2 a few questions and for each of the questions, P_2 took longer than P_1 expected to respond, P_1 recognizes a pattern. P_1 realizes that P_2 responds more slowly in general than it had expected and so it revises its expectation, noting that P_2 has a longer typical pause length for conversations.

Listing 5. Example 3 Dialog in Alfred without Metacognition

```
(t=0) Alfred: "Welcome."
(t=1) User: "Send Metroliner to Baltimore."
(t=2) Alfred: "Command sent to domain."
(t=3) Alfred: "Please enter another command."
...
(t=103) Alfred: "Please tell me what to do now."
(t=104) Alfred: "Please tell me what to do now."
...
(t=150) User: "Send Northstar to Richmond."
(t=151) Alfred: "Command sent to domain."
(t=152) Alfred: "Please enter another command."
...
(t=252) Alfred: "Please tell me what to do now."
(t=253) Alfred: "Please tell me what to do now."
...
(t=300) User: "Send Bullet to Washington."
(t=301) Alfred: "Command sent to domain."
(t=302) Alfred: "Please enter another command."
...
(t=402) Alfred: "Please tell me what to do now."
(t=403) Alfred: "Please tell me what to do now."
...
```

Listing 6. Example 3 Dialog in Alfred with Metacognition

```
(t=0) Alfred: "Welcome."
(t=1) User: "Send Metroliner to Baltimore."
(t=2) Alfred: "Command sent to domain."
(t=3) Alfred: "Please enter another command."
...
(t=103) Alfred: "Please tell me what to do now."
...
(t=150) User: "Send Northstar to Richmond."
(t=151) Alfred: "Command sent to domain."
(t=152) Alfred: "Please enter another command."
...
(t=252) Alfred: "Please tell me what to do now."
...
(t=300) User: "Send Bullet to Washington."
(t=301) Alfred: "Command sent to domain."
(t=302) Alfred: "Please enter another command."
...
(t=450) User: "Send Metroliner to Buffalo."
```

We implemented our two metacognition techniques using a particular dialog agent, Alfred. Alfred acts as an interface between a human user and a task-oriented domain. As input, it accepts English sentences which it then parses and takes as commands to be sent to a specific domain. We consider the problem of Alfred encountering conversational pauses of varying length when interacting with a human user. Alfred has expectations about the typical pause length associated with a particular user, and is able to detect when an expectation has been violated.

We have implemented a version of Alfred which uses metacognition to handle situations similar to the three examples above. We are presently focused on Alfred's expectations concerning interaction with the human user.

We will focus on the implementation of the two systems with Alfred, but much of the following discussion is applicable to any host system. In our implementation of internal metacognition, we combine the cognitive and metacognitive capabilities, creating an interleaved cognitive and metacognitive reasoning within Alfred. For our external implementation of metacognition, we used our MCL2, which Alfred communicates with through monitor calls.

IV. External Metacognition using MCL2

First, we will discuss the architecture where the host is connected to an external metacognitive system. In this architecture, the host initially gives the metacognitive system its set of expectations. The metacognitive system then determines (via observations also provided by the host) when expectations have been violated and recommends how the host should respond to such violations.

One important design problem in this architecture involves knowledge sharing. Initially, the host sends its expectations to the metacognitive system, and the host must also send updates about the current state of the world in order for it to reason about possible violations. A key question arises: how often should the host system send information to the metacognitive system? As the host sends more information, there is more overhead incurred in sending information between the host and the metacognitive component.

We have a particular implemented metacognitive module called MCL2. MCL2 is capable of accepting expectations

 ISBN: 978-1-61208-340-7

and information about the current state of the world from a host, reasoning about expectations, and sending suggestions to the host when it notes an expectation violation. The host communicates with MCL2 through monitor calls in which it shares information about particular sensor readings. The host can perform monitor calls at any time; there is no specified frequency of monitor calls from the host.

In our implementation, Alfred provides MCL2 with an expectation for a typical pause length, *expected_pause(100)*; at each step, Alfred increments its current waiting time, *curr_wait_time(t)*, and sends this information to MCL2. When the current waiting time exceeds the expected pause length (*curr_wait_time(101)*), MCL2 notes that an expectation has been violated and provides the host with a suggestion as to how to respond. Currently, MCL2's suggestion is for the host to prompt the user, so Alfred then prompts the user with "Please tell me what to do now." Since Alfred is sending information to MCL2 at every time step, Alfred now sends the current wait time (*curr_wait_time(102)*) to MCL2. MCL2 only keeps track of the expectation and the current information being sent to it by the host. It receives *curr_wait_time(102)* from Alfred and treats it as a new expectation violation so MCL2 again sends a suggestion to prompt the user. This happens at every time step until the user enters a command to Alfred, at which time Alfred would reset its wait time (assert *curr_wait_time(0)*) and send that to MCL2. This is not the desired behavior of an intelligent agent. When a user is prompted, the system should give the user time to respond to the prompt before prompting again. Therefore, MCL2 needs to maintain another expectation for an appropriate response time associated with a prompt (*expected_response_time(100)*).

Another design problem which is even more complicated is that of deciding what exactly it means to implement a suggestion given to the host by the metacognitive system. In the case of MCL2 and Alfred, when MCL2 sends the suggestion to Alfred that it should prompt the user, MCL2 expects a response from Alfred indicating if the suggestion was a success or a failure. However, this does not make sense in the context of time-related expectations. If MCL2 tells Alfred to prompt the user, and Alfred does so, then MCL2's suggestion has been implemented, but both MCL2 and Alfred must wait in order to see if the suggestion was a failure or a success, that is, if the effect occurs. The suggestion is a failure if after the prompt, the user does not respond within the *expected_response_time* and it is a success if the user responds within that amount of time. However, is this truly a failure if the user simply takes longer to respond than expected? After all, if the user responds at step 102, the *expected_response_time* has been exceeded, but the prompting was successful.

In order to handle Examples 1-3 when connecting Alfred with MCL2, we used two expectations: *in_set(sensor_pause_id, num_pause_violations, 0, 1, 2, 3)*, and *discrete_range(sensor_pause_id, pause_length, 0, 100, add(1))*. The first expectation states that the value for *num_pause_violations* can only be 0, 1, 2, or 3. If it is any other value, there is a violation. The second expectation says that the value for *pause_length* must be between 0 and 100 in increments of 1. The value of *num_pause_violations* is incremented for each user input which required a prompt. If Alfred starts up and the user walks away, Alfred will prompt the user at step 101, and again at step 202, and so on. If we consider each one of these a violation; then, at step 404, Alfred would change its expectation. There is no need for Alfred to change its expectation if there is no user there. So, we do not consider repeated prompts for the same user input to be separate violations. If a user requires two prompts before a response, then that would be one violation and *num_pause_violations* would be incremented by one. On the fourth violation of the expectation for *pause_length*, the expectation for *num_pause_violations* is violated. When this expectation is violated, it means that Alfred has been repeatedly noticing the same expectation violation and the most probable source of the problem is a model error, so the expectation must be revised. This system of two expectations works well because it accounts for user error. If a user walks away, Alfred will not change its expectation, and if a user is distracted in some way and takes a long time to respond to one prompt, but from then on continues responding in a reasonable amount of time, Alfred will not change its expectation. This is generally a good idea as an agent should not change its expectation based off of one violation. More information is needed in order to determine if there is an internal or external error occurring.

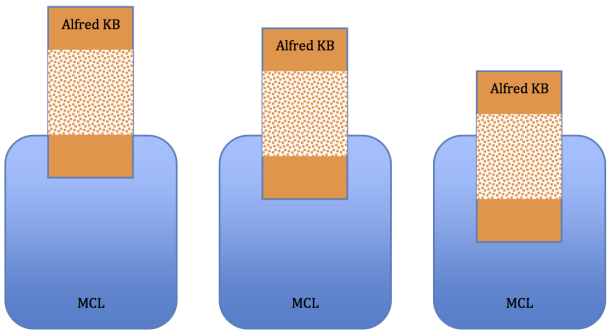

Figure 4. Amount of knowledge being shared between Alfred and MCL2 in Examples 1-3 from left to right.

This implementation of Alfred with MCL2 is fully functioning with the pause time example. However, Alfred is doing most of the reasoning. Alfred is keeping track of the current waiting time, as well as the number of pause violations, and sending all of this information to MCL2 at each time step. In this framework, MCL2 is doing very little to add to the overall system, and it is not doing anything Alfred, or any similar host, could not do itself. The design problem of knowledge sharing becomes very complex when connecting a host system with an external metacognitive module. External metacognition requires that the host decide what to share with the external component and when to share it. Figure 4 shows the knowledge sharing between Alfred and MCL2 in Examples 1 through 3 discussed earlier. The figure shows Alfred's KB overlapping with MCL as the portion which is being shared. The orange portion of Alfred's KB that is overlapping with MCL is the general knowledge the Alfred shares with MCL, which is not related to pause time. The orange dotted portion of Alfred's KB is Alfred's knowledge about pause time. In Example 1, there is no overlap between the orange part of Alfred's KB and MCL. In the second example, Alfred sends some of its KB concerning pause time to MCL2 and in the

 ISBN: 978-1-61208-340-7

final example even more of the pause time knowledge is shared with MCL2.

As implemented, MCL2 requires the host to periodically send a subset of its observations using monitor calls. Thus, whether an expectation violation gets noted in a timely manner depends on whether the appropriate observations are being sent to MCL2 and the frequency at which the host issues monitor calls. If the host shares very little information with MCL2, such as in Alfred's pause time example, then flaws in the host's initial knowledge base cannot be found or corrected by MCL2. For these reasons, we decided to focus on designing and implementing the second framework (Figure 3), where the host has cognitive and metacognitive internal capabilities.

V. Interleaved Metacognition using Active Logic

In this version, Alfred has full metacognitive and cognitive abilities, including expectations about itself and the world in which it is situated. Alfred has expectations that the user will respond to a prompt, that a user will respond with a certain type of answer, and that the user will respond within a specified amount of time. Alfred's expectations for interleaved metacognition are similar to those when connected with MCL2. It has an expectation for user pause length (or when it should receive user input), and an expectation for an appropriate number of violations before revising its expectation.

Alfred's expectations concerning the amount of time associated with a particular result are represented as time intervals, because Alfred expects a user response between two time steps. Initially, Alfred has the expectation of user input within 100 steps, represented in a predicate in its knowledge base as *in_set(pause_sensor_id, user_input, 0, 100, add(1))*. The predicate specifies the start and end points of the interval in which the user should respond. If the current time step exceeds the endpoint of the expected pause interval, Alfred notes that its expectation has been violated. When Alfred's expectation is violated, it prompts the user with "Please tell me what to do now." This is Alfred taking action to fix the expectation violation, but the violation will not be fixed until the user responds to Alfred's prompt. When Alfred prompts, it must wait for user input, so now the expectation is *in_set(pause_sensor_id, user_input, 100, 200, add(1))*, giving the user another 100 steps to respond to the prompt.

Alfred also has expectations about its expectation violations which look like *in_set(sensor_pause_id, num_pause_violations, 0, 1, 2, 3)*, exactly the same as with MCL2. Each time a violation of the expectation associated with *user_input* is violated, then the property *num_pause_violations* is increased. Once *num_pause_violations* reaches a value greater than 3, the expectation is violated, and Alfred knows that it needs to revise its expectation for the property *user_input* so that it can more effectively communicate with the human user.

Interleaved metacognition has lesser communication overhead than external, as all knowledge is shared between the cognitive and metacognitive components. With all information being shared, all expectations can be monitored properly and all expectation violations can be detected. Interleaved metacognition is implemented in time-tracking Active Logic [5], so the metacognition and cognition processes proceed in parallel, step-by-step. In Active Logic, a step is the fundamental measure of time passage. Since both the cognition and metacognition are being processed internally, the same concept of a step is shared by both, and therefore new observations are handled at the same time by both the metacognition and cognition processes.

VI. Comparing Interleaved and MCL2

Consider a more general situation in which we either have interleaved metacognition or MCL2, where we are no longer just considering the pause time example. If in the case of MCL2, say we have a host with three sensors and it is sharing 60% of its initial belief set with the external module. If there is one anomaly detected, the knowledge being shared by the host is the same as prior to the anomaly. If there are several anomalies, the percentage of knowledge being shared is the same. This is counter-intuitive and not necessarily the behavior that we want from the connection between the host and an external metacognitive module. If an anomaly occurs, the host should share more information with MCL2 in order for MCL2 to better correct the problem. Another problem is even if there are anomalies not detected by MCL2 - because they are a part of the 40% not being shared - the amount of knowledge sharing remains the same. Therefore, these anomalies can never be corrected, and this, in principle, is against the entire point of the metacognitive component. In order for the metacognitive process to be effective, the host must be able to share any part of its KB with it, so that all anomalies can be detected and corrected appropriately. Interleaved metacognition provides just that very easily. The metacognitive external module, MCL2, however, is limited by its reliance on the host to share the required parts of its KB in a timely manner.

Figure 5 shows different scenarios of knowledge sharing for external metacognition. The shaded region is the portion of the knowledge base that is being shared with the external module for each scenario. The 10th scenario shares 100% of the KB, making it equivalent to interleaved metacognition. Only the violations that occur in the shaded area of the KB will be noticed when using an external module. Any violations that occur in the KB above the shaded area will go unnoticed with external metacognition.

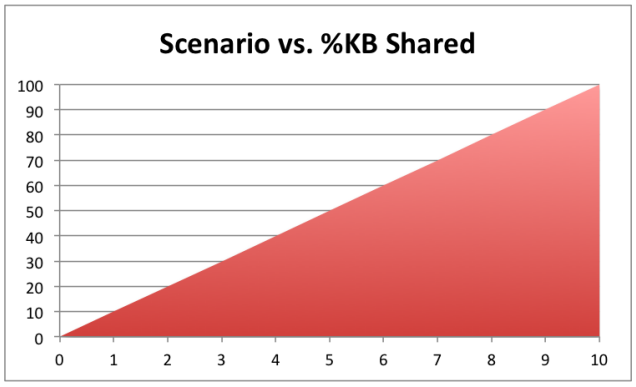

Figure 5. Different knowledge sharing scenarios vs the amount of knowledge being shared.

We note that the effectiveness of MCL2 is also dependent on the frequency of "monitor" calls. Going back to the pause

 ISBN: 978-1-61208-340-7

time example, if Alfred only sent updates to MCL2 every 100 timesteps, MCL2 would only have available that information about the user's response. If Alfred had the expectation of a response within 100 timesteps, and the user consistently responded late, MCL2 would be unable to tell the difference between a 1-timestep delays and 99-timestep delays. Interleaved MCL does not have a dependency on the host to specify when to process information, and so can note and act upon any anomalies without waiting for a host to signal. We are currently working on an improved version of MCL2 that does not have these constraints.

One significant benefit to using external MCL with MCL2 is that the external metacognitive component does not need to be rewritten for each host system. MCL2 can be connected to any host system. Internal metacognition requires that the metacognitive portion be rewritten for each host system, which is quite a bit of work. The entire N-A-G cycle must be rewritten inside of the host system; but, with MCL2, it can just be interfaced with the host system with very few changes being made to the host system.

VII. Conclusion and Future Work

In our research, we have found that an interleaved implementation of metacognition is much more useful than an external connection with MCL2. An external connection requires that a large amount of information be shared between the host and the metacognitive module in order for external metacognition to work properly with our current implementation of MCL2. However, if the host must communicate to the external metacognitive component a large portion of its knowledge base, then there seems to be little to no advantage to using an external metacognitive component like MCL2. A host-initiated data sharing model like MCL 2, causes significant overhead for timely sharing of information by the host to MCL. Instead, the host could easily perform metacognition interleaved with the cognition and not waste time and space with external metacognition. An external metacognitive module could be useful if the host only needed to share a small amount of information with it, but in this case, flaws in the hosts initial knowledge base (unshared) could not be exposed with that limited metacognition, as that information is not being shared with the external module. Another option would be to have a KB that is completely shared between the metacognitive component and the host without the host initiating the sharing. An agent with internal metacognitive capabilities allows for 100% knowledge sharing and therefore the ability of the agent to detect all expectation violations.

Acknowledgment

This material is based upon work supported by ONR Grant # N00014-12-1-0430.

References

[1] N. Alechina, B. Logan, H. N. Nguyen, and A. Rakib, "Logic for coalitions with bounded resources," Journal of Logic and Computation, 2009, vol. 21, no. 6, pp. 907-937.

[2] G. Alexander, A. Raja, and D. Musliner, "Controlling Deliberation in a Markov Decision Process-Based Agent," in Proceedings of the 7th International Conference on Autonomous Agents and Multiagent Systems (AAMAS 2008), Estoril, Portugal, 2008, pp. 461-468.

[3] G. Alexander, A. Raja, E. Durfee, and D. Musliner, "Design Paradigms for Meta-Control in Multiagent Systems," Proceedings of AAMAS 2007 Workshop on Metareasoning in Agent-based Systems, 2007, pp. 92-103.

[4] M. Anderson and B. Lee, "Metalanguage for Dialog Management," in 16th Annual Winter Conference on Discourse, Text and Cognition, 2005.

[5] M. Anderson, T. Oates, W. Chong, and D. Perlis, "The metacognitive loop I: Enhancing reinforcement learning with metacognitive monitoring and control for improved perturbation tolerance," Journal of Experimental and Theoretical Artificial Intelligence, vol. 18, no. 3, 2006, pp. 387-411.

[6] M. Anderson and D. Perlis, "Logic, self-awareness and self-improvement: The metacognitive loop and the problem of brittleness," Journal of Logic and Computation, vol. 15, no. 1, 2005, pp. 21-40.

[7] M. Canale, "From Communicative Competence to Communicative Language Pedagogy," in Language and Communication, J. Richards and R. Schmidt, Ed., New York: Longman, 1983, pp. 2-27.

[8] F. Dylla, A. Ferrein, E. Ferrein, and G. Lakemeyer, "Acting and Deliberating using Golog in Robotic Soccer - A Hybrid Architecture," in Proceedings of the 3rd International Cognitive Robotics Workshop (CogRob 2002), Edmonton, Alberta, Canada, 2002.

[9] S. Fox and D. Leake, "Using Interospective Reasoning to Refine Indexing," in Proceedings of the Fourteenth International Joint Conference on Artificial Intelligence, Montreal, Quebec, Canada, 1995, pp. 391-397.

[10] E. A. Hansen and S. Zilberstein, "Monitoring and control of anytime algorithms:A dynamic programming approach," Artificial Intelligence, 2001, vol. 126, no. 1-2, pp. 139-157.

[11] D. Hymes, "On Communicative Competence," in Sociolinguistics: Selected Readings, J. B. Pride and J. Holmes, Ed., Harmondsworth: Penguin Books, 1972, pp. 269-293.

[12] D. Josyula, "A Unified Theory of Acting and Agency for a Universal Interfacing Agent," Ph.D. dissertation, University of Maryland, College Park, 2005.

[13] D. P. Josyula, S. Fults, M. L. Anderson, S. Wilson, and D. Perlis, Application of MCL in a Dialog Agent, in Papers from the Third Language and Technology Conference, 2007.

[14] E. McNany, D. Josyula, M. T. Cox, M. Paisner, and D. Perlis, "Metacognitive Guidance in a Dialog Agent," The Fifth International Conference on Advanced Cognitive Technologies and Applications, IARIA, 2013, pp. 137-140.

[15] S. McRoy, "Abductive Interpretation and Reinterpretation of Natural Language Utterances," Ph.D. dissertation, University of Toronto, 1993.

[16] A. Nuxoll and J. Laird, "Enhancing intelligent agents with episodic memory," Cognitive Systems Research, 2012, pp. 17-18, 3448.

[17] A. Raja and V. Lesser, "A Framework for Meta-level Control in Multi-Agent Systems," Autonomous Agents and Multi-Agent Systems, 2007, vol. 15, no. 2, pp. 147-196.

[18] U. Ramamurthy and S. Franklin, "Memory Systems for Cognitive Agents," in Proceedings of the Symposium on Human Memory for Artificial Agents, AISB'11 Convention, York, United Kingdom, 2011, pp. 35-40.

[19] C. Rieger, "Conceptual Memory: A Theory and Computer Program for Processing the Meaning Content of Natural Language Utterances," Ph.D. dissertation, Stanford University, 1974.

[20] M. Schmill, M. T. Cox, and A. Raja, "The Metacognitive Loop and Reasoning about Anomalies," in Metareasoning: Thinking about Thinking, Cambridge, MA: MIT Press, 2011, pp. 183-198.

 ISBN: 978-1-61208-340-7

Recognition of Unspoken Words Using Electrode Electroencephalograhic Signals

May Salama, Loa'ay ElSherif, Haytham Lashin, Tarek Gamal
Computer Engineering Dept.
Faculty of Engineering at Shoubra, Benha University
108 Shoubra St. Cairo, Egypt
emails: {msalama@megacom-int.com, thefieryarroow@hotmail.com, haytham.lashin@yahoo.com, tarek_egypte@yahoo.com}

***Abstract*—In this paper, the use of electroencephalograhic signals in recognizing unspoken speech is investigated. The aim of the work is to recognize two words, namely, Yes and No by using a single electrode electroencephalograhic device. Yes and No were selected based on the fact that they are the basic answers of any disabled person. The single electrode device was chosen because of its ease of setup, adjustment, and light weight; hence, most suitable also for disabled. Several neural networks were trained with 7 subjects. Online and offline testing were carried out on male and female subjects in semi quiet environment. Average recognition results reached were 57% for online testing and 59% offline, whereas maximum value for offline was 68% and online 90%. The novelty of the work is using a single electrode device, as all previous work was done on multi-electrode devices.**

Keywords-electroencephalograhic signal; unspoken speech; recognition.

I. INTRODUCTION

Brain computer interface (BCI) is a communication between a person and a computer without physical movement. A signal emitted from the brain is measured, processed and interpreted into action on the computer. An electroencephalograhic (EEG) device records electrical signals from the brain using single or multiple electrodes. According to Graimann et al. [1], a BCI must have four components: 1- record activity directly from the brain, 2- must provide feedback to the user, 3- must do that in real time, 4- the user must choose to perform a mental task whenever a goal is needed to be achieved.

Recognizing unspoken speech is getting more attention due to its importance in many fields. One field is verbal disability of some people, while another is security field, where it is unsafe to speak in the presence of others. There are two approaches concerning recognition of unspoken speech; words and blocks (syllables). Wester and Shultz [2] implemented a system to recognize unspoken speech in five modalities using 20 electrode EEG device. The system used the blocks approach, as well as words approach. In continuation to Wester's work, Wester and Schultz [2] and Calliess [3] showed that the block wise presentation produced better results. He reached a 15.5% better than random guess, a best of 87.3%. Calliess [3] also raised the question whether the results of Wester and Schultz [2] were due to temporal brain artifacts. Two hypotheses were investigated by Porbadnigk [4]. First, Silent speech can be recognized based on EEG signals. Second, unspoken speech cannot be recognized based on EEG signals and that the good results reached by Wester and Schultz [2] were due to the temporal patterns that were recognized. The conclusion was that "It could be shown that except for the block mode which yielded an average recognition rate of 45.50%, all other modes had recognition rates at chance level". This was justified by the fact that block data would contain less noise and that the block mode made it easier to think about words in a consistent way. It was also concluded from work of Porbadnigk [4], that temporal artifacts are superimposed over the signal under investigation in block mode.

Some studies conducted by Wester and Schultz [2], Calliess [3], and Porbadnigk [4] were done in 2009, where a 16 channel EEG channels using 128 cap montage was used to recognize 5 words. Porbadnigk et al. [5] showed that the block mode yielded an average recognition rate of 45.5% and it dropped to chance level for other modes.

A research for recognizing unspoken 5 words using 21 subjects was carried out by Torres-García et al. [6]. These subsets were used to train four classifiers: Naïve Bayes (NB), Random Forests (RF), support vector machine (SVM), and Bagging-RF. The accuracy rates were above 20%.

The paper is organized in seven sections. After the introduction, overview of the system is presented in Section II. Section III shows feature extraction methods. Section IV discusses classification methods applied, while Sections V and VI investigate the testing results and their validation. Section VII concludes the paper and the future work.

II. SYSTEM OVERVIEW

A. Scope and limitations

The scope of words to be recognized is 2 arabic words "Yes" and "No" using the single electrode Neurosky Mindwave Mobile headset [7] to acquire brain signals. The device consists of a headset, an ear-clip, and a sensor arm. The headset's reference and ground electrodes are on the ear clip and the EEG electrode is on the sensor arm, resting on the forehead above the eye. It safely measures and outputs the EEG power spectrums (Alpha waves, Beta waves, Theta waves, Delta waves), NeuroSkyeSense meters (attention and mediation) and eye blinks. The headset is rated at 60 Hz. Neurosky device has been selected for our experiments because of its affordable price and its light weight that enables the user to wear it for a long time although it has

 ISBN: 978-1-61208-340-7

only one delectrode which limits the features carried in the data acquired.

B. Dataset collection

Data were collected from many subjects. During the course of work, it was proven that training with seven subjects was enough for the objective. Accordingly, brain signals of seven subjects have been recorded in a quiet room to prevent any possible distractions. A reading session consists of 14 readings for one subject, each reading 14 seconds recording of EEG signals. The subject closes his eyes to prevent eye-blink artifacts. Moreover, the subject should not move any muscle to prevent muscle artifacts. The readings are further used to train different classifiers.

C. Recording Setup

Subjects were all Egyptians whose mother tongue is Arabic. They were not under any medication and had no diseases. Their ages were between 22 and 23. Each subject was presented to 14 "Yes" questions and 14 "No" questions.

The subject sits on a chair in a quiet room and wears the headset that is connected with the laptop via Bluetooth.

The subject is asked a Y/N question. He presses the "start button".

The subject starts to think of the answer, while the recording is processing for 14 seconds.

The Neurosky support development kit (SDK) drops the data recorded on the first two seconds and the last two seconds to ensure subject's concentration.

III. FEATURE EXTRACTION

The NeuroSky SDK offers the values of low Alpha, high Alpha, low Beta, high Beta, Delta, Gamma and Theta waves. It gives a single value for each wave every one second. Alpha and Beta waves are more related to mental activities and thinking. Low alpha, high alpha, low beta and high beta were selected to be the classifying features. Delta waves were discarded because they only appear in baby brain waves, Gamma waves were discarded because they appear during recognizing object or sound tasks, and Theta also were discarded, as they only appear in young children or during idle tasks. The minimum, maximum and average values for each of the 4 considered waves were calculated giving a feature vector of 12 values for each sample. Ten samples were acquired.

The NeuroSky SDK also offers the value of Raw EEG data acquired, with a sampling rate of 512 Hz. Based on the work of Ting et al. [8], wavelet packet decomposition was applied to get 6-level decomposition tree using the Sym8 wavelet, and the first 6 nodes from level 6, which have the respective frequency bands (0-8, 8-16, 16-24, 24-32, 32-40, 40-48) Hz were selected. The average coefficient and the band energy for each node were calculated which gives a feature vector of 12 values for each sample. The next phase is to input the vectors to the classifiers.

IV. CLASSIFICATION

Four classifiers and ensemble network were used:

1) Support Vector Machine (SVM)

Matlab function svmtrain was chosen with a variety of kernel functions: linear, Quadratic, RBF with sigma values 0.2, 0.4, 0.6, 0.8, 1 and Polynomial. Matlab code, e.g.,

```
struct = svmtrain(train , target_train , 'kernel', 'rbf', 'rbf_sigma', 0.2);
output = svmclassify(struct , test2);
```

With SVM, as the number of classes increases, the prediction time increases significantly. Also, with large classes, the training time increases significantly.

2) Discriminant Analysis (DA)

It was shown by Shashua [9], that the decision hyper planes for binary classification obtained by SVMs is equivalent to the solution obtained by Fisher's linear discriminant on the set of support vectors. It was also shown by Gallinari et al. [10], that the neural networks classifiers are equivalent to DA. That justifies using DA algorithm for classification of our work. Both linear and quadratic functions were used for classification.

3) Self-Organizing Map (SOM)

An enhancement step was added to the SOM architecture: First, data are classified into the maximum number of clusters (unsupervised). Second, these clusters are mapped in a supervised mode into one of 2 clusters based on majority concept.

4) Feed Forward Back-propagation (FFBP)

Various multi layer networks were used, each with different layer-neuron combinations. This was done by trial and error starting with single layer-5 neuron network ending with 156 networks combinations.

5) Ensemble network

Ensemble networks or combining multiple classifiers aim to reduce generalization error and to improve the classification performance over individual classifiers, as has been presented by Avnimelech and Intrator [11], Hansen and Salamon [12], Hashem and Schmeiser [13], and Sharkey [14]. Two types of combinational networks were tested. Each used the same classifiers as above: DA, SOM and SVM. The 2 types are: 1- Two-stage network with the combinations SOM→DA, SOM→SOM, SOM→SVM. It means that the output of SOM is fed as input for DA, SOM and SVM networks, respectively 2- Voting network composed of SOM, DA and SVM, where simple majority voting was applied on the outputs of the classifiers.

V. TESTING AND RESULTS

Data collected are placed in 12 files. Each file's data are arranged in one of two ways: Firstly, Random arrangement, where "Yes" and "No" are scattered in a random way in the file. This type of files will be named "randomly arranged file". Secondly, Sequence arrangement, where "Yes" is placed before "No" or vice versa. This type of files will be named "sequentially arranged file'. Testing was carried out in 2 modes: 1- Offline mode: separating data acquisition and classification phases into two groups. One group is for

 ISBN: 978-1-61208-340-7

classification and the other group is used for testing. Signals used in offline were primarily concerned with the 7 subjects and the conditions mentioned in the earlier section. 2- Online mode: based on prior training of the network, new data signals from various subjects are examined for classification. Signals used covered different subjects to validate the work done. Subjects participating in testing were of different genders and ages. Experiment conditions also varied, where it involved quiet, as well as noisy environment, and eyes open also. Classifiers were applied to raw data, as well as Alpha and Beta signals.

A. *Offline testing with Raw Data*

The following are the hit rates achieved when using raw data with different classifiers. The charts show the result for sample tested files, while the Tables show the min, max and average values. The testing was carried with 60%-40% train-test ratios based on different trials' results.

1) *DA classifier*

DA classifier is not affected by the data arrangement, so, results from random files are the same as sequential files. Figure 1 shows the average hit rates for 6 files with various random data arrangements using linear and quadratic functions. For two files, both functions gave equal results. Linear function was better in 3 files, while quadratic was better in one. So, it could be concluded that linear function gave on average better results. Table I shows the min, max and average values for DA classifier.

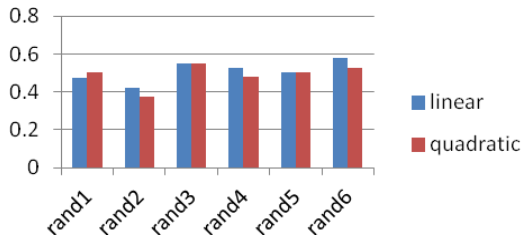

Figure 1. Hit rates for DA classifier

TABLE I. MIN, MAX AND AVERAGE VALUES FOR DA CLASSIFIER

Min value	Max value	Average value
0.3717	0.5769	0.49843

2) *SOM classifier*

A modification was done on regular SOM network as follows: 1- samples are first classified into the largest possible number of clusters, n. Starting with n= 2, then increasing the number of clusters until classification remains the same in two successive iterations. 2- the n clusters are remapped to two clusters with majority rule, i.e., classes with "Yes" samples greater than "No" are mapped to "Yes" cluster and the same for "No". A fragment code is shown in figure 2.

```
// train phase.  Constructor with rate 0.7
        Som = new SOMCSharp(0.7)
// preparing the input
        Som.prepare_C(train, test);
// start is training main method. It takes learning rate and continues to repeat training until stable conditions.
// we start with level=1 i.e., 2 clusters
// check for stability conditions applied, if "Yes stop training
// else increase level (number of clusters)
        Som.start(0.7);
// start method calls leveltrain() method which starts the weights with a fixed value of 0.5 and update weights in train() method according to distances
    // test phase where test() method computes hit rate
    int SOMout = Som.test_C(data);
```

Figure 2. Fragment code showing flow of instructions

Figure 3 shows the average hit rates for 6 files, with various data arrangements and various sigma, using SOM classifier. The tests show that for sigma= 0.5, 0.7, 0.9, the best results are obtained, except for one file. Table II shows the min, max and average values achieved.

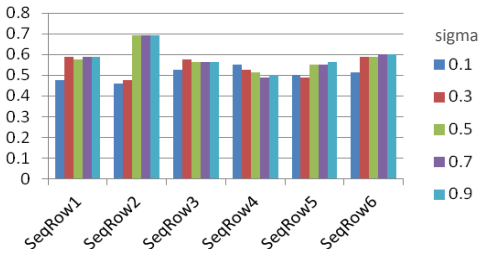

Figure 3. Hit rates for SOM classifer.

TABLE II. MIN, MAX AND AVERAGE VALUES FOR SOM CLASSIFIER

Min	Max	Average
0.4615	0.6923	0.55854

3) *SVM classifier*

Matlab was used to test and train networks. SVM classifier experienced no changes when the arrangement of data changed from random to sequential. Figure 4 shows the values with different mapping functions and permutations (P1-P6).

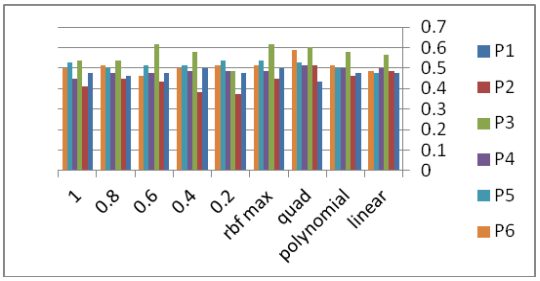

Figure 4. Hit rates for SVM classifier.

 ISBN: 978-1-61208-340-7

Table III shows the min, max and average values for SVM classifier.

TABLE III. MIN, MAX AND AVERAGE VALUES FOR SVM CLASSIFIER

Min value	Max value	Average value
0.3718	0.6154	0.4962

4) FFBP

Different networks have been tried starting from 1 layer/5 neurons, 1 layer/10 neurons, 2 layers/5 neurons, 2 layers/10 neurons, 3 layers/ 5 neuron and 10 neurons reaching 156 combinations. Also various training functions like trainbr, trainbfg, traincgb were applied. In all the combinations, the best result achieved was way far from the other networks. It was concluded that FFBP network results should not be listed.

B. Offline testing with Alpha and Beta signals

The same percentage of train-test data was used; 60%-40% with the same classifiers but using the Alpha and Beta signals. Results are as follows:

TABLE IV. OFFLINE RESULTS WITH ALPHA AND BETA SIGNLS

Network	Min value	Max value	Average value
DA	0.5147	0.641	0.448
SOM	0.4744	0.6795	0.5599
SVM	0.4231	0.641	0.5531

Comparing results in Table IV and in Tables I-III, we conclude that the best average offline results were obtained from SOM networks with Raw data and with Alpha and Beta signals. It proves that the modification done on the network enhanced the performance with offline testing. Average efficiencies were 55.8 and 55.9%. Maximum values were 69 and 67.9%.

Ensemble networks were also tested and the results are presented below.

1) Ensemble Networks

Alpha and Beta signals were used in offline testing with Ensemble networks. In the ensemble multistage network, the first network was always SOM based on the results shown in Table IV. Slightly better average result was achieved, 0.5666.

For the voting system that comprised of DA network, SVM network, and SOM network and based on majority function, average result further improved to reach 0.5933. The improvement in both cases was on the expense of time. Results are shown in Table V.

Accordingly, for offline recognition of unspoken two words, the most suitable network is a Voting system with simple majority function applied on Alpha and Beta signals. The Voting network comprises DA, SVM, and SOM.

TABLE V. ENSEMBLE NETWORKS' RESULTS

Network	Min value	Max value	Average value
SOM → DA	0.42	0.5512	0.4902
SOM →SOM	0.6538	0.4487	0.5516
SOM →SVM	0.4261	0.6391	0.5666
VOTING system	0.551	0.6667	0.5933

C. Online testing

Online testing was carried out using the DA, SVM, SOM and Voting networks on male and female subjects of age groups 19-23 years to identify the network that gives the best result. The testing environment was a college hall with open windows and open door having 40-60 students. Table VI shows the average efficiencies for this testing.

TABLE VI. AVERAGE ONLINE EFFICIENCIES

Network	Efficiency
DA	0.485
SVM	0.60
SOM	0.49
VOTING	0.51

It could be seen that DA, SOM and Voting gave nearly equal results, while SVM gave a remarkably better result. Further online testing in the same environment was carried out using SVM to find average result. Table VII shows the results.

TABLE VII. ONLINE TESTING WITH SVM ON MALE/FEMALE SUBJECTS

Male/Female	No of Subjects	Min value	Max value	Average value
Male	17	0.3	0.9	0.564
Female	10	0.3	0.8	0.57

The average efficiency is less than that attained by offline. This is an expected result, although the maximum value reached in online testing is much higher.

1) Random subjects

The online system was further tested in a two day exhibition (Egyptian Engineering Day) with 60-80 subjects per day. Subjects were males and females visitors between 19-23 years old. They stopped randomly to try the system. The recording environment was the exhibition booth, while asking the people around to stay quiet, as there was enough noise from the surroundings. The result was 56.7%.

 ISBN: 978-1-61208-340-7

VI. VALIDATION

Our target was to help disabled young children to communicate. Children need basically "Yes" and "No" words to interact. The device used in this work is light weight with only 1 electrode. The electrode is put directly on the forehead. Signal transfer is done via Bluetooth. It is very suitable for disabled adults also, as in case mentioned by Graimann et al. [1]. All previous work listed hereunder was based on 5 words recognition using a multi electrode device. The cap used for recordings is made of spandex type fabric and is equipped with many electrodes, up to 128. The electrodes have to be filled with conductive gel. The subject wears the cap and it has to be tight. The cap is then attached to the subject with straps that are connected to a band, which is attached around the supper part of the body. The target subject for those researches was normal adults like astronauts, divers, soldiers in battle who need to communicate. Difference in target subjects justifies the difference in number of words to be recognized. Table VIII represents a summary of results for the work presented and other work.

TABLE VIII. SUMMARY OF THE CURRENT WORK WITH PREVIOUS WORK

Research	Scope	Average efficiency
Wester and Shultz [2]	5 words 21subjects 16 electrodes	- 42%
Calliess [3]	5 words 16 electrodes used 23 subjects	- 15.5 % better than Wester and Shultz [2] (49%)
Porbadnigk [4]	5 words 16 electrodes used 23 subjects	- 45.5% for block - By chance for separate words
Porbadnigk et al. [5]	5 words 21subjects 16 electrodes	- 45.5% for block - By chance for separate words
Torres-García et al. [6]	5 words 21 subjects 16 electrodes used	- 20%
Our work	2 words 7 subjects 1 electrode used	- Offline 56% - Online 57%

VII. CONCLUSION AND FUTURE WORK

In this work, different ways of recognizing unspoken speech have been investigated using a single electrode EEG device. The unspoken speech comprised of 2 words; "Yes" and "No". Seven subjects were used for training. The hit rate for unspoken speech recognition depended on the subject's concentration and absence of artifacts. A modification to SOM network classification was made by making the classification a two step process. This improved the results of the SOM network in offline testing. Offline average hit rate of 59% was reached. An online average hit rate of 57% was achieved. It is worth mentioning that the ensemble network performed well only in offline, while failed in online, which is contrary to Avnimelech and Intrator [11], Hansen and Salamon [12], Hashem and Schmeiser [13], and Sharkey [14]. Other researches in the same field used multi-electrode EEG devices (up to 16 electrodes) to recognize 5 words with average recognition rates ranging between 20% and 49%. The future work is to use a single electrode device to recognize more than 2 words since such a device is much easier and lighter to wear and to adjust for certain cases as the disabled children.

REFERENCES

[1] B. Graimann, B. Allison, and G. Pfurtscheller, "Brain–computer interfaces: a gentle introduction", The Frontiers Collection, pp. 1-27, Springer-Verlag Berlin Heidelberg, 2010, doi :10.1007/978-3-642-02091-9_1.

[2] M. Wester and T. Schultz, "Unspoken speech -speech recognition based on electroencephalography". Masters thesis, Institut für Theoretische Informatik Universität Karlsruhe (TH), Karlsruhe, Germany, 2006.

[3] J. Calliess, "Further investigations on unspoken speech. - findings in an attempt of developing EEG-based word recognition", Bachelor work, Interactive Systems Laboratories Carnegie Mellon University, Pittsburgh, PA, USA and Institut fuer Theoretische Informatik Universitaet Karlsruhe (TH), Karlsruhe, Germany, 2006.

[4] A. Porbadnigk, "Eeg-based speech recognition: impact of experimental design on performance". Institut fuer Algorithmen und Kognitive Systeme, Universitaet Karlsruhe (TH), Karlsruhe, Germany, 2008.

[5] A. Porbadnigk, M. Wester, J. Calliess, and T. Schultz, "EEG-based speech recognition: impact of temporal effects", 2nd International Conference on Bio-inspired Systems and Siganl Procesing (Biosignals 2009), Porto, Portugal, pp. 376-381.

[6] A. Torres-García, C.A. Reyes-García, and L. Pineda, "Toward a silent speech interface based on unspoken speech," Proc. Biosignals 2012 (BIOSTEC), Vilamoura, Algarve, Portugal, SciTePress, Feb 2012, pp. 370-373.

[7] http://neurosky.com/products-markets/eeg-biosensors/hardware/, April 2014.

[8] W. Ting, Y. Guo-zheng, Y. Bang-hua, and S. Hong, "EEG feature extraction based on wavelet packet decomposition for brain computer interface", ScienceDirect, Measurement 41, (2008), pp. 618-625. Available online from: www.sciencedirect.com.

[9] A. Shashua, "On the equivalence between the support vector machine for classification and sparsified Fisher's linear discriminant". Neural Process Lett 9(2):129–139, 1999.

[10] P. Gallinari et al., "On the relations between discriminant analysis and multilayer perceptrons". Journal Neural Networks, vol. 4 issue 3, pp. 349–360, 1991, doi: 10.1016/0893-6080(91)90071-C.

[11] R. Avnimelech and N. Intrator, "Boosted mixture of experts: an ensemble learning scheme," Neural Computation., vol. 11, pp. 483–497, Feb 1999, MIT press, doi: 10.1162/089976699300016737.

[12] L. Hansen and P. Salamon, "Neural network ensembles," IEEE Trans. Pattern Analysis and Machine Intelligence, vol. 12, no. 10, pp. 993–1001, Oct 1990, B.001.

[13] S. Hashem and Schmeiser, "Improving model accuracy using optimal linear combinations of trained neural networks," IEEE Trans. Neural Networks, vol. 6, no. 3, pp. 792–794, May 1995, doi: 10.1109/72.377990.

[14] A. Sharkey, "Multi-net systems, combining artificial neural nets: ensemble and modular multi-net systems", Berlin, Germany: Springer-Verlag, 1999, pp. 1–30.

 ISBN: 978-1-61208-340-7

Motorsport Driver Workload Estimation in Dual Task Scenario

A Methodology for Assessing Driver Workload in a Racing Simulator

Luca Baldisserri, Riccardo Bonetti, Francesco Pon
Direzione Gestione Sportiva - Ferrari Driver Academy
Ferrari spa
Maranello (MO), Italy
luca.baldisserri@ferrari.com, riccardo.bonetti@ferrari.com,
francesco.pon@ferrari.com

Leandro Guidotti, Maria Giulia Losi, Roberto Montanari, Francesco Tesauri
RE:Lab srl
Reggio Emilia, Italy
leandro.guidotti@re-lab.it, giulia.losi@re-lab.it,
roberto.montanari@re-lab.it, francesco.tesauri@re-lab.it

Simona Collina
Università Suor Orsola Benincasa
Napoli, Italy
simona.collina@unisob.na.it

***Abstract* — The study aims to define a methodology to assess driver workload by means of a racing simulator applying the dual task paradigm. The experimental plan consists of a series of secondary tasks (i.e., math calculation, imaginative, monitoring and communication tasks) to be performed in a driving simulated context. The preliminary results evidenced that the methodology is a fundamental step forward in order to improve driving abilities of young professional drivers. The described methodology puts the basis for the definition of training programmes for managing high workload racing situations.**

Keywords - Distraction; driver; dual task; motorsport; multitasking; racing; simulator; stress; track; training; workload.

I. INTRODUCTION AND BACKGROUND

This work and the reported experimental plan are intended to define a methodology for assessing the level of cognitive load of young motorsport drivers involved in advanced training programs for single-seater racing cars. The aim of the described methodology is to evaluate potential variation in performance due to the increase of mental workload. Drivers involved in test sessions are engaged in driving in a racing simulator (i.e., primary task) while they are asked to perform also one or more secondary tasks.

Studying the performance of drivers and their "multitasking" skills implies the measurement of their performance first, and the identification of their level of adaptability to increasing workload. The ability and adaptability of multitasking are prominent features of many professions, where the simultaneous management of multiple activities is required and it is sometimes in conflict or in competition over physical and cognitive resources. When multitasking, people can become overloaded as working memory and attentional resources are exhausted [2]. They might also become anxious and frustrated when task challenges outweigh cognitive resources [10]. Furthermore, overall performance can be negatively affected when the demands of one task interfere with those of another task [5]. For instance, a common multitasking everyday situation is the concurrent use of mobile phones while driving, which have been demonstrated to impair driving by, for instance, delaying break reaction times and affecting object detection [4]. Although many studies have shown a generalized impact on attention related to driving distraction tasks, recent research has focused on "supertaskers" [6], by examining individual differences in the performance of multitasking.

In order to highlight abilities of "supertaskers", this study carried out on the short-term working memory [1] that constitutes a field of fundamental analysis to make predictions about the level of resource adaptability. Different skills are required for performing tasks simultaneously, and one must activate different cognitive structures according to tasks, such as the central executive system, the visual-spatial notebook and the phonological loop.

The presented methodology aims to measure the level of racing driver cognitive workload while driving in a simulated circuit, establishing a relationship between the observed cognitive workload and the variation of the driving performance in different scenarios of the dual task paradigm.

The paper is structured as follows: Section II presents the methodology and the design of experiment in details. Section III describes the test protocol and the execution of the experiment. Section IV presents the results of the test. In Section V, the results, the presented methodology, and the related impact are discussed. Conclusion and references close the paper.

II. METHODOLOGY

The methodology for the evaluation of cognitive workload in racing environment has been designed to reach

 ISBN: 978-1-61208-340-7

two main goals. On the one side, the objective is to identify the cognitive profile of each individual driver, by assessing the cognitive load. On the other side, once the driver cognitive profile has been outlined, a specific training programme can be identified in order to enhance the abilities and the adaptability of drivers in complex situations. This objective can be achieved by making some target activities automated according to the driver cognitive profile, thus reducing the cognitive and attentional resources allocated to those specific tasks.

In order to outline the cognitive profile, two different kinds of test can be assigned: (1) computer-based tests about cognitive resources and (2) tests in driving and not driving conditions in simulators. Concerning the former point, Individual Differences Measures (IDMs) can be collected assigning to users a series of computer-based tasks to be performed concerning each cognitive structure (i.e., central executive system, visual-spatial notebook, phonologic loop) [2].

In this research, we focused on the latter point, i.e., on the methodology for the assessment of the cognitive workload in driving a racing simulator applying a dual task paradigm. The Dual-Task Paradigm [3] is characterized by a series of secondary tasks assigned in concurrency with the primary driving task.

The reference methodology is the Multi-Attribute Task Battery (MATB) [2], which is used widely in the avionic domain. MATB consists in 4 different tasks simultaneously submitted to users at flight simulators. According to this methodology, the types of secondary tasks drivers might be asked to carry out while driving are reported below.

- Perform complex math calculation (e.g., to count backwards of 7 steps from an assigned number).
- Imaginative task (e.g., mental imagery task).
- Monitoring of system status and tracking (e.g., to indicate an event by pushing a button on the steering wheel or to check the number of engine revolutions).
- Communication task (e.g., to listen to instructions and questions via radio and to answer properly).

Each task has 4 different levels of complexity: automatic (0), low (1), medium (2), high (3).

The Dual-Task Paradigm is aimed to collect objective and subjective measures as well as qualitative and quantitative data to be analysed for assessing if the driver performance improve or decrease, whenever the cognitive workload changes itself due to the variation in the difficulty of the secondary tasks as schematised in Fig. 1.

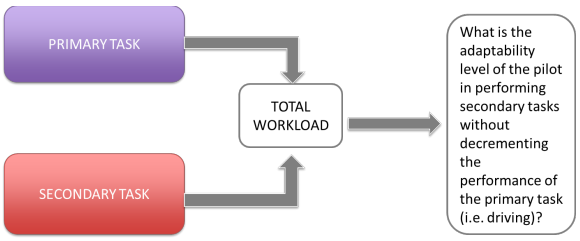

Figure 1. Double task paradigm.

The evaluation of the cognitive workload of racing drivers allows researchers to assess the relationship between workload and changes in the driving performance and then to plan training programmes that may take the cognitive profile of each driver into account for the improvement of his adaptability to multitasking. The estimation of the residual cognitive abilities while performing a Dual-Task Paradigm tests is identified as the result of the comparison between the baseline performance (e.g., the lap time in the driver comfort range) and the performance in terms of lap times carried out experiencing a secondary task.

The methodology applied for the assessment of the cognitive profile of racing driver comes from the assumption that all track, racing, and practice conditions shall be taken into account, and that the driver physical status can change during the driving session. These aspects may be responsible for a significant variation in the level of mental workload while driving. Hence, the following scenarios and conditions have been identified as relevant for test sessions.

- Monitoring of internal and external conditions of the cockpit (e.g., weather, engine revolutions, fuel level).
- Managing radio communication with garage.
- Visualizing data on the steering wheel display.
- Psychophysical degradation related to a high level of mental workload (e.g., sweating or tiredness).

The experimental design has been tailored also by considering some requirements of the driving academy involved in research and, of course, the experimental requirements. They are briefly described below.

- Users should be racing drivers of single-seater vehicles with experience in motorsport domain and should be involved in training programmes.
- Users should be young (i.e., 14 to 22 year old) in order to evaluate future training programs.
- Test sessions need to be carried out in a controlled environment as a lab.
- The main asset required is a single-seater driving simulator for racing. A fully dynamic and immersive racing simulator would be best.
- Material for interviews and collection of data (e.g., datasheet, notebooks, test protocols, chronometer, questionnaires) should be prepared in advance and available at sessions.
- Additional displays should be necessary if visual secondary tasks (e.g., reading of a value; acknowledge following a visual warning) are experienced.
- Radio equipment for remote communication between driver and interviewers should be present.

As far as it concerns the primary task, users are asked to drive in a simulated selected track at the maximum of their skills and performance. The driving performance, measured in terms of lap time within the comfort range of lap times, is considered as baseline. Users are then asked to perform secondary tasks aimed at stimulating each interested cognitive structure (i.e., phonologic loop, visual-spatial notebook and central executive system), either individually

 ISBN: 978-1-61208-340-7

or in association. The goal assigned to the driver is to maintain a level of performance within the comfort lap time range, both in cases of exclusive primary task and in dual task conditions.

Relevant dependent variables are collected in terms of subjective and objective measures. Subjective measures consist of both qualitative data (i.e., post-task comments) and quantitative data, such as NASA-TLX (i.e., Task Load Index) questionnaire, about mental workload [11], and SEQ (i.e., Single Ease Question), about perceived difficulty to carry out tasks [8]. Quantitative objective data are collected by measuring the driving performance in terms of lap time in baseline as well as in dual task conditions, by identifying explicit driving errors (e.g., off-track, over-steering) or modifications in driving behaviours (i.e., by collecting most relevant indicators such as the usage of throttle, brakes, steering wheel, and gear shift), and the number of right/wrong answers reported to secondary task, when asked. The number of answers is considered a measure of efficiency, whereas the speed and correctness in answering are measures of effectiveness. Also direct observation of driving style could be considered, if quantitative data are not available.

According to the identified relevant variables, appropriate tools are used for the collection of measures. In particular, “think-aloud” comments will be written down by observers, numeric values will be reported on scales as answers to questionnaires, and vehicle data will be recorded by the telemetry software of the driving racing simulator.

Different types of data analysis can be performed:

- Analysis and clustering of significant comments, annotations, and answers to open-ended questions.
- Descriptive statistical analysis describing each aspect of interest (e.g., frequency of answering, rate of perceived difficulty in driving, the reported subjective mental workload).
- Inferential statistical analysis of the impact of the dual task on the primary task (i.e., performance in lap time) carried out for subjects and for items.
- Analysis of statistical regression to assess which one of the variables considered is predictive of the performance of the other one, by correlating both the linguistic and the visual-spatial tests to see how much they influence the driving task.

Testing the driver performance in a racing simulator environment cannot disregard some constraints that might affect the testing procedure. In particular, a higher workload level can arise compared to the experience of driving on track with a real single-seater vehicle. This increased workload might be due to the lack of feedbacks from the external environment and to the effort of the racing driver who artificially recreates mentally inputs in order to generate specific driving behaviours. Furthermore, the selection of young racing drivers implies different technical skills and different levels of automations while driving. Depending on the track configuration and on the technical skills of the driver, a track can be more or less difficult to be covered in terms of mental workload. For instance, the "Fiorano" track in Italy can be considered familiar for the Ferrari Driver Academy racing drivers and it is assumed to imply a medium level of mental workload compared to the "Monza" track, which generates a variable level of mental workload depending on the track segments and on the number and type of corners. Other minor aspects could impact the workload, for instance the use of a standardized rather than a customized steering wheel for each racing driver can influence the level of familiarity and the automatic driving procedures. Moreover, the variable and permanent conditions of real tracks are missing, such as the high or low grip feeling, the weather conditions, and the presence of other vehicles that can only be simulated. It is not possible to simulate this variability and to control it as an independent variable in order to increase the difficulty level due to changing external context conditions.

III. TESTING OF METHODOLOGY

The test protocol has been designed for sessions on a fully dynamic and immersive single-seater driving simulator for racing, as shown in Fig. 2.

Figure 2. Racing driving simulator facilities

The test session has been carried out on the 13th of March 2013 involving one young professional driver of the Ferrari Driver Academy, 19 years old. The simulated single-seater vehicle has been his "F3 Euro Series" in the simulated track of "Autodromo Nazionale Monza", Italy (5793 km, 8 corners, clockwise). The track is represented in Fig. 3.

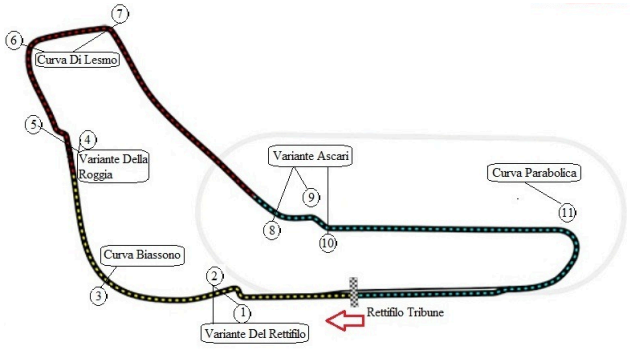

Figure 3. Autodromo Nazionale Monza

 ISBN: 978-1-61208-340-7

The test session lasted about 120 minutes and it consisted of 40 laps with 3/4 minutes of stop between each test run.

The test protocol has been designed considering 1 run of warm-up, aimed at identifying the "comfort lap time range" for the driver and 1 run for each task session. Each run consists of 1 out-of-garage lap and 3 timed laps.

The comfort lap time range (i.e., minimum lap time and maximum lap time) for the involved user is within 1:46.200 - 1:47.200 in Monza track, considering a comfort variance of 2%. The baseline sessions, in which the driver is asked to focus only on the primary task, are followed by SEQ and NASA-TLX questionnaires. After that, a sequence of randomly selected test run including secondary tasks is assigned to the driver. The user performs, firstly, only the secondary task, in not driving conditions, and he is then asked to fill in SEQ. Then, he experienced the secondary task in driving conditions, followed by SEQs referring both to primary and to secondary tasks, and by the NASA-TLX questionnaire about perceived mental workload. The baseline is repeated three times, at the beginning, in the middle and at the end of the test session. In the performed test session, the randomized task sequence has been: B, T1, T3, T2, B, T5, T4, B, which are described below.

- T1 = Math identification if an assigned number is grater or less than 45 (in not driving and driving conditions).
- T2 = Count backwards of 3, step by step, starting from an assigned number (in not driving and driving conditions).
- T3 = Count backwards of 7, step by step, starting from an assigned number (in not driving and driving conditions).
- T4 = Count backwards of 13, step by step, starting from an assigned number (in not driving and driving conditions).
- T5 = Count the number of letters of a given word (in not driving and driving conditions).
- B = Baseline run.

The user was alone in the driving simulator room. During test sessions, the researcher was able to communicate with the user through one-way at a time radio. As in real "F3 Euro Series" racing context, user had to press a button on the steering wheel in order to enable communication and let researcher hear him while speaking. Also, the researcher had to press button to be heard by user. These actions are mutually exclusive. The researcher has been in charge of the task assignment, such as to provide to the user the list of numbers according to the given task.

After each test phase, SEQ has been provided to the driver. It is a 7-points scale item from "Very difficult" to "Very Easy" to be self reported by the user. The objective of the measure is to evaluate the perceived easiness of the primary task (i.e., driving performing a lap time within the comfort range) not experiencing (i.e., in baseline) or experiencing the secondary tasks, and also the perceived easiness of the secondary task itself, in stationary and driving conditions. SEQ has concerned the following topics.

In baseline - "How do you evaluate the driving task on track? (i.e., how difficult or easy it has been?)"

After experiencing the secondary task stationary - "How do you evaluate the 'secondary task'? (i.e., how difficult/easy has it been?)"

After experiencing the dual task while driving - "How do you evaluate the driving task on track while you are performing the 'secondary task'? (i.e., how difficult/easy has it been?)"

After experiencing the dual task while driving - "How do you evaluate the 'secondary task' while driving on track? (i.e., how difficult/easy has it been?)"

After each driving session, both in baseline and in dual task, the user is also asked to fill in the six scales of NASA-TLX questionnaire. RTLX (i.e., Raw NASA-TLX) version of the questionnaire has been considered [11].

The driving performances have been recorded by Atlas software for telemetry. It collected data from different channels (e.g., brake, accelerator, steering wheel angle, speed, engine revolution, gear, wheel speed, etc.) and the press of the buttons on the steering wheel.

IV. RESULTS

The data analysis has shown that it is possible to point out specific remarks about dual task performance in the motorsport driving domain by carrying out test sessions applying the described methodology.

With respect to lap timing, a remarkable impact on performance has been registered according to the type of secondary task. Timings in dual task conditions are higher (M_a= 01:47.5) in comparison with those in baseline conditions (M_a= 01:46.7). In three occasions, the lap time is higher than the comfort range threshold (i.e., between 01:46.2 and 01:47.2), as shown in Fig. 4 and in Table I.

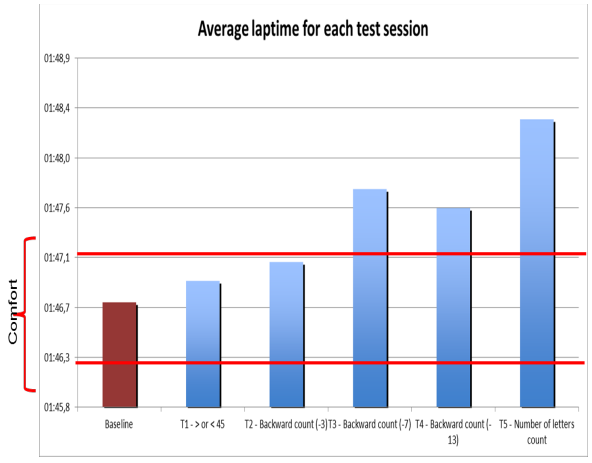

Figure 4. Average lap time

TABLE I. AVERAGE LAP TIME

Test session	Average laptime
Baseline	01:46,7
T1 - > or < 45	01:46,9
T2 - Backward count (-3)	01:47,1
T3 - Backward count (-7)	01:47,7
T4 - Backward count (-13)	01:47,6
T5 - Number of letters count	01:48,3

The perceived mental workload by NASA-TLX and the self-reported changes depend on the type of secondary task, as shown in Fig. 5 and Table II.

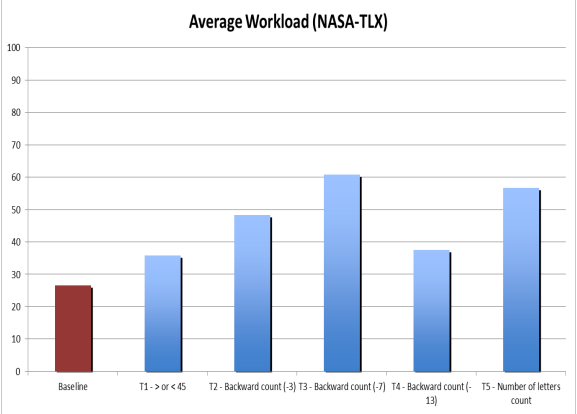

Figure 5. Average Workload (NASA-TLX)

TABLE II. NASA-TLX RESULTS

Test session	Average Workload (NASA
Baseline	26,67
T1 - > or < 45	35,83
T2 - Backward count (-3)	48,33
T3 - Backward count (-7)	60,83
T4 - Backward count (-13)	37,50
T5 - Number of letters count	56,67

The perceived easiness while performing the dual task changes among the tasks themselves and it changes for the same task in stationary or driving conditions, as shown in Fig. 6.

The secondary tasks that are considered the most demanding and that seem to have a greater impact on lap times and on perceived mental workload are the backward counting of -7 steps (NASA-TLX score 60,83 and easiness 3/2/2) and the identification of the number of letters in a word (NASA-TLX score 56,67 and easiness 3/4/3). Nevertheless, an effect of self-learning may have happened while performing the secondary tasks.

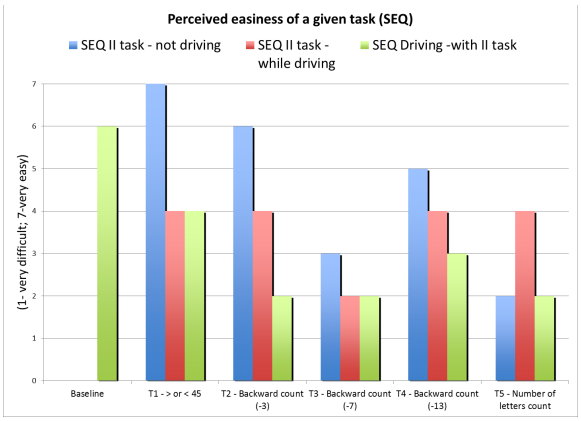

Figure 6. Perceived easiness of tasks

The times for answering to assigned sub-tasks reflect the difficulties perceived while performing the tasks, as shown in Fig. 7.

All the surveys and the results seem to be consistent with the perceived easiness, the errors occurred in the answers provided to secondary tasks (Fig. 8), workload, and the level of performance (i.e., lap time).

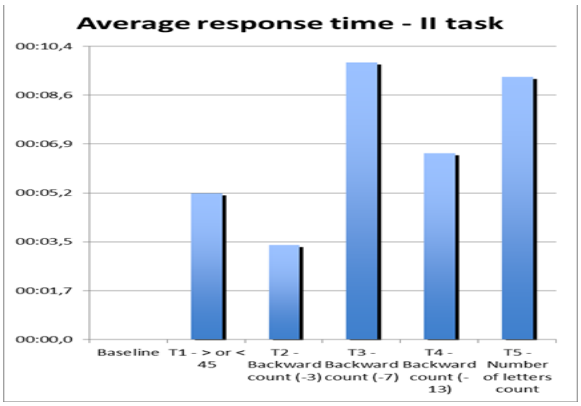

Figure 7. Average response time

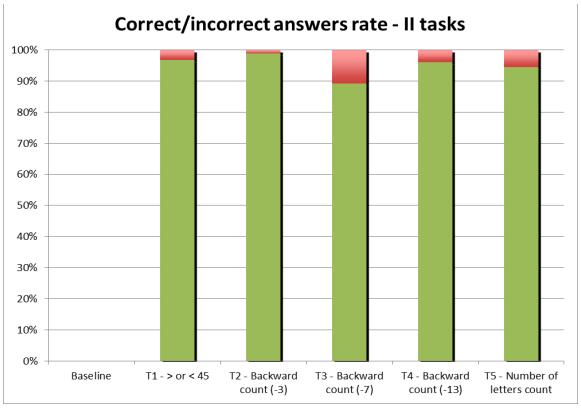

Figure 8. Correct answer rate

 ISBN: 978-1-61208-340-7

TABLE III. ERRORS AND RESPONSE TIME

Test session	Item Number	Errors	% errors	Average time per item
Baseline				
T1 - > or < 45	62	2	3,23%	00:05,2
T2 - Backward count (-3)	96	1	1,04%	00:03,3
T3 - Backward count (-7)	33	4	12,12%	00:09,8
T4 - Backward count (-13)	49	2	4,08%	00:06,6
T5 - Number of letters count	35	2	5,71%	00:09,3

The user involved in the test session has a maximum error rate counting back of 7 steps task (i.e., 12,12 % of error rate) and he takes more time (i.e., 00:09.8) to carry out sub-tasks rather than other dual tasks, as reported in Table III.

V. IMPACT AND DISCUSSION

A methodology to analyse the multitasking ability of a young motorsport driver while performing a dual task paradigm on a racing simulated track has been designed. A preliminary test has been carried out. Researchers collected and analysed data to evaluate if any degradation could be detected in the driving performance due to the concurrency with increasing demanding cognitive tasks.

Findings cannot be considered statistically relevant due to the narrow sample of users, but it has served the scope to identify and to test the designed methodology for data collection and data analysis. Thus, it can be considered an indicator of the expected impact of cognitive workload on the driving performance in a racing context.

Driver has autonomously and constantly performed the requested dual tasks. The secondary tasks seemed to induce a diversified level of workload pressure, pointed out by the self-reported data, perceivable also by the tone of the voice and by the speed of the answers provided by the user.

In some conditions, driver has not immediately answered to or performed the secondary task, but he took some time to complete the task assigned. From the observation, it seemed that, when approaching the corners of the Monza track, the driver was focused exclusively on the primary task and he started performing the secondary task only after the completion of the manoeuvre.

Learning strategies in the answering to dual task requests (e.g., to count -30 or -3 when asked to count back of 13) does not seem to influence the performance of the dual task and the global impact it has on the primary task. Driver encountered an initial physical difficulty, reported as a speech comment, when pushing the “radio” button while changing the gear or when approaching the corners. Furthermore, possible relevant changes in the driving performance by analysing the telemetry channels shall be assessed and interpreted. The survey in baseline conditions and double task will allow an interpretation of the driving style in the different conditions of mental workload.

VI. CONCLUSION

Research findings shall be considered as interpretations referred to collected data and to the descriptive results presented. There are no specific considerations and interpretations about the performance and driving style in different test sessions. There are no interpretations related to or statistic interferences among the data collected. For practitioners and researchers, it shall be highlighted that motorsport, together with the avionic domain, is a well suited context for the goal of testing multitasking ability of young drivers and the impact of workload on the driving performance. Training programmes can be easily defined thanks to the results gathered by applying the methodology, with the aim of improving the performance of the driver by increasing his/her multitasking ability and the ability to face concurrent task on cognitive resources. Although only one user has been involved in the tests performed so far, the expected impact has been verified by the collected data: the young professional driver registered large variations in the driving performance in terms of lap time, due to the secondary tasks. In addition to that, the methodology applied has been solid, coherent and correct in terms of results. It is also in line with the studies that have been carried out in the last years concerning the dual task paradigm. In order to enhance the obtained results, the objective will be to consolidate the methodology by involving a larger sample of drivers in test sessions as a way to identify areas of improvement and to evaluate if such improvements have been reached thanks to the training activity.

VII. REFERENCES

[1] A. Baddley, Human Memory: Theory and Practice, Lawrence Erlbaum Associates, London, UK, 1990.

[2] B. Morgan, S. D’Mello, R. Abbott, G. Radvansky, M. Haass, and A. Tamplin, "Individual Differences in Multitasking Ability and Adaptability", Human Factors: The Journal of the Human Factors and Ergonomic Society, vol. 55, 2013, pp. 776-788.

[3] C.D. Wickens, "Processing resources and attention", Multiple Task Performance, Taler & Francis, Ltd., Bristol, UK, 1991, pp. 3-34.

[4] D. L. Strayer, F. A. Drews, and W. A. Johnston, "Cell phone induced failures of visual attention during simulated driving", Journal of Experimental Psychology: Applied, vol. 9, 2003, pp. 23-52.

[5] E. M. Altmann and W. D. Gray, "An integrated model of cognitive control in task switching", Psychological Review, vol. 115 (3), 2008, pp. 602–639.

[6] J. M. Watson and D. L. Strayer, "Supertaskers: Profiles in extraordinary multitasking ability", Psychonomic Bulletin & Review, vol. 17 (4), 2010, pp. 479-485.

[7] J. R. Comstock, and R. J. Arnegard, The Multi-Attribute Task Battery for human operator workload and strategic behaviour research, National Aeronautics and Space Administration Technical Memorandum No. 104174, Washington D.C., USA, NASA, 1992.

[8] J. Sauro and J. S. Dumas, "Comparison of three one-question, post-task usability questionnaires", Proceedings of CHI, ACM, Boston (MA), USA, 2009, pp. 1599-1608.

[9] L. Angell et al., Driver Workload Metrics Project, Task 2 Final Report, CAMP Driver Workload Metrics, Report No: DOT HS 810 635, U.S. Department of Transportation NHTSA, USA, 2006.

[10] M. Csikszentmihalyi, Beyond boredom and anxiety, Jossey-Bass, San Francisco (CA), USA, 1975.

[11] S. G. Hart, “NASA-TLX Load Index; 20 years later”, Proceedings of the Human Factors and Ergonomics Society 50th Annual Meeting, Santa Monica (CA), USA, 2006, pp. 904-908.

 ISBN: 978-1-61208-340-7

ACT-R Meets Usability

Or why Cognitive Modeling Is A Useful Tool To Evaluate The Usability Of Smartphone Applications

Nele Russwinkel
nele.russwinkel@tu-berlin.de

Sabine Prezenski
sabine.prezenski@zmms.tu-berlin.de

Dep. of cognitive Modeling in dynamic HMS
TU Berlin
Berlin, Germany

***Abstract*—The usability of two different versions (A and B) of a smartphone shopping list application is evaluated via user tests and cognitive modeling. The shopping list application allows users to select different products out of different stores. Version A has less menu-depth than version B. The results show that less product-search time is required for version B. This benefit of version B over A declines, as users become more experienced. Advantages of modeling approaches and disadvantages of empirical data are discussed. It is shown that cognitive modeling approaches with ACT-R are a powerful tool for model based usability testing.**

Keywords-usability; cognitive modeling; ACT-R; mobile applications;

I. INTRODUCTION

Nowadays, smartphones and mobile applications are part of our everyday life. Application numbers are growing rapidly [1]. Successful applications obviously have a high usability. Evaluating usability with conventional usability testing requires time and money. Therefore, a pressing question is how the usability of applications can be guaranteed without costs exploding. In this paper, we will present our idea and first results of how cognitive modeling with ACT-R can serve as substitute for extensive usability testing. We will show how learning in Apps will proceed and also deal with the interesting question of version update (or switching) effects.

Cognitive architectures, such as ACT-R (Adaptive Control of Thought-Rational) [2] offer a computable platform that represents well established theories about human information processing. With cognitive architectures it is possible to simulate cognitive mechanisms and structures, such as visual perception or memory retrieval. These are organized in different modules and these modules communicate via their interfaces to the production system which are called buffers. ACT-R is a hybrid architecture, which means that is has symbolic (knowledge representations, such as chunks and rules called productions) and subsymbolic components (activation of chunks and utility of productions).

What exactly is usability? Standard ISO 9241-11 specifies usability as effectiveness, efficiency and satisfaction. Standard ISO-9241-110 describes general ergonomic principles for the design of dialogues between humans and information system, outlining seven import criteria (suitability for the task, suitability for learning, suitability for individualization, conformity with user expectations, self descriptiveness, controllability, and error tolerance).

Nielson`s Usability heuristics describe ten general principles for interaction design, for example that consistency and standards should be applied [3]. There are also more specialized heuristics for mobile applications [4]. Developers should apply these heuristics when designing applications. Another, more technical way, to deal with usability is via pattern matching methods [5].

Other popular methods to assess usability of mobile applications are expert reviews or user data, which can be collected via questionnaires, qualitative methods (e.g., think aloud protocol) or usability tests. Particularly information about subjective satisfaction can only be obtained with qualitative measurements. Nevertheless quantitative user testing allows assessment of a wide range of usability criteria; e.g., task completion time as a measure for efficiency, the number of successful task completions as a measure for effectiveness, the number of and kind of mistakes give information about suitability for the task, conformity with user expectations, self descriptiveness, controllability and error tolerance. Suitability for learning can be measured via comparison of several runs [6].

In a review on different studies on usability of mobile applications R. Harrison et al. [7] stress, the importance of cognitive load of applications for successful usage. They also emphasize the difficulty of assessing cognitive load via heuristics or standards. Cognitive models can be powerful tools, when dealing with questions concerning cognitive load.

Cognitive models can serve as a substitute for (quantitative) user tests. User models build with ACT-R can simulate the interaction with a certain task. Cognitive modeling has two advantages over real user tests; first of all no human participants are needed when good and evaluated models exist and second, important information about underlying cognitive processes can be discovered.

 ISBN: 978-1-61208-340-7

Implications from these findings can then be used in designing further applications.

So far some first approaches were developed that combine modeling with usability. CogTool is a user interface prototyping tool, which is based on keystroke-level modeling and produces a simplified version of ACT-R code [8]. After the user manually compiled a storyboard, CogTool produces a cognitive model, which runs along the pathway as identified in the storyboard. CogTool then predicts how long a skilled user requires to complete the task [4]. CogTool has several limitations: It is not possible to let the model explore the interface since the model only runs along the ideal-pathway as defined by the storyboard. Therefore, information about potential user-errors or influence of workload cannot be achieved. MeMo- is a Usability Workbench for Rapid Product Development which can simulate user interactions with the system [9]. On the basis of task, possible solution pathways are searched by the model and deviations from these pathways are then generated; Different user groups (e.g., elderly users, novice users) are taken under consideration [9], which is clearly an advantage of MeMo over CogTool. Another advantage with MeMo persists in the potential of the model to produce errors. A clear disadvantage of MeMo arises due to the fact that it is not a cognitive modeling tool- important concepts about human cognition are not implemented.

In the following, we will first introduce a new tool that connects applications with a cognitive architecture to directly enable cognitive models to interact with an interface. Then we will describe our general approach. Afterwards, we will introduce the application we used and the usability study we conducted including the results. In the discussion section, the empirical results as well as the different modeling approaches are discussed for three main topics: Comparing app versions, whether learning occurs and switching effects between versions. Lastly, we draw conclusions and explain the further process of the approach.

II. APPROACH

Our approach towards modeling the usability of interfaces differs from those described above: We developed a tool called „Hello Android" [10]. This tool enables a direct connection of the cognitive architecture with a Smartphone application via a TCP/IP protocol. In this vein, the user model can directly interact with the application, press buttons and in turn the model can perceive changes on the interface as well. The tool has many advantages for the modeler; first of all no mock-up version of the app or possible pathways need to be created, which saves a lot of time, compared to CogTool or MeMo. Secondly, we will model the application using the full possibility and functions of the ACT-R architectures, which allows investigating a great number of different aspects of how the app affects human information processing and individual differences (e.g., memory, experience or age). Thirdly, with our modeling approach we can evaluate processing time of an application as well as different kind of user mistakes. Main requirement for the usage of our approach are skills in modeling with ACT-R. The modeler just needs to know how to write (or change) productions and have rudimentary knowledge of the subsymbolic part of ACT-R. No lisp-programming is needed.

III. STUDY

Our study compares two slightly different versions of a shopping list application for Android. Both versions allow users to choose products out of either an alphabetically ordered list or via categorical search. The chosen products are then added to a list. Menu depth differs between the two versions: version A has one menu level more than version B. The first page of the application is the same for both versions: three buttons are presented: "overview", "shops" and "my list". For both versions, when selecting "overview" one gets a list of the alphabet. Three or two letters are always grouped together on one button, e.g., "ABC", "DEF"…. Selecting one of those buttons then results in an alphabetical ordered list of the products. For example, when clicking on ABC, all possible products, with product names beginning from A to C appear in a list. A click on a small checkbox in the right of the product selects it. If you click on shops, then for both versions a list of seven shops (bakery, drugstore, deli, greengrocer, beverage store, stationery, and corner shop) appears. Each of these shops is represented by a button. For version B, selecting one of the shops results in an alphabetical ordered list of the products available in that particular shop. For example, by clicking on greengrocers all items that can be found in a greengrocers store are presented (apples, bananas, blueberries, cherries, etc.). A click on a small checkbox in the right of the product selects it as well. For version A, the shops each have seven subcategories. For example, when selecting greengrocers, one is presented with the subcategories exotic fruits, domestic fruits, tuber vegetables, herbs, seeds and nuts, mushrooms and salads. When selecting a subcategory, a list of products that can be found under this subcategory, appears. Again, a click on a small checkbox in the right of the product selects it. For both versions, selecting "My List" from page one results in a shopping list which comprises the selected products plus information about the store in which the products are available.

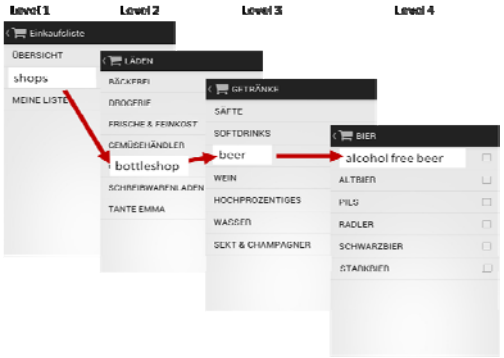

Figure 1: Version A of the shoppinglist application- Version B is similar, except that Level 3 *"Getränke"* is missing.

 ISBN: 978-1-61208-340-7

Sixteen voluntary student participants (seven male and nine female, $mean_{age}$=22) took part in the study. After receiving standardized oral instructions participants were asked to select a list of products. For each trial, a product was read to participants by the investigator and participants had to find the product. He or she could select the product either via the "Overview" path or search the stores. After selecting a product, participants were asked to return to the first page and then the next trial started. After selecting eight products, participants were asked to read the shopping list (in order to assure learning of the store categories) and then the next block started, this time the items were the same but presented in a different sequence. After completing the second block, the investigator presented the participant the other version and the two blocks of trials were repeated. Half of the participants first worked with version B and half started with version A.

A. *Results*

In the following section, preliminary results are presented (see figure 1). This paper focuses on the mean trial time for the different blocks, which is defined as the time difference from when the participant leaves the start page until the item is selected. For participants of group "A first- B second", the mean trial time of block 1 of version A is 10.67 sec and decreases approximately 4 seconds for block 2 (mean trial time 6.11 sec). After switching from version B "B second", time decrease to 4.96 sec and reaches 4.43 sec for B second-expert (block 4). For participants of group "B first- A second" a trial in the first block has a mean duration of 8.74 sec and a trial in the second block a mean duration of 4.02 seconds. After participants switch to version A "A second", time increase to 6.56 sec and decreases again to 4.42 seconds.

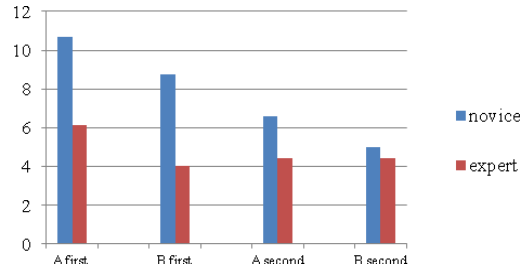

Figure 2: mean trial time for the different conditions

IV. DISCUSSION

The next passage explains how modeling captures usability aspects and depicts explanations for the effects found in the data.

B. *Comparison of both versions:*

Empirical: Version B is overall faster than version A, especially for novice users. The benefit of version B over A decreases and almost reaches nil, as block 4 for version A and version B (expert) show. Explanation: Obviously, more required clicks in version A are probably not the reason for the benefit of version B over A for novice users.

Modeling: The building of expectations-chunks takes longer for version A than for version B, because there are more interaction steps in A and therefore, more encoding of these steps is required. Furthermore, for version A more semantic knowledge (which shop holds which subcategory and which subcategory holds which product) is needed, but the knowledge of subcategory is unnecessary for version B. Version A also takes longer because the extra semantic knowledge needs more encoding in chunks for subsequent use. For both versions, knowledge is learned via trial and error. Useful pre knowledge is probably available (and provided in declarative memory) but especially for some categories pre knowledge is less obvious and those product-category pairs have to be learned. The first step in the model is to try to retrieve the information about categories, e.g., in which category a certain product might be found. If the retrieval is not successful the next step for the model is to search a different category. If this is successful the connection between product and category is encoded in declarative memory. An unsuccessful retrieval takes longer than a successful one and also requires more productions to proceed. The plus of productions takes a lot of time (each production takes about 50ms). Once the subject has acceptable knowledge about category membership, there are more successful then unsuccessful retrievals. As a consequence the mean trial duration decreases.

C. *Does Learning occur?*

Empirical: Our data shows a clear learning effect, as participants become more familiar with the application the mean trial duration decreases- there also seems to be a learning transfer from version A to version B.

Modeling: Production compilation is a useful ACT-R mechanism to model learning. In the beginning, for every interaction step a memory retrieval of the next processing step is required. After a few trials often used information is integrated in the productions. Trial duration decreases, since retrieval time is redundant and proceeding productions are integrated. Furthermore, retrieved expectancies can give detailed information were the next relevant button will be located. Therefore, eye- and finger-movements can be prepared early and initiated more quickly with practice. Because no additional information needs to be learned when switching from version A to B (note that version A includes all menu-structures of version B, but has more menu depth), the above mentioned learning processes are not disturbed and learning continues.

D. *Are there switching effects?*

Empirical: A switching effect occurs when participants familiar with version B change to version A. This becomes apparent in the increase of time from B first expert to A second. Nevertheless, participants using version A second still profit from version B, since A second is faster than A first.

Modeling: Switching from version B to A irritates the users, because they end up with a menu they did not expect and are not familiar with. In terms of the user model, this means they do not have instruction chunks that give the

 ISBN: 978-1-61208-340-7

information what is to do next. They have to go back and search for the back button and then learn the items that belong to the new categories. This takes time because it causes a number of additional productions to fire. But after a few trials, new category-product pairs are learned and the switching effect disappears. In the opposite case, users end up earlier with the final (more familiar) list that is already encoded in the expectancy chunks. They do not have to learn new category members and do not need to encode representations to declarative memory; therefore, fewer productions have to fire and mean trial duration is low.

V. CONCLUSION

Conclusion over the usability of the two versions

Both versions are suitable for users, but version B is slightly faster than version A. The benefit of version B decreases as user experience increases. Shallow menu structures are more convenient for novice users. Both versions of the application are easy to learn. Switching from version A to B has additional time cost in the beginning, whereas switching from B to A has not. We showed that user models can provide informed interpretations about the causes of usability, e.g., differences between versions can be explained through specific learning processes; a finding that is not possible with conventional usability tests.

Outlook

In the near future, we will further investigate our data, with a stronger focus on potential user errors, data fitting and mobile context. Cognitive modeling of the usage of Smartphone applications with ACT-R is a promising approach for usability research. The goal of our research is to develop guidelines for ACT-R modelers describing the most relevant modeling concepts for usability of applications. These guidelines will raise the opportunity to quickly develop user models and improve and evaluate the usability of applications. As the number of new applications on the market further increases, cognitive modeling provides the solution for affordable and capacious usability testing.

ACKNOWLEDGMENT

We would like to thank the students of Human Factors Engineering for their engagement in data collection and all members of our team for support. Special thanks to Lisa Doerr. Thanks also to Gabi Taenzer and Steffen Vaupel for the programming of the application.

REFERENCES

[1] J. Koetsier, *Google Play will hit a million apps in June* [Online]. Available from: http://venturebeat.com/2013/01/04/google-play-will-hit-a-million-apps-in-2013-probably-sooner-than-the-ios-app-store/ 2013.01.04.

[2] J. R. Anderson, How Can the Human Mind Occur in the Physical Universe?, New York: Oxford University Press , p. 304, 2007.

[3] J. Nielsen, Usability engineering. Morgan Kaufmann Pub, 1994.

[4] L. Kuparinen, J. Silvennoinen, and H. Isomäki, "Introducing Usability Heuristics for Mobile Map Applications," Proceedings of the 26th International Cartographic Conference, Dresden, Germany, 2013.

[5] J. Engel, C. Herdin, and C. Maertin, "Exploiting HCI Pattern Collections for User Interface Generation," Proceedings of the 4th International Conference on Pervasive Patterns and Applications, (IARIA Proceedings) Nice, France, pp. 36-44, 2012.

[6] D. Zhang and B. Adipat, "Challenges, Methodologies, and Issues in the Usability Testing of Mobile Applications," International Journal of Human-Computer Interaction, vol 18, pp. 293-308, September 2005, doi:10.1207/s15327590ijhc1803_3.

[7] R. Harrison, D. Flood, and D. Duce, "Usability of mobile applications: Literature review and rationale for a new usability model," Journal of Interaction Science, vol. 1, pp. 1-16, January 2013.

[8] L. Teo, B. E. John, and P. Pirolli, "Towards a Tool for Predicting User Exploration," CHI '07 Extended Abstracts on Human Factors in Computing Systems. pp. 2687–2692, New York, NY, USA: ACM, 2007, doi:10.1145/1240866.1241063.

[9] S. Möller, K.-P. Engelbrecht, and R. Schleicher,. "Predicting the Quality and Usability of Spoken Dialogue Services," Speech Commun., vol. 50, pp. 730–744, August/September 2008, doi:10.1016/j.specom.2008.03.001.

[10] S. Linder, P. Büttner, S. Vaupel, G. Taenzer, and N. Rußwinkel, „Towards an Efficient Evaluation of the Usability of Android Apps by Cognitve Models," Kognitive Systeme, Universität Duisburg-Essen, in press.

 ISBN: 978-1-61208-340-7

HORUS: a Configurable Reasoner for Dynamic Ontology Management

Giovanni Lorenzo Napoleoni, Maria Teresa Pazienza, Andrea Turbati
Department of Enterprise Engineering
University of Rome Tor Vergata
Rome, Italy
e-mail: giovannilorenzo.napoleoni@gmail.com,
{pazienza, turbati}@info.uniroma2.it

***Abstract*—This paper introduces HORUS (Human-readable Ontology Reasoner Unit System), a configurable reasoner which provides the user the motivations for every inferred knowledge in the context of a reasoning process. We describe the reasoner, how to write an inference rule and check which explicit knowledge was used to infer a new one. Real cases examples will be provided to show the capabilities of our reasoner and the associated language developed to express inference rules. We show how HORUS allows the user to understand the logical process over which each new RDF triple has been generated.**

Keywords—Ontology Management; Reasoner; Formal Language

I. INTRODUCTION AND MOTIVATION

The Semantic Web is becoming more and more popular and easy to work with. Ontologies are used as a common base to all the applications which rely on such a framework. Main features of an ontology are:

- The use of a specified standards, such as Resource Description Framework (RDF) [1];
- The possibility to infer knowledge from existing one.

The process of inferring new knowledge, from the existing one, is delegated to reasoners. They take in input a vocabulary, the data stored in the ontology and a list of rules and produce new knowledge, hopefully in the same standard in which the ontology is written. A list of existing reasoners can be found at [2]. They differentiate for:

- The rules they are able to use in the inference process;
- Under which license they are distributed, inside which tool they can be used;
- The language in which they are written (e.g., Java, C++, etc.);
- The possibility to accept new rules without the need to change most of their source code;
- Performances in the inference process.

Once a reasoner has been chosen, it is possible to use it:

- Standalone as a tool to infer new knowledge that is saved in a particular serialization (with or without the analyzed knowledge base);
- As a component, inside a framework to immediately observe the inferred knowledge.

Generally, the task of visualizing the results of any tool embedded inside a framework is finalized to both validate its output and produce some performance metrics (such as precision or recall). The validation process for a reasoner is very different: in fact as a list of inference rules is used, a reasoner is characterized on which inference is able to run, its scalability regarding the size of the ontology it analyzes and the time it needs to process it.

By analyzing different reasoners, we discover that they can be really optimized regarding the execution time while both customization and visualization processes are generally lacking, even if they are important and useful, as discussed in [3] (see as an example the use of the framework Protégé (version 3.4.8) [4] and the bundled reasoner Pellet (version 1.5.2) [5]). In this case, a user is not able to know immediately which rules the reasoner will apply. The sole possibility is to consult its home page, [6] for Pellet 2.0. New rules can be added using the language SWRL [7]. Protégé 3.4.8 provides inferred knowledge generated from the selected reasoner, specifying that it has been inferred, without showing which underling knowledge was used in the inference process and why such new knowledge has been produced. There are several contexts in which users could be interested to follow the reasoning process, as for:

- Learning how it behaves;
- Comparing results in different application domains;
- Comparing results with his own expectations related to previous/personal conceptualizations.

Protégé 4.3 has a new system to manage reasoners (Protégé 3.x and Protégé 4.x are used depending on the Ontology characteristics and the existing plug-in). It has two bundled reasoners, FaCT++ [8] and HermiT [9]; but other reasoners can be downloaded and installed. It is also able to provide an explanation to why an inferred knowledge has been (temporarily) added to the selected ontology, but this explanation consists of just the list of explicit triples used by the current reasoner, without showing the other inferred knowledge produced and successively used along the reasoning process, so for complex reasoning it can be difficult to follow the entire process.

For all these reasons, we decided to develop a new reasoner characterized by the following features:

- Being open source;
- Implemented as a Java library;

 ISBN: 978-1-61208-340-7

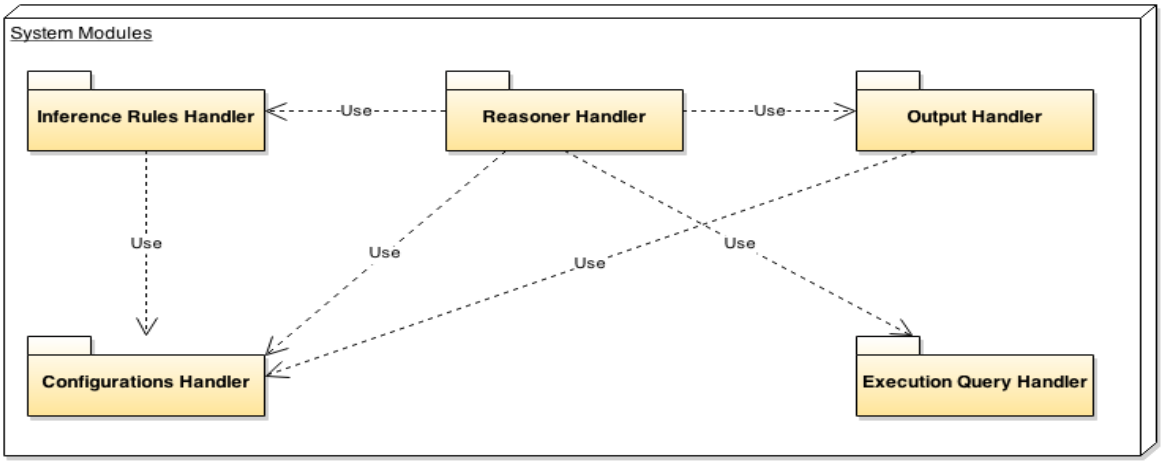

Figure 1. Reasoner Achitecture

- Easy to add new rules using an intuitive language based on the RDF family standard;
- The inference process would point out the list of RDF triples (explicit and inferred ones) used to produce every inferred triple.

In such an approach, the end user is totally aware of the inference process; as a consequence he can evaluate how much it fits his approach to reasoning.

In the rest of the paper, we describe first in Section II the architecture on which the reasoner is based on. Then, in section III, we present the language used to express the inference rules providing some real case examples. In Section IV we show how the reasoner allows the user to understand the logical process over which each new RDF triple has been generated. Finally, in Section V, we present our conclusions.

II. ARCHITECTURE AND IMPLEMENTATION

The architecture of the reasoner Human-readable Ontology Reasoner Unit System (HORUS) is shown in Fig. 1. A modular approach has been adopted to make easy to change any module without modifying the other ones.

First, the configuration parameters are read by the *Configuration Handler* and passed to the *Reasoner Handler*. Then, all inference rules are parsed by the *Inference Rules Handler*. The language in which these rules are written will be discussed in detail in Section III. HORUS does not have any hard-coded inference rule, each rule used by the reasoner is written in the developed language, so a user will be able to see what the reasoner is able to infer, without the need to read its source code. This is a first aspect of configurability.

Once the reasoner is configured, each inference rule is executed by the *Execution Query Handler*, which, in the current implementation, uses SPARQL SELECT [10], taking advantage for any improvement provided by the triple store the reasoner is used with. To avoid any dependency on the specific technology regarding a triple store, HORUS uses the OWL-ART API [11] middle layer which enable an abstraction layer over different RDF triple store technologies. In the current implementation, the reasoner has been tested with these API in conjunction with a Sesame2 implementation [12]. All the inference rules are executed in one or more iterations, until the reasoner is able to infer no further knowledge, or the number of iterations specified during the configuration is achieved.

Finally, the output of the inference process is shown to the user by the *Output Handler*.

III. LANGUAGE

Hereafter, we describe the language defined to specify the *inference rules* and *consistency rules* to be used by the reasoner, that follow a similar syntax while their objective is totally different. The former rule is used to deduce new knowledge (using either already existing or inferred in a previous iteration), the latter does not produce any knowledge, it is used to check if the ontology causes an inconsistency (two or more axioms which contradict each other). In the following, first we explain the syntax adopted for the rules and then we provide some real case rules.

A. Rule syntax and use

The simplified grammar of the language developed for these rule is shown in Fig. 2.

Each rule starts with the word *rule* followed by its type. There exist two possible rule types: inference rule (called *new rule*) and consistency rule (*new consistency rule*).

Successively, the name and an id are provided. The id must be unique and it is used to refer to a specific rule. Then, the list of premises used by the reasoner follows. They check if in the current iteration this rule is able to generate new knowledge. Generally at least two premises are required to

```
parseInferenceRule : (new_rule)+;
new_rule : (rule_info) (premise)+ (filter)* (conclusion)+;
rule_info : 'rule: ' type 'name: ' NAME 'id: ' ID ;
type : 'new rule' | 'new consistency rule';
premise : 'premise: ' triple;
triple : 'subject: ' value 'predicate : ' value 'object: ' value;
filter : 'filter: ' '?' VAR LOGIC_OPERATOR '?' VAR;
value : ('?' VAR) | IRI | BNODE | SINGLEVALUE ;
conclusion : ('conclusion: ' triple ) | ('conclusion: ' 'false' );
```

Figure 2. Simplified rule grammar

 ISBN: 978-1-61208-340-7

have a meaningful rule. Each premise is constituted by three elements: a *subject*, a *predicate* and an *object*. Since in the grammar the reasoner works on RDF datasets, we decided to adopt the same terminology used in RDF. The meaning of the premises is that the reasoner searches the RDF datasets for all the RDF graph which satisfy all the premises of a given rule. Each element of a premise can be one of the following:

- a variable (introduced by the symbol *?* as it is done in the SPARQL grammar);
- an IRI (starting with the symbol <, containing a URI an ending a > or alternatively a prefix followed by a local name);
- a BNODE (using the same syntax in RDF, a *_:* followed by a name), used when we are not interested in the particular value, we just need that it exists, as it is done in SPARQL;
- a SINGLEVALUE, which is a typed literal containing a number.

These premises can be optionally followed by zero or more filter constrains. In the grammar shown in Fig. 2, each filter is represented as being just a comparison between two elements to avoid possible confusion when reading it.

In the real grammar used by HORUS it is possible to define complex comparison using Boolean expression, so it is possible to have a filter which uses the *or* Boolean operator to join several simple comparison. See example later on.

The last part of each rule is the conclusion. When dealing with an inference rule, the conclusion contains one or more triples. These triples are used by the reasoner to know the RDF graph that can be inferred using the current rule. The syntax used by each conclusion is similar to the one used for the premises, because in both cases the reasoner is dealing with RDF triples. The variables used in the conclusion contain the value(s) bound by the reasoner during the inference process. In the retrieve phase of the inference process, the reasoner can retrieve more than one RDF graph which satisfy all the premises of the inference rule. The reasoner then iterates over all the retrieved RDF graphs, and, for each graph, it creates all the RDF triples by using the templates stated in the conclusion section of the rule.

When dealing with a consistency rule, the conclusion can only be *false*. In fact, if the reasoner is able to find at least one RDF graph which satisfies all the premises and the filters, then the ontology contains an inconsistency, so the reasoner generate no new RDF triples; it just needs to save the RDF triples which generated the inconsistency (or at least what has been labeled by the current rule as an inconsistency) to show them to user.

B. Inference and Consistency rules example

To better understand what is possible to achieve by using the previously described grammar, we provide a few real case rules. By first we present the content of a file containing two simple rules; then, we discuss a more complex rule which uses a filter to deal with cardinality restriction regarding the definition of a class; finally, we show an example of a consistency rule

```
type : new rule
name: Transitive
id: 1
premise: subject: ?p predicate: rdf:type object:
        owl:TransitiveProperty
premise: subject: ?a predicate: ?p object: ?b
premise: subject: ?b predicate: ?p object: ?c
conclusion: subject: ?a predicate: ?p object: ?c

type : new rule
name: Symmetric
id: 2
premise: subject: ?p predicate: rdf:type object:
        owl:SymmetricProperty
premise: subject: ?a predicate: ?p object: ?b
conclusion: subject: ?b predicate: ?p object: ?a
```

Figure 3. Two simple Inferemce Rule

1) Simple Inference rules

In the definition of an ontology, it is common to have a property defined as transitive and/or symmetric. The rules used for this particular task are shown in Fig.3. The first one, called *Transitive*, and identified by the id 1, consists of three premises and one conclusion. In the premises, we use the prefix and local name instead of the complete URI (while we suggest to use the complete URI to avoid any confusion). The first premise states that we are interested in all resources which have as one type the value *owl:TransitiveProperty*. We then need to find all the RDF triple of the form *?a ?p ?b* and *?b ?p ?c*, where ?p is bound to a resource (a property in this case) which is *owl:TransitiveProperty* and the variable *?b* of the second premise must bound to the same resources used with the variable *?b* of the third premise. At any iteration, the reasoner searches for any RDF graph which satisfies these three triples and for every graph it applies the conclusion. The reasoner searches for the graph not only in the original ontology, but also in all the inferred triples obtained in the previous application of the rules, so it combines both explicit and inferred knowledge. In this case, there is only one conclusion, *?a ?p ?c*, stating that this triple, where each of the variable is bound to the value found in the query execution phase, should be added to the inferred list of new triples. This triple (or these triples if more than one RDF graph was found) are added to the list of the inferred new triples only if the following two conditions are met:

- The new triples were not already represented in the original ontology;
- The new triple has not been already generated in a previous application of either this or other rules.

When adding a new triple, the reasoner stores the triples which were used in the inferred process, to show them in the log file and in a graph GUI to the user (see Section IV).

The other rule, called *Symmetric* and having id:2 is similar to the first one. Having two premises and one conclusion, it is searching for the resources having type *owl:SymmetricProperty*. It is important to notice that even if two rules share a variable with the same name (in this case the variables *?a , ?p* and *?b*) each variable has the rule itself

type : new rule
name: **ComplexSubClass**
id: 13
premise:subject:?p1predicate:rdfs:subPropertyOf
object: ?p2
premise: subject: ?class1 predicate: owl:equivalentClass
object: ?equiClass1
premise: subject: ?equiClass1 predicate: rdf:type
object: owl:#Restriction
premise: subject: ?equiClass1 predicate: owl:onProperty
object: ?p1
premise: subject: ?equiClass1 predicate: owl:minCardinality
object: ?card1
premise: subject: ?class2 predicate: owl::equivalentClass
object: ?equiClass2
premise: subject: ?equiClass2 predicate: rdf:type
object: owl:Restriction
premise: subject: ?equiClass2 predicate: owl:onProperty
object: ?p2
premise: subject: ?equiClass2 predicate: owl:minCardinality
object: ?card2
filter: ?card1 >= ?card2
conclusion: subject: ?class1 predicate: rdfs:subClassOf
object: ?class2

Figure 4. Complex Inferemce Rule

as its scope, so binding in a rule a variable to a particular value has no effect on the application of another rule.

2) Inference Rule with a Filter

We now describe a more complex rule using the filter after the premises. The idea behind this rule is that if a class *?class1* is defined as equivalent to a class having *minCardinality* on property*?p1* equal to *?card1* AND a second class *?class2* is equivalent to a class having *minCardinality* on property *?p2* equal to *?card2* AND if the value associated to *?card1* is greater or equal to *?card2* AND if the property bound to *?p1* is *subProperty* to the property bound to *?p2*, THEN we can infer *?class1* is a *subClass* of *?class2*.

This complex inference is represented by the rule written in Fig. 4, in which, to infer that a class is a subClass of another class, we need to analyze their restrictions. This rule is constituted by nine premises, one filter and one conclusion. The nine premises can be divided into three sets:

- The first one has just the first premise and regards two properties, *?p1* and *?p2* where *?p1* is a subProperty of *?p1;*
- The second one deals with the definition of a class, *?class1*, and its equivalent class, *?equiClass1*, which has a restriction regarding the *minCardinality*, having value *?card1*, on the property *?p1*. This second set is formed by 4 premises (from premise 2 to premise 5);
- The third and final set is equivalent to the second one, by replacing the variable with *?class2*, *?equiClass2*, *?card2* and *?p2*. Its premises are from premise 6 to premise 9.

The filter is used to check and compare the values of the two cardinalities. In this case the cardinality associated to the first class, *?class1*, is greater or equal to the cardinality associated to the second class, *?class2*.

type : new consistency rule
name: **Same_and_Different**
id: 6
premise: subject: ?a predicate: owl:sameAs object: ?b
premise: subject: ?a predicate: owl:differentFrom object: ?b
conclusion: false

type : new consistency rule
name: **MaxCard_consistency**
id: 12
premise: subject: ?x predicate: owl: maxCardinality
object: "0"^^xsd:nonNegativeInteger
premise: subject: ?x predicate: owl:onProperty object: ?p
premise: subject: ?u predicate: rdf:type object: ?x
premise: subject: ?u predicate: ?p object: ?y
conclusion: false

Figure 5. Consistency Rule

3) Consistency Rule

The three previously described rules highlighted what are the possible inferences that are possible in HORUS. Now, we discuss how to write a rule which is used to check if the ontology, and all the inferred RDF triples, violates any constraint. Fig. 5 contains two consistency rules.

The first one, named *Same_and_Different*, is used to check if there exist two resources (classes in this case) which are defined, or inferred, to be simultaneously *sameAs* and *differentFrom*. In such a case, there is obviously an inconsistency in the vocabulary used in the ontology, because two axioms are mutually exclusive.

The second rule is more complex, it states the presence of an inconsistency if a class *?x* has *maxCardinality* equals to 0 on property *?p* and then in the RDF dataset we have an instance of class *?x*, which has the property *?p*. In this second case as well, the only possible conclusion is *false*.

IV. REASONER USE AND RESULT VISUALIZATION

We now describe how to use HORUS and how to visualize reasoning results. Since it has been developed as a library, it will be invoked inside another tool. Two possible solutions have been developed:

- Inside a simple stand alone Java program;
- Inside a Semantic Turkey Extension.

In the rest of this section, we will describe how use the reasoner into Semantic Turkey framework.

Semantic Turkey [13][14] supports an ontology editor developed as an extension of the popular web browser Firefox [15] with a client/server architecture. One main feature is its extendibility, achieved by developing new extensions by using both Java plugin framework OSGi Felix [16] and the Firefox extension mechanism. Each Semantic Turkey extension consists of two part:

- A Java implementation, which extends the server side and is written completely in Java;
- A Firefox extension, written in JavaScript and XUL (client side) and responsible for the interaction with the user taking advantages of the Firefox GUI.

 ISBN: 978-1-61208-340-7

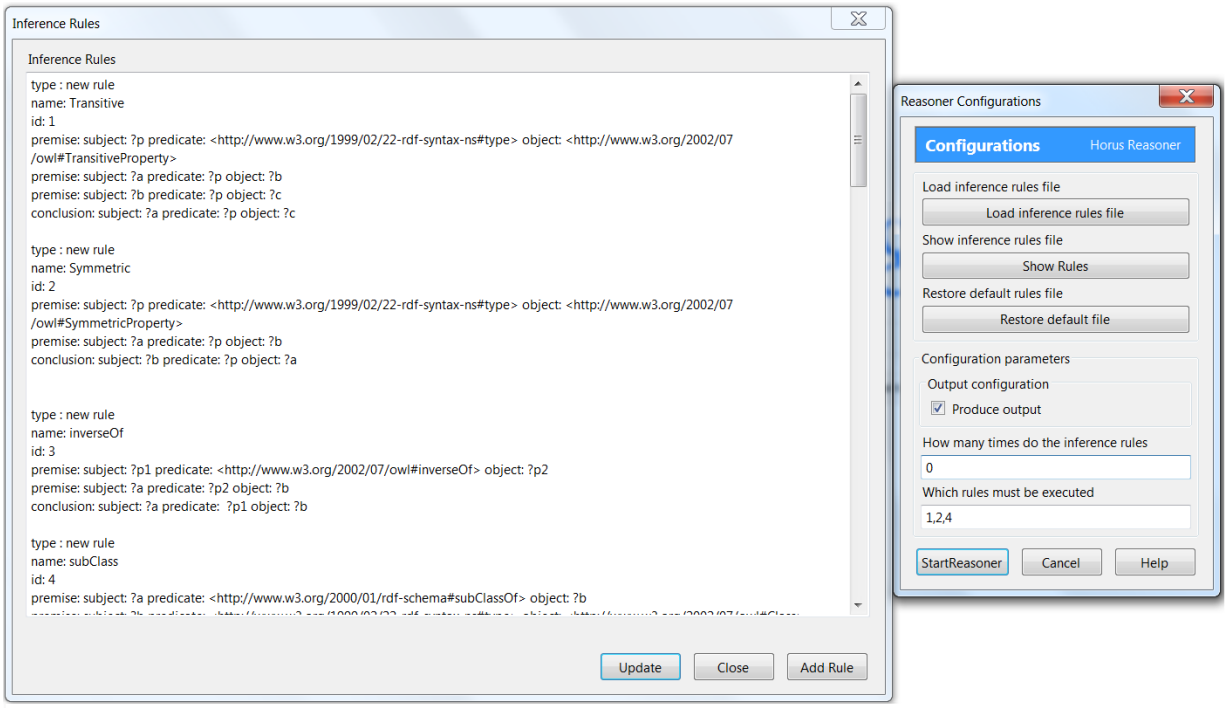

Figure 6. HORUS inside Semantic Turkey

HORUS was placed inside a Semantic Turkey extension, which can be download from [17] with its source code and the source code of the reasoner as well. Since the reasoner needs at least one inference rule to work, in the downloadable package, a file containing several working and tested inference rules is provided. In what follows, an evidence of configurable property oh HORUS is described.

When the reasoner is executed inside Semantic Turkey, the user has the possibility to decide which file containing the inference/consistency rule to load, which rule among them to use, how many iterations the reasoner should do (if it select 0 then the reasoner will stop only when no new knowledge can be inferred). An example of the presented GUI can be seen in Fig. 6. It is possible to write new rules using a dedicated GUI, which in the next release of the tool will provide a better assistance to the user for this task.

Once the user has selected which rule file to load and which rules to use, he can launch the reasoning process on the ontology currently managed by Semantic Turkey.

At the end of the reasoning, the inferred RDF triples are added in the current ontology in a different graph, which can be deleted at any moment by the user for several reasons (for example the ontology has changed and the inferred triples are no longer valid, because they cannot be derived from the new ontology).

The user is able to check all the inferred knowledge in two complementary ways:

- In the logger file, containing all inferred RDF triples with all the knowledge used to generate them and the name of the rule used in the process;
- in a graph, where each node is an RDF triple (explicit or inferred) and each link states which RDF triples were used to generate other triples.

An example of the result graph can be seen in Fig. 7. In this case, we have execute HORUS on a small ontology dealing with some geographical information about Lazio, a region in Italy. At the center of the graph, for example, we have the triple *Roma locatedIn Italia* generated using three (explicit) triples:

- LocatedIn type TransitiveProperty;
- Roma locatedIn Lazio;
- Lazio locatedIn Italia.

On the left side we have another triple, *Ariccia locatedIn Italia*, which has been inferred from the explicit:

- LocatedIn type TransitiveProperty;
- Ariccia locatedIn Roma.

and the previous inferred:

- Roma locatedIn Italia.

Finally, on the left side of the GUI in Fig. 7, we see a series of button that can be used to switch between the graph representation or the text one (the logging file) and to delete all the inferred triple (by deleting the RDF graph in the ontology in which they are stored). Using the GUI interface the user is also able to filter the results, to concentrate its attention to just a particular RDF inferred triple and the knowledge that was used to produce it.

The consistency rules are not shown in the graph representation, they are present only in the logging file.

V. CONCLUSION

In this article, we have presented a first implementation of HORUS, a new reasoner whose main features are:

- Possibility to write new inference and consistency rules by using an intuitive language based on some concepts of RDF standard and SPARQL filter;

 ISBN: 978-1-61208-340-7

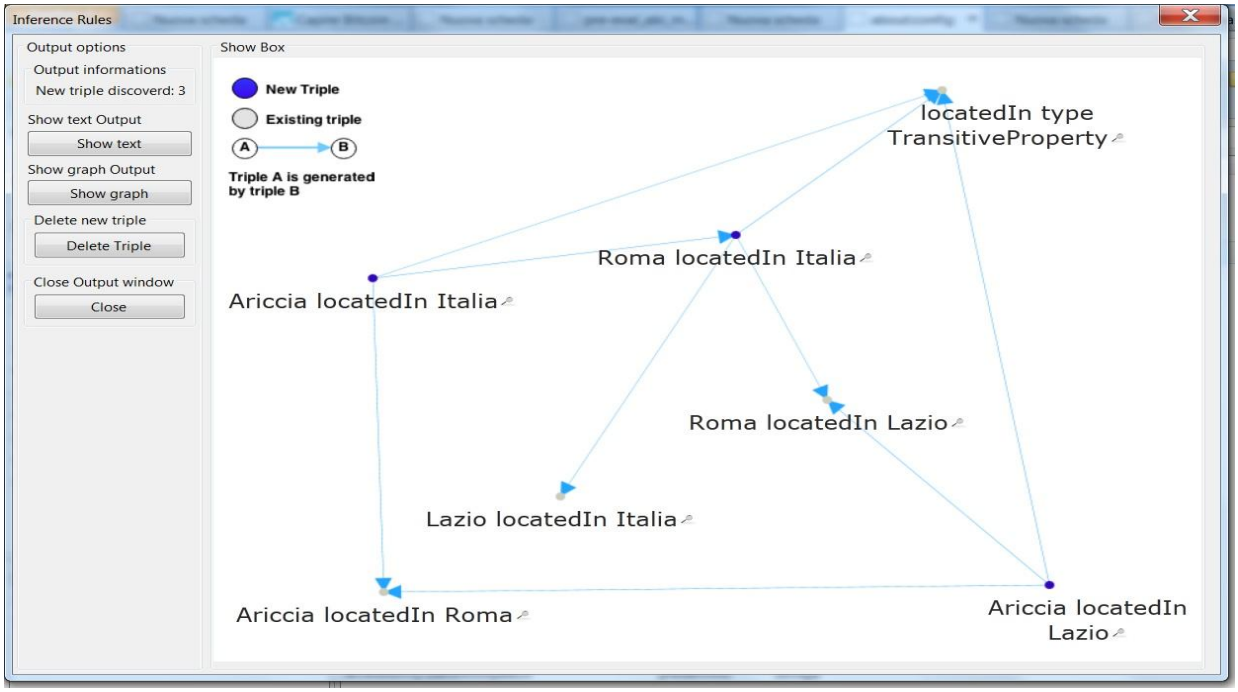

Figure 7. Inferred RDF triples in a graph

- Being aware of why each new triple was inferred by consulting a graphical representation or by reading a logging file containing all the motivations for each decision taken by the logger.

Possible applications are foreseen in context as:

- Educational use, to teach ontologies and inferences;
- Understanding why inferred triples were generated;
- Understanding which axioms should be changed or deleted in the ontology to prevent an undesired inference.

In fact, knowledge representation and reasoning techniques can be used for modeling background knowledge (e.g., in the form of ontologies) and to reason over them for logic-based verification.

REFERENCES

[1] W3C, Resource Description Framework (RDF), 2004. [Online]. Available: http://www.w3.org/RDF/ [retrieved: Apr, 2014]

[2] Description Logic Reasoners. [Online]. http://www.cs.man.ac.uk/~sattler/reasoners.html [retrieved: Apr, 2014]

[3] M. Horridge, J. Bauer, B. Parsia, and U. Sattler, "Understanding Entailments in OWL," in Fifth OWLED Workshop on OWL, Karlsruhe, Germany, 2008.

[4] J. Gennari, et al. "The evolution of Protégé-2000: An environment for knowledge-based systems development," International Journal of Human-Computer Studies, 2003, vol. 58, n. 1, pp. 89–123.

[5] E. Sirin, B. Parsia, B. C. Grau, A. Kalyanpur, and Y. Katz, "Pellet: A practical owl-dl reasoner," Web Semantics: science, services and agents on the World Wide Web, 2007, vol. 5, no. 2, pp. 51-53.

[6] Pellet FAQ: Single Page Version [Online]. http://clarkparsia.com/pellet/faq/single-page#rules [retrieved: Apr, 2014]

[7] SWRL: A Semantic Web Rule Language Combining OWL and RuleML. [Online]. http://www.w3.org/Submission/SWRL/ [retrieved: Apr, 2014]

[8] D. Tsarkov and I. Horrocks, "FaCT++ Description Logic Reasoner: System Description," in Proceedings of the Third International Joint Conference on Automated Reasoning, Seattle, WA, Springer-Verlag, 2006, pp. 292-297.

[9] A. Farmer, A. Gill, E. Komp, and N. Sculthorpe, "The HERMIT in the Machine: A Plugin for the Interactive Transformation of GHC Core Language Programs," in Proceedings of the 2012 Haskell Symposium (Haskell '12), New York, NY, USA, 2012, pp. 1-12.

[10] SPARQL Query Language for RDF. [Online]. http://www.w3.org/TR/rdf-sparql-query/ [retrieved: Apr, 2014]

[11] Official OWL ART API website. [Online]. http://art.uniroma2.it/owlart/ [retrieved: Apr, 2014]

[12] J. Broekstra, A. Kampman, and F. van Harmelen, "Sesame: A Generic Architecture for Storing and Querying RDF and RDF Schema," in The Semantic Web - ISWC 2002: First International Semantic Web Conference, Sardinia, Italy, 2002, pp. 54-68.

[13] M. T. Pazienza, N. Scarpato, A. Stellato, and A. Turbati, "Semantic Turkey: A Browser-Integrated Environment for Knowledge Acquisition and Management," Semantic Web, Jan 2012, vol. III, no. 3, pp. 279-292.

[14] Semantic Turkey Homepage. [Online]. http://semanticturkey.uniroma2.it [retrieved: Apr, 2014]

[15] Firefox Homepage. [Online]. http://www.mozilla.org/en-US/firefox/new/ [retrieved: Apr, 2014]

[16] Apache Felix Homepage. [Online]. http://felix.apache.org/ [retrieved: Apr, 2014]

[17] HORUS Homepage. [Online]. https://code.google.com/p/reasoner [retrieved: Apr, 2014]

 ISBN: 978-1-61208-340-7

An Ontology and Brain Model-based Semantic Discovery and Visualization System

Xia Lin, Mi Zhang, Yue Shang, Yuan An
College of Computing and Informatics
Drexel University
Philadelphia, PA, USA
{xlin, mz349, ys439, ya45}@drexel.edu

Abstract— **A system was built to let the user click on a location of a brain model to explore neuroscience ontology terms related to the location. The user can explore further the related terms and related documents through a visualization interface and learn new concept or document relationships derived from the ontology and annotated document collections. This paper discusses the semantic technologies used to build the system and introduces various features of the visualization interfaces. It concludes that semantic technologies can be integrated with visual brain models and ontologies to support visual semantic exploration and discovery.**

Keywords-Information visualization; Brain models for information retrieval; Semantic browsing; Neuroscience ontology; Visual interface design

I. INTRODUCTION

Ontology, modeling, and visualization are three knowledge representation techniques for neuroscience research. Their methodologies are related and complement to each other, but the connections among them are not so obvious. Ontology, as a formal language, seeks to explicitly define concepts and concept relationships for the purposes of concept retrieval, semantic concept lookup, concept linking, and semantic inferences [1][2]. Through the standardized classes, instances, and relationships, ontology helps facilitate data interoperability and provides linkages between research data and literature. The Neuroscience Information Framework Project [3] represents a good example of how comprehensive ontologies can unite a domain's literature, data, and research projects. Modeling, while mostly theory or data driven, seeks to represent complex natural systems (such as the neural system or brain) through mathematical or graphical models in order to reveal the most relevant relationships of the underlying data [4]. It can also help to define concept and concept relationships. Various brain map projects such as Talairach Atlas [5] and Allen Brain Atlas [6] are good examples of using models' layers, locations, and views to unify concepts, data, functions, and other relevant information [7]-[9]. Both ontology and modeling will be more effective if modern visualization techniques can be applied to them. Like ontology and modeling, visualization makes implicit relationships explicit. It takes advantages of human visual capability to allow users to explore and understand large amount of data and make visual inferences among the data [10]. It facilitates interaction with data and allows researchers to select different views or to zoom in to specific locations to explore data or concepts and their relationships.

To experiment how to bring ontology, modeling, and visualization together for interactive concept exploration and semantic discovery, a collaborative project funded by the U.S. National Science Foundation and several major industrial partners was carried out in the Center on Visual and Decisions Informatics (CVDI) in our university. In the following, we present a semantic discovery and visualization system we are implementing and discuss how a brain-model and ontologies have enhanced functionality of the system.

The rest of the paper is organized as follows. Section II provides an overview of the system with detailed descriptions of each system component. Section III discusses semantic technologies used to build the system. Section IV shows and discusses several visual interfaces of the system, and finally, Section V provides a summary of the project.

II. SYSTEM OVERVIEW

The main goal of the project is to create an innovative system for information retrieval and semantic discovery on neuroscience literature. With permission and support from the publisher Elsevier, we downloaded about 1 million documents related to neuroscience from hundreds of Elsevier's journals and books for this experimental system. Each of the documents includes full text of the documents and the metadata created by the publisher, both in XML format.

Through initial requirements analysis and discussion with neuroscientists, we recognized that ontologies, brain models, and visualizations should be the key considerations for the systems. The Neuroscience Information Framework (NIF) Standard Ontology was chosen for the project as it is considered both an ontology and an extended framework for concept-based indexing and retrieval [11]. The ontology composes of a collection of Web Ontology Language (OWL) modules covering distinct domains of bio-medical areas such as anatomy, molecule, disease, and organism, etc. The

 ISBN: 978-1-61208-340-7

ontology can be downloaded as OWL files and can be imported into Protégé, the popular ontology creation and editing tool [12].

While the ontology is well constructed and easy to download, the challenge we faced is how to annotate the very large neuroscience document collection (about 1 million documents) with this very large ontology (more than 108k classes). This is a scale-up issue of annotation. Thus the first component of the system we developed is an annotation tool called SemIntegrator, which can be used either through the APIs or through the Protégé interface.

We also learn that domain experts often need to work with both a comprehensive ontology and a specialized ontology most relevant to their own specialties. Thus, we include several specialized ontologies in the system also. Linking concepts in multiple ontologies, however, is another challenge we faced. The second component of the system is an ontology linking tool and a faceted-based interface that integrates two or more ontologies for searching, browsing, and exploration. A unique feature of the interface is to let the user search in one ontology and browse in another.

The third component of the system is an ontology-based visualization and exploration interface where one can click on a specific location of the brain map to find relevant terms from two or more ontologies and then click on the terms for searching and browsing. Details of the interface will be described in the later sections.

III. SYSTEM TECHNOLOGY

The core technology of our system includes semantic annotation, semantic integration, and semantic visualization, as shown in Figure 1.

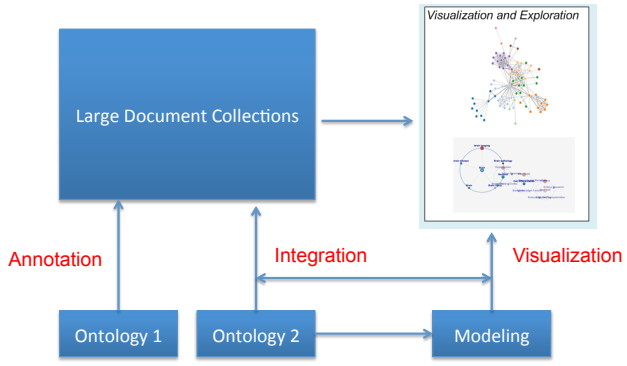

Figure 1. Overview of the semantic technologies used for the system.

A. Semantic Annotation

Our focus on semantic annotation is to apply information extraction techniques to identify in the documents all occurrences of ontology concepts and enrich the metadata of the documents with the identified concepts. An annotation component of our system was developed for this purpose. The component was first developed as a plugin of Protégé and then as a stand-alone Web service made available through Application Programming Interfaces (API). Protégé is an open source toolkit that can be used to build, alter and search ontologies [13]. It is extensible and offers API for researchers to work with ontologies in OWL format.

The annotation process we implemented involves several open-source packages (Fig. 2). First, Protégé is used to parse the OWL-formatted ontology files. Lingpipe [14] is then used to implement the term matching. The matching terms are saved into Trie, also called "prefix tree", which is a data structure used to improve search efficiency [15]. Chunk is an interface in Lingpipe that specifies a slice of a character sequence and used to match the article with terms in Trie. Levenshtein distance [16] is used here to calculate the similarity of two strings. The Levenshtein distance between two strings is the minimum number of single-character operation (three kinds of operation: insertion, deletion and substitution) that can change on string to the other.

Using SemIntegrator, we were able to process the whole Elsevier neuroscience document collection and, on average, 72 concepts are annotated for each document. In addition, a set of Java/Java-script modules was created to bridge those open-source packages and make them work together for the multiple ontologies and the document collections.

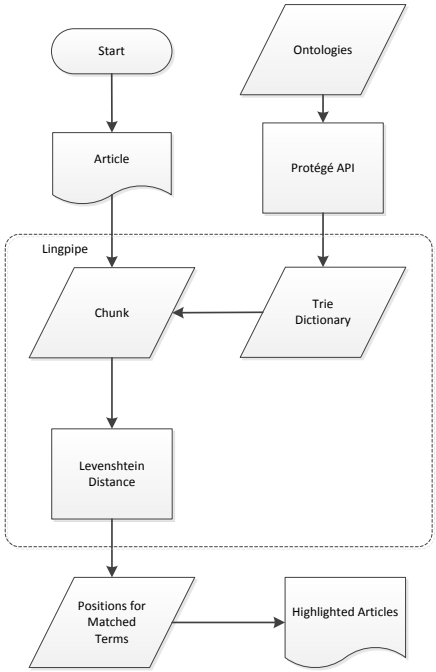

Figure 2. The overall process of semantic annotation.

B. Semantic Integration

Linking concepts in one ontology to concepts in another ontology is semantic integration [17]. In this project, we use SemIntegrator created in this project to annotate multiple ontologies to the same collection, and then use the collection as the bridge to link two or more ontologies. Here, we use an example to illustrate how it works.

 ISBN: 978-1-61208-340-7

Say a researcher is interested in exploring associations between human brain dysfunctions and brain structures. There are well-developed ontologies on each side, the Allen Brain Atlas Ontology [6] for brain structures and the NIF-Dysfunction ontology for brain dysfunctions. But, there are no direct associations between concepts in the two ontologies even though they are clearly related and the concepts often appear in the same documents. Using SemIntegrator, we can annotate documents with both ontologies and highlight the annotated concepts from each ontology with a different color (Fig. 3). This allows the reader to make associations among the concepts from different ontologies. From the highlighted result, the reader can quickly scan the article by reading terms highlighted in one color, say the term "Alzheimer's Disease," and find the correlated brain regions highlighted in a different color, such as the terms "degeneration in parietal lobe," "frontal cortex" and "cingulate gyrus" that show potential associations with "Alzheimer's Disease." The reader can further explore the unfamiliar terms such as "cingulate gyrus" through our visualization interface to find the correlation of this concept with other entities.

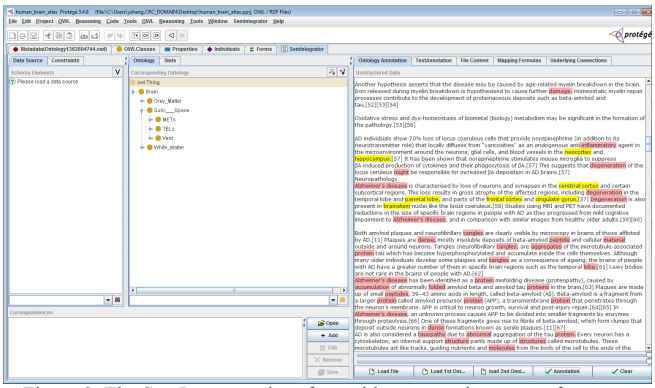

Figure 3. The SemIntegrator interface with annotated concepts from two ontologies highlighted in different colors.

Another way to realize semantic integration is through search engines. Our system uses the Apache Solr indexing service [18] to index the document collection after the metadata have been enriched with multiple ontologies. Since Solr is a facet-based indexing, each ontology could be treated as a facet and the user has the option of searching by a particular ontology and displaying terms of other ontologies. This creates a very useful function of linking related concepts from multiple ontologies and using them for searching and browsing. Fig. 4 shows an example of the Solr-based interface where both NIF ontology terms and the original Elsevier indexing terms related to the query are shown. The user can click on either type of term to narrow down search results or search in one type of the terms and browse through documents that have been annotated by another type of the terms.

C. Semantic Visualization

Visualization may be applied to neuroscience research in many different ways [10][19]. For this system, our focus is on semantic concept visualization, or visualizing knowledge structure of ontologies and document collections through meaningful concept displays [20]. One of the main advantages of ontologies is the rich concept relationships existed within the ontologies and the annotated document collections. Some of those relationships are explicitly defined. Some can be derived from their semantic relationships or co-occurrence relationships. Some can only be discovered through computational learning algorithms. These relationships essentially form a knowledge structure that can assist users in navigating and exploring both the conceptual space and the document space of the domain, particularly if the knowledge structure can be visualized in an interactive visual interface. In our system, we have implemented such an interactive interface with learning and visualization algorithms such as PFNet, D3.js, Gephi, and Sigma.js [21]-[24]. Details of the interface are described in the next section.

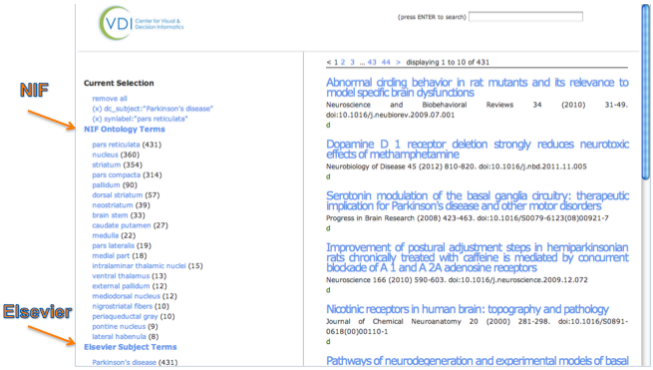

Figure 4. The search interface of the system that allows searching in one ontology and browsing in another.

IV. THE VISUALIZATION INTERFACE

The visualization interface is implemented to assist users in exploring semantic relationships among the concepts and let users follow the relationships for document browsing, exploration and discovery. Figure 5 (at the end of the paper) shows an example of the visualization interface.

The interface is divided into three main parts. The top-left is an interactive brain map, which consists of six areas of the human brain, including frontal lobe, parietal lobe, temporal lobe, occipital lobe, cerebellum and brain stem. Each of the brain area is filled with a different color. The user can zoom in or out the map by clicking on a specific brain area of the map. When a specific area of the map is clicked, a list of concept, function and dysfunction terms associated with that area will be shown in the bottom-left of the interface. This helps the user to quickly find concepts and functions related to a certain brain location.

When the user scans through the list of concepts, functions or dysfunctions, they can choose to explore any of them by clicking on a term to bring up either a hierarchical or associative concept display on the right-hand side of the interface. The hierarchical display visualizes the hierarchical structure of the ontology. The user can follow the visual display to see a concept's parent, children, or sibling terms.

 ISBN: 978-1-61208-340-7

Each of the terms on the visual display is also clickable – the user can click on any of them to expand the structure or show a new hierarchical structure.

The associative concept display shows concept relationships not based on the ontology itself but on the annotated document collections. On the display, the size of a node is decided by the frequency of the concept occurred in all the articles of the collection, and the color of the node indicates which brain part the concept is related to. The links and distance of nodes are based on the co-occurrence of the annotated terms in the whole corpus. Through Solr indexing, extensive computation was done to calculate the co-occurrence of any two concepts of the ontology in the collections of a million documents. When the user clicks on a term, the system will first select the top twenty concepts that have the highest co-occurrence frequencies with the term, and then generate a co-occurrence matrix of 20 by 20 for these 20 terms. The Pathfinder algorithm [21] is then applied to the matrix to generate a meaningful display of semantic relationships of the concepts.

Through the hierarchical and associative displays, the user will be able to explore concept relationships both in the ontology and the collections, and use them complementarily for their semantic exploration and discovery. Moreover, during the user's interaction with the visual interface, a search query is automatically generated and updated, and the number of search results is shown (on the bottom-left corner). The user can click on the results to retrieve relevant documents any time during the interactive exploration.

When the user moves from the concept space to the document space, he or she can also browse the document cluster map where each node is a document and each link indicates sharing of concept terms (Fig. 6). The cluster map was first generated using Gephi [23] and then used sigmajs [24] to provide interactive functions. By interacting with both the concept maps and document maps, the user can explore semantic relationships of terms and documents at both the global level (with all the documents) and at the detailed and focused levels.

V. SUMMARY

In this article, we presented a semantic discovery and visualization system that has two distinct features. One is the capability of annotating full text documents with concepts from multiple ontologies. The other is the set of visual interactive functions that link ontology concepts to a brain model for browsing and exploration. The system has showed promising results. The next step for us is to test and evaluate the system while continuously improving the implementation of the system. Through this paper, we hope to bring the attention of the research community to the central idea of the system: using ontologies, modeling, and visualization together to support semantic exploration and discovery.

ACKNOWLEDGMENT

This research was conducted at the Center for Visual and Decision Informatics (CVDI). The support of the Center's industrial members was gratefully acknowledged. Thanks in particular are due to the industrial member Elsevier who provides the data and feedback for this project. This research is also partially funded by the NSF IIP 1160960.

REFERENCES

[1] S. D. Larson and M. E. Martone, "Ontologies for neuroscience: What are they and what are they good for?" Frontiers in Neuroscience, 3(1), 60-67, 2009.

[2] Y. Le Franc, et al. "Computational neuroscience ontology: A new tool to provide semantic meaning to your models," BMC Neuroscience, 13(suppl 1), 2012, p. 149.

[3] NIF. Neuroscience Information Framework. http://neuinfo.org [retrieved: April 5, 2014].

[4] D. Sterratt, B. Graham, A. Gillies, and D. Willshaw, Principles of Computational Modelings in Neuroscience, Cambridge University Press, 2011.

[5] BrainMap. http://brainmap.org. [retrieved: April 5, 2014].

[6] Allen Brain Atlas. http://www.brain-map.org/ [retrieved: April 5, 2014].

[7] A. P. Alivisatos, M. Chun, G. M. Church, R. J. Greenspan, M. L. Roukes, and R. Yuste, "The Brain Activity Map Project and the Challenge of Functional Connectomics," Neuron, vol. 74 (6), June 2012 , pp. 970-974.

[8] A. R. Laird, J. L. Lancaster, and P. T. Fox, "BrainMap," Neuroinformatics, 3(1), March, 2005, pp.65-77.

[9] A. R. Laird, et al., "The BrainMap strategy for standardization, sharing, and meta-analysis of neuroimaging data," BMC Research Notes, 2011, 4:349.

[10] Emilio Badoer, (ed.) Visualization techniques: From Immunohistochemistry to Magnetic Resonance Imaging (Neuromethods). Humana Press, 2012.

[11] D. Gardner, H. Akil, G.A. Ascoli, and D. M. Bowden, "The Neuroscience Information Framework: A Data and Knowledge Environment for Neuroscience," *Neuroinform*, 2008, pp. 149–160.

[12] D. Rubin, N. Noy, and M. Musen, "Protégé: A Tool for managing and using terminology in radiology," *Journal of Digital Imaging*, 2007, pp. 34-46.

[13] Protégé, "Protégé: A open source ontology editor and knowledge-base framework," Available at: http://protégé.stanford.edu [retrieved: April 5, 2014].

[14] Alias-I, "LingPipe 4.1.0." http://alias-i.com/lingpipe [retrieved: April 5, 2014].

[15] J. Bentley and R. Sedgewick, "Ternary search trees," Dr. Dobb's Journal, April, 1998.

[16] D. Hirschberg, "Serial computations of Levenshtein distances." In A. Apostolico and Z. Galil (eds.), *Pattern matching algorithms*, pp. 123 - 141. Oxford University Press, 1997.

[17] N. F. Noy, "Semantic integration: a survey of ontology-based approaches," *SIGMOD Rec.* 33(4), 2004, pp. 65-70.

[18] Apache Solr, "Apache Solr: open source enterprise search platform," Available at: http://lucene.apache.org/solr/ [retrieved: April 5, 2014].

[19] P. Mutton and J. Golbeck, "Visualization of semantic metadata and ontologies," Proceedings of the *Seventh International Conference on Information Visualization," 2007,* pp.300 – 305.

 ISBN: 978-1-61208-340-7

[20] X. Lin and J. Ahn, "Challenges of knowledge structure visualization," Classification & Visualization: Interfaces to Knowledge, Proceedings of the International UDC Seminar, October 2013, pp 73-87.

[21] R. W. Schvaneveldt, Pathfinder Associative Networks. Westport, CT, US:Ablex Publishing, 1990.

[22] M. Bostock, V. Ogievesky, and J. Heer, "D3: Data-driven documents," IEEE Transaction on Visualization and Computer Graphics, 17(12), Dec. 2011, pp. 2301-2309.

[23] Gephi, "Gephi, an open source graph visualization and manipulation software," Available at: https://gephi.org/ [retrieved: April 5, 2014].

[24] SIGMAJS. "Sigma.js: an open-source lightweight javaScript library," Available at: http://sigmajs.org/ [retrieved: April 5, 2014].

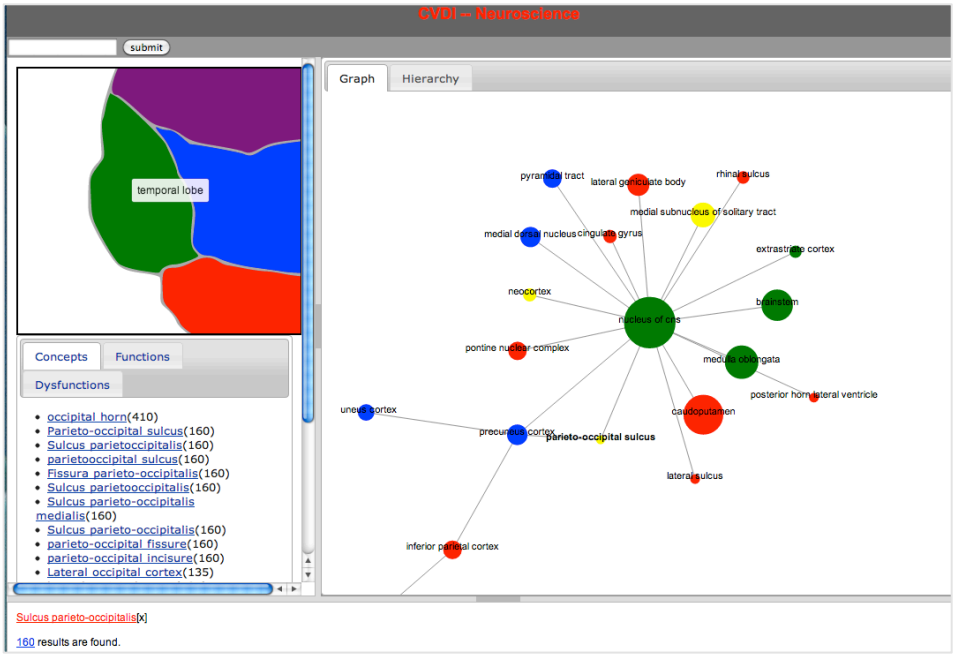

Figure 5. An example of the model-based interface and associative concept maps.

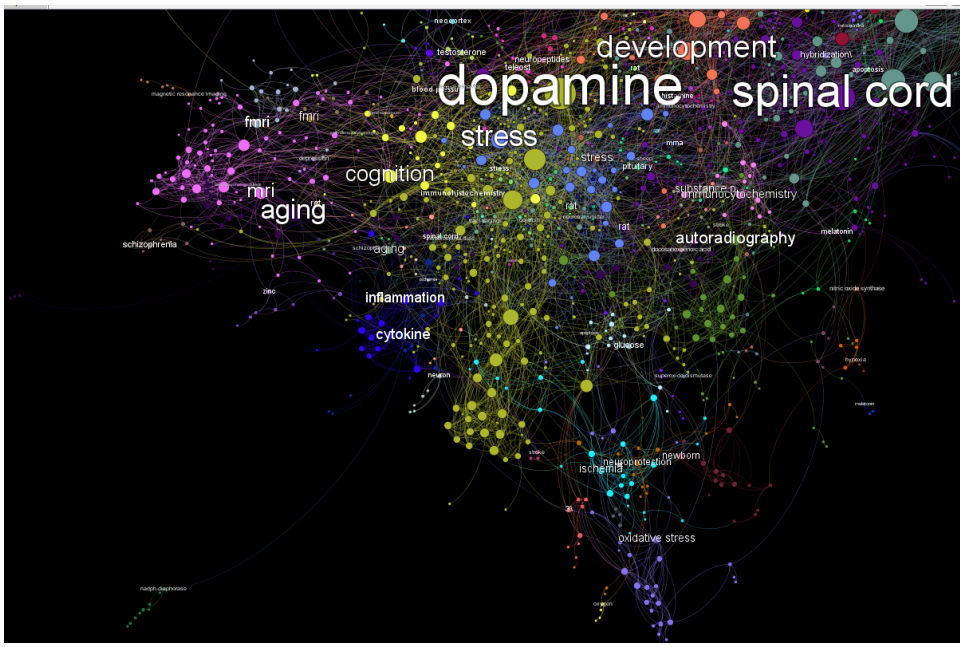

Figure 6. An example of the grobal mapping based on the relationships of the annotated concept terms over the whole collection.

Linked Closed Data Using PKI: A Case Study on Publishing and Consuming data in a Forensic Process

Tamer Fares Gayed, Hakim Lounis
Dépt. d'Informatique
Université du Québec à Montréal
Succursale Centre-ville, H3C 3P8,
Montréal, Canada
gayed.tamer@courrier.uqam.ca lounis.hakim@uqam.ca

Moncef Bari
Dépt. de Didactique
Université du Québec à Montréal
Succursale Centre-ville, H3C 3P8,
Montréal, Canada
bari.moncef@uqam.ca

***Abstract*—The main aim of the Linked Open Data (LOD) project is to publish data publicly without access restriction in order to be consumed upon Unified Resource Identifier (URI) resolution. The latter provides more description about the resources being represented through the resolvability and discoverability of more others resources. Sometimes, data/resources need to undergo an access restriction to be consumed only on a small scale for keeping its confidentiality. However, while the power of the LOD resides in the resolvability of more URIs related to the resources in hand, a curious question imposes itself: how can we achieve a compromise between URI resolvability and access restriction? This paper discusses how the represented data cam be secured. It illustrates how the Public Key Infrastructure (PKI) can be applied to restrict the access to confidential resources of represented data being published using the Linked Data Principles (LDP), while maintaining the resolvability of such restricted resources. This brings out a new era of research related to the counter part of LOD, a research topic called the Linked Closed Data (LCD). A good example to elaborate this compromise question is a case study retrieved from the Cyber Forensics (*CF*) field where the tangible Chain of Custody (*CoC*) is represented using the LDP to exploit the resolvability feature of such principles on different resources of the Electronic-*CoC* (*e-CoC*). The latter should also obey an access restriction in order to be shared only between role players who published the data and juries who are going to consume it.**

Keywords-Linked Open Data; Linked Data Principles; Linked Closed Data; Public Key Infrastructure; Digital Certificates, Cyber Forensics, Chain of Custody.

I. INTRODUCTION

The classical way for publishing and accessing documents in the World Wide Web (WWW) [12] is through hypertext links, which allow users to navigate over the Hyper Text Markup Language (HTML) documents using browsers and search engines [1].

Today, the WWW has radically altered the way to share information [15]. The interrelation is not just between documents but it has evolved to also link the data within these documents (i.e., Linked Data-LD), using the same web aspects (URI [13], Hyper Text Transfer Protocol-HTTP [2]). Thus, the HTTP URIs are used not only to identify web documents but also real objects and abstract concepts in the world, the fact that allows the latter to be dereferenceable/resolvable (i.e., it means that HTTP clients can look up the URI using the HTTP and retrieve a description of the resource that is identified by this URI).

While the primary unit of the hypertext web are the HTML connected by untyped hyperlinks, the LD uses the Resources Description Framework (RDF) [3] to link such data using typed statements allowing arbitrary link of things (i.e., resources) in the WWW. The web aspects are then called the technology stack or LDP, which encompasses three components: URI, HTTP, and RDF [14]. The most visible project using this technology stack is LOD [20][4]. This project and its derivative [27] attracted the interest of many researchers of the data cloud to construct several cloud-based LD management systems [24][25][26].

Generally, the LOD aims to bootstrap the web of data by identifying existing data sets that are available under open licenses [17] (i.e., converting them to RDF according to the LDP, and publishing them publicly on the Web). The openness (i.e., no license and no access restrictions) and resolvability of resources are two likely factors in the success of this project.

The knowledge representation concept has been persistent at the centre of the field of Artificial Intelligence (AI) since its founding conference in the mid 50's. This concept is described by Davis & al. with five distinct roles [43]. The most important role is the definition of knowledge representation as a surrogate for things. In this paper context, the *e-CoC* is constructed through the LDP as a surrogate of the tangible one. Later, the resources of *e-CoC* will be then consumable by humans and machines.

However, several times, URI/URL resources need to obey some access restriction, where a specific set of people are those who are authorized to access such resources. LDP should be bended to realize the adaptation of publishing and consuming the resources on a small scale without loosing the resolvability feature of these resources. Thus, a compromise question arises in this case, how we can realize the access restriction over certain URI/URL resources while keeping the resolvability feature of the same resources. In addition, this question brings out a new era of research called the LCD [20], where the publisher would take step of imposing access restrictions to protect his information [21][7] from anonymous consumption. A very good example to elaborate this idea, is a case study retrieved from the CF field, where the tangible *CoC* is represented using the LDP (i.e., the work

 ISBN: 978-1-61208-340-7

in [7], listed all the advantages of using LDP to represent tangible *CoC*). As well, this work explained in a theoretical way, how the represented resources could obey an access restriction using PKI. The framework depicted in [7] provides a PKI layer, which explains how the represented resources can be shared between role players and the juries. Current paper will not only explain how this scenario can be implemented and applied, but it is also considered as a bridge connecting two recent works; the work published in [19] and [21].

The work provided by Rajabi et al. in [19], explained theoretically how PKI is used to achieve the trustworthiness of LD and how different datasets are exchanged in a trusted way. The work provided by M. Cobden et al. in [21], outlined in a vision paper, the need to have an access restriction on the LOD. Each work apart does not provide the complete picture to realize the LCD using PKI. In [19], the work explains how the PKI can be used to secure the resources of LD, but did not put the scope on how such stuffs can be implemented and applied, and how this work can bring out a new era of research related to the counter part of LOD (i.e., LCD). However, in [20] the work outlined the need of the LCD in certain domain (e.g., business and finance), but did not refer to the PKI solution, or how the LCD can be realized. Thus, this paper complements and completes the half picture of both works, by explaining how the PKI and digital certificates are used to restrict the access of resources in the LD cloud while keeping the resolvability of such resources, and then resulting the LCD.

This paper is organized as follows: the next section, discusses the state of the art of URI identifications, the LOD Project, PKI and Digital Certificates, and *CoC* in CF. Section 3 explains in a linked data manner, how PKI is applied to LOD. Section 4 provides methodology and experimentation explaining how the digital certificates can be used to share LD resources between the role player and juries. Finally, last section summarizes and concludes the depicted work.

II. STATE OF THE ART

A. URI Identifications

URI is a string of characters used to identify a name or a web resource. URI and HTTP are the two essential technologies of the web upon which the LD relies on. As mentioned in the last section, we use URI to identify any entity that exists in the world. On the web, any URI is always accompanied by the HTTP, which makes the entity being represented, deferenceable/resolvable to more resources. Both technologies were integrated with HTML to structure and link web documents. Nowadays, the data presented in these documents are integrated with the RDF to structure and link different data and resources.

An RDF consists of three slots called triple: resources/subject, properties/predicate, and objects. In addition, resources are entities retrieved from the web (e.g., persons, places, web documents, pictures, abstract concepts/resources, etc.). RDF resources are represented using URIs, of which URLs are subset. Resources have properties (attributes) that admit a certain range of values or can be attached to another resource. As well, the object field can be also a literal value or a resource [16].

The essential thing to publish data is to have a unique domain/namespace minted by a unique URL owned by the publisher [14] (e.g., [38], where "*mydomain*" is a unique namespace in the WWW space) and the URI HTTP are used to relate and identify objects and abstract concepts, thereby maximizing the discoverability of more data/resources. Therefore, a common practice called contents negotiating is used by an HTTP mechanism [2] that sends HTTP headers with each request to indicate what kinds of documents are requested (i.e., is it an HTML or RDF content). The receiver (i.e., the side that receives the HTTP request or Server) can then inspect these headers and select an appropriate representation of resources. The content negotiation uses two different types of URIs [13][44][45]:

- **303 URIs (known as 303 redirect):** the server redirects the client HTTP request to see another URI of a web document, which describes the concept in question. First, HTTP request is triggered for the initial request and the second is triggered when the request is redirected to the retrieval of the appropriate format.
- **Hash URIs:** this type avoids two http requests used by the 303 URIs. Its format contains the base part of the URI and a fragment identifier separated from the base by a hash symbol. When a client requests hash URI, the fragment part is stripped off before requesting the URI from the server. This means that the hash URI does not necessarily identify a web document and can be used to identify real-world objects.

Using the first type of URI, publisher publishes in his own server (i.e., his own domain) the description of any concept using two types of representation: HTML documents containing a human readable representation about a concept, and RDF documents about the same concept. Publisher can also use three different patterns to describe a resource (e.g., resource 'x') [18]:

- URI identifying resource 'x' itself [35].
- URI identifying the serialized RDF document (i.e., RDF/XML [10], Turtle document [11] or N3) describing resource 'x' [36].
- URI identifying the HTML document describing resource 'x' [37].

Using the second type of URI pattern, publisher can define different resources and use then the Hash URI to serve an RDF/XML file containing the definition/terminology for each resource.

B. Linked Open Data Project

After the resources are represented and identified using URIs, they will be connected using RDF links, creating a global data graph that spans data sources and enable the resolvability of such resources to a new data source. The LOD cloud project has been constructed upon this basic structure (see Figure 1).

Thus, the LOD is based on the LDP, where URI resources are linked using typed RDF links to other resources within the same or to other data set. Two types of links can be used; links to navigate forward and others to navigate backward between resources.

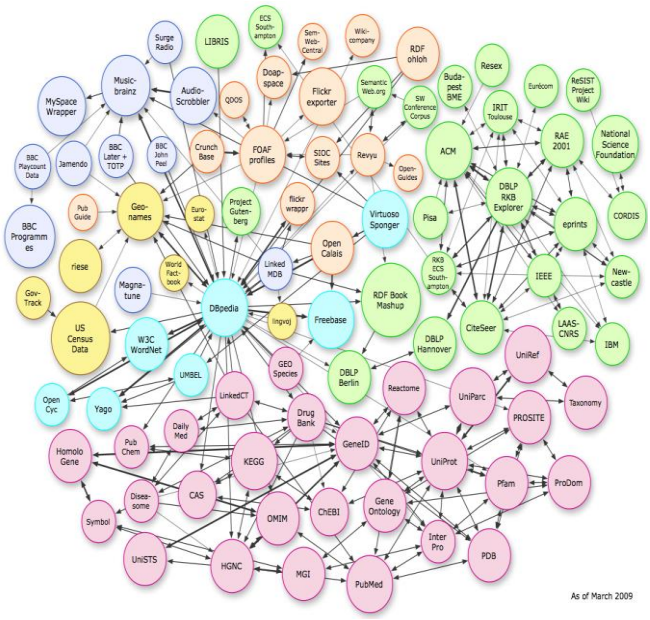

Figure 1. Linking open data cloud diagram

For example, if we have an RDF triple connecting two resources x and y, and we need to move forward from x to y, then this RDF triple should appear in the document describing the resource y. This triple is then called incoming link because it allows to navigate back to resource x. Same case, for the outcoming link, where the RDF triple should appear in the document describing the resource x and allows to navigate forward to resource y [9]. Figure 1 shows the LOD cloud diagram, where each links exists between items in the two connected data sets. Some data sets are connected together using whether, the outcoming links, the incoming links, or both.

C. PKI and Digital Certificates

PKI is a combination of softwares and procedures providing a mean to create, manage, use, distribute, store, and revoke digital certificates [47][48][49][50][51][52]. PKI called Public Key because it works with a key pair: the public key and the private key

A digital certificate is a piece of information (e.g., like a passport) that provides a recognized proof of a person/entity identity. It uses the key pair managed by the PKI to exchange securely the information in order to create trustworthiness between data provider and data consumer in a network environment [5] (i.e., trustworthiness occurs when receiver ensures the identity of the sender. This is called non-repudiation).

Any certificate contains (see Figure 2) the identity of the certificate owner, such as distinguisher's name, and information about the CA (issuer of certification), such as CA's signature of that certificate, and general information about the expiration and the issue date of that certificate [6]. Digital certificate alone can never be a proof of anyone's identity.

A third trusted party is needed to confirm and sign the validity and authority of each certificate and share securely the cryptographic key pair. This party is called Certification Authority (CA).

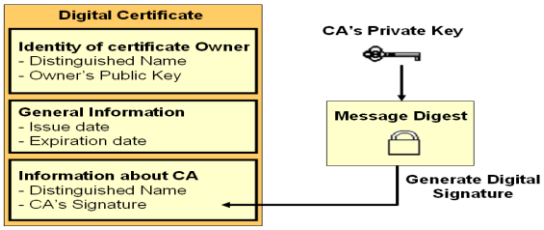

Figure 2. Digital certificate

Since a CA (e.g., VeriSign Inc., Entrust Inc., Enterprise Java Bean Certificate Authority-EJBCA, etc.) relies on public trust, it will not put its reputation on the line by signing a certificate unless it is sure of its validity, the fact that makes them acceptable in the business environment. All digital certificates provide the same level of security, whether they are created by a well-known issuer, or by unknown one. Usually, the information providers request their certificates from well-known parties when they provide services and information with large segment in society. In this paper, the authors imitate the issuer party and create CA certificate instead of buying it from well-known trusted party.

Before going further in how to adapt the digital certificates to the LD, this section should simply underline some important points related to the digital certificates:

1) Purposes

A digital certificate has various security purposes and can be used to [47]:

- Allow only the authorized participant (sender/receiver) to decrypt the encrypted transmitted information (i.e., encryption).
- Verify the identity of either sender or recipient (i.e., Authentication).
- Keep the privacy of transmitted information only to the intended audience (i.e., privacy/Confidentiality).
- Sign different information in order to ensure the integrity of information and confirms the identity of the signer of such information (i.e., digital signatures). Digital signatures also solve the non-repudiation problem by not allowing the sender to dispute that he was the originator of the sent message.

2) Protocols

In the field of Information and Communication Technology (ICT), the digital certificate is called SSL/TLS certificate because it uses two essential protocols; the SSL and the TLS [22]. The Former is the short version of the Secure Socket Layer. This protocol is used to describe a

 ISBN: 978-1-61208-340-7

security protocol underlying a secure communication between a server and a client. After upgrading this protocol with some encryption standards, the protocol got another acronym called TLS, which is standing for Transport Layer Security. Both protocols are based on the public key cryptography [7]. They are used to establish a secure connection over the HTTP. Classically, the HTTP establishes an unencrypted connection without using the SSL and TLS (i.e., if there is some intruder around monitoring the communication between server and client, he can come with all plain data packages of such transferred data). HTTP is then extended to HTTPS to secure the connection and encrypt all the transferred data with the SSL (i.e., HTTP + SSL/TLS = HTTPS) [46].

3) Creation Phases

The creation of a digital certificate passes by four phases (see Figure 3) using the OpenSSL tool [8]. First step, the requester (client/server/CA) generates his own pair of keys (i.e., key file), then he creates a request (i.e., req or csr format file) to the trusted party to issue for him/her a certification (i.e., crt format file). The trusted party (i.e., CA) signs the request and issues the certificate using his own private key (i.e., when the CA is the requester of the certificate, then this certificate is considered a self-signed certificate/root certificate). The created certificate is then transformed to an exportable format (i.e., p12 format) for sending it to the requester.

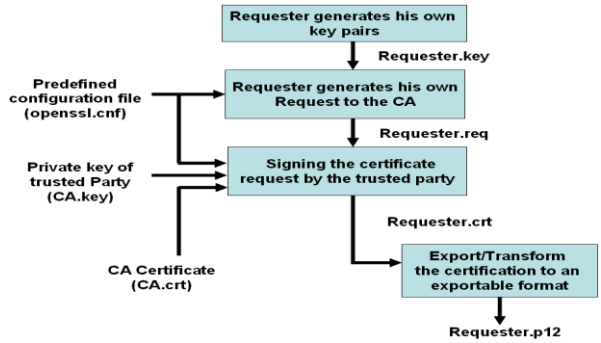

Figure 3. Procedures for creating a digital certificate using openSSL tool

4) Types and Exchange

There exist three types of digital certificates. Figure 4 presents an abstract scenario where Alice and Bob want to share information over a secure connection (i.e., HTTPS).

Firstly, Alice and Bob should determine a third trusted party called the CA. The latter is responsible to issue SSL/TLS certificates for both of them in order that each can identify himself/herself to the other. CA issues two types of certificates.

- **Server certificate***:* this certificate is issued by the CA and it is used by Alice (i.e., suppose that she is the owner of the information) to identify herself to her authorized clients, like Bob. When Bob tries to access this server, he will be sure that he accessed the right server. Otherwise, Bob will not trust Alice information.

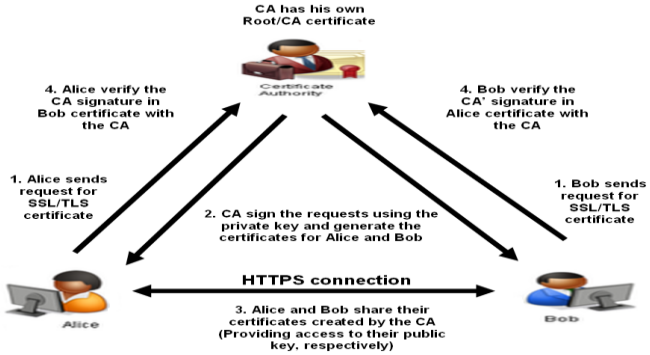

Figure 4. Sharing SSL/TLS certificates

- **Client certificate**: the CA issues this certificate, and it is used by Bob (i.e., suppose he is the consumer of Alice' information) to identify himself to Alice Alice will not allow any one to access her information unless he has a certificate known by her.
- **CA certificate:** CA also has the own certificate to sign the certificate requests received from the clients and servers. In addition, this type of certificate answers the question of how Alice and Bob ensure the identities of each others. Alice would know that Bob is the right person by verifying that his certificate is signed by the common trusted part authority (CA), as well as for Bob. Both know each others through the CA certificates.

From the definitions mentioned above, we notice that there is no distinguishable difference between the server certificate and the client certificate; both use the certificates to identify themselves to the other. However, the only difference that distinguishes both is about who is providing the information and who will go to consume it.

D. Chain of Custody in Cyber Forensics

Digital forensic is a technique for acquiring, preserving, examining, analyzing, and presenting digital evidences to the court of law. *CoC* is a chronological document that accompanies these evidences along the investigation process in order to avoid later allegations or any tampering attempt in such evidences. It provides useful information by answering 5 Ws and 1 H questions. The 5 Ws are the When, Who, Where, Why, What and the 1 H is the How.

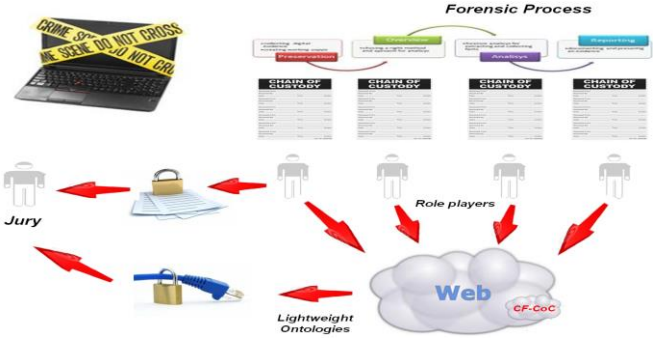

Figure 5. Abstract scenario of tangible and electronic *CoC*

According to the literature, CF includes different forensic models [19][21][26][28][32][33], each model containing a set of forensics phases, where each phase is accompanying by a tangible *CoC* describing all forensic tasks (see Figure 5).

Classically, any crime scene should obey an investigation process using a forensics model. Role player of each phase prepares his *CoC* describing all investigation tasks performed in this phase. Later, each role player submits the *CoC* securely to jury in a sealed envelope.

The work published in [7] depicts the need to transform such *CoCs* from documents to electronic data. This work proposed a framework to construct a *CF-CoC* web application hosted somewhere on the web cloud (i.e., domain known by role players and jury, e.g., [39]). The role players can use this application [7] to generate lightweight ontologies using RDF schema (RDFS) [42], representing each phase in the forensic model. Each lightweight Ontology (i.e., with big 'O') contains a set of build-in terms (i.e., retrieved from the semantic web) and custom terms (i.e., created by the role players) describing all the tasks and procedures of this phase. As the represented information should not be published publicly, the framework proposes a PKI layer that protect and foster the published information only between the role players (i.e., who published the data) and the juries (i.e., who will go to consume such data). This layer ensures the identities and authorization of all players in a forensic process.

III. ADAPTING PKI TO LOD

In this section, we will discuss how digital certificates can be applied to LOD to publish and consume data on a small scale. In other words, this section describes how digital certificates are used to restrict the access of certain resources and at the same time, such resources will be resolvable to more resources.

Referring to Figure 1 of the linking open data cloud diagram, we find several data sets interrelating using outer and/or inner links. Each data set is published in a unique domain owned only by the publisher of this data set over the WWW space. Each data set contains set of URI resources that are interrelated between each other, within the same data set or to an outer data set.

Now, imagine that the owner of a data set wants to publish resources using the technology stack/LDP of the LD (URI, HTTP, and RDF) and having such resources resolvable within the LOD cloud, but at the same time, he wishes to publish them in a manner that any anonymous parties on the web space cannot access them.

The idea to realize both features at the same time (i.e., resolvability and access restrictions of resources) resides in the digital certificates. The latter can be used to restrict the resolvability of resources in a one-way manner. With other words, the resources are restricted using digital certificates to be forward resolvable, but not backward resolvable unless the owner of such resources specify and list his authorized clients existing outer of his domain to access his resources. Same concepts can be applied between data sets/resources in the LOD cloud, where each data set owns a digital certificate(s). Thus, publisher of the resources can accomplish his publication task through an enhanced technology stack using a secure access protocol (i.e., HTTPS). Therefore, the current technology stack is transformed from (URI, HTTP, and RDF) to (URI, HTTPS, and RDF).

Imagining a scenario will be as follow: assuming that the publisher (server) and consumer (client) of the LD have already a common trusted party to issue their certificates. The publisher has a domain name named by an IP [40] (i.e., for simplicity consider this IP is corresponding to a domain string name in [39]) to publish his resources in the LOD cloud. The publisher of this domain wants only someone called: 'Jean-Pierre' to consume his resources from his domain within the LOD cloud. In this case, the publisher of the data has restricted the access to his resources to a specific consumer, but he is still able to dereference his resources and resolve them to retrieve more resources outside his dataset/domain. Publisher will be also able to move back to his domain using the backward link, because he owns the server certificate for this domain. Any other anonymous party outside this domain will not be able to access the resources of [39]. If the publisher wants someone else rather than 'Jean-Pierre' accesses his resources, this person should have a client certificate signed by the same trusted party.

Talking in a linked data manner, we can not only consider the client side as a person (i.e., as Jean-Pierre to access restricted resources), but the client side can also be a dataset or a resource within a data set that can access other resources in another data set using outer links (i.e., by moving backward to the publisher resources). In addition, another important point should be underlined; Jean-Pierre/dataset/resources can react also as a server side, if we look to the picture from the inverse direction.

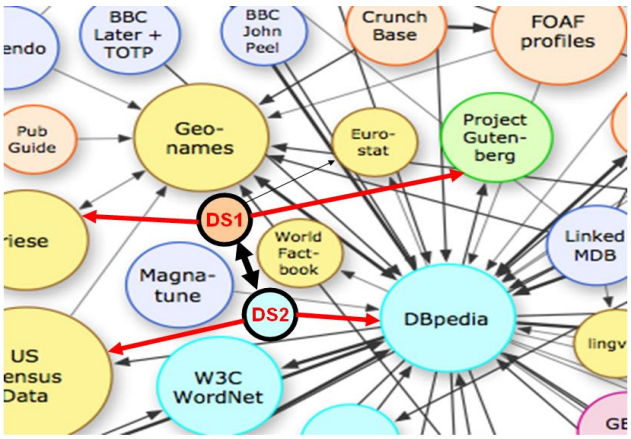

Figure 6. Client/Server certificate between two data sets

Thus, Jean-Pierre/dataset/resource may have also a server certificate for his/its domain and allows the access to only people/dataset/resource that has a client certificate to his/its domain.

To illustrate this idea, Figure 1 of the LOD cloud is zoomed-in, resulting in Figure 6. Let us consider that we have two data sets DS1 and DS2 residing in two different

domains. Each domain represents a data set. Both of them are interrelated between each others using inner and outer links. As well, both data sets are related with other data sets in the LOD cloud.

DS1 and DS2 can be client and server at the same time. If we look from the DS1 to DS2, we will see an outer link from DS1 to DS2 and vice-versa. DS1 is considered as a client trying to access the server DS2. Thus, DS1 will have a client certificate for its domain to identify itself to the server certificate installed in the DS2 domain. Now, let us consider if we have the contrary view; DS2 should has then a client certificate to access the server DS1 resources. However, for any other data sets around the scope of DS1 and DS2, they will not be able to resolve their resources with resources from DS1 and DS2 (i.e., at this time, DS1 and DS2 act as servers and requires client certificates from their surrounded data sets). Therefore, the resources of DS1 and DS2 have access restriction while their resources are resolvable with different resources from the LOD cloud, but the latter cannot resolve their resources from the two data sets, DS1 and DS2.

Furthermore, the certificates cannot only used on the level of datasets (i.e., including all resources), but can also be issued on the level of a specific resource within the datasets. This can be realized by issuing the certificate using one of the three URI patterns provided in section 2.

IV. METHODOLOGY

This section explains how the digital certificates are created, installed, and used over a LD set. The experimentation is applied on a scenario between a role player and the jury to share LDP resources. This scenario is explicit. The server part is the side where the *CF-CoC* web application is hosted and owned by jury (i.e., we can see the jury as a provider, because he owns the *CF-CoC* application on his server, at the same time he is a consumer, because he will consume the data that will be published by the role player). The client part is the role player, who will use the *CF-CoC* web application to define, create, and publish the resources over this domain (i.e., we can see the role player as a consumer, because he uses the *CF-CoC* application, at the same time he is a publisher, because he will publish the data to jury using the *CF-CoC*). Role players and juries request digital certificates from the CA. The role player must have a client certificate to identify himself to the server. Jury can be also considered as a client to his server when he will consume such published data. Because jury owns a server certificate, he does not need to have another client certificate to consume the published resources (i.e., the case when the server requires a client certificate takes place when the server acts as a client to access another server. In this case, a client certificate is needed by the first server to access the second server). In our case, we have only one server [39] where the data is published and consumed.

In addition, the server provides to the CA, beside his certificate request, a list containing the names of all role players who are authorized to participate in the current forensic case.

A. Work Environment

The operating system used in this experimentation is Windows XP, accompagning with the Internet Information Services (IIS) [34] and the OpenSSL tool [8]. IIS simulate the machine as a server, and the OpenSSL tool is used to create the digital certificates.

1) Internet Information Services (IIS):

It is a group of internet web servers created by Microsoft. It includes two main protocols; the File Transfer Protocol (FTP) and HTTP. When installing the IIS on a machine, the web application on this machine considered as a visual basic application that lives on web server and responds to requests from the browser by processing into HTML interface code result.

2) OpenSSL

This tool implements the SSL v2/v3 and TLS. Both layers are used to create the digital certificates.

B. Creating Digital Certificates

This section explains how to create the digital certificate using the four procedures mentioned above (see Figure 3). Before creating the server and client certificate, a CA certificate will be created to sign both client and server requests (i.e., in this scenario, we will create manually a CA instead to buy it from a well-reputated CA). Usually, a well-known CA provider (e.g., VeriSign Inc, Entrust Inc, etc) provides the CA certificate. In this scenario, a CA self-signed certificate is manually created.

1) Self-Signed Certificate:

Before starting, the CA key is generated, *RootCA.key* of length 2048 bits (2 bytes).

openssl genrsa –out RootCA.key 2048

The *RootCA.key* is then used to generate the certificate request *RootCA.csr* by providing the country name (i.e., C=CA), the organization name (i.e., O=Cyber Forensics Institution), and the common name of the certificate (i.e., CN=CF-CA)

openssl req -new -key RootCA.key -out RootCA.csr -config openssl.cnf -subj "/C=CA/O=Cyber Forensics Institution/CN=CF-CA/"

After generating the RootCA.csr, the request is signed using the RootCA.key to generate the requested certificate (*crt* format, *RootCA.crt*), but in this type of certificate, the CA itself will sign the certificate, that's why it is called self-signed certificate:

openssl req -x509 -days 365 –in RootCA.csr -out RootCA.crt -key RootCA.key -config opensslCA.cnf -extensions v3_ca

 ISBN: 978-1-61208-340-7

Finally, the exportable format p12 is generated to transform the *RootCA.crt* into an exportable format *RootCA.p12*

openssl pkcs12 -export -in RootCA.crt -inkey RootCA.key -certfile RootCA.crt -out RootCA.p12

Figure 7. CA self signed certificate

2) Server Certificate:

The server certificate is created for two goals: it lets the role player ensures the identity of the server, as well it is used to check for the client certificate.

As we mentioned in last section, assume that the IP in [40] is corresponding to the server in [39]. This certificate will be issued for the juries to install it on their server. This server will host the *CF-CoC application* [7], which will be used by the role player. Thus, the CA will issue and sign a certificate for this IP name.

First, the *Server.key* is generated using the following command:

openssl genrsa -out Server.key 2048

The *Server.key* is then used to generate the certificate request *Server.csr* by providing the country name (i.e., C=CA), the organization name (i.e., O=Cyber Forensics Institution), and the common name of the certificate (i.e., CN=192.168.2.12).

openssl req -new -key Server.key -out Server.csr -config openssl.cnf -subj "/C=CA/O=Cyber Forensics Institution/CN=192.168.2.12/"

After generating the *Server.csr*, the request is signed using the CA certificate *RootCA.crt* and the key *RootCA.key* to generate the requested certificate (i.e., *Server.crt*).

openssl ca -days 365 -in server.csr -cert RootCA.crt –out Server.crt -keyfile RootCA.key -config opensslserver.cnf -extensions server

Because the server certificate is signed by the CA, the *openssl* command uses a build in parameter called '*ca*', to declare that the server certificate will be signed by the CA using its key (*RootCA.key*).

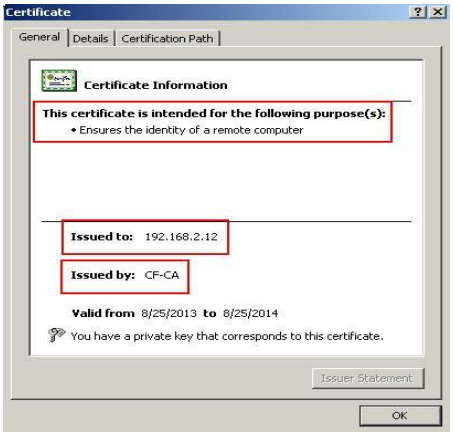

Figure 8. Server digital certificate

3) Client Certificate:

The role player authenticates himself to the server through the client certificate. Without this certificate, the role player will not be able to access *CF-CoC* application to construct different ontologies for each forensic phase and publish different resources.

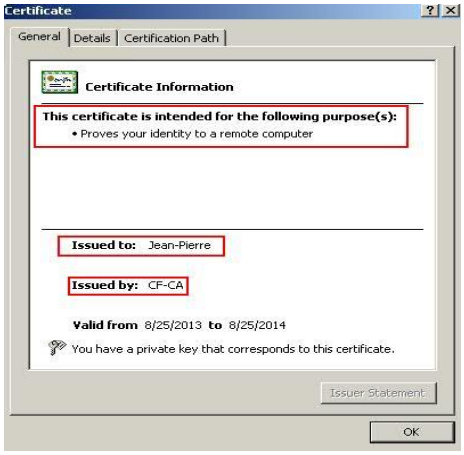

Figure 9. Client digital certificate

First, the *Client.key* is generated using the following commands:

openssl genrsa –out Client.key 2048

The *Client.key* is then used to generate the certificate request *Client.csr* by providing the country name (i.e., C=CA), the organization name (i.e., O=Cyber Forensics Institution), and the common name of the certificate (i.e., CN=Jean-Pierre).

openssl req -new -key Client.key -out Client.csr -config openssl.cnf -subj "/C=CA/O=Cyber Forensics Institution/CN=Jean-Pierre/"

After generating the *Client.csr*, the request is signed using the CA certificate (*RootCA.crt*) and key (*RootCA.key*) to generate the requested certificate (i.e., *Server.crt*).

openssl ca -days 365 -in Client.csr -cert RootCA.crt -out client.crt -keyfile RootCA.key -config opensslclient.cnf -extensions client

As shown in the last three figures (7, 8, and 9), we noticed that each certificate has its own purpose(s). Purpose(s) of a certificate depends on its type. The type of certificate is defined using the *-extension* in the creation of *crt* certificate. The *–extension* parameter calls the proper module for each certificate type. For example, it calls the *opensslCA.cnf, opensslServer.cnf,* and *opensslClient.cnf* for the CA, server, and client certificates, respectively. However, the *openssl.cnf* contains general configuration of all types of certificates.

C. Installation of Digital Certificates

Before installing the certificate, the CA sends to the jury and the role player their own certificates. Jury installs his certificate on his server and role player installs his certificate on his browser.

1) Self-Signed Certificate:

After creating the CA certificate, the CA sends to the server and client his certificate (i.e., p12 format without the private key of the CA certificate). By clicking on the p12 file (i.e., exportable format), a wizard will be launched to install the CA certificate in the trusted root folder of the current browsers for both server and client. By firstly installing this certificate on the server and client machines, their browsers will automatically identify the issuer of the client and server certificates.

2) Server Certificate:

The CA sends the server certificate to the jury. The latter then starts the installation of the server certificate. Installation of server certificates on Windows XP passes by two phases:

- Running the Microsoft Management Console and follow the steps in [29].
- Installing server certificates using the steps mentioned in [23].

3) Client Certificate:

Installing the client certificate is the same as the CA certificate, but at this time, the wizard installs the certificate in the client/ Personal folder of the browser.

D. Experimentation

This section shows how the scenario is enrolled after the role player and jury install their certificates:

- The client accesses the site by typing the URL of the server 192.168.2.12
- Because the remote server (i.e., where the *CF-CoC* web application is hosted) owns a server certificate, it requires then that his clients also owns a client certificate owned by the same trusted party (In this case, the *CF-CA*), otherwise the browser responded with a blank page (See Figure 10).

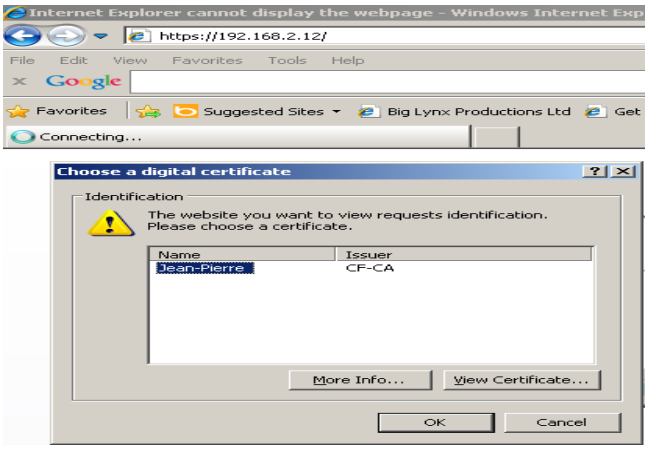

Figure 10. Server requires Client Digital certificate

- Once the server identifies the client certificate, it redirects the client to *CF-CoC* web application (see Figure 11).

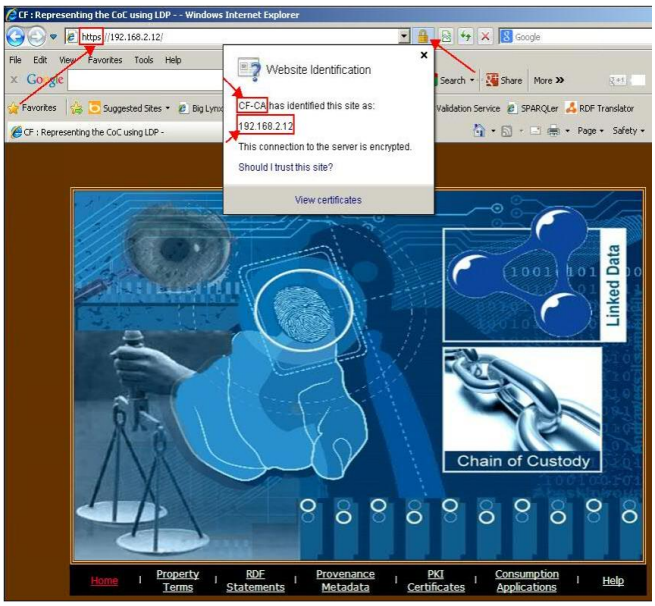

Figure 11. Redirection to the Restricted Resources

- Once the role player accesses the application, he starts to publish the ontologies and creates terms describing the forensic phase in hand (See Figure 12, 13).

As we see in Figure 11, the server certificate is installed and shown in the top of the screen as a yellow lock. By clicking on the lock, it will show who issued the certificate (i.e., CA) for this page and to whom it was issued (i.e., [40]).

 ISBN: 978-1-61208-340-7

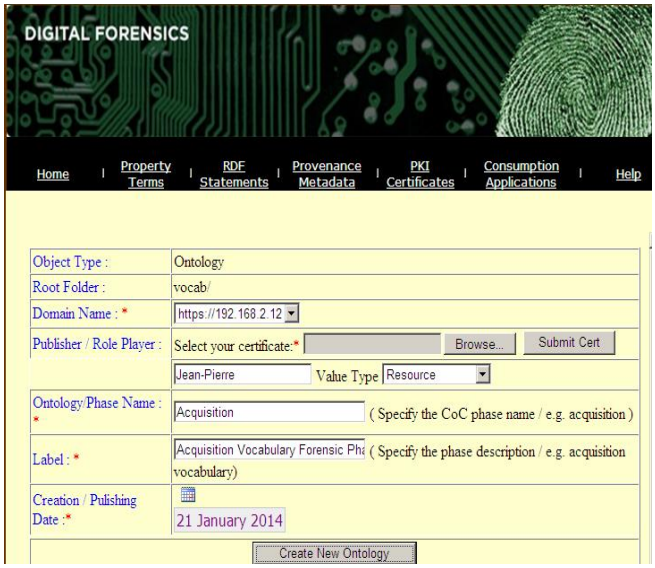

Figure 12. Create lightweight Ontology phase

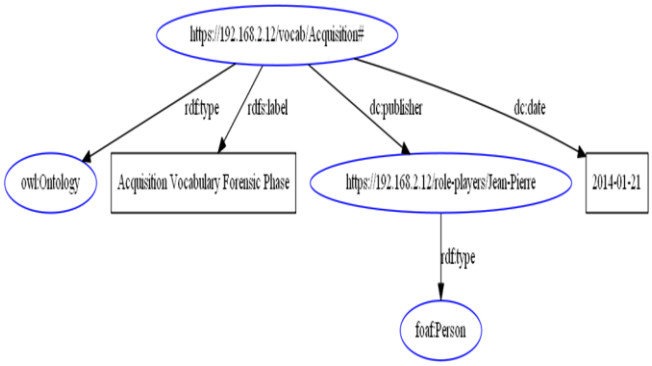

Figure 13. Ontology Acquisition phase

Once the role player finishes the publication task, the resources will be available to jury for consumption, as he owns a server certificate of the server, which allows him to view and access such resources published on his server. Resource as Jean-Pierre (see Figure 13) will be resolvable to more extra resources in the same domain [39] or to external domain [41]. However, Jean-Pierre will not be accessible from external resources outer the former domain.

As we mentioned in the last section, a certificate can not be created only for resources on the server but it can be issued for a specific resource on a server. For example, if we imagine that we have a resource 'x' in DS1, and the latter resides in the domain [35], then the field of the certificate called 'issued to' (see Figure 8) will be assigned the complete URL of the resource 'x' (e.g., *CN=192.168.2.12/resources/x).*

V. Conclusion And Future Works

This paper discusses in details how the technology stack/linked data principle of the linked data is adapted to publish data into a small scale while keeping the resolvability of these published resources. The idea is elaborated on a case study retrieved from the CF field, where the tangible *CoC* are represented using LDP. The represented resources are shared in a small scale between the role player and jury through the public key infrastructure approach. This paper opens the door to a new era of research representing the counter part of the LOD, called the LCD, which share all the advantages of the LOD, but with consumption restriction. Therefore, the technology stack (URI, HTTP, and RDF) is enhanced to include the secure access mechanism (URI, HTTPS, and RDF). The work presented in this paper is a bridge connecting dual works; the work proposed in [19] and in [21]. In addition, it underlines that the digital certificates cannot be issued only for datasets, but also for resources within these datasets. Furthermore, the current work provides with technical details the complete scenario of how to use digital certificates to bend resources from LOD to LCD, in order to answer the compromise question between the resolvability of resources and their access restrictions.

According to our knowledge, we are the first who introduced the PKI with the juridical *CoC.* On the other hand, we are implementing the two remaining layers of the framework; provenance layer and consumption layer, and we are working with a cyber criminality laboratory to define different metrics in order to evaluate our *CF-CoC* framework.

References

[1] I. Jacobs and N. Walsh, "Architecture of the World Wide Web," Volume One – W3C Recommendation", http://www.w3.org/TR/webarch/ [retrieved: Mar, 2014].

[2] R. Fielding, "Hypertext Transfer Protocol" -- HTTP/1.1. Request for Comments: 2616, http://www.w3.org/Protocols/rfc2616/rfc2616.html [retrieved: Jan, 2014].

[3] G. Klyne and J. Carroll, "Resource Description Framework (RDF): Concepts and Abstract Syntax," - W3C Recommendation, 2009, http://www.w3.org/TR/rdfconcepts/ [retrieved: Jan, 2014].

[4] Linking Open Data, W3C SWEO Community Project, http://www.w3.org/wiki/SweoIG/TaskForces/CommunityProjects/LinkingOpenData [retrieved: Feb, 2014].

[5] Securing Digital Identities & Information, Entrust, http://www.entrust.com/what-is-pki/#whatis [retrieved: Feb, 2014],

[6] R. Perlman, "An overview of PKI trust models, In IEEE network," vol. 13, pp. 38-43, 1999.

[7] T. F. Gayed, H. Lounis, and M. Bari, "Cyber forensics: Representing and Managing Tangible Chain of Custody Using the Linked Data Principles," The international conference on Advanced Cognitive technologies and Application (IARIA), Valencia, pp. 87-96, 2013.

[8] Official Site of OpenSSL Project, http://www.openssl.org/ [retrieved: Dec, 2013].

[9] K. Alexander, R. Cyganiak, M. Hausenblas, and J. Zhao, "Describing Linked Datasets - On the Design and Usage of VoiD, 'the Vocabulary Of Interlinked Datasets'," WWW 2009 Workshop : Linked Data on the Web LDOW2009, Madrid, Spain, (2009)

[10] D. Beckett, "RDF/XML Syntax Specification (Revised)," - W3C Recommendation.http://www.w3.org/TR/rdf-syntax-grammar/ [retrieved: Jan, 2014].

[11] D. Beckett and T. Berners-Lee, "Turtle - Terse RDF Triple Language," - W3C Team Submission. http://www.w3.org/TeamSubmission/turtle/, 2008 [retrieved: Jan, 2014].

[12] T. Berners-Lee et al., "The World-Wide Web," Communications of the ACM," Vol 37, No. 8, pp. 76-82, 2009.

 ISBN: 978-1-61208-340-7

[13] T. Berners-Lee et al., "Uniform Resource Identifier (URI): Generic Syntax. Request for Comments: 3986," (2005), http://tools.ietf.org/html/rfc3986 [retrieved: Feb, 2014].

[14] C. Bizer, R. Cyganiak, and T. Heath "How to publish Linked Data on the Web," 2007 http://www4.wiwiss.fu-berlin.de/bizer/pub/LinkedDataTutorial/. [retrieved: Feb, 2014].

[15] I. Jacobs and N. Walsh, "Architecture of the World Wide Web," W3C Recommendation., 2004, Volume One, http://www.w3.org/TR/webarch/ [retrieved: Jan, 2014].

[16] G. Klyne and J. Carroll, (2004), "Resource Description Framework (RDF): Concepts and Abstract Syntax," - W3C Recommendation, http://www.w3.org/TR/rdfconcepts/, 2004 [retrieved: Feb, 2014].

[17] P. Miller, R. Styles, and T. Heath, "Open Data Commons, a License for Open Data," Proceedings of the first Workshop about Linked Data on the Web (LDOW), 2008.

[18] L. Sauermann and R. Cyganiak, "Cool URIs for the Semantic Web," W3C Interest Group, Note 2008, http://www.w3.org/TR/cooluris/ [retrieved: Mar, 2014].

[19] E. Rajabi, M. Kahani, and M. Angel Silicia, "Trustworthiness of Linked Data Using PKI," World Wide Web Conference (www2012) Lyon, France, 2012.

[20] C. Bizer, T. Heath, and T. Berners-Lee, "Linked Data— The Story So Far," International. Journal on Semantic Web and Information Systems, Vol 5, No 3, pp. 1-22, 2009.

[21] M. Cobden, J. Black, N. Gibbins, L. Carr, and N. R. Shadbolt, "A Research Agenda for Linked Closed Dataset," Workshop on consuming Linked Data, Vol 782, ISWC, 2011. [Vision paper]

[22] Extended Validation SSL Certificate: The Next Generation High Assurance SSL Certificate, http://www.evsslcertificate.com/ssl/description-ssl.html [retrieved: Mar, 2014].

[23] Server Certificate Installation Instructions, Microsoft Developer Network: http://msdn.microsoft.com/en-us/library/ms751408.aspx [retrieved: Feb, 2014].

[24] M. Hausenblas, R. M. Grossman, A.Harh, and P. Cudré-Mauroux, "Large-Scale Linked Data Processing – Cloud Computing to the Rescue," CLOSER, pp. 246-251, Mar 2012.

[25] C. Bizer, A. Jentzsch, and R. Cyganiak, "State of the LOD Cloud," 2004, http://lod-cloud.net/state/ [retrieved: Jan, 2014].

[26] P. Mika and G. Tummarello, "Web semantics in the clouds," IEEE Intelligent Systems, Vol 2, pp. 82–87, 2008.

[27] R. L. Grossman et al., "An overview of the open science data cloud," In Proceedings of the 19th ACM International Symposium on High Performance Distributed Computing (HPDC '10), ACM. pp. 377-384, 2010.

[28] Technical Working Group for Electronic Crime Scene Investigation, Electronic Crime Scene Investigation, "A Guide for first responders, United States Department of Justine," 2001, pp.1-81.

[29] IIS Management Microsoft Management Console (MMC), Microsoft, http://support.microsoft.com/kb/892987 [retrieved: Feb, 2014].

[30] E. Casey, "Digital Evidence and Computer Crime - Forensic Science," Computers and the Internet, 3rd Edition. Academic Press, pp. 1-807, 2011, ISBN: 978-0-12-374268-1.

[31] S.O. Ciardhuain, "An extended model of CC investigations," International Journal of digital Evidence, Vol. 3, pp. 1-22, 2004.

[32] Y. Yusoff, R. Ismail, and Z. Hassan, "Common Phases of Computer Forensics Investigation Models," International Journal of computer science and information technology (IJCSIT), Vol. 3, No 3, pp. 17-31, June 2011.

[33] M. D. Köhn, J. H. P. Eloff, and M. S. Olivier, "UML modeling of Digital Forensic Process Models (DFPMs)," in Proceedings of the ISSA 2008 Innovative Minds Conference, Johannesburg, South Africa, pp. 32-36, July 2008.

[34] Internet Information Services, Microsoft, http://www.iis.net/ [retrieved: Mar, 2014]

[35] Virtual Example: http://www.mydomain.com/resource/x.

[36] Virtual Example: http://www.mydomain.com/resource/x.rdf.

[37] Virtual Example: http://www.mydomain.com/resource/x.html.

[38] Virtual Example: http://www.mydomain.com.

[39] Cyber Forensics-Chain of Custody, Tamer Gayed, www.cyberforensics-coc.com [retrieved: Oct, 2013].

[40] Local Network IP, http://192.168.2.12 [retrieved: Jan, 2014].

[41] Friend of a Friend, http://xmlns.com/foaf/0.1/ [retrieved: Jan, 2014].

[42] RDF Schema 1.1, http://www.w3.org/TR/rdf-schema/ [retrieved: Feb, 2014].

[43] R. Davis , H. Shrobe, and P. Szolovits, "What is a knowledge representation?," AI Magazine, Vol 14(1), pp.17-3, 1993.

[44] L. Sauermann, R. Cyganiak, (2008): Cool URIs for the Semantic Web. W3C Interest Group Note, http://www.w3.org/TR/cooluris/ [retrieved: Jan, 2014].

[45] D. Raggett, A. L. Hors, and Ian Jacobs "Html 4.01 specification - w3c recommendation," http://www.w3.org/TR/html401/, 1999 [retrieved: Mar, 2014].

[46] Internet X.509 Public Key Infrastructure Certificate Management Protocols: https://tools.ietf.org/html/rfc2510 [retrieved: Mar, 2014].

[47] D. Richard, V. C. Hu, W. Timothy, and S. Chang, "Introduction to Public Key Technology and the Federal PKI Infrastructure," National Institute of Standards and Technology (NIST), U.S. Government publication, 2011.

[48] T. Moses "Trust Management in the Public Key Infrastructure," Entrust Technologies", January 1999. [White paper]

[49] National Institute of Standards and Technology. Public Key Infrastructure Technology, ITL Bulletin :. http://www.nist.gov/itl/lab/bulletns/archives/july97bull.htm [retrieved: Apr, 2014]

[50] J. Davies, "Implementing SSL/TLS Using Cryptography and PKI," Indianapolis, Indiana: Wiley Publishing Inc, 2011.

[51] E. Barker et al., "Recommendation for Key Management Part 3: Application-Specific Key Management Guidance," NIST Special Publication 800-57, 2013 Edition.

[52] D. Kuhn, V. Hu, W. Polk, and S. Chang, "Introduction to Public Key Technology and the Federal PKI Infrastructure," NIST Special Publication 800-32, 2013 Edition.

 ISBN: 978-1-61208-340-7

Using Reservoir Computing for Wind Ramp Events Classification and Prediction

Tatyana M. P. Santos, Mêuser J. S. Valença
Polytechnic School of Pernambuco, POLI-UPE
Recife, Brazil
{tmps, meuser}@ecomp.poli.br

***Abstract*—The increasing use of wind power as source of electricity motivates a continuous improvement of the accuracy of wind power forecasts. There is a considerable value in optimizing forecasts systems to provide the best performance in an environment where the wind power production increases and/or decreases by a large amount over a short period of time. This paper presents a model that uses Reservoir Computing to classify energy production variations in wind farms, known as ramp events. This method is compared with two other approaches: one that uses a MLP network and the other is based in Persistence. The tests were performed and the results are given for real cases, reaching up over 90% of success rate.**

Keywords-ramp events; wind power forecast; reservoir computing; neural networks; mlp.

I. INTRODUCTION

In recent years, with the large-scale expansion of wind farms, the percentage of energy derived from wind sources is increasing rapidly. Thus, the demand for more reliable wind energy is driving the need for detection and prediction of ramp events [1].

There are wind power predictive models that are based on physical characteristics, of the weather, of the terrain, and thus dependent on the physical aspects. Recent research works in wind power forecasting, however, have focused on associating uncertainty estimates to these point forecasts, using historical measurements and machine learning algorithms to induce a predictive model [2][3]. In the following section, there are some examples of works done in this area, but no model was found, even among those which use machine learning algorithms, with the same techniques compared in this work for the same purpose (classify and predict ramp rates).

The series representing power generation in wind farms are very dynamic, predisposed to many variations. These series oscillate a lot in short periods of time, since it suffers various influences of physical and meteorological factors, which requires the use of a technique that handles very well with this volatility.

If properly applied, these works have much to add in wind power generation, increasing significantly the value of this modality in our energy matrix.

Today, a major difficulty when it comes to the prediction accuracy of wind power is to provide a forecast able to handle extreme situations, these situations that still rely heavily on the activities of end users, who need to develop procedures that meet the electricity demand, as well as maximizing the economic and environmental benefits. These extreme events are associated with large deviations on power generation compared with what was expected. The severity of these events depends on the speed with which they occur and when they occur, because the demand for electricity is also highly uncertain. The sooner these events are planned, the most effective are the procedures [2][3].

One solution to be considered is to try to determine in advance, and with the best possible accuracy, the timing, the amplitude and the width of the variations of the power generated. In this work, we try to optimize this type of solution using this *Reservoir Computing* model.

The remaining of this paper is organized as follow. Section 2 presents some related work, Section 3 addresses the proposed model based on *Reservoir Computing*, a recurrent neural network approach, whose structure is discussed, in addition with how it was applied and why it was chosen. Still talking about the proposed model, it was explained a little about ramp events, bringing the concept and defining the parameters considered in this work. In Section 4, the experiments are presented, showing the improvements compared to the results from a model using a *Multi-Layer Perceptron* (MLP) neural network and a second model based on the Persistence concept. Section 4 also explains a little about the common use of Persistence models as a reference predictor. The final remarks and future works are discussed in the conclusion section.

II. RELATED WORK

As discussed in introduction, physical-based models are still most common in this area, such as weather and terrain-based. These models use to determine relationships between the physical aspects and wind farms output power [4][5][6].

The other approach is the mathematical modelling, in which statistical and/or artificial intelligence methods are used to find the relationship between historical data sets and wind farms output power [7][8][9][10].

In the last decade, there was strong research effort on the improvement of wind power predictions using meteorological forecast data from Numerical Weather Prediction (NWP) systems. NWP systems uses mathematical models of the atmosphere and oceans to predict the weather based on current weather conditions data.

In the European project ANEMOS, several prediction models (multi-model approach) were applied and compared for the prediction of selected wind farms located in areas

 ISBN: 978-1-61208-340-7

with different characteristics. The ANEMOS project develops intelligent management tools for addressing the variability of wind power.

In other studies, strong improvements, up to about 20%, were obtained by using the data of different NWP models or ensemble models as input data for the wind power prediction models [11][12][13].

Within the short-term context, time series based models have shown a better performance than NWP models for horizons up to few hours [14][15][16]. These models, as the model brought in this paper, try to learn and replicate the dynamic shown by certain time series, for instance the power output time series of a wind farm.

For wind ramps forecasting, there are studies which showed improvements of predictions by using statistical and/or artificial methods too [17][18][19] [20].

Any work was found related to our case study regarding with *Reservoir Computing*.

III. PROPOSED MODEL

A. Theoretical background

There are certain complex situations and problems which are part of our reality. These facts have stimulated and continue boosting research aimed at bringing computing solutions to what could not be solved in a most trivial way. Many interesting and challenging problems in engineering also do not have direct solution using heuristic methods or algorithms explicitly programmed. These problems are prime candidates for the application of machine learning methods [21], which share the common property of learning by example and being able to generalize these examples in a "smart" way to new entries yet unseen.

A large subclass of machine learning methods is formed by Artificial Neural Networks, which are very abstract connectionist models of how the brain makes computing. They consist of networks of simple and non-linear computational nodes that communicate values via weighted connections, i.e., having their respective weights. Mainly, these weights are computed through features extracted from examples in such way that the desired behavior of the network is reached. If the network has a recurrent structure, i.e., with feedback loops, then it will have a memory of past inputs, which allows it to make the processing of temporal signals making them powerful computational nonlinear methods [21].

In Fig.1, there are two examples of neural networks topologies. At left, a feedfoward network, without feedback, where the signal travels through the network in a single direction. At right, a recurrent network, with feedback loops, that provide memory of past input, as explained above.

These recurrent neural networks are, however, notoriously difficult to train. A new learning paradigm called *Reservoir Computing* (RC) was introduced, allowing the use of recurrent neural networks alleviating the consuming and difficult phase of training. This idea was emerged simultaneously from the Echo State Networks [22] and Liquid State Machines [23] approaches, proposed independently and in periods very close (2001 and 2002 respectively). In both networks, the architecture consists of a recurrent network of neurons, we call this reservoir, which is built randomly and not trained initially, and a separate linear output layer, trained by simple one-shot methods [21], i.e., do not require large data sets or multiple training rounds, leaving to the discretion of the modeler doing training in batches, if desired.

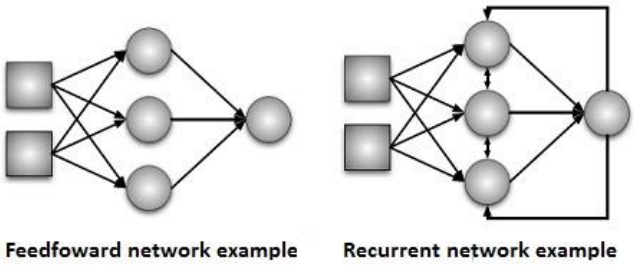

Figure 1. Differences between network topologies.

Fig. 2 below shows a schematic representation of a network with *Reservoir Computing* approach. The fixed connections and randomly formed are indicated with a solid line, the trained connections are indicated with a dashed line.

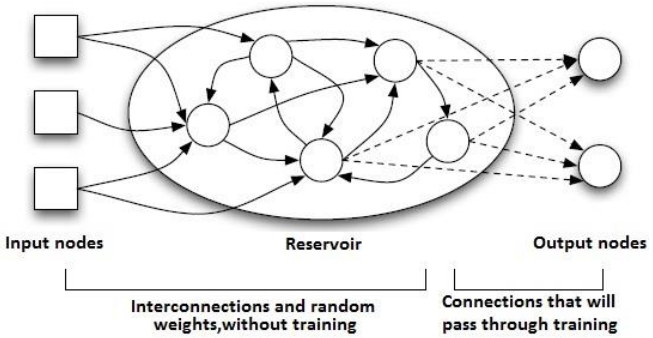

Figure 2. Schematic representation of a network with *Reservoir Computing* approach.

Since its introduction, *Reservoir Computing* has attracted much attention in the community of neural networks, due to the combination of simplicity of use and its good performance in a variety of difficult benchmark tasks [21]. Therefore, *Reservoir Computing* is used in our proposed model in the classification of ramp events task. Basically, ramp events can be understood as a variation on the nominal power greater than a threshold that lasts for a certain period of time. A more concrete definition about ramp events is presented in the following section.

B. Databases preparation for ramp events classification

Recently, the wind power industry began to evaluate the nature of ramp events. There is still no universal acceptance threshold to detect them [22], the most commonly used concept is the one that defines the ramp event as a variation that exceeds a minimum percentage of the nominal power (V_{min}) in a wind farm within a time period less than or equal to a maximum (T_{max}) [2][22], that is, when there is an

alteration in the output power that has an amplitude sufficiently large for a relatively short period of time [3]. It is difficult to find a consensus between the values for V_{min} and T_{max}, because they usually depend on geographical situation, climate and complexity of the terrain and end up being set "arbitrarily" by the solution modeler [2].

Fig. 3 below shows an example based on Ferreira [3] where the ramps are defined as a change in power of at least 50% of the capacity over a maximum duration of 4 hours.

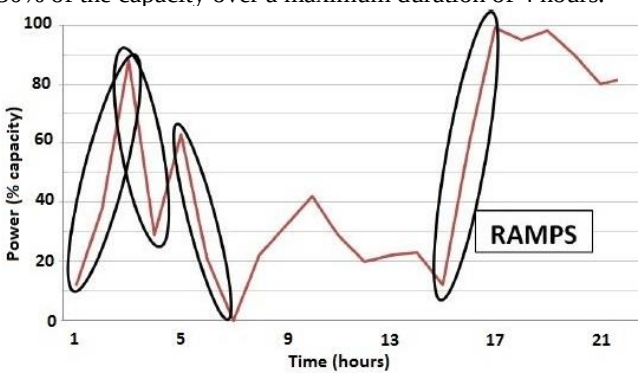

Figure 3. Ramp event definition: for this image, a change in power of at least 50% of the capacity over a maximum duration of 4 hours (Ferreira, 2010).

In this work, the behavior of the databases fairly reflected what was previously said, the values for V_{min} and T_{max} vary considerably according to local conditions of the wind farm. To define the parameters and continue favoring the individual behavior of generation in each wind farm, we chose not to set a universal value for V_{min} and T_{max}, but to do it according to the number of events observed in accordance with the variation of these parameters. The ramp should be a sparse event, not repeated many times, so the event does not become widespread throughout the generation. To process the data, we assume that the number of values found above the threshold V_{min} should be about 10% of total. To find these quantities of values observed at each threshold, the following process was made:

1) Apply filters that make it possible to view the percentage of variation of the series;

2) Count occurrences for each variation percentage;

3) For each variation percentage, check how much the ramps of this threshold represent in relation to the whole.

For the first step of the process, we based on an approach that does not work directly with the sign of the power generated in the farm, but turns the signal into a more appropriate representation. This strategy is used by Bossavy et al. (2010), who consider n differences in the amplitude of the power generated. In this procedure, let (p_t)t as the time series of wind power, and (p_t^f)t as the filtered signal associated, obtained by the following equation:

$$p_t^f = \text{mean}\ \{p_{t+h} - p_{t+h-n_{am}}\ ;\ h = 1, \ldots, n_{am}\} \qquad (1)$$

In (1), the n_{am} comes from the amount of differences in power measurements to be considered in the average (n_{am} = number of averaged differences of measures). The filtered signal (p_t^f)t measures variations of the wind power series (p_t)t. The ramp event then corresponds to a time interval where the absolute value of the filtered signal (p_t^f)t exceeds a threshold t>0. The ramp time is the point where the filtered signal (p_t^f)t reaches a local maximum. Figures 4, 5, and 6 demonstrate part of the analysis done until we could choose the appropriate n_{am}.

In Fig. 4 below, there is a part of the power generation time series on Farm A (p_t)t and absolute values of the filtered signal (p_t^f)t with parameter n_{am} = 2. Ramps in power series coincide with the local peaks of the filtered signal. Considering the threshold of 20% of the nominal power, for example, we observe 6 ramp events on this stretch.

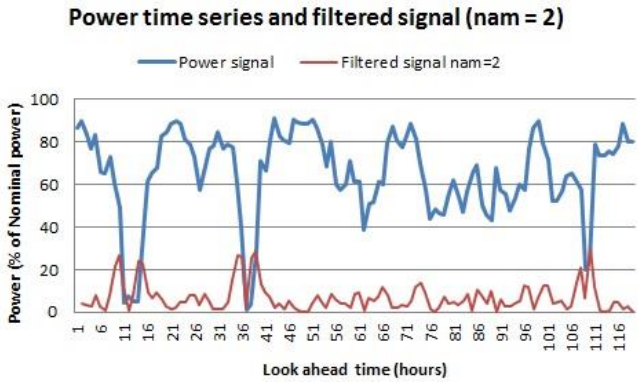

Figure 4. Part of the power generation time series on Farm A (p_t)t and absolute values of the filtered signal (p_t^f)t with parameter n_{am} = 2.

In Fig. 5 below, the parameter n_{am} was set as 5. Considering the threshold of 20% of the nominal power too, 4 ramp events can be observed on this stretch. The identification of the ramps observed at t = 108 and 110 in Fig. 4 is lost, this happens because lower values of n_{am} do the filtered signal (p_t^f)t be more sensitive to variations in power series occurred in shorter periods of time.

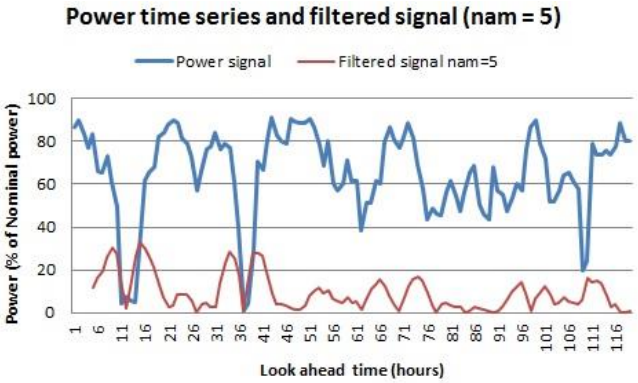

Figure 5. Part of the power generation time series on Farm A (p_t)t and absolute values of the filtered signal (p_t^f)t with parameter n_{am} = 5.

$$\alpha + \beta = \chi. \qquad (1) \qquad (1)$$

In Fig. 6 below, the parameter n_{am} was set as 10. It is possible to observe that bigger values of n_{am} will result in a filtered signal increasingly less sensitive to variations in the generated power.

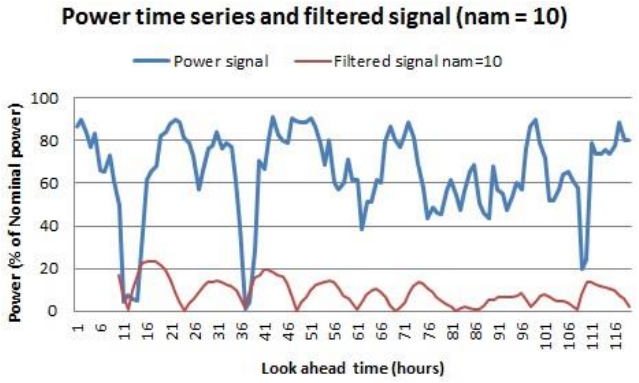

Figure 6. Part of the power generation time series on Farm A (p_t)t and absolute values of the filtered signal (p_t^f)t with parameter n_{am} = 10.

This work was done using power generation time series of three wind farms in Brazil, here we call them Farm A, Farm B and Farm C. These wind farms range in capacity 54.6, 70.56 and 126 MW respectively. This dataset is available for research purpose under request. The following figures were extracted from the Farm A series.

With the three power series used as case study in this paper (Farm A, Farm B and Farm C), using the previously detailed definition, the value of n_{am} remained 5 for the three cases and the thresholds were defined as: 15% to the Farm A, 20% to the Farm B and 40% for the Farm C.

890 values were found exceeding the threshold of 15% over a period of 5,855 hours with measurement occurring 30 to 30 minutes in the Farm A, 1236 values exceeding the threshold of 20% over a period of 8,784 hours (one year) with measurement occurring 30 to 30 minutes in the Farm B and 1,243 values exceeding the threshold of 40% over a period of 8,784 hours (one year) with measurement occurring 30 to 30 minutes in the Farm C.

The series were transformed into an hourly measurement before setting the n_{am}s, then n_{am} = 5 means 5 hours and n_{am} = 2 means 2 hours, i.e., for the Farm A, for example, the definition of the ramp is a variation of 15% in a period of 5 hours or less.

Figure 7 portrays these situations more easily and also shows that we would have more examples of ramps opting to use n_{am} = 5 instead of n_{am} = 2. This figure also presents that choosing a threshold below 15%, 10% for example, more ramps could be observed, however, as said previously, would increase greatly the sensitivity of the filter and the whole generation would be filled with ramps, generalizing too much the event.

In the following section, the experiments and results of ramp events classification are discussed. Then, the objective was to train the model to signalize in which periods the ramp events may occur.

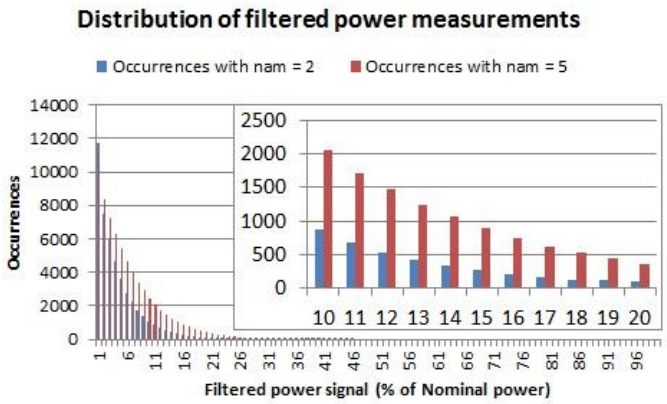

Figure 7. Filtered signal (p_t^f)t of Farm A considering n_{am} = 2 and n_{am} = 5 to verify the amount of occurrences exceeding all thresholds.

In addition with the proposed system based on *Reservoir Computing*, the experimental results of systems based on the both methods are presented: MLP network and a Persistence model.

IV. EXPERIMENTS AND RESULTS COMPARISONS FOR WIND RAMPS CLASSIFICATON

A. *Used settings*

The experiments were made using the last 24 hours to predict 24 hours ahead, but it can be parameterized for other options.

For neural networks, both of the *Reservoir* and for the MLP, we used 48 input neurons and 48 output neurons. The 48 entries relate to a full day of measurement, occurring in 30 to 30 minutes, the 48 output neurons correspond to 5-hour intervals (each interval has 10 values, since the measurement are arranged in 30 to 30 minutes) from the first hour of the day until the 9th measument of the subsequent month, since this was the maximum period set for detecting ramp events using 100% of power from one day. To find the amount of neurons in the hidden layer and other settings specifics to each type of network (interconnectivity rate and warm up cycles for RC and the learning rate and moment for MLP), we performed tests between possible configurations, explained in the following section, comparing the percentage of correct classifications (*Success Rate*) and checking if the choice had generalization capability to perform a good classification over all wind farms in study. These values will be showed and discussed in results comparisons section.

B. *Results comparisons*

To compare the classifications performed by the models employed in this work, and choose the best one, we used Success Rate (SR), as said before.

1) *Reservoir Computing*

With RC, as shown in Table I, we have achieved a success rate of 76.85% with standard deviation of 4.49 in Farm A, 80.48% with standard deviation of 3.93 in Farm B and 91.52% with standard deviation of 2,71 in Farm C.

 ISBN: 978-1-61208-340-7

TABLE I. RESULTS FOR CLASSIFICATION USING A RC MODEL

	Success Rate	Deviation
Farm A	76.85%	±4.49
Farm B	80.48%	±3.93
Farm C	91.52%	±2.71

The tests were conducted always incrementing the number of neurons in the hidden layer, starting with 5 neurons until 100, the rate of interconnectivity between the neurons of the hidden layer, from 50% to 100%, and the amount of warm up cycles from 1 to 100, but after 4 warm up cycles, any positive difference detected is very low.

Figures 8, 9 and 10 below show how the success rate changes due to the number of neurons for Farms A, B and C. The x-axis and y-axis correspond to executions and the number of neurons, respectively.

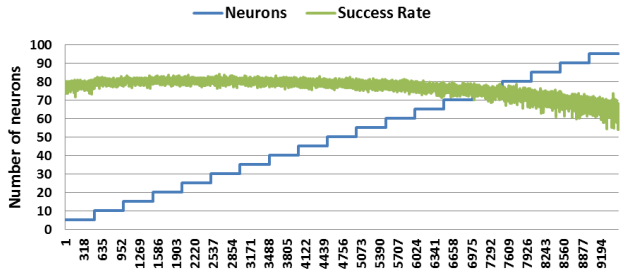

Figure 8. Changes in Success Rate according to the number of neurons in the hidden layer for Farm A data.

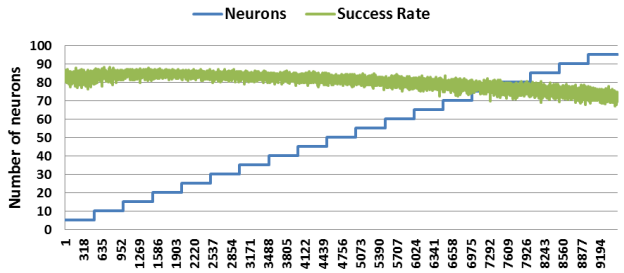

Figure 9. Changes in Success Rate according to the number of neurons in the hidden layer for Farm B data.

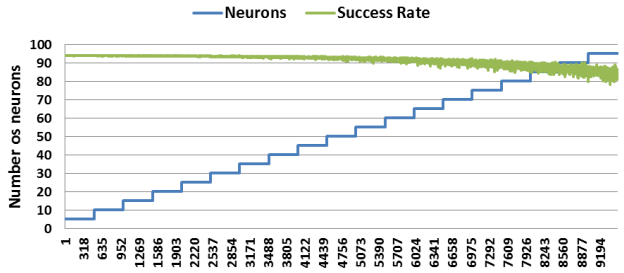

Figure 10. Changes in Success Rate according to the number of neurons in the hidden layer for Farm C data.

The blue line, referring to the number of neurons, remains at the same level during a sequence of executions because other parameters are changed (warm-up cycles and rate of interconnectivity).

Despite the small deviation, it's important to mention that each wind farm presented a different configuration for the best result. This information is on the Table II below:

TABLE II. BEST RESULTS FOR CLASSIFICATION USING RC MODEL

	Number of neurons in hidden layer	Interconnectivity rate	Warm up cycles	Success Rate
Farm A	30	64%	36	84.02%
Farm B	10	76%	11	88.13%
Farm C	10	94%	66	93.93%

2) *MLP*

With the MLP tool, no significant difference was detected in results between the tested configurations. This scenario occurred for the three wind farms used as case study.

According to Table III below, in Farm A, the success rate ranged an average of 71.57% with standard deviation of 0.49 in Farm B, ranged an average of 83.07% with standard deviation of 0.52 and in Farm C, ranged an average of 90.28% with standard deviation of 0.30.

TABLE III. RESULTS FOR CLASSIFICATION USING MLP MODEL

	Success Rate	Deviation
Farm A	71.57%	±0.49
Farm B	83.07%	±0.52
Farm C	90.28%	±0.30

Despite the small deviations, it's important to mention that each wind farm presented a different configuration for the best result. This information is on the Table IV below:

TABLE IV. BEST RESULTS FOR CLASSIFICATION USING MLP MODEL

	α	β	Number of neurons in hidden layer	Success Rate
Farm A	0.7	0.4	10	72.35%
Farm B	0.6	0.3	120	83.76%
Farm C	0.4	0.7	45	91.87%

3) *Persistence*

As Kariniotakis [24] reports, it is worthwhile to use operationally an advanced tool for wind forecasting only if this is able to outperform naive techniques resulting from simple considerations without special modeling effort. Such simple techniques are used as reference to evaluate advanced ones. The most commonly used reference predictor is Persistence. This approach states that the future wind generation will be the same as the last measured power value.

Despite its apparent simplicity, this model might be hard to beat for the first look-ahead times (up to 4-6 hours). This is due to the scale of changes in the atmosphere, which are relatively slow, in order of days [24].

 ISBN: 978-1-61208-340-7

Here, it was considered that the occurrence of ramps the next day is the same as the present day, at the same moments. For example, if we had ramp events at 12 o'clock today, we will consider the occurrence of ramps at 12 o'clock tomorrow. Assuming that, the moments that this model hits the occurrence of ramps will be counted in the success rate. The Table V below shows the results found for wind farms A, B and C:

TABLE V. RESULTS FOR CLASSIFICATION USING A PERSISTENCE MODEL

	Success Rate
Farm A	41.87%
Farm B	43.92%
Farm C	12.87%

C. Improvement calculation

The improvement between the RC model and the two other reference models was calculated, based, for classification, on the best success rate found.

The improvement is calculated as in (2):

$$Improvement = \frac{SR_{model1} - SR_{model2}}{SR_{model1}} * 100 \quad (2)$$

The results obtained are shown in the Table VI below:

TABLE VI. IMPROVEMENT CALCULATION BETWEEN COMPARED MODELS FOR CLASSIFICATION

Compared models	**Wind farm**	***Improvement***
Reservoir Computing x MLP	A	13.89%
	B	4.96%
	C	2.19%
Reservoir Computing x Persistence	A	50.17%
	B	50.16%
	C	86.30%
MLP x Persistence	A	42.13%
	B	47.56%
	C	85.99%

With the used metric, the RC model has shown better results than the MLP and the Persistence model, as we can see above.

As the RC model offers recurrence between neurons, it was expected that it would provide better results, as discussed in theoretical background in Section 3. This expectation was met.

Besides the recurrence, *Reservoir Computing* has a simpler way of training, as explained in Section 3 too. This feature helps to create models that tend to use less processing time compared with other recurrent neural networks.

CONCLUSION AND FUTURE WORK

In this work, a model that uses a recurrent neural network with differentiated learning method, called *Reservoir Computing*, was proposed for trying to promote better results in ramp events classifications and in power generation forecast in wind farms. A MLP neural network and a Persistence model were used as reference models.

The results indicate that the proposed model has better performance compared with reference models for classifying ramp events, reaching up over 90% of success rate.

As prospects for future works, is suggested the investigation of new options of input variables and architectures for the RC, as well as further support to indicate the amplitude of wind energy ramp events.

REFERENCES

[1] C. Kamath, "Understanding Wind Ramp Events through Analysis of Historical Data," Proc. IEEE PES Transmission and Distribution Conference and Expo (T&D), Apr. 2010, pp. 1-6.

[2] A. Bossavy, R. Girard, and G. Kariniotakis, "Forecasting Uncertainty Related to Ramps of Wind Power Production," Proc. European Wind Energy Conference & Exhibition (EWEC 2010), Apr. 2010, pp. 20-23.

[3] C. Ferreira, J. Gama, L.Matias, A. Botterrud, and J. Wang, "A Survey on Wind Power Ramp Forecasting", Argonne National Laboratory Technical Report, Chicago, USA, 2010.

[4] H. G. Beyer, D. Heinemann, H. Mellinghoff, K. Mönnich, and H. P. Waldl, "Forecast of Regional Power Output of Wind Turbines," Proc. European Wind Energy Conference & Exihibition (EWEC 1999), Mar. 1999, pp. 1070-1073.

[5] G. Giebel et al., "Short-term Forecasting Using Advanced Physical Modelling – The Results of the Anemos Project, Results from mesoscale, microscale and CFD modeling," Proc. European Wind Energy Conference & Exihibition (EWEC 2006), Feb. 2006.

[6] M. Lange, and U. Focken., "Physical Approach to Short-Term Wind Power Prediction," Berlin: Springer-Verlag, p. 208, 2006.

[7] G. Giebel, L. Landberg, G. Kariniotakis, and R. Brownsword, "The State-Of-The-Art on Methods and Software Tools for Short-Term Prediction of Wind Energy Production," Proc. European Wind Energy Conference & Exihibition (EWEC 2003), Jul. 2006.

[8] T. S. Nielsen et al., "Short-term Wind Power Forecasting Using Advanced Statistical Methods," Proc. European Wind Energy Conference & Exihibition (EWEC 2006), Feb. 2006.

[9] I. Sánchez, "Short-term prediction of wind energy production," International Journal of Forecasting, vol. 22, Jan.-Mar. 2006, pp. 43 – 56, doi:10.1016/j.ijforecast.2005.05.003.

[10] R. Jursa, "Wind power prediction with different artificial intelligence models," European Wind Energy Conference & Exihibition (EWEC 2007), May 2007.

[11] L. von Bremen, "Optimal linkage of different NWP models with neural networks for offshore wind power predictions," Sixth International Workshop on Large-Scale Integration of Wind Power and Transmission Networks for Offshore Wind Farms, Oct. 2006, pp. 291-296.

[12] M. Lange et al., "Optimal combination of different numerical weather models for improved wind power predictions," Sixth International Workshop on Large-Scale Integration of Wind Power and Transmission Networks for Offshore Wind Farms, Oct. 2006, pp. 273-276.

[13] G. Gregor et al., "Wind Power Predictions using Ensembles," Risø National Laboratory, Technical Report, Roskilde, Denmark, Sep. 2005.

[14] A. Costa, "Mathematical/Statistical and Physical/Meteorological Models for Short-term Prediction of Wind Farms Output," Ph. D Thesis, Escuela Técnica Superior de Ingenieros Industriales, Universidad Politécnica de Madrid, 2005.

 ISBN: 978-1-61208-340-7

[15] G.Giebel, R. Brownsword, G. Kariniotakis, M. Denhard, C. Draxl, "The state of the art in short-term prediction of wind power – A literature overview," ANEMOS EU Project, Technical Report, 2011.

[16] H. Zheng, and A. Kusiak, "Prediction of Wind Farm Power Ramp Rates: A Data-Mining Approach," Journal of Solar Energy Engineering, vol. 131, Jul. 2009, pp. 031011-1–031011-8, doi:10.1115/1.3142727.

[17] C. Gallego, A. Costa, and A. Cuerva, "Improving short-term forecasting during ramp events by means of Regime-Switching Artificial Neural Networks," Proc. 8th European Conference on Applied Climatology (ECAC 2010), Adv. Sci. Res., Sep. 2010, pp. 55-58, doi:10.5194/asr-6-55-2011.

[18] D. Lee, "Short-Term Wind Power Ensemble Prediction Based on Gaussian Processes and Neural Networks," IEEE Transactions on Smart Grid, vol. 5, Jan. 2014, pp. 501-510, doi: 10.1109/TSG.2013.2280649.

[19] R. Sevlian and R. Rajagopal, "Detection and Statistics of Wind Power Ramps," IEEE Transactions On Power Systems, vol.28, Jan. 2013, pp. 3610-3620, doi: 10.1109/TPWRS.2013.2266378.

[20] A. Couto, P. Costa, L. Rodrigues, V. Lopes, and A. Estanqueiro, "Impact of Weather Regimes on the Wind Power Ramp Forecast," Twelfth International Workshop on Large-Scale Integration of Wind Power and Transmission Networks for Offshore Wind Farms, Oct. 2013.

[21] D. Verstraeten, "Reservoir Computing: computation with dynamical systems,", Doctoral Thesis, Eletronics and Information Systems, Gent, Ghent University, 2009.

[22] H. Jaeger, "The "echo state" approach to analysing and training recurrent neural networks," GMD - German National Research Institute for Computer Science, Report 148, 2001.

[23] W. Maass, T. Natschlaeger, and H. Markram, "Real-time computing without stable states: A new framework for neural computation based on perturbations," Neural Computation, vol. 14, Nov. 2002, pp 2531-2560, doi:10.1162/089976602760407955.

[24] G. Kariniotakis, P. Pinson, N. Siebert, G. Giebel, and R. Barthelmie, "The State of the Art in Short-term Prediction of Wind Power – From an Offshore Perspective," Proc. Ocean Energy Conference ADEME-IFREMER, Oct. 2004.

 ISBN: 978-1-61208-340-7

Missing Categorical Data Imputation for FCM Clusterings of Mixed Incomplete Data

Takashi Furukawa
Graduate school of Engineering
Hokkai-Gakuen University
Sapporo, Japan
Email: 6512103t@hgu.jp

Shin-ichi Ohnishi
Faculty of Engineering
Hokkai-Gakuen University
Sapporo, Japan
Email: ohnishi@hgu.jp

Takahiro Yamanoi
Faculty of Engineering
Hokkai-Gakuen University
Sapporo, Japan
Email: yamanoi@hgu.jp

***Abstract*—The Data mining is related to human congnitive ability, and one of popular method is fuzzy clustering. The focus of fuzzy c-means (FCM) clustering method is normally used on numerical data. However, most data existing in databases are both categorical and numerical. To date, clustering methods have been developed to analyze only complete data. Although we, sometimes, encounter data sets that contain one or more missing feature values (incomplete data) in data intensive classification systems, traditional clustering methods cannot be used for such data. Thus, we study this theme and discuss clustering methods that can handle mixed numerical and categorical incomplete data. In this paper, we propose some algorithms that use the missing categorical data imputation method and distances between numerical data that contain missing values. Finally, we show through a real data experiment that our proposed method is more effective than without imputation, when missing ratio becomes higher.**

Keywords-clustering; incomplete data; mixed data; FCM.

I. INTRODUCTION

Clustering is the most popular method for discovering group and data structures in datasets in data intensive classification systems. Fuzzy clustering allows each datum to belong to some clusters. Thus data are classified into an optimal cluster accurately [1]. The k-means algorithm is the most popular algorithm used in scientific and industrial applications because of its simplicity and efficiency. Whereas k-means gives satisfactory results for numeric attributes, it is not appropriate for data sets containing categorical attributes because it is not possible to find a mean of categorical value. Although, traditional clustering methods handle only numerical data, real world data sets contain mixed (numerical and categorical) data. Therefore, traditional clustering methods cannot be applied to mixed data sets. Recently, clustering methods that deal with mixed data sets have been developed [4][5].

Moreover, when we analyze real world data sets, we encounter incomplete data. Incomplete data are found for example through data input errors, inaccurate measures, and noise. Traditional clustering methods cannot be directly applied to data sets that contain incomplete data, so we need to treat such data. A common approach to analyzing data with missing values is to remove attributes and/or instances with large fractions of missing values. However, this approach excludes partial data from analytical consideration and hence compromises the reliability of results. Therefore, we need analytical tools that handle incomplete categorical data, a process that is called imputation. To date, many imputation methods have been proposed, but most apply only to numerical variables. Thus, when analyzing categorical data or mixed data containing missing values, one has to eliminate from consideration data with missing values. Moreover, an imputation method applicable to fuzzy clustering is rare.

Fuzzy c-means (FCM) clustering is a very popular fuzzy extension of k-means. However, FCM for mixed data cannot be applied to data that contains missing data. Therefore, we use the imputation method for missing categorical data, and then we apply FCM clustering for mixed data. If we encounter missing numerical data, we use the partial distance [7] instead of the Euclidean distance.

In this paper, we describe the development of a fuzzy clustering algorithm for mixed data with missing numerical and categorical data. The next section introduces the FCM algorithm. Section III presents the clustering algorithm for mixed data. Sections IV and V introduce the missing categorical imputation method, and the notion of distance between data that contain missing values. Section VI proposes a fuzzy clustering algorithm that can treat mixed incomplete data. Finally, Section VI shows through a real data experiment that our proposed method is more effective than without imputation, when missing ratio becomes higher.

II. FUZZY c-MEANS CLUSTERING

The FCM algorithm proposed by Dunn [1] and extended by Bezdek [2] is one of the most well-known algorithms in fuzzy clustering analysis. This algorithm uses the squared-norm to measure similarities between cluster centers and data points. It can only be effective in clustering spherical clusters. To cluster more general datasets, a number of algorithms have been proposed by replacing the squared-norm with other similarity measures [3]. The notation that we use throughout is as follows. Let $\boldsymbol{x}_i = (x_{ij}), i = 1, \ldots, n, j = 1, \ldots, m$ is a feature value of the i^{th} data vector, c is the number of clusters. $\boldsymbol{b}_c = (b_{c1}, \ldots, b_{cm})^{\mathsf{T}}$ is the cluster center of the c^{th} cluster, u_{ci} is the degree to which x_i belongs to the c^{th} cluster. Then, u_{ci} satisfies the following constraint

$$\sum_{c=1}^{C} u_{ci} = 1, \ i = 1, \ldots, n \tag{1}$$

 ISBN: 978-1-61208-340-7

The FCM algorithm for solving (2) alternates the optimizations of L_{fcm} over the variables u and b

$$L_{fcm} = \sum_{c=1}^{C}\sum_{i=1}^{n} u_{ci}^{\theta}\left(\sum_{j=1}^{m}(x_{ij}-b_{cj})^2\right) \quad (2)$$

where θ is the fuzzification parameter ($\theta > 1$). Minimizing the u values of (2) are less fuzzy for values of θ near 1 and fuzzier for large values of θ. The choice $\theta = 2$ is widely accepted as a good choice of fuzzification parameter.

III. Fuzzy c-means clustering for mixed databases

The FCM algorithm has been widely used and adapted. However, only numerical data can be treated; categorical data cannot. When we analyze categorical data, we have to implement a quantification of such data. For example, suppose we obtained n sample data that have m categorical data consisting of K_j categories.

Then, the j^{th} item data can be expressed as an $(n \times K_j)$ dummy variable matrix $G_j = \{g_{ijk}\}, i = 1,\ldots,n, k = 1,\ldots,K_j$

$$g_{ijk} = \begin{cases} 1, & \text{data } i \text{ contains category } k \\ 0, & \text{otherwise} \end{cases} \quad (3)$$

Honda et al. proposed a method that combined the quantification of categorical data and the fuzzy clustering of numerical data [6]. The variables up to $(m-q)$ are numerical; the rest is categorical. Calculating

$$L = \sum_{c=1}^{C}\sum_{i=1}^{n} u_{ci}^{\theta}\left(\sum_{j=1}^{m-q}(x_{ij}-b_{cj})^2 + \sum_{j=m-q+1}^{m}(\boldsymbol{g}_{ij}^{\mathsf{T}}\boldsymbol{q}_j - b_{cj})^2\right) \quad (4)$$

where $\boldsymbol{q}_j$ is a categorical score, which can be computed as follows

$$\boldsymbol{q}_j = \left(G_j^{\mathsf{T}}\left(\sum_{c=1}^{C} U_c^{\theta}\right)G_j\right)^{-1}\left(\sum_{c=1}^{C}\boldsymbol{b}_{cj}G_j^{\mathsf{T}}U_c^{\theta}\mathbf{1}_n\right) \quad (5)$$

To obtain a unique solution, we impose the following constraint.

$$\mathbf{1}_n^{\mathsf{T}}G_j\boldsymbol{q}_j = 0 \quad (6)$$

$$\boldsymbol{q}_j^{\mathsf{T}}G_j^{\mathsf{T}}G_j\boldsymbol{q}_j = n \quad (7)$$

Algorithm: Fuzzy c-means algorithm for mixed databases

1. Initialize membership $u_{ci}, c = 1,\ldots,C, i = 1,\ldots,n$ and cluster center $b_{cj}, c = 1,\ldots,C$, then normalize u_{ci} satisfying (1).
2. Update category score $\boldsymbol{q_j}, j = m-q+1,\ldots,m$, using (5) according to constraint conditions (6) and (7). We then interpret $\boldsymbol{g}_{ij}^{\mathsf{T}}\boldsymbol{q}_j$ as the j^{th} numerical score x_{ij}.
3. Update cluster center b_{cj} using

$$b_{cj} = \frac{\sum_{i=1}^{n} u_{ci}^{\theta}x_{ij}}{\sum_{i=1}^{n} u_{ci}^{\theta}} \quad (8)$$

4. Update membership u_{ci} using

$$u_{ci} = \left(\sum_{l=1}^{C}\left(\frac{D_{ci}}{D_{li}}\right)^{\frac{1}{\theta-1}}\right)^{-1} \quad (9)$$

where

$$D_{ci} = \|\boldsymbol{x}_i - \boldsymbol{b}_c\|^2 \quad (10)$$

If $\boldsymbol{x}_i = \boldsymbol{b}_c$, $u_{ci} = 1/C_i$

5. Let ϵ judgment value for convergence. Compare u_{ci}^{NEW} to u_{ci}^{OLD} using

$$\max_{c,i}\|u_{ci}^{\mathrm{NEW}} - u_{ci}^{\mathrm{OLD}}\| < \epsilon \quad (11)$$

If true then stop, otherwise return to Step 2.

IV. Missing categorical data imputation method

Recently, missing data imputation has been recognized and developed as an important task. However, we are not accustomed to combining the clustering algorithm and the imputation method. Most missing data imputations are restricted to only numerical data. There are a few methods that permit missing categorical data or mixed data imputation [8][9]. If attributes and/or instances are missing, we do not apply the clustering algorithm. Instead, we apply the imputation method to fill the missing values, and then we can apply the clustering algorithm. In this paper, we use the missing categorical data imputation method, a"novel rough set model based on similarity", as proposed by Sen et al. [7].

DEFINITION 1. (Missing Attribute Set) An incomplete information system is denoted $S =< U, A, V, f >$; with attribute set $A = \{a_k | k = 1,2,\ldots,m\}$; V is the domain of the attribute. $V = V_k$, V_k is the domain of the attribute a_k, which is the category value. $a_k(x_i)$ is the value of attribute a_k of object x_i, and "$*$" means missing value. The missing attribute set (MAS) of object x_i is defined as follows:

$$MAS_i = \{k \mid a_k(x_i) = *, k = 1,2,\ldots,m\}$$

DEFINITION 2. (Similarity between objects) For two objects $x_i \in U$ and $x_j \in U$, their similarity $P_k(x_i, x_j)$ of attribute a_k is defined as

$$P_k(x_i,x_j) = \begin{cases} 1, a_k(x_i) = a_k(x_j) \wedge a_k(x_i) \neq * \wedge a_k(x_j) \neq * \\ 0, a_k(x_i) \neq a_k(x_j) \vee a_k(x_i) = * \vee a_k(x_j) = * \end{cases} \quad (12)$$

Then the similarity of the two objects of all attributes is defined as:

$$P(x_i,x_j) = \begin{cases} 0, \exists a_k \in A(a_k(x_i) \neq a_k(x_j) \wedge a_k(x_i) \neq * \\ \wedge a_k(x_j) \neq * \\ \sum_{k=1}^{m} P_k(x_i,x_j), others \end{cases} \quad (13)$$

The similarity matrix is $M(i,j) = P(x_i, x_j)$.

DEFINITION 3. (Nearest undifferentiated set (NS) of an object) The NS of object $x_i \in U$ is defined as a set NS_i of objects that have a maximum similarity:

$$NS_i = \{j \mid (M(i,j) = \max_{x_k \wedge k \neq i}(M(i,k))) \wedge M(i,j) > 0\}$$

Algorithm: Missing Categorical Data Imputation

1. Set parameter $num = 0$ to record the quantity of imputation data in the current iteration; for all the $x_i \in U$, if x_i has missing attribute, compute its missing attribute set MAS_i and nearest undifferentiated set NS_i;

2. For all the objects x_i that have missing attributes, which means $MAS_i \neq \phi$, do the perform loop for all the $k \in MAS_i$ in order:

2.1 if $|NS_i| = 0$,
break(to deal with the next missing attribute object);

2.2 if $|NS_i| = 1$, assume $j \in NS_i$ and $a_k(x_j) \neq *$, then:

$$a_k(x_i) = a_k(x_j);$$

$num++$;

2.3 if $|NS_i| \geq 2$,

2.3.1 If there exists $m, n \in NS_i$ satisfied $(a_k(x_m) \neq *) \wedge (a_k(x_n) \neq *) \wedge (a_k(x_m) \neq a_k(x_n))$, set:

$$a_k(x_i) = *;$$

2.3.2 Otherwise, if there exists $j_0 \in N$ and $a_k(x_{j0})$: $num++$;

3. if $num > 0$, return to Step 1, otherwise, go to step 4;

4. End. Other methods can be used.

V. Distances between data that contain missing values

In some situations, the feature vectors in $X = \{\boldsymbol{x}_1, \ldots, \boldsymbol{x}_n\}$ can have missing feature values. Any data with some missing feature values are called incomplete data. The original FCM algorithm and the FCM algorithm for mixed databases is a useful tool, but it is not directly applicable to data that contain missing values. Hathaway et al. proposed four approaches to incomplete data[7]: the whole data strategy (WDS), the partial distance strategy (PDS), the optimal completion strategy (OCS), and the nearest prototype strategy (NPS). In WDS, if the proportion of incomplete data is small, then it may be useful to simply delete all incomplete data and apply FCM to the remaining complete data. WDS should be used only if $\frac{n_p}{n_x} \leq 0.75$, where $n_p = |X_P|$ and $n_s = |X| \cdot m$. The cases when missing values $\|X_M\|$ are sufficiently large that the use of the WDS cannot be justified entails calculating partial (squared Euclidean) distances using all available (non-missing) feature values, and then scaling this quantity by the reciprocal of the proportion of components used. For this study, we used the PDS approach for mixed databases containing incomplete data.

In the PDS approach, the general formula for the partial distance calculation of D_{ci} is

$$D_{ci} = \frac{m}{I_i} \sum_{j=1}^{m} (x_{ij} - b_{cj})^2 I_{ij} \tag{14}$$

where

$$I_{ij} = \begin{cases} 0 & (x_{ij} \in X_M) \\ 1 & (x_{ij} \in X_P) \end{cases} \text{ for } 1 \leq i \leq n, 1 \leq j \leq m \tag{15}$$

$$I_i = \sum_{j=1}^{m} I_{ij} \tag{16}$$

$$X_P = \{x_{ij} | \text{ the value for } x_{ij} \text{ is present in } X\}$$

$$X_M = \{x_{ij} | \text{ the value for } x_{ij} \text{ is missing from } X\}$$

For example, let $m = 3$ and $n = 4$. Denoting missing values by *,

$$X = \begin{bmatrix} 1 \\ * \\ * \\ 4 \\ * \end{bmatrix}$$

Then, $X_P = \{x_1 = 1, x_4 = 4\}$, $X_M = \{x_2, x_3, x_5\}$, and

$$\begin{aligned} D_{ci} &= \|\boldsymbol{x}_i - \boldsymbol{b}_c\|_2^2 \\ &= \|(1 \ * \ * \ 4 \ *)^{\mathsf{T}} - (5 \ \ 6 \ \ 7 \ \ 8 \ \ 9)^{\mathsf{T}}\|_2^2 \\ &= \frac{5}{(5-3)}((1-5)^2 + (4-8)^2) \end{aligned} \tag{17}$$

The PDS version of the FCM algorithm, is obtained by making two modifications of the FCM algorithm. First, we calculate D_{ci} in (10) for incomplete data according to (14) – (16). Second, we replace the calculation of $\boldsymbol{b}$ in (8) with

$$b_{cj} = \frac{\sum_{i=1}^{n} u_{ci}^{\theta} I_{ij} x_{cj}}{\sum_{i=1}^{n} u_{ci}^{\theta} I_{ij}} \tag{18}$$

VI. FCM for mixed databases with incomplete data

For clustering analysis, treating missing data becomes especially important when the fraction of missing values is large and the data are of mixed type. We combine the FCM algorithm for mixed databases with the imputation method and the PDS approach to construct a FCM algorithm for mixed databases containing missing values. Here, we assume incomplete mixed data x_{ij}, $i = 1, \ldots, n$, $j = 1, \ldots, m$, the values up to $m - q$ correspond to numerical data and the rest is categorical. The dummy valuable matrix $G_j = \{g_{ijk}\}$, $k = 1, \ldots, K_j$, is described in equation (3). Applying the FCM algorithm to mixed databases that contain incomplete data is considered as follows:

Algorithm: FCM for mixed databases containing incomplete data

1. If there are missing categorical data, use the imputation algorithm described in Section IV, and separate the complete categorical data $x_{ij} (i = 1, \ldots, n, j = m - q + 1, \ldots, m)$

2. Initialize membership u_{ci} and cluster center b_{cj}, then normalize u_{ci} satisfying $\sum_{i=1}^{n} u_{ci} = 1$, $i = 1, \ldots, n$.

3. Update the category score

$$\boldsymbol{q}_j = \left(G_j^{\mathsf{T}} \left(\sum_{c=1}^{C} U_c^{\theta} \right) G_j \right)^{-1} \left(\sum_{c=1}^{C} \boldsymbol{b}_{cj} G_j^{\mathsf{T}} U_c^{\theta} \mathbf{1}_n \right) \tag{19}$$

according to the following constraint conditions:

$$\mathbf{1}_n^{\mathsf{T}} G_j \boldsymbol{q}_j = 0 \tag{20}$$

 ISBN: 978-1-61208-340-7

$$\boldsymbol{q}_j^{\mathsf{T}} G_j^{\mathsf{T}} G_j \boldsymbol{q}_j = n. \tag{21}$$

We interpret $\boldsymbol{g}_{ij}^{\mathsf{T}} \boldsymbol{q}_j$ to be the j^{th} numerical score x_{ij}.

4. Update cluster center b_{cj} using

$$b_{cj} = \frac{\sum_{i=1}^{n} u_{ci}^{\theta} I_{ij} x_{cj}}{\sum_{i=1}^{n} u_{ci}^{\theta} I_{ij}} \tag{22}$$

5. Update membership u_{ci} using

$$u_{ci} = \left(\sum_{l=1}^{C} \left(\frac{D_{ci}}{D_{li}} \right)^{\frac{1}{\theta-1}} \right)^{-1} \tag{23}$$

where D_{ci} is calculated form

$$D_{ci} = \frac{m}{I_i} \sum_{j=1}^{m} (x_{ij} - b_{cj})^2 I_{ij} \tag{24}$$

6. Let ϵ be a set value to judge convergence. Then compare u_{ci}^{NEW} to u_{ci}^{OLD} using

$$\max_{c,i} \| u_{ci}^{\mathrm{NEW}} - u_{ci}^{\mathrm{OLD}} \| < \epsilon \tag{25}$$

If true, then stop, otherwise return to Step 3.

VII. Experimental Results

In this section, we show the performance of our algorithm for mixed incomplete data.

We use credit approval datasets from UCI Machine Learning Repository which have 683 samples, 15 attributes(6 is numerical and the rest categorical), and 53 missing values. Table I lists the type of attribute("N" is numerical and "C" is categorical) and the number of missing values. This database has its own real classification result, i.e., each sample has been classified into 2 groups "+" or "−".

Fig. 1 the result for this incomplete mixed data using the proposed fuzzy clustering method; The number of samples with membership value over 10 intervals between 0 and 1 are found. 77% of the "+" group samples have high membership in cluster1 and almost all of "−" group samples are strongly classified in cluster 2. The fuzzification parameter θ is 1.2. The result shows that our proposed method is applicable for these real data.

Next, we compared following four methods; (I) Using Imputation method for categorical missing values, PDS for non-imputation missing values and numerical missing values (Imp + PDS). (II) Using imputation method for categorical missing values, WDS for non-imputation missing values and PDS for numerical missing values (Imp + PDS + WDS). (III) Using PDS for all missing values (PDS). (IV) Using WDS for all missing values (WDS).

Fig. **??** shows the results of these 4 methods. This graph's positive area indicate numbers of "+" group samples that have membership value to cluster1, and area of negative indicate "-" group samples data to cluster2. Results of (II) and (IV) have enough high membership samples (from 0.9 to 1.0).

Finally, we change missing ratio (from 0.7% to 0.9% and 1.2%) and apply four methods. Results are shown in Fig. 3 to 6. (II)Imp+PDS+WDS and (III)PDS cannot classify enough when missing ratio is high (1.2%) in Fig. 4 and 5. Further in Fig. 6, (IV)WDS have a lot of samples that cannot be used in any missing ratio (especially in high missing ratio), because this method except all sample data which contain missing values(describe value of 0 in each graph). From these point of view, (I) Imp+PDS can be better method for these dataset as shown in Fig. 3.

TABLE I. ATTRIBUTES AND MISSING VALUES

Attribute	type	Category	Missing
A_1	C	2	12
A_2	N	-	12
A_3	N	-	0
A_4	C	4	6
A_5	C	3	6
A_6	C	14	6
A_7	C	9	6
A_8	N	-	0
A_9	C	2	0
A_{10}	C	2	0
A_{11}	N	-	0
A_{12}	C	2	0
A_{13}	C	3	0
A_{14}	N	-	13
A_{15}	N	-	0

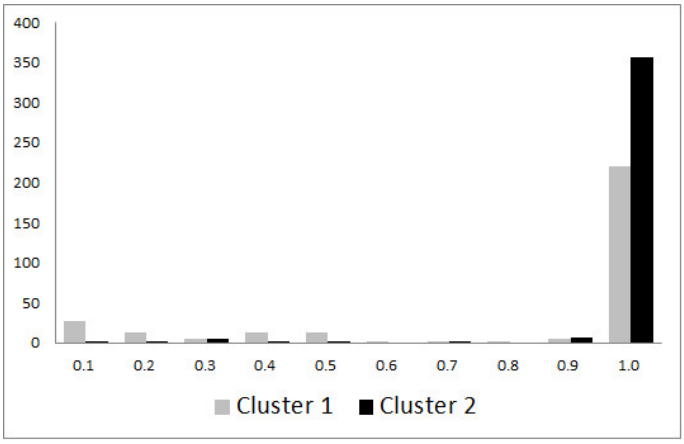

Fig. 1. Fuzzy Clustering Result(Real data)

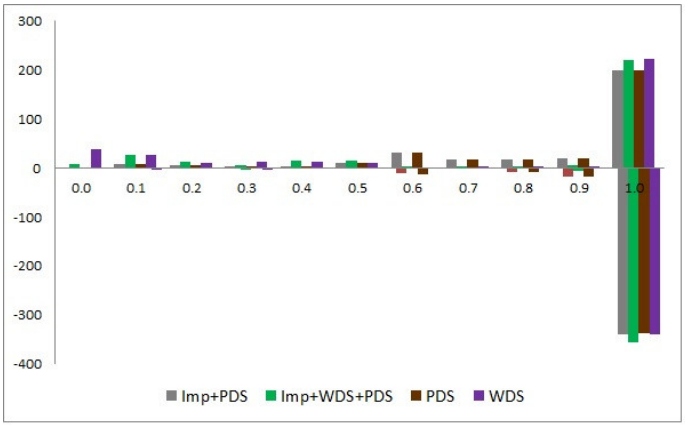

Fig. 2. Comparing four methods

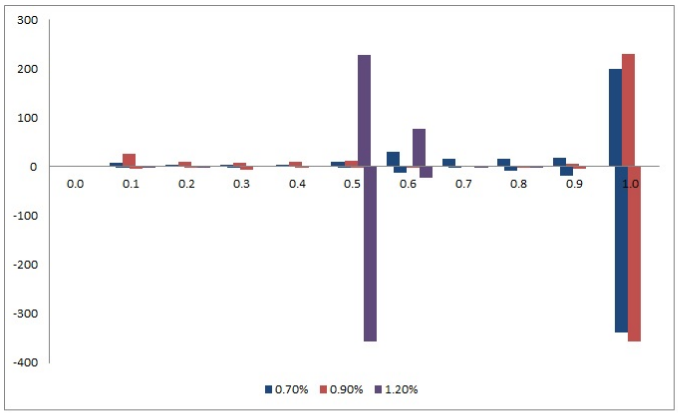

Fig. 3. Missing Result of PDS (I)

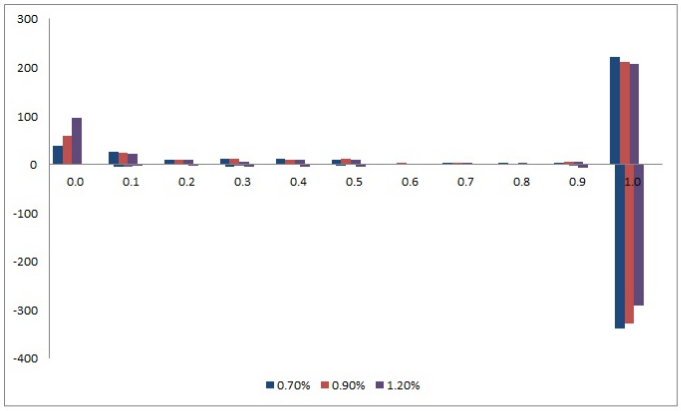

Fig. 4. Missing result of WDS (II)

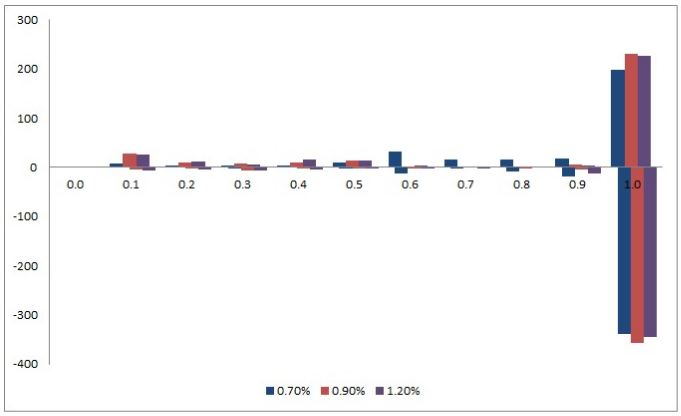

Fig. 5. Missing result of Imp + PDS (III)

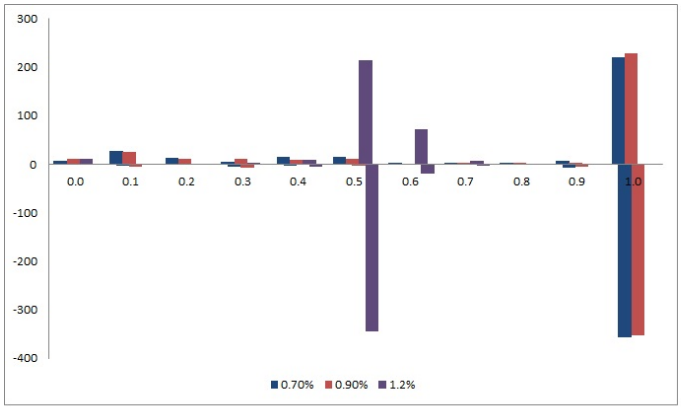

Fig. 6. Missing result of Imp + WDS + PDS (IV)

VIII. CONCLUSION

In this paper, we discussed a FCM clustering algorithm that handles mixed data containing missing values. In our study, we applied the imputation method to missing categorical data before clustering, followed by the FCM clustering algorithm. When we encountered numerical missing data, we used the PDS (and WDS) distance for numerical missing data. A real data experiment shows that our proposed method is more effective than without imputation, when missing ratio becomes higher. To obtain better performance during the clustering analysis for mixed data containing missing values, we plan to apply our algorithm to another datasets, too.

REFERENCES

[1] J. C. Dunn, A Fuzzy Relative of the ISODATA Process and Its Use in Detecting Compact Well-Separated Clusters, Journal of Cybernetics 3: 32-57, 1973.

[2] J. C. Bezdek, Pattern Recognition with Fuzzy Objective Function Algorithms, Plenum Press, 1981

[3] W. Sen, F. Xiaodong, H. Yushan, and W. Qiang, Missing Categorical Data Imputation Approach Based on Similarity, IEEE International conference on Systems, Man, and Cybernetics, 2012.

[4] Y. Naija, K. Blibech, S. Chakhar, and R. Robbana, Extension of Partitional Clustering Methods for Handling Mixed Data, IEEE International Conference on Data Mining Workshop, 2008.

[5] K. L. Wu and M. S. Yang, Alternative c-means clustering algorithms, Pattern Recognition vol. 35, pp. 2267-2278, 2002.

[6] K. Honda and H. Ichihashi, Fuzzy c-means clustering of mixed databases including numerical and nominal variables, Cybernetics and Intelligent Systems, 2004 IEEE Conference on, vol. 1, 2004

[7] R. J. Hathaway and J. C. Bezdek, Fuzzy c-means Clustering of Incomplete Data, IEEE Transactions on Systems, Man and Cybernetics, Part B, Vol.31, No. 5, pp.735-744, 2001

[8] K. Bache and M. Lichman, UCI Machine Learning Repository [http://archive.ics.uci.edu/ml]. Irvine, CA: University of California, School of Information and Computer Science [retrieved: Feb. 2014]

 ISBN: 978-1-61208-340-7

Evaluating AOU e-Learning Platform Based on Khan's Framework

Bayan Abu-Shawar
IT Department, Arab Open University, Jordan
b_shawar@aou.edu.jo

***Abstract*—The rapid growth of online world and the great evolution in digital technology open new horizons in different domains including education one. Blended learning and e-Learning approaches are new trends that are based on using computers as a medium to deliver and share educational materials which makes education available anytime, and anywhere. Khan suggested eight dimensional e-learning framework which serves as a base to help institutions to plan, design, implement and evaluate their e-learning programs. This paper discusses whether learning management systems at Arab Open University (AOU) meet the eight dimensional e-learning frameworks suggested by Badrul Khans. A detailed description of Khan's framework and the LMS used at Arab Open University are included in this paper. We claim that the AOU LMS is a good framework for e-learning based on these eight dimensions.**

Keywords-e-Learning platform; Khan's framework; LMS; e-Learning; blended learning.

I. INTRODUCTION

The growth of Internet-based technology has brought new opportunities and methodologies to education and teaching represent in e-learning, online learning, distance learning, blended learning and open learning. These approaches are typically used in place of traditional methods and mean that students deliver their knowledge though the web rather than face-to-face tutoring.

E-learning is a new trend of education systems, which implies the "use of Internet technology for the creation, management, making available, security, selection and use of educational content to store information about those who learn and to monitor those who learn, and to make communication and cooperation possible." [1].

Kruse [2] addressed the benefits of e-learning for both parties: organization and learners. Advantages of organizers are reducing the cost in terms of money and time. The money cost is reduced by saving the instructor salaries, and meeting room rentals. The reduction of time spent away from the job by employees may be most positive shot. Learning time reduced as well, the retention is increased, and the contents are delivered consistently. On another hand, learners are able to find the materials online regardless of the time and the place; it reduces the stress for slow or quick learners and increases users' satisfaction; increases learners' confidence; and more encourages students' participations.

In order to make such e-learning or blended learning works effectively a well-designed framework is needed. Khan's [3] framework offers eight factors that help in planning, designing, and evaluating e-learning materials, e-learning authoring tools, and e-learning platforms, such as Learning Management systems (LMS). The framework dimensions are: institutional, pedagogical, technological, interface design, evaluation, management, resource support, and ethical. Khan's framework aims to serve as a self-assessment instrument for institutions to evaluate their e-learning readiness or their opportunities for growth [4].

In this paper, the e-learning platform of the AOU is described in Section II. Khan's framework is presented in Section III. Section IV investigates AOU e-learning platform in terms of Khan's framework. A comparison between University of Jordan and AOU is discussed in Section V. Section VI presents conclusion.

II. THE E-LEARNING PLATFORM OF THE AOU

Arab Open University was established in 2002 in the Arabic region, and adopted the open learning approach. An open learning system is defined as "a program offering access to individuals without the traditional constraints related to location, timetabling, entry qualifications."[5].

The aim of AOU is to attract large number of students who cannot attend traditional universities because of work, age, financial reasons and other circumstances. The "open" terminology in this context means the freedom from many restrictions or constraints imposed by regular higher education institutions which include the time, space and content delivery methods.

Freed et al. [6] claimed that the "interaction between instructors and students and students to students remained as the biggest barrier to the success of educational media". The amount of interaction plays a great role in course effectiveness [7]. For this purpose and to reduce the gap between distance learning and regular learning, the AOU requires student to attend weekly tutorials. Some may argue that it is not open in this sense; however, the amount of attendance is relatively low in comparison with regular institutions. For example, 3 hours modules which require 48 hours attendance in regular universities, is reduced to 12 hours attendance in the AOU.

In order to give a better service to students and tutor, to facilitate accessing the required material from anywhere, and to facilitate the communication between them, an e-learning platform is needed. A learning platform "is software or a combination of software that sits on or is accessible from a network, which supports teaching and learning for practitioners and learners." [18]. A learning platform is considered as a common interface to store and access the prepared materials; to build and deliver learning activities such quizzes and home-works; support distance learning and

 ISBN: 978-1-61208-340-7

provide a set of communication possibilities such as timetables, videos, etc.

AOU has partnerships with the United Kingdom Open University (UKOU) [19] and according to that at the beginning the AOU used the FirstClass system as a Computer Mediated Communication (CMC) tool to achieve a good quality of interaction. The FirstClass tool provides emails, chat, newsgroups and conferences as possible mediums of communication between tutors, tutors and their students, and finally between students themselves. The most important reason behind using FirstClass was the tutor Marked Assignment (TMA) handling services it provided. However, the main servers are located in the UKOU which influences the control process, causes delays, and totally depends on the support in UKOU for batch feeds to the FirstClass system [8].

To overcome these problems, AOU uses Moodle [17] as an electronic platform. Moodle is an open-source Course Management System (CMS) used by educational institutes, business, and even individual instructors to add web technology to their courses. A course management system is "often internet-based, software allowing instructors to manage materials distribution, assignments, communications and other aspects of instructions for their courses." [9] CMS's, which are also known as Learning Management Systems (LMS) or Virtual Learning Environments (VLE), are web applications, meaning they run on a server and are accessed by using a web browser. Both students and tutors can access the system from anywhere with an Internet connection.

The Moodle community has been critical in the success of the system. With so many global users, there is always someone who can answer a question or give advice. At the same time, the Moodle developers and users work together to ensure quality, add new ,modules and features, and suggest new ideas for development [10][11]. Moodle also stacks up well against the feature sets of the major commercial systems, e.g., Blackboard and WebCT [12]. Moodle provides many learning tools and activities such as forums, chats, quizzes, surveys, gather and review assignments, and recording grades.

Moodle was used in AOU mainly to design a well formed learning management system which facilitates the interaction among all parties in the teaching process, students and tutors, and more over to integrate the LMS with the Student Information System (SIS).

In addition that Moodle is easy to learn and use, and that it is popular with large user community and development bodies. Moodle is flexible in terms of:

- Multi-language interface,
- Customization (site, profiles),
- Separate group features, and pedagogy.

III. KHAN'S E-LEARNING FRAMEWORK

Khan [3] suggested eight factors of e-learning framework that provides a structure to help institutions reviewing e-learning initiatives and programs to achieve the desired learning outcomes. Each dimension represents "a category of issues that need to be considered in order to create successful e-learning experiences" [4]. The question: "What does it take to provide the best and most meaningful open, flexible, and distributed learning environments for learners worldwide?" [4] originates the idea of Khan's framework. The framework aims to guide planning, designing, and implementing online programs and materials. Figure 1 shows the eight dimensional e-learning framework which are listed below:

- Pedagogical dimension, which mainly concerns of issues related to teaching and learning such as course contents, how to design it, how to offer it to target audience and how the learning outcomes will be achieved.
- Technological dimension examines issues related to hardware, software and infrastructure. E-learning environment, LMS, server capacity, bandwidth, security and backup are also covered in this dimension.
- Interface design dimension concerns the overall look and feel of an e-learning program. Interface design encompasses web and content design, navigation, web accessibility, and usability testing.
- Evaluation dimension addresses the evaluation of e-learning at institutional level, evaluation learning assessments.
- Management dimension refers to the maintenance and modification of the learning environment, it also addresses issues related to quality control, staffing and scheduling.
- Resource support dimension related to all technical and human resources support to create meaningful online environment which includes web-based, digital libraries, journals, and online tutorials.
- Ethical dimension considers issues related to social and political influence, diversity, and legal issues such as plagiarism, and copy rights.
- Institutional dimension includes three sub dimensions: issues of administrative affairs related to financial aid, registration, payment, graduation and grades; issues of academic affairs related to accreditation policy, faculty and support staff, and class size; issues of student services related to e-learning which covers everything from counseling and library support to book store, internships, and alumni affairs.

 ISBN: 978-1-61208-340-7

Figure 1. Khan's framework [4]

IV. IMPLEMENTING KHAN'S FRAME WORK AT AOU E-LEARNING PLATFORM

AOU adopted the blended learning approach, which is a hybrid of both face to face tutoring and online learning. So, students attend face to face tutorials once a week for each course; at the same time all learning materials are provided online for students.

Moodle was used in AOU to design a well formed e-learning platform and learning management system (LMS). To guarantee security issue, upon launching the LMS site, a unified webpage, as shown in Figure 2, is used, where users are asked for their authentication. LMS users are classified into six categories according to their authorities: administrator, creator, an editing-tutor, non-editing tutor, student, and guest where each one has different roles as listed below:

- Administrator can create courses, course sections, and create course module blocks and can create new user names for new tutors and students. Admin can add discussion forums, add chat rooms, messaging system, add announcement, add any offline or online activities for any course,
- *Creator* has responsibilities according to course level such as: creating course sections, adding students to their sections, assigning tutors to their sections, and adding module blocks and references.
- Editing-tutor can do all creation activities related to the course level that he is assigned to such as adding: lecture notes, references, assignments, online quizzes, etc.
- Non-Editing tutor can use web site as it without any privilege to create new activities. However, he is able to insert grades for assignment quizzes, giving feedback to students, share in the discussion forums, etc.
- A student can use the course website to download files and assignment, re submit assignment after solving, do online quizzes, fill online questionnaire related to course and another one to evaluate tutor. Moreover, the student plays the major role in discussion forums with other students and with his/her tutor.
- A guest can observe the activities going on the site depending on his level as course level or category level but he could not do any interaction

Figure 2. AOU e-learning platform starting page

The infrastructure of LMS is composed mainly of authoring tool, and activities tool. Publishing learning materials by adding text, creating files, or any content management is achieved by authoring tool. Communication medium is achieved via activities tool that provides ability to create chat rooms, discussion forums, messaging system, online quizzes, and grading. Each website of a module provides online chatting between student and tutor, different forums that enables students to communicate with each other and with their tutor sharing their ideas, problems and solutions. According to LMS infrastructure, and security issues the technological dimension is guaranteed.

After authentications, another webpage is appeared that it shows a list of modules students register on, or the tutor is teaching, the user can select the module he/she wants where another module website is presented. The module website is designed to enable learners to study it online, where learning outcomes of each module, and each unit is identified. The website of module is divided into weeks according to module calendar, where each week has its lecture notes, or slides, in addition to video lectures that is offered for students. Based on that the pedagogical dimension is considered where in addition to face-to face tutoring, online tutoring is also available any time.

Ethical dimension is achieved based on the fact that all students have the same rights and etiquette regardless of gender, age or disabilities. In terms of assignments, and exams there are strict rules applied in case of plagiarism. AOU staff has also the same rights, and duties.

In addition to online material, AOU has an agreement with EPESCO, IEEE, Enrolled and other digital libraries so

AOU staff and students can access this digital library with its journals, and publications. According to this, the support report dimension is also guaranteed.

In general, the interface of LMS has attraction look and feels appearance in terms of colors, standardization, standardization, and organizations per module. This interface is easy to use and user friendly, it needs only an hour lecturing to teach new students how to use it. Based on this, the Khan's interface design dimension is applied at AOU e-learning platform.

In terms of evaluation dimension, AOU evaluates each module and each tutor through online questionnaires. Face-to-face monitoring is also applied to evaluate monitoring is also applied to evaluate tutor teaching strategy; based on results of this evaluation, modifications and developments are taken in both dimension tutors and modules. Moreover, the management dimension is taking into account modifications and updating in all program levels including LMS platform. For example, a lot of inner house enhancements were applied on LMS, such as integrate the LMS with the SIS and the Human Resource System (HRS). In addition, to release students from being restricted to textual learning contents only, learning materials are provided as: textual lecture notes, video lectures by registering lectures using MS-Producer, and animation presentation through PowerPoint application.

Finally, in respect to institutional dimension, we need to elaborate the three sub-dimensions applied at AOU as follows:

- Issues *of administrative affairs:* AOU have specific fees related to faculties and registration; it provides financial aid for students and also has regulation to fund excellent students. At the same time, AOU has different sources of financial aid from Higher Ministry of Education and head quarter in Kuwait to fund research and projects issues. AOU follows a standard scale for full time employee salary and the part timer.
- Issues *of academic affair:* AOU follows the regulations and standards of Higher Ministry of Education in terms of graduation and grading system. Since AOU has a partnership with Open University (OU) in United Kingdome, the accreditation policy of OU is applied at AOU where accreditation is conducted with OU team every four years, to discuss any required changes in curriculum based on market needs. For teaching purposes, most class rooms are equipped with data show that is connected to computer; also the class size ranged from 25 to 30 students.
- Issues *of student services:* A lot of services are provided to students in AOU such as: connecting to the SIS to do online registration, obtaining their grades, perform learning activities through the LMS, such as submitting assignments, do online quizzes, and retrieve resources through AOU digital library subscriptions. There is a book store to provide students with their required books, and establishing the student affair department to solve student problems, to encourage them practicing their hobbies, and establishing graduation alumni. AOU offers internship for the tutors to get PhD degree from UK universities under certain regulations.

From the above description, we can figure out that AOU e-learning platform applied Khan's eight dimensional e-learning framework in a digitization way. All services provided by AOU for students or staff are part of LMS, which facilitate online accessing via e-Learning platform.

V. COMPARING E-LEARNING PLATFORMS BETWEEN AOU AND UNIVERSITY OF JORDAN

University of Jordan (JU) is both a modern as well as old institution of Higher Education in Jordan. Established in 1962, the University has, since then, applied itself to the advancement of knowledge no less than to its dissemination [13].

E-learning came to assist accomplishing the educational system in JU. In order to give a better service to students and tutors, to facilitate accessing the required material from anywhere, and to facilitate the communication between them, an e-learning platform is needed.

JU is using Blackboard as an electronic platform. Blackboard is a web-based system that supports and manages various aspects of learning and teaching. Blackboard provides many learning tools and activities such as course announcements, course documents, self-assessment quizzes and online testing, discussion forums, surveys, electronic assignment submissions, and links to external Web pages.

Blackboard has been used in JU mainly to design a well formed virtual learning environment which facilitates the interaction among all parties in the teaching process, students and tutors. Moreover, in addition to being easy to use and learn, Blackboard is a multi-language platform - since JU is using both Arabic and English in its computerized systems, and can be customized (site, profiles).

JU Blackboard system was designed as a modification to the existing system; it was developed by students as a graduation project [14]. The following summarizes the benefits of using the blackboard system in JU:

- Providing a web-based system for students and staff in order to have a direct effective communication channel.
- Giving students valuable information to complete their learning process through course outlines, notes, assignments, quizzes, etc.
- Facilitating learning activities by providing students with valuable channels of communication such as discussion boards with staff, even with students themselves.
- Enhancing the utilization of existing learning tools and making them more attractive for students and staff.

 ISBN: 978-1-61208-340-7

- Giving staff more depth and control over their accounts.
- In addition to blackboard features, the enhanced system will add new features such as discussion boards, emails service, playing media files, etc.
- Enhancing knowledge sharing, and building relationships with the students themselves.
- Ensuring that students are timely updated with information regarding courses and other valuable announcements.
- JU and AOU developed various systems, including the e-learning system, the Student Information System (SIS), and the Human Resource System (HRS). However, JU had the advantage of providing more useful tools for university staff and students, including the registration using SMS system, the e-library system, and the automated exams system.
- On the other hand, although the JU systems have one integrated data base, these systems are separated in the interface, where users of AOU can access most of its systems using a unified interface. JU used Blackboard in its e-learning system, while AOU used Moodle. Moodle is an open source CMS used by educational institutes, business, and even individual instructors to add web technology to their courses. More details about this system and the differences between Blackboard and Moodle can be found in [15][16][17].

VI. CONCLUSION

The e-learning becomes widely used as a way of teaching in the education community. The need for learning management systems to deliver the courses online becomes a significant issue. Khan's e-learning framework served as an instrument to guide institutions to plan, design, implement and evaluate their e-learning programs. In this paper we present Khan's framework, AOU blended learning approach, and we conducted that AOU e-learning platform implemented Khan's eight dimensional e-learning framework: pedagogical, technological information, interface, ethics, management, report support, evaluation and institution dimension. A comparison between the e-learning platform in JU and AOU was discussed.

REFERENCES

[1] Mikic, F. and Anido, L. Towards a standard for mobile technology. Proceedings of the International Conference on Networking, International Conference on Systems and International Conference on Mobile Communications and Learning Technologies (ICNICONSMCL'06). 2006, pp. 217-222.

[2] Kruse, K. The Benefits and Drawbacks of e-Learning. [Online]: http://www.corebiztechnology.com/software_article_elearning_d.htm. [Retrieved: May, 2014].

[3] Khan, B. H. (Ed.). (1997). Web-based instruction. Englewood Cliffs, NJ: Educational Technology Publications.

[4] Khan, B. H. (2001). A framework for Web-based learning. In B. H. Khan (Ed.), Web-based training. Englewood Cliffs, NJ: Educational Technology Publications.

[5] P. Karampiperis and D. Sampson. Designing Learning Services for Open Learning Systems Utilizing IMS Learning Design. In Proceeding of 4th IASTED Int. Conf. on web-based Education (WBE 2005), Swaziland, 2005, pp. 165-170.

[6] Freed, K. A History of Distance Learning, Retrieved June 25, 2004 from http://www.media-visions.com/ed-distlrn.html

[7] Rovai, A.P. and Barnum, K.T. On-line course effectiveness: an analysis of student interactions and perceptions of learning. Journal of Distance Education, 18(1), 57-73, 2003.

[8] Hammad, S., Al-Ayyoub, A.E., and Sarie, T. Combining existing e-learning components towards an IVLE. EBEL 2005 conference. [Online] http://medforist.grenobleem.com/Contenus/Conference%20Amman%20EBEL%2005/pdf/15.pdf

[9] M.C. Lohman. Effects of Information Distributions Strategies on Student Performance, and Satisfaction in a Web-Based Course Management System. International Journal for the Scholarship of Teaching and Learning, vol. 1, no. 1, 2007, pp. 1-17.

[10] Giannini-Gachago D., Lee M., and Thurab-Nkhosi D. Towards Development of Best Practice Guidelines for E-Learning Courses at the University of Botswana. In Proceeding Of Computers and Advanced Technology In Education, Oranjestad, Aruba, 2005.

[11] Louca, S., Constantinides, C., and Ioannou, A. Quality Assurance and Control Model for E-Learning. In proceeding (428) Computers and Advanced Technology in Education - 2004.

[12] Cole, J. Using Moodle, O'Reilly, First edition, July 2005

[13] University of Jordan. URL: http://www.ju.edu.jo. [retrieved: May, 2014].

[14] N. Al-Assaf. JU Blackboard System. Graduation project, King Abdullah II School for Information Technology, The University of Jordan, summer term 2009.

[15] D. Giannini-Gachago, M. Lee, and D. Thurab-Nkhosi. Towards Development of Best Practice Guidelines for E-Learning Courses at the University of Botswana. In proceeding of Computers and Advanced Technology In Education, Oranjestad, Aruba, 2005.

[16] S. Louca, C. Constantinides, and A. Ioannou. Quality Assurance and Control Model for E-Learning. In Proceeding (428) Computers and Advanced Technology in Education. 2004.

[17] J. Cole. Using Moodle. 1st edition, O'Reilly. 2005.

[18] B. AbuShawar. Learning Management System and its Rlationship with Knowledge Management. Proceedings of the International Conference on Intellignet Computing and Information Systems. (2009), pp.738–742.

[19] Open University. URL: http://www.open.edu/openlearn/. [retrieved: May, 2014].

 ISBN: 978-1-61208-340-7

Emotion Classification Based on Bio-Signals Using Machine Learning Algorithms

Eun-Hye Jang, Byoung-Jun Park, Sang-Hyeob Kim, Myung-Ae Chung
IT Convergence Technology Research Laboratory & Creative Future Research Laboratory
Electronics and Telecommunications Research Institute
Daejeon, Republic of Korea
{cleta4u, bj_park, shk1028, machung}@etri.re.kr

Yeongji Eum, Jin-Hun Sohn
Department of Psychology, Brain Research Institute
Chungnam National University
Daejeon, Republic of Korea
petitaudrey@hanmail.net, jhsohn@cnu.ac.kr

***Abstract*—In human-computer interaction researches, one of the most interesting topics in the field of emotion recognition is to recognize human's feeling using bio-signals. According to previous researches, it is known that there is strong correlation between human emotion state and physiological reaction. Bio-signals takes noticed lately because those can be simply acquired with some sensors and are less sensitive in social and cultural difference. We have applied four algorithms, linear discriminant analysis, Naïve Bayes, decision tree and support vector machine to classify emotions, happiness, anger, surprise and stress based on bio-signals. In this study, audio-visual film clips were used to evoke each emotion and bio-signals (electrocardiograph, electrodermal activity, photoplethysmo-graph, and skin temperature) as emotional responses were measured and the features were extracted from them. For emotion recognition, the used algorithms are evaluated by only training, 10-fold cross-validation and repeated random sub-sampling validation. We have obtained very low recognition accuracy from 28.0 to 38.4% for testing. This means that it needs to apply various methodologies for the accuracy improvement of emotion recognition in the future analysis. Nevertherless, this can be helpful to provide the basis for the emotion recognition technique in human-machine interaction as well as contribute to the standardization in emotion-specific autonomic nervous system responses.**

Keywords-emotion classification; bio-signal; feature extraction; machine learning algorithm

I. INTRODUCTION

Recently, one of the most interesting fields in Human Computer Interaction (HCI) is to understand human's feeling and to categorize emotions. Some engineers and psychologists have tried to analyze facial expressions, voices, gestures and bio-signals in an attempt to recognize emotions [1][2]. In particular, studies to recognize human's feeling using various bio-signals have gradually increased, because signal acquisition by non-invasive sensors is relatively simple and physiological responses by emotion are less sensitive in social and cultural difference. Emotional states are recognized by some signals reflect physiological responses such as heartbeat, respiration, skin temperature and, so on. For example, Electrocardiograph (ECG) is a signal to detect the electrical activity of the heart through electrodes attached to the outer surface of the skin and reflects emotional states such as tension or stress. Also, Electrodermal Activity (EDA) is a physiological signal that can characterizes changes in the electrical properties of the skin owing to the activity of the sweat glands and a good indicator of arousal level due to external sensory and cognitive stimuli [3][4]. Skin Temperature (SKT) is an important and effective indicator of emotion states and reflects Autonomic Nervous System (ANS) activity. Photoplethysmograph (PPG) is also a signal that indicates pulsation of chest wall and great arteries followed by heartbeat, and measures activities of the sympathetic and para-sympathetic nervous system. Many previous studies have already examined that there is a strong relation between physiological responses and human's emotional states [5]. For example, in research reviewed 134 studies about ANS activity [6], anger is related to ANS responses such as a modal response pattern of reciprocal sympathetic activation and increased respiratory activity, particularly faster breathing, and ANS responses of fear point to broad sympathetic activation including cardiac acceleration, increased myocardial contractility, vasoconstriction, and electrodermal activity. Emotion recognition using bio-signals has been mostly performed by machine learning algorithms (e.g., Fisher's Linear Discriminant (FLD) [7], Support Vector Machine (SVM) [8] and so on). For example, Picard and colleagues at MIT Lab [1] have conducted a recognition accuracy of over 80% on average which seems to be acceptable for realistic applications using linear pattern recognition method. In this paper, we introduce the analysis processes such as signal processing, features extraction and deduction for classification of emotions (happiness, anger, surprise and stress) based on bio-signals and results of emotion classification using some machine learning algorithms. To induce four basic emotions, ten emotional stimuli sets which have been verified their appropriateness and effectiveness by replicate experiments were used in experiment. ECG, EDA, SKT and PPG as bio-signals are acquired by MP100 Biopac system Inc. (USA) [9] and analyzed to extract features for emotional pattern dataset. To classify four emotions, four machine learning algorithms, which are Linear Discriminant Analysis (LDA) [7], Classification And Regression Tree (CART) [10], Naïve Bayes [7] and Support Vector Machine (SVM) [8] are used. The results will offer information about the emotion recognizer with feature selections using bio-signlas induce by four emotions.

 ISBN: 978-1-61208-340-7

II. EXPERIMENTAL METHODS

Twelve subjects (males: 20.8 years±1.26, females: 21.2 years±2.70) participated in this study. They are normal persons who did not report any history of medical illness or psychotropic medication. A written consent was obtained before the beginning of the experiment.

A. *Emotion Induction Experiment*

To effectively induce the four emotions (happiness, anger, surprise and stress), forty emotional stimuli, which consist of 10 sets for the four emotions, are used in the experiments. Those are constituted 2~4 min long audio-visual film clips which are captured originally from movies, documentary and TV shows. The stimuli for happiness have included scenes such as victory, wedding or laughing and scenes such as massacre, beating, or attack for anger induction, scenes of a sudden or unexpected scream etc., as the stimuli for surprise, and audio/visual noise on screen for stress. Audio-visual film clips take advantage that these have the desirable properties of being readily standardized, involving no deception, and being dynamic rather than static. They also have a relatively high degree of ecological validity, in so far as emotions are often evoked by dynamic visual and auditory stimuli that are external to the individual [11].

In preliminary study, to verify whether each emotional stimulus induce real emotion or not, we had examined the appropriateness and effectiveness of them. The appropriateness means consistency (%) between target emotion designed by experimenter and label of subjects' experienced emotion. The effectiveness is the emotion intensity by subjects' rating on a 1 to 11 point Likert-type scale (e.g., 1 being "least happy" or "not happy" and 11 being "most happy"). Twenty-two college students, that are different group from participants in the experiment, categorize their experienced emotion and rate intensity of their categorized emotion on emotional assessment scale after presentation of each emotion stimuli.

The emotional stimuli have the appropriateness of 92.25% and the effectiveness of 9.3 point on average of 10 sets as shown in the results (Table 1). The appropriateness of each stimulus is ranged from 75 to 100% and the effectiveness comes out from 8.0 to 10.3 point as shown in results. This means that the selected stimuli can provoke each emotion, suitably and effectively.

The procedures for main experiment are as like figure 1. Subjects have introduced to experiment procedures and have an adaptation time in the laboratory setting. Then they are attached electrodes on their wrist, finger, and ankle for bio-signals measurement. Bio-signals have recorded for 60 sec prior to the stimulus presentation (baseline) and for 2 to 4 min during the stimulus presentation as emotional state, then for 60 sec after presentation of stimulus for debriefing. Subjects have rated the emotion that they experienced during presentation of the stimulus on the emotion assessment scale. This procedure is conducted on each of the four emotions for 10 times.

TABLE I. THE APPROPRIATENESS AND EFFECTIVENESS OF EMOTIONAL STIMULI

	HAP	ANG	SUR	STR	M
1	100% (8.4)	75% (9.7)	75% (9.3)	92% (9.3)	83% (9.5)
2	100% (8.9)	75% (9.9)	92% (9.7)	100% (9.1)	94% (9.6)
3	100% (8.8)	75% (9.7)	100% (9.7)	100% (8.8)	93% (9.3)
4	100% (9.6)	75% (9.5)	100% (9.9)	100% (8.9)	95% (9.7)
5	100% (9.6)	92% (9.8)	83% (9.6)	100% (9.3)	94% (9.6)
6	100% (9.3)	92% (9.4)	83% (9.6)	100% (8.8)	95% (9.5)
7	100% (9.3)	92% (8.9)	100% (9.5)	92% (9.3)	92% (9.3)
8	92% (8.0)	83% (9.2)	83% (9.4)	100% (9.3)	92% (9.2)
9	100% (9.7)	92% (9.5)	83% (8.6)	100% (9.1)	96% (9.4)
10	92% (8.8)	92% (9.7)	75% (10.3)	100% (9.3)	91% (9.5)
M	98% (9.1)	84% (9.5)	89% (9.5)	98% (9.1)	92% (9.3)

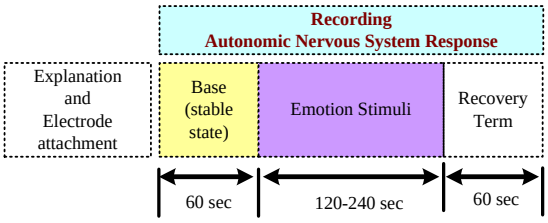

Figure 1. Experimental protocol for emotion induction

B. *Measurement of Bio-signals*

The MP100WS and AcqKnowledge (version 3.8.1) (Biopac Systems Inc., USA) were used to acquire the data and analyse them. The sampling rate was fixed at 250 Hz for all the channels and appropriate amplification and band-pass filtering were performed. Figure 2 shows an example of the obtained signals from device. The ECG was measured from both wrists with the two-electrode method its basis from the left ankle (Lead I) as reference. The respiration sensor measured expansion and contraction of the chest cavity using a Hall effect sensor attached around the chest with a Velcro band. EDA was measured from two Ag/AgCl electrodes attached to the index and middle fingers of the left hand. PPG and SKT were measured from the little finger and the ring finger of the left hand, respectively. PPG allows

 ISBN: 978-1-61208-340-7

non-invasive recording of arterial-blood-volume pulses at the finger.

Data for 30 sec from the baseline and another 30 sec from each emotional state were used in the analysis. The emotional states are determined by the result of subject's self-report (scene that emotion is most strongly expressed during presentation of each stimulus). Total 360 signal data except for severe artefact effect by movements, noises, etc. are used for analysis.

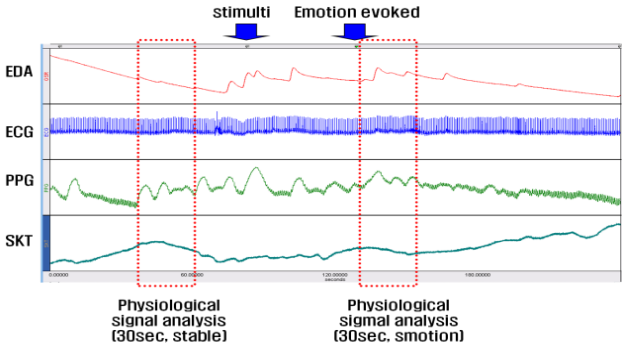

Figure 2. The example of bio-signals measures

C. Feature Extraction

27 features extracted from the bio-signals and used to analysis (Table 2). The features extracted from EDA, which was down-sampled to 100Hz after low-pass filtering the signal, are skin conductance level (SCL), average of skin conductance response (mean SCR) and number of skin conductance response (NSCR). Figure 3 shows the example of EDA signal. These are features which show statistically significant change between baseline and emotion state by paired t-test (using SPSS ver.18.0).

TABLE II. THE FEATURES EXTRACTED FROM BIO-SIGNALS

Bio-signal		Features	
EDA		SCL, NSCR, meanSCR	
SKT		meanSKT, maxSKT	
PPG		meanPPG	
ECG	Time domain	Statistical parameter	meanRRI, stdRR, meanHR, RMSSD, NN50, pNN50
		Geometric parameter	SD1, SD2, CSI, CVI, triangular index, TINN
	Frequency domain	FFT	apLF, apHF, nLF, nHF, LF/HF ratio
		AR	apLF, apHF, nLF, nHF, LF/HF ratio

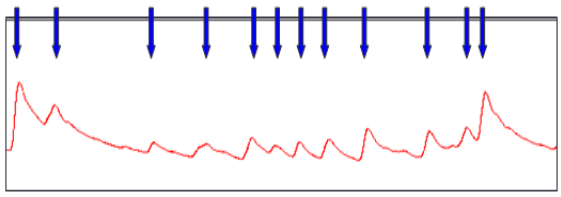

Figure 3. The example of EDA signals (200 sec)

Figure 4 is the law signal of ECG during 10 sec and the example of RRI tachogram extracted from ECG. RRI (msec) is the time interval between two R-peaks in the ECG.

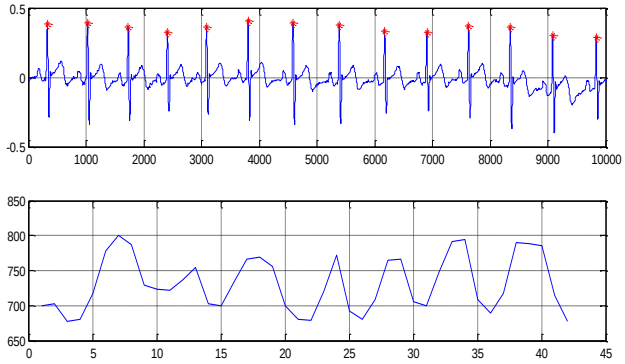

Figure 4. ECG signal (10 sec) and RRI tachogram (30 sec)

For extracting an emotional feature based on bio-signals, ECG analysis in the time (statistical and geometric approaches) and frequency domain (FFT and AR) was performed. RRI and heart rate (HR) offers the mean RRI (mean RRI) and standard deviation (std RRI), the mean heart rate (mean HR), RMSSD, NN50 and pNN50. RMSSD is the square root of the mean of the sum of the squares of differences between successive RRIs. NN50 is the number of RRI with 50msec or more and the proportion of NN50 divided by total number of RRI is pNN50. In addition to those, RRI triangular index (RRtri) and TINN are extracted from the histogram of RRI density as a geometric parameter. RRtri is to divide the entire number of RRI by the magnitude of the histogram of RRI density and TINN is the width of RRI histogram (M-N) as shown in Figure 5.

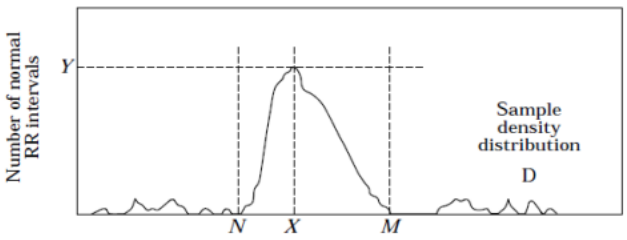

Figure 5. Histogram of RRI

The relations between RRI (n) and RRI (n+1) are called Lorentz or Poincare plot [12] as shown in Figure 6. Here, n

and n+1 are n-th and n+1-th values of RRI, respectively. In the figure, L is the direction that is efficient for representing data, and T is the orthogonal direction of L. The standard deviations, SD1 and SD2, are gotten for T and L directions, respectively. The cardiac sympathetic index (CSI) is calculated by CSI = 4SD2/4SD1 and the cardiac vagal index (CVI) is obtained from CVI = log10 (4SD1 * 4SD2) as an emotional feature. SD1, SD2, CSI and CVI reflect short term Heart Rate Variability (HRV), long term HRV, sympathetic nerve activity and parasympathetic activity, respectively.

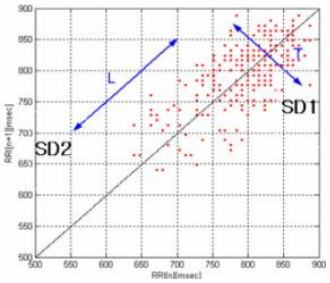

Figure 6. Lorentz plot of RRI

Also, we used the fast FFT and the AR power spectrum. Figure 7 shows Power spectrum density of FFT and AR on frequency domain. The band of low frequency (LF) is 0.04~0.15 Hz and the high frequency (HF) is 0.15~0.4Hz. The total spectral power between 0.04 and 0.15 Hz is apLF and the normalized power of apLF is nLF. apHF and nHF are the total spectral power between 0.15 and 0.4 Hz and the normalized power, respectively. L/H ratio means the ratio of low to high frequency power. These are resulted by averaging FFT and AR. LF and HF are used as indexes of sympathetic and vagus activity, respectively. The L/H ratio reflects the global sympatho-vagal balance.

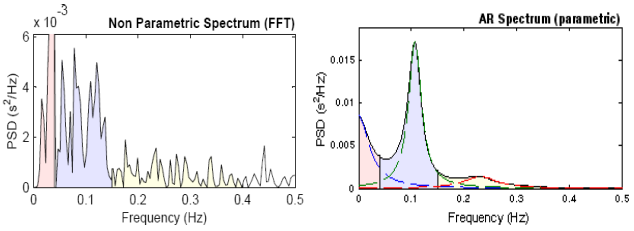

Figure 7. Power spectrum density of FFT (left) and AR (right)

The mean skin temperature (mean SKT) and maximum skin temperature (max SKT) and the mean amplitude of blood volume changes (mean PPG) are gotten from SKT and PPG, respectively.

D. Machine Learning Algorithm for Emotion Rrecognition

Fisher's LDA is one of the linear models to find a linear combination of features which characterizes or separates two or more classes of objects and is used in statistics, pattern recognition and machine learning. LDA finds the direction to project data on so that between-class variance in maximized and within-class variance in minimized, and then offers a linear transformation of predictor variables which provides a more accurate discrimination [7]. In LDA, the measurement space is transformed so that the separability between the emotional states is maximized. The separability between the emotional states can be expressed by several criteria.

$$W^{*} = \arg \max \left\{ \frac{W^{T} S_{B} W}{W^{T} S_{W} W} \right\} \quad (1)$$

CART is one of decision tree and nonparametric technique that can select from among a large number of variables those and their interactions that are most important in determining the outcome variable to be explained [10]. The fundamental principle underlying tree creation is that of simplicity. We prefer decisions that lead to a simple, compact tree with few nodes. In formalization this notion, the most popular measure is the entropy impurity (or occasionally information impurity):

$$i(N) = -\sum_{j} P(\omega_j) \log_2 P(\omega_j) \quad (2)$$

where, $P(\omega_j)$ is the fraction of patterns at node N that are in class ω_j. By the well-known properties of entropy, if all the patterns are of the same category, the impurity is 0; otherwise it is positive, with the greatest value occurring when the different classes are equally likely.

The Naïve Bayes algorithm is a classification algorithm based on Bayes rule and particularly suited when the dimensionality of the inputs is high [7]. When the dependency relationships among the features used by a classifier are unknown, we generally proceed by taking the simplest assumption, namely, that the feature are conditionally independent given the category, that is,

$$p(\omega_k \mid \mathrm{X}) \propto \prod_{i=1}^{d} p(\chi_i \mid \omega_k) \quad (3)$$

This so-called naïve Bayes rule often works quite well in practice, and it can be expressed by a very simple belief net.

SVM is the well-known emotion algorithms and non-linear model that support vector classifier can be extended to nonlinear boundaries by the kernel trick. SVM is designed for two class classification by finding the optimal hyperplane where the expected classification error of test samples is minimized and has utilized as a pattern classifier to overcome the difficulty in pattern classification due to the large amount of within-class variation of features and the overlap between classes, although the features are carefully extracted [8]. The distance from any hyperplane to a pattern y is |g(y)|/||a||, and assuming that a positive margin b exists

$$zk\ g(yk) / \|a\| \geq b,\ k = 1, \ldots, n; \quad (4)$$

The goal is to find the weight vector a that maximizes b. Here, zk is the class of k-th pattern, b is margin and g(y) is a linear discriminant in an augmented y space,

$$g(y) = aTy \quad (5)$$

III. EMOTION CLASSIFICATION

To examine the difference physiological responses of among four emotions, one-way ANOVA was performed using SPSS ver.18.0. We could identified that there are significant the differences in NSCR, meanSCR, meanPPG, TINN and FFT L/H ratio ($p<.05$) (Table 3). Results of post-hoc test (LSD) showed that the change of NSCR during stress is higher than other emotions, happiness, anger and surprise, and meanSCR induced by surprise increase more than other emotions significantly.

TABLE III. RESULT OF ONE-WAY ANOVA BY 28 FEATURES

Features		SS	df	MS	P
NSCR	between	30.451	3	10.150	.01
	within	986.756	357	2.604	
	sum	1017.206	360		
meanSCR	between	10.503	3	3.501	.00
	within	204.954	357	.541	
	sum	215.457	360		
meanPPG	between	4.130	3	1.377	.05
	within	245.480	357	.648	
	sum	249.610	360		
TINN (ms)	between	34.624	3	11.541	.05
	within	849.876	357	5.379	
	sum	884.500	360		
FFT L/H ratio	between	112.024	3	37.341	.04
	within	6125.350	357	16.162	
	sum	6237.374	360		

For recognition accuracy of emotions, the four machine learning algorithms were evaluated on only Training (TR), 10-fold Cross-Validation (CV) and Repeated Random Sub-sampling Validation (RRSV). For TR, the entire dataset is used to build a recognizer and evaluate the built recognizer. We have also applicated CV and RRSV cosidering that TR has the overfitting problem. In 10-fold cross-validation, the entire dataset is partitioned into 10 equal size subsets. Of the 10 subsets, a single subset is retained as the testing data for testing the recognizer, and the remaining 9 subdatasets are used as training data to build a recognizer. In RRSV, the 70% of the whole emotional patterns are selected randomly for training, the remaining patterns are used for testing purposes and this is repeated 10 times.

TABLE IV. RESULT OF EMOTION RECOGNITION ON FEATURE SPACE WITH 28 FEATURES

Machine Learning Algorithms	TR	CV	RRSV	
			Training	Testing
LDA	48.2	33.4	52.3±2.4	29.3±4.3
CART	86.7	35.8	83.3±1.1	34.3±5.6
Naive Bayes	77.7	43.7	78.9±1.4	38.4±5.9
SVM	100	31.9	100.0±0.0	28.0±4.9

We have performed feature normalization and the related parameters of algorithms using default values, which have offered with toolbox. Table 4 shows the recognition results by using the TR, CV and RRSV for 28 features. The accraccy of emotion recognition have higher values for training than testing. The CV exhibits the results for testing. To apply to real system, we have to discuss in the view point of testing. For 28 features, the results of emotion recogntion for CV has range of 31.9 to 43.7% when all emtions are recognized for test dataset. The accuracy of recognition for RRSV shows in range 28.0 to 38.4% for testing.

IV. CONCLUSIONS

The aim of this study was to classify four emotions, happiness, anger, surprise and stress, induced by audio-visual stimuli. For this, we have gotten the bio-signals based on ANS responses of the evoked emotions. Also, twenty-eight features have been analyzed and extracted from these signals. For four emotions classification, we have used four machine learning algorithms, namely, LDA, CART, Naïve Bayes, and SVM. The results were reported by only TR, CV and RRSV. However, we have only obtained very low recognition accuracy from 28.0 to 38.4% for testing and this means that there is a problem with improvement of recognition accuracy for the four emotions, becuase recognition results showed the low accuracy for testing. To apply to real system, we have to discuss in the view point of testing and this means that it needs to apply various methodologies for the accuracy improvement of emotion recognition in the future analysis. We will investigate various methodologies for dealing the accuracy improvement of emotion recognition in the future research (e.g., the deduction of the features such as NSCR or mean SCR are significant differences among emotions by statistical methods, data normalization or the use of enhanced algorithm). Although bio-signal offers a great potential for the emotion recognition in computer systems, in order to effectively exploit the advantages of bio-signals, there are limitations, such as standardization on the emotional model, the measures and feature extraction of bio-signals, signal patterns, and model for pattern recognition and classification [13]. Nevertheless, our result can be useful in developing an emotion recognition system based on bio-signals in HCI.

 ISBN: 978-1-61208-340-7

ACKNOWLEDGMENT

This research was supported by the Converging Research Center Program through the Ministry of Science, ICT and Future Planning, Korea (2013K00 0329 and 2013K000332).

REFERENCES

[1] R. W. Picard, E. Vyzas, and J. Healey, "Toward machine emotional intelligence: Analysis of affective physiological state," IEEE Transaction on Pattern Analysis and Machine Intelligence, vol. 23, 2001, pp. 1175-1191.

[2] F. Nasoz, K. Alvarez, C. L. Lisetti, and N. Finkelstein, "Emotion recognition from physiological signals using wireless sensors for presence technologies," Cognition, Technology and Work, vol. 6, 2004, pp. 4-14.

[3] W. Boucsein, Electrodermal activity, New York: Plenum Press, 1992.

[4] C. Maaoui and A. Pruski, Emotion recognition through physiological signals for human-machine communication. in Cutting Edge Robotics 2010, Vedran Kordic (Ed.), 2010, pp. 317.

[5] P. D. Drummond and S. H. Quah, "The effect of expressing anger on cardiovascular reactivity and facial blood flow in Chinese and Caucasian," Psychophysiology, vol. 38, 2001, pp. 190-196.

[6] S. D. Kreibig, "Autonomic nervous system activity in emotion: A review," Biological psychology, vol. 84, 2010, pp. 394-421.

[7] R. O. Duda, P. E. Hart, and E. G. Stork, Pattern Classification, 2nd ed-4th print, John Wiley and Sons, Inc., New York, 2000.

[8] P. D. Wasserman, Advanced Methods in Neural Computing, New York, Van Nostrand Reinhold, 1993.

[9] https://www.biopac.com/

[10] L. Breiman, J. H. Friedman, R. A. Olshen, and C. J. Stone, Classification and Regression Trees. Wadsworth, 1984.

[11] J. J. Gross and R. W. Levenson, "Emotion elicitation using films," Cognition and Emotion, vol. 9, 1995, pp. 87-108.

[12] O. M. Doyle, I. Korotchikova, G. Lightbody,W. Marnane, D. Kerins, and G. B. Boylan, "Heart rate variability during sleep in healthy term newborns in the early postnatal period," Physiological Measurement, vol.30, 2009, pp.847-860.

[13] J. Arroyo-Palacios and D. M. Romano, "Towards a Standardization in the Use of Physiological Signals for Affective Recognition Systems," Proceedings of Measuring Behavior 2008, Maastricht, The Netherlands, August 2008, pp. 121-124.

 ISBN: 978-1-61208-340-7

Cognitive Robotics: For Never was a Story of More Owe than This

Emanuel Diamant
VIDIA-mant
Kiriat Ono , Israel
email : emanl.245@gmail.com

Abstract— **We are now on the verge of the next technical revolution – robots are going to invade our lives. However, to interact with humans or to be incorporated into a human "collective" robots have to be provided with some human-like cognitive abilities. What does it mean? – Nobody knows. But, robotics research communities are trying hard to find out a way to cope with this problem. Meanwhile, despite abundant funding these efforts did not lead to any meaningful result (only in Europe, only in the past ten years, Cognitive Robotics research funding has reached a ceiling of 1.39 billion euros). In the next ten years, a similar budget is going to be spent to tackle the Cognitive Robotics problems in the frame of the Human Brain Project. There is no reason to expect that this time the result will be different. We would like to try to explain why we are so unhappy about this.**

Keywords – Cognitive robotics; information; physical information; semantic information.

I. INTRODUCTION

From the beginning, it was a fascinating idea: to create human-like living beings that would help and assist us in our tedious everyday duties. The history has preserved many famous stories about such undertakings – Pygmalion and his Galatea, Talos the guard of Crete (both from the ancient Greek mythology), Maharal's Golem from the late 16th century Prague, Frankenstein's monster of the early 19th century.

In the year 1920, that was Karel Capek who gave them their present-day name – Robots. In 1942, Isaac Azimov was the first who introduced the term – Robotics. In 1959, the first real, not imagined and not legendary, industrial robot had entered the factory floor and, strictly speaking, has heralded the beginning of the robotics era. Then, at the end of the past century, robots start to appear in our human surroundings.

It has immediately become clear that, to work with humans (in cooperation and in tight interaction with them), robots have to possess some human-like cognitive abilities. What does it mean "to possess human-like cognitive abilities"? – Nobody knew then, nobody knows today. But that does not matter – the robotics research community enthusiastically started to cope with the challenge, endorsed with ample budget funding provided by the USA Defence Advanced Research Projects Agency (DARPA) and the European Union Research and Technological Development (EU RTD) programme. We would like to provide a short account of these efforts.

II. MARCH TO THE GLORIOUS FUTURE

As it was just said above, the DARPA in USA and the European Commission in Europe are today the most prominent supporters of scientific and technological progress, which are operating worldwide and are promoting an extensive range of critically important research initiatives. In the past 10-15 years, Cognitive Robotics was certainly one among them.

A. DARPA's Projects on Cognitive Robotics

The DARPA has always posited itself as an authority aimed to address a wide range of technological opportunities directed to meet the national security challenges. Endorsed with a budget of up to $2.8 billion (in FY 2013), it pursues its objectives through a wide range of R&D programs [1]. Cognitive Robotics does not appear in DARPA's programme as a bundle of programs grouped by a common theme; on the contrary, in DARPA's practice Cognitive Robotics is handled as a collection of separate programs that share a common target issue. The list of Cognitive Robotics and Cognitive-Robotics-related programs launched in the years 2001-2013 can be seen in Table I.

DARPA's efforts on robotics are focused primarily on military and defence-related applications with a clear goal to bring real-time, integrated, multi-source intelligence to the battlefield. DARPA does not strive to replace the warrior with a robot, but it believes that it is possible to improve the abilities of individual warfighter by combining technological achievements with human brain cognitive capacities thus making information understanding and decision-making far more effective and efficient for military users. So, it tries hard, on one hand, to revolutionize the underlying technologies (for unmanned sensor systems and battlefield information gathering) and, on the other hand, to merge them with the next generation computational systems that will have some human-like cognitive capabilities (such as reasoning and learning capabilities) and levels of autonomy which are beyond those of the today's systems. The spectrum of programs presented in Table I reliably represents this DARPA's approach to Cognitive Robotics R&D.

 ISBN: 978-1-61208-340-7

TABLE I. DARPA'S PROJECTS ON COGNITIVE ROBOTICS

Cognitive Computing Systems (CoGS)	2008 – ….....
DARPA's Neovision project (NEOVISION2)	2009 – ……
Video and Image Retrieval and Analysis Tool (VIRAT)	2011 – ……
Autonomous Robotics Manipulation Program (ARM)	2011 – ……
DARPA Robotics Challenge (DRC)	2012 – ……
DARPA's Insight Program (DIP)	2013 – ….....
Biologically Inspired Cognitive Architectures (BICA)	2005 - 2007
The Cognitive Technology Threat Warning System (CT2WS)	2007 – ……
Cognitive Assistant that Learns and Organizes (CALO)	2003 - 2008
Personalized Assistant that Learns (PAL)	2003 - 2008
Augmented Cognition (AugCog)	2001 - 2006

B. The European programs on Cognitive Robotics

European Union research is conducted in a frame of research programmes called Framework Programmes for Research and Technological Development, in short Framework Programmes farther abbreviated as FP1 to FP8.

Cognitive Robotics related issues start to appear in the FP5 programme and then, respectively, continue to evolve and expand in the following FP6 and FP7 work programmes. Contrary to DARPA's approach, EU R&D activities are clustered to several main "themes" that are further segmented into "challenges", which are further divided into "objectives" in frame of which the individual projects are carried out. Cognitive Robotics in the Frame Programmes FP6 and FP7 is represented as a Challenge (Challenge 2) of the Information and Communication Technologies (ICT) theme (Theme 3). At the time of the transition from FP5 to FP6, when subdivision to Challenges was not yet introduced, Cognitive Robotics and its related issues such as Cognitive Vision and four other particular items appear straight as objectives in the Information Society Technologies (IST) theme (see Table II).

TABLE II. ROBOTICS IN FP5

Area	No. of projects	Total cost (M€)	Total EC funding (M€)
IST Demining	8	30,6	15,6
IST FET Neuro-IT	15	32,4	23,1
IST FET General	17	39,2	25,7
IST Cognitive Vision	8	24,2	17,3
GROWTH etc.	24	63,2	34,9
Total	72	**189,7**	116,5

TABLE III. COGNITIVE ROBOTICS IN FP6

Year	Objective	Total cost (M€)
2002 Work Programme	IST2002 - IV.2.1 Cognitive vision systems IST2002 - VI.2.2 Presence Research: Cognitive sciences and future media	? ?
2003-2004 Work Programme	2.3.1.7 Semantic-based Knowledge Systems 2.3.1.8 Networked Audiovisual systems and home platforms 2.3.2.4 Cognitive Systems 2.3.4.2.(vii) : Bio-inspired Intelligent Information Systems Proactive initiatives (i) Beyond robotics	55 60 25
2005-2006 Work Programme	2.4.6 Networked Audio Visual Systems and Home Platforms 2.4.7 Semantic-based Knowledge and Content Systems 2.4.8 Cognitive Systems 2.4.11 Integrated biomedical information for better health	63 112 45 75
	Total	**435**

 ISBN: 978-1-61208-340-7

TABLE IV. COGNITIVE ROBOTICS IN FP7

Year	Call	Objective	Budget (M€)
2007	Call 1	ICT-2007.2.1 Cognitive systems, interaction, robotic ICT-2007.4.2 Intelligent content and semantics ICT-2007.8.3 Bio-ICT convergence	96 51 20
2008	Call 3	ICT-2007.2.2 Cognitive systems, interaction, robotics ICT-2007.4.3 Digital libraries and technology-enhanced learning ICT-2007.4.4 Intelligent content and semantics ICT-2007.8.5 Embodied Intelligence	97 50 ? ?
2009	Call 4	ICT-2009.2.1: Cognitive Systems and Robotics ICT-2009.2.2: Language-Based Interaction	73 26
2010	Call 6	ICT-2009.2.1: Cognitive Systems and Robotics ICT-2009.2.2: Language-Based Interaction	80 30
2011	Call 7	ICT-2011-7 Cognitive Systems and Robotics	73
2012	Call 9	ICT-2011-9 Cognitive Systems and Robotics	82
2013	Call 10	ICT-2013.2.1 Robotics, Cognitive Systems & Smart Spaces, Symbiotic Interaction ICT-2013.2.2 Robotics use cases & Accompanying measures	67 23
		Total	**768**

Juxtaposing Table II, Table III, and Table IV, it can be seen how from a Cognitive Vision objective in FP5 (a Cognitive Robotics related topic) Cognitive Robotics has evolved to a full-blown Challenge (Challenge 2) in the FP6 and FP7 programmes, steadily growing from 190 M€ in FP5 to near 1.2 billion euros in the next FP6 and FP7 programmes (435 M€ for FP6 + 768 M€ for FP7).

III. DECEIVED EXPECTATIONS

During all these times, the declared goals of Cognitive Robotics programmes were: (As it follows from DARPA's News Releases) "to create adaptable, integrated intelligence systems aimed to augment intelligence analysts' capabilities to support time-sensitive operations on the battlefield" [11]. And in another document – "The objectives (of DARPA's programs) are not to replace human analysts, but to make them more effective and efficient by reducing their cognitive load and enabling them to search for activities and threats quickly and easily" [12].

Objectives of Challenge 2 programs in the EU research initiative have been far more ambitious – The FP6 Workprogramme for years 2003-2004 states: (The objective is) "to construct physically instantiated or embodied systems that can perceive, understand (the semantics of information conveyed through their perceptual input) and interact with their environment, and evolve in order to achieve human-like performance in activities requiring context-(situation and task) specific knowledge, etc. The development of cognitive robots whose "purpose in life" would be to serve humans as assistants or "companions". Such robots would be able to learn new skills and tasks in an active open-ended way and to grow in constant interaction and co-operation with humans" [4].

These objectives (almost in similar words) are repeatedly declared in all further Work programmes. For example, the 2011-2012 Workprogramme says that in these words: "Challenge 2 focuses on artificial cognitive systems and robots that operate in dynamic, nondeterministic, real-life environments… Actions under this Challenge support research on engineering robotic systems and on endowing artificial systems with cognitive capabilities" [8].

Careful examination of the outcome that results from both the DARPA's programs and from the FP5-FP7 objectives leads to a univocal conclusion – the announced goals of all these programs have never been reached!

The explanation of this phenomenon is very simple – people try to provide robots with human-like cognitive abilities, but at the same time the same people are devoid of even a slightest understanding about what does the notion of "human-like cognitive abilities" really mean.

During the past years, the problem has become obvious and has been even mentioned in the 2011-2012 Workprogramme: "Hard scientific and technological research issues still need to be tackled in order to make robots fit for rendering high-quality services, or for flexible manufacturing scenarios. Sound theories are requisite to underpinning the development of robotic systems and providing pertinent design paradigms, also informed by studies of natural cognitive systems (as in the neuro- and behavioural sciences) [8].

 ISBN: 978-1-61208-340-7

Even more definite was the statement of the year 2013 Work programme – "An additional research focus targeted under this challenge will address symbiotic human-machine relations, which aims at a deeper understanding of human behaviour during interaction with ICT, going beyond conventional approaches. The work on cognitive systems and smart spaces and on symbiotic human-machine relations is not restricted to robotics" [13].

This promise was also left unfulfilled. At the end of 2013, Cognitive Robotics research has moved to and has tightened itself with the human brain research activities.

IV. NEW HOPES

At the beginning of year 2014, both Europe and USA will launch ambitious programmes for human brain research. In the USA, the programme is called the Brain Research through Advancing Innovative Neurotechnologies (BRAIN) Initiative and it was announced by President Barack Obama on April 2013. Its accomplishment will be led by the National Institutes of Health (NIH), DARPA, and the National Science Foundation (NSF) [14].

In Europe, the Human Brain Project is a ten-year project, consisting of a thirty-month ramp-up phase, funded under FP7, with support from a special flagship ERANET, and a ninety-month operational phase, to be funded under Horizon 2020 programme. The project, which will have a total budget of over 1 billion Euros, is European-led with a strong element of international cooperation. The goal of the project is to build a completely new ICT infrastructure for neuroscience, and for brain-related research in medicine and computing, catalysing a global collaborative effort to understand the human brain and its diseases and ultimately to emulate its computational capabilities [15].

The main features of the two projects are collected in the Table V.

As it follows from the Table V, Cognitive Robotics is not among the main goals of the two Flagship initiatives, but it is definitely among their main purposes. In the European Human Brain Project it appears as the "Cognitive Architectures" line in the list of the HBP topics. In the American BRAIN Project Cognitive Robotics issues are hidden behind the "Link neuronal activity to behaviour" topic.

V. AN ATTEMPT TO PREDICT THE FUTURE

In attempt to predict the future results of these two projects, let us juxtapose them with something that is well known to us and that we are quite familiar with. We mean the enduring and persistent study of National Economics. While the human nervous system can be seen as the driving force behind the behaviour of a single human, national economics can be seen as the driving force behind the behaviour of a whole human society. Both are complex distributed systems whose efficient operation is supported by an all-embracing communication system. In the Human brain that is the Nervous system, in the National Economics this is the Transportation system.

From Table VI, one can see that the principal features of the Transportation system are well reflected in both brain research projects. Only one feature "What is being transported?" is missing in the future brain studies. A proper answer to the question "What is being transported in the Nervous system between different brain parts?" should be "Information". But, for unknown reasons, that is left undefined in both future mega-projects. And the consequences of this omission are predictable.

TABLE V EUROPEAN AND AMERICAN HUMAN BRAIN PROJECTS

Parameter	European HB Project	American BRAIN Project
Duration	10 years.	long-lasting programme
Funding	$ 1.35 billion.	$110 million in the 2014 fiscal year supposed to ramp up this commitment in subsequent years
Main Topics	- Human and mouse neural channelomics. - Genotype to phenotype mapping the brain. - Identifying, gathering and organizing neuroscience data. - **Cognitive architectures.** - Novel methods for rule-based clustering of medical data. - Neural configurations for neuromorphic computing systems. - **Virtual robotic environments, agents, sensory & motor systems.** - Theory of multi-scale circuits.	- Generate a census of brain cell types - Create structural maps of the brain - Develop new, large-scale neural network recording capabilities - Develop a suite of tools for neural circuit manipulation - **Link neuronal activity to behavior** - Integrate theory, modeling, statistics and computation with neuroscience experiments - Delineate mechanisms underlying human brain imaging technologies - Create mechanisms to enable collection of human data for scientific research - Disseminate knowledge and training

 ISBN: 978-1-61208-340-7

TABLE VI JUXTAPOSING HUMAN BRAIN PROJECTS

Economic system	**Human brain system**	
Transportation system	Nervous system	
System's Features	American BRAIN Project	European HB Project
Network topology (road and pathway maps)	The Brain Connectome Project	Neural channelomics Neuroinformatics platform
Network dynamics (Traffic) Transportation means, time tables, hubs, congestions	The DARPA's SyNAPSE Project	Neuromorphic computing platform
What is being transported (through the network) Raw materials, Goods, Freights.	**(Information)**	**(Information)**

On the other hand, the reason of this omission is also fully understandable: we don't know what Information is and how it is being transported (processed) in the brain. (That the brain is an information processing system is a widely accepted hypothesis in the scientific community). So, it will be wise to try to understand what information is.

VI. WHAT IS INFORMATION

While a consensus definition of information does not exist, we would like to propose a definition of our own (borrowed and extended from the Kolmogorov's definition of information, first introduced in the mid-sixties of the past century):

Information is a linguistic description of structures observable in a given data set [16].

Two types of structures could be distinguished in a data set – primary and secondary data structures. The first are data elements aggregations whose agglomeration is guided by natural physical laws; the others are aggregations of primary data structures which appear in the observer's brain guided by the observer's customs and habits. Therefore, the first could be called Physical data structures, and the second, Meaningful or Semantic data structures. And their descriptions should be accordingly called **Physical Information** and **Semantic Information**.

This subdivision is usually overlooked in the contemporary data processing approaches leading to mistaken and erroneous data handling methods and techniques.

In [17], E. Diamant presents a list of publications on the subject and a more extended explanation of information description duality can be found. Meanwhile, it is important to explain the consequences that immediately pop up from this assertion. And which are critically important for the right definition of the notion of cognition. In the light of this just acquired knowledge, we can certainly posit that **cognitive ability is the ability to process information**. And that is what our brains are doing, and that is what we are striving to replicate in our Cognitive Robots designs.

First of all, physical information is carried by the data and therefore can be promptly extracted from it. At the same time, semantic information is a description of observer's arrangement of the physical data structures and therefore it can not be extracted from the data, because semantics is not a property of the data, it is a property of an observer that is watching and scrutinizing the data. As such, semantics is always subjective and it is always a result of mutual agreements and conventions that are established in a certain group of observers, or a future group of robots and humans that act as a team sharing a common semantic understanding (semantic information) about their environment. An important sequel of this is that the semantic information can not be learned autonomously, but it should be provided to a cognitive robot from the outside (semantics has to be taught and not learned, as it is usually requested by all workprogrammes).

Another important corollary that follows from the new understanding of information nature is that information description is always a linguistic description, that is, a string of symbols which can take a form of a mathematical formula (don't forget that mathematics is a sort of a language) or a natural language item – a word, a sentence, or a piece of text. That is a very important outcome of the new theory considering that contemporary approaches to the problem of information processing are assuming computer involvement in the processing task. However, contemporary computers are data processing machines which are not supposed to process natural language texts which are carrying semantic information.

Finally, we would like to provide some examples of widespread misunderstandings that appear in the Calls of proposals issued by DARPA and EU Commission: In the "ICT Work Programme 2009/2010, (C(2009) 5893)" [7], in its "Part 4.2 Challenge 2: Cognitive Systems, Interaction, Robotics" the problem that Robotic systems have to cope with is specifies as "extracting meaning and purpose from bursts of sensor data or strings of computer code…" This is

 ISBN: 978-1-61208-340-7

a false and a misleading statement – sensor data does not possess semantics, and therefore, meaning and purpose can not be extracted from it.

DARPA's Document "Deep Learning" (RFI SN08-42) states that: "DARPA is interested in new algorithms for learning from unlabeled data in an unsupervised manner to extract emergent symbolic representations from sensory input…" Again, that is a false and a misleading statement – symbolic representations (semantics) could not be learned from data.

VII. CONCLUSION

Cognitive Robotics R&D is a very important branch of contemporary science that is paving the road to the next technological revolution – smart robots that are invading our everyday lives. Until now, the extensive research efforts of the Cognitive Robotics field investigators have been derailed by a wrong understanding about the essence of information, in general, and semantic information, in particular. We hope that the paper will contribute to some changes in this situation.

REFERENCES

[1] DARPA's Mission in a Changing World, DARPA Framework 2013, Available: http://www.hsdl.org/?view&did=735402 retrieved: March, 2014.

[2] P. Karp and T. Skordas, "Robotics in the IST Programme", 22nd JCF Meeting, 16 - 18 October 2003, Madrid, Spain, Available: http://www.nsf.gov/eng/roboticsorg/documents/EU_000.pdf retrieved: March, 2014.

[3] 2002 Work programme, Available: ftp://ftp.cordis.europa.eu/pub/ist/docs/b_wp_en_200201.pdf retrieved: March, 2014.

[4] 2003-2004 Workprogramme, Available: ftp://ftp.cordis.europa.eu/pub/ist/docs/wp2003-04_final_en.pdf , retrieved: March, 2014.

[5] 2005-06 Work Programme, Available: ftp://ftp.cordis.europa.eu/pub/ist/docs/ist_wp-2005-06_final_en.pdf , retrieved: March, 2014.

[6] 2006 Work Programme Fourth Update, Available: ftp://ftp.cordis.europa.eu/pub/ist/docs/wp_4th_update_en.pdf , retrieved: March, 2014.

[7] Updated work programme 2009 and work programme 2010, Available: ftp://ftp.cordis.europa.eu/pub/fp7/ict/docs/ict-wp-2009-10_en.pdf, retrieved: March, 2014.

[8] Updated work programme 2011 and work programme 2012, Available: ftp://ftp.cordis.europa.eu/pub/fp7/ict/docs/ict-wp-2011-12_en.pdf , retrieved: March, 2014.

[9] Work programme 2013, Available: http://cordis.europa.eu/fp7/ict/docs/ict-wp2013-10-7-2013.pdf retrieved: March, 2014.

[10] ICT Challenge 2: Cognitive Systems and Robotics, Available: http://cordis.europa.eu/fp7/ict/programme/challenge2_en.html retrieved: March, 2014.

[11] DARPA advances video analysis tools, Available: http://www.darpa.mil/NewsEvents/Releases/2011/2011/06/23_DARPA_advances_video_analysis_tools.aspx . retrieved: March, 2014.

[12] Unified Military Intelligence Picture Helping to Dispel the Fog of War, Available: http://www.darpa.mil/NewsEvents/Releases/2013/09/05.aspx retrieved: March, 2014.

[13] ICT Work programme 2013, Available: http://cordis.europa.eu/fp7/ict/docs/ict-wp2013-10-7-2013.pdf retrieved: March, 2014.

[14] BRAIN Working Group Interim Report, Available: http://www.nih.gov/science/brain/09162013-Interim%20Report_Final%20Composite.pdf retrieved: March, 2014.

[15] The Human Brain Project, Available: https://www.humanbrainproject.eu/documents/10180/17648/TheHBPReport_LR.pdf/18e5747e-10af-4bec-9806-d03aead57655 , retrieved: March, 2014

[16] E. Diamant, "Let Us First Agree on what the Term "Semantics" Means: An Unorthodox Approach to an Age-Old Debate", In M. T. Afzal, Ed., "Semantics - Advances in Theories and Mathematical Models", pp. 3 – 16, InTech Publisher, http://www.intechopen.com/statistics/35998 retrieved: March, 2014

[17] E. Diamant, "Brain, Vision, Robotics, and Artificial Intelligence", Available: http://www.vidia-mant.info, retrieved: March, 2014.

 ISBN: 978-1-61208-340-7

Mechanical Cognitivization

Gideon Avigad
Mechanical Engineering Department
Ort Braude College of Engineering
Karmiel, Israel
e-mail: gideona@braude.ac.il

Avi Weiss
Mechanical Engineering Department
Ort Braude College of Engineering
Karmiel, Israel
e-mail: avi@braude.ac.il

***Abstract*— The common approach for training robots is to expose them to different environmental scenarios, training their controllers to have the best possible commands when untrained scenarios are encountered. When humans train, they do the same. They try new manipulations by performing within different environments. However, humans training (and in fact development from infancy to maturity) also includes a type of training which, although claimed to improve cognitive capabilities, has not, to date, been adopted for the training of robots. This type of training involves the restriction of manipulation capabilities while performing different tasks, e.g., climbing with just one hand. The hereby reported upon research aims at exploring the invigorating idea that such training would enhance the robustness of robots and moreover may increase our understanding of why humans utilize such training in the first place. The main idea has been patented and is here published by a new name: Mechanical Cognitivization (MC).**

Keywords-cognitive robotics; developmental robotics; evolutionary algorithms.

I. INTRODUCTION

Robots are ubiquitous in performing industry related tasks and operating within hazardous environments. However, they scarcely participate in day to day tasks. In contrast, humans are those doing most of such jobs. The human competencies to perform arduous and complicated tasks while controlling and maneuvering a multi-degrees-of-freedom body are truly amazing. Through repeatedly executing different tasks, the human brain learns how to control the complex body.

Observing the humans' activities, two of them are of interest to the current research. The first is associated with sport related training. For example, while training, climbers often use different techniques such as climbing with one hand tied, without hands at all (on sloping walls) and blindfolded. Clearly, such situations are not envisaged in the actual climbing and are all training techniques that are intended to improve the climbers' sense of balance. Such restriction of movement, as a way to train, may be found in other sports (e.g., swimming, martial arts, and more). The other activity is also related to training under restricted movement, and involves the way human capabilities are developed from day one. Babies' brains are trained on a non-fully developed body. In contrast to calves, they cannot stand, walk or run. Yet, the evolution calls for such a slow development and compels using restricted capabilities. Maybe, this is due to the fact that in many situations, just some of the body's abilities need to be used and the body has to train also these sub-manipulations. It should be noted that in many sports, it is acknowledged that it is better to start young and let the body and mind adapt to the specific demands of that field of sport.

In contrast to the above, the major developments, as related to robots' learning and cognition were made with respect to the competencies of their artificial brains to learn, conceptualize, perform offline-planning based on anticipation and more [1]. However, these brains utilized fully developed bodies/embodiments. This is not to say that simultaneous evolution of solutions and their controllers were not investigated, but rather that such a development always considered one defined model for the body with a related controller [2].

The research proposed here suggests exploring the novel idea of enhancing the robustness of robots through training them while considering their final bodies/embodiments as well as their restricted-modes (less capable versions). It is contemplated that such training would enhance the robustness of robots to perform untrained maneuvers as well as to cope with malfunctions and unexpected working conditions. Moreover, such training is envisaged to be more optimally facilitated by specific bodies when compared to others. Therefore, optimization has to be incorporated. The basic idea has been patented [3].

In order to better elucidate the idea, suppose that a Robotic Climber (CR) that climbs on a wall that has poles sticking out of it, has to be developed. The left panel of Figure 1 depicts one possible mechanical configuration (body) for such a CR. The CR should now be trained to maneuver up and to grasp one of the poles (A or B).

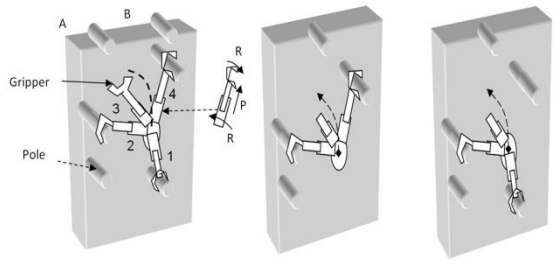

Figure 1: CR having four links is trained using all of them (left panel) and using restricted modes (middle and right panels).

 ISBN: 978-1-61208-340-7

The idea suggested here is that while training this CR's controller, not only this body should be utilized, but also its restricted modes. Two of such restricted modes are depicted in the middle and right panels of the figure. Clearly, performing such a maneuver by utilizing one of the restricted modes might be associated with degraded performances (e.g., bigger integral of the square error, measured while considering the planned and the actual performed maneuver). Restricted modes may include the following restrictions: a. Using just some of its mechanical capabilities, such as restricting some of the links from moving, that is if the robot has four arms/links, it will be restricted to use three/two of them or not using its gripper, b. Restricting the movement of the arms/links to less than their full possible extent, c. Deliberately imposing friction at joints, d. Changing the stiffness of links, e. Restricting the performances of actuators, by for example: reducing the power supply to the actuators or using weaker actuators (smaller motors).

The paper is organized as follows. In Section II, the background for the current study is given. In Section III, a description of the already attained results is given. This is followed by Section IV, where a discussion and envisaged future work are given.

II. BACKGROUND

Over the past several decades, a great deal of research attention has been directed at cognition and its implementation for artificial brains. The inspiration provided by human beings toward producing a machine that will copy human abilities is evident. Different models of cognition have been adopted to produce artificial cognitive systems or cognitive architectures. Cognitive architectures [1] represent attempts to create unified theories of cognition, i.e., theories that cover a broad range of cognitive issues, among them attention, memory, problem-solving, decision-making, learning. These theories consider several aspects, including psychology, neuroscience, and computer science. Examples of such architectures are EPIC [4], and ACT-R [5]. Some of these architectures have been claimed to be more adequate than others for use as cognitive brains for robots. This distinction [1], is rooted in the differences between the "cognitivist" and the "emergent" philosophies of cognition. The philosophy of emergent cognition contends that the relationship between the cognitive architecture and the body it is controlling (e.g., robots) is essential to the development of cognition. An associated philosophy is embodied cognition [6][7], which states that cognition can be influenced and biased by states of the body and that abstract cognitive states are grounded in states of the body. Among the architectures that facilitate this view is the biologically plausible brain-inspired neural-level cognitive architecture proposed by Shanahan [8], in which cognitive functions such as anticipation and planning are realized through internal simulation of interaction with the environment.

Several approaches have been proposed to improve the response of artificial entities to specific stimulations by circumventing complex cognitive architecture. For example, the computational model of perception and action for cognitive robots discussed by Haazebroek et al. [9] embraces the view that there is a direct route from perception to action that may bypass cognition [10]. A related approach is morphological computing [11][12][13], in which the idea is to design the mechanical structure to respond directly to a stimulus. This response is a result of the special morphology (shape, materials inter-relation among parts) of the structure. For example, in [14], the special features of a hand (Yoki hand) partially built from flexible deformable materials enable it to easily grasp different objects with no need for controller feedback. This notion has gained a great deal of interest, and for the past several years workshops have been dedicated to considering different aspects of morphological computing, such as artificial skin and stretchable sensors, compliant actuators and mechanisms, and soft materials in robotics.

Most relevant to the current paper are studies conducted by Mark Lee's group at Aberystwyth, UK. Their research is related to Developmental Robotics [15]. According to this approach, which is rooted in the way babies develop, cognitive development is achieved through staged growth of cognition as the sensomotoric competencies gradually and sequentially improve. In several publications [16][17] [18], Lee's group introduced and developed what they term as 'constraint lifting'. At each stage, learning takes place with certain constraints imposed on the sensomotoric system. At the next stage, some of these constraints are removed or 'lifted'. For example, learning hand-eye coordination in manipulating a robotic arm has been investigated. In that case, as learning progressed, constraints imposed on moving parts of the robot (e.g., using the fingers) were 'lifted'.

The proposed research focuses on the enhancement of cognition by considering the mechanical structure, as is the case in morphological computing. Here, however, the cognitive architecture is of vital importance, and the mechanical structure and its possible restricted modes (permutations of the final structure) are utilized for training the cognitive architecture. This means that the mechanical structure is the driving force for the enhancement of cognition. Moreover, the current project involves several basic differences from the works, such as [18]: a) In contrast to the sequential staged growth, MC may be enhanced simultaneously. b) In the proposed approach, constraining manipulations may take place any time along the robot's life time. c) In our research, a search for embodiments that will optimally benefit from the MC training will be conducted.

III. PROMISING INITIAL RESULTS

Mathematical functions rather than a model of a CR were used to elucidate the concept of MC and to demonstrate its potential. A polynomial function Y(x) of order m, where x is a vector of inputs (e.g., location of poles), is used to represent the "environment" (the climbing wall) to which the CR must adapt (i.e., climb in the best way). In other words, Y(x) may be viewed as a planned route for the robot to follow. The CR's controller is a neural net (NN) whose outputs are the coefficients of a polynomial of order n, $y(x) = a_1 x^n + a_2 x^{n-1} + \ldots + a_n$. Each output may be viewed as a control signal (here a coefficient) to a motor of a

manipulator that moves a robotic arm. By means of kinematics, the sum of the arm's movements results in the location of the CR on the wall, where the summing is represented by y(x). One way to enhance the training is to minimize the error, $Error = Y(x) - y(x)$. Figure 2 depicts the correlation between the CR case and the function representation.

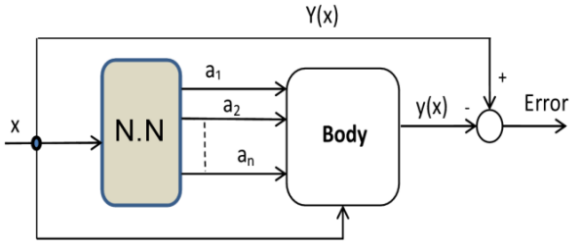

Figure 2. The correlation between the CR and the related function representation.

In order to train the net to provide output adequate to the environment (a function of order m), the artificial learning system is set, as depicted in Figure 3.

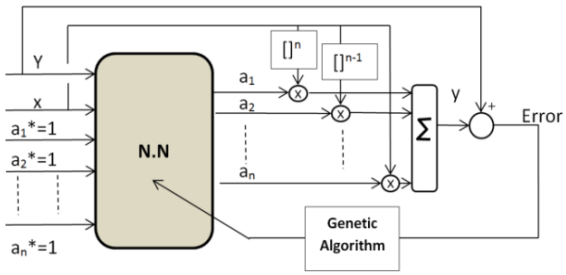

Figure 3. The artificial NN with no restricted modes.

The input to the NN is a list of K, x and corresponding Y(x) values that are fed sequentially to the net. The net has n extra inputs (flags), namely: $[a_1^*, a_2^*, \ldots . a_n^*]$. These flags serve as the feedback to the controller and indicate the condition of related outputs. That is, if all outputs are functioning (no restriction of movement is associated with the manipulator's links), the value of the corresponding flag will be set to one, while if there is a restriction (unable to move due to a malfunction) a value of zero will be assigned to that flag. In the non-restricted training mode these flags are all set to one, indicating that no restriction is imposed on outputs and that all of them participate in estimating a function Y(x). A genetic algorithm was used to tune the net's weights so as to minimize the error. The results of the training are in the form of weights that for each input [x, Y(x)] produce a different set of outputs that best fit the target function Y(x). In the restricted mode, training the NN uses different sets of inputs, exploiting not more than the former system's available resources (K pairs). 1/n of the inputs, were pairs fed to the net together with all the flags, which were set to one as in the unrestricted mode. For the next 1/n inputs, the first output was prohibited and the corresponding flag was set to zero, as shown in Figure 4.

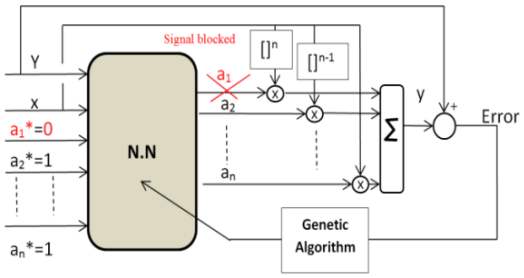

Figure 4. The artificial NN training setting for a restricted mode.

The implication of this training is that the weights are now trained to produce only n-1 outputs so as still to provide the best fit to the original function (environment). The other available resources were used to train the restricted modes by repeating this procedure for all other outputs while setting the corresponding flags to zero. In another version of this training, the available resources were divided among the restricted mode training such that more than one output was restricted. The left panel of Figure 5 depicts a target function as a dashed curve.

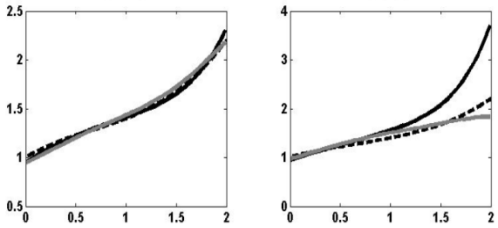

Figure 5. Left panel: The two NNs are trained to follow a function, right panel: Restricted mode shows better performances in following a function.

The trained non-restricted and restricted net outputs for a new arbitrary set of x points are shown in that panel by the black and the grey curves, respectively. Next, the performances of these differently trained entities have been compared while considering different scenarios: A. Malfunction in one or more of the outputs: In this scenario the environment is not altered (i.e., the same function has to be correlated) and the two different systems must still fit it. As stated in the patent, the MC-based system provides feedback that informs the net that there is a problem by setting the corresponding flag to zero. Because such situations have been included as part of the MC training, the performances of the related entity are expected to be superior. B. Environmental changes: In these scenarios, all flags are set to one (no malfunctions). This means that the two systems must perform in an untrained environment. A change in the environment is simulated by changing Y(x) by altering the coefficients (including setting one or several to zero) and the powers (not using only integers as powers). This is tested practically by entering a new set of inputs pairs (x, Y(x)) that corresponds to these changes. The right panel of Figure 5 depicts a common situation in which the MC approach showed merit. Here again, the target function, the non-restricted-mode trained function and the MC trained

 ISBN: 978-1-61208-340-7

function are designated by dashed, black and grey curves, respectively.

These scenarios yielded the following observations: a) As expected, the superiority of the MC training was unquestionable for scenario A. b) For scenario B, no conclusive conclusions could be made, although as the n-m difference grew (possibly related to more degrees of freedom associated with the CR), the statistical success of the MC training became more profound. This observation clearly implies that, depending on possible environmental changes, some entities (order of n) will benefit more from MC training. c) If planning is taken into account, that is, if the different performances resulting from the different restricted-mode models are assessed before action is taken, the superiority of the MC is unquestionable. This means that at least one of the flags is deliberately set to zero, prohibiting at least one of the outputs so as to best fit the function at hand (the new environment). Thus, the CR may choose whether to use all of its arms in order to best fit the needed maneuver. A decision to deliberately prohibit movement may also be the result of failing to advance along a route and trying a different strategy for advancement.

IV. CONCLUSION AND FUTURE WORK

The suggested idea is to enhance the robustness of robots in performing within changing environments and tasks by optimizing and training them while exploiting their final mechanical configuration as well as their restricted mode configurations. Restricted modes are modes where part of the mechanical capabilities, are restricted. This means that such training should take into account multi-models (kinematics and dynamics) while training the entity to perform within different scenarios. The dependency of the controller's tuning, which may be related to cognition, on the mechanical structure and its related restricted modes, for the sake of inducing cognition, has been termed here as Mechanical cognitivization. For now, it seems that the success of the MC would be, for all scenarios, dependent upon optimizing the entity itself in order for it to fully exploit this type of training. It is noted that the main envisaged drawback of such optimized entities is that they will probably be more complicated and therefore will cost more. Although for the cases where planning is possible, success is more easily obtained.

As for future work, we intend to further exploit the use of functions in order to explore the fundamentals of MC optimization and training. However, due to the fact that the correlation between functions and robots is not always apparent, the idea will be examined through evolving embodiments and simulating their performances within artificial environments. More futuristic plans include testing the MC by using learning by demonstrations and more.

V. ACKNOWLEDGMENTS

This research was supported by a Marie Curie International Research Staff Exchange Scheme Fellowship within the 7th European Community Framework Programme.

VI. BIBLIOGRAPHY

[1] D. Vernon, G. Metta, and G. Sandini, "A Survey of ArtificialCognitive Systems: Implications for the Autonomous Development of Mental Capabilities in Computational Agents," Evolutionary Computation, IEEE Transactions on, vol.11, no.2, pp.151-180, April 2007.

[2] M. Mazzapioda, A. Cangelosi, S. Nolfi, "Evolving morphology and control: a distributed approach," In Proceedings of the Eleventh IEEE Congress on Evolutionary Computation (CEC'09), May 2009, pp 2217-2224.

[3] G. Avigad, and A. Weiss,, "Method and System for Developing Cognitive Responses in a Robotic Apparatus", US Non Provisional Application No.: PCT/IL2013/050906.

[4] D. Kieras and D. Meyer, "An overview of the epic architecture for cognition and performance with application to human-computer interaction," Human-Computer Interaction, vol. 12, no. 4, 1997.

[5] P. Langley, "An adaptive architecture for physical agents," Proc. IEEE/WIC/ACM International Conference on Intelligent Agent Technology. Compiegne, France: IEEE Computer Society Press, 2005, pp. 18–25.

[6] L. Shapiro, The Mind Incarnate. Cambridge, MA: MIT Press, 2004.

[7] L. Shapiro, Embodied Cognition. NY: Routledge Press, 2011.

[8] M. P., Shanahan, "Emotion, and imagination: A brain-inspired architecture for cognitive robotics," in Proceedings AISB 2005 Symposium on Next Generation Approaches to Machine Consciousness, April 2005, pp. 26–35.

[9] P. Haazebroek, S. Van Dantzig, and B. Hommel. A computational model of perception and action for cognitive robotics, Cognitive Processes. vol. 12, no. 4, pp. 355–365, Nov 2011.

[10] JR. Simon, AP. Rudell (1967) "Auditory S-R compatibility: the effect of an irrelevant cue on information processing". J Appl Psychol, vol. 51, pp. 300–304.

[11] R. Pfeifer, F. Iida, and G. Gomez, "Morphological computation for adaptive behaviour and cognition" International Congress Series vol. 1291, pp. 22-29, 2006.

[12] R. Pfeifer and G. Gomez In B. Sendhoff et al. (Eds.) Morphological Computation – Connecting Brain, Body, and Environment,: Creating Brain-Like Intelligence, LNAI 5436, pp. 66–83, 2009. Springer-Verlag Berlin Heidelberg 2009.

[13] T.M. Kubow, R.J. Full, "The role of the mechanical system in control: a hypothesis of self-stabilization in hexapedal runners", Philosophical Transactions, Royal Society. Lond., B vol. 354, pp. 849– 861, May 1999.

[14] H. Yokoi, et al., Mutual adaptation in a prosthetics application, in: F. Iida, R. Pfeifer, L. Steels, Y. Kuniyoshi (Eds.), Embodied Artificial Intelligence, vol. 3139, Springer LNAI, 2004, pp. 146– 159.

[15] M. Asada, K. Hosoda, Y. Kuniyoshi, H. Ishiguro, T. Inui, Y. Yoshikawa, M. Ogino, and C. Yoshida, "Cognitive Developmental Robotics: A Survey," IEEE Transactions on Autonomous Mental Development, vol. 1, no. 1, pp. 12-34, May 2009.

[16] M. H. Lee, Q. Meng, and F. Chao, "Developmental learning for autonomous robots," Robotics and Autonomous Systems, vol. 55, no. 9, pp. 750–759, 2007.

[17] M. Huelse, S. McBride, and M. Lee, "Fast Learning Mapping Schemes for Robotic Hand–Eye Coordination," Cognitive Computation, vol. 2, no. 1, pp. 1–16, 2010.

[18] J. Law, M. Lee, M. Huelse, and A. Tomassetti, "The infant development timeline and its application to robot shaping" Adaptive Behavior 19 (5), 335-358.2011

 ISBN: 978-1-61208-340-7

A Design of Memory-based Learning Classifier usign Genteic Strategy for Emotion Classification

Momory-based Learing Classifier for Emotion Classification

Byoung-Jun Park, Eun-Hye Jang,
Sang-Hyeob Kim, Chul Huh
IT Convergence Technology Research Laboratory
Electronics and Telecommunications Research Institute
Daejeon, Republic of Korea
{bj_park, cleta4u, shk1028, chuh}@etri.re.kr

Myung-Ae Chung
IT Convergence Services Future Technology Research
Electronics and Telecommunications Research Institute
Daejeon, Republic of Korea
machung@etri.re.kr

***Abstract*—In this study, we discuss emotion classification for seven kinds of emotion (happiness, sadness, anger, fear, disgust, surprise, stress) in the psycho-physiological research. Seven emotions are evoked by stimulus formed on audio-visual film clips, and then physiological signals of autonomic nervous system responses are measured for the reaction of stimulation. Additionally, seven different emotions will be classified by the proposed classification methodology using physiological signals. We introduce a classification methodology on memory-based learning that dwells upon the usage of genetic strategy (Genetic Algorithms). Genetic algorithms (GAs) take selection problems of instances and features of memory into two level optimization processes. In the first level, GAs chooses *P* % of instances as a set of memory comes from instances with *c* classes. In the second level of the optimization process, GAs is instrumental in the formation of a core set of features that is a collection of the most meaningful and discriminative components of the original feature space. In classification problems, it becomes important to carefully select instances and establish a subset of features in order to achieve a sound performance of a classifier. The study offers a complete algorithmic framework and demonstrates the effectiveness of the approach for the classification of seven emotions. Numerical experiments show that a suitable selection of instances and a substantial reduction of the feature space could be accomplished and the classifier formed in this manner is characterized by high classification accuracy for the seven emotions based on physiological signals.**

Keywords-memory-based learning; emotion classification; pysiological signals; genetic algorithms

I. INTRODUCTION

Recently, the most popular research in the field of emotion recognition on human-computer interaction is to recognize human's feeling using various physiological signals. In the psycho-physiological research, it is known that there is strong correlation between human emotion state and physiological reaction. Emotion plays an important role in contextual understanding of messages from others in speech or visual forms. For affective communication between user and computer, it has to consider how emotions can be recognized and expressed during human-computer interaction and emotion recognition is one of the key steps towards emotional intelligence in advanced human-machine interaction. Psychologists and engineers have tried to analyze facial expressions, vocal emotions, gestures, and physiological signals in an attempt to understand and categorize emotions. Many previous studies on emotion have reported that there is correlation between basic emotions such happiness, sadness, anger, fear, etc. and physiological responses [1]-[3]. Recently, emotion recognition using physiological signals has been performed by various machine learning algorithms (e.g., Fisher's Linear Discriminant, k-Nearest Neighbor algorithm, Neural Networks, and Support Vector Machine , etc.[4]-[8]).

The objective of this study is to achieve dataset on multi-physiological signals for seven emotions induced by an emotional stimulus and to develop memory-based learning classifier driven by genetic algorithms. Firstly, in order to get physiological signals for emotions, we use 10 different emotional stimuli set to induce seven emotions, i.e., happiness, sadness, anger, fear, disgust, surprise and stress under the same conditions. We identify emotion-specific physiological responses induced by these emotional stimuli. To induce each emotion, ten emotional stimuli sets which have been tested their suitability and effectiveness, are used in experiment. Physiological signals, namely, Skin temperature (SKT), photoplethysmography (PPG), electrodermal activity (EDA) and electrocardiogram (ECG) are acquired by MP100 Biopac system Inc. (USA) and analyzed to extract features for emotional pattern dataset.

For emotion classification, we use one of the techniques of evolutionary optimization, namely, genetic algorithms (GAs) [9]-[10]. In order to improve classification speed and accuracy of a classifier, suitable formations of a set of instance and features are required. GAs embraces two optimization processes, that is, choosing *P* % of instances as a set of memory comes from patterns with seven classes (emotions) and forming a core set of features that is a collection of the most meaningful and discriminative components of the original feature space. Numerical experiments are carried out and it is shown that a suitable selection of prototypes and a substantial reduction of the feature space could be accomplished that is also accompanied with a higher classification accuracy.

 ISBN: 978-1-61208-340-7

The study is organized into five sections. We outline the measurements of physiological signal induced by seven emotion stimuli in Section II. Section III covers all necessary development issues by the optimization scheme. Numeric experimental studies are presented in Section IV while Section V offers some concluding comments.

II. STIMULI AND PHYSIOLOGICAL SIGNALS FOR SEVEN EMOTIONS

In this study six males (20.8 years±1.26) and six females (21.2 years±2.70) students participated. None of the subjects reported any history of medical illness or psychotropic medication and any medication that would affect the cardiovascular, respiratory, or central nervous system. A written consent was obtained before the beginning

A. *Emotional stimuli*

As shown in Fig. 1, seventy emotional stimuli (7 emotions x 10 set) are used to successfully induce emotions. Emotional stimuli are selected the 2-4 min long audio-visual film clips which are captured originally from movies and TV. Audio-visual film clips have widely used because these have the desirable properties of being readily standardized, involving no deception, and being dynamic rather than static [11]-[14].

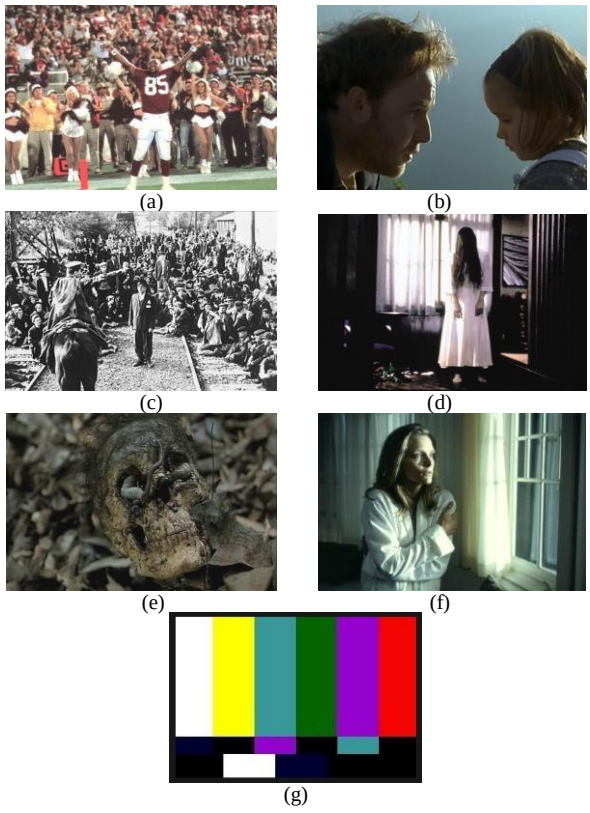

Figure 1. Examples of emotional stimuli; (a) Happiness: victory, wedding, laughing, etc., (b) Sadness: death of parents/lover, separation, longing for mother, etc., (c) Anger : massacre, beating, attack, etc., (d) Fear : ghost, haunted house, scare, etc., (e) Disgust: body in pieces, vomiting, etc., (f) Surprise: sudden or unexpected scream etc., and (g) Stress : audio/visual noise on screen, etc.

TABLE I. SUITABILITY AND EFFECTIVENESS OF EMOTIONAL STIMULI

Emotion set	Happiness	Sadness	Anger	Fear	Disgust	Surprise	Stress
1	100% (8.4)	92% (9.5)	75% (9.7)	75% (10)	75% (10.2)	75% (9.3)	92% (9.3)
2	100% (8.9)	100% (9.1)	75% (9.9)	100% (9.9)	92% (10.8)	92% (9.7)	100% (9.1)
3	100% (8.8)	100% (8.7)	75% (9.7)	83% (9.8)	92% (9.9)	100% (9.7)	100% (8.8)
4	100% (9.6)	100% (9.7)	75% (9.5)	92% (9.6)	100% (10.4)	100% (9.9)	100% (8.9)
5	100% (9.6)	100 (9.3)	92% (9.8)	92% (9.7)	92% (9.7)	83% (9.6)	100% (9.3)
6	100% (9.3)	100% (9.3)	92% (9.4)	92% (9.7)	100% (10.3)	83% (9.6)	100% (8.8)
7	100% (9.3)	75% (8.9)	92% (8.9)	83% (9.6)	100% (9.3)	100% (9.5)	92% (9.3)
8	92% (8.0)	100% (9.0)	83% (9.2)	100% (9.3)	83% (10.2)	83% (9.4)	100% (9.3)
9	100% (9.7)	100% (9.2)	92% (9.5)	100% (9.3)	100% (10.1)	83% (8.6)	100% (9.1)
10	92% (8.8)	100% (9.3)	92% (9.7)	75% (8.7)	100% (10.1)	75% (10.3)	100% (9.3)

The used audio-visual film clips are examined their suitability and effectiveness by preliminary study. After being presented each film clip, twenty-two college students rate the category and intensity of their experienced emotion on emotional assessment scale. The result shows that emotional stimuli have the suitability of 93% and the effectiveness of 9.5 point on average. The suitability of each stimulus is ranged from 75 to 100% and from 8.4 to 10.4 point in the effectiveness as shown in Table I. The suitability of emotional stimuli means the consistency between the target emotions designed to induce each emotion and the categories of participants' experienced emotion. The effectiveness is determined by the intensity of emotions reported and rated by the subjects on a 1 to 11 point Likert-type scale (e.g., 1 being "least happy" or "not happy" and 11 being "most happy").

B. *Physiological signals*

The dataset of physiological signals such as SKT, EDA, PPG, and ECG are collected by MP100 Biopac system. SKT is an important and effective indicator of emotion states and reflects autonomic nervous system activity. Variations in the SKT mainly come from localized changes in blood flow caused by vascular resistance or arterial blood pressure. EDA is a method of measuring the electrical conductance of the skin, which varies depending on the moisture of the skin, caused by sweat. PPG is a signal derived from light absorption changes in pulse oximeters in contact with the skin. The change in the light absorption reflects a change in the blood flow rate. Thus, the PPG signal is subordinate to pulse pressure, i.e., the difference between systolic and diastolic pressure in the arteries. Lastly, ECG is a transthoracic (across the thorax or chest) interpretation of the electrical activity of the heart over a period of time, as detected by electrodes attached to the surface of the skin and recorded by a device external to the body.

 ISBN: 978-1-61208-340-7

TABLE II. TABLE TYPE STYLES

Physiological signals			Features
EDA			SCL, NSCR, meanSCR
SKT			meanSKT, maxSKT
PPG			meanPPG
ECG	Time domain	Statistical parameter	meanRRI, stdRRI, meanHR, RMSSD, NN50, pNN50
		Geometric parameter	SD1, SD2, CSI, CVI, RRtri, TINN
	Frequency domain	FFT	FFTapLF, FFTapHF, FFTnLF, FFTnHF, FFTLF/HFratio
		AR	ARapLF, ARapHF, ARnLF, ARnHF, ARLF/HFratio

SKT electrodes are attached on the first joint of non-dominant ring finger and on the first joint of the non-dominant thumb for PPG. EDA is measured with the use of 8 mm AgCl electrodes placed on the volar surface of the distal phalanges of the index and middle fingers of the non-dominant hand. Electrodes are filled with a 0.05 molar isotonic NaCl paste to provide a continuous connection between the electrodes and the skin. ECG electrodes are placed on both wrists and one left ankle with two kinds of electrodes, sputtered and AgCl ones. The left-ankle electrode is used as a reference.

The signals are acquired for 1 minute long baseline state prior to presentation of emotional stimuli and 2-4 minutes long emotional states during presentation of the stimuli. The obtained signals are analyzed for 30 seconds from the baseline and the emotional state. The emotional states are determined by the result of participant's self-report.

C. Feature extraction

For seven emotions, 28 features extracted from the physiological signals and used to analysis are shown in Table II. Skin conductance level (SCL), average of skin conductance response (meanSCR) and number of skin conductance response are obtained from EDA. The mean (meanSKT) and maximum skin temperature (maxSKT) and the mean amplitude of blood volume changes (meanPPG) are gotten from SKT and PPG, respectively. ECG is analyzed in the view point of time domain and frequency domain. Analysis in time domain is divided into the statistical and the geometric approaches and in frequency domain is dealt with FFT and AR.

III. DESIGN OF MEMORY-BASED LEARINIG CLASSIFIER

For the classification of seven emotions, the proposed classifier is a type of memory-based learning that uses only specific instances to solve classification problem. Namely, the classifier is a method for classifying objects based on the closest training samples called memorized instances in the feature space. This classifier embraces two selection problems to classify a new pattern to a class. One is the selection of instance to be memorized and another is feature selection.

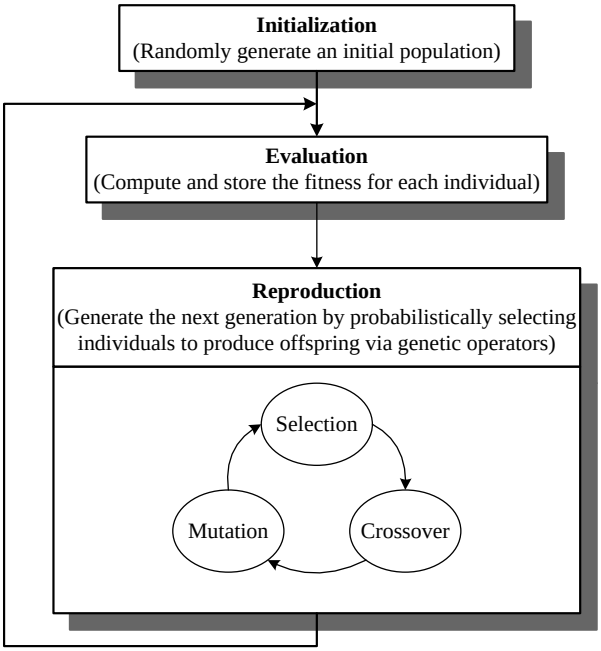

Figure 2. General Flowchart of Genetic Algorithms

To format instance to be memorized, we start with choose *P* % of patterns using GAs. The classifier generates classification predictions using only P % of patterns. The classifier does not use any model to fit and only is based on distance between a pattern and memorized instance. Given a set of N instance, the classifier finds the one instance closest in feature space to an unknown pattern, and then assigns the unknown pattern to the class label of its nearest instance. The underlying distance between a pattern and an instance is measured by weighted Euclidean one,

$$\|\mathbf{x}-\mathbf{y}\|^2 = \sum_{i=1}^{n} \frac{(x_i - y_i)^2}{\sigma_i^2} \quad (1)$$

where **x** and **y** are the two patterns in the *n*-dimensional space and σ_i is the standard deviation of the *i*-th feature whose value is computed using the instance set.

Secondly, once the instances to be memorized have been formed, we reduce feature space by choosing a core set of features encountered in the problem. Those features are regarded as the most essential ensemble of features that, organized together, exhibit the highest discriminatory capabilities. We use GAs to choose *d* % of features which minimizes the classification error.

GAs have proven to be useful in optimization of such problems because of their ability to efficiently use historical information to obtain new solutions with enhanced performance and a global nature of search supported there [9][10]. GAs are also theoretically and empirically proven to support robust search in complex search spaces. The search of the solution space is completed with the aid of several genetic operators. There are three basic genetic operators used in any GAs - supported search that is reproduction,

 ISBN: 978-1-61208-340-7

crossover, and mutation. Reproduction is a process in which the mating pool for the next generation is chosen. Individual strings are copied into the mating pool according to their fitness function values. Crossover usually proceeds in two steps. First, members from the mating pool are mated at random. Second, each pair of strings undergoes crossover as follows: a position l along the string is selected uniformly at random from the interval [1, l-1], where l is the length of the string. Two new strings are created by swapping all characters between the positions k and l. Mutation is a random alteration of the value of a string position. In a binary coding, mutation means changing a zero to a one or vice versa. Mutation occurs with small probability. Those three operators, combined with the proper definition of the fitness function, constitute the main body of the genetic computing. A general flowchart is visualized in Fig. 2.

As a generic search strategy, the GAs has to be adjusted to solve a given optimization problem. There are two fundamental components that deserve our attention: a fitness function, and a representational form of the search space. Given the wrapper mode of instance formation and feature selection, we consider the minimization of the classification error as a suitable fitness measure. There could be different choices of the search space considering that an optimal collection of features could be represented in several different ways. Here, we adopt the representation scheme of the search space in the form of the n-dimensional unit hypercube (N is the number of patterns while n denotes the number of features of emotional dataset). The content of a chromosome is ranked viz. each value in this vector is associated with an index the given value assumes in the ordered sequence of all values encountered in the vector (The elements of a chromosome for prototypes and features are ranked separately.). Considering that we are concerned with d % of all features, we pick up the first $d \times n$ ($0<d<1$) entries of the vector of the search space. This produces a collection of features forming the reduced feature space. This mechanism of the formation of the feature space is portrayed in Fig. 3. For the entire patterns, the prototype formation is carried out in the same manner as we encountered in the feature selection.

Given the instance formation and the feature selection, we consider the minimization of the classification error to be a suitable fitness measure of GAs.

$$Fitness = 1/\left(1+\frac{\text{Number of misclassified patterns}}{\text{Number of patterns}}\right) \quad (2)$$

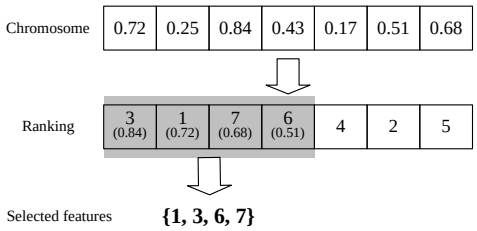

Figure 3. GAs formation of the reduced feature space; here, n=7 while the assumed reduction of the space results in 4 features viz. {1, 3, 6, 7}.

There are two stopping conditions for seven emotion classification: (a) the algorithm terminates if the objective function does not improve during the last 100 generations, otherwise (b) it terminates after 500 iterations. The size of the population is related to the dimensionality of the search space.

IV. RESULTS OF EMOTION CLASSIFICATION

The numerical studies presented here provide some experimental evidence behind the effectiveness of the GAs approach. The detailed setup of an extensive suite of experiments is reflective of the methodology we outlined in the previous sections. The two essential parameters that we use in the assessment of the performance of prototype and feature selection are the percentage of features (denoted by "d") forming the core of the reduced feature space and the percentage of the data forming the instance set (P) optimized by the GAs. The results are reported for the testing data sets for various values of "P" and "d".

In this paper, for the optimization of the classification of seven emotions, GAs uses the serial method of real type, roulette-wheel in the selection operator, one-point crossover in the crossover operator, and uniform in the mutation operator. More specifically, we use the following values of the parameters: maximum number of generations is 500; the number of populations is 100, crossover rate is 0.75, and mutation probability is set to 0.1.

For the seven emotions dataset given as multi-physiological signals, the relationship between the percentage of features used in the GAs optimization, values of "P" and the resulting classification accuracy is presented in Table III. Here, "No. of F" is the number of selected features for d % of entire features, "AVG" and "STD" indicate average and standard deviation, respectively. The classification accuracy was computed over 10-fold realization of the experiments, namely, for each combination of the values of the parameters (d and P), the experiments was repeated 10 times by running GAs. Fig. 4 shows the result of fitness function of GAs for d=30 and P=70. There is an evident effect of the "optimal" subsets of the instance and the feature space: clearly the subsets leads to better classification results when compared with the outcomes of the classifier operating on the entire feature space.

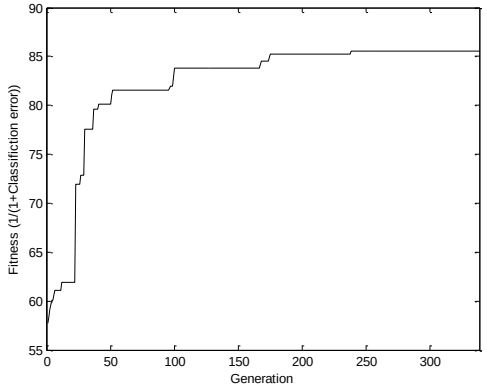

Figure 4. Fitness function of GAs for d=30 and P=70

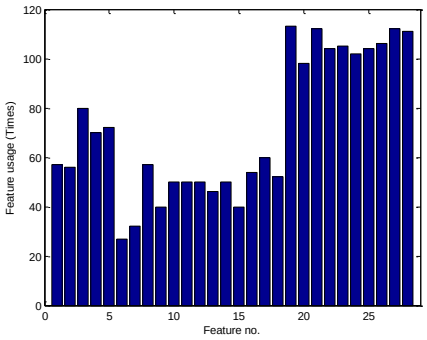

(a) Feature usage index over all values of d and P

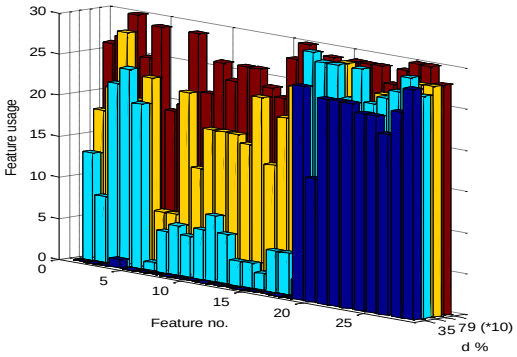

(b) Feature usage index over all P for each d

Figure 5. Cumulative number of occurrence of individual features

TABLE III. CLASSIFICATION ACCURACY FOR SEVEN EMOTIONS

d % (No. of F)	*P* %			AVG±STD over *P*
	30	50	70	
30(8)	44.4 ± 1.96	64.0 ± 0.92	83.0 ± 2.26	63.8 ± 16.15
50(14)	27.7 ± 2.05	36.9 ± 5.56	38.6 ± 3.22	34.4 ± 6.17
70(20)	24.3 ± 0.83	27.6 ± 0.69	31.9 ± 1.64	27.9 ± 3.32
90 (28)	24.5 ± 0.84	26.6 ± 0.95	30.2 ± 1.27	27.1 ± 2.60
100(28)	24.6 ± 0.85	26.4 ± 0.95	31.1 ± 1.31	27.4 ± 2.98

TABLE IV. COMPARISON OF THE CLASSIFICATION ACCURACY OF THE PROPOSED METHOD AND OTHER METHODS

Method		**Accuracy (%)**	**Features**
CART		21.7 ± 3.6	28
C4.5		16.1 ± 1.2	28
kNN		45.3 ± 2.3	28
FLD		20.3 ± 1.8	28
NN		18.0 ± 1.0	28
PNN		16.3 ± 1.9	28
RBFs		17.4 ± 1.2	28
SOM	Supervised	16.3 ± 1.9	28
	Unsupervised	15.4 ± 3.2	28
SVM		17.8 ± 3.1	28
Proposed Methodology		83.0 ± 2.26	8

With the increasing values of "*d*", the classification accuracy of seven emotions decreases substantially; in the case of *P*=30% it drops from 44.4 to 24.3 when increasing the number of features from 10% to 70%. Conclusively, the use of all features dropped accuracy of classification for seven emotions. Changes in the values of "*P*" have far less effect on the classification rate, however, the distinguished result was occurred in *d*=30 and *P*=70. From these results, we observe that the number of suitable features is 8 and 70 % of dataset are required as the prototype for the seven emotion recognition using multi-physiological signals. We report the number of occurrences of the features in Fig. 5. This indicator becomes more illustrative and offers an interesting view at the suitability of the features when forming various reduced feature spaces and using different prototype set sizes. In case of *d*=30 % for the classification of seven emotions, namely, the number of features is 8, we have gotten that classification accuracy is 83 % for P=70.

For the classification of seven emotions, Table 4 contrasts the classification accuracy (%) of the proposed method with other well-known methods studied in the literatures [5]-[8]. These machine learning algorithms are standard algorithms, which have been applied to various and lots of fields. For more information, refer to [5]-[8].

As abovementioned, the experiments are reported for the 10 times using a split of data into 70% training and 30% testing subsets, namely, 70% of the whole patterns are selected randomly for training of all methods and the remaining patterns are used for testing purposes. The results are averaged over 10 times for testing dataset. The experimental results reveal that the proposed approach and the resulting model outperform the existing methods both in terms of the simpler structure and better prediction (generalization) capabilities on feature space reduced 70% of entire feature space.

While the experimental results provide sound evidence behind the selection process showing that the reduced feature spaces led to the better classification results than those obtained in some previous studies, they are also quite revealing in showing that the reduction of the feature space could exhibit different effectiveness. In some cases, the reduction of the dimensionality of the feature space could be high but there could be cases where the elimination of subsets of features could not be strongly justifiable

V. CONCLUSION

In this study, we have discussed the acquisition of multi-physiology signals using emotion stimuli and the design of a classification methodology for seven emotions. The emotion stimuli used to induce a participant's emotion were evaluated for their suitability and effectiveness. The result showed that emotional stimuli have the suitability of 93% and the effectiveness of 9.5 point on average. Twenty eight features have been extracted by means of the statistical and the geometric approaches in time and frequency domain from physiological signals such as EDA, SKT, PPG and ECG. These signals have been induced by emotional stimuli. In order to improve the classification accuracy using physiological signals for seven emotions, we have

 ISBN: 978-1-61208-340-7

introduced a memory-based learning classifier using the evolutionally mechanism for the seven emotions expressed by physiological signals. The optimization process of forming the instance and the feature space is reflective of the conjecture on the importance of forming a set of instance and a core set of features whose discriminatory capabilities emerge through their co-occurrence in these set. The methodology of feature selection becomes legitimate considering that we immediately see the result of the reduction of the feature space being translated into the corresponding classification rate. The use of the instance is also justifiable considering that this classification scheme is the simplest that could be envisioned in pattern classification. The proposed classifier will lead to better chance to recognize human emotions by using physiological signals in the emotional interaction between man and machine.

ACKNOWLEDGMENT

This research was supported by the Converging Research Center Program through the Ministry of Science, ICT and Future Planning, Korea (2013K000329).

REFERENCES

[1] R. W. Picard, E. Vyzas, and J. Healey, "Toward Machine Emotional Intelligence: Analysis of Affective Physiological State," IEEE Transactions Pattern Analysis and Machine Intelligence, vol. 23, no.10, 2001, pp.1175-1191.

[2] A. Haag, S. Goronzy, P. Schaich, and J. Williams, "Emotion Recognition Using Bio-Sensors: First Step Towards an Automatic System," Affective Dialogue Systems, Tutorial and Research Workshop, 2004.

[3] F. Nasoz, K. Alvarez, C. L. Lisetti, and N. Finkelstein, "Emotion Recognition from Physiological Signals for Presence Technologies," International Journal of Cognition, Technology and Work, Special Issue on Presence, vol. 6, no. 1, 2003, pp. 4-14.

[4] M. Murugappan, N. Ramachandran, and Y. Sazali, "Classification of human emotion from EEG using discrete wavelet transform," Journal of Biomedical Science and Engineering, vol. 3, 2010, pp. 390-396.

[5] J. R. Quinlan, C4.5 Programs for Machine Learning, San Mateo, CA: Morgan Kaufmann, 1992.

[6] R. O. Duda, P. E. Hart, and D. G. Stork, Pattern classification, 2nd ed. Wiley-Interscience, New York, 2000.

[7] P. D. Wasserman, Advanced Methods in Neural Computing, New York, Van Nostrand Reinhold, 1993, pp. 35–55.

[8] S. Parsa and S. A. Naree, "A New Semantic Kernel Function for Online Anomaly Detection of Software," ETRI Journal, vol.3 , no. 2, 2012, pp. 288-291.

[9] D. E. Goldberg, Genetic Algorithms in search, Optimization & Machine Learning, Addison-Wesley, 1989.

[10] S. A. Taghanaki, M. R. Ansari, B. Z. Dehkordi, and S. A. Mousav, "Nonlinear Feature Transformation and Genetic Feature Selection: Improving System Security Decreasing Computational Cost," ETRI Journal, vol.34, no.6, 2012, pp 847-857.

[11] J. J. Gross and R. W. Levenson, "Emotion elicitation using films," Cognition and Emotion, vol. 9, pp. 87-108, 1995.

[12] R. S. Lazarus, J. C. Speisman, A. M. Mordkoff, and L. A. Davidson, "A Laboratory study of psychological stress produced by an emotion picture film," Psychological Monographs, vol. 76, 1962, pp. 553.

[13] M. H. Davis, J. G. Hull, R. D. Young, and G. G. Warren, "Emotional reactions to dramatic film stimuli: the influence of cognitive and emotional empathy," Journal of personality and social psychology, vol. 52, 1987, pp. 126-133.

[14] D. Palomba, M. Sarlo, A. Angrilli, A. Mini, and L. Stegagno, "Cardiac responses associated with affective processing of unpleasant film stimuli," International Journal of Psychophysiology, vol. 36, 2000, pp. 45-57.

 ISBN: 978-1-61208-340-7

A HMM Model Based on Perceptual Codes for On-Line Handwriting Generation

Hala Bezine Wafa Ghanmi Adel M. Alimi
REGIM-Lab: Research Group on Intelligent Machines Laboratory, University of Sfax,
National School of Engineers, BP 1173, 3038.
Sfax, Tunisia
hala.bezine@ieee.org; wafa.ghanmi@hotmail.fr; adel.alimi@ieee.org

***Abstract*—This paper handles the problem of synthesis of online handwriting that can be reconstructed by several methods such as those of movement or shape simulation techniques and computational methods. Indeed, this work presents a probabilistic model using the Hidden Markov Models for the classification of perceptual sequences, starting from global perceptual codes as input and ending with a class of number probabilities as output. In fact, the algorithm analyzes and learns the handwriting visual codes features. In order to recover the original handwriting shape, and to generate new ones via the generated perceptual sequences, we investigate the polynomial approximation methods such us the Bezier curves and Bspline interpolation. The performance of the proposed model is assessed using samples of scripts extracted from Mayastroun Database. In experiments, good quantitative agreement and approximation is found between human handwriting data and the generated trajectories and more reduced representation of the scripts models are designed.**

Keywords-Human reading; Cursive handwriting synthesis; Hidden Markov Models; Global perceptual codes; Beta-elliptic model.

I. INTRODUCTION

Despite the invasion of the computer and various technologies, such as keyboard and mouse, reducing the importance of handwriting, this latter attaches a great value on communication for a large majority of individuals. As a result, the emergence of so different and significant progress, such as tablet PC, interactive whiteboard or pen-based devices allow the implementation of recognition, production and handwriting synthesis systems.

Various cognitive and psychological studies have been performed on a number of participants to observe their behavior during the reading process. It has been demonstrated that vision is considered as the most advanced sensor for human and provides the widest range of information to our body in general and to writing in particular. As stated in many previous studies, perception and handwriting synthesis are highly correlated and formed a cognitive loop: the visual perception process extracts relevant features from the external environment to enable the motor system to act [14]. So the handwriting process can be considered as a sensory-motor task in which the component of perception corresponds to the shape of the letter and the neuromuscular system assumes the formation of the script trajectory [7][8]. On the other hand, the problem of handwriting generation has been addressed for a long time and there are many studies in this field such as [9][11][12][16][18]. These ones try to generate handwriting scripts focusing on movement dynamic characteristics or handwriting shape features. Other research studies suppose that generation and visual perception of human movements are strongly correlated and that complex handwriting trajectories should be formed from the superposition of elementary building blocks [5]. In such a way, the visuo-motor correspondence could explain that Humans tend to provide motor commands which have similar kinematic properties to their neuro-muscular system. In this paper we have to analyze the interactions between the handwriting synthesis task and the cognitive functions which are integrated during learning of handwriting movements.

The most of previous studies focused respectively on one of the perception or the production processes involved in handwriting generation task without handling with the interaction between both of them as two interrelated parts of the complete feedback loop [10]. As well, because the handwriting depends on both the perceptual skills and production, the formation of an online acquired script was more effective in the improvement of these two capabilities. In this context, the purpose of our work is to develop a handwriting generation model by using the visual codes extracted from on-line handwritten scripts. We propose to use specific statistical models: the hidden Markov models for their dominant impact in the treatment of writing and their handling of any type of sequences (image, speech, writing traces, etc...). Because of their nature, these models are deemed the most adequate to our task involving the handwriting classification and the generation of sequential data.

This paper is organized as follows: in Section 2, the proposed approach is detailed and we present the principle characteristics of the detection of the global perceptual codes. In the second part of Section 2, we briefly introduce the Hidden Markov model, we summarize the observation

 ISBN: 978-1-61208-340-7

extraction step. Then we detail the training and classification process. In the third part of Section 2, we describe our approach for fitting the partial contours i.e. GPC through conventional geometrical approach. Then we deal with some experimental results made on MAYASTROUN database [15]. Finally, we present some conclusions and further works.

II. THE PROPOSED MODEL

In this section, we describe on-line handwriting classifier and model for synthesis of scripts. An appropriate HMM model is used for each sample of the lexicon. In our concept, only one model is constructed for the different class of digits (each digit in lexicon), then for the classification task of an input digit, the score for matching the digit to each model is computed, and the class related to the model that has the maximum score gives the result of the classification. This approach is reasonable for small lexicon size. The samples of digits are extracted from the MAYASTROUN database [15].

The system that we have developed for modelling and classification of online handwritten scripts is shown in Fig.1.

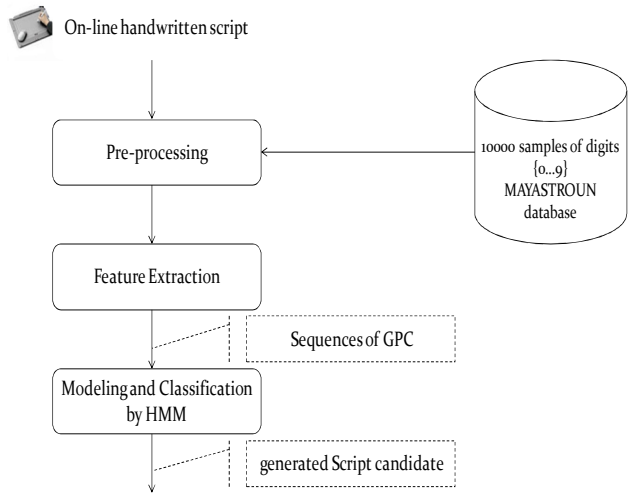

Figure 1. The architecture of the proposed model.

Firstly, the scripter writes on a digitizing tablet using a special stylus. So that the user's written scripts are captured as they are being formed by sampling the (x,y) coordinates corresponding to the pen position. Then, the acquired handwriting data is smoothed by a low pass-filtering type Chebychev. In this connection, each handwriting trace "isolated digit" is composed of at least one segment and each segment comprises multiple strokes. Moreover a segment is defined as a trace which is drawn continuously and during such movement the pen is touching the digitizing tablet.

Regarding to the feature extraction stage, each script, i.e trace, is represented as a feature vector, which becomes its identity. In other words, it resides in the selection and the extraction of important features. Our purpose is to achieve a transformation of the original data space into a fixed dimension vector space which contains all of the relevant information necessary to the modeling step with HMM. Since the proposed model is classified as well as generative model, we can choose the most probable digit from the HMM. The most probable digit can be interpreted as the most representative digit pattern that each model has. If our proposed model successfully learns the concept of digits from training data, then it can generate natural shapes.

A. Feature Extraction

Because of the human visual system is selectively activated in response to global form, we have investigated the properties of the GPC extractor composed of ten GPCs which have been already accomplished in previous studies [13]. As shown in [13], a GPC is a combination of a set of elementary perceptual codes (EPCs) according to well defined criteria. For this task, the authors have used the beta-elliptic model for on-line handwriting segmentation scripts [2].

1) The Beta-Elliptic Model for Handwritten Segmentation

In the context of the beta-elliptic theory, a rapid handwriting movement is resulted from the activation of a sufficient number of neuromuscular subsystems, to get a smoothest trajectory characterized by a curvilinear velocity profile fitted by a Beta function and an elliptic stroke in the static domain.

As shown in (1), the Beta equation depends on the set of parameters *(t, t_0, t_1, t_c, p, q)* where t_0 is the starting time, t_1 is the ending time, t_c is the instant where the curvilinear velocity reaches its maximum. p and q are intermediate parameters which describe the beta profile shape [1][3][4].

$$\beta(t, t_0, t_1, p, q) = \left[\frac{t_1 - t}{t_1 - t_c}\right]^p \left[\frac{t - t_c}{t_c - t_0}\right]^q \quad (1)$$

and

$$t_c = \frac{p * t_1 + q * t_0}{p + q} \quad (2)$$

According to these kinematic features, we check the different static characteristics. Based on the assumption that each stroke is represented in the static domain by an elliptic arc characterized by a and b which are respectively the dimensions of the large and the small axes of the elliptic shape. x_0 and y_0 are the Cartesian coordinates of the elliptic center relative to the orthogonal reference *(o, x, y)*. The angle θ defines the deviation of the elliptic portion as presented in (3) [2].

$$\theta = tan^{-1}\left(\frac{(y_1 - y_0)}{(x_1 - x_0)}\right) \quad (3)$$

For complex handwriting movements, each handwriting trace is composed of at least one segment and each segment comprises multiple strokes. Each stroke is characterized by

ten features in both the kinematic and static domain. The reader is referred to [2] for more details.

2) The Elementary Perceptual Codes Extractor

Following the approach of the beta-elliptic model, we carried on with the detection of the perceptual codes. Firstly, for each elliptic stroke, we assigned an elementary perceptual code (EPC) [13]. According to the to the deviation angle θ, we have identified four types of strokes: *Shaft, Valley, Left oblique shaft, Right oblique shaft*). Each one has the opportunity to belong to both separate intervals of the trigonometric circle and depending on the trigonometric sense, we have defined the positive part going from 0 to π and the negative range going from 0 to - π. i.e. the stroke number two (valley), belongs to both intervals containing each one a positive and a negative part. It takes into account both sides of the trigonometric circle (positive and negative) to indicate the direction of writing which is consistent with the trigonometric direction. The number of strokes of an appropriate handwriting trace is predefined by the Beta-elliptic model and this latter is equal to the number of EPC.

3) The Global Perceptual Codes Extractor

Assuming that human vision does not detect readily the elementary perceptual codes comprised in the original trace, but more general forms [13], we have used the global perceptual codes (GPCs) extracted previously in [13]. According to pre-defined criteria and by the means of genetic algorithms, these GPCs are obtained by collecting the EPCs [13] already detected. We have defined ten GPCs classified into both categories; simple and complex ones, as shown in Fig 2. In order to take into account the Arabic lexicon, we have considered the letter "Ain" as a complex perceptual code referenced by number ten. As a result, we obtained a set of CPGs forming the initial script that will be used for online handwriting classification modeling step [14][15].

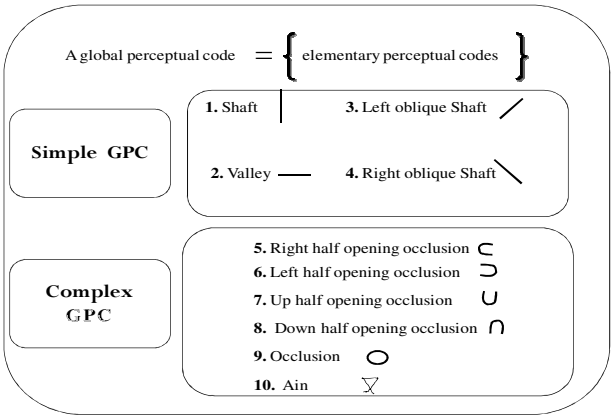

Figure 2. The different global perceptual codes.

In order to obtain more satisfying handwriting generation system and to simulate how Human understand and recognize handwriting, we adopt these global perceptual codes (GPCs) and the Hidden Markov Models to classify the different patterns of digits.

B. Modelling and Classification by HMM

The handwriting perception and learning can be viewed as a problem of probabilistic learning at high level. Indeed the learning of new characters affects not only the temporal characteristics but also influences the composition of the GPC sequences and the whole shape.

The extraction of knowledge from sequentially structured data is a complex problem appearing in various fields of applications [6]. In this study, we check to develop a single model of representation that comprehensively summarizes all structured data identifying correspondences or differences in data sets. Hidden Markov Models (HMM) appear as one of the best approaches adopted for sequences treatment, due to their ability to handle with sequences of variable lengths, and secondly their capability to model the dynamics of phenomena described by sequences of events. Thus, we propose to use a discrete HMM for the modeling and classification task, the observations sequences are identified to sequences of discrete values corresponding to sequences of GPCs. An important issue that must be resolved before putting the system into use is to decide how many states the digits model should composed. For our case, each digit has different number of states that reflects the number of GPCs that the digit has. As a result, the states number for a HMM model is varied with respect to the modeled handwritten digit proprieties.

1) Overview of Hidden Markov Models

A Hidden Markov Model (HMM) [17] is a kind of stochastic model that is similar to a finite states machine in which transitions and results are stochastic. Otherwise, a HMM is a sequence of observations as a piecewise stationary process. This model combines the advantages of a states machine and probability distributions between states. The HMM registers the observations as probability functions of an appropriate state and the input data is described as a hidden stochastic process.

More formally, it may be represented by a set of features namely N, M, A, B and π. The values associated to these characteristics can be used to produce the observations sequences. These characteristics are detailed below:

- N : the number of hidden states within the model.
- M: the number of observations symbols per state.
- $A = \{a_{ij}\}$: the state transition probability distributions;

$a_{ij} = P(q_{t+1} = S_j \,|\, q_t = S_i),\ 1 \le i, j \le N$

- $B = \{b_j(k)\}$: the emission probability distribution in the state j;

$b_j = P(v_k \text{ at } t \,|\, q_t = S_j),\ 1 \le j \le N, 1 \le k \le M$

- $\pi_i = \{\pi_i\}$: the prior probability of being in the state i at the beginning of the observations;
$\pi_i = P(q_1 = S_i), 1 \leq i \leq N.$
- $O = \{ O_1 O_2 O_3 \ldots O_T\}$ where O_t is an observation from the set of possible symbol observations and T is the number of observations in the sequence.

To initiate a HMM characterized by a compact notation $\lambda = (N, A, B, \pi)$, an initial state will be chosen based on the prior distribution π and t is set at 1. $\sum_j a_{ij} = 1$, $\sum_t b_i(O_t) = 1$, $\sum_i \pi_i = 1$, $a_{ij}, b_i(O_t), \pi_i \geq 0$, for all i, j, t.

2) Observations Extraction

We summarized the different steps of feature extraction as shown in Fig 3, starting with an original handwritten digit and ending with an observation which is equivalent to a sequence of global visual codes as output.

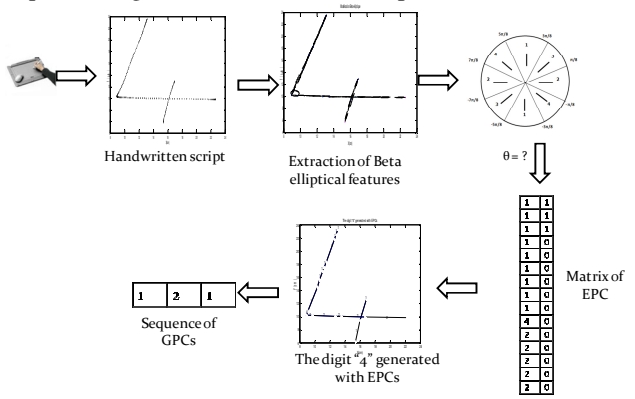

Figure 3. Example of the feature extraction step.

A GPC is a combination of a set of elementary perceptual codes (EPCs) according to well defined criteria. In other words, just like a script is defined as a sequence of GPC, each GPC may be defined as an alternating sequence of EPCs. In fact, we extend the conventional representation of observation sequence as following:

Handwritten digit = {GPC}+
GPC = EPC. EPC.{EPC}+

where "+" denotes repetition and "." indicates concatenation. Indeed, we consider the list of GPCs extracted from a handwritten digit as observations for our model. These observations are then classified into corresponding digit categories.

3) HMMs Structure and Training

To define the architecture of the model, we must take into account the topology as well as the number of states according to our case. The most adopted topology to our system is of ergodic type. In this type of structure, each state can be reached or visited by any other state and the transition to itself is permitted: that is to say that all states communicate among themselves. According to a graphical representation, all states are interconnected by arrows which indicate the direction of transition and the corresponding probability.

Only one model is built to represent every handwritten digit. Such one is formed with an ergodic digit models. Figure 4 shows the modeling of each digit class by a HMM.

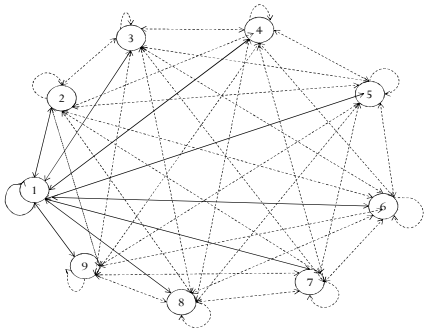

Figure 4. Graphical representation of the proposed model: an ergodic HMM with nine states.

We handle the different types of GPCs as possible symbols that can formed the set of ten digits and we notice the absence of GPC "ain" in the composition of the different sequences and the presence of other ones. So we treat nine GPC instead of ten. In others words, GPCs are considered as states.

Taking into account the above remarks, the design of HMM characterized by a compact notation $\lambda = (N = 9, A, B, \pi)$ has led to the diagram shown in Fig. 4, with:

• Nine discrete states: 1, 2, 3 ... 9, which define the hidden states of the HMM.
• O_1, O_2, O_3 and O_{10} denote the observations of the HMM.
• a_{ij} denote the transition probabilities between the different states of the model .
• $P(O_j|i)$ represent the emission probabilities of observation.

In the training phase, the goal is the estimation of model parameters (A, B, π) for all possible digits that best approximate the digit. The learning of the HMM model parameters corresponding to the classes of sequences is performed by the Baum- Welch algorithm [17]. This latter allows us to adjust and recompute the parameters of each sequence by maximizing the likelihood value over several iterations. In another words, it adjusts the parameters of the HMM model in order to maximize the probability $P(O|\lambda)$ of generating a sequence O of observations which is already contained in the training data.

Thus, a set of reasonable re-estimation values for π, A and B is given. We save the new settings of each class model for the use in the next step as depicted in Fig.5.

Various digits prototypes were used for the experiments. These ones were collected from college and secondary school students without imposing any stylistic constraints or restriction while writing. The system is trained with 10000 digits written by 100 writers. The number of training samples per class was 700.

 ISBN: 978-1-61208-340-7

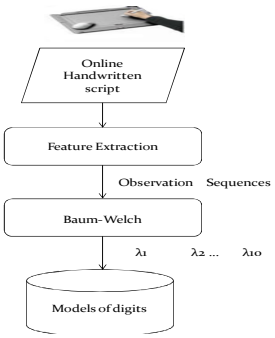

Figure 5. Scheme of the learning data.

4) HMMs Classification

Up to now, we have defined the structure of a HMM, its characteristics and how it can be created. Starting from many kinds of sequences, we would like to distinguish between them. To solve this task, we need a sequence classifier.

Given a sample of sequence or an observation digit obtained from an on-line handwriting digit or generated by HMM, our task can be expressed as the determination of the best observation sequence out of the HMM model and its classification.

During this phase, and in order to select the best class and make a decision, we use the classical classification likelihood values which are computed in the previous step by the HMM model such as described in Fig. 6.

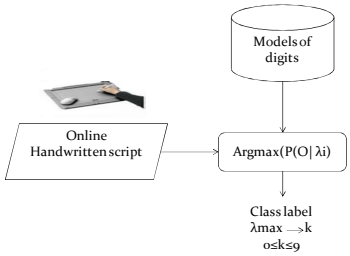

Figure 6. Digits classifier and the evaluation of HMMs Models.

The classifier takes the digit to be classified as a sequence of discrete observations O and the decision function is based on the maximum likelihood criterion. For each HMM model λi, the classifier calculates the probability P(Oλi) and we collect the correspondent probability value. So, in order to find the most near optimal sequence, we use the maximum likelihood criterion and the best one represents the observation of digit with maximum probability.

C. Handwriting Generation

Various approximating methods have been proposed including the interpolation and the B-spline [21] or Bezier curves [19][20], to generate the cursive handwriting. The main objective of the interpolation, for example, is to interpolate unknown data from points. In this case, the value of the approximated function between these points can be estimated. In other case, the interpolation involves passing a curve by a subset of points extracted from the set of GPCs composing a given script. Our task of generation can be expressed as the fitting of handwriting trajectory by a small number of points in the 2D plane defining the different GPCs. We describe our approach for fitting the partial contours i.e. GPCs through those conventional geometrical approach such that: Bezier curves and B-splines.

A simple GPC is a straight or nearly straight trace that has different directions and is composed of points. For the case of the simple GPCs, the linear interpolation method have been used, in which each pattern of data is fitted by a line segment connecting the extreme points of two neighboring GPC i.e. the tail and head of each of them. These ones correspond to local features representing maximums or minimums of the curvilinear velocity signal of the handwriting trace as shown in Table.I.

TABLE I. THE DIFFRENT GPC AND THE CORRESPONDING CONTROL POINTS

Code	GPC Shape	Control Points
1		$\{(x_i, y_i), (x_f, y_f)\}$
2		$\{(x_i, y_i), (x_f, y_f)\}$
3		$\{(x_i, y_i), (x_f, y_f)\}$
4		$\{(x_i, y_i), (x_f, y_f)\}$
5		$\{(x_i, y_i), (x_k, y_k), \dots (x_f, y_f)\}$
6		$\{(x_i, y_i), (x_k, y_k), \dots (x_f, y_f)\}$
7		$\{(x_i, y_i), (x_k, y_k), \dots (x_f, y_f)\}$
8		$\{(x_i, y_i), (x_k, y_k), \dots (x_f, y_f)\}$
9		$\{(x_i, y_i), (x_k, y_k), \dots (x_f, y_f)\}$

With 2<=k<=4

According to Table.1, the local features representing the spatial information of the different GPCs namely two points for the simple GPC such as the starting point $P_i(x_i, y_i)$ and the ending point $P_f(x_f, y_f)$. While a complex GPC may be defined by five points. In addition to the starting and ending points, we have k points having the maximum or minimum curvature as well as points of zero crossing curvature.

In fact, each GPC may be expressed as follow:

Simple GPC $= \{(x_i, y_i), (x_f, y_f)\}$

Complex GPC $= \{(x_i, y_i), (x_k, y_k), \dots (x_f, y_f)\}$

Due to the variability of handwriting style, the number of main control points is different from a script to another and from one sample to another and we are obliged to add new ones especially when the original points are sparse i.e. assuming that many points are missed between both P_i and P_f, it is necessary to generate new points between them. We explore the idea of modeling the sequence of control points

 ISBN: 978-1-61208-340-7

positions of handwritten digit to best fit via Bezier curve or B-spline. In this sense, we investigate the feature extraction step to compute these latter which are required for the implementation of the polygonal approximations.

We conducted experiments which show the ability of handwriting modeling of the proposed method. First of all, we applied our system to digit generation and classification. Moreover, and in order to test our system, we have carried out several experimentations on MAYASTROUN Database [15].

As depicted in Fig.7, an example of the handwriting digit "4" is generated. The associated controls points computed for such digit are represented in Fig 7.(a). , There are four control points for all the extracted GPCs namely Left oblique Shaft, Valley and Shaft. These ones are generated from the learned model. All the sample points are integrated together by respectively Bezier Curve in Fig. 7.(b). and B-spline in Fig.7(c) to yield a cursive handwritten digit.

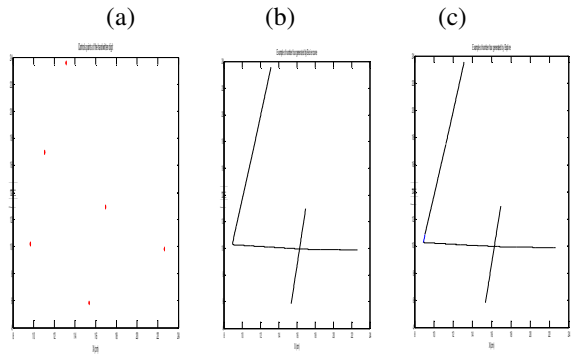

Figure 7. (a) The controls points. (b) The digit "4" generated by Bezier curves, (c) The digit "4" generated by Bsplines.

Another example of script is carried out, which is the digit "3", as shown in Fig.8. This one is made of two GPCs: two Left half opening occlusion. Figure 8.(b). presents the model fitted by Bezier curve while Fig8.(c). shows the approximation of the digit via B-spline.

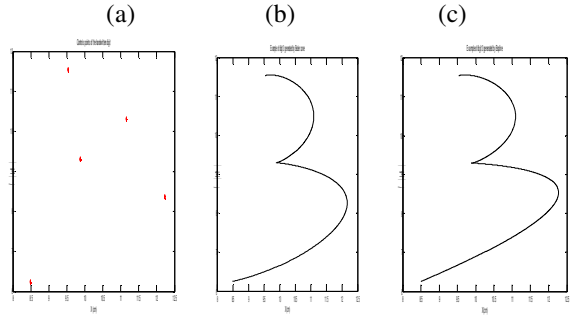

Figure 8. (a) The controls points. (b) The digit "3" generated by Bezier curves, (c) The digit "3" generated by Bsplines.

We give another example of digit "6" in Fig.9. which have some complex GPCs. Figure 9.(a) shows the distribution of the different control points that characterize these latter. An instantiation of the digit is then generated by Bezier curve as well as by B-spline.

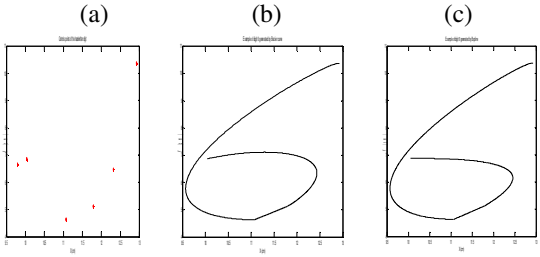

Figure 9. (a) The controls points. (b) The digit "6" generated by Bezier curves, (c) The digit "6" generated by Bsplines.

To evaluate our method, we use a measure of similarity between the original acquired data and regenerated one to analyze and provide information to help make a decision on the results provided. The degree of similarity [22] between the original script and the script generated is measured with the following equation (4):

$$S(S_o, S_g) = 1 - \frac{\sqrt{\sum_{i=1}^{n}((x_{oi}-x_{gi})^2+(y_{oi}-y_{gi})^2)}}{n} \quad (4)$$

with:

$S(S_o, S_g)$ is the degree of similarity between the original script (S_o) and generated script (S_g).

(x_{oi},y_{oi}) are the i-th point coordinates in the original script.

(x_{gi},y_{gi}) are the i-th point coordinates in the generated script.

n is the number of points of the original writing.

We note that:

1. $S(S_o, S_g) \in [0, 1]$
2. $S(S_o, S_g) = 1 \Rightarrow S_o = S_g$
3. $S(S_o, S_g) = \alpha \Rightarrow S_g$ (generated script) is similar with α degree to the S_o (original script).

This degree helps us to compare different results between generated scripts via B-spline and Bezier curve.

TABLE II. THE SIMILARITY DEGREE OF SAMPLE OF DIGITS.

Digits	The similarity degree with Bezier curves	The similarity degree with B-spline
Digit '4'	0.121	0.215
Digit '3'	0.252	0.824
Digit '6'	0.432	0.864

As shown table II, we note the variance of the similarity degree from one digit to another and between the two adopted approximating method namely B-spline and Bezier curves. We remark that B-spline method gives better results for fitting than Bezier curves as the GPC curvature decreases. We conclude that the B-spline can generate handwritten digits with acceptable performance.

 ISBN: 978-1-61208-340-7

These results can be enhanced by increasing the number of control points.

III. CONCLUSION

In this paper, we presented a system for the synthesis of on line handwriting scripts using global perceptual codes. In such away, having a set of GPCs and in order to generate more variant and natural handwriting shapes, we have applied a conditional algorithm to obtain the set of variants scripts. For this task, the HMMs models have been successfully applied. Starting from many kinds of GPCs sequences we differentiate between them as possible symbols that can formed the set of ten digits. Then we have adopted the geometric fitting method to approximate the different GPCs sequences: we have tried to collect the perceptual codes by the means of geometrical methods i.e. a GPC is approximated by an n^{th} order polynomial.

The variability of the similarity degree is due to the style of the writer handwriting and to the complexity of extracted global perceptual codes. The representation of handwriting script by GPCs is a good way to minimize the amount of data, and promising results are obtained. In order to enhance the degree of similarity and the handwriting generation performance, we opt to use genetic algorithms to check the set of optimized control points belonging to every global perceptual code. Our proposed model can be applied for different applications purposes such us automated generating training data for recognition systems, and simplifying the understanding of human handwriting especially for young students. Therefore, it can be used for teaching of handwriting and integrated as a tool of handwriting learning.

ACKNOWLEDGMENT

The authors would like to acknowledge the financial support of this work by grants from General Direction of Scientific Research (DGRST), Tunisian, under the ARUB 01/UR/11/02 program.

REFERENCES

[1] M.A. Alimi. “Beta Neuro-Fuzzy Systems”, TASK Quarterly Journal, Special Issue on “Neural Networks” edited by W. Duch and D. Rutkowska, vol. 7 (1), pp. 23-41, 2003.

[2] H. Bezine."Contribution au Développement d’une Théorie de Génération de l’Ecriture Manuscrite", PhD, Univ. of Sfax, 2006.

[3] H. Bezine, M. A. Alimi and N. Sherkat: “Generation and Analysis of Handwriting Script with the Beta-Elliptic Model”, Int. J. of Simulation, vol. 8, n° 2, pp. 45-65, 2007.

[4] H. Bezine, M. Kefi, and M. A. Alimi. “On the Beta-Elliptic Model for the Control of Human Arm Movements”. IJPRAI, 21 (1): 5-19, 2007.

[5] S. Bouaziz, and A. Magnan, "Contribution of the Visual Perception and Graphic Production Systems to the Copying of Complex Geometrical Drawings: A Developmental Study". Cognitive Development, 22(1), 5–15. doi:10.1016/j.cogdev.2006.10.002, 2007.

[6] P. Dreuw, P. Doetsch, C. Plahl and Ney H. “Hierarchical Hybrid MLP/HMM or rather MLP Features for a Discriminatively Trained Gaussian HMM: A Comparison for off-line Handwriting Recognition”, Int. Conf on Image Processing, ICIP’2011, pp. 3541-3544, 2011.

[7] S. Edelman, and T. Flash. “A Model of Handwriting”, Biological Cybernetics, vol. 57, pp. 25-36, 1987.

[8] G.V.Galen, J. Weber. “On-line Size Control in Handwriting Demonstrates the Continuous Nature of Motor Programs”. Acta Psychol. vol. 100, pp. 195-216, 1998.

[9] G. Gangadhar, J.Denny and V.C. Srinivasa. “An Oscillatory Neuromotor Model of Handwriting Generation”. IJDAR, pp. 69-84, 2007.

[10] E. Gilet, J. Diard and P. Bessie`, “Bayesian Action–Perception Computational Model: Interaction of Production and Recognition of Cursive Letters,” , journal pone, pp.1-23, 2011.

[11] J.M. Hollerbach, “An Oscillation Theory of Handwring”. Biological Cybernetics. vol. 39, pp. 139-156, 1981.

[12] C. V. Jawahar, A. Balasubramanian, and A. M. Namboodri, “Retrieval of Online Handwriting by Synthesis and matching”, Int. J. of Pattern Recognition, vol 42, pp. 1445-1457, 2009.

[13] M. Ltaief, S. Njah, H. Bezine, and M. A. Alimi, “Genetic Algorithms for Perceptual Codes Extraction”, Int. J. of Intelligent Learning Systems & Applications, vol 4, pp. 256-265, 2012.

[14] D.Marr, and S. Cermak,“Predicting Handwriting Performance of early Elementary Students with the Developmental test of Visual Motor Integration”, Perceptual and Motor Skills. vol. 95, pp. 661-669, 2002.

[15] S. Njah, B.Nouma, H. Bezine, and A.M. Alimi, “MAYASTROUN: A Multilanguage Handwriting Database”, Frontiers in Handwriting Recognition ICFHR, 2012, Bari, 308 – 312, 2012

[16] R. Plamondon, W. Guerfali, “The Generation of Handwriting with Delta-Lognormal Synergies”,Bio.Cyb., vol. 78, pp. 119-132, 1998.

[17] Rabiner, L., “A tutorial on HMM and Selected Applications in Speech Recognition”. Proc. IEEE 77 (2), pp. 257–286, 1989.

[18] L. Schomaker, “Simulation and Recognition of Handwriting Movements: a Vertical Approach to Modeling Human Motor Behavior”. Ph. D Thesis, Nijmegen University, Netherlands, 1991.

[19] L.Shao and H. Zhou. “Curve Fitting with Bezier Cubics”. Graphical Models and Image Processing. vol. 58, pp. 223-228. 1996.

[20] N.Taweechai and D. Natasha, “ Approximating Online Handwritten Image by Bézier Curve”. 10th IEE Int. Conf. Computer Graphics, Imaging and Visualization (CGIV), Los Alamitos, USA, pp. 33-37, 2013.

[21] J. Wang, C. Wu, Y. Xu, H. Shum and L. Ji, “Learning-Based Cursive Handwriting Synthesis,” Proc. of the Eighth Int. Workshop on Frontiers in Handwriting Recognition (IWFHR’02), 2002.

[22] L. Yanhong, L. O. David and Q. Zheng. “Similarity Measures Between Intuitionistic Fuzzy (vague) Sets: A Comparative Analysis”. Pattern Recognition Letters 28:278–285, 2007.

 ISBN: 978-1-61208-340-7

How to Make Robots Feel and Social as Humans

Building attributes of artificial emotional intelligence with robots of human-like behavior

Aleksandar D. Rodić and Miloš D. Jovanović
Institute Mihailo Pupin
University of Belgrade
Belgrade, Serbia
e-mail: {aleksandar.rodic, milos.jovanovic}@pupin.rs

***Abstract*—Paper contributes to building attributes of artificial Emotional Intelligence (EI) aimed to be implemented in robots of human behavior as advanced intelligent robot interface. The main research objective of the paper regards to searching is it possible and how to make robots emotive and sociable as humans. For this purpose, the Meyers-Briggs theory on human personality, known from personality psychology, is employed for mapping human psychological traits and development of robot EI-controller. A customized multi-input and multi-output fuzzy inference model is designed to fit human affective and social attributes. The assumed fuzzy structure makes core of the robot EI-controller. Developed intelligent robot interface was implemented with small Aldebaran's Nao humanoid robot used to validate control performances and EI model developed. In the paper, was presented how the developed intelligent robot interface can be used for mapping different human personality traits and temperaments to the machine. Accuracy of the model used for building robot interface was verified by tests with human examinees by using corresponding on-line psychological tests – questionnaires.**

Keywords-emotional intelligence; emotion-driven behavior; social robots; embodied mind; affective computing;

I. INTRODUCTION

To function in a complex and unpredictable physical and social environment humans are faced with applying their physical and intellectual resources to realize multiple goals in an intelligent and flexible manner. Two distinct and complementary information processing systems – *cognition* and *emotion* enable humans achieving of these goals by operating simultaneously [1]. The cognitive system is responsible for interpreting and making sense of the world, whereas the emotion system is responsible for evaluating and judging events to assess their overall value with respect to the human (e.g., positive or negative, desirable or undesirable, hospitable or harmful, etc.) [2]. When operating in the proper balance, the emotion system modulates the operating parameters of the cognitive system and the body to improve the overall mental and physical performance of the human. The scientific literature documents the beneficial effect of emotion on creative problem solving, attention, perception, memory retrieval, decision-making, learning, etc.

The fact that emotions are considered to be essential to human reasoning suggests that they might play an important role in autonomous robots as well [3][4].Today's autonomous robots can certainly improve their ability to function in complex environments and to behave appropriately in partnership with people. Using the properties of natural intelligence as a guide, a robot's cognitive system would enable it figure out what to do, whereas the emotion system would help it to do so more flexibly in complex and uncertain environments, as well as help the robot behave in a socially acceptable and effective manner with people [4].

In order to interact with social partners (whether it is a device, robot or another person), it is essential to have a good conceptual model of how the social partners operates [5]. With such a model, it is possible to explain and predict what the interlocutor is about to do, its reasons to doing it, and how to elicit a desired behavior from it. The work in this paper focuses on developing emotionally-driven and sociable robots for envisioned applications where the robot interacts with a person or another robot as a partner. The field of social robots and safe Human-Robot Interaction (HRI) opens new areas of applications like: healthcare, caretaking, assistance, edutainment and entertainment.

The paper is organized in seven sections. In Section 1, a brief introduction into the topics considered in the paper is given. Progress beyond the state-of-the-art is pointed out in Section 2. Necessary theoretic background as a platform for building of the EI model is given in Section 3. Section 4 addresses to modeling of human affective and social behavior dealing with concept and solutions. Model validation and implementation of EI interface with the small Nao humanoid robot are given in Sections 5 and 6. The paper is concluded in Section 7.

II. PROGRESS BEYOND STATE-OF-THE-ART

Modeling of natural intelligence, artificial EI, embodied mind and embodied cognition are emerging research fields. They were thoroughly explored by many scientists in natural, human and technical sciences in the last decade.

Inspired by models of natural intelligence in biological systems, Breazeal [2] [6] designed an architecture that features both - cognitive system and Emotion System (ES). Both systems operated in parallel and are deeply intertwined to foster optimal functioning of the robot in its environment. The overall architecture was comprised of a distributed network of interacting agent-like processes that excite and inhibit one another by spreading activation. For modeling of

 ISBN: 978-1-61208-340-7

the ES, a learning structure for dynamically deciding the appropriate number of kernels, were applied [6]. This work resulted in development the sociable machine Kismet [7], an expressive robotic creature with perceptual and motor modalities, tailored to natural human communication channels.

Beginning with an outline of the theoretical and methodological commitments of standard cognitive science, Shapiro then examined philosophical and empirical arguments surrounding the traditional perspective [8].

Varela et al. have highlighted several themes clearly [9]: our dualistic tendencies to distinguish between subject and object, and the reification of representation in our framing of experience - both projected outward (idealism) onto objects in the world that can then contain and give shape to our inner representations, or assimilated symbols of an independent world 'out there' (realism).

Brooks theorized on the importance of emotional intelligence in predicting individual and group success [10]. Drawing off of a variety of disciplines including psychology, economics and cognitive research, Brooks made a case for the power of the unconscious mind in influencing our interactions, beliefs and decisions. We are products of our emotions, he said. “Emotions enable us to value things. We can’t make decisions if we can’t value things.” Brooks stressed out that “the mere act of affection rewires connections in our brains”.

Authors of this paper contribute beyond the recent research results in this field by searching for the answer how to make robots feel and sociable as humans. They go even further trying to give the answer how to make robot psyche to be of predefined (requested) human-like personality traits. The solution proposed in this paper concerns with design of an appropriate model of human affective and social behavior based on personality psychology that also takes into account real interior and exterior constraints.

III. THEORETIC BACKGROUND

The platform for development mathematical model of human emotionally driven and social behavior is the Meyers-Briggs theory on personality [11] widely used in personality psychology. According to this theory, the personality type and temperament dominantly influence human psychological behavior.

A. Personality Type

Personality psychology is a branch of psychology that studies personality and its individual differences [12]. According to the theory, "personality" is a dynamic and organized set of characteristics possessed by a person that uniquely influences individual cognitions, emotions, motivations, and behaviors in various situations. Personality also refers to the pattern of thoughts, feelings, social adjustments, and behaviors consistently exhibited over time that strongly influences one's expectations, self-perceptions, values, and attitudes. It also predicts human reactions to other people, problems, and stress [13] [14]. This scientific discipline uses the Myers-Briggs Type Indicator (MBTI) assessment as a psychometric questionnaire designed to measure psychological preferences in how people perceive the world and make decisions [15]. The MBTI sorts psychological differences into four opposite pairs, i.e., dichotomies (Extravert-Introvert, Sensing-iNtuitive, Feeling-Thinking and Perceiving-Judging). That results in 16 possible psychological, i.e., personality types. None of these types are better or worse. However, Briggs and Myers theorized that individuals naturally prefer one overall combination of type differences [12].

B. Human Temperament

Under the notion “temperament” it is assumed in psychology, unlike to the term “personality”, the individual kinds of the psyche traits that determine dynamics of human psychological activity [16]. The temperament traits are expressed in an even manner in any activity nevertheless to its’ content, goals and motives, remaining invariant in the later years and which, in their interconnections, characterize the type of temperament [16]. The temperaments are (Fig. 1): *sanguine* (pleasure-seeking and sociable), *choleric* (ambitious and leader-like), *melancholic* (introverted and thoughtful), and *phlegmatic* (relaxed and quiet), Fig. 1.

A temperament type can be determined by filling corresponding questionnaires (tests) available at the Internet as well as corresponding personality tests [17] [18].

IV. MODELING EMOTIONS

While the artificial intelligence copes with tasks such as pattern recognition, context understanding, reasoning, decision making, etc., the emotional intelligence is responsible with humans for self-awareness, self-management, awareness of others and relationship management [19]-[21]. According to the theory of personality, human emotional reactions primarily depend on three factors [13]: (i) personality type, (ii) personality character, and (ii) temperament. These factors are mainly determined by genetic code and acquired by a birth. Also, behavior of individuals is strongly influenced by additional exterior and interior factors (Fig. 2). Under the term “exterior world” our physical and social environment (such as events, situations, acts or relationships with other persons) are assumed. The “interior stimuli” mainly concerns with our physical and psychological conditions (regarding to body and psyche) such us senses of fatigue, pain, disease, etc. Under the same term, the feelings like love, depression, anger, hatred, fear, satisfaction, etc., are assumed, too. The “social factors” regard to the conditions that influence some features of individual behavior.

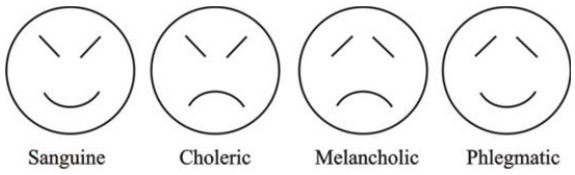

Figure 1. Emotion representation of four temperament types.

 ISBN: 978-1-61208-340-7

The "social factors" includes the following: family and school education, influence of companions, religion and affiliation to the social groups such as political parties, civil communities, clubs, etc.

To derive generic model of a human psychological behavior the following assumptions can be assumed. The considered biological system, such as human psyche, can be approximated by a deterministic, dynamic, non-linear, multi-input and multi-output (MIMO) system of arbitrary complexity. The input and output variables of the emotion-driven behavior (EDB) model are hardly measurable. They can be quantified (rated) by using corresponding psychological questionnaires [17], [18].

The variables of interest required for modeling EDB include qualitative information regarding personality profile, physical and social environment, emotional and health conditions, social factors, etc. They are quite heterogeneous, defined in the form that is more symbolic and descriptive than measurable and numerical. Generally, humans use to behave (in psychological sense) in a fuzzy manner by using corresponding linguistic variables. That means people use their different natural skills of sensing, symbolic and phonetic communication (e.g., body and facile gestures, phonetic meanings, etc.) to express their emotional state – feelings, mood, etc. Due to a fuzzy nature of human behavior, the modeling approach to be assumed in this paper as appropriate solution consequently belongs to the knowledge-based type. It assumes utilizing of a fuzzy logic system structure. Accordingly, the appropriate model structure of emotionally-driven and social behavior can be represented by a three-stage block structure presented in Fig. 2. It consists of three fuzzy logic blocks FIS-1 to FIS-3 where everyone contributes particularly to shaping of outcome event-driven emotional reaction(s).

Human affective behavior is generated and profiled by influence of three input variables (information carriers) that are: (i) "trigger-event" that arouses different psychological reactions, (ii) "behavior profiler" that shapes event-driven behavior in a way to fit particular personal profile of individual whose behavior need to be modeled, and (iii) "behavior booster/inhibitor" that intensifies or weakens the expressiveness of the affective manifestations of individual. The trigger-event (e.g., situation, interpersonal relationship, interaction or just an act) provokes (excites) corresponding affective reactions (mood) with individuals. It is well known that some persons react more intensively in emotional sense (depending on their personality type and temperament) to the same trigger-event than others.

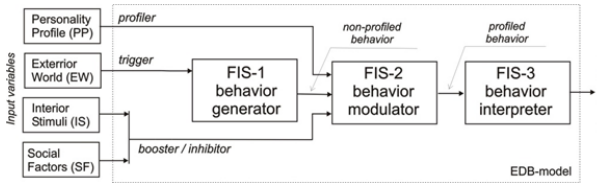

Figure 2. Block-structure of the emotionally-driven behavior model consists of behavior generator, modulator and interpreter.

These personality differences can be modeled by introducing corresponding "behavior profiler". The "behavior profiler" modulates usual (generally expected) emotional reactions characteristic for this trigger-event. It is done in a way to imitate reactions characteristic for the particular personality profile and temperament of the individual whose behavior need to be modeled. The "behavior booster/inhibitor" in the model presented in Fig. 2 serves to intensify or weaken the intensity of emotional reactions depending on dominant personality traits and temperament type.

Fuzzy model blocks FIS-1, FIS-2 and FIS-3 (Fig. 2) are assumed to be of Mamdani type. The input and output variable vectors at the particular fuzzy blocks are of the arbitrary number depending on how comprehensive model wish to be developed. In the model presented in Fig. 2, the corresponding input/output membership functions of the FIS-1 to FIS-3 blocks are either the Gauss curves or Sigmoid functions. The number of fuzzy rules synthesized in the model varies depending on how comprehensive and accurate model is required. The proposed model architecture (Fig. 2), with three fuzzy blocks aligned in a cascade, enables easy monitoring of the model state variables.

Trigger-events to be considered in the model, presented in Fig. 2, can be rather numerous. The list of the trigger-event attributes used for modeling of human emotional behavior in this paper is given in [22]. At this stage of research, this number of event attributes is limited to approximately n1=50. This amount of attributes satisfies modeling requirements of majority usual scenarios to appear in everyday practice. The actual number of event attributes can be in principle very high - the larger number of trigger-event attributes in the model, the more comprehensive, accurate and complex model is. The number of emotions (moods) n2, modeled in the paper, is higher than the number of trigger-event attributes n1 (middle column, Fig.3). The right column, presented in Fig. 3, contains emotional reactions, i.e., attributes of reactions, caused by trigger-events. They are modulated by use of the fuzzy rules that take into account personality traits and temperament of the individual whose affective and social behavior is modeled. To clarify the methodology applied, the event "birthday anniversary", taken as an example, represents combination of several particular event attributes such as: cheerful, funny, surprising, sociable, etc. To build a model, every particular event attribute as well as emotion state of the individual has to be quantified (rated) in an appropriate way. It can be done in a way presented in Fig. 4. Such an approach leads to correct definition of linguistic fuzzy variables as appropriate inputs to the corresponding fuzzy model blocks. For example, if take the attribute "cheerful" as a variable, its' rating can be accomplished in the following way: (i) *not at all* (0%), (ii) *somewhat* (<25%), (ii) *very* (25-75%) and (iii) *entirely* (>75%). Concerning fuzzy rules of the model, they are determined based on the semantic-graph whose reduced (not complete) form is presented in Fig. 3. According to this graph, the following fuzzy rule, as an example, can be derived:

 ISBN: 978-1-61208-340-7

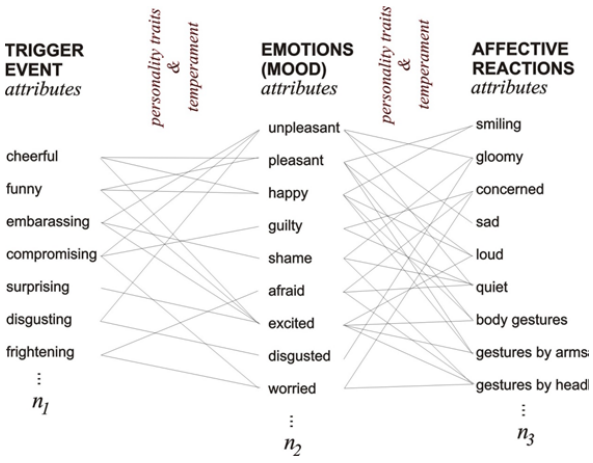

Figure 3. Example of functional interconnections between the trigger events, produced emotions and corresponding affective reactions.

if (*event*.is.*cheerful*) than (*mood*.is.*pleasant*) and (*mood*.is.*happy*) and (*mood*.is.*excited*).

By designing of the model rules, it is also necessary to take into account the influence of the personality profile of individual as well exterior and interior constraints.

The model designed in this paper includes 75 fuzzy rules, n1=20 trigger-event attributes, n2=35 emotion attributes and n3=20 different affective reactions. The number of rules can be much higher in the case of a more accurate and comprehensive model. Being we have implemented this model to a small humanoid robot with limited capabilities the number assumed was enough numerous to verify the performances of the designed robot EI-controller. More details regarding model building are given in [22].

Additionally, attributes of social behavior regard to interpersonal ability of communication and self-adaptation to group or team. The properties such as sociability (easiness of communication with others), cooperativeness, compatibility with others, interpersonal synergy, reliability and responsibility for the community interest, mutual tolerance,

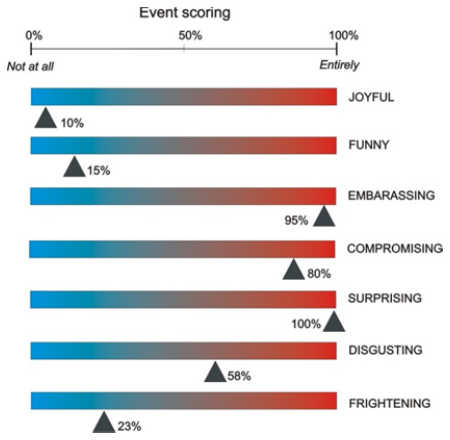

Figure 4. Example of rating (quantification) trigger-event attributes according to degree of experiance.

feel of belonging community, etc., are properties based on highly developed degree of EI. Brooks [10] pointed out that emotions are the motor-power of human individual and collective behavior. Attributes of social behavior of individuals strongly depend on personality profile and temperament but also on social constraints such as family education, companions, club memberships, religion, etc.

V. MODEL VALIDATION

Model validation is accomplished experimentally by involving human examines in this procedure to provide reference values. Ten persons of different gender and age were requested to fill out the personality type and temperament test. Both questionnaires are available on Internet [17] [18]. The same examinees were asked also to fill out the questionnaires to assess their affective reactions (response) to the imagined (hypothetical) set of trigger-events taken from the life practice. The results were systematized and presented in [22]. In the paper, a characteristic trigger event, arousing emotional behavior, is chosen for model verification.

Trigger event example: *At the dinner table, someone told a funny joke. While laughing, you have suddenly burped loudly.*

The chosen event is experienced in a different way by interviewed persons. Model validation was done by comparison of the results obtained by testing human examinees (of known personality profiles) with corresponding results obtained by simulation of the generic model proposed in the paper. In such a way, the objectivity of model assessment is achieved.

Also, the model sensitivity test upon variation of exterior and interior factors (personality traits, social factors and interior stimuli) was done. The emotion trigger-event assumed in this simulation experiment has the attributes presented in Fig. 4. These attributes are independently rated by anonymous human examinees. The model of EI presented in Section IV is simulated taking into account the parameters that correspond to the following test-cases:

C-1: Personality type *INTJ* (Introvert=60%, iNtuitive=57%, Feeling=78%, Judging=69%); Temperament: *Sanguine*=80%; Interior stimuli: *none*; Social factor: *none*;

C-2: Personality type *ESTP* (Extrovert=60%, Sensing=57%, Thinking=78%, Perceiving=69%; Temperament: *Sanguine*=80%; Interior stimuli: *none*; Social factor: *none*;

C-3: Personality type *ESTP*; Temperament: *Choleric*=80%; Interior stimuli: *none*; Social factor: *none*;

C-4: Personality type *ESTP*; Temperament: *Phlegmatic*=80%; Interior stimuli: *none*; Social factor: *none*;

C-5: Personality type *ESTP*; Temperament: *Phlegmatic*=80%; Interior stimuli: *completely moody*; Social factor: *none*;

C-6: Personality type *ESTP*; Temperament: *Phlegmatic*=80%; Interior stimuli: *none*; Social factor: *strict family education*;

Simulation results presented in Table 1 represent the rated feelings (affective reactions) obtained by model simulation. Feeling attributes (Table 1) were aroused by the

 ISBN: 978-1-61208-340-7

TABLE I. SIMULATION RESULTS: TABLE OF FEELING RATES

	C-1	C-2	C-3	C-4	C-5	C-6
Feeling rate	*%*	*%*	*%*	*%*	*%*	*%*
Unpleasant	50.49	51.72	51.84	45.89	45.94	46.55
Guilty	84.82	87.98	85.78	67.88	70.36	72.69
Shame	97.41	97.41	95.45	79.82	79.82	82.70
Frightened	49.86	51.48	51.63	45.62	45.71	46.29
Excited	45.80	48.80	49.37	42.60	43.13	43.35
Disgusted	43.49	46.32	46.98	40.33	40.98	41.07
Warried	48.37	50.88	51.13	44.83	45.00	45.52

imposed trigger-event example and modulated by corresponding interior and exterior factors such as: personality traits, temperaments, emotional states and social factors. The presented results validate model sensitivity upon variation of the previously mentioned factors. By comparing the feeling indicators presented in the columns C-1 and C-2 of Table 1, it is evident that an ESTP person demonstrates emotions in a more intensive way than one IFTJ person. Also, an ESTP choleric person (C-3) is more sensitive than corresponding sanguine (C-2) and phlegmatic (C-4) persons. A moody person (C-5) and a person that is subjected to the strict social constraints (e.g., family education) are slightly more sensitive than others with the same temperament and personality. Affective reactions that are generated by the model proposed in Section IV commonly can be displayed by the feeling charts, as presented in Fig. 5.

The obtained simulation results and verification of model properties make us believe that the EI model designed in this paper can be effectively implemented with robots to enable them to feel and be social as humans. In the next section it will be demonstrated.

VI. IMPLEMENTATION OF ROBOT EI-INTERFACE

Robot interface (software algorithms), based on the model of human affective and social behavior developed in this paper, is implemented in the controller of the Aldebaran's Nao humanoid robot [23]. Block-diagram of the high-level control structure is presented in Fig. 6.

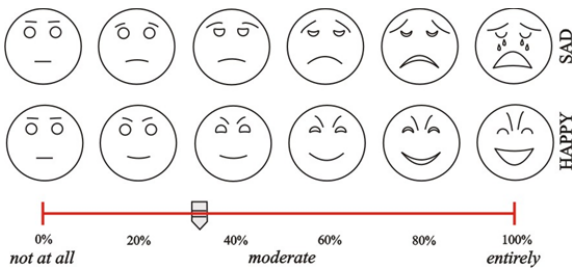

Figure 5. Example of feeling charts. Mood rating scale with respect to the sadness and happiness

A. Software Implementation

As a widely used open robotic platform, the Nao robot provides a relatively fine possibility of simple implementing advanced control algorithms through the Naoqi robotic application [23]. The Naoqi application is an open and fully accessible software module which provides easily access through all major ports of the Nao robot. The Naoqi application is embedded Nao software that includes fast, secure and reliable development platform. It allows easy implementation of new features that can improve functions of the Nao robot. The Naoqi allows an implementation of algorithms that share its Application Programming Interface (API) to the other systems and supports the development of modules that run on the Nao platform or on a remote PC system. Software development can be accomplished in Windows, Mac OS, or Linux environment. A software package that collects signals from the visual system of the robot is written in Open CV. Through the Naoqi, the application gathers information from one of the video cameras implemented in the head of the Nao robot. It is not possible at once to combine signals from both cameras due to the configuration of the controller built into the Nao robot. So, images from selected high-definition camera are transmitted to remote PC, via Naoqi implemented software applications by wireless communication.

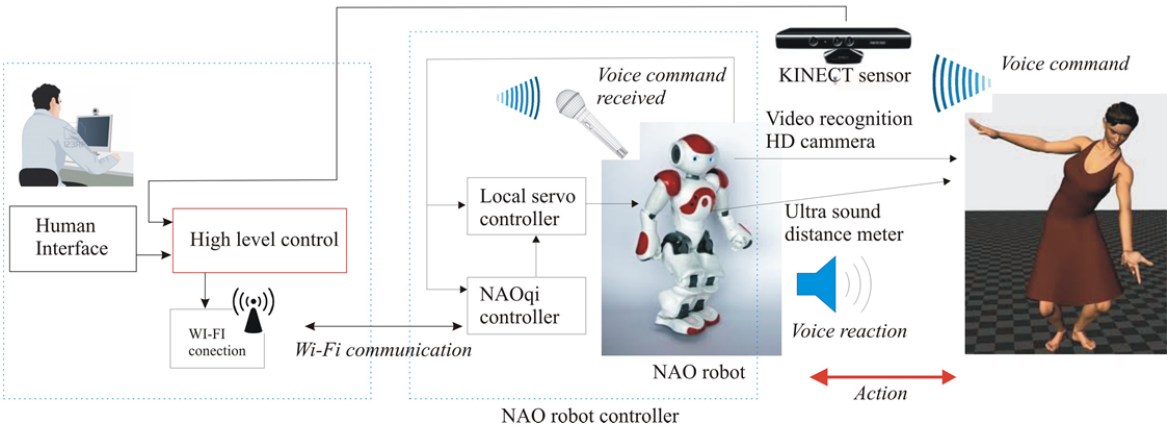

Figure 6. High-level system description. The control block-diagram of the NAO humanoid with EI-controller.

 ISBN: 978-1-61208-340-7

Remote PC provides signal processing and recognition of individuals based on face recognition applications. When the Nao robot observes and locates the person for possible cognitive interaction, an ultrasound sensor is activated to determine the distances to the interlocutors. Based on the vision algorithms and signals from ultrasonic rangefinder, the distance between Nao and interlocutor is obtained and estimated and modules of cognitive analysis are activated. Cognitive analysis module of persons, together with face recognition module, analyze the condition of the interlocutor, based on the movement of arms and legs of the interlocutors, coordinate all the parameters of cognitive analysis and decide about the emotional state of the interlocutor. In accordance with all analyzed cognitive parameters of the interlocutor, a conclusion is made and desired movement of the Nao robot are generated achieving its' hands, and at the same time it is generated desired audio message that Nao robot directs to the interlocutor. So, the audio system is included into the algorithm. Namely, entire action is initiated by the voice. The block diagram of the overall cognitive task is shown in Fig. 6.

B. Embodiment of Social Behavior Attributes in Robot

Attributes of social behavior were implemented in Nao robot controller as an advanced EI-interface. The task of EI-controller is to enable robot some basic functions of social behavior attributes characteristic for behavior in groups. Bearing in mind the real technical constraints of the hardware, some of the particular attributes of social behavior, shown in the semantic graph in Fig. 7, were implemented with the Nao robot. Principle of implementation of fuzzy model in realization of some features of social behavior is similar to the principle of implementation the functions of affective behavior presented in Fig. 3. In this case, instead of a trigger-event, physical and social environment arouse corresponding emotional reactions and interpersonal relationship (communication, collaboration, etc.) between robot and others. In the paper, Nao robot is requested to express some elements of social behavior based on relativelly modest perceptive capabilities. They are based on embedded robotic vision, external Kinetic sensor (for gesture recognition) and speach recognition system. Fuzzy model, that is core of the control interface implemented in Nao robot, includes variables that carry on neccessary information regarding stimuli received from social environemnt such as audio and physical incentives: invitation voice, salutation, body and arms gestures, dialog sequences, etc.

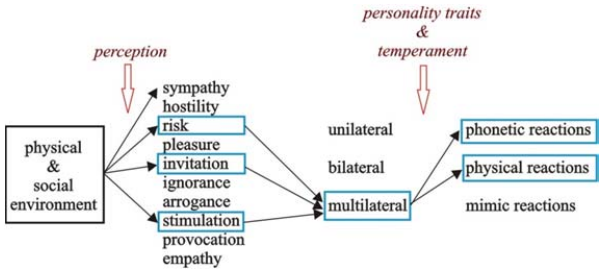

Figure 7. High-level semantic diagram of Nao robot social behavior.

Robot also checks for possible risks of interacting with others by recognizing exsitance of some irregular physical gestures originating from the interacting persons. Also, type of communication, assuming unilateral, bilateral or multilateral modus, determines character of robot interaction.

Nao robot interacts with social environment by using its' audio interface (microphones and speakerphones) and physical gestures through movements of body and arms. The rating scale of phonetic and physical reactions implemented in the Nao robot is presented in Fig. 8.

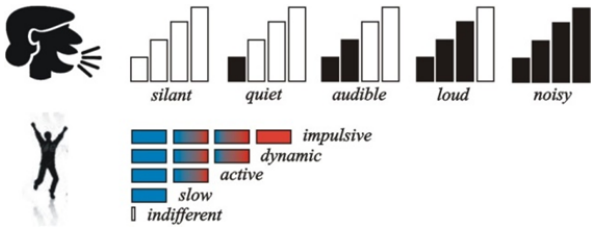

Figure 8. Rating scale of phonetic and physical reactions implemented with Nao robot.

C. Experiments with Nao Robot

The task „teamwork" is a typical scenario that includes attributes of social behavior. In this case, temperamental and strongly motivated individuals accomplish this task easier and in a more efficient way than ones with weak temperament and low motivation. In this example, group of junior researchers from laboratory invites (stimulates by voice) Nao robot to join them and salute (Fig. 9). Nao robot, having an advanced EI interface, recognizes calls, locates persons in the surrounding, recognizes their gestures and responses them by stretching arm forward and speaking the kind words. In such a way, robot expresses its' social behavior as presented in Fig. 9. In this experiment, personality traits of a joyful, sociable and temperamental individual are imposed to the NAO robot. The experiment was repeated by changing robot parameters (features) making robot to be a "person" of properties that regards to a reserved (introverted) and melancholic person.

Figure 9. NAO robot demonstrates EI capabilities by communicating with young reserchers from the IMP Robotics Laboratory.

 ISBN: 978-1-61208-340-7

By comparison of robot affective reactions obtained in the previously mentioned experimental sessions, the expected validation of the proposed modeling concept is achieved.

VII. CONCLUSION AND FUTURE WORK

The paper concerns with development of robot EI interface designed to ensure advance robot capabilities – emotional and social behavior as humans. Developed interface is based on generic model of natural emotional intelligence that includes human emotion-driven and social behavior. EI model is synthesized by implementing multi-input and multi-output fuzzy inference system. The purpose of artificial EI in robots is to increase the autonomy through building advance cognitive features such as: emotion understanding, self-management, managing relationship with others, etc. The novelties given in the paper regards to modeling approach of human affective and social behavior attributes based on theory taken from personality psychology. Model takes into account personality traits, type of temperament as well as interior and exterior constraints – emotional conditions, social factors, etc. Model validation was done by comparison of experimentally acquired indicators from human examinees and indicators obtained by model simulation. Convergence of experimentally obtained and simulation results indicates that developed EI-model can be used with robots for embodiment of mind and cognitive capabilities. The EI-interface was implemented with NAO humanoid robot. It was demonstrated how Nao robot demonstrate some attributes of social behavior based on its' EI-controller. Additional model extension and validation are planned in the future by using extensive experimental results with human examinees. The model structure will be upgraded by including new attributes of emotion and social behavior. In such a way, the EI-model will become more comprehensive and accurate.

ACKNOWLEDGMENT

The research in the paper is funded by the Serbian Ministry of Science under the grants TR-35003 and III-44008. It is partially supported by the SNSF IP project IZ74Z0_137361/1 as well by the Serbia-Portugal "COLBAR" research project under the grant 451-03-02338/2012-14/12. The authors express thanks to the scientists from the Department of Experimental Psychology, Faculty of Human Sciences, University of Belgrade, for the valuable suggestions and expertize.

REFERENCES

[1] R. Picard, Affective computation. MIT Press, Cambridge, MA. 1997.

[2] C. Breazeal, "Function Meets Style: Insights from Emotion Theory Applied to HRI", IEEE Transactions in Systems, Man, and Cybernetics, Part C, 34(2), 2003, pp. 187-194.

[3] J. H. Busher, Human Intelligence its Nature and Assessment, Harfer Torbchbooks, NewYork, 1973.

[4] J. Weng et al., "Autonomous mental development by robots and animals", Science, vol. 291, 2001, pp. 599–600.

[5] D. Norman, "How might humans interact with robots", Keynote address to the DARPA/NSF Workshop on Human-Robot Interaction, San Luis Obispo, CA., 2001, pp. 72-78.

[6] C. Breazeal, Designing sociable robots. MIT Press. Cambridge. 2002.

[7] Sociable machines – the Kismet robot. http://www.ai.mit.edu/ /projects/sociable/baby-bits.html [retrieved: April, 2014].

[8] L.Shapiro, Embodied Cognition (New Problems of Philosophy), Routledge Taylor & Francis Group, London and NewYork, ISBN-10: 0415773423 | ISBN-13: 978-0415773423, 2010.

[9] F. J. Varela, E. Rosch, and E. Thompson, The Embodied Mind: Cognitive Science and Human Experience, MIT Press, 1992.

[10] D. Brooks, The Social Animal: The Hidden Sources of Love, Character, and Achievement, Books Inc. - The West's Oldest Independent Bookseller, Published by Random House, ISBN-10: 140006760X, ISBN-13: 9781400067602, 2011.

[11] I. Myers-Briggs and P. Myers, Gifts Differing: Understanding Personality Type. Mountain View, CA: Davies-Black Publishing. 1995.

[12] Personality psychology. http://en.wikipedia.org/wiki/Personality_psychology [retrived: April, 2014].

[13] G. D. Myers, Psychology (9th ed.). New York: Worth Publishers. 2010.

[14] F. J. Winnie and W. J. Gittinger, "An introduction to the personality assessment system", Journal of Clinical Psychology, Monograph Supplement, 38, 1973, pp. 1-68.

[15] MBTI. http://en.wikipedia.org/wiki/Myers-Briggs-Type-Indicator [retrived: April, 2014].

[16] Temperament types. http://en.wikipedia.org/wiki/Four-temperaments [retrived: April, 2014].

[17] On-line personality test. http://www.16personalities.com/free-personality-test [retrived: April, 2014].

[18] On-line temperament test. http://neoxenos.org/wp-content/blogs.dir/1/files/temperaments/temperament_test.htm [retrived: April, 2014].

[19] H. D. Kluemper, "Trait emotional intelligence: The impact of core-self evaluations and social desirability" Personality and Individual Differences, 44(6), 2008, pp. 1402-1412.

[20] D. J. Mayer and P. Salovey, What is emotional intelligence? In: P. Salovey & D. Sluyter (Eds.), Emotional development and emotional intelligence: Implications for educators, pp. 3-31, New York: Basic Books, 1997.

[21] V. K. Petrides, R. Pita, and F. Kokkinaki, "The location of trait emotional intelligence in personality factor space", British Journal of Psychology, 98, 2007, pp. 273-289.

[22] A. D. Rodić and K. M. Addi, „Mathematical Modeling of Human Affective Behavior Aimed to Design Robot EI-Controller",A. Rodic´ et al. (eds.), New Trends in Medical and Service Robots, Series: Mechanisms and Machine Science 20, DOI: 10.1007/978-3-319-05431-5_10, Springer International Publishing Switzerland, 2014, pp. 141-162.

[23] NAO robot. www.aldebaran-robotics.com/en/Discover-NAO/Key-Features/open-source.html [retrived: April, 2014].

 ISBN: 978-1-61208-340-7

A Study of Retrieval Algorithms of Sparse Messages in Networks of Neural Cliques

Ala Aboudib, Vincent Gripon, Xiaoran Jiang
Electronics Department
Télécom Bretagne (Institut Mines-Télécom)
Brest cedex 3, France
e-mail: name.surname@telecom-bretagne.eu

The authors are also with the Laboratory for Science and Technologies of Information, Communication and Knowledge, CNRS Lab-STICC, Brest, France.

***Abstract* – Associative memories are data structures addressed using part of the content rather than an index. They offer good fault reliability and biological plausibility. Among different families of associative memories, sparse ones are known to offer the best efficiency (ratio of the amount of bits stored to that of bits used by the network itself). Their retrieval process performance has been shown to benefit from the use of iterations. In this paper, we introduce several rules to enhance the performance of the retrieval process in recently proposed sparse associative memories based on binary neural networks. We show that these rules provide better performance than existing techniques. We also analyze the required number of iterations and derive corresponding curves.**

Keywords – associative memory; sparse coding; parsimony; iterative retrieval; threshold control

I. INTRODUCTION

Associative memories are alternatives to classical index-based memories where content is retrieved using a part of it rather than an explicit address. Consider for example accessing a website using a search engine instead of a uniform resource locator (URL). This mechanism is analogous to human memory [*1*] and has inspired many neural-networks-based solutions such as [*2*] [*3*].

A new artificial neural network model was proposed recently by Gripon and Berrou [*4*]. It employs principles from information theory and error correcting codes and aims at explaining the long-term associative memory functionality of the neocortex. This model was proved to outperform the celebrated Hopfield neural network [*3*] in terms of diversity (the number of messages the network can store) and efficiency (the ratio of the amount of useful bits stored to that of bits used to represent the network itself) [*5*]. It was later extended in [*6*] to a sparser version based on the Willshaw-Palm associative memory model [*2*] [*7*].

The key difference between the models proposed in [*6*] and [*2*] is the use of specific structures in the network. This is done by grouping neurons into clusters within which connections are not authorized (multi-partite graph). These clusters are considered analogous to cortical columns [*4*] of mammalian brains within which nodes are likened to micro-columns. This is supported by Mountcastle [*8*] who suggests that a micro-column is the computational building block of the cerebral neo-cortex. In addition, here are some reasons to motivate the use of clusters:

- It is believed that micro-columns in each cortical column react to similar inputs. The concept of clustering is meant to imitate this stimulus-similarity-based grouping. A consequence is the possibility to use this network for retrieving messages from inaccurate observations. This type of retrieval is addressed by Gripon and Jiang in [*9*].
- Clusters allow for simple and natural mapping between non-sparse input messages and sparse patterns representing them in the associative memory. In the case where clusters are all of size 1 each, a model equivalent to the classical Willshaw-Palm networks is obtained, where input messages have to be sparse.
- It was observed that micro-columns usually have many short inhibitory connections with their neighbors [*10*] [*8*], which means that the activation of one micro-column causes all of its near neighbors to be deactivated. This is due to the locally limited energy supply of the brain. This mechanism is represented by the local winner-takes-all rule introduced in [*4*].
- Using clusters allows for introducing guided data recovery in which a prior knowledge of the location of clusters containing the desired data can significantly enhance performance. A detailed study of this type of data retrieval is available in [*6*].

In this paper, we consider the extended version of the model proposed in [*6*]. We introduce several retrieval rules including adaptations of those proposed by Willshaw [*2*], Palm [*11*], Schwenker [*12*] and Gripon and Berrou [*4*]. We also propose new ones and make a comparison of these regarding performance and number of iterations.

The rest of this paper is organized as follows: in Section II, we describe the general architecture of the network model we use. Section III introduces a generic formulation of the retrieval algorithm on such structures. Then, the following five sections develop each step of this algorithm. For each step, different rules are reviewed if available. Some of these rules have been proposed in previous papers, and others we introduce here for the first time. In Section IX, performance comparisons of several combinations of retrieval rules are presented. Section X is a conclusion.

II. NETWORK TOPOLOGY AND STORING MESSAGES

This section focuses on the neural-network-based auto-associative memory introduced by Gripon and Berrou in [*4*]. It is dedicated to defining this network and describing how it can be extended to store variable-length messages.

A. *Architecture*

The network can be viewed as a graph consisting of n vertices or units initially not connected (zero adjacency matrix) organized in χ parts called clusters with each vertex belonging to one and only one cluster. Clusters are not necessarily equal in size but for simplicity, they will be all considered of size l throughout this work. Each cluster is given a unique integer label between 1 and χ, and within each cluster, every vertex is given a unique label between 1 and l. Following from this, each vertex in the network can be referred to by a pair (i, j), where i is its clus-

 ISBN: 978-1-61208-340-7

ter label, and j is the vertex label within cluster i. For biologically-inspired reasons [*13*] [*14*], and as explained in [*6*], a unit in this model is chosen to represent a cortical micro-column instead of a single biological neuron which is why we shall not use the term "neuron".

At a given moment, a binary state v_{ij} is associated with each unit (i,j) in the network. It is given the value 1 if (i,j) is active and 0 if it is idle. Initially, all units are supposed to be idle. The adjacency matrix (also called the weight matrix w) for this graph is a binary symmetric square matrix whose elements take values in {0,1}. In this representation, a zero means an absence of a connection while a 1 indicates that an undirected (or a symmetric) connection is present. Note that despite the fact that physiological neural networks are known to be asymmetric, we argue that units in the proposed model represent populations of tens of neurons, and therefore can be mutually connected.

Row and column indexes of the weight matrix are (i,j) pairs. So in order to indicated that two units (i,j) and (k,s) are connected, we write $w_{(i,j)(k,s)} = 1$. All connection combinations are allowed except those among units belonging to the same cluster, resulting in a χ-partite undirected graph. When the memory is empty, w is a zero matrix.

B. *Message Storing Procedure*

We now describe how to store sparse messages using this network. This methodology has been first introduced in [*6*]. Suppose that each message consists of χ submessages or segments. Some of these segments are empty, i.e., they contain no value that need to be stored, while the rest has integer values in $\{1,..,l\}$. For the sake of simplicity, let us consider that all messages contain the same number of submessages c. Only those nonempty submessages are to be stored while empty ones are ignored. For example, in a network with $\chi = 6$ and $l = 12$, a message $m = \{,10,7,,12,11\}$ with $c = 4$ has two empty segments (the 1st and the 4th) while the remaining ones have values that need to be stored. In order to store m, each nonempty segment position i within this message is interpreted as a cluster label, and the segment value j is interpreted as a unit label within the cluster i. Thus, each nonempty segment is associated with a unique unit (i,j). So the message m maps to the 10th unit of the 2nd cluster, the 7th unit of the 3rd cluster, the 12th unit of the 5th cluster and the 11th unit of the 6th (last) cluster. A single message is not allowed to use more than one unit within the same cluster because, by definition, connections are not allowed within a cluster.

Then, given these c elected units in c distinct clusters, the weight matrix of the network is updated according to (1) so that a fully connected subgraph (clique) is formed of these selected units.

$$w_{(i,j)(k,s)} = 1 \quad \text{if} \quad i \neq k \quad \text{and} \quad m_i, m_k \neq 0 \qquad (1)$$

where $w_{(i,j)(k,s)}$ refers to the undirected connection between (i,j) and (k,s) which are two units associated to message segments m_i and m_k, respectively. i and k are cluster indices while j and s are unit indices.

The value of the parameter c can be unified for all stored messages, or it can be variable. A description of how to choose an optimal value of c is provided in [*6*] where c is considered identical for all messages.

It is important to note that if one wishes to store another message m' that overlaps with m, i.e., the clique corresponding to m' shares one or more connections with that of m, the value of these connections, which is 1, should not be modified. Such a property is called the nondestructivity of the storing process. As a direct consequence, the network's connection map is the union of all cliques corresponding to stored messages.

It is worth noting that when $l = 1$, the structure of this network becomes equivalent to the Willshaw-Palm model.

III. THE RETRIEVAL PROCESS

The goal of the retrieval process introduced in this paper is to recover an already stored message (by finding its corresponding clique) from an input message that has undergone partial erasure. A message is erased partially by eliminating some of its nonempty segments. For example, if $m = \{,1,8,,10,12\}$ is a stored message, a possible input for the network is $\overline{m} = \{,,,10,12\}$.

The core of the retrieval process can be viewed as an iterative twofold procedure composed of a dynamic rule and an activation rule. Figure 1 depicts the steps of the retrieval process:

```
Insert an Input Message.
Apply a dynamic rule.
Phase 1:
   Apply an activation rule.
   Apply a dynamic rule.
Phase 2:
  While (stopping criterion is not attained) {
      Apply an activation rule.
      Apply a dynamic rule.
   }.
output ← active units.
```

Figure 1. The generic algorithm for the retrieval process.

Each step of the algorithm of Figure 1 is described in detail in the next sections.

IV. INPUT MESSAGE INSERTION

An input message should be fed to the network in order to trigger the retrieval process. For example, suppose that we have a stored message $m = \{7,1,5,11,,\}$. Suppose now that we wish to retrieve m from the partially erased input $\overline{m} = \{,,5,11,,\}$. In order to do that, all units corresponding to nonempty segments should be activated. That is, a unit (i,j) associated with the segment of $\overline{m}$ at position i whose value is j is activated by setting $v_{ij} = 1$. So, $\overline{m}$ activates two units: (3,5) and (4,11). Having a number of active units, a dynamic rule should be applied.

V. DYNAMIC RULES

A dynamic rule is defined as the rule according to which unit scores are calculated. We will denote the score of a unit (i,j) by λ_{ij}. Calculating units' scores is crucial to deciding which ones are to be activated. A score is a way of estimating the chance that a unit belongs to a bigger clique within the set of active units and thus the chance that it belongs to the message we are trying to recover. In principle, the higher the score the higher this chance is. Two dynamic rules have been already introduced, namely, the Sum-of-Sum [*4*] and the Sum-of-Max [*15*] rules. We also introduce for the first time what we call the Normalization rule.

A. *The Sum-of-Sum Rule (SoS)*

The Sum-of-Sum is the original rule. It states that the score of a unit (i,j) denoted by λ_{ij} is simply the number of active units connected to (i,j) plus a predefined memory effect γ which is only added if (i,j) is active. Scores should be calculated for all of the units in the network. This Sum-of-Sum rule can be formalized by the following equation:

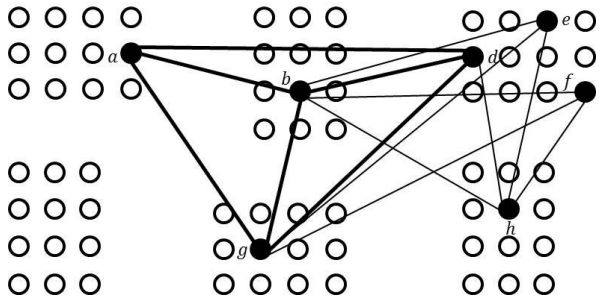

Figure 2. Dynamic rule application phase. Black-filled units are active.

$$\forall i \text{ and } j, 1 \le i \le \chi, 1 \le j \le l: \\ \lambda_{ij} = \gamma v_{ij} + \sum_{k=1}^{\chi} \sum_{s=1}^{l} w_{(i,j)(k,s)} v_{ks}. \quad (2)$$

Although intuitive, this rule has a major problem which is that in some cases, the scores give a false estimate of the chance that a given unit belongs to a bigger clique within the set of active units. To clarify this point we consider the example of Figure 2 where black circles represent active units at an iteration $t > 1$. The clique we wish to restore is $abdg$ which is maximal in size. Now, we will see what happens when we calculate the scores of units a and h given a memory effect $\gamma = 1$ where a is part of the searched message while h is not. According to the Sum-of-Sum rule, unit a has a score of 4 while unit h has a score of 5. This result indicates that the latter unit is more likely to belong to a bigger clique than the former because it has a higher score. This observation is not true since most of the active units connected to h belong to the same cluster and by conception, a message can only contain at most one unit per cluster. In order to solve this problem, the Sum-of-Max and the Normalization dynamic rules can be applied.

B. *The Normalization Rule (Norm)*

In the Normalization rule that we introduce here, units' scores are calculated using the following equation:

$$\lambda_{ij} = \gamma v_{ij} + \sum_{k=1}^{\chi} \frac{1}{|v_k|} \sum_{s=1}^{l} w_{(i,j)(k,s)} v_{ks}. \quad (3)$$

where $|v_k|$ is the number of active units in cluster k. Equation (3) states that the contribution of a unit (k, s) to the score of another unit connected to it is normalized by the number of active units in cluster k. That is, if the cluster k contains x active units, then the contribution of the unit (k, s) becomes $1/x$. So, by applying this rule to the network of Figure 2, unit h gets a score of 3 and unit a gets a score of $3\frac{1}{3}$ which is a result that privileges the activation of the latter unit and thus solves the Sum-of-Sum rule problem.

C. *The Sum-of-Max Rule (SoM)*

According to the Sum-of-Max rule, the score of a unit (i, j) is the number of clusters in which there is at least one active unit (k, s) connected to (i, j) plus the memory effect γ if (i, j) is active:

$$\lambda_{ij} = \gamma v_{ij} + \sum_{k=1}^{\chi} \max_{1 \le s \le l} \left(w_{(i,j)(k,s)} v_{ks} \right). \quad (4)$$

So referring back to Figure 2, and according to (4), unit a has a score of 4 whereas unit h has a score of 3. This is a more satisfying result than the one obtained by the Sum-of-Sum rule since it indicates that the latter unit, although connected to more active units, is less likely to belong to a bigger clique within the set of active units than unit a.

Moreover, it has been shown in [*15*] that for the particular case, when $c = \chi$, the Sum-of-Max rule guarantees that the retrieved massage is always either correct or ambiguous but not wrong. An ambiguous output message means that in some clusters more than one unit might be activated among which one is the correct unit.

VI. ACTIVATION RULES

The activation rule is applied for electing the units to be activated based on their scores after the application of a dynamic rule. So basically, a unit (i, j) is activated if its score λ_{ij} satisfies two conditions:

- λ_{ij} is greater or equal than a global threshold that may be chosen differently for each activation rule.
- $\lambda_{ij} \ge \sigma_{ij}$ where σ_{ij} is the activation threshold proper to unit (i, j). [*16*]

The difference between the two thresholds defined above is that σ_{ij} could be set differently for each unit, so it can be used to control a unit's sensitivity to activation. For a very large value of σ_{ij}, (i, j) is inhibited. This is helpful for excluding a group of units from the search of a certain message in order to save time. The global threshold has a unique value independent of any individual unit. So it is used to elect units to be activated in a competitive activation process. For example, in a winner-take-all competitive process, this threshold could be dynamically set to the value of the highest score in the network in order to activate only units with the highest score.

The activation rule should be able to find two unknowns: The subset of clusters to which the message we are trying to recover belongs, and the exact units within these clusters representing the submessages. Two activation rules are introduced in this paper: the Global Winners Take All rule (GWsTA) which is a generalization of the Global Winner Take All (GWTA) rule, and an enhanced version of the Global Losers Kicked Out (GLsKO) rule initially presented in [*17*] .

A. *The GWsTA Rule*

The GWTA rule introduced in [*6*] activates only units with the network-wide maximal score. The problem with this rule is that it supposes that units belonging to the message we are looking for have equal scores. It also supposes that this unified score is maximal which is not necessarily the case. It has been shown in [*6*] that spurious cliques, i.e., cliques that share one or more edges with the clique we are searching, might appear and render the scores of the shared units of the searched clique higher than others'.

For example, in the network of Figure 2, if the searched clique is $abdg$, then bdh is an example of a spurious one. Now, by applying the Sum-of-Max rule on the black units which are supposed to be active, and considering $\gamma = 1$, we get the scores: $\lambda_a = 4,\ \lambda_b = 5,\ \lambda_d = 5,\ \lambda_e = 4,\ \lambda_f = 4,\ \lambda_g = 4,\ \lambda_h = 3.$ Thus, according to the GWTA rule, only units b and d will be kept active and the clique $abdg$ is lost. This is caused by the spurious clique bdh which increases the scores of b and d.
The generalization of the GWTA rule we propose is meant to account for this problem.

The behavior of the Global Winners Take All rule is the same in both phases of the retrieval process. It elects a subset of units with maximal and near-maximal scores to be activated. In other words, it defines a global threshold θ at each iteration, and only units that have at least this threshold are activated.

In order to calculate this threshold at a given iteration, we first fix an integer parameter α. Then we make a list compromising the α highest scores in the network including scores that appear more than once. For example, if the units scores in a network with a total number of units $n = 10$ are

 ISBN: 978-1-61208-340-7

$\{25, 18, 25, 23, 23, 19, 18, 19, 18,17\}$ and $\alpha = 7$, then our list becomes $\{25, 25, 23, 23, 19, 19, 18\}$. The minimum score in this list which is 18 becomes the threshold θ. Then we apply the equation:

$$\forall i \text{ and } j, 1 \le i \le \chi, 1 \le j \le l: \quad v_{ij} = \begin{cases} 1, & \lambda_{ij} \ge \theta \text{ and } \theta \ge \sigma_{ij} \\ 0, & \text{otherwise} \end{cases} \tag{5}$$

It is worth noting that this activation rule is equivalent to the retrieval rule proposed by Willshaw [*2*] in that units are activated by comparing their scores to a fixed threshold θ.

One problem with this rule is that the choice of an optimal α for a certain message size would not be adapted for other message sizes. This limits the possibility of using this rule for retrieving messages of variable sizes. Moreover, this rule always activates a subset of units with maximal and near-maximal scores. But in some cases, when the number of stored messages reaches a high level, the units with the near-maximal score do not necessarily belong to the searched message.

B. *The GLsKO Rule*

As we have seen, The GWsTA rule needs a prior knowledge of the value of the message size c in order to retrieve a message. This means that if c is not available at retrieval, the rule may not be able to correctly retrieve information. The Global Losers Kicked Out (GLsKO) rule is designed to address this problem by being independent of any prior information about c which should also enable it to retrieve variable-sized messages more efficiently than the GWsTA rule. In order to achieve this, the GLsKO rule has a behavior in *phase 1* of the retrieval process that differs from that of *phase 2* as follows:

Phase 1:
Apply the GWTA rule.
Phase 2:
Kick losers out.

In *phase 1*, the GWTA rule is applied resulting in the activation of a subset of units to which the searched message is guaranteed to belong. After this, the activation thresholds of inactive units are set to infinity because we are no more interested in searching outside the already activated units.

In *phase 2*, the rule changes behavior, so, at each iteration, it makes a list compromising the β lowest nonzero scores of the active units only. For example, if the set $\{25, 18, 25, 23, 23, 19, 18, 19, 17,17\}$ represents the scores of active units in a network with a total number of units $n = 10$ and we fix $\beta = 3$, then the list of lowest scores becomes {18,19,18,19,17,17}. After that, a threshold θ equal to the maximum score in the latter list is set, and only units with scores greater than θ are kept active. This can be described by the following equation:

$$\forall i \text{ and } j, 1 \le i \le \chi, 1 \le j \le l: \quad v_{ij} = \begin{cases} 1, & \lambda_{ij} > \theta \text{ and } \theta \ge \sigma_{ij} \\ 0 \text{ and } \sigma_{ij} \to \infty, & \text{otherwise} \end{cases} \tag{6}$$

The reason why σ_{ij} is set to an infinitely large value is that after the first phase of the algorithm, a subset of units is activated. The clique corresponding to the message we are looking for is guaranteed to exist in this subset given that we are dealing with partially erased messages. So, setting σ_{ij} in this fashion ensures that units that have failed to be active upon the first phase would be out of the search scope throughout the retrieval process.

We propose to enhance the performance of the GLsKO rule by controlling the number of units μ to be deactivated. This is only interesting when $\beta = 1$. For example, if we set $\beta = 1$ in the network example of the previous paragraph, we get the following list of scores {17,17}. If μ is not specified, all losers are deactivated. But by setting $\mu = 1$, only one of these two units is randomly chosen to be deactivated. This may be useful if we wish to exclude losers one at a time and thus reduce incautious quick decisions.

VII. STOPPING CRITERIA

Since the retrieval process is iterative, a stopping criterion should be used in order to put this process to an end. In parts *A* and *B* of this section we review the two classic criteria that are already in use. In parts *C* and *D*, we propose two new ones that are supposed to enhance performance.

A. *A Fixed Number of Iterations (Iter)*

A stopping criterion can be defined as a predefined number of iterations of the retrieval process. So dynamic and activation rules are applied iteratively, and when a counter announces that the desired number of iterations is attained, the retrieval process terminates and the activated units are taken for the retrieved message. The problem with this approach is that the stopping criterion which is a simple iteration counter is independent of the nature of retrieved message. That is, the activated units after the last iteration are not guaranteed to form a clique corresponding to an already stored message. This stopping criterion is only interesting with the GWsTA rule.

B. *The Convergence Criterion (Conv)*

This criterion states that if the set of active units at iteration $t + 1$ is the same as that of iteration t, the retrieval process is taken as converged so it terminates and the result is output. The convergence criterion is only compatible with the GWsTA rule. In the case of the GLsKO rule, one or more active units are deactivated in each iteration. So it is not possible to have the same set of active units throughout two subsequent iterations.

C. *The Equal Scores Criterion (EqSc)*

The idea we propose here is that when all scores of active units are equal, the retrieval process terminates and the result is output.

D. *The Clique Criterion (Clq)*

This new criterion depends on the relationship between the number of activated units and their scores. If the activate units form a clique the retrieval process terminates. Thus, the retrieved message is more likely to make sense though it is not necessarily the correct result. In order to check if the activated units form a clique, we define the set of active units as $\{a_i \mid i = 1,2, \dots, |A|\}$, $\lambda(a_i)$ as the score of the active unit a_i and ρ as an integer, then we apply the procedure shown in Figure 3:

$\forall\, 1 \le i, j \le |A|$.
If
  $\lambda(a_i) = \lambda(a_j) = \rho$ and $|A| = \rho - (\gamma - 1)$.
Then
  output the result.
terminate the retrieval process.

Figure 3. The Clique stopping criterion (Clq).

To make sense of this stopping criterion, we take an intuitive situation when $\gamma = 1$. In this case, the stopping criterion is that when all active units have an equal score which is equal to the number of these units, a clique is recognized, so the process terminates and the result is output.

It is worth noting that when using the GWsTA rule, it is always preferable to combine any stopping criterion with the Iter criterion so that when any one of them is satisfied the process terminates which prevents infinite looping.

VIII. RESULTS

We have seen that there are many possible combinations of dynamic, activation rules and stopping criteria in order to construct a retrieval algorithm. In this section we will demonstrate the performance of some of these combinations. All messages used for the following tests are randomly generated from a uniform distribution over all possible message values. Reported retrieval error rates for a given number of stored messages are averaged over 100 trials. However, no significant difference was found between average error rates and error rates resulting from single trials. All the tests were written in C++, compiled with g++ and executed on a Fedora Linux operating system.

A. *Comparing Dynamic Rules*

Figure 4 shows that both the SoM and the SoS dynamic rules give a similar performance. The Norm rule was found to give the same results also, but it is not shown in the figure for clarity. This is not the case with the original network introduced in [*4*] where the Sum-of-Max rule was proved to give better results [*15*]. This is an interesting phenomenon that is worth studying. It may indicate that the major source of retrieval errors in this sparse version of the network is not related to the different methods of calculating units' scores. This renders the differences in performance due to the use of different dynamic rules insignificant.

B. *Comparing Retrieval Strategies*

We notice in Figure 5 that the GWsTA ($\alpha = 12$) rule gives a better performance than the GWTA (equivalent to GWsTA with $\alpha = 1$) rule used with the Conv stopping criterion with 30 iterations allowed at most. This is due to the fact that the former rule has a better immunity to the phenomenon of spurious cliques described in Section VI.A. We also notice that the GWsTA ($\alpha = 12$) rule gives even a lower error rate when the memory effect γ is set to a large value such as 1000. This is because

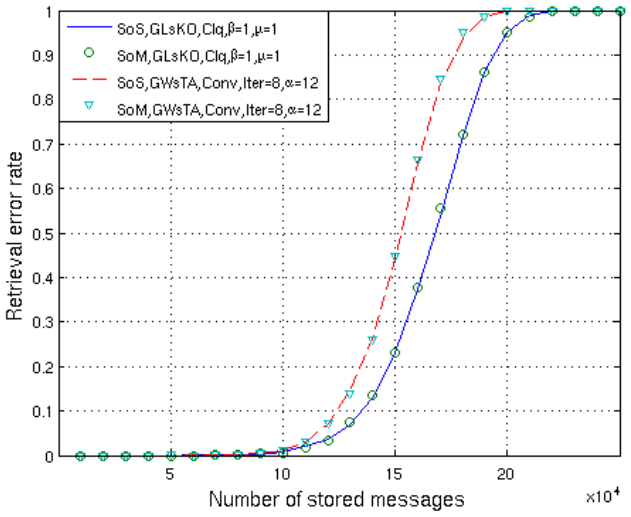

Figure 4. Influence of dynamic rules on retrieval error rates in a network with $\chi = 100, l = 64, c = 12, \gamma = 1, \sigma_{ij} = 0$ initially, with 3 segments of partial erasure in input messages.

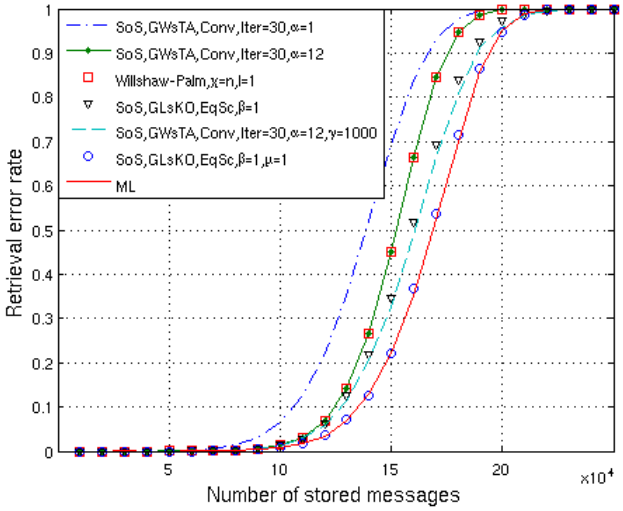

Figure 5. Influence of activation rules on retrieval error rates in a network with $\chi = 100$, $l = 64$, $c = 12$, $\gamma = 1$ if not stated otherwise, $\sigma_{ij} = 0$ initially, with 3 segments of partial erasure in input messages.

setting γ to a very large value restrains the search to only a limited region of the network where the target message is thought to exist. This is due to the fact that a large value of γ guarantees that active units always get higher scores than other ones. So, in subsequent iterations, the set of active units would most often be the same or a subset of the previous active set. In all cases, the GLsKO ($\alpha = 1$, $\mu = 1$) rule using the EqSc or the Clq (not shown on the figure for clarity) stopping criterion has the lowest error rate which almost achieves the performance of the brute force Maximum Likelihood retrieval algorithm (ML) (which is a simple exhaustive search for a maximum clique) for 3 erased input submessages out 12. This is because the GLsKO rule configured with such parameter values searches for the output in a limited subset of units resulting from *phase 1* and excludes only one unit at a time before testing for the stopping criterion. This is proved by the degraded performance shown in Figure 6 of this same rule but without specifying a value of μ which results in the exclusion of more than one unit at a time rendering the retrieval process less prudent and more susceptible to bad exclusions.

We also notice that when a Willshaw-Palm network with $n = 6400$ units is used with the GWsTA ($\alpha = 12, \gamma = 1$) rule, the same performance as in a clustered network is obtained.

C. *The Number of Iterations*

Figure 6 shows that the average number of iterations required to retrieve a message is relatively constant for all rules up to 140000 messages learnt. Beyond this, the number of iterations required for the GLsKO and the GWsTA rules with $\gamma = 1$ begins to increase rapidly. It is worth emphasizing that the maximum number of iterations we allowed for the GWsTA rule is 30 so the constant level reached by the curve representing this rule with $\gamma = 1$ in Figure 6 is just a result of that constraint. However, the number of iterations for the GWsTA rule with $\gamma = 1000$ increases only slightly approaching an average of 3.3 up to 250000 messages stored.

The reason for this explosion of the number of iterations in the case of the GLsKO rule is that the number of units activated after the first phase increases with the number of stored messages. So more iterations would then be needed in order to exclude losers and thus shrink the set of active units. In the case of the GWsTA rule with $\gamma = 1$, all units in the network are concerned with the search for a message in each iteration. So when the number of stored messages increases, the connection density in the network gets higher and it then would be more likely that new winners appear in each iteration violating the Conv criterion.

 ISBN: 978-1-61208-340-7

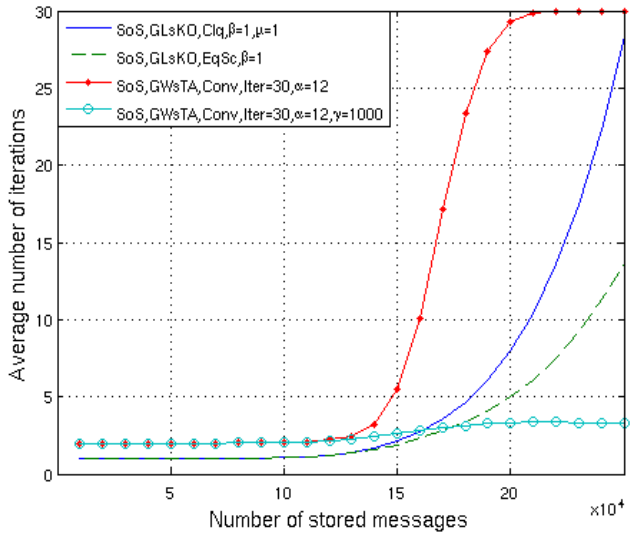

Figure 6. Average number of iterations for different scenarios in a network with $\chi = 100, l = 64, c = 12,$ $\gamma = 1$ if not stated wise, $\sigma_{ij} = 0$ initially, with 3 segments of partial erasure in input messages.

Setting γ to 1000 limits the possibility of the apparition of new winners in each iteration and consequently decreases the number of iterations needed before satisfying the Conv criterion.

IX. Conclusion and Future Work

In this paper, we analyzed the performance of retrieval algorithms on extensions of a recently proposed sparse associative memory model. We demonstrated and compared the performance of these algorithms when using partially erased messages as inputs. We also provided comparisons between the model proposed in this paper and the Willshaw-Palm model where we proved that the clustering constraint applied to the model we use which decreases the number of available connections does not necessarily affect performance when comparing with the Willshaw-Palm model.

We found that our modified version of the GLsKO activation rule combined with the equal scores or the clique stopping criteria gives the best results in terms of retrieval error rate but with a rapidly increasing number of iterations. Actually, the second phase of the GLsKO rule along with the clique criterion can be viewed as an operation equivalent to searching the maximum clique among active units. This is a famous NP-complete problem. However, many suboptimal solutions were suggested for this problem (or equivalently, the minimum vertex cover problem) such as [*18*] [*19*] and many more. We believe that such suboptimal solutions are adaptable to our problem and can be integrated in our retrieval algorithm in the future in order to give a better performance with a more reasonable number of iterations.

Finally, the retrieval algorithms presented in this work are all synchronous in the sense that, at each iteration, dynamic and activation rules are always applied to all clusters. In future work, we will consider asynchronous methods which can take into account the fact that some clusters may reach their final state before others, so application of dynamic and activation rules could then be limited to only a subset of clusters. We also aim at extending the scope of the algorithms presented in this paper to deal with other types of input messages, such as distorted ones in which some submessages have slightly modified values from their origin.

Acknowledgment

The authors would like to thank Zhe Yao and Michael Rabbat at McGill University for interesting discussions that helped leading to the proposal of the new retrieval techniques introduced in this paper. We also acknowledge funding from the NEUCOD project at the electronics department of Télécom Bretagne and support from the European Research Council (ERC-AdG2011 290901 NEUCOD).

References

[1] J. R. Anderson and G. H. Bower, Human associative memory.: Psychology press, 2013.

[2] D. J. Willshaw, O. P. Buneman, and H. C. Longuet-Higgins, "Non-holographic associative memory," Nature, vol. 222, pp. 960-962, 1969.

[3] J.J. Hopfield, "Neural networks and physical systems with emergent collective computational abilities," in Proceedings of the National Academy of Science, USA, vol. 79, 1982, pp. 2554-2558.

[4] V. Gripon and C. Berrou, "Sparse neural networks with large learning diversity," IEEE Transactions on Neural Networks, vol. 22, no. 7, pp. 1087-1096, 2011.

[5] V. Gripon and M. Rabbat, "Maximum Likelihood Associative Memories," in Proceedings of the IEEE Information Theory Workshop (ITW), 2013, pp. 1-5.

[6] B. K. Aliabadi, C. Berrou, V. Gripon, and X. Jiang, "Learning sparse messages in networks of neural cliques," IEEE Transactions on Neural Networks and Learning Systems, August 2012, in press.

[7] G. Palm, "Neural associative memories and sparse coding," Neural Networks., vol. 37, pp. 165-171, 2013.

[8] V. B. Mountcastle, "The columnar organization of the neocortex," Brain, vol. 120, no. 4, pp. 701-722, 1997.

[9] V. Gripon and X. Jiang, "Mémoires associatives pour observations floues," in Proceedings of XXIV-th Gretsi seminar, September 2013, in press.

[10] D. P. Buxhoeveden and M. F. Casanova, "The minicolumn hypothesis in neuroscience," Brain, vol. 125, no. 5, pp. 935-951, 2002.

[11] F. T. Sommer and G. Palm, "Improved bidirectional retrieval of sparse patterns stored by Hebbian learning," Neural Networks, vol. 12, no. 2, pp. 281-297, 1999.

[12] F. Schwenker, F. T. Sommer, and G. Palm, "Iterative retrieval of sparsely coded associative memory patterns," Neural Networks, vol. 9, no. 3, pp. 445-455, 1996.

[13] L. Cruz et al., "A statistically based density map method for identification and quantification of regional differences in microcolumnarity in the monkey brain," Journal of Neuroscience Methods, vol. 141, pp. 321-332, 2005.

[14] E. G. Jones, "Microcolumns in the cerebral cortex," PNAS, vol. 97, no. 10, pp. 5019-5021, 2000.

[15] V. Gripon and C. Berrou, "Nearly-optimal associative memories based on distributed constant weight codes," in Proceedings of Information Theory and Applications Workshop, USA, 2012, pp. 269-273.

[16] W. S. McCulloch and W. Pitts, "A logical calculus of the ideas immanent in nervous activity," The Bulletin of Mathematical Biophysics, vol. 5, no. 4, pp. 115-133, 1943.

[17] X. Jiang, V. Gripon, and C. Berrou, "Learning long sequences in binary neural networks," in The Fourth International Conference on Advanced Cognitive Technologies and Applications (COGNITIVE 2012)

 ISBN: 978-1-61208-340-7

IARIA, 2012, pp. 165-170.

[18] X. Xu and J. Ma, "An efficient simulated annealing algorithm for the minimum vertex cover problem," Neurocomputing, vol. 69, no. 7, pp. 913-916, 2006.

[19] X. Geng, J. Xu, J. Xiao, and L. Pan, "A simple simulated annealing algorithm for the maximum clique problem," Information Sciences, vol. 177, no. 22, pp. 5064-5071, 2007.

[20] Z. Yao, V. Gripon, and M. G. Rabbat, "A massively parallel associative memory based on sparse neural networks," Submitted to IEEE Transactions on Neural Networks and Learning Systems, arXiv:1303.7032v1 [cs.AI].

 ISBN: 978-1-61208-340-7

Cognitive Linguistic Representation of Legal Events

Towards a semantic-based legal information retrieval

Anderson Bertoldi, Rove Chishman, Sandro José Rigo, Thaís Domênica Minghelli
Universidade do Vale do Rio dos Sinos (UNISINOS)
São Leopoldo, Brazil
andersonbertoldi@yahoo.com, rove@unisinos.br, rigo@unisinos.br, thaisdomenica@hotmail.com

***Abstract*—An important role of an attorney in Brazil is to search Brazilian courts databases in order to find precedent decisions to base their requests on. This paper discusses the initial efforts that have been made towards the development of a legal knowledge base, composed by semantic frames, to improve Brazilian courts information retrieval systems. Linguistic methods are applied to recognize possible legal event structures to be described in legal documents. Afterwards, based on the linguistic theory of Frame Semantics, the participants and props of legal events are described. This is a work in progress that will involve both legal and linguistic description as well as system development. With this legal knowledge base, the results expected are the improvement of the legal information retrieval system of Brazilian courts databases, using semantic representation of Brazilian legal events.**

Keywords-knowledge representation; semantic modeling; semantic frames; legal information retrieval.

I. INTRODUCTION

This paper presents a project in progress whose aim is to represent legal knowledge to replicate the possible cognitive connections that a law specialist makes in the moment he/she is analyzing a legal document. This project applies the Frame Semantics theory [1][2] for the semantic modeling of legal events. Legal events are represented as semantic frames and relations among these semantic frames are established in order to reproduce the connections of knowledge that specialists have to make to understand legal documents.

In Brazil, usually, before filing a lawsuit, attorneys search the online databases of Brazilian courts for similar cases. In this search they look for precedent decisions to decide whether a lawsuit has chance to be accepted for the judge and to base the request that originates the suit. Despite the efforts to improve their Information Retrieval (IR) systems, Brazilian court databases still do not work with semantic annotation of their documents, which could improve the search results. As a consequence, lawyers, when looking for precedent decisions, have to deal with a huge amount of documents. The proposal of this project is to develop a knowledge base composed by semantic frames describing the legal knowledge related to legal terms/words. These resources will be used to annotate a legal corpus aimed to be applied together with an automatic corpus annotation tool.

To discuss this topic, this paper is structured as follows. Section II presents the problem that motivates this research. As IR systems of Brazilian courts return a huge amount of documents, lawyers spend too much time reading documents to separate meaningful to non-meaningful documents. Section III presents the solution proposed in this project. Using linguistic methods to describe the meaning of the legal terms/words, this project expects to develop a set of semantic tags for legal text annotation. Section IV discusses the expected results as well as the steps that have to be accomplished in order to build a semantic-based legal information retrieval system. Section V presents the related work in which this research is based on. Section VI discusses the possible contributions of this work with respect to legal information retrieval system of Brazilian courts and with respect to the previous work in the areas of Frame Semantics and legal information retrieval.

II. THE PROBLEM

When specialists search the online databases of Brazilian courts, such as the State Court of Appeal [3] or the Federal Court of Appeal [4], looking for precedent decisions to base the lawsuit request on, they need to provide a combination of words to get better results. Let us consider, for example, an attorney who is working on a divorce case. He needs to make a request of child support and, therefore, he looks for the jurisprudence of the State Court of Appeal. He will need to provide to the IR system a combination of words, such as *alimentos* (*food*) and *divórcio* (*divorce*) or *alimentos* (*food*) and *pensão* (*alimony*).

This example demonstrates that the IR systems of the Brazilian courts search their databases by string patterns, not by the meaning of the legal terms/words. The search result is a huge amount of legal documents stored in the court database. The specialist has to spend a considerable part of his/her time just reading documents that were returned to find which documents are really meaningful for his/her intents.

The assumption explored in this project is that describing the meaning of the legal terms/words and establishing relations among these terms, with the support of FrameNet [5] formalism, the result will be a knowledge base that can provide valuable resource to the IR system improvements in order to return better results. The framework to implement and use this knowledge base comprises the development of additional components that expand both the documents

 ISBN: 978-1-61208-340-7

indexing and the term searching operations of the existing IR systems.

III. THE SOLUTION PROPOSED

The solution proposed by this project is to build a knowledge base describing the meaning of the legal terms/words through semantic frames. The theory concerned about semantic frames is called 'Frame Semantics' and was proposed by the linguist Charles Fillmore, inspired by the previous work of Marvin Minsky [6].

A semantic frame is a schematic structure which describes the role of the participants and props of an event or state [1]. This schematic structure is evoked by lexical units. According to Frame Semantics, lexical units work like a trigger that makes the speaker retrieve in his/her mind related concepts that help to understand the meaning of a certain concept. For instance, in order to understand the meaning of 'buying' the speaker needs to understand the meaning of 'selling'. The lexical units 'buy' and 'sell' evoke a frame of commercial transaction. To understand the concept of commercial transaction, speakers must understand concepts that are related to a commercial transaction, such as 'seller', 'buyer', 'goods', and 'money'.

The proposal presented here is to develop legal semantic frames based on the study of legal documents and to describe the meaning of legal lexical units relating lexical units to semantic frames. After storing semantic frames and lexical units in a knowledge base, this knowledge base could be used as a component of a legal IR system, providing knowledge reasoning capability to IR systems.

The methodology adopted to develop legal semantic frames is majorly based in non-automatic linguistics methods. First, a collection of legal texts is compiled and, based on linguistic methods, the most relevant lexical units of the texts are described, relating them to a specific semantic frame. For instance, the lexical unit *acusação* (*charges*) evokes a semantic frame of 'Charging.' Fig. 1 shows an example of relations among semantic frames for Charging frame.

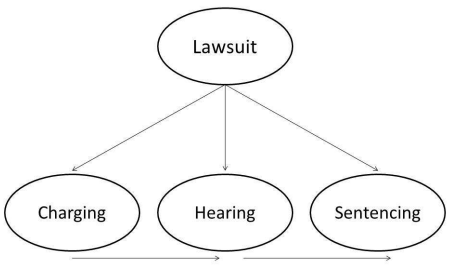

Figure 1. Relations among semantic frames.

Concepts related to Charging frame include the 'Prosecutor,' the authority in Brazilian legal system responsible for taking a suspect to the court, the 'Judge,' the authority responsible in the Brazilian legal system for saying if the suspect can be suited or not, the 'Suspect,' the person that is suspect to have committed an infraction or a crime, and the 'Charges,' the infraction or the crime committed. Once the legal events are described as semantic frames, it is possible to establish relations among semantic frames, pointing which legal action comes first. In this moment, the project has had a moderate progress having described about ten legal frames related to the lawsuit process.

The Lawsuit frame has as participants and props 'Type of Action,' which indicates the type of lawsuit that was filled against a defendant (administrative, criminal, familiar), 'Author,' who is the person that goes to the court with a request, 'Defendant,' who is the person that is been suited, and 'Concrete case,' which is the legal base that gives the author the right to make a legal request. Fig. 2 shows a schematic representation of the Lawsuit frame.

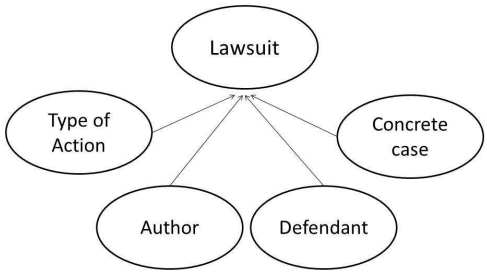

Figure 2. Participants and props of Lawsuit frame

After having developed a set of legal semantic tags organized by semantic frames, the project intends to annotate legal texts to develop a learning corpus. The assumption is that if the legal databases of the Brazilian legal courts present a more fine-grained semantic annotation, the IR system could be able to return documents related closely to the topic that the specialist needs when he searches court databases for precedent decisions. Fig. 3 shows an example of semantically annotated sentences of legal documents.

Antonio Jair da Costa$_{[AUTHOR]}$ **ajuizou** ação$_{[TYPE\ OF\ ACTION]}$ contra o Instituto Nacional Do Seguro Social – INSS$_{[DEFENDANT]}$.

[*Antonio Jair da Costa filed a lawsuit against the National Institute of Social Security – INSS.*]

Figure 3. Example of annotated sentences

Fig. 3 shows an example of annotation based on semantic frame. The participants of the lawsuit are pointed with the

semantic tags AUTHOR and DEFENDANT. The tag TYPE_OF_ACTION indicates if the lawsuit is, for instance, criminal or civil.

What this project intends is to describe the knowledge that a specialist has about legal terms/words when he/she is reading a legal document. The representation of these legal events in a knowledge base, with the FrameNet [5] foundation could reproduce the cognitive connections that specialists make when they are reading a legal document. Once this database was developed, the semantic tags could be used for documents annotation, following others frame-based annotation projects [7][8][9].

This project has been developed by a multidisciplinary group, counting with linguists, lawyers, and computer science specialists. Despite all the steps described until this point being manually-based, further steps will include the knowledge base implementation, the manual annotation of legal corpora, the development of an automatic document annotation tool, and the integration of the knowledge base to the IR system of the Brazilian court.

The automatic document annotation tool is aimed to allow improvements in the indexing process of the IR system. Since the semantic frames and the semantic tags being described allow an approach not syntactically based, but rather semantically based, it consists in the first step to include the results of the developed knowledge base in the IR system operation. Therefore, the expected outcome of this tool is the possibility of document indexing operations based on the semantic frames related to legal knowledge, which is a more precise approach than the word-based indexing traditionally observed in IR systems.

The integration of these resources with the IR system will be done through the implementation of semantic treatment modules to be applied together with the existing document indexing module and information retrieval module. In the first one, the improvements obtained are related to the use of semantic frames in the indexing process. In the second one, the outcomes are due to the change in the traditional search operations, shifting from word-based search operations to semantic-based operations.

IV. EXPECTED RESULTS

The target of this project is, first, to apply a linguistic theory to legal knowledge modeling and, second, to improve a practical implementation. This project expects to develop a semantic-based legal IR system to help specialist in searching legal documents in the online Brazilian court databases. An important step in this direction is to find a partner court that is willing to provide legal documents for this research project and to support the implementation of a frame-based IR system. Some negotiation process was started with The National Council of Justice (CNJ) [10] to provide the legal documents for this research project.

Considering the amount of manual work that will be needed to develop a legal frame-based knowledge database, the expectation is that in five years the linguistic and conceptual part of the project could be ready. Once the search in the legal database can be done by the content of the documents, the specialist will receive documents more related to the intents of their search, saving a precious time spent only to look for precedent decisions.

V. RELATED WORK

Since Frame Semantics [1][2] was proposed, a number of studies and applications were developed. The first project to apply the principles of Frame Semantics was FrameNet [5]. FrameNet is a computational lexicographic project that has been developing a lexical database describing the meaning of English lexical units relating them to semantic frames. After the development of FrameNet, many projects started to develop FrameNets for different languages. Here are just some examples: Japanese FrameNet [11], Spanish FrameNet [12], German FrameNet [13], Swedish FrameNet [14], and Brazilian FrameNet [15][16].

Another application of FrameNet is in semantic annotation. Gildea and Jurafsky propose an automatic method of using FrameNet semantic tags for automatic annotation [7]. Padó and Lapata suggest an automatic method to annotate multilingual corpora using FrameNet semantic tags [17][18]. The Salsa project opts for manual corpus annotation with semantic frames [8]. Other FrameNet applications include the use of frame-based lexicons for foreign language education [19] and sentiment analysis [20].

In the legal domain, Venturi [9] applies the FrameNet semantic tags to the annotation of legislative texts. According to Venturi's findings [9], despite being created from English lexicon, FrameNet semantic labels can be applied for semantic annotation of Italian legislative texts with no significant mismatches. In previous work [21][22], the authors point the necessity to develop a set of frames for Brazilian legal system. Differently from legislative texts, semantic frames and tags to annotate Brazilian court decision change significantly. This is the reason why this project suggests the development a set of semantic frames for Brazilian legal system.

VI. CONCLUSION AND FUTURE WORK

This paper was concerned to present a semantic-based information retrieval project. Only the linguistic part of the knowledge base development was addressed here. This project has been developed for a multidisciplinary research group integrated by linguists, lawyers and computer scientists. The legal knowledge database development requires a huge amount of lexicographic work to select the legal terms/words that will be described, as well as conceptual work to design semantic frames to represent the meaning of these terms/words.

The expected contribution of this work is to improve the legal information retrieval of court databases, optimizing the time specialists spend looking for meaningful documents on legal databases. Moreover, this work tries to find a solution for a practical problem using linguistic studies for knowledge representation. This project is an initiative towards a semantic-based information retrieval system, trying to meet the needs of the Brazilian society.

 ISBN: 978-1-61208-340-7

ACKNOWLEDGMENT

The authors acknowledge the financial support given by the Brazilian research support agencies CNPQ, CAPES and FAPERGS. The authors thank the valuable comments of the reviewers.

REFERENCES

[1] C. J. Fillmore, "Frame Semantics," in Linguistics in the Morning Calm, The Linguistic Society of Korea, Ed. Seoul: Hanshin, 1982, pp. 111-137.

[2] C. J. Fillmore, "Frames and the semantics of understandings," in Quaderni di Semantica, vol. 6, no. 2, 1985, pp. 222-254.

[3] Rio Grande do Sul State Court of Appeal/Tribunal de Justiça do Estado do Rio Grande do Sul. [Access: 2014, 03]. Available at: www.tjrs.jus.br.

[4] Regional Federal Court of Appeal/Tribunal Regional Federal da 4ª Região. [Access: 2014, 03]. Available at: www.trf4.gov.br.

[5] C. J. Fillmore, C. R. Jonhson, and M. R. L. Petruck, "Background to FrameNet," International Journal of Lexicography, vol. 16, no. 3, Sep. 2003, pp. 235-250.

[6] M. Minsky, "A framework for representing knowledge," Artificial Intelligence Meno no. 306, Cambridge: Massachusetts Institute of Technology, 1974.

[7] D. Gildea and D. Jurafsky, "Automatic labelling of semantic roles," Computational Linguistics, vol. 28, no. 3, Sep. 2002, pp. 245-288.

[8] A. Burchardt et al., "Using FrameNet for the semantic analysis of German: annotation, representation, and automation," in Multilingual FrameNets in computational lexicography: methods and applications, H. C. Boas, Ed., Berlin/New York: Mouton de Gruyter, pp. 209-244, 2009.

[9] G. Venturi, "Semantic annotation of Italian legal texts: a frame-based approach," Constructions and Frames, vol. 3, no. 1, 2011, pp. 46-79.

[10] Coselho Nacional de Justiça/National Council of Justice [Access: 2014, 03]. Available at: www.cnj.jus.br.

[11] K. H. Ohara, "Frame-based contrastive lexical semantics in Japanese FrameNet: the case of risk and kakeru," in Multilingual FrameNets in computational lexicography: methods and applications, H. C. Boas, Ed., Berlin/New York: Mouton de Gruyter, pp. 163-182, 2009.

[12] C. Subirats, "Spanish FrameNet: a frame-semantic analysis of the Spanish lexicon," in Multilingual FrameNets in computational lexicography: methods and applications, H. C. Boas, Ed., Berlin/New York: Mouton de Gruyter, pp. 136-162, 2009.

[13] H. C. Boas, "Semantic frames as interlingual representations for multilingual lexical databases," in International Journal of Lexicography, vol. 18, no. 4, Dec. 2005, pp. 445-478.

[14] L. Borin, M. Forsberg, and B. Lyngfelt, "Close Encounters of the fifth kind: some linguistic and computational aspects of the Swedish FrameNet ++ project," in Veredas, vol. 17, no. 1, 2013, pp. 28-43.

[15] M. M. M. Salomão, "FrameNet Brasil: a work in progress," in Calidoscópio, vol. 7, no. 3. Sep./Dec. 2009, pp. 171-182.

[16] T. T. Torrent and M. Ellsworth, "Behind the labels: criteria for defining analytical categories in FrameNet," in Veredas, vol. 17, no. 1, 2013, pp. 44-65.

[17] S. Padó and M. Lapata, "Cross-lingual projection of role-semantic information," in Proc. Of Human Language Technology Conference and Conference on Empirical Methods in Natural Language, Vancouver: Association for Computational Linguistics, 2005, pp. 859-866.

[18] S. Padó, Cross-lingual annotation projection models for role-semantic information. PhD Thesis. Saarbrücken: Universität des Saarlandes, 2007.

[19] H. C. Boas and R. Dux, "Semantic frames for foreign language education: towards a German frame-based online dictionary," in Veredas, vol. 17, no. 1, 2013, pp. 82-100.

[20] J. Ruppenhofer, "Extending FrameNet for sentiment analysis," in Veredas, vol. 17, no. 1, 2013, pp. 66-81.

[21] A. Bertoldi and R. Chishman, "Developing a frame-based lexicon for the Brazilian legal language," in Proc. Of International Workshop on Artifitial Intelligence Approaches to the Complexity of Legal Systems (AICOL-III), AI Approaches to the Complexity of Legal Systems – Models and Ethical Challenges for Legal Systems, Legal Language and Legal Ontologies, Argumentation and Software Agents, vol. 7639, Berlin/ Heidelberg: Springer-Verlag, 2012, pp. 256-270.

[22] A. Bertoldi and R. Chishman, "Applying Frame Semantics for the Description of the Brazilian Law." in Veredas, vol. 17, no. 1, 2013, pp. 117-133.

 ISBN: 978-1-61208-340-7

Automatic Classification of Cell Patterns for Triple Negative Breast Cancer Identification

Juan Luis Fernández-Martínez*, Ana Cernea*, Enrique J. deAndrés-Galiana*,
Primitiva Menéndez-Rodríguez†,
José A. Galván‡ and Carmen García-Pravia†
*Mathematics Department, Oviedo University,
Email: jlfm@uniovi.es, cerneadoina@uniovi.es, ej.deandres@gmail.com
†Hospital Universitario Central de Asturias, Oviedo
Email: tiva@hca.es, carmen.garciapravia@gmail.com
‡Institute of Pathology, University of Bern
Email: josegalvan6@hotmail.com

***Abstract*—This paper is devoted to presenting a methodology in Artificial Intelligence and Cognition for the optimization of basal cell patterns classification. Different unsupervised and supervised learning techniques are applied to the analysis, diagnosis and prognosis of cell patterns classification for Triple Negative Breast Cancers (TNBC), a group of cancers that, together with basal-like breast cancers, have a very bad prognosis. For that purpose, different machine learning algorithms are performed on histological images, and on a list of pathological and immunohistochemical variables currently used in medical practice. The main objective is to design a biomedical robot able to assist physicians with the kind of histological grade of different subgroups of TNBC samples in order to optimize the treatment protocol. The proposed methodology is performed on a database of 116 patients. The results show that pathological and immunohistochemical variables and histological images provide complementary information to improve the classification of TNBC samples.**

Keywords–Artificial Intelligence; Cognition; Cell Patterns; Triple Negative Breast Cancers (TNBC); Machine Learning.

I. INTRODUCTION

Breast cancer (or neoplasia) is a very heterogeneous disease. This term encompasses a variety of entities with distinct morphological features and clinical behaviors. For a long time, breast tumors have been classified according to their morphologic features (histologic type and grade) to ascertain prognostic outcome in patients. Subsequently, molecular markers (the expression of estrogen and progesterone receptor and human epidermal growth factor 2 receptor) were used to provide additional predictive power. Therefore, Triple Negative Breast Cancers (TNBC) refers to any breast cancer characterized by the absence of Estrogen Receptors (ER), Progesterone Receptors (PR) and Human Epidermal Growth Factor 2 Receptors (HER2). This classification is important from a clinical and therapeutic point of view, since TNBC are resistant to targeted therapies, because they do not express these receptors [13]. Statistics showed that TNBC account for approximately $15\% - 25\%$ of all breast cancer cases. Recently, a molecular classification based on gene expression profiles classified tumors into five groups that were not detected using traditional histopathologic methods. This classification includes the basal-like tumors group [17]. These tumors are defined by: (1) the lack of ER, PR, and HER2 expressions; (2) the expression of one or more high-molecular-weight/basal cytokeratins (CK5/6, CK14); (3) the lack of expression of ER and HER2 in conjunction with expression of CK5/6; and (4) the lack of expression of ER, PR, and HER2 in conjunction with expression of CK5/6. Also, from a morphological point of view both basal-like and triple negative breast cancers share a predominance of high histologic grades. The analysis of gene expression profiles showed that 77% of basal-like tumors were of TNBC phenotype [17].

The treatment for TNBC is adjuvant chemotherapy and radiotherapy. Unfortunately, response to chemotherapy does not correlate with overall survival. In addition, most recurrences are observed in TNBC during the first and third years after therapy, and most deaths take place in the first five years. The survival decreases after the first metastatic event. Therefore, in this heterogeneous group of tumors, new identification and classification techniques are necessary to establish a better diagnosis and prognosis, and to outline appropriate therapies. [6].

The main objective of this research is to design a biomedical robot able to help physicians with the diagnosis of different subgroups of TNBC in order to optimize their treatment protocol. The first aim of this research is to analyze the possibility of performing an automatic histological grade prediction using different biometric attributes of TNBC images and also a list of currently-used pathological and immunohistochemical variables. The methodology used in this paper is inspired by previous research works [7][8]. The preliminary conclusion of this study is that the use of both pieces of information (immunohistochemical markers and histological images) might improve the accuracy of TNBC histological grades classification and survival.

The structure of this paper is as follows: Section II describes the database of histological images and pathological, clinical and immunohistochemical variables; Sections III and IV describe the machine learning methods used in both cases. Section V presents the histological image attributes, and finally, Section VI draws the conclusion and future research work.

 ISBN: 978-1-61208-340-7

II. DATABASE DESCRIPTION

A. Histological Images

A cohort of 105 Caucasians women diagnosed in the Hospital Universitario Central de Asturias (Spain) with TNBC and ages between 30 and 94 years were enrolled in this study, which was developed in accordance with the last version of the Helsinki Declaration of 1975 [21]. Tumor samples were obtained from surgical resection. They were fixed in 10% formaldehyde and paraffin embedded, then cut $4\mu m$ thick, mounted on treated slides, and stained with H&E stain (Hematoxylin and eosin stain). Finally, the sections were studied and photographed at two different resolutions (100X and 400X) using an Olympus light microscope. Most of the cancers in this cohort were classified in histological degrees 2 (20 samples) and 3 (89 samples), and only two samples were in degree 1. Also, a few samples have a histological degree, which is unknown. This methodology will be used in the future to asses the histological grade of the TNBC samples, and to analyze the possibility of predicting the patients survival.

B. Pathological and Clinical Variables

The pathological and clinical variables description is important to understand the different classification problems involved in this analysis, and the way the histological grade of the TNBC is established in medical practice. The Nottingham Histologic Score system (the Elston-Ellis modification of Scarff-Bloom-Richardson grading system [2], [5]) has been applied to establish the histological grades of the TNBC cancers. This system is based on the ability of the tumor to form structures similar to the ducts where the tumor has originated, on the similarity between the cancer cells and the original benign cells and finally on its proliferative activity. The histological grade will be used as the class for the different machine learning classification problems presented in this paper.

In order to assign the grade score, several factors are taken into account: **(1) Tubular structure formation**: the score increases with the percentage of tumor area forming glandular/tubular structures, as follows: score 1: $> 75\%$ of tumor area forming glandular/tubular structures; score 2: 10% to 75% of tumor area forming glandular/tubular structures; score 3: $< 10\%$ of tumor area forming glandular/tubular **(2) Nuclear pleomorphism**: the score increases with variation of size and shape of cells, as follows: score 1: Small nuclei with little increase in size in comparison with normal breast epithelial cells, regular outlines, uniform nuclear chromatin, little variation in size; score 2: Cells larger than normal with open vesicular nuclei, visible nucleoli, and moderate variability in both size and shape; score 3: Cells with vesicular nuclei, often with prominent nucleoli, exhibiting marked variation in size and shape. **(3) Mitotic rate**: The mitotic count score depends on the field diameter of the microscope used by the pathologist. The pathologist will count how many mitotic figures are seen in 10 high power fields. Using a high power field diameter of 0.50 mm, the criteria are as follows: score 1: less than or equal to 7 mitoses per 10 high power fields; score 2: 8-14 mitoses per 10 high power fields; score 3: equal to or greater than 15 mitoses per 10 high power fields.

The final total score is used to determine the histological grade of a TNBC sample, as follows:

- Histological grade 1: tumors with a total score between 3 and 5;
- Histological grade 2: tumors with a total score between 6 and 7;
- Histological grade 3: tumors with a total score between 8 and 9.

In the present case, most TNBC samples were classified with grades 2 (20 samples) and mainly 3 (89 samples). Higher scores are usually correlated with the worse prognostic.

Other currently used variables include: **(1) TNM stage**: The pathologic stage of breast cancer takes into consideration the tumor size (T) and the presence of any lymph nodes metastases (N) or distant organ metastases (M). **(2) Differentiation**: it is a combined measure of the tubular formation and the pleomorphism. It is a descriptor provided by the medical experts based on visual inspection of the histological images. This histological variable is expected to be highly correlated in medical practice to the histological grade of the different TNBC samples. **(4) Vascular and perineural invasion**: binary variable indicating the presence or absence of tumor cells inside the vessels and nerves, respectively. **(5) Necrosis**: binary variable indicating the presence of death cells. This variable is correlated with the TNBC aggressiveness. **(6) In situ component**: binary variable indicating the absence of invasion of tumor cells into the surrounding tissue. Most of these variables are provided by the pathologist by visual inspection of the TNBC images.

C. Immunohistochemical variables

The following immunohistochemical variables are also currently monitored: **(1) Estrogen receptors** (ER), Progesterone receptors (PR) and Androgen receptors (AR) nuclear expression: Hormone receptor status is important because these variables serve to decide whether the cancer is likely to respond to hormonal therapy or other treatments. **(2) Human epidermal growth factor receptor 2** (HER-2): HER2 testing is performed to assess prognosis and to determine suitability for trastuzumab therapy. **(3) Ki67 expression**: The percentage of Ki-67 ($< 2\%$, $2 - 20\%$ and $> 20\%$) can be used to aid in assessing the proliferative activity of normal and neoplastic tissue. **(4) Bcl-2 expression**: Bcl-2 is specifically considered as an important anti-apoptotic protein and classified as an oncogene. Bcl-2 expression is associated with a better prognosis [4]. **(5) E-cadherin expression**: Reduction or loss of E-cadherin expression is associated with invasive carcinoma and possibly metastasis in a variety of carcinomas [16]. **(6) P53 expression:** is also a maker used in breast cancer, but its significance in predicting clinical outcome remains controversial. **(7) CK-5/6** and **CK-14 expression**: are helpful markers in the identification of breast cancer with a basal phenotype. **(8) COL11A1**: is a stromal marker of invasion [10].

All these variables but COL11A1 have been described in the literature as useful for TNBC description.

It is important to note that the histological grade estimation of the TNBC samples is established in medical practice as it

 ISBN: 978-1-61208-340-7

has been shown in this section, using the pathological, clinical and immunohistochemical variables that are measured for each patient, and also by visual inspection of the histological images after surgical resection. Therefore, and up to our knowledge, no biomedical robot exists to automatize these approaches, to integrate both types of information, and to assist physicians with the diagnostic. This decision has very important consequences on the prescribed treatment for the patient.

III. MACHINE LEARNING USING PATHOLOGICAL AND IMMUNOHISTOCHEMICAL VARIABLES

The aim of this section is to analyze the most discriminatory pathological and immunohistochemical variables of the histological grade. Data preprocessing includes in this case the imputation of the clinical variables that have not been measured for some patients in real practice and the normalization of these variables in the interval $[0, 1]$ according to their own empirical cumulative distribution. The imputation algorithm that is used is based on the nearest neighbor estimator. Its workflow is as follows: (1) Finding the subset S_{fi} of samples (patients) that are fully-informed for all the control variables. (2) For each patient k that is not fully-informed, finding the set of variables $\mathbf{m}_k(var_1 : var_q)$ that are missed. These variables are interpolated using the values of the same variables corresponding to the nearest fully-informed patient f_k in S_{fi}:

$$\mathbf{m}_k^*(var_1 : var_q) = \mathbf{m}_{f_k}(var_1 : var_q). \quad (1)$$

In order to measure the similarity between patients we use the cosine criterion induced by the Euclidean scalar product defined over the set of fully-informed variables in the current sample (patient):

$$cos(\mathbf{m}_k, \mathbf{m}_j) = \frac{\mathbf{m}_k \cdot \mathbf{m}_j}{\|\mathbf{m}_k\|_2 \|\mathbf{m}_j\|_2}, \quad (2)$$

where $\mathbf{m}_k$ and $\mathbf{m}_j$ stand for the vectors of fully-informed variables in patients k and j. Once the variables are imputed, the normalization of variable $\mathbf{var_j}$ is based on the p-percentile concept: $P(\mathbf{var_j} \leq c_p) = p$, by assigning the probability p to the value c_p of the attribute $\mathbf{var_j}$. Figure 1 shows the normalized pathological and immunohistochemical variables. The samples are arranged by their histological grades (2 to 3) beginning by the top of the image. It can be observed the high variability of these variables within the different classes (histological grades).

To perform machine learning, we have first used feature selection methods to finding the minimum-size list of most discriminatory variables. For that purpose, we defined the Generalized Fisher's ratio of the attribute j, for a binary classification problem, as follows [9]:

$$FR_j = \frac{(\mu_{j1} - \mu_{j2})^2}{\sigma_{j1}^2 + \sigma_{j2}^2}, \quad (3)$$

where is μ_{j1} a measure of the center of the distribution of the attribute j in class i, and σ_{ji} is a measure of its dispersion within the class i. The Fisher's ratio (GFR) can be also generalized for multiclass classification as follows:

$$GFR_j = \sum_{i=1}^{N_c} \sum_{k=i+1}^{N_c} \frac{(\mu_{ji} - \mu_{jk})^2}{\sigma_{ji}^2 + \sigma_{jk}^2}, \quad (4)$$

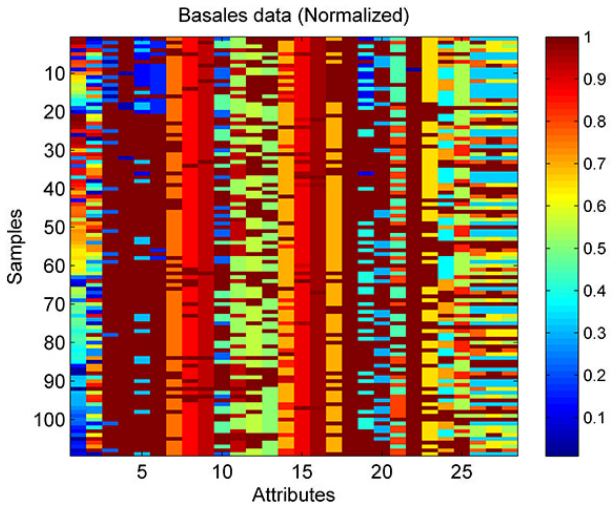

Figure 1. Normalized pathological and immunohistochemical array. The samples are ordered by their histological grade (first 20 samples with degree 2, followed by 89 samples with histological degree 3.

where N_c is the number of classes, j is the attribute index and i, k the classes indices. This feature selection method looks for attributes that are homogenous within each class (low intra-class dispersion) and show a high separation between the center of the corresponding distributions (inter-class distance). Most discriminatory attributes correspond to higher Fisher's ratios. The algorithm to find the minimum-size list of features is based on Recursive Feature Elimination, that is:

1) Attributes are ranked by the decreasing value of their Fisher's ratio.
2) Beginning by the tail of the list we calculate the accuracy of the different set of attributes, that are formed by dropping one attribute at each time. The set with the optimum accuracy and minimum size is therefore selected.
3) Finally, the accuracy of this reduced set of the attributes in the class prediction is based on Leave-One-Out method, using the average distance on the reduced set of attributes. The class with the minimum distance is assigned to the sample test. The average accuracy is calculated by iterating over all the samples.

The classification problem is linearly separable when this simple algorithm provides high accuracies. In the case where these accuracies decrease, other nonlinear classification algorithms should be used instead. If despite all these modifications, there is no improvement in the accuracy, this would mean that the data set (data and class) is noisy.

Table 1 shows the list of attributes selected by the Fisher's ratio (FR) analysis using the median and the mean to describe the centers of the distribution of the corresponding classes. These attributes are ranked by decreasing discriminatory power (Fisher's ratio) in the case of the median. In the case of the mean, the Ki67 expression should be in the third position. Five of the eight attributes in these lists are in common: *Mitotic count, Differentiation, AR expression, Ki67 expression and Tubular Formation*. The reduced base of features with the highest accuracy $(96, 4\%)$ is composed by the four first

 ISBN: 978-1-61208-340-7

Table I. LIST OF MOST DISCRIMINATORY ATTRIBUTES AND THEIR CORRESPONDING FISHER'S RATIOS USING THE MEDIAN AND THE MEAN.

Attributes	FR median	FR mean
Mitotic count (10HPF)	4.56	2.00
Differentiation	4.55	2.41
AR expression	2.60	0.64
Tubular Formation	2.46	0.56
Insitu	2.06	-
T	2.05	-
N	1.99	-
Ki67 expression	1.78	0.94
pro-CollA1 intensity	-	0.24
Bcl2 expression	-	0.22
pro-Coll1A1 Score	-	0.21

markers (*Mitotic count, Differentiation, AR expression, and Tubular Formation*). Only four patients are wrongly predicted using these attributes. Also, using the mean the two first markers (*Differentiation and Mitotic count*) provide an accuracy of 94.4%. Other list of features with high accuracy (93.6%) includes HER2, PR expression, nipple and/or skin invasion, ER, AR and Ki67 expressions. Interesting, the main attributes in these lists coincide with those used by medical experts to asses the histological grade of TNBC samples, nevertheless, these lists also show other attributes that are important for this automatic classification and were not directly used by the pathologists.

We have also analyzed the possibility of predicting the median survival of the different patients. This analysis has shown that the best markers to predict survival (with 78% of accuracy) are: E-cad expression, tumor size, perineural invasion, tubular formation, differentiation, and TNBC subtype. The accuracy of this prediction is lower than in the former case (histological grade), showing that this problem is not very well linearly separable using these attributes. Other additional variables, such as the kind of treatment followed by the patient, should be also used. The use of a nonlinear neural network classifier (extreme learning machine) [12] improved the accuracy of the prediction till 84%.

IV. MACHINE LEARNING USING HISTOLOGICAL IMAGES

The second aim of this research is to analyze the possibility of performing an automatic histological grade prediction using different biometric attributes of TNBC images corresponding to different histological grades taken at two different resolutions. These pattern images have been chosen by expert pathologists in this field. Figure 2 shows different histological images at two different resolutions for cancers in degrees 1, 2 and 3. It can be observed that the main differences reside on the histological variables that have been described in the previous section, that are visually assessed by medical experts. The question resides in the possibility of capturing these characteristics using image processing techniques and machine learning.

A. The automatic image classification problem

The automatic image recognition problem consists in assigning a class to a new incoming image $I \notin B_d$, given a database of TNBC color training images

$$B_d = \left\{ I_k \in S_{(n,m,3)}\left(\mathbf{N}\right) : k = 1, \ldots, N \right\}, \qquad (5)$$

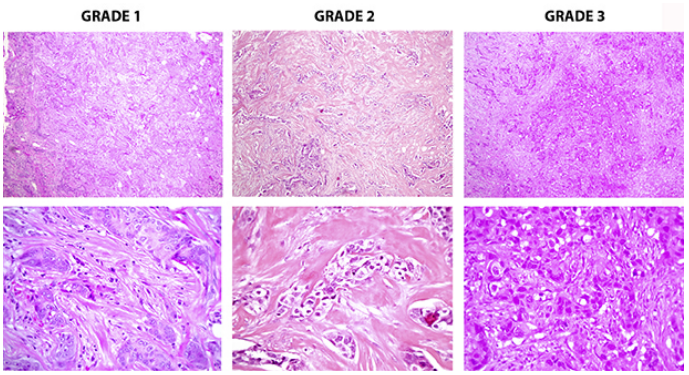

Figure 2. Basal images at two resolutions (100x and 400x magnification) for TNBC with three different histological grades. In the present case the histological grade 1 is very bad represented (only two samples).

that are characterized by a set of histological grades (labels) annotated by medical experts

$$C_d = \left\{ c_k \in \{1, 2, ..., N_c\}, k = 1, \ldots, N \right\}. \qquad (6)$$

In this definition, $S_{(n,m,3)}$ is the space of color images of size $m \times n$, and N_c is the number of classes (3 in this particular case). To perform the classification it is necessary to construct a learning algorithm $C^* : S_{(n,m,3)} \rightarrow C_d$ for the class prediction:

The classification is based on a nearest neighbor algorithm [15]:

1) First, finding the image $I_k \in B_d$ such as:
$$d\left(I, I_k\right) = \min d\left(I, I_j\right), I_j \in B_d, \qquad (7)$$
where d is a suitable distance (or norm) criterium defined over $S_{(n,m,3)}$.
2) Once this image has been found, assigning the class as follows: $C_I^* = C_{I_k} = C_k$.

The images are represented by a feature vectors calculated for each individual method of analysis (or attribute). Naming $\mathbf{v}_i^k \in \mathbf{R}^{s_k}$ the feature vector of image I_i according to the attribute k, the distance between two images I_i and I_j is defined as follows:

$$d\left(I_i, I_j\right) = \|\mathbf{v}_i^k - \mathbf{v}_j^k\|_p, \qquad (8)$$

where p is a certain norm defined over the k-attribute space $(\mathbf{R}^{s_k})$.

The final classification will be performed by consensus [14]:

1) From every individual non-supervised classifier built using the different attributes, we retain the first N_f images that are closer to I. Based on this classification a matrix $M \in M_{Nf \times Na}$ is built, containing the N_f image candidates for each of the N_a attributes and their corresponding histological grades. The score of image I according to the attribute j $(j = 1, N_a)$ to belong to the class k $(k = 1, N_c)$ is established as follows:
$$s_{jk} = \frac{1}{f_k} \frac{N_{jk}}{N_f}, \qquad (9)$$

 ISBN: 978-1-61208-340-7

where f_k is the sampling frequency of class k in the training database (examples) and N_{jk} is the number of images belonging to class k within the N_f candidates found for attribute j.

2) The final score for a new incoming image I to belong to class k is calculated as follows:

$$S_k = \sum_{j=1}^{N_a} s_{jk} w_j = \mathbf{s}_{jk} \cdot \mathbf{w}, \;\; k = 1, N_c \qquad (10)$$

where $\mathbf{s}_{jk}$ is the score assigned by attribute j to class k and $\mathbf{w}$ is a vector of weights corresponding to the trust factors assigned to any individual classifier (attribute). After calculating the scores for all the classes, the final classification of the test image I is performed by selecting the class with the major score. Eventually, the number of candidate images (N_f), the sampling frequencies (f_k), and the trust factors ($\mathbf{w}$), can be optimized (supervised learning) using global algorithms, such as PSO.

V. Image Attributes

In this paper, we have used the following list of attributes, statistical based (histogram and variogram), spectral (discrete cosine transform), and image segmentation/regional descriptors (edges, texture and Zernike Moments). In this case all attributes will be calculated as global descriptors since TNBC image comparison should not be pixel-based.

A. PCA analysis using attributes of the histological images

In this section, we analyze the possibility of discriminating the different histological grades of the TBNC samples by means of unsupervised classification using the Principal Component Analysis (PCA). PCA aims at finding the orthogonal basis by diagonalizing the experimental covariance matrix of training images [18]:

$$S = \sum_{k=1}^{N} (X_k - \mu)(X_k - \mu)^T, \qquad (11)$$

where $X_k \in \mathbf{R}^{Npixels}$ transformed into $1-D$ column vectors, $\mu = \frac{1}{N}\sum_{k=1}^{N} X_k$ is the images sample mean, N is the number of sample images contained in the learning database, and N_{pixels} is the number of pixels of each image. The eigenfaces u_k are the eigenvectors of S, corresponding to the largest eigenvalues. The dimensionality reduction from N_{pixels} to q parameters, is obtained by retaining the q first eigenfaces $\mathbf{u}_k$, spanning most of the database variability. Figure 3 shows the PCA plot in two dimensions (two first PCA coordinates) of the different TNBC images at 10X resolution. We also show the TNBC samples that have positive androgen receptors (AR). This information is important since it implies a different type of TNBC (apocrine carcinoma). Apocrine carcinoma is a subtype of TNBC that expresses androgen receptor (AR), but often lacks estrogen receptor (ER) and progesterone receptor (PR). It is possible to observe that TNBC samples with $HG = 2$ are mainly located on three different clusters, surrounded by samples with $HG = 3$. Also, most of the $HG2$ samples correspond to apocrine type. Taking this fact into account, it seems that non-apocrine $HG2$ samples are only located in very restricted areas of the PCA diagram. Figure 4 shows the 10 first mean PCA coefficients for TNBC images with histological grades 2 and 3. It can be observed that biggest differences occur high-order harmonics (4th). This attribute is expected to have a medium discriminatory power on TNBC images.

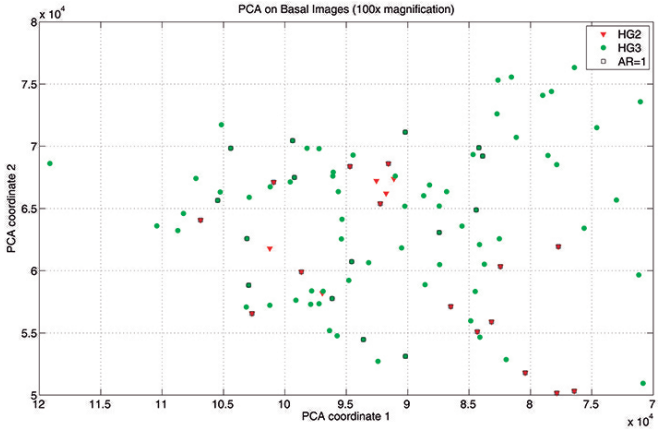

Figure 3. PCA plot (two first PCA coordinates) of the basal images corresponding to the histological grades 2 (HG2) and 3 (HG3), at 100x magnification. We also show the samples with positive androgen receptor ($AR = 1$).

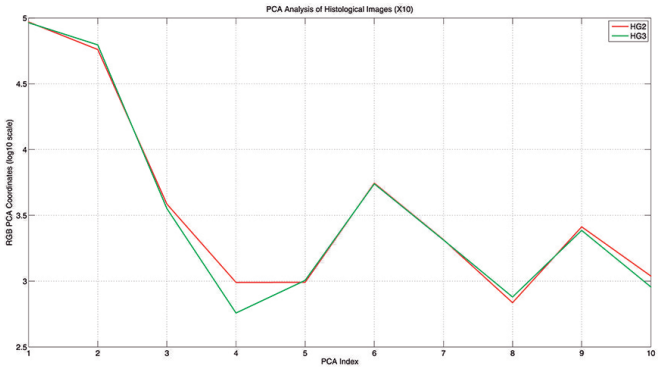

Figure 4. Mean 10 first PCA coefficients for HG2 and HG3 images. It can be observed that the biggest difference occurs for PCA number 4. PCA with higher indexes correspond to increasing high frequency harmonics in the images.

B. Color Histograms

An image histogram describes the frequency of the brightness in the image. The shape of the histogram provides information about the nature of the image [20]. For a gray-scale digital image I the histogram represents the discrete probability distribution of the gray-levels in the image. For this purpose the gray-scale space ($[0, 255]$ for an `8-bit` image) is divided into L bins, and the number of pixels in each class n_i, $(i = 1, L)$ is calculated. In this case the attribute vector has dimension L:

$$H_I = (n_1, ..., n_L). \qquad (12)$$

Relative frequencies can be also used by dividing the absolute frequencies n_i by the total number of pixels in the image. In the case of RGB images, the histogram is calculated for each color channel I_R, I_G and I_B, and then all the channels histograms are merged together, as follows:

$$H_I = (H(I_R), H(I_G), H(I_B)). \qquad (13)$$

 ISBN: 978-1-61208-340-7

Figure 5 shows the relative histograms of the color channels for TNBC images with HG2 and HG3. It can be observed that the major differences occur in the green channel, being its relative frequency lower than those of the red and blue channels. This attribute is expected to have a medium discriminatory power for TNBC images.

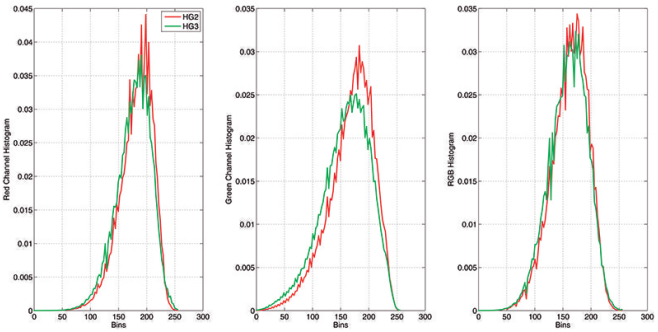

Figure 5. Mean histograms for HG2 and HG3 images. We show a different histogram for each color channel. The biggest differences between classes HG2 and HG3 occur in the green color channel.

C. Variogram

The variogram of an image describes the spatial distribution in each color channel. In spatial statistics the variogram describes the degree of spatial dependence of a spatial random field or stochastic process, the gray-scale in this case. For a given value of vector h, defined by a modulus and direction, the variogram is an index of dissimilarity between all pairs of values separated by vector h. The omnidirectional variogram is the mean of the p-absolute difference between the color values of the $N(h)$ pairs of pixels that are located at the same distance h:

$$\gamma_i(h) = \frac{1}{N(h)} \sum_{k=1}^{N(h)} |c_i(x_k) - c_i(x_k + h)|^2. \qquad (14)$$

To compute the variogram each color channel (matrix) is transformed into the corresponding color vector $c_i(x)$. Typically $N(h)$ is limited to one third of the total number of pixels. The number of classes that have been considered in this case was $N(h) = 100$. Variograms are usually used to analyze spatial continuity and anisotropies. The sill of the variogram is related to the color channel variability, its range to the spatial continuity, and its nugget (origin value) to the image low scale variabilities. Figure 6 shows the omnidirectional variograms of the three color channels for TNBC images with HG2 and HG3. It can be observed that the major differences occur in all the channels, being the blue and green the most discriminatory with respect to this attribute. The green channel also shows the biggest nugget. This attribute is expected to have a high discriminatory power for TNBC images.

D. Texture Analysis

Texture analysis of an image consists in analyzing regular repetitions of a pattern. In this paper, we use the spatial gray level co-occurrence matrix to describe an image texture. The gray level co-occurrence matrix (GLCM), or spatial dependence matrix of an image I is an estimate of the second-order

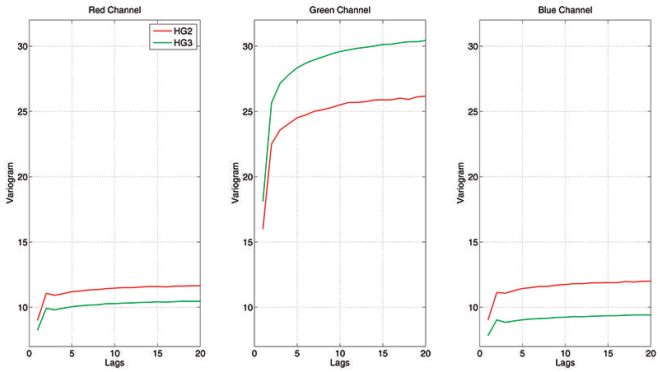

Figure 6. Mean variograms for HG2 and HG3 images. The biggest differences in the sill occur in the green and blue channels.

joint probability function $P_{d,\theta}(i,j)$ of the intensity values of two pixels i and j located at a distance d apart (measured in number of pixels) along a given direction θ. Typically the GLCM is calculated for different pairs of d and θ. Different statistical moments can be calculated from the GLCM matrix, such as contrast, homogeneity, squared energy, correlation and entropy [1]. In the present case, we have used a lag $d = 1$ for the directions 0, 45, 90 and 135. Figure 7 shows the texture moments of the three color channels for TNBC images with HG2 and HG3. The conclusions are similar than in the case of variogram. This attribute is expected to have a high discriminatory power for TNBC images.

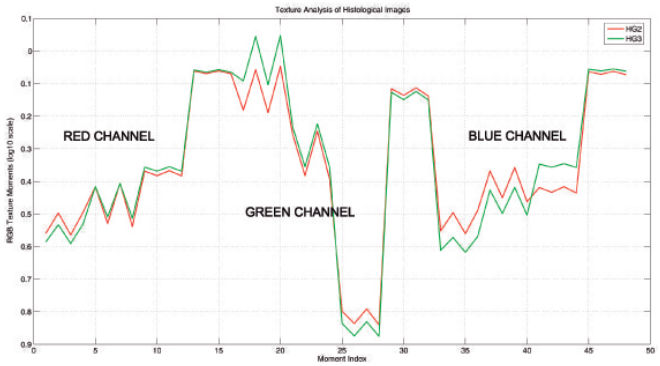

Figure 7. Mean texture coefficients for HG2 and HG3 images. The biggest differences also occur in the green and blue channels.

E. Edges Detection

Edges are determined by sets of pixels where there is an abrupt change in intensity. If a pixel's gray level value is similar to those around it, there is probably not an edge at that point. However, if a pixel has neighbors with widely varying gray levels, it may represent an edge. Thus, an edge is defined by a discontinuity in the gray-level values. More precisely, we can consider an edge as a property associated to a pixel where the image function $f(x,y)$ changes rapidly in the neighborhood of that pixel. Related to f, an edge is a vector variable with two components: magnitude and direction. The edge magnitude is given by the gradient of the pixels intensities function, and its direction is perpendicular to the

 ISBN: 978-1-61208-340-7

gradient's direction:

$$|\nabla f(x,y)| = \sqrt{\frac{\partial f}{\partial x}^2 + \frac{\partial f}{\partial y}^2}, \quad (15)$$

$$\theta(x,y) = arctg\left(\frac{\partial f}{\partial y}, \frac{\partial f}{\partial x}\right) \pm \frac{\pi}{2}. \quad (16)$$

To compute the partial derivatives of $f(x,y)$ we have used the Canny edge detection operator [3], which is one of the most commonly used in image processing, due to its property of detecting edges in a very robust manner in the case of noisy images. The edge detection algorithm provides an image of the same size than the original image on which this analysis is performed. To produce the edge attributes we use a compression of edge image using the DCT. In the present case this analysis provides an attribute vector of dimension 48 for each image. Figure 8 shows the DCT-edges moments of the three color channels for TNBC images with HG2 and HG3. The main differences occur for the first coefficients in each color channel. This attribute is expected to have a low/medium discriminatory power for TNBC images.

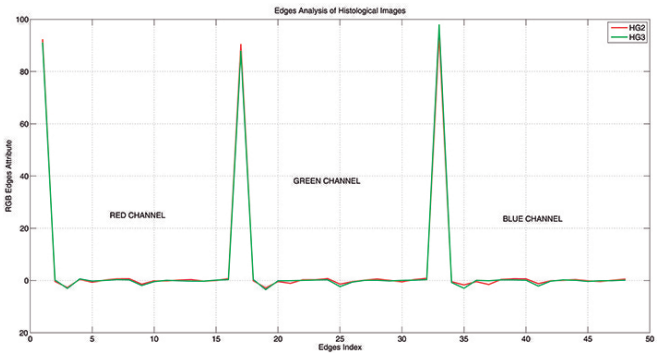

Figure 8. Mean edges vectors (after compression by the DCT) for HG2 and HG3 images. In this case we plot consecutively the first 16 DCT-edges coefficients of each color channel. No big differences are visually observed.

F. Discrete Cosine Transform (DCT)

DCT is a free-covariance model reduction technique that attempts to decorrelate 2D images by projecting the rows and columns of the incoming image into cosines of increasing frequency [11]. DCT is a discrete Fourier transform that expresses a signal in terms of a sum of sinusoids with different frequencies and amplitudes. For an image I_k the DCT is defined as follows:

$$D(u,v) = c(u)c(v)\sum_{i=0}^{s-1}\sum_{j=0}^{n-1} D_{(i,j)} \quad (17)$$

$$D_{(i,j)} = I_k(i,j)\cdot \cos\frac{\pi(2i+1)u}{2s}\cos\frac{\pi(2j+1)v}{2n}, \quad (18)$$

with $u = 0, ..., s-1$, $v = 0, ..., n-1$, and

$$c(\alpha) = \begin{cases} \frac{1}{\sqrt{N}}, & if \quad \alpha = 0, \\ \sqrt{\frac{2}{N}}, & if \quad \alpha \neq 0. \end{cases} \quad (19)$$

N is either the number of rows (s) or columns (n) of the image. The DCT can be expressed in matrix form as an orthogonal transformation [7].

$$D_{CT} = U_{DC} I_k V_{DC}^T, \quad (20)$$

where matrices U_{DC} and V_{DC} are orthogonal. This transformation is separable and can be defined in higher dimensions. The feature vector of an image I_k is constituted by the $q_1 - q_2$ block of D_{CT}, $D_{CT}(1:q_1, 1:q_2)$, where q_1, q_2 are determined by energy reconstruction considerations using the Frobenius norm of the image I_k. Figure 9 shows the DCT coefficients of the three color channels for TNBC images with HG2 and HG3. As in the previous case the main differences occur for the first coefficients in each color channel. This attribute is expected to have a low/medium discriminatory power for TNBC images.

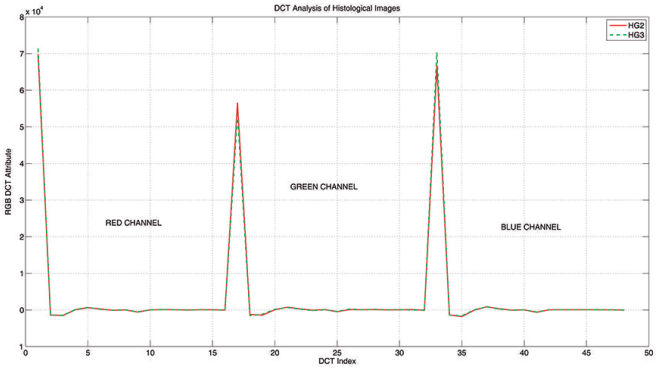

Figure 9. Mean DCT coefficients for HG2 and HG3 images. In this case we plot consecutively the first 16 DCT coefficients of each color channel. No big differences are visually observed.

G. Zernike Moments

Zernike polynomials are a sequence of polynomials that are orthogonal on the unit disk, and are widely used as basis functions for image analysis. Due to the orthogonality of Zernike polynomials, Zernike moments are image descriptors used in many applications due to their properties of orthogonality and rotation invariance. In biomedical applications, Zernike moments have been used as shape descriptors to classify benign and malignant breast masses [19]. Figure 10 shows the Zernike moments for the TNBC images of degree 2 and 3 for polynomials of order 10. This analysis provided an attribute of dimension 36x3 for each color image in this case. Although Zernike moments has been previously applied as shape descriptors to classify benign and malignant breast tissues [19], the differences do not seem very important in this particular case and occur mainly for higher order polynomials in the green and blue channels. This attribute is expected to have a medium discriminatory power.

Finally, as a compendium of all these analysis, Figure 11 shows the PCA plots in 2D (similar to figure 3) of all the attributes that have been commented. It can be observed that the HG2 and HG3 samples are located differently in each of these diagrams. Using the above mentioned image attributes, the unsupervised machine learning algorithm commented in section IV-A provided an accuracy of 86.8%, which is slightly higher than the majority voting algorithm (80%). Future research will be devoted to this important problem.

 ISBN: 978-1-61208-340-7

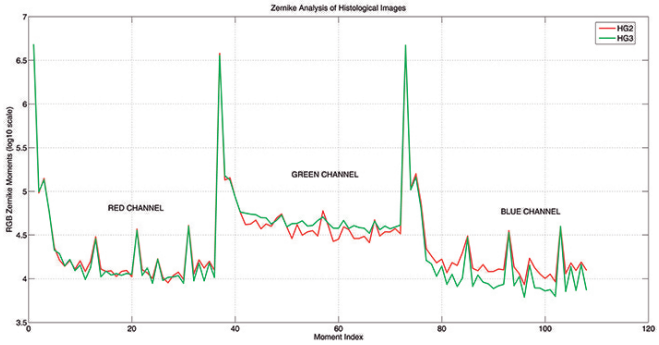

Figure 10. Mean Zernike moments for polynomials of order 10, for HG2 and HG3 images. The biggest differences occur in the green and blue channels.

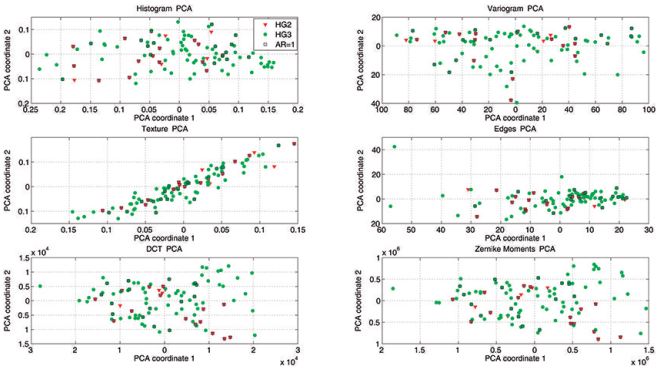

Figure 11. PCA plots (two first PCA coordinates) for all the attributes used in the analysis of the histological images.

VI. Conclusions and Future Research

In this paper, we have explored the possibility to design a biomedical robot able to assist physicians on the kind of histological grade/survival of different subgroups of TNBC samples in order to optimize their diagnosis/treatment and prognosis. Very promising preliminary results are shown using pathological and immunohistochemical variables and histological images of a cohort with 105 patients. Future research will include the possibility of using other supervised learning techniques and global optimization methods (PSO) to optimize the machine learning parameters and to improve the accuracy of the classification. Also, it is expected that the use of both pieces of information (pathological and immunohistochemical variables and histological images) will provide complementary information, improving the accuracy in the classification of TNBC samples (histological grade and survival).

Acknowledgment

The authors want to acknowledge the *Hospital Central de Asturias (Oviedo, Spain)* for providing all the facilities to acquire and treat the TBNC samples.

References

[1] M. H. Bharati, J. J. Liu, and J. F. MacGregor, Image texture analysis: methods and comparisons. *Chemometrics and Intelligent Laboratory Systems*, 72(1), 2004, pp. 57-71.

[2] H. J. Bloom and W. W. Richardson, Histological grading and prognosis in breast cancer; a study of 1409 cases of which 359 have been followed for 15 years, *British journal of cancer* 11 (3), 1957, pp. 359377.

[3] J. Canny, A computational approach to edge detection. *IEEE Transactions on Pattern Analysis and Machine Intelligence*, 8(6), 1986, pp. 679-698.

[4] S. J. Dawson et al., BCL2 in breast cancer: a favourable prognostic marker across molecular subtypes and independent of adjuvant therapy received, *British Journal of Cancer.* 103(5), 2010, pp. 668-75.

[5] C. W. Elston and I. O. Ellis, Pathological prognostic factors in breast cancer I. The value of histological grade in breast cancer: experience from a large study with long-term follow up. In *Histopathology*, 19, 1991, pp. 403-10.

[6] O. Fadare and F. A. Tavassoli, Clinical and pathologic aspects of basal-like breast cancers. In *Nat Clin Pract Oncol.* 5(3), 2008, pp. 149-59.

[7] J. L. Fernández-Martínez and A. Cernea, Numerical analysis and comparison of spectral decomposition methods in biometric applications. *International Journal of Pattern Recognition and Artificial Intelligence (IJPRAI)*, 28(1), 2014, pp.14560-14593.

[8] J. L. Fernández-Martínez, A. Cernea, E. García-Gonzalo, J. Velasco and B. Ketan Panigrahi, Aligned PSO for Optimization of Image Processing Methods Applied to the Face Recognition Problem, In *Swarm, Evolutionary, and Memetic Computing (SEMCCO), Springer Berlin Heidelberg*, Lecture Notes in Computer Science, 8297, 2013, pp 642-651.

[9] R. A. Fisher, The use of multiple measurements in taxonomic problems. *Annals Eugen*, 7, 1936, pp. 179-188.

[10] C. García-Pravia et al., Overexpression of COL11A1 by cancer-associated fibroblasts: clinical relevance of a stromal marker in pancreatic cancer. In *PLoS One.* 8(10), 2013, e78327.

[11] Z. M. Hafed and M. D. Levine, Face recognition using the discrete cosine transform. *Int. J. Comput. Vision*, 43(3), 2001, pp. 167-188.

[12] G. B. Huang et al., Extreme learning machine: Theory and applications. *Neurocomputing*, 70, 2006, pp. 489501.

[13] E. A. Rakha et al., Breast cancer prognostic classification in the molecular era: the role of histological grade. In *Breast Cancer Research,* 12(14), 2010, pp. 12-207.

[14] L. Rokach, Ensemble-based classifiers. *Artificial Intelligence Review*, 33(1-2), 2010, pp. 1-39.

[15] G. Shakhnarovich, T. Darrell, and P. Indyk, *Nearest-Neighbor Methods in Learning and Vision: Theory and Practice (Neural Information Processing)*, The MIT Press, 2006.

[16] S. M. Siitonen et al., Reduced E-cadherin expression is associated with invasiveness and unfavorable prognosis in breast cancer. *American Journal of Clinical Pathology,* 105, 1996, pp. 394-402.

[17] T. Sørlie et al., Gene expression patterns of breast carcinomas distinguish tumor subclasses with clinical implications. In *Proc Natl Acad Sci USA* 98(19), 2001, pp. 10869-10874.

[18] M. Turk and A. Pentland, Eigenfaces for recognition. *Journal of Cognitive Neuroscience*, 3(1), 1991, pp. 71-86.

[19] A. Tahmasbi, F. Saki, H. Aghapanah, and S.B. Shokouhi, A Novel Breast Mass Diagnosis System based on Zernike Moments as Shape and Density Descriptors, *Proceeding of 18th Iranian Conference of Biomedical Engineering (ICBME)* , 2011, pp.100-104.

[20] S. E. Umbaugh. *Computer Vision and Image Processing: A Practical Approach Using CVIPtools*. Number ISBN 0-13-264599-8. Prentice Hall Professional Technical Reference, 1998.

[21] World Medical Association, Declaration of Helsinki - Ethical Principles for Medical Research Involving Human Subjects, *The Journal Of the American Medical Association (JAMA)*, 2013, Volume 310(20), pp.2191-2194.

 ISBN: 978-1-61208-340-7

An Interval Type-2 Fuzzy Neural Network for Cognitive Decisions

Gang Leng, Anjan Kumar Ray, Thomas Martin McGinnity, Sonya Coleman, Liam Maguire, Philip Vance
Intelligent Systems Research Centre, Faculty of Computing and Engineering
University of Ulster, Magee Campus, Londonderry, U.K.
e-mail: gang.leng@gmail.com, {ak.ray, tm.mcginnity, sa.coleman, lp.maguire, p.vance}@ulster.ac.uk

***Abstract*—In an ambient assisted living environment, raw data can often be very noisy making is difficulty to interrupt by a decision and reasoning system. To help reduce the effects of noise, we propose a decision and reasoning system which combines an interval fuzzy system and a self-organising fuzzy neural network (SOFNN) is presented in this paper. The method exploits the use of a trained standard SOFNN structure from a fuzzy neural network to initialise the proposed approach. Simulation results show that the proposed structure is more suitable for uncertain situations demonstrating a high level of robustness.**

Keywords- interval type-2 fuzzy system; self-organising fuzzy neural network; cognitive decisions; modelling capability; robustness.

I. INTRODUCTION

Robotic UBIquitous COgnitive Network (RUBICON) [16] is an EU project that aims to create a self-sustaining, self-organizing, learning and goal-oriented robotic ecology, which consists of four layers: Learning Layer, Control Layer, Cognitive Layer and Communication Layer. The Cognitive Layer obtains events from the Learning Layer and generates goals for the Control Layer. The Cognitive Layer is described in detail in [1] and includes a cognitive reasoning and decision module.

The objective of the cognitive decision module is to generate decisions signal by integrating the status outputs determined by the cognitive reasoning module, taking into account current and historical information. These decision signals are then used to set the actual goals for the Control Layer so as to attempt to ensure that the RUBICON ecology behaves appropriately. Ultimately, the RUBICON system will be embedded in real environments where, potentially, the collected data will be noisy. To minimise the impact of noise and the inherent uncertainty of the generated status outputs, the decisions module is expected to show a high level of robustness.

A Self-Organising Fuzzy Neural Network (SOFNN) has a degree of robustness [2][3]. However, the membership functions of a SOFNN are type-1 fuzzy systems, which are presented as crisp numbers. This limits the ability of the network to model uncertainty. Type-2 fuzzy sets have been extended from type-1 fuzzy sets by Zadeh [4] and are attracting increasing attention. The advantage of type-2 fuzzy systems is that the membership functions can be presented as a fuzzy set, not simply as crisp numbers. This enhances the ability of the network to handle the uncertainty in the rule base [5], which is vitally important for deployment in real applications, such as the RUBICON ecology. In this work, the combination of an interval type-2 fuzzy system and a SOFNN, denoted as SOFNN-IT2, has been proposed for the cognitive decision module.

Background information on the SOFNN and an interval type-2 fuzzy system are presented in Section II. Section III presents the proposed SOFNN-IT2 learning method. Simulation results in Section IV are presented to verify the proposed method in terms of its modelling capability and robustness. The work is summarised in Section V.

II. BACKGROUNDS

A. Overview of SOFNN

A Self-Organising Fuzzy Neural Network (SOFNN) [2] is a hybrid network which has the capability to model and forecast a complex nonlinear system. The SOFNN is a five-layer network, namely, the input layer, the Ellipsoidal Basis Function (EBF) layer, the normalised layer, the weighted layer, and the output layer, as shown in Figure 1.

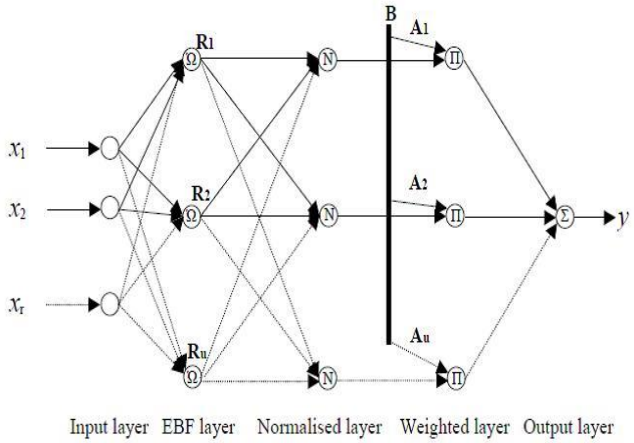

Figure 1. Structure of SOFNN.

In the EBF layer, each neuron is a T-norm of Gaussian fuzzy membership functions [2] belonging to the inputs of the network. Every Membership Function (MF), thus, has its own distinct centre and width, which means every neuron has both a centre vector and a width vector and the dimensions of these vectors are the same as the dimension

 ISBN: 978-1-61208-340-7

of the input vector. Figure 2 illustrates the internal structure of the *j*th neuron, where $X = [x_1\, x_2 \cdots x_r]$ is the real valued input vector, $C_j = [c_{1j}\, c_{2j} \cdots c_{rj}]$ is the centre vector in the *j*th EBF neuron, and $\Sigma_j = [\sigma_{1j}\, \sigma_{2j} \cdots \sigma_{rj}]$ is the width vector in the *j*th neuron.

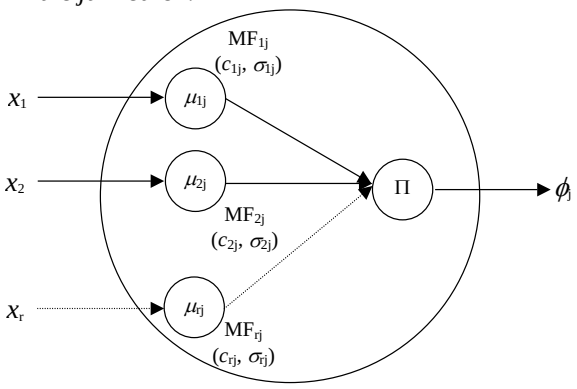

Figure 2. Structure of the *j*th neuron R_j with c_j and σ_j in EBF layer.

The SOFNN is thus constructed based on EBFs consisting of a centre vector and a width vector. The adding approach is based on the geometric growing criterion [6] and the ε-completeness of fuzzy rules [7]. The pruning method is based on the Optimal Brain Surgeon (OBS) method [8] and depends on the second order derivative of the objective function with respect to the parameters of each neuron, i.e., the Hessian matrix [2]. The Hessian matrix can be easily obtained as part of the proposed on-line parameter learning algorithm. Further information on this network is available from [2] and [3].

The SOFNN can be used for on-line learning and the adding and pruning strategies have the self-organising capability to produce a fuzzy neural network with a flexible structure that grows in order to minimise the training error. The SOFNN has demonstrated good performance in applications of function approximation, complex system identification, and time-series prediction [2] [3].

B. Interval Type-2 Fuzzy System

An Interval Type-2 Fuzzy Logic System (IT2FLS) is shown in Figure 3. This is similar to a Type-1 FLS (T1FLS) containing a fuzzifier, rule base, fuzzy inference engine, and output processing. The main difference is that a type-2 FLS has a type-reducer in the output processing. The type-reducer has the ability to generate a type-1 fuzzy set from a type-2 fuzzy set. The defuzzifier then can defuzzify this type-1 fuzzy set to a crisp number. IT2FLSs have demonstrated better ability to handle uncertainties than their type-1 counterparts [9].

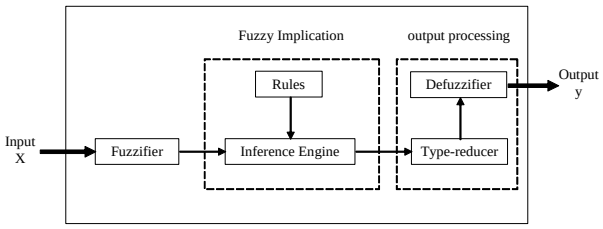

Figure 3. Interval type-2 fuzzy logic system (IT2FLS).

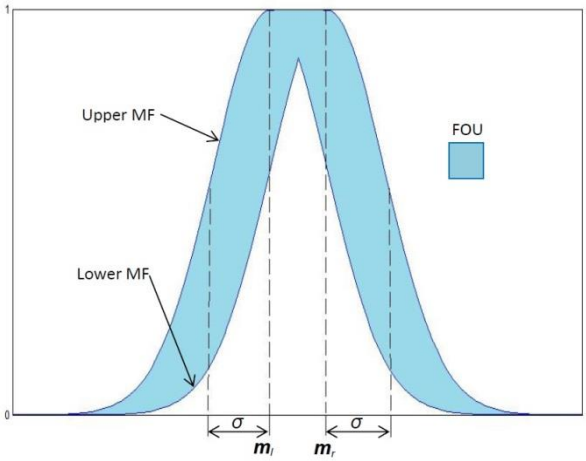

Figure 4. Interval type-2 Gaussian primary membership function.

Figure 4 illustrates the Footprint of Uncertainty (FOU) of an interval type-2 Gaussian primary Membership Function (MF). This MF can be represented by the two bounding MFs: upper MF and lower MF. For the *i*th type-2 fuzzy rule R_i, the *j*th input variable x_j has the interval type-2 fuzzy set $\tilde{A}_j^i$ which has a Gaussian primary MF with the standard deviation σ_j^i and the uncertain mean m_j^i within the range $[m_{jl}^i, m_{jr}^i]$, i.e.,

$$\mu_{\tilde{A}_j^i} = \exp[-\frac{(x_j - m_j^i)^2}{2\sigma_j^{i\,2}}] \equiv N(m_j^i, \sigma_j^i, x_j)\ , \qquad m \in [m_{jl}^i, m_{jr}^i],\ \ \mu_{\tilde{A}_j^i} \in [\underline{\mu}_{\tilde{A}_j^i}, \bar{\mu}_{\tilde{A}_j^i}] \tag{1}$$

The FOU of this MF for the input x_j can be represented as an upper MF

$$\bar{\mu}_{\tilde{A}_j^i} = \begin{cases} N(m_{jl}^i, \sigma_j^i; x_j), & x_j < m_{jl}^i \\ 1, & m_{jl}^i \le x_j \le m_{jr}^i \\ N(m_{jr}^i, \sigma_j^i; x_j), & x_j > m_{jr}^i \end{cases} \tag{2}$$

and a lower MF

$$\underline{\mu}_{\tilde{A}_j^i} = \begin{cases} N(m_{jr}^i, \sigma_j^i; x_j), & x_j \le \dfrac{m_{jl}^i + m_{jr}^i}{2} \\ N(m_{jl}^i, \sigma_j^i; x_j), & x_j > \dfrac{m_{jl}^i + m_{jr}^i}{2} \end{cases} . \tag{3}$$

For a type-2 Takagi-Sugeno (TS) model [10][11], the type-2 fuzzy rule R_i can be represented as

$$R_i: IF\ x_1 is N([m_{1l}^i, m_{1r}^i], \sigma_1^i)\ and\ x_2 is N([m_{2l}^i, m_{2r}^i], \sigma_2^i),$$
$$THEN\ y^i = [a_{0l}^i, a_{0r}^i] + [a_{1l}^i, a_{1r}^i]x_1 + [a_{2l}^i, a_{2r}^i]x_2 \quad (4)$$

where y^i is the output of the ith rule and $[a_{kl}^i, a_{kr}^i]$ is the interval set of the parameter for TS model.

The type-reducer [12][13] reduces the outputs of the rules to the type-1 output of the system as an interval-valued fuzzy set $[y_l, y_r]$. This type-1 interval-valued fuzzy set can be defuzzified as

$$y = \frac{y_l + y_r}{2}. \quad (5)$$

III. SOFNN-IT2 LEARNING

An algorithm combining SOFNN and IT2FLS has been developed for the cognitive decision module to attain a high level of robustness. The strategy for development exploits the following steps:

1. A trained SOFNN structure, which is a type-1 fuzzy structure, is obtained following learning.
2. This type-1 fuzzy structure is then initialised as a type-2 fuzzy structure.
3. The initialised type-2 structure is trained off-line, based on gradient descent and Kalman filter algorithms. The obtained type-2 fuzzy neural structure can be represented as a set of type-2 fuzzy rules similar to (4).
4. The final output of the system can be generated after information has passed through type-reduction and defuzzification.

The method to obtain a SOFNN structure has been described in [2] and [3]. Details on attaining the final output of the system by type-reduction and defuzzification can be found in [12] and [13]. Steps 2 and 3 are outlined in the following sections.

A. Initialise Type-1 Structure to Type-2 Structure

The structure of the SOFNN can be represented as a set of type-1 fuzzy rules, for example

$$R_i: IF\ x_1 is N(m_1^i, \sigma_1^i)\ and\ x_2 is N(m_2^i, \sigma_2^i),$$
$$THEN\ y^i = a_0^i + a_1^i x_1 + a_2^i x_2. \quad (6)$$

Firstly, we initialise the centres of the Gaussian membership function in the IF-part as

$$[m_k^i - \delta m_{0k}^i, m_k^i + \delta m_{0k}^i],$$
$$i.e.,\ m_{kl}^i = m_k^i - \delta m_{0k}^i,\ m_{kr}^i = m_k^i + \delta m_{0k}^i, \quad (7)$$
$$k = 1, 2, ...$$

and then initialise the parameters in THEN-part as

$$[a_n^i, \delta s_{0n}^i],\ i.e.,\ a_{nl}^i = a_n^i - \delta s_{0n}^i,\ a_{nr}^i = a_n^i + \delta s_{0n}^i, \quad (8)$$
$$n = 0, 1, 2, ...$$

where δm_{0k}^i and δs_{0n}^i are predefined values. This is the initial type-2 structure of the system, similar to (4). Thus, the parameters m_{kl}^i, m_{kr}^i, σ_k^i, a_n^i and δs_n^i should be adapted during the learning process.

B. Proposed Training Algorithm

The proposed training algorithm is based on the gradient descent and Kalman filtering algorithms.

Considering the objective function

$$E = \frac{1}{2}[y(t) - y_d(t)]^2 \quad (9)$$

where $y(t)$ and $y_d(t)$ are the real and desired outputs of the system, respectively. Parameters of the IF-part are tuned by the gradient descent algorithm as:

$$m_{kl}^i(t+1) = m_{kl}^i(t) - \eta \frac{\partial E}{\partial m_{kl}^i} \quad (10)$$

$$m_{kr}^i(t+1) = m_{kr}^i(t) - \eta \frac{\partial E}{\partial m_{kr}^i} \quad (11)$$

$$\sigma_k^i(t+1) = \sigma_k^i(t) - \eta \frac{\partial E}{\partial \sigma_k^i} \quad (12)$$

where η is a learning rate.

For training purposes, the output of the system can be described in matrix form as

$$y = \mathbf{W_2}\boldsymbol{\Psi}. \quad (13)$$

Similar to [2][14][15], $\mathbf{W_2}$ is relevant to parameters of the THEN-part and $\boldsymbol{\Psi}$ is a matrix obtained by parameters of the IF-part and input data. Parameters of the THEN-part $\mathbf{W_2}$ can be updated by executing the Kalman filtering algorithm

$$\mathbf{W_2}(t+1) = \mathbf{W_2}(t) + Q(t+1)\boldsymbol{\Psi}(t+1)[y_d(t+1) - \mathbf{W_2}(t)\boldsymbol{\Psi}(t+1)] \quad (14)$$

$$Q(t+1) = Q(t) - \frac{Q(t)\boldsymbol{\Psi}(t+1)\boldsymbol{\Psi}^T(t+1)Q(t)}{1 + \boldsymbol{\Psi}^T(t+1)Q(t)\boldsymbol{\Psi}(t+1)}. \quad (15)$$

The proposed training algorithm, combining the gradient descent and Kalman filtering algorithms is performed in one iteration for each incoming training data and repeated for incremental offline learning. The trained type-2 fuzzy neural network is thus obtained. This network is employed as the RUBICON cognitive decision module to generate the decision signal to set the actual goals for Control Layer.

IV. SIMULATION

For the purposes of validating the approach, a synthesised dataset consisting of 4500 samples was used as input to the reasoning module [1], which generates the data needed for the decision module. These data describe typical events in a domestic environment, one of the application areas of the RUBICON project's ecology. Figure 5 shows the inputs to the decision module are status outputs from the reasoning module [1], and the outputs of the decision

 ISBN: 978-1-61208-340-7

module (the SOFNN-IT2) are decision signals to set actual goals. The decision module receives 10 status outputs from the reasoning module plus an additional 10 one-step-back status outputs to make a combined set of 20 inputs. These status outputs are then categorised into 1 of 7 goals by the decision module. The status outputs and goal labels are listed in Table I and Table II, respectively.

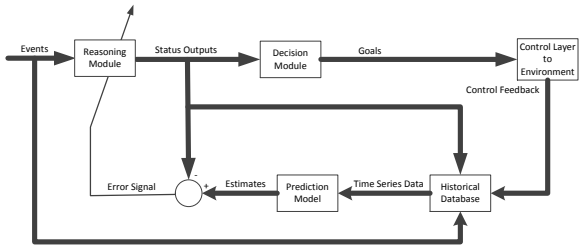

Figure 5. Block diagram of Cognitive Layer.

TABLE I. LIST OF STATUS OUTPUTS

ID	Status Outputs
1	User Exercising
2	User Relaxing
3	User in Kitchen
4	Phone Ringing Confirmed
5	Visitor at Door
6	User Cook Activity
7	Fire Alert
8	Burglary Alert
9	Dripping Alert
10	Cleaning Situation

TABLE II. LIST OF GOALS

ID	Goals
1	Bring Drink for User
2	Set Bath for User
3	Bring Phone for User
4	Attend Door
5	Attend Drip
6	Suspend Clean
7	Attend Fire

A. *Testing of Modelling Capability*

The first 3900 points of the data set were used as the training data of the decision module, and the remaining 600 points as the testing data. Using the algorithm outlined in the previous section a type-2 structure, SOFNN-IT2, is then obtained. The results of training and testing of the SOFNN-IT2 are shown in Table III, where RMSE is the Root Mean Square Error between the output of the network and the desired decision signal of the goal (i.e., target) and CD is the percentage of correct decision in terms of goals against desired goal data. Figures 6 to 8 give results of the decision signal of the goal, "Bring Drink for User", and type-2 membership functions (MFs) of selected inputs.

TABLE III. RESULTS OF SOFNN-IT2

ID	Goals	Number of Rules	Result	SOFNN-IT2	
				Training	Testing
1	Bring Drink for User	4	RMSE	0.1373	0.1195
			CD	94.92	97.17
2	Set Bath for User	3	RMSE	0.1636	0.1326
			CD	92.36	94.17
3	Bring Phone for User	33	RMSE	0.1553	0.1297
			CD	93.79	96.33
4	Attend Door	11	RMSE	0.1223	0.0856
			CD	96.56	99.00
5	Attend Drip	9	RMSE	0.1425	0.1319
			CD	93.03	94.67
6	Suspend Clean	3	RMSE	0.0945	0.1115
			CD	96.15	94.33
7	Attend Fire	3	RMSE	0.1080	0.1093
			CD	97.21	97.17

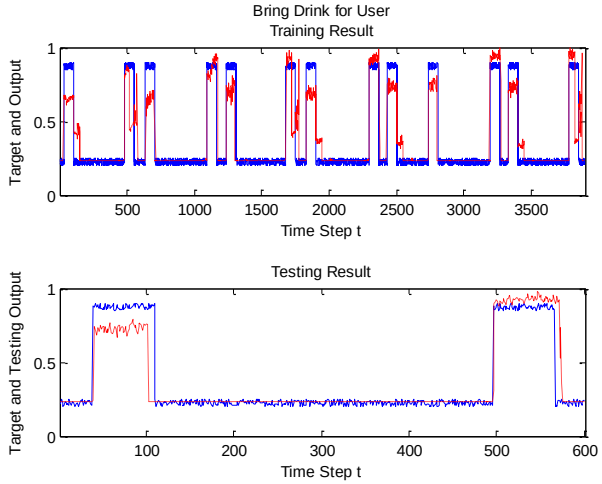

Figure 6. Results of Bring Drink for User.

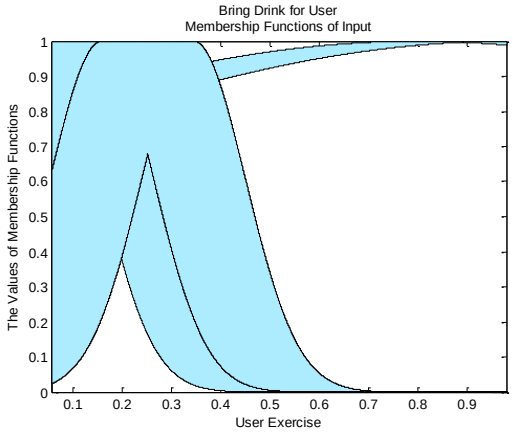

Figure 7. MFs of current input User Exercising.

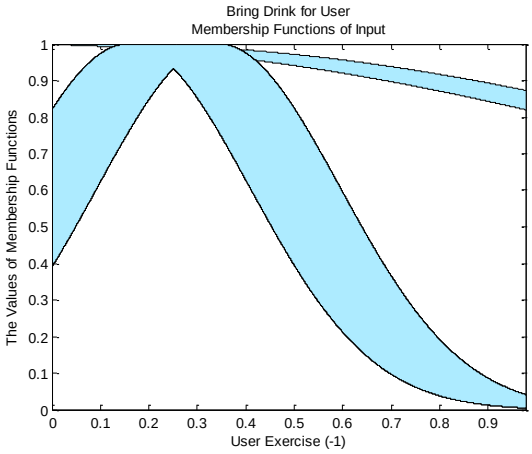

Figure 8. MFs of one-step-back input User Exercising.

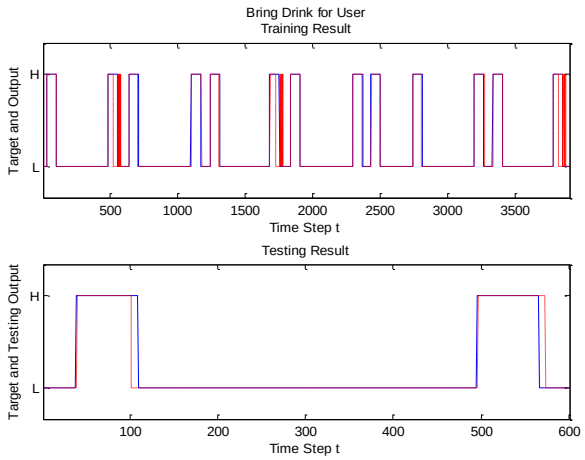

Figure 9. Results of Bring Drink for User's decision goals.

In Figure 6, the red line represents outputs of the decision model and the blue line represents targets. As an example, Figure 9 shows the results for the goal "Bring Drink for User". In Figure 9, the red line represents the goals obtained by the decision module and the blue line represents desired goals. In Figure 9, H is the high-level signal which triggers the actual goal, L is the low-level signal. Any decision signal with a confidence greater than 0.5 is defined as the high-level goal data; otherwise it is defined as the low-level goal data. These results prove that the obtained type-2 system, SOFNN-IT2, has the capability to model the complex input-output relationship to achieve high accuracy decisions.

B. Testing of Robustness

To investigate the robustness of the type-2 network SOFNN-IT2, its type-1 counterpart network SOFNN is used for comparison. Inputs for the obtained SOFNN and SOFNN-IT2 structures are a combination of current and one-step-back historical data from the reasoning module. The 20 inputs are combined with white-noise to assess the robustness of both networks. White-noise is chosen from the different standard deviations listed in Table IV. Again, the RMSE is between the output with noise inputs and the output without noise inputs. Table IV provides the results for both the SOFNN and SOFNN-IT2 for the goal "Bring Drink for User".

TABLE IV. RESULTS OF SOFNN AND SOFNN-IT2 FOR BRING DRINK FOR USER

No.	White Noise (SD)	Result	SOFNN	SOFNN-IT2
1	σ=0.00001	RMSE	1.16E-05	3.66E-06
		CD%	98.84	95.24
2	σ=0.0001	RMSE	0.0001	3.48E-05
		CD%	98.84	95.24
3	σ=0.001	RMSE	0.0012	0.0004
		CD%	98.84	95.24
4	σ=0.01	RMSE	0.0116	0.0038
		CD%	98.84	95.29
5	σ=0.1	RMSE	0.124	0.0731
		CD%	96.29	93.62
6	σ=0.15	RMSE	0.1569	0.1525
		CD%	70.38	86.27
7	σ=0.2	RMSE	0.177	0.2214
		CD%	71.67	79.96
8	σ=0.25	RMSE	0.1914	0.2512
		CD%	73	77.71
9	σ=0.3	RMSE	0.2034	0.2676
		CD%	72.18	76.67

Figure 10 and Figure 11 plot the trends of RMSE and CD% against increased noise on the inputs for the goal "Bring Drink for User".

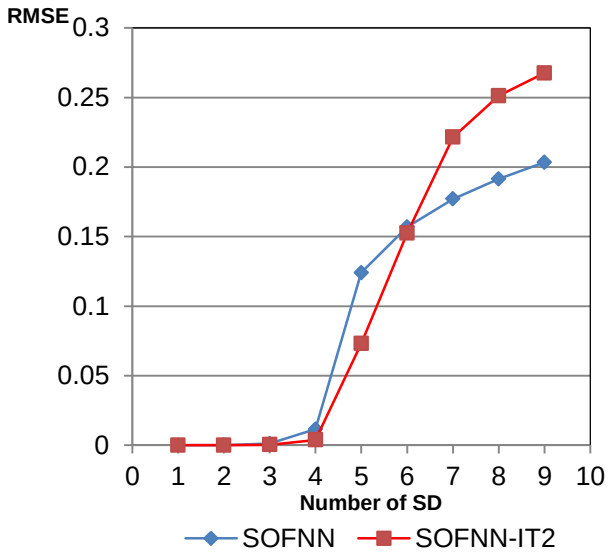

Figure 10. Results of Bring Drink for User's decision goals.

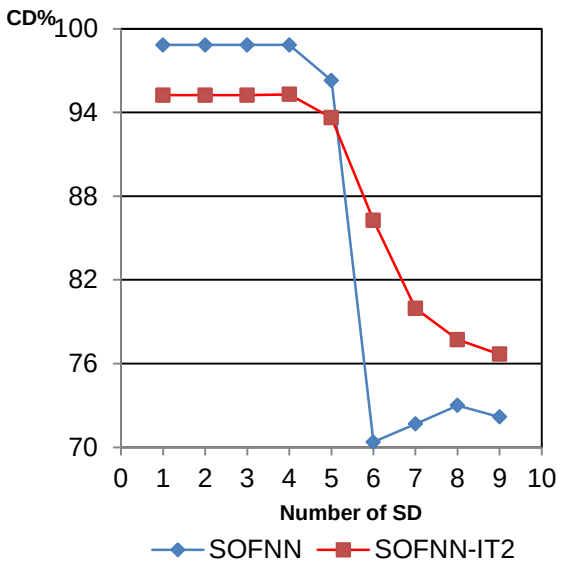

Figure 11. Results of Bring Drink for User's decision goals.

It is observed that the RMSEs of SOFNN and SOFNN-IT2 decrease as the standard deviation of the white-noise is decreased. This means that the SOFNN and SOFNN-IT2 both have a degree of robustness. For white-noise with $\sigma \leq 0.1$, the RMSEs of the SOFNN-IT2 for all outputs are smaller than those of the SOFNN and the CDs are similar. This illustrates that the SOFNN-IT2 is more robust to noise than the SOFNN. Furthermore, for increased white-noise, the CDs of the SOFNN-IT2 are better than those of the SOFNN, though the RMSEs of the SOFNN-IT2 are slightly larger than those of the SOFNN. These results show that, compared with its type-1 counterpart structure, the type-2 structure is more suitable for addressing uncertain situations with a high level of robustness.

V. CONCLUSION

A type-2 fuzzy neural network SOFNN-IT2, based on a SOFNN and interval type-2 fuzzy reasoning, has been proposed in this paper. The obtained type-1 SOFNN structure is firstly initialised to a type-2 SOFNN-IT2 structure and then the final type-2 SOFNN-IT2 structure is generated by the proposed training algorithm. Extensive testing of the cognitive decisions module using this SOFNN-IT2 algorithm has demonstrated that the approach is highly robust to noise and that performance is improved (compared to the traditional SOFNN approach) when considerable noise or uncertainty is present in the inputs. This is a very important attribute for RUBICON as it will be deployed in a real world environment, and thus, subject to uncertainty and noisy inputs.

ACKNOWLEDGMENT

The authors would like to acknowledge support of the European Commission. This work is partially supported by the EU FP7 RUBICON project (contract no. 269914) [16].

REFERENCES

[1] G. Leng, A. K. Ray, T. M. McGinnity, S. Coleman, and L. Maguire, "Online sliding window based self-organising fuzzy neural network for cognitive reasoning," Cognitive 2013, Valencia, Spain, pp. 114-119, 27 May-1 June 2013.

[2] G. Leng, G. Prasad, and T. M. McGinnity, "An on-line algorithm for creating self-organizing fuzzy neural networks," Neural Networks, vol. 17, pp. 1477-1493, 2004.

[3] G. Leng, T. M. McGinnity, and G. Prasad, "An approach for on-line extraction of fuzzy rules using a self-organising fuzzy neural network," Fuzzy Sets and Systems, vol. 150, no. 2, pp. 211-243, 2005.

[4] L. A. Zadeh, "The concept of linguistic variable and its application to approximate reasoning," Information Sciences, vol. 8, pp. 199–249, 1975.

[5] J. M. Mendel, Uncertain Rule-Based Fuzzy Logic System: Introduction and New Directions, Upper Saddle River, NJ: Prentice-Hall, 2001.

[6] V. Kadirkamanathan and M. Niranjan, "A function estimation approach to sequential learning with neural networks," Neural Computation, vol. 5, pp. 954-975, 1993.

[7] C. C. Lee, "Fuzzy logic in control systems: fuzzy logic controller – Part I and II," IEEE Transactions on Systems, Man, and Cybernetics, vol. 20, no. 2, pp. 404-435, 1990.

[8] B. Hassibi and D. G. Stork, "Second order derivatives for network pruning: Optimal brain surgeon," in Advances in Neural Information Processing Systems, 4, Morgan Kaufman, pp. 164-171, 1993.

[9] D. Wu, "On the fundamental differences between interval type-2 and type-1 fuzzy logic controllers," IEEE Transactions on Fuzzy Systems, vol. 20, no. 5, pp. 832-848, 2012.

[10] T. Takagi and M. Sugeno, "Fuzzy identification of systems and its applications to modeling and control," IEEE Transactions on Systems, Man, and Cybernetics, vol. 15, no. 1, pp. 116-132, 1985.

[11] M. Sugeno and G. T. Kang, "Structure identification of fuzzy model," Fuzzy Sets and Systems, vol. 28, pp. 15-33, 1988.

[12] Q. Liang and J. M. Mendel, "Interval type-2 fuzzy logic systems theory and design," IEEE Transactions on Fuzzy Systems, vol. 8, no. 5,pp. 535–550, 2000.

[13] J. M. Mendel, R. I. John, and F. Liu, "Interval Type-2 Fuzzy Logic Systems Made Simple," IEEE Transactions on Fuzzy Systems, vol. 14, no. 6, pp. 808-821, 2006.

[14] C.-F. Juang and Y.-W. Tsao, "A self-evolving interval type-2 fuzzy neural network with online structure and parameter learning," IEEE Transactions on Fuzzy Systems, vol. 16, no. 6, pp.1411-1424, 2008.

[15] Y.-Y. Lin, J.-Y. Chang, N. R. Pal, and C.-T. Lin, "A mutually recurrent interval type-2 neural fuzzy system (MRIT2NFS) with self-evolving structure and parameters," IEEE Transactions on Fuzzy Systems, vol. 21, no. 3, pp. 492-509, 2013.

[16] http://fp7rubicon.eu/

 ISBN: 978-1-61208-340-7

Robust Detection and Tracking of Regions of Interest for Autonomous Underwater Robotic Exploration

A. Alejandro Maldonado-Ramírez, L. Abril Torres-Méndez
Robotics and Advanced Manufacturing Group
CINVESTAV Campus Saltillo
Ramos Arizpe, Coahuila, MEXICO
Emails: alejandro.maldonado.ramirez@gmail.com, abril.torres@cinvestav.edu.mx

Edgar A. Martínez-García
Lab. de Robótica, Inst. of Eng. and Tech.
Universidad Autónoma de Cd. Juárez
Juarez, Chihuahua, Mexico
Email: edmartin@uacj.mx

***Abstract*—Autonomous robotic exploration of unstructured and highly dynamic environments is a complex task, particularly, in underwater environments. An underwater robot needs to quickly detect a region of interest and then track it for a certain period of time in order to plan for the next trajectory; all of these while keeping its motion control stable. In this paper, we present a novel approach that robustly detects and tracks regions of interest in underwater video streams at frame rate. First, to detect relevant regions in an image, our approach combines two existing visual attention schemes with some improvements to adjust it to underwater scenes. Second, a scaled version of the resulting image is segmented by using a superpixel segmentation algorithm, and each relevant point is associated to a superpixel descriptor. The descriptor helps to track the same region as long as it results interesting for the visual attention algorithm. The experimental results demonstrate that our approach is robust when tested on different videos of underwater explorations.**

Keywords-visual attention models; regions of interest; superpixel segmentation; feature tracking; underwater vision

I. INTRODUCTION

The development of simple sensory motor skills for tracking an object of interest starts at early stages of life, this involves motion of eyes, head and even tongue and/or hands (in newborns), which together with cognitive skills, direct the way to explore the surrounding environment [3], [15]. As we grow and get more mobility, we develop more sophisticated exploratory skills, which can be transferred and adapted to new objects or scenes. It is at this point that the exploration fully involves active perception and navigation skills [6]. However, the goal of exploration is not just to navigate and look around in the environment but to build hypotheses about the data, in other words, to build knowledge about what it is sensed. This knowledge depends on the type of environment and the application for which the exploration is required [5]. For a robotic system, for example, the goal of exploring a natural habitat may be to prevent natural disasters. In any case, a key aspect in the exploration task is to know what features are relevant in an environment in order to learn about it and take important decisions while interacting with it.

The detection and tracking of relevant regions in an scene is a fundamental part of any autonomous robotic exploration task [16]. Particularly, in underwater environments, it may result complex. On one hand, the inherent physical properties of marine environments cause geometrical distortions, such as color distortions, dynamic lighting conditions and suspended particles (known as "marine snow"), resulting in poor visibility thus hindering computer vision tasks. On the other hand, this type of environments are unstructured and highly dynamic. Since exploration is implicitly linked to motion, the tracking of relevant features must be stable enough to allow for smooth movements for the suitable control of the robotic system.

In this research work, we present a real-time visual attention model to robustly detect and track relevant underwater features with the aim of exploring coral reefs. The real-time characteristic in robotics applications is fundamental since the tracked relevant features will help to direct the exploration trajectories in subsequent captured images while estimating the relative robot pose.

The outline of the paper is as follows. Section II presents the related work. Section III describes our model and its implementation. The experimental results and discussion are presented in Section IV. Finally, in Section V the conclusions and future work are given.

II. RELATED WORK

The use of visual attention models to find regions of interest in images is a common preprocessing tool for a variety of applications. However, for practical applications, the main challenge for designing these systems lies in their real-time performance requirements. Particularly, when applied to video streams at frame rate. Two of the more popular ones, due to their easy implementation, flexibility and fast computation are the Neuromorphic Vision Toolkit (NVT) proposed by Itti *et al.* [12] and the attention system called Visual Object detection with a CompUtational attention System (VOCUS) by Frintrop *et al.* [10]. The Focus Of Attention (FOA) is the place in the image that draws the attention of the system. Itti *et al.* [12] obtained the FOA by using a Winner-Take-All neural network. Frintrop *et al.* [10] simply find the point with the highest saliency value by scanning every point, and the most salient region is determined by seed region growing.

Recently, visual attention models have been used in robotic applications [5]. There has been likewise underwater applications of these models. For example, Walther *et al.* [17] and Edgington *et al.* [7] detect objects and potentially interesting visual events for humans in order to label the frames of a video

 ISBN: 978-1-61208-340-7

stream as interesting or boring. In both research work, the NVT [12] model is used and the videos were recorded by a Remotely Operated Vehicle (ROV). Barat and Rendas [4] present a visual attention system for detection of manufactured objects. Their model is based on the minimum description length test for detecting the motion of contrasting neighboring regions. After that a statistical snake is adapted to determine the boundary of the object. Lobato *et al.* [13] use intensity, motion and edge maps as features for their visual attention model to detect the Norway lobsters and help scientist to quantify them.

In all these works, the visual attention models are used for aiding humans in the task of analyzing video streams. In our case, we want that the visual attention model leads the robot motion by automatically detecting and tracking features that are considered of interest for exploration. Particularly, we are interested in transferring abilities to an Autonomous Underwater Vehicle (AUV) in order to detect regions of interest without human supervision while successfully navigating the environment. Visual attention models for autonomous underwater exploration require an strict real time performance.

As hardware limitations in underwater robots are still an issue, we need to rely on fast computational algorithms.

III. METHODOLOGY

In this section, we describe our visual attention model for underwater scenes.

The general structure of our methodology (see Fig. 1) combines two methods with some improvements to adjust it to be used in underwater scenes – the NVT [12] and the VOCUS method [10].

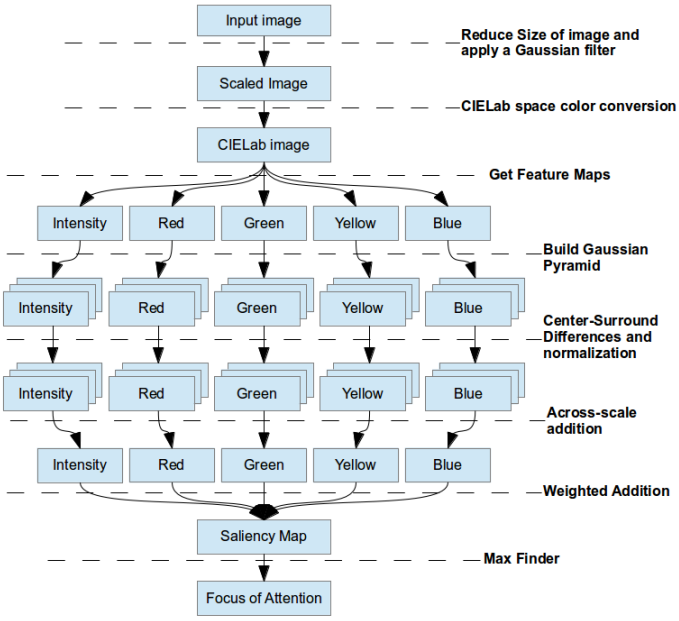

Figure 1. General diagram of our visual attention algorithm.

Given that underwater environments are unstructured, *i.e.*, the existing objects lack of specific orientation and shape, our attention model relies strongly on the intensity and color information. Therefore, the use of a color space capable of highlighting colors that are different from the color of seawater is crucial. As pointed out, this represents a challenge given that visibility conditions in open water are not always ideal and color tonality tends to diminish significantly. The space color we choose is the CIELab. This color model has the characteristic of being perceptually uniform and also that its a and b channels naturally encompass the green-red and blue-yellow contrast colors, which turns to be perfect for underwater image analysis and processing. By assigning weights to each of the five color channels (intensity, green, red, blue and yellow) the focus of attention can be directed to a certain object or characteristic. This is specially important since water absorbs color abruptly with depth thus limiting its detection.

Furthermore, our model needs to be robust to dramatic changes in illumination, which are very common for underwater images or videos. By considering only the chromatic channels a and b of the CIELab color space, our model does not consider abrupt changes in brightness in images as these tend to be smooth in the chromatic channels. This turns out to be fine for our purposes.

An important aspect to consider in any computational visual attention system is how to highlight the relevant parts of each feature. This is usually done by using a center-surround mechanism (also called *center-surround difference*), which is inspired in cells of the human visual receptive field [14].

For exploration tasks, keeping track of the same focus of attention, or one near a previous one at different image frames, is of particular importance. First, it allows the robot to lead its motion in a smooth manner avoiding sudden maneuvers, which may cause the system to become unstable. Secondly, for the navigation part, it is important to have an estimate of the current pose of the robot, thus, by tracking the same feature (natural landmark in our case), it would allow the robot to estimate its relative pose by means of triangulation.

Our strategy to achieve this is based on the fact that once a region of interest is identified as FOA, this region should be kept as FOA as long as it results interesting for the attention system. In other words, the robot needs to robustly keep track of the same or very similar FOA for a certain period of time in order to make inferences about it, to estimate its relative pose, and finally, to plan the motion to the next relevant region to be explored. To achieve this behavior we apply a superpixel segmentation technique based on the Simple Linear Iterative Clustering (SLIC) algorithm [2]. The information captured at each superpixel forms a *descriptor*, which helps to discriminate the FOA at the current frame by considering the FOAs in the previous frame. By doing this, the algorithm tries to keep the same region as FOA in consecutive frames.

In the following sections, we describe in more detail each of the steps involved in our visual attention model.

A. Preprocessing of the image

The input RGB image is scaled to a size of 320×240 pixels and then blurred with a Gaussian filter. After that, the image is converted to the CIELab color space to extract a particular color from an image (Section III-B).

B. Getting the features maps

We use intensity and color (red, yellow, green and blue) as features. The intensity map corresponds to the $L-$channel of the CIELab image. The colors are extracted from the a and b

 ISBN: 978-1-61208-340-7

channels, as described in [8], as follows,:

$$F_i(x,y) = V_{max} - \|ab(x,y) - p\|, \quad (1)$$

where F_i is the i^{th} feature map, $V_{max} = 255$ in 8-bit depth images, $p = (a_d, b_d)$ is the desired color to extract (only the a and b component are used) and $ab(x,y)$ is the ab-channel of the image. The color feature maps are gray-scale images in which the intensity indicates how near is the desired color to the original color of the pixel. As it was previously mentioned, there is no need of using the orientation feature, since underwater environments are unstructured.

C. Getting the conspicuity maps

The conspicuity maps tell us where the most relevant regions are in an specific feature map. We are going to have five conspicuity maps at the end of this process. One for intensity and four for each of the colors.

The first step to calculate the conspicuity maps is to build a Gaussian pyramid. The number of levels used in the pyramid depends on the size of the image and the size of the relevant regions to be found [9]. In the algorithm, we use a $3-$level pyramid, *i.e.*, three scales $s_n = \frac{1}{2^n}$ with $n = \{0,1,2\}$. We obtain three maps F_{in} for each feature map.

Once the pyramids are built, the center-surround differences are applied. The center-surround differences are implemented as in [9], but using filter operations.

$$D_{in\sigma}(x,y) = center - surround \quad (2)$$

$$center = F_{in}(x,y) \quad (3)$$

$$surround = K(\sigma) * F_{in}(x,y) \quad (4)$$

$$K(\sigma) = \frac{1}{(2\sigma+1)^2 - 1} \begin{bmatrix} 1 & \dots & 1 \\ \vdots & 0 & \vdots \\ 1 & \dots & 1 \end{bmatrix}_{(2\sigma+1)\times(2\sigma+1)} \quad (5)$$

where $*$ is the convolution operator. We use $\sigma = \{3,4\}$.

After the center-surround differences are applied, each of the resultant maps $D_{in\sigma}(x,y)$ is normalized in a range of $[0,M]$ (in our case, we set $M = 1$). Then, all the obtained maps from the same feature are added across-scale in s_2. This way, we obtain a conspicuity map C_i for each feature.

D. Getting the saliency map

To calculate the saliency S map we normalize each of the conspicuity maps, then we weigh each with a value w_i and add them into a single saliency map S. By changing the values of w_i, we can give a preference to certain color feature.

$$S(x,y) = \sum_i w_i C_i(x,y). \quad (6)$$

It is worth noting that the saliency map is a gray-scale image in the scale s_2. The most relevant parts of the image appear brighter in the saliency map.

The way to fuse the maps into a single one (the scaled feature maps into a conspicuity map and conspicuity maps into a saliency map) is called a *naive* strategy [11]. We have also implemented the normalization operator $N(\cdot)$ [12],[11] to fuse the maps.

Finally, in order to give priority to relevant points that are close to the most relevant point in a saliency map, each value of saliency in the map is weighted as follows:

$$w = e^{-a\sqrt{(x_c-x)^2+(y_c-y)^2}}, \quad (7)$$

where (x_c, y_c) are the coordinates of the most relevant point $\mathbf{c}$, (x,y) are the coordinates of the other points of the image and a is a positive value. This way the points nearer to $\mathbf{c}$ are more likely to be chosen as the next relevant points by the algorithm.

We compared the relevant regions obtained with our method to those obtained with the model of the non-iterative $N(\cdot)$ normalization and the model of the iterative normalization using a dataset of non-underwater images, containing natural and man-made objects. Two examples of natural outdoor scenes are shown in Fig. 2 (top and middle rows). As our interest is in underwater scenes, we carry on this comparison using a dataset of underwater images containing only natural structures (rocks, coral reefs, fishes). The last row of Fig. 2 shows an example with an underwater scene. Each of the relevant regions detected is surrounded by a circle. It can be observed that the relevant regions detected by our model are all on the rock formation whereas the regions detected with the other models are mostly on areas like sand or sea water, which are not of relevance for exploration tasks.

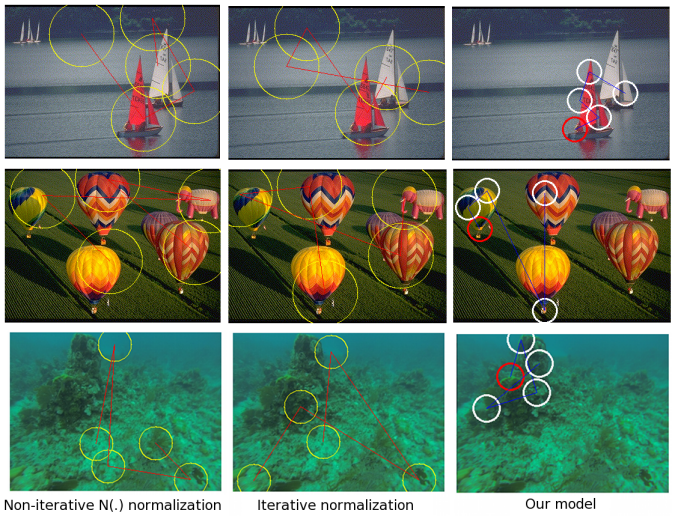

Figure 2. Comparison results on the detection of relevant regions (indicated by circles) in non-underwater an underwater scenes by using the $N(\cdot)$ normalization (left), the iterative normalization (middle) and our visual attention model (right).

In general, good results are obtained for still images, however for a video sequence of a coral reef, the results were not satisfying for our purpose (underwater robotic exploration) because the focus of attention changed its position arbitrarily from one frame to the next one. Therefore, a robust tracking of FOA is fundamental (more details in Section III-E).

E. Robust tracking of focus of attention

We find the most relevant point (FOA) by scanning all the values of saliency in the map and choosing the one with the highest value, then we set the surrounding points to zero in a given radius. We repeat this process until we find the n most saliency points. It is important to recall that we want

 ISBN: 978-1-61208-340-7

the algorithm to find a relevant region and be able to find the same relevant region in the next image frame, that is, we want to keep track of the relevant region for few more subsequent images if and only if this region is still among the n most saliency ones. We are interested in this behavior because it will lead the movement of a robot during an exploration. Having abrupt changes of the FOA from one frame to next one may cause an erratic motion.

To tackle this problem, we segment the smallest image in the 3-level pyramid (*i.e.*, an image of 80×60 for an input image of 320×240) in m superpixeles using the SLIC algorithm [2]. Each superpixel is a set of pixels with similar features and it is characterized by a $5-$dimensional vector of the form $\mathbf{c}$=$[L_c, a_c, b_c, x_c, y_c]$. The n most relevant points are described with a descriptor $\mathbf{c}$ of the superpixel they belong. Once we have the descriptor of each saliency point, we choose the closest (the most similar) to the descriptor of the FOA from the previous frame. The chosen region become the FOA of the current frame. The distance (similarity) measure is based on the SSD metric as in [2], but without using the L component:

$$dist(p_1, p_2) = \sqrt{\left(\frac{d_s}{n_s}\right)^2 + \left(\frac{d_c}{n_c}\right)^2}, \quad (8)$$

$$d_s = \sqrt{(a_{p_1} - a_{p_2})^2 + (b_{p_1} - b_{p_2})^2},$$

$$d_c = \sqrt{(x_{p_1} - x_{p_2})^2 + (y_{p_1} - y_{p_2})^2},$$

where n_c and n_s are the normalization factor for the distance in the color space and the image space, respectively. These values were set as described in [1]. Fig. 3 illustrates the use

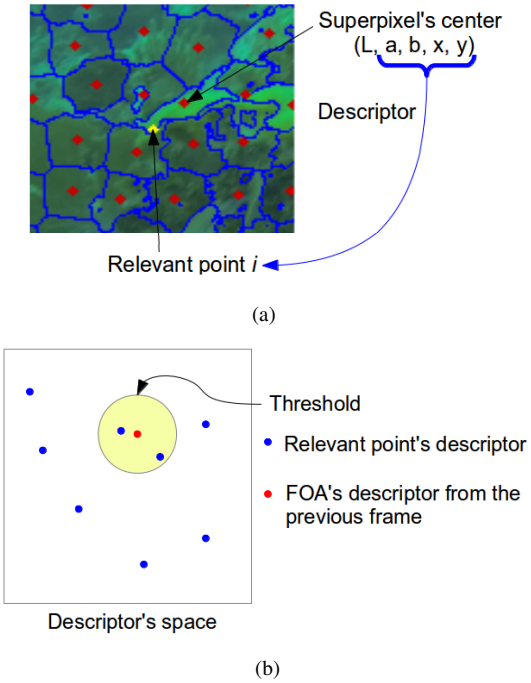

Figure 3. Finding the next focus of attention. (a) Superpixels are used to associate a descriptor to each relevant point. (b) The distance defined in (8) is used to find the next focus of attention. The relevant point descriptors inside the yellow circle represent the FOA candidates.

of superpixels to achieve a stable tracking of similar FOAs in a region of interest. If the distance from the closest saliency descriptor to the previous FOA descriptor is greater than a defined threshold (yellow circle in Fig. 3b), the distances are ignored and the point with the highest saliency value is chosen as the new FOA.

IV. Experimental Results

Before conducting the experiments, we tested our algorithm with different image resolutions to analyze their performance. The complexity of the algorithm is $O(N)$, where N is the total number of pixels in the image. The average processing time, in a 2.1GHz dual-core processor, for an image of 640×480 is 184 ms. We select to use the 320×240 resolution (49 ms) as the behavior of the detected FOA was better (with less abrupt changes). Also, some parameters, related to regions considered as relevant in underwater scenes, needed to be tuned before running our algorithm. We conducted visual tests with 32 people (16 women and 16 men) in an age range of $20-30$ years old. In the experiment, each person was asked to select the region(s) in an underwater image that attracted more their attention. A set of eight images were shown to each person.

Fig. 4a depicts some examples of the regions of interest chosen by people. Each column shows the regions selected in an image. With this information, we train our algorithm by assigning to each color feature a weight. In Fig. 4b, some regions of interest chosen by our visual attention algorithm are shown. It can be observed that the regions detected by the algorithm resembles the ones detected by people. We carried

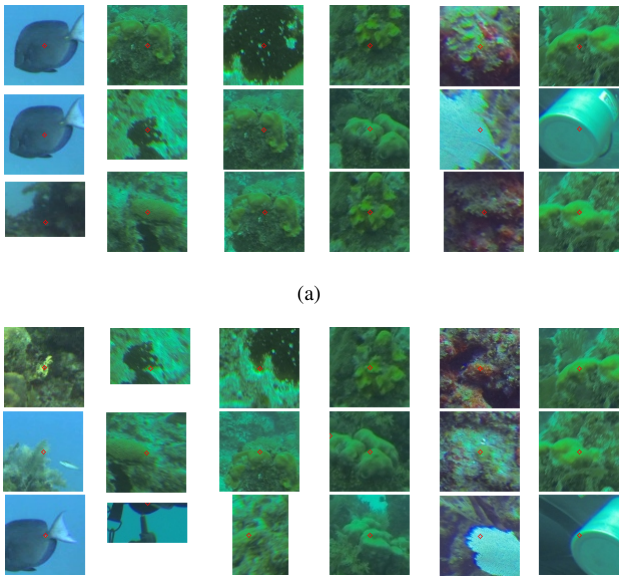

Figure 4. Some of the region of interests selected by (a) people and by (b) our visual attention algorithm. A column shows the snapshots considered as FOAs in each of the images.

out a set of experiments using two different underwater videos taken during a dive exploration of the coral reef of Mahahual, Costa Maya. The first video (Video 1) is a 30 fps video in which the diver's camera motion is mainly forward. The second video has also a frame rate of 30 fps but the camera's motion is mainly a rotation around its vertical axis and it is

 ISBN: 978-1-61208-340-7

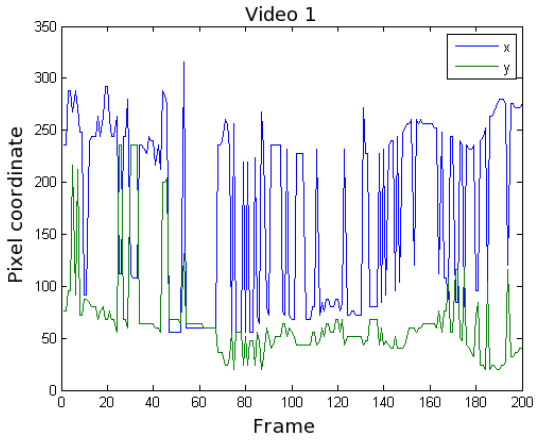

(a) Position of FOA during forward motion.

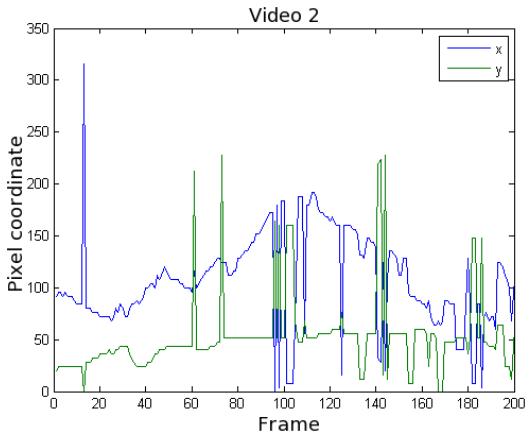

(b) Position of FOA during rotational motion.

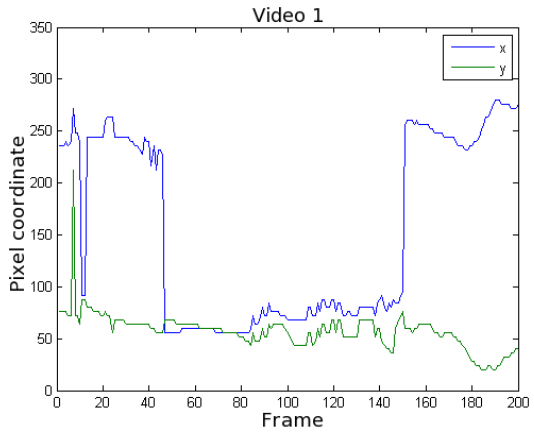

(c) Position of FOA during forward motion (using superpixel descriptors for each saliency point).

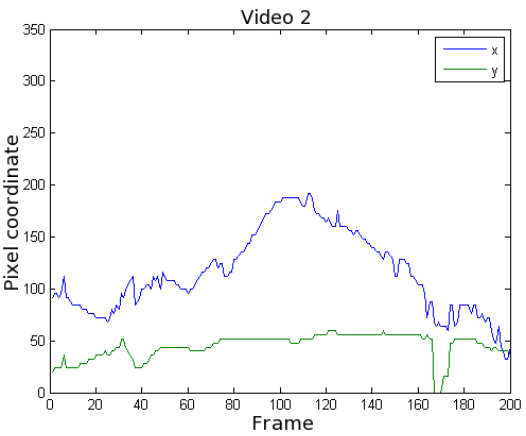

(d) Position of FOA during rotational motion (using superpixel descriptors for each saliency point).

Figure 5. Position of the FOA on the image plane. (a) The FOA is chosen by using directly the point with the highest saliency map. (b) The FOA is chosen using the superpixel descriptors for each saliency point in order to keep a FOA in the same region on a given number of consecutive frames, avoiding with this, an erratic motion in the robot.

slower than Video 1. We use Video 1 to test the performance of the algorithm in forward motion and the Video 2 for rotational motion. The experiments were done in 200 consecutive frames on each video.

In the first experiment, the FOA was chosen by using only the information provided by the saliency map obtained from the visual attention algorithm, *i.e.*, the point with the highest saliency value on the map. Figures 5a-b show the graphs of the (x, y) images coordinates of the FOA obtained at each frame for Videos 1 and 2, respectively. As we can see, there are some abrupt changes in the position of the FOA from one frame to the next one, especially on forward motion. In general, this can be considered as a good behavior because an exploration task implies that the focus of attention changes over time. However, when the FOA only stays for a very short period of time (*i.e.*, in very few consecutive frames), then this may become a problem as the abrupt uncontrolled changes of position of the FOA may cause an erratic movement in the robot. To solve this, we segment the image in superpixels. From the saliency map we take the n most relevant points and describe them with the a, b, x and y component of the superpixel they belong to. Figures 5c-d show the results of the FOA obtained at each frame for Videos 1 and 2 but now using the superpixel descriptors.

Once we have the descriptor of each saliency point, we choose the closest (the most similar) to the FOA of the previous frame. The similarity measure is calculated using (8). It is important to mention that if the distance from the closest saliency point to the previous FOA is greater than a defined threshold then we ignore the distances and the point with the highest saliency value is chosen as the new FOA. It can be observed that the FOA still takes arbitrary regions in the image, but once a new FOA is obtained, it stays almost in the same region on several consecutive frames. The effect of the improvement to the visual attention algorithm can be seen more clearly on the plot of Video 1. We can obtain less abrupt changes in the FOA by adjusting the threshold for the similarity measure between a previous FOA and the new saliency points. In the previous experiment, for Video 1, this threshold was 2 (Figures 5c and 6a). We observed that the greater the value of the threshold the less abrupt changes in the FOA. Fig. 6b shows results when applying a threshold value of 2.5 and using the naive normalization. Each time the distance overpasses the threshold, we extract a snapshot of the FOA and its surrounding region (pixels) to see how different these

 ISBN: 978-1-61208-340-7

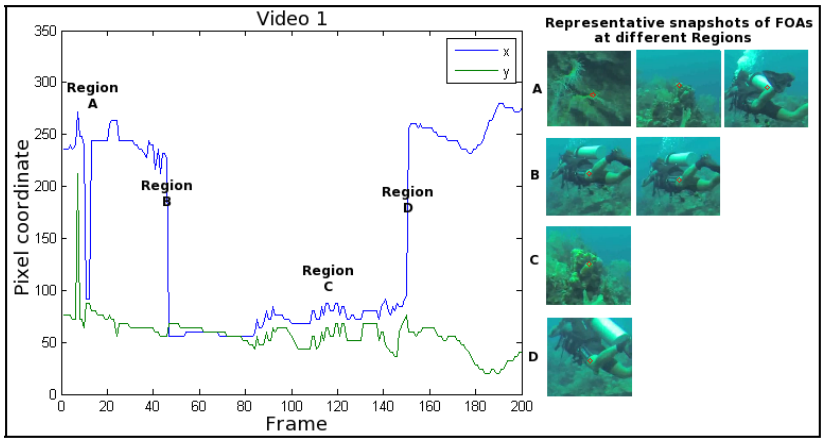

(a) Position of FOAs with their representative snapshots at each change (indicated by regions A, B, C and D) when using a threshold of 2.

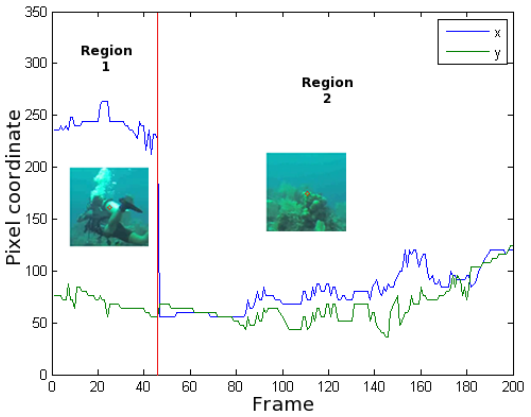

(b) Position of FOAs with two relevant regions when using a threshold of 2.5.

Figure 6. Relevant regions captured at each change of FOA.

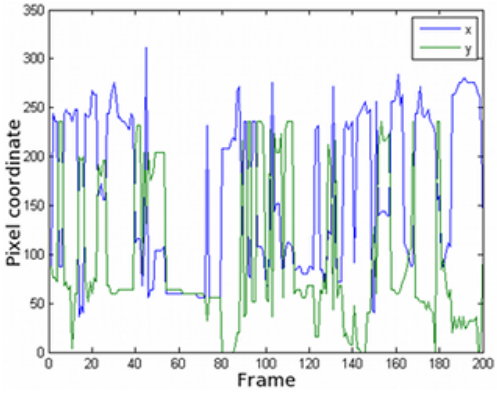

(a) Position of FOA points.

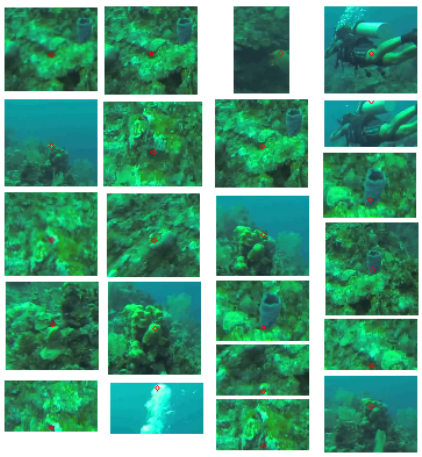

(b) Relevant regions detected.

Figure 7. Position of FOA points with some of the associated relevant regions when using the $N(\cdot)$ operator.

regions are. As it can be seen in Fig. 6a, when the threshold was set to 2 the algorithm found 10 relevant regions, although many of them represent almost the same scene. Instead, when the threshold was set to 2.5 (see Fig. 6b) the algorithm found only 2 relevant regions.

We carried out an additional experiment, in which our algorithm was tested using the $N(\cdot)$ operator in order to compare the results with those obtained using the naive normalization (Fig. 6b). We can observe in the plot of Fig. 7a that the position of the FOA changes abruptly when the $N(\cdot)$ operator is used; about 57 relevant regions were found using this operator (Fig. 7b). Even so, this may be useful in an offline program to find all the possible relevant regions or in a training phase.

Finally, as poor visibility is a common problem in underwater environments, we want to see how our algorithm performs in this type of conditions. Fig. 8 shows the position of the FOA and a snapshot of the relevant regions found when running our algorithm. Despite of the poor visibility, parts like the hand of the diver, the blue triangle in the red ball or the yellow tube are detected.

V. Conclusion and Future Work

We have presented a novel approach which robustly detects regions of interest in underwater video streams and tracks them under forward and rotational movements. As it is shown in the experiments, the robustness of this approach is mainly due to two parts. The first part is the visual attention model that can determine relevant regions of an underwater image even if the geometry or shape of the environment to explore is unknown, making it ideal when dealing with unstructured environments.

The other important part is the use of the superpixels as a descriptor, because it summarizes the information of color and position of the similar set of pixels, thus reducing the computational time significantly.

Our approach turns out to be also robust for tracking saliency zones even in scenes with poor visibility conditions.

As future work, we want to test our approach in real underwater explorations performed by our robotic system. Also, further analysis on the training process is needed in order to determine the concurrence of FOAs annotated by the users with those detected by our algorithm. Finally, the approach could be extended to track more that one region of attention.

 ISBN: 978-1-61208-340-7

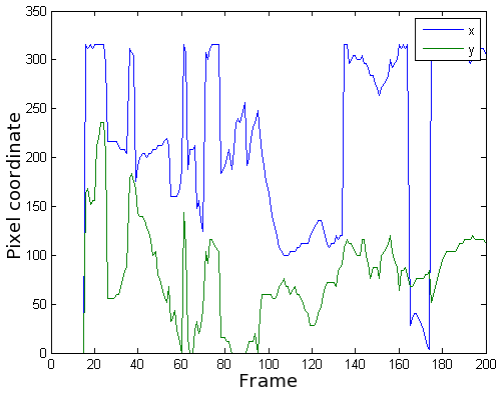

(a) Position of FOA points.

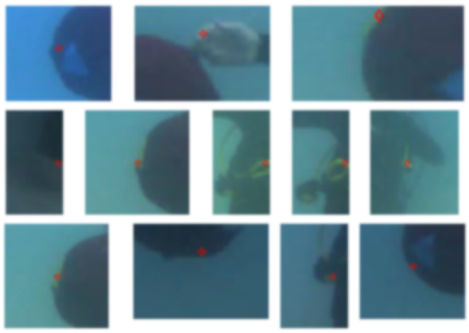

(b) Relevant regions detected.

Figure 8. Results of applying our visual attention algorithm in underwater environments with poor visibility.

This will help to plan ahead the robot's trajectories, which leads to a better exploration.

ACKNOWLEDGMENT

The authors would like to thank CINVESTAV and CONACyT for funding this project, and to the Robotics Lab of Universidad Autónoma de Ciudad Juárez for its collaboration.

REFERENCES

[1] R. Achanta, A. Shaji, K. Smith, A. Lucchi, P. Fua, and S. Susstrunk, "SLIC superpixels compared to state-of-the-art superpixel methods," IEEE Transactions on PAMI **34** (2012), no. 11, 2274–2282.

[2] R. Achanta, A. Shaji, K. Smith, A. Lucchi, P. Fua, and S. Süsstrunk, "SLIC superpixels", Tech. report, EPFL, 2010.

[3] James Mark Baldwin, *Mental development in the child and the race: Methods and processes*, Macmillan, 1906.

[4] C. Barat and M.-J. Rendas, "A robust visual attention system for detecting manufactured objects in underwater video," OCEANS, 2006, pp. 1–6.

[5] M. Begum and F. Karray, Visual attention for robotic cognition: a survey," IEEE Transactions on Autonomous Mental Development **3** (2011), no. 1, 92–105.

[6] Bennett I. Bertenthal, *Origins and early development of perception, action, and representation*, Annual review of psychology **47** (1996), no. 1, 431–459.

[7] D.R. Edgington, K.A. Salamy, M. Risi, R. E. Sherlock, D. Walther, and C. Koch, "Automated event detection in underwater video," OCEANS, vol. 5, 2003, pp. P2749–P2753 Vol.5.

[8] S. Frintrop, "VOCUS: a visual attention system for object detection and goal-directed search", Ph.D. thesis, Rheinische Friedrich-Wilhelms-Universität Bonn, 2006.

[9] S. Frintrop, "Computational visual attention," Computer Analysis of Human Behavior (A. A. Salah and T. Gevers, eds.), Springer London, 2011, pp. 69–101.

[10] S. Frintrop, G. Backer, and E. Rome, "Goal-directed search with a top-down modulated computational attention system," Pattern Recognition (W. G. Kropatsch, R. Sablatnig, and A. Hanbury, eds.), Lecture Notes in Computer Science, vol. 3663, Springer Berlin Heidelberg, 2005, pp. 117–124.

[11] L. Itti and C. Koch, "A Comparison of Feature Combination Strategies for Saliency-Based Visual Attention Systems," Journal of Electronic Imaging **10** (1999), 161–169.

[12] L. Itti, C. Koch, and E. Niebur, "A model of saliency-based visual attention for rapid scene analysis," IEEE Transactions on Pattern Analysis and Machine Intelligence **20** (1998), no. 11, 1254–1259.

[13] P. Lobato-Correia, P. Y. Lau, P. Fonseca, and A. Campos, "Underwater video analysis for Norway lobster stock quantification using multiple visual attention features," 15th European Signal Processing Conference, 2007.

[14] S. Palmer, "Vision Science, Photons to Phenomenology," The MIT Press, 1999.

[15] J. Piaget, *The origins of intelligence in children*, New York: Int. Univ. Press, 1952.

[16] S. Thrun, S. Thayer, W. Whittaker, C. Baker, W. Burgard, D. Ferguson, D. Hannel, M. Montemerlo, A. Morris, Z. Omohundro, and C. Reverte, *Autonomous exploration and mapping of abandoned mines*, IEEE Robotics Automation Magazine **11** (2004), no. 4, 791.

[17] D. Walther, D. R. Edgington, and C. Koch, "Detection and tracking of objects in underwater video," Proc. of the IEEE Computer Society Conference onComputer Vision and Pattern Recognition (CVPR), vol. 1, 2004, pp. I–544–I–549.

 ISBN: 978-1-61208-340-7

Creating Confidence Intervals for Reservoir Computing's Wind Power Forecast

Use of Maximum Likelihood Method and the Distribution-based Method

Breno Menezes. Mêuser Valença
Escola Politécnica de Pernambuco
Universidade de Pernambuco
Recife, Brasil
Emails: (bamm, meuser)@ecomp.poli.br

***Abstract*—The world is increasing the investments in electricity production from renewable sources, such as wind farms, although, the variable power production of wind farms must be balanced by other sources of energy, such as thermal units. As the amount of electric energy generated by the wind represents a higher percentage in the electric grid, it becomes more important to do accurate wind power forecasts and confidence intervals to support the system's operation and reduce its costs. In order to generate the confidence intervals, the forecasting error is often assumed to follow a Gaussian distribution. A wrong assumption can have a huge impact on the confidence intervals. This work proposes an evaluation of the forecasting error distribution generated by a Reservoir Computing network forecast in different timescales and the confidence intervals generated using the maximum likelyhood method and the distribution based method.**

Keywords-Reservoir Computing; Confidence Intervals; Maximum Likelihood Method; Distribution Fit.

I. INTRODUCTION

Following the ideas of sustainable growth, the World is increasing the use of wind to generate electrical energy. As an alternative to fossil fuels, it is plentiful, renewable and widely distributed around the globe [1]. The problem involving this source of energy is that the wind might be inconsistent as it is strongly influenced by the weather conditions and other sources of energy are needed to cover the deficit from wind farms.

As the participation of wind farms in the electrical grid is raising, the challenge to maintain the balance between power generation and load is even harder. Another sources of energy must be kept in order to compensate eventual changes in the wind power output. In this scenario, it is very important to have accurate wind power forecasts. As the forecast improves its accuracy, the need of other sources of energy, such as thermal units, are minimized, representing a cost reduction to the system. The cost of wind power forecast errors in a single plant is around €15,000 - 18,000 per MW of installed capacity [2], which is the production capacity of a plant.

In order to improve the wind power forecast, which is mostly represented as a single value, confidence intervals can be built. They represent a range of estimated values for a certain probability. These intervals increase the amount of information of the prediction, making it easier to operate the system. There can be different intervals for distinct timescales. This kind of estimation is important because the system must be able to anticipate the needed load by increasing the generation from other sources, such as hydroelectric power, like Brazil, or slow starting thermal units. And this is why it is really important to have forecasts done with results for every hour to one day ahead.

The generation of confidence intervals is highly correlated to the forecast error distribution. It is very common to assume that the errors can be represented by a Gaussian distribution in every timescale. This assumption can create errors and the system may overestimate or underestimate wind power generation, and this represents extra costs to the system operation [2].

Some studies have concluded that these errors are better represented using a Cauchy or Weibull distribution when compared to a Gaussian or Beta distribution [3]. One of the objectives of this work is to study the error distribution of a wind power forecast generated by a Reservoir Computing network using data from a real wind farm in Brazil. This work will evaluate which distribution represents better the error in different timescales doing a distribution fit, in order to improve the forecast (Figure 1).

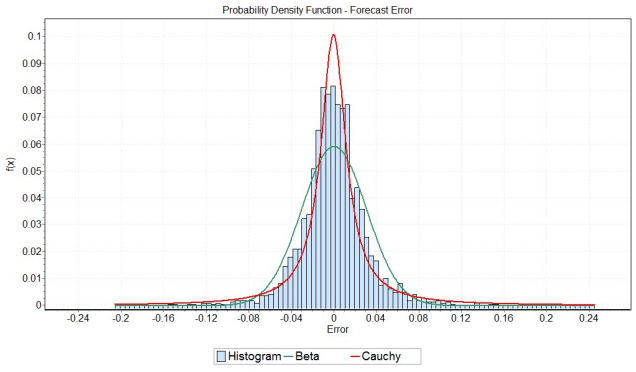

Figure 1. Normal vs. Cauchy Distribution.

After finding the distribution that fits better the forecast errors, it will be possible to compare the confidence intervals generated. The method used to generate the interval is proposed by Nandeshwar [4], the maximum likelihood method. The method assumes that a prediction has two uncertainty sources. The first one is related to the prediction error and the second one is related to the error generated by the network

 ISBN: 978-1-61208-340-7

when trying to predict its own error. The maximum likelihood method uses these two values to generate an upper and a lower limit to represent the confidence interval. The final objective is to compare and evaluate the confidence intervals generated for distinct timescales using values from the distribution that fit better with forecast values.

This paper is organized as follows. Section II contains the basic explanation about *Reservoir Computing* and its training. All the information about the distribution fit problem is explained in Section III. Details about confidence intervals and the methods to generated them used on this paper are reported in Section IV. Section V explains the methodology used, giving details about the database used, how the network was trained and how the distribution fit was done. The results are shown on Section VI and the conclusions in Section VII.

II. Reservoir Computing

Artificial Neural Networks are mathematical models of computer intelligence based on the behavior of the human brain and its basic unit, the neuron. Inspired by the biological neuron, the artificial neuron was modeled. It is capable of processing entering signals (inputs) and generating one or more outputs, representing a synapse [5].

A Multi Layer Perceptron network (MLP) determines new rules for neurons' organization. Unlike the previous networks, it has a hidden layer. This new layer is responsible for the non linearity of MLP, making it possible to solve non-linearly separable problems, like the most of real problems.

The Reservoir Computing is presented as a network of several layers including the principle of recurrences in its links. Thus, the network is no longer feed-forward and the signal propagates through the network in several directions.

One of the ideas that gave rise to the Reservoir Computing network was the Echo State Network [6]. It is characteristic of it that a neuron in the middle layer can be interconnected, including with itself. This topology creates cycles within the network, and the signal propagated "echoes" by these recurrences. The network creates a kind of signals memory. The signals lose strength with time as they propagate through cycles (Figure 2).

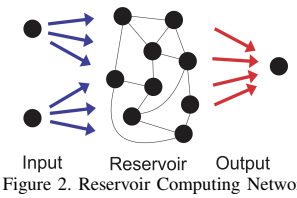

Figure 2. Reservoir Computing Network.

The topology of the network does not allow the use of simple training methods as used in MLP, the backpropagation method. The difference is caused by the recurrences. The method used in this work uses the matrix inversion (JAMA) to adjust the weights connected to the output layer. The other weights are determined once and remain the same during the whole training.

With these characteristics, Reservoir Computing is proposed to be a powerful tool to solve dynamic problems related with time processing and continuous values just like the wind power prediction [7], and this is why it was chosen. Because of its recent implementation, some of the Reservoir Computing's properties are not theoretically based and they are set empirically.

III. Distribution Fit

As the Reservoir Computing returns a set of predicted values using the input data, the error can be calculated subtracting it from the real values for each output. Some information of theses errors need to be extracted in order to generate the confidence intervals. One of them is the error distribution, which is often assumed to be Gaussian/Normal, and it is not true for all the cases. This kind of mistake can have a huge impact on the confidence interval accuracy [2].

Probability distribution fitting, or just distribution fitting, is a way to fit a probability distribution function to a data set by observing data characteristics to adjust the distribution's parameters. Doing this it is possible to predict the probability of occurrence of a certain phenomenon. There are many distributions of which some can represent a data set better than others, depending on the data characteristics. The distribution giving a close fit is supposed to lead to good predictions.

The distributions evaluated in this work are normal, beta, cauchy and weibull distribution. Each of these will be fit to the set of errors generated by the network and the results will be compared. The Kolmogorov-Smirnov test will be used to decide which distribution fits better to the set of errors. As the model have predictions for every half an hour for 24 hours, there can be a variation of which distribution fits better depending on the timescale. The prediction may present different results for a short timescale (+00:30 or +01:00) when compared to a long range timescale (+24:00) for example.

IV. Confidence Intervals

In a prediction model, the output value does not represent much information to the user. To use it in a proper way there is a need to know how much reliable the model is, or how certain it is about the outputs. Because even a unstable model may present random good results for a period of time.

The confidence intervals have as its objective measure the reliability and also aggregate information to the results presented. Instead of estimating one single value, a interval of probable estimates is given. The range of this interval will determine the quality of the results presented for a specific problem. If the interval is too wide, it means that the reliability is low and the model shows unstable results. If the interval is thin, it means that the results are constant and the model is reliable.

With higher probabilities wider will be the intervals. But if it is too wide, it means that the results are poor on information about the problem. In a ideal situation, the model will generate a thin interval for a high value of probability of containing the occurred value. The value of probability is chosen by the needs of the user.

In other models based on neural networks, confidence intervals are implemented using traditional linear statistical models [8].

In neural networks prevision based models, the confidence intervals have generally been set grounded by traditional linear statistic models [8]. However, as neural networks are non-linear models those linear methods are not always appropriate so that new proposals are being tested, such as the maximum likelihood method.

 ISBN: 978-1-61208-340-7

A. Maximum Likelihood Method

To create a confidence interval, it is necessary to set an upper and a lower limit from the chosen probability and the results obtained in network training.

In this work, we applied the maximum likelihood method [4] proposed by Nandeshwar. The method assumes that there are two sources of uncertainty in a interval prediction model:

- The first is the noise variance (σ_v^2), calculated from the variance calculation standard equation (2) applied to absolute errors (1).
- The second is the uncertainty's variance (σ_w^2), calculated from a separate network variance (2) errors that aims errors generated by the first network training. This second variance is related to the network's ability to predict the error itself.

$$Error = |occurred\_value - calculated\_value| \quad (1)$$

$$\sigma = \frac{1}{n-1}\sum_{i=1}^{n}(Error_i - \widehat{Error})^2 \quad (2)$$

where:

$Error_i$ = Errors regarding the i entry.

$\widehat{Error}$ = Errors average.

The total variance is determined by the sum of the two previously calculated variances (3).

$$\sigma_{total}^2 = \sigma_v^2 + \sigma_w^2 \quad (3)$$

The calculation of the confidence interval is done using (4). Given a predicted value f(x):

$$f(x) - t * \sigma_{total}^2 < f(x) < f(x) + t * \sigma_{total}^2 \quad (4)$$

where t is the extracted value of the t Student's table. In this work the largest possible degree of freedom has been chosen combined with an alpha value of 5%.

The algorithm on Figure 3 shows the steps to generate the confidence interval using the maximum likelihood method.

1 Divide the database into training data and test data;
2 Normalize data;
3 Train the network;
4 Calculate the error variance σ_v^2 (2);
5 De-normalize data;
6 Calculate errors (calculated - occurred);
7 Normalize data again;
8 Train a new network with the same inputs, aiming errors calculated in step 6;
9 Calculate this network's error variance, σ_w^2 (2);
10 De-normalize data;
11 Calculate σ_t^2 (3);
12 Select the appropriate confidence level and find its value in the t Student's table;
13 Calculate the range for the values obtained with the test data (4).

Figure 3. Maximum Likelihood Method.

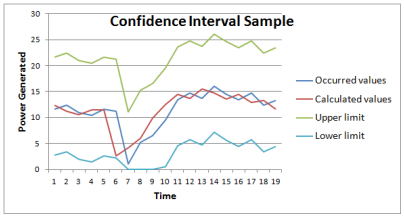

Figure 4. Confidence Interval sample.

The confidence interval validation is made using the occurred and the calculated values. When applying the interval, the occurred values must be within the range of the interval with the same probability used to choose the value of t in the t Student's table (Figure 4).

V. METHODOLOGY

A. The Database

In order to achieve the objectives of this work, a real database was used. The data come from a real wind farm in Brazil containing measurements for every 30 minutes including wind speed, direction and generated power. Each value represent a mean calculated from every windmill in the farm. They also include the date it was measured, the standard deviation, minimum and maximum value for each type of data. The installed capacity of this wind farm is 54.61MW.

In total, there are 11712 measurements. Therefore, a few values are missing due to problems during the measurement. This instants are not using during the network training. All values chosen to be the inputs on the network's training are values of mean generated power. The whole data is spited in 3: training, cross validation and testing set.

Before using the data for training, it must be normalized (step 2 on the algorithm show on Figure 3). This is done using a linear transformation 5. The data will be represented on a interval between 0.25 and 0.75.

$$x = \frac{(x - x_{min}) * (b - a)}{x_{max} - x_{min}} + a \quad (5)$$

where:

x_{max} = Maximum value found on the real data.

x_{min} = Minimum value found on the real data.

a = Minimum value for the normalized data.

b = Maximum value for the normalized data.

Doing this the network will deal with values that are alike attributing the same importance to a low and a high value. The de-normalization (step 5 on the algorithm show on Figure 3) is done using this same equation in a reverse way.

B. Reservoir Computing

The Reservoir's structure is an important factor that could determine a good or bad performance for the wind power forecast task. As being a result of recent studies, some network properties are determined empirically.

In this work, a Reservoir Computing network with three layers was created. The first one represent the inputs. To set the number of inputs, the linear correlation was evaluated and it was decided to use 7 past values to be the inputs. Too much past values may confuse the network and too few values may not give enough information to the network. The hidden

 ISBN: 978-1-61208-340-7

layer was set up with 20 neurons determined empirically. Both of these two layers have the sigmoid logistic as the activation function. The output layer has 48 neurons, each one representing one of the 48 instants of half an hour a head that are needed to be predicted. The number of outputs has been chosen according to other existing methods that are already applied on ONS (Brazilian electric system operator).

On the hidden layer, there is a 20% probability of existing a connection between two neurons where it could be positive or negative by the same chance. This probability value determines the amount of recurrences in the network.

Based on previous work this Reservoir Computing network has a little improvement from the basic version. It has connections between the input layer and the output layer. This feature leads to better results.

The training uses 75% of the database, where 50% is used for initial training and 25% is used for cross-validation. The rest is used for tests where values that never have been shown to the network are used to evaluate its results.

The training can be stopped if a maximum number of cycles have occurred or if the network is not improving itself anymore. For this evaluation, the mean squared error is calculated using (6). If the error stops decreasing it means that the network has been stable and need no further training.

$$MSE = \frac{1}{n}\sum_{i=1}^{n}(x_{calc_i} - x_{obs_i})^2 \quad (6)$$

The last part of training is the test phase. The predicted values generated on the test phase are used to evaluate the results of the network and also to create the confidence intervals. The error for each timescale is calculated by subtracting the real value minus the predicted value, doing this we get a set of errors for each one of the outputs. As the Reservoir presents predictions for distinct timescales, the confidence intervals may present different behaviors. For each one, the distribution fit is applied in order to find a probability distribution to represent the errors in a certain timescale and generate a better confidence intervals.

C. Distribution Fit

The distribution fit can be done by adjusting the parameters of a certain probability distribution using the characteristics of a set of values. In this work, the normal, beta, cauchy and weibull distribution are adjusted to the sets of errors obtained on the Reservoir's training. To evaluate which one is more similar to the error set, the Kolmogorov-Smirnov test is used. This test is used to compare a sample with a reference probability distribution.

Using this method, it is possible to rank the four distributions for errors in each timescale. As the errors present distinct behaviors for different timescales, it is possible the rank have variations for each scale and this will make it possible to choose the best distribution for each case.

VI. Results

A. Maximum Likelihood Method

In order to evaluate the behavior of the maximum likelihood method applied over the prediction of generated power done by a Reservoir Computing network, the hit rate of the confidence interval must be observed. This means that the number of real values inside the boundaries created by the confidence intervals must be coherent to the confidence level chosen, in this case 95%.

TABLE I. Maximum Likelihood results table.

Maximum likelihood method results				
	Sigma V	Sigma W	Sigma T	Hit Rate
+00:30	4.311594	4.302589	6.09115	96.71%
+12:00	13.61194	13.5954	19.2358	99.63%
+24:00	11.8412	11.8304	16.74022	98.56%

The results can be observed on Table I. As the prediction has different properties for distinct time scales the results are shown in 3 moments: Half hour ahead, 12 hours ahead and 24 hours ahead.

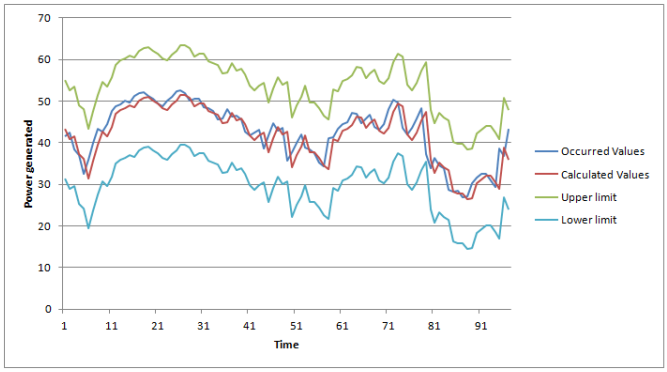

Figure 5. Maximum likelihood interval for +00:30.

The results show that the predicted values are really close to the real values (Figure 5) and the prediction error present low variance for a short range of time (+00:30). This statement can be observed on the corresponding line on Table I.

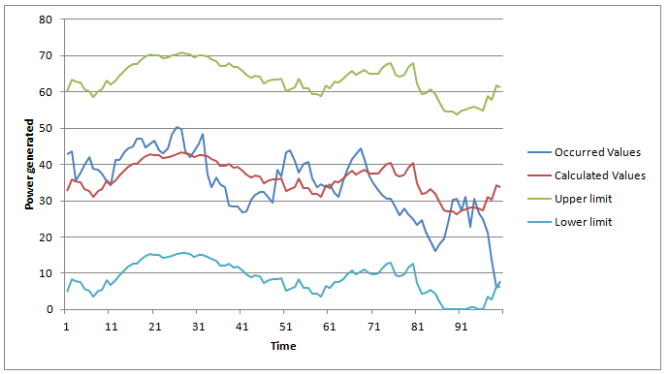

Figure 6. Maximum likelihood interval for +24:00.

For instants that are far ahead, 12 or 24 hours ahead, and the correlation with past values is lowered the Reservoir does not show constant results and the error variation is increased (Table I). For this reason, the confidence intervals generated are wider (Figure 6) and the hit rate is increased because of the interval's range. This means that the Reservoir has poor results on these timescales, which can be justified by the low correlation caused by the randomness of the wind in a larger

 ISBN: 978-1-61208-340-7

TABLE II. Distribution Fit +00:30 results table.

	Kolmogorov-Smirnov	
Distribution	Statistic	Rank
Cauchy	0.05301	1
Normal	0.07168	2
Beta	0.0719	3
Weibull	0.12251	4

TABLE III. Distribution Fit +12:00 results table.

	Kolmogorov-Smirnov	
Distribution	Statistic	Rank
Beta	0.03576	1
Weibull	0.04459	2
Normal	0.04569	3
Cauchy	0.10767	4

timescale, compromising the prediction and the confidence interval's quality.

B. Distribution Based Method

Before generating the confidence intervals using the distribution based method, the distribution fit must be evaluated using the Kolmogorov-Smirnov test. It may be observed that for each timescale there was a distribution that fits better with the errors set (Tables II, III, IV), and this one will be used as a reference to generate the confidence interval.

For half an hour ahead (+00:30), the probability distribution that fit better with the forecast error distribution was cauchy (Figure 7). The K-S test pointed it as being the most similar between to the error distribution. The normal and beta distribution had similar results and weibull showed the poorest result for this time scale (Table II).

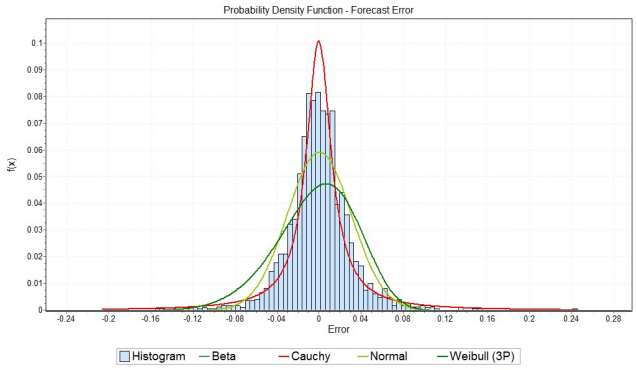

Figure 7. Distribution Fit +00:30.

TABLE IV. Distribution Fit +24:00 results table.

	Kolmogorov-Smirnov	
Distribution	Statistic	Rank
Weibull	0.01944	1
Beta	0.02041	2
Normal	0.02492	3
Cauchy	0.09133	4

For Twelve hours ahead (+12:00), cauchy did not present the same results as for half an hour ahead, it was actually the worst in the Kolmogorov-Smirnov test (Table III). For this timescale the winner distribution was beta followed by weibull and normal in this order (Figure 8).

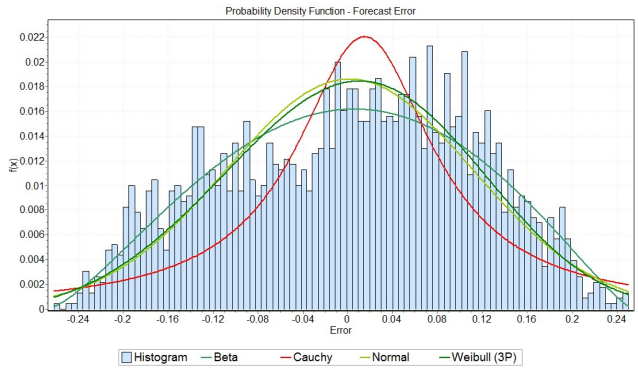

Figure 8. Distribution Fit +12:00.

For twenty four hours ahead, presenting a large variation between the predicted values and the real values, the distribution that fit better with the error distribution was weibull (Table IV), followed by beta, normal and cauchy (Figure 9).

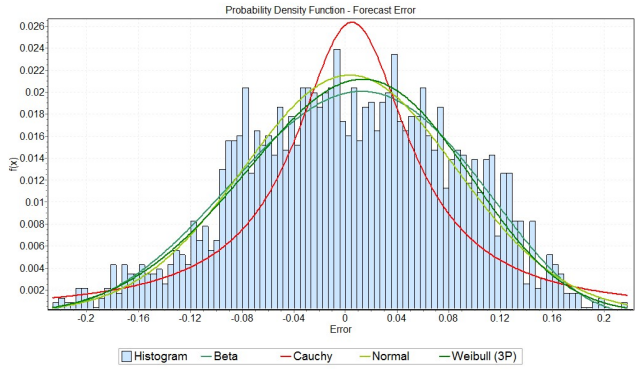

Figure 9. Distribution Fit +24:00.

Having the results previously mentioned, it is possible to generate the confidence intervals based on the right probability distribution. As seen, the error may be represented better by a certain distribution in a timescale, and this one will be chosen to create the intervals for that instant.

Generated for a half an hour ahead timescale, the first confidence interval will use the cauchy distribution (Table II). As it is fit to the error distribution, the values are extracted from it according to the confidence level chosen, 95%. Being the distribution asymmetric, two values must be extracted, one for the positive side and one for the negative side. These values are -0.164 and 0.184. To establish the upper and lower limit of the confidence interval these values must be multiplied with the installed capacity of the wind farm and then added the calculated value (Reservoir's output).

Part of the interval for +00:30 may observed on Figure 10. It was obtained a hit rate of 98.2668% (real values inside the confidence interval's range).

 ISBN: 978-1-61208-340-7

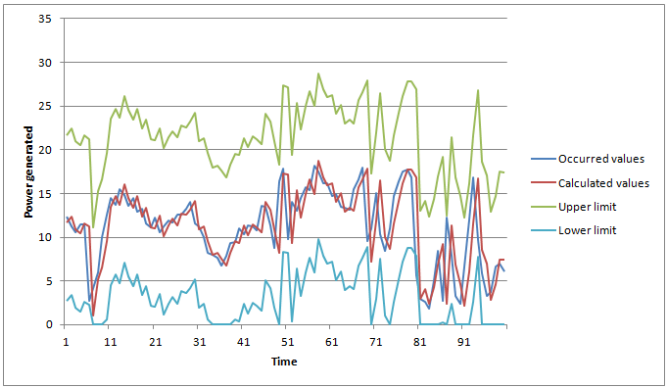

Figure 10. +00:30 Confidence interval sample.

Using beta distribution, the confidence interval generated for a +12:00 timescale may be observed on Figure 11. The values extracted from the distribution are -1.66 and 1.64, also following the 95% confidence level. The hit rate was 88.99%.

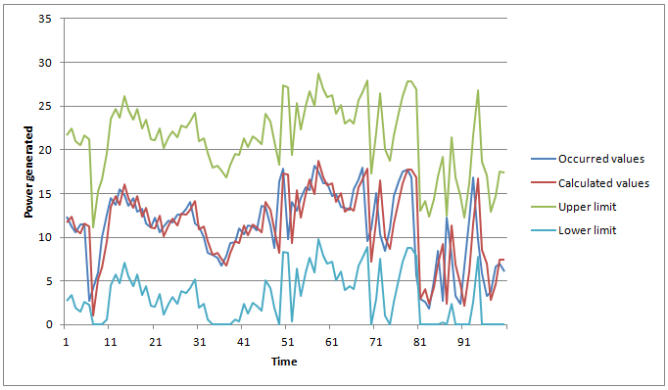

Figure 11. +12:00 Confidence interval sample.

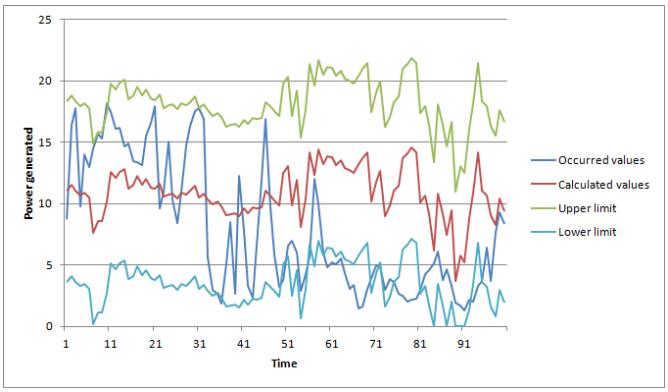

Figure 12. +24:00 Confidence interval sample.

For twenty four hours ahead (+24:00) and using the weibull distribution, a sample of the confidence interval for this timescale may be observed on Figure 12. The values extracted from this distribution are -1.36 and 1.33 and the hit rate is 90.1646%.

VII. Conclusion and Future Work

Analyzing the presented results, it is possible to take a few conclusions about the generation of confidence intervals applied on the wind power forecast done with Reservoir Computing. Also, it is possible to compare the two methods used in this work.

The maximum likelihood method showed coherent results for a short range timescale (+00:30). The confidence interval has a hit rate close to what it was proposed (95%) and it is not too wide. For the cases where the Reservoir Computing did not generate stable results and the error variation was high (+12:00 and +24:00), the maximum likelihood method did not show good results. As the variation is high, the intervals show a wide range for the same 95% confidence level.

The distribution based method presented good results for all three timescales. In all of them the confidence interval's width is quite similar and the hit rate is close to what it was proposed, the 95% of confidence level. This proves that a distribution analysis is worth done in order to improve the generation of the confidence intervals.

Comparing the result of these two techniques, it is possible to conclude that they show similar results for sets that present a distribution with low variation. In the other case, where there is some large variation, the distribution fit helped the creation of better confidence intervals with the same confidence level but with a shorter range.

In the future works, these techniques will be applied to other set of data that have different characteristics in order to compare the results. Also, another model must be tested in the prediction to check if this result are only related to the Reservoir Computing's outputs. Other techniques to generate confidence intervals must be evaluated.

References

[1] A. L. Sá, "Wind energy: principles and aplications." [Online] Avaliable from: http://www.cresesb.cepel.br/ , acessed on August 09th, 2012.

[2] B. Hodge and M. Milligan, "Wind power forecasting error distribution over multiple timescales," *To be presented at the Power & Energy Society General Meeting*, 2011.

[3] B. Hodge, A. Florita, K. Orwig, D. Lwe, and M. Milligan, "A comparison of wind power and load forecasting error distributions," *Presented at the 2012 World Renewable Energy Forum*, 2012.

[4] A. R. Nandeshwar, "Models for calculating confidence intervals for neural networks," Master's thesis, West Virginia University, 2006.

[5] M. J. S. Valenca, *Fundamentos das Redes Neurais*. Livro Rapido, 2011.

[6] M. Lukosevicius and H. Jaeger, "Reservoir computing approaches to recurrent neural network trainning," *Computer Science Review*, vol. 3, August 2009, pp. 127–149.

[7] D. Verstraeten, *Reservoir Computing: computation with dynamical systems*. PhD thesis, Ghent University, 2009.

[8] D. S. Moore, *The Basic Practices of Statistics*. W.H. Freeman and Company, 3rd ed., 2005.

 ISBN: 978-1-61208-340-7

A Comparative Study of Neural Network Techniques to Perform Early Diagnosis of Alzheimer's Disease

Lara Dantas and Mêuser Valença
Polytechnic School of Pernambuco
University of Pernambuco
Recife, Brazil
Email: {ldc, meuser}@ecomp.poli.br

***Abstract*—The life expectancy of the population in most developed countries is growing every day and hence there is an increase of several age-related diseases. In Brazil, about 1.2 million people have Alzheimer's disease (AD), now considered the most common type of dementia in the population. Although it is a degenerative and irreversible disease, if diagnosed early, medications may be administered to slow the progression of symptoms and provide a better quality of life for the patient. Previous studies with classifiers contained in the software Weka using a database with values of 120 blood proteins, and they noticed that they could classify the patient may or may not be diagnosed with AD with an accuracy rate of 94% and 85%, respectively. Thus, this study aims to use a new connectionist approach called Reservoir Computing (RC) to perform early diagnosis of a patient with or without AD, also compare these results with those obtained using a Neural Network Multi-Layer Perceptron (MLP). This article also envisions to utilize the Random Forest Algorithm to select proteins from the original set and, thus, create a new protein signature.**

Keywords–Reservoir Computing; Alzheimer's Disease; Neural Network.

I. INTRODUCTION

More developed countries are undergoing a major demographic shift. The older segments of the population are growing at a faster rate, and therefore, there is an increase in age-related diseases, especially progressive dementia disorders. First described by psychiatrist Alois Alzheimer in 1907, Alzheimer's Disease (AD) is today the most common cause of dementia in the elderly population.

According to the Brazilian Institute of Geography and Statistics (IBGE) and the World Health Organization (WHO), there are 1.2 million people with AD in Brazil. It is believed that only 5% of the patients developed the disease at an early stage, i.e., before 65 years of age. In patients where the AD started after 65 years old, it is estimated that between 10% and 30% of cases started after 85 years old [1].

AD is a degenerative disease that causes irreversible death of several brain cells, the neurons. The patient suffering from this disease has a brain with microscopic pathologic lesions, known as neuritic plaques, and neurofibrillary tangles [2]. In addition, the brain of a person with Alzheimer's is much smaller than the brain of a healthy person.

This disease develops in each patient in a unique way; however, there are several symptoms common to all of them, for example, loss of memory, language disorders, depression, aggression, among others.

Initially, the patient loses episodic memory, i.e., memory that holds information of events and their spatio-temporal relations. Thus, the old facts and the facts that just happened are easily forgotten.

With the progress of the disease, semantic memory is also lost, i.e., lexical knowledge, rules, symbols are forgotten and the patient begins to lose its cultural identity [3].

Although it is an irreversible disease, if it is discovered in its early stage, medications may be administered to slow the progression of symptoms and prolong the patient's welfare [4]. Thus, it is extremely important that mechanisms are developed for the prediction of AD in the whole population.

In the literature, Herbert et al. [5] conducted a study using a database of 120 samples of proteins contained in plasma of several patients. He concluded in his research that a combination of 18 of the 120 available proteins enabled the realization of early diagnosis of AD with a accuracy rate of 91% using a set of tests with data from 92 patients who were diagnosed with AD or not.

In addition, he also used another set of tests containing data from 47 patients diagnosed with Mild Cognitive Impairment (MCI). For this set, the accuracy rate was 81%. These values were calculated from the average success rates found for all classifiers used in clinical trials for both sets [6].

Afterwards, Gòmez [6] conducted a study using 20 different classifiers available in the software Weka and set various signatures with 18, 10, 6 and 5 proteins. These proteins were all contained in the set described by Herbert et al. The 10 protein signature reached a accuracy rate of 89% using the AD test set and of 66% for the MCI test set. These success rates were also calculated from the average values of the 20 classifiers used [6].

Since the results available in the literature use only classification techniques provided by the software Weka [7], this work will use a new connectionist approach called Reservoir Computing (RC) [15] to perform the classification of a patient, given the set of 5 and 10 proteins defined by Gòmez et al.

In order to compare the results obtained using the RC, the classification was also performed using a Multiple-Layer Perceptron neural network (MLP). This topology is widely used and it has a good performance for classification problems [8].

In addition to that, a study using the Random Forest Algorithm [9] was conducted in order to select a new signature of 10 proteins for the prediction of the Alzheimer's Disease and another for the diagnosis of MCI. This step was performed to reduce costs for the diagnosis since Gòmez used paid sofware and other techniques for variable selection.

 ISBN: 978-1-61208-340-7

This article is organized into several sections. The first section contains information about the operation, structure and simulation of Reservoir Computing. The next section describes the methodology used throughout this work, i.e., what is the database used and how it is organized, the experiments and statistical analysis that was performed. Finally, there is a section that displays the results and the last one with the conclusions obtained in this work.

II. *Reservoir Computing*

Recurrent Neural Networks (RNN) were created to enable the solution of dynamic problems. This is accomplished through a feedback of a neuron in a layer i to that found in some previous layer, $i - j$. This neural network topology has a better resemblance to the operation and behaviour of the human brain [10].

In 2001, a new approach for the design of the training of a RNN was proposed by Wolfgang Mass called Liquid State Machine (LSM) [11]. At the same time, but independently, the same approach was described by Herbert Jaeger and called Echo State Machine (ESN) [12].

Both ESN and LSM networks have the Echo State Property (ESP) [13], i.e., due to the recurrent network connections, information from previous entries are stored. However, these data are not stored for an infinite period of time, and as well as the human brain, old information must be forgotten over time. Thus, the neural network has a rich set of information from the past and present therefore enhancing its applicability to dynamic systems [14].

In 2007, Verstraeten coined the term Reservoir Computing (RC) that unified the concepts described in ESN and LSM. Since then, this term is used in literature to illustrate learning systems which are represented by a dynamic recurrent neural network [15].

The RC is composed of three parts: an input layer, which as the MLP, represents the input variables of the problem, a reservoir, which can be seen as a large distributed and dynamic RNN with fixed weights, and a linear output layer called readout.

Figure 1 represents the RC topology with two neurons in the input layer, three in the reservoir and one neuron in the output layer.

A. *Construction and Simulation of RC*

The RC used in this work was developed in the Java programming language to make use of the object-oriented paradigm. This framework was created in order to solve classification and prediction problems and it was validated by three Benchmarks available: Iris species, Thyreoide cancer and diabetes.

The first step to be taken in order to prepare the RC and perform the data set classification is configuring its architecture. Thus, it is necessary the amount of neurons that will be used in input and output layers and the reservoir itself is defined.

Furthermore, several RC parameters should also be determined. Being a recent methodology, there are no studies that

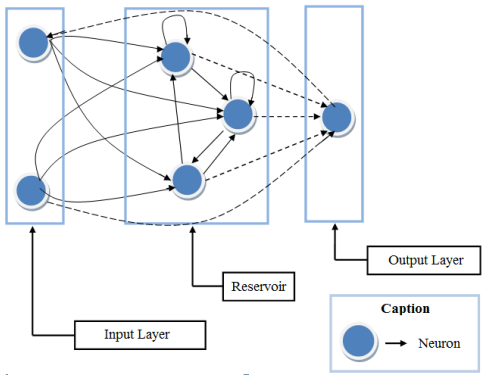

Figure 1: RC architecture. The dashed lines represent the weights that should be adjusted during the training of the network.

prove how many neurons in the reservoir are necessary so that the neural network has better performance, or the rate of connectivity between these neurons. Therefore, for this work, values were defined based on some empirical tests performed.

Once the architecture of the neural network is determined, the next step is to generate the weight matrices connecting the input layer to the reservoir, W_{in}, and the matrix with the weights between neurons in the reservoir, W_{res}. Both matrices are generated with random values between -1 and 1.

Studies claim that the matrix W_{res} must have a spectral radius equal to 1 to provide a more numerical stability [16], i.e., when W_{res} is initialized, it must have its values changed as follows:

- Initially it must be decomposed into singular values;
- Then, W_{res} should have its values changed until the maximum value of the main diagonal of the eigenvalues matrix is less than or equal to 1.

To perform the simulation of the RC, the database is divided into three sets: training, used to perform the update of the states of the neurons of the reservoir, cross-validation, used to stop the training of the neural network, and test set, used to calculate the RC classification rate [17].

The states of the neurons in the reservoir must be initialized to zero. Since this is a recurrent network and RC stores its states (M_{est}) in a matrix, it is necessary that the final values found by the network are not so influenced by this initialization. Therefore, the literature suggests that before start training, a set of cycles called warm up is executed in order to perform updates in the states of the neurons in the reservoir and overlook the influence of the initial value. The states are updated according to (1) [15]:

$$x[k+1] = f(W_{res}x[k] + W_{in}u[k]) \quad (1)$$

where, $W_{in}u[k]$ represents the matrix containing the result of the product of the values derived from the input layer by the weights connecting these neurons to the reservoir at a time k and $W_{res}x[k]$ is the matrix with the states of the neurons from

 ISBN: 978-1-61208-340-7

the reservoir at the same time k. The result will be assigned to $x[k+1]$, i.e., the state of the neuron RC in an instant forward will be the result of calculating the activation function of the neuron from the sum of the two parcels described above. In this work, the activation function used was the hyperbolic tangent according to 2.

$$f(net_i) = \frac{e^{net_i} - e^{-net_i}}{e^{net_i} + e^{-net_i}} \quad (2)$$

Once the period of warm up is over, the training of the RC can be initialized. The first step should be to load the training set and perform the update of the states of the reservoir, noting that the matrices W_{in} and W_{res} should not be changed. They are randomly generated during construction of the RC, as described in the previous section, and should not be adjusted.

Still during training, the weights matrix that connects the neurons of the input layer to the output (W_{inout}) and the one that connects the reservoir to the output must be calculated by the pseudo-inverse of Moore-Penrose. As they are non-square matrices and their determinants can approach zero, it is necessary to calculate the pseudo-inverse.

At the end of each training cycle, a cross validation cycle should be initiated. This process should be repeated until the stopping criteria is reached and the training set is finalized. During the process of cross-validation, the matrices W_{inout} and W_{out} should remain being readjusted.

When the process of training is finished, the testing process begins. The set of tests is presented to the RC and at this time, all the weights matrices, W_{in}, W_{res}, W_{inout} and W_{out}, should remain unchanged, as the matrix M_{est}. At this point, the classification error is calculated. These values will be used in the future to make the necessary comparisons.

The behaviour of the RC can be best viewed through the algorithm described in Figure 2.

Pseudocode of RC

```
1  Set the number of neurons in the input layer ;
2  Set the number of neurons in the reservoir layer ;
3  Set the number of neurons in the output layer ;
4  Randomly generate the weights of Win matrix between
   -1 e 1;
5  Randomly generate the weights of Wres matrix between
   -1 e 1;
6  Normalize the weights of Wres matrix so that the
   spectral radius of the matrix is smaller than or equal to
   1;
7  while until the end of the number of warm up cycles do
8  |  updates the states of the neurons of the RC;
9  end
10 while until the stopping criterion is reached do
11 |  for each value of the input set do
12 |  |  updates the states of the neurons of the RC;
13 |  end
14 |  Calculates the Moore-Penrose inverse matrix to find
   |  the weights connecting the RC to the output layer;
15 |  Calculates the Moore-Penrose inverse matrix to find
   |  the weights connecting the input layer to the output
   |  layer;
16 |  for each value of the cross-validation set do
17 |  |  updates the states of the neurons of the RC;
18 |  end
19 |  Calculates the output values of the RC;
20 |  Calculates the RMSE;
21 |  Checks if the stopping criterion has been reached;
22 end
23 for each value in the set of tests do
24 |  updates the states of the neurons of the RC;
25 end
26 Calculates the output values of the RC;
27 Calculate the accuracy rate;
```

Figure 2: Reservoir Computing pseudocode

III. METHODOLOGY

A. Database

The database used in the development of this work was the same used by Gòmez et al. in his publication. It has values of 120 proteins found by analysis of blood samples from different patients. The ultimate goal of the database is to classify whether a patient can be diagnosed or not with AD or MCI [6].

In his work, Gòmez et al. [6] subdivided the database in 2 sets. The first set contained the results of blood samples of 83 patients. Of these 83 patients, 68 were allocated to the training process of the chosen classifier. The data for the remaining 15 patients were used in the process of cross-validation of the classifier, i.e., a process that determines the optimal point to stop its training [8].

The second set, used in the testing process of the classifier, has two options. It could be used to diagnosis AD and in this case, this set will contain the samples related to the 92 patients that could be diagnosed with AD. The second option is use this set to perform diagnosis of MCI. In this other case, the test set will contain blood samples related to 47 patients with a possible diagnosis of MCI.

Aiming a comparison with the signatures previously defined by Gòmez et al. [6], two new signatures of 10 proteins were proposed. One of them used to perform the diagnosis of Alzheimer's Disease and another for MCI.

The Random Forest algorithm was executed 30 times and in each of the simulations, a signature of 10 proteins was defined. To choose the best signature among 30 proposals, a new classifier was used to determine which one got a better classification rate.

Thus, the Support Vector Machine (SVM) was chosen to perform 30 executions with each signature. Thus, an average of the classification rates was calculated, besides the analysis of the standard deviations. The signature that obtained the best average classification rate was chosen to be used later by the RC and the MLP.

It is important to mention that Gòmez defined the same signature for both cases, that is, the signature composed by 10 proteins is used for the AD and MCI testing sets.

Table I shows the signatures of proteins that are contained in Gòmez et al. work and which are used in this study.

In this work, 4 databases were prepared in order to reproduce the experiments described by Gòmez et al., using the MLP and the RC. They were:

- 1 database for testing the signature of 10 proteins defined by Gòmez et al. with the DA set of tests, called

TABLE I: Representation of the proteins contained in each one of the signatures used.

Abbreviation	Signature	Proteins
S1	**10 proteins signature defined by Gòmez et al.**	CCL7/MCP-3, CCL15/MIP-1d, EGF, G-CSF, IL-1a, IL-3, IL-6, IL-11, PDGF-BB, TNF-a [6]
S2	**10 proteins signature defined by the Random Forest for AD test set**	IL-1a, TNF-a, G-CSF ,PDGF-BB, IGFBP-6, M-CSF, EGF, IL-3, GDNF, Eotaxin-3
S3	**10 proteins signature defined by the Random Forest for MCI test set**	IL-1a, PDGF-BB, EGF, TNF-a, RANTES, FAS, GCSF, MIP-1d, FGF-6, IL-11

now by **Database 1**;

- 1 database for testing the signature of 10 proteins defined by Gòmez et al. with the MCI set of tests, called now by **Database 2**;
- 1 database for testing the signature of 10 proteins defined by Random Forest Algorithm with the DA set of tests, called now by **Database 3**;
- 1 database for testing the signature of 10 proteins defined by Random Forest Algorithm with the MCI set of tests, called now by **Database 4**;

All databases described above maintained the organization used by Gòmez et al. regarding the division of values for the training, cross validation and testing set.

1) Pre-processing of data: To properly execute the training of the neural network it is necessary that your data is normalized, i.e., the input values of the neural network must be contained in the same numerical range. This is important since very different values can influence the training and generate a loss in the generalization ability of the neural network [8].

One of the most commonly used normalization techniques in literature is the linear transformation and it was the one chosen for this work. Equation (3) is the formula used to normalize the values of the database.

$$y = ((b - a) \times (\frac{x - x_{min}}{x_{max} - x_{min}})) + a \quad (3)$$

In (3), a and b represent the maximum and minimum values that the data should take. In this work, it was used the value of -0.85 for a and 0.85 for b, as the activation function chosen for this neural network is the Hyperbolic Tangent. Therefore, the values contained in the database must be between -1 and 1.

B. Simulations

As described above, in order to compare the results obtained with RC, it was used a neural network MLP. Table II shows which parameters were chosen to perform the simulations with the RC and MLP. They were obtained through empirical testing and the settings that showed the lowest mean squared errors in the cross-validation procces were chosen.

After defining the settings of the RC and the MLP, 30 simulations were performed with each of the databases in each of the chosen neural network topologies in this work. This number is considered ideal to perform more meaningful statistical comparisons [18].

TABLE II: Representation of the parameters used for the simulations with the RC and MLP

Parameters	RC value	MLP value
RC connectivity	20%	Not applicable
Number of neurons in the input layer	10	10
Number of neurons in the RC	4	Not applicable.
Number of neurons in the hidden layer	Not applicable	20
Number of neurons in the output layer	2	2
Number of warm up cycles	100	Not applicable.
Activation function of neurons in the reservoir or hidden layer	Hyperbolic Tangent	Hyperbolic Tangent
Activation function of neurons in the output layer	Linear	Linear
Learning rate	Not applicable.	0.7
Momentum	Not applicable.	0.4

C. Statistical Analysis

When all the simulations were completed, it was necessary to perform a sequence of statistical tests in order to scientifically validate the results. For this, it was used the R mathematical software, since it contains all the implementations of the tests used. This software uses as default a level of significance (α) previously defined with the value of 0.05.

Before using a parametric test on a data set is necessary to check whether the samples are normally distributed and if they have statistically equal variances. If these two assumptions are validated, one can apply a parametric test, otherwise it must be used a non-parametric test.

Thus, it was applied the Shapiro-Wilk test to verify whether or not the samples were normally distributed and the F-test to verify whether or not the samples were drawn from the same population, i.e., if their variances were statistically equal.

As none of the four datasets met these two premises at the same time, it was not possible to perform the Student's T-test. Thus, it was chosen the Wilcoxon Rank-Sum Test, since it is a non-parametric test, i.e., makes no assumptions about the probability distribution of the samples.

IV. RESULTS

After all simulations were performed with the databases, it was calculated the arithmetic mean for each set of simulations and Table III displays those values found.

When applied the Wilcoxon Rank-Sum Test for each of the four cases, the results found were that the MLP has a statistically better performance than the RC, except for the case 2. Thus, with the 10 proteins signature defined by Gòmez et al. and MCI test set, the test indicated there is not statistical differences between the results obtained with both techniques.

In order to verify the performance of the new proposed signatures, simulations with RC and MLP topologies were

 ISBN: 978-1-61208-340-7

TABLE III: Representation of the average accuracy rates after the 30 experiments

Database	Average accuracy rate with RC / Standard Deviation	Average accuracy rate with MLP / Standard Deviation
Database 1	86.62% / 0.026	93.44% / 0.017
Database 2	69.29% / 0.024	68.15% / 0.018
Database 3	90.57% / 0.022	94.31% / 0.008
Database 4	76.59% / 0.047	78.86% / 0.031

TABLE IV: Comparison of the results with the new protein signature proposal obtained with RC, MLP and the ones available in literature.

Protein Signature	RC - Maximum value	MLP - Maximum value	Results found by Gòmez et al.
New 10-protein signature for AD	96.73%	95.65%	93%
New 10-protein signature for MCI	89.36%	82.97%	66%

performed for both the diagnosis of AD and MCI. The results were compared with those found by the same neural networks when the signatures used were the ones defined by Gòmez et al.

In all cases, the classification rate showed improvement when the new signatures were used for both architectures. After the Wilcoxon Rank-Sum test, this statement was confirmed statistically. The maximum and average values are also bigger than those described by Gòmez et al.

Table IV summarizes the maximum values found in the simulations of the RC and MLP. Those results were found using the new signature proposoal with 10 proteins. The Table IV also display the results obtained in the work of Gòmez et al. using ther own signature [6].

From Table IV, it can be concluded that the RC obtained results consistent with those described by Gòmez et al. and succeeded in reaching a maximum value greater than the average found in the literature.

V. Conclusion and Future Work

Nowadays, Alzheimer's disease is one of the most common diseases in the elderly population. More recently, the number of patients has grown significantly since the life expectancy in most developed countries has increased.

AD is a degenerative disease, i.e., brain cells will deteriorate and there is no way to reverse the disease. However, the earlier the drugs are administered, the better the quality of life of the patient since the medication will slow the progression of symptoms.

Thus, this study aimed to verify the performance of a new connectionist neural network approach called Reservoir Computing to early classify if a patient can be diagnosed with AD or not. Moreover, another goal was to make a comparison of the performance of the RC with the MLP neural network, and also with the results available in the literature.

From the statistical tests and simulations, it can be concluded that the MLP presented a superior performance in most cases, although the RC have obtained maximum values higher than the MLP and available in the literature. This can be explained by the fact that the RC is more suitable for use in dynamic systems as it has a good storage capacity.

It is also possible to conclude that the 2 new signatures proposed achieved better results when compared to those showed by Gòmez et al. Furthermore, they also had better perfomance when compared to the results obtained from the same neural network topologies when the signatures used were the ones proposed by Gòmez et al.

Unlike the RC, the MLP has a better ability to approximate non-linear functions and does not contain the property to store the previous state of its neurons, i.e., does not have recurrence.

As future work, it is intended to conduct a comparative study between the RC non-linear approach capability and storage capacity of the network, in order to assess the appropriate parameters to obtain better results.

It will be also carried out a thorough study on parametrization of the RC, such as the definition of the spectral radius size, how many neurons should be placed in reservoir, the degree of connectivity between these neurons. Furthermore, in order to address dynamic problems, recurrence will be implemented between the neurons of the output layer with the reservoir.

Finally, it is intended to invest in more variable selection techniques in order to further optimize the results and to reduce the number of proteins in the signatures used to perform early diagnosis of Alzheimer and MCI.

References

[1] H. Portal. Portal of the brazilian health [retrieved March, 2014] [Online]. Available: http://portal.saude.gov.br/saude/ (2012)

[2] R. Green, Diagnosis and Treatment of Alzheimer's Disease and Other Dementias. Editora de Publicações Científicas Ltda., 2001.

[3] M. Paulo, Dementia of Alzheimer type: diagnostic, treatment and social aspects. Editora de Publicações Científicas Ltda., 1997.

[4] E. Giusti and V. Surdo, Alzheimer's care and family counseling: psychological needs and treatment of dementia. Gryphus, 2010.

[5] H. Charles, Y. Takeda-Uchimura, B. Adam, S. Ray and B. Markus. "Classification and prediction of clinical Alzheimer's diagnosis based on plasma signaling proteins" Nat Med, vol. v13, 2007, pp. 1359 - 1362.

[6] M. Gómez and P. Moscato, "Identification of a 5-protein biomarker molecular signature for predicting alzheimer's disease," PLos One, vol. v3, 2008, p. 12p.

[7] S. David and R. Peter, WEKA Experimenter Tutorial for Version 3-5-8, 2008.

[8] M. Valença, Fundamentals of Neural Networks: Examples in Java, 2nd ed. Livro Rápido, 2009.

[9] StatSoft. Random forests. https://www.statsoft.com/Textbook/Random-Forest. [retrieved: May, 2014]

[10] M. Valença, Applying Neural Networks: A Complete Guide, 1st ed. Livro Rápido, 2005.

[11] W. Maass, Motivation, theory, and applications of liquid state machines. Imperial College Press, 2011.

[12] H. Jaeger, "The echo state approach to analysing and trainning recurrent neural networks," German National Resource Center for Information Technology, Tech. Rep., 2010.

[13] M. Massar and S. Massar, "Mean-field theory of echo state networks," PHYSICAL REVIEW E, vol. 87, 2013.

 ISBN: 978-1-61208-340-7

[14] M. Lukoševičius, A practical guide to applying echo state networks. Springer Berlin Heidelberg, 2012, pp. 659-686.

[15] D. Verstraeten, "Reservoir computing : computation with dynamical systems," Ph.D. dissertation, Ghent University. Faculty of Engineering, Ghent, Belgium, 2009.

[16] A. Ferreira, Araújo, "A method for design and training reservoir computing applied to prediction of time series," Ph.D. dissertation, Universidade de Federal de Pernambuco, 2001.

[17] M. Kulkarni and C. Teuscher, "Memristor-based reservoir computing," in Proceedings of the IEEE/ACM International Symposium on Nanoscale Architectures (NANOARCH'12), Amsterdam, 2012, pp. 226-232.

[18] N. Juristo and A. Moreno, M., Basics of Software Engineering Experimentation. Kluwer Academic Publishers, 2001.

 ISBN: 978-1-61208-340-7

Using Reservoir Computing for Forecasting of Wind Power Generated by a Wind Farm

Bruna Cavalcanti Galle de Aguiar and Mêuser Jorge Silva Valença
Polytechnic School of Pernambuco
University of Pernambuco
Recife, Brazil
Email: {bcga, meuser}@ecomp.poli.br

***Abstract*—One of the main challenges today is the growing global energy demand. In order to meet this need, the most widely used energy sources are oil, natural gas and coal. The main problem with these sources is due to the fact that, besides being extremely polluting, they are non-renewable sources. Therefore, renewable sources are becoming essential for humanity. Among many of them, the wind is the most promising choice. Wind farms have their potential directly related to the wind power, which requires good estimates of this variable in order to build effective strategies and plans. However, this task presents great difficulties due to the complex characteristics of the wind, such as the high variability of its velocity and direction. This paper aims to use the technique of Reservoir Computing for the prediction of wind power generated by a wind farm and compare its performance with the one produced by the Multi-Layer Perceptron, another type of artificial neural network and the most widely used for this purpose. At the end, it will be possible to analyse the results and conclude which one is more appropriate for predicting wind power.**

Keywords*—*Reservoir computing; forecasting of wind power, artificial neural network, MLP.

I. INTRODUCTION

One of the major challenges today is the growing global energy demand. In order to meet this need, the most widely used energy sources are petroleum, natural gas and coal. The main problem with these sources is due to the fact that, besides being extremely polluting, they are non-renewable sources, i.e., will be exhausted from nature within a few years. According to the International Energy Agency (IEA), if we do not reduce the average consumption recorded in recent decades, the world reserves of oil and natural gas will be exhausted in 100 years and those of coal in 200 years [1]. Thus, the use of renewable energy sources has become essential. They will also help to combat environmental degradation.

Renewable energy, for the reasons cited above, is becoming increasingly important to humanity. The main advantage of renewable energy are: it is clean, safe, abundant and, therefore, does not impact the environment in a negative way. Among the various sources available in the world, the wind is the most promising choice. This is explained due to its constant availability anywhere and its production is now considered cost competitive [2].

Due to the randomness of wind generation, it is not possible to guarantee a fixed amount of energy to the electrical system. In addition to that, there is the increasingly high investment of several governments in this type of energy in order to meet the high power consumption in recent years. Thus, in order to help countries whose energy matrix now includes the wind as an alternative source, the forecast wind power has proven to be crucial for developing strategies and appropriate, efficient and inexpensive planning. This forecasting depends mainly on wind power. Various models are used to perform it, several of them including artificial intelligence. This work aims to use an architecture of Artificial Neural Network (ANN) called *Reservoir Computing* (RC) and analyse its performance.

Although there are already models using the most common types of ANNs, such as Multi-Layer Perceptron (MLP), the *Reservoir Computing* was chosen for having an architecture in which artificial neurons are interconnected and organized in a more similar way to the human brain (a metaphor that is the origin of ANNs, as the name implies)[3].

This characteristic of the RC architecture allows this technique to represent systems with dynamic behaviour, which are difficult to be represented in neural networks, such as MLP [4]. Therefore, learning the dynamic characteristics which represent the temporal series of the wind power becomes a more suitable task for the RC.

Due to this, it is expected that its performance on forecasting is better than that obtained by the other ANNs. Hence, the prediction would be more accurate and increase efficiency in the planning and use of wind energy, encouraging its use in many place and, at the same time, preserving the environment.

This paper is organized as follows. Section II introduces the Reservoir Computing technique, its structure and how it is created, used and trained. Section III presents the methodology used during this work, such as the database used and the ANNs configurations. Results can be found in Section IV. Conclusions and future works are given in Section V.

II. RESERVOIR COMPUTING

In addition to feed forward architectures, such as the MLP, widely used in time series forecasting, Recurrent Neural Networks (RNN) began to emerge. In this new type of network, there is the addition of recurrent connections to existing feed forward architectures. These connections transform the system into a complex dynamic system and one more suitable for solving temporal problems. In the case of this project, it becomes an attractive option because the problem to be solved, the forecast of wind power, is temporal in nature. Figure 1 shows the structure of a feed forward and recurrent network [5].

The RNNs are computational models capable of creating internal memory required to store the history of input patterns through their recurrent connections [5].

In 2001, a new proposal for the design and training of RNNs was suggested independently by Wolfgang Maass [6] called Liquid State Machine (LSM) and Herbert Jaeger [7] called Echo State Networks (ESN). Verstraeten proposed the unification of these two approaches into a single term called Reservoir Computing. Since then, RC began to be adopted in the literature as a generic name for learning systems that consist of a recurrent network dynamics with simple computational nodes combined with a simple output function [8].

 ISBN: 978-1-61208-340-7

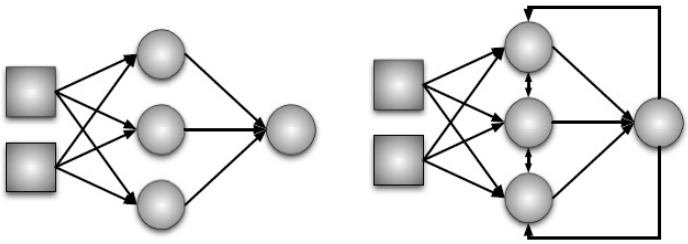

Fig. 1: Structure of a feed forward (left) and recurrent network (right)

[Fonte: [4]]

A reservoir computing system consists of two main parts: a reservoir and a linear output layer. The reservoir is a non-linear dynamical system with a recurrent topology composed of processing nodes. The connections between nodes are randomly generated and are globally rescaled in order to achieve a proper dynamic state. An important property of the RC is that the reservoir has fixed weights, that is, its training is not necessary. Only the output layer is trained, therefore, it has an output function. This function can be, for example, a classifier or linear regression algorithm [4].

The fact that only the output layer needs to be trained allows the use of the same reservoir for the solution of different tasks simultaneously by keeping the same inputs.

An interesting feature of RC is one based on ESNs, a property called echo. This property defines the effects of a previous state x (n) and an input value at a future state x (n +1) should gradually decrease with the passage of time k (i.e. k $\rightarrow$ infinity) and should not persists, or be amplified.

Due to recurrent connections, information on past entries is stored in the network. Because of this, the network contains a rich set of non-linear transformations and mixtures of input signals of past and present (called echoes) times.

A. Creating and Using Reservoirs

In the following text, it is assumed that the RC system consists of N reservoir nodes, M inputs and P outputs.

1) Creating the input and reservoir connections:

1) Construct an MxN input to reservoir weight matrix W_{in}. The weights are drawn from a random distribution or discrete set. If all input signals are fed to all reservoir nodes, then all elements of this matrix are non-zero. Otherwise, there will be null elements.
2) Construct an NxN reservoir interconnection weight matrix W_{res}. The values for the weights are again drawn from a distribution or a discrete set of values (e.g.,[-1, 1]).
3) Rescale the weight matrix globally such that the reservoir has a suitable dynamic excitability. The most common way to do this is to tune the spectral radius of W_{res}. The spectral radius of a matrix is its largest absolute eigenvalue. A value close to 1 is usually proposed as a good starting point for optimizations of ESNs.

2) Simulating the Reservoir and training and testing read-out:

1) Construct a dataset D and split it in 3 sets: training, cross validation and tests.
2) The network state at time k is denoted as x[k] and an input at the same time as u[k]. For every sample, we initialize x[0] = 0. Before starting the training, the first 100 cycles are called warm up. During the warm up, the neural network forgets its initial states and loses the influence of value zero. As soon as the warm up finishes, the training is started and the neural network is simulated recursively.
3) After every sample is simulated, state matrices of the training set are concatenated into a large state matrix A.
4) Compute the output weights. In this project, to perform this calculation, we used the Moore-Penrose [9] generalized matrix or pseudo-inverse due to the fact that the matrix A is not square. These calculations will be done automatically by a Java routine called JAMA.
5 After a sample entry is trained, cross-validation is performed in order to check if the training can now be finalized. The Mean Square Error (RMSE) is calculated and stored for each cross-validation done.
6) After training, the network is simulated with the test set and the Mean Absolute Percentage Error (MAPE) is calculated. These errors are stored for subsequent statistical tests. In this project, we used the Normalized Mean Absolute Error (NMAE).

Through the NMAEs calculated for network performance with the RC and MLP techniques, it will be possible to compare which architecture is the best choice for the prediction of wind power.

III. METHODOLOGY

A. Database

The database used in the experiments was provided by the brazilian Operador Nacional de Sistena Elétrico (ONS) or National Operator of Electrical System. The ONS is the body responsible for the coordination and control of the operation of generation and transmission of electricity in the national interconnected system [10].

Data for average wind power are daily and the period in which they were measured and collected goes from December 1, 2011 until July 31, 2012. They were observed from 30 to 30 minutes and the available data are: average wind speed, direction and power. From all these attributes, we will only use the power of the wind. Through experiments, it was noted that only this variable achieves good results.

Each wind farm has an installed power capacity associated with it. This value indicates the maximum power that can be produced by the farm. The database used belongs to a wind farm with a capacity of 54.61 MW.

B. Pre-processing of data

The first step in the stage of pre-processing data is the normalization of values. This step aims to prevent high values from influencing too much the calculations of the ANN while low values go unnoticed. It is necessary to ensure that the variables at different intervals receive equal attention during the training. Moreover, the variables should have their values proportional to the boundaries of the activation function used in the output layer. If the activation function chosen is the

 ISBN: 978-1-61208-340-7

logistic sigmoid, their values are limited between [0 and 1], then the data are usually normalized between [0.10 and 0.90] and [0.15 to 0.85] [11].

The normalization is calculated using the formula described in (1):

$$y = \frac{(b-a)(x_i - x_{min})}{(x_{max} - x_{min})} + a \quad (1)$$

where:

- y = normalized value;
- x_i = original value;
- x_{min} = minimum value of x;
- x_{max} = maximum value of x;
- a e b = limits chosen. In this work, a = 0.15 e b = 0.85.

C. Measure Network Performance

In case of wind power prediction, the usual error descriptors, such as MAPE and Mean Absolute Error (MAE), are given as a percentage of the installed capacity of a particular wind farm. In this work, it was defined that the network performance would be measured by the Normalized Mean Absolute Error (NMAE).

D. Predicting Wind Power with MLP

Although it is widely used in many researches, the MLP requires that several of its parameters are configurable and the choice of each directly influences the final outcome of the prediction.

Below are the main parameters of the MLP and Backpropagation algorithm:

- Number of neurons in the input layer;
- Number of neurons in the hidden layer (only one hidden layer);
- Number of neurons in the output layer;
- Activation function;
- Stopping criterion;
- Learning Rate;
- Momentum.

The number of entries varied in order to be possible to make an analysis of the impact of a larger amount of inputs, like 48 or a smaller number of inputs, such as 7 and if this alteration made any difference in the wind power prediction. As noted, it did not matter if the number of neurons in the input layer was 7 or 48. For the purpose of expediting the training, we chose the value of 7 inputs.

The output is always 48 wind power values, thus the predictions are one day ahead.

The algorithm used is the Backpropagation and the activation function chosen for the neurons is the logistic sigmoid. This function returns values in the interval [0, 1].

The stopping criterion used was cross-validation, with 50% of the set of values for training, 25 % for cross-validation and the remaining 25 % for testing.

Several tests were performed to define the learning rate, momentum and number of neurons in the hidden layer. The best results correspond to the values of 0.8 for the learning rate, 0.2 for the momentum and 6 neurons in the hidden layer.

The MLP used has been implemented in the JAVA programming language and in the Eclipse development environment [12].

E. Predicting Wind Power with RC

Like the MLP, the Reservoir Computing technique has several parameters that require configuration. Taking into account that it is a recent area of research, the choice of these settings can not be considered ideal and is often performed randomly. One way to do this is to evaluate each chosen value and determine if it was better or worse for the network performance. This process is repeated until a value is considered optimal, which does not necessarily means the best.

Below are the parameters whose settings were required to be defined during this project:

- Number of neurons in the input layer;
- Number of neurons in the output layer;
- Number of neurons in the reservoir;
- Activation function of the reservoir;
- Activation function of the output layer;
- Initialization of weights;
- Connection rate of the reservoir;
- Number of warm up cycles;
- Stopping criterion.

The number of inputs remains the same as used in the MLP, since it is necessary to keep this parameter with the same value of the prior neural network in order to perform statistical tests. The same applies to the number of outputs. The RC will have 48 neurons in the output layer to predict one day ahead.

The number of neurons in the reservoir is one of the parameters for which there is no fixed criterion that defines it. It was chosen randomly after checking the NMAE at the end of each training. It was observed that the ideal number of neurons in the reservoir was 20.

As mentioned in Section II, the weights of the input layer to the reservoir and the weights of the reservoir are randomly generated from a random distribution.

The reservoir states are initialized to zero (0). Because of this, as also mentioned in Section II, it was decided to add to the network a phase called warm up. During the warm up, it is not necessary to find the weights of the output layer, or to calculate an output value. This warm up phase is done just to update the states of the reservoir and remove the dependence on the initial state. The number of cycles chosen for warm-up was 10.

The connection rate of the reservoir neurons was 20%. That is, only 20 % of the connections have weight values different from zero associated to them.

The stopping criterion used was also cross-validation, with 50% of the set of values for training, 25 % for cross-validation and the remaining 25 % for testing.

The activation function chosen in the reservoir was the logistic sigmoid. In the output layer, the selected function was linear one.

During this work, we implemented a Neural Network with the technique of RC in the programming language Java and the Eclipse development environment. Figure 2 is a synthesized form of how this ANN works.

F. Statistical Tests

After 30 trainings with each type of neural network [13], statistical tests were performed to assess which technique has the best performance in the prediction of wind power or if their results can be considered statistically equivalent.

Among various tests in the literature, there are the t-student

 ISBN: 978-1-61208-340-7

```
Set the number of neurons in the input layer ;
Set the number of neurons in the reservoir layer ;
Set the number of neurons in the output layer ;
Randomly generate the weights of Win matrix between -1 e 1;
Randomly generate the weights of Wres matrix between -1 e 1;
Normalize the weights of Wres matrix so that the spectral radius of the matrix is smaller than or equal to 1;
while until the end of the number of warm up cycles do
    updates the states of the neurons of the RC;
end
while until the stopping criterion is reached do
    for each value of the input set do
        updates the states of the neurons of the RC;
    end
    Calculates the Moore-Penrose matrix inverse to find the weights connecting the output layer to the RC;
    for each value of the cross-validation set do
        updates the states of the neurons of the RC;
    end
    Calculates the output values of the RC;
    Calculates the RMS;
    Checks if the stopping criterion has been reached;
end
for each value in the set of tests do
    updates the states of the neurons of the RC;
end
Calculates the output values of the RC;
Calculates the NMAE// in case of wind power prediction;
```

Fig. 2: Pseudo-code of RC

test and the Wilcoxon Rank-Sum test. To apply t-student test, it is necessary to begin using the Shapiro-Wilk test in order to check whether or not the data are normally distributed. If they are considered normal samples, then we performed an F test to verify if the variance can be considered originated from the same population. By passing these tests, we applied t-student test for unpaired data. If samples are not considered normal, nor pass the F test, then we apply the Wilcoxon Rank-Sum test.

IV. RESULTS

The training of the MLP and the RC was conducted with three settings, as mentioned in the previous section, until the best result was achieved. The following three settings were tested: 7, 24 and 48 entries. As it shown in table I, the NMAE did not vary significantly if the number of inputs were altered.

TABLE I: Executions for determining the ideal number of inputs

Number of input neurons	RC	MLP
7	18.04%	23.54%
24	18.47%	24.03%
48	18.23%	24.07%

30 simulations were performed for each topology and the average NMAEs can be found in Table II.

TABLE II: Average Normalized Mean Absolute Errors Values

Topology	Average NMAE
RC	18.02 %
MLP	24.47%

In addition to calculating the average normalized mean absolute error, a graphic was constructed to better show the behaviour of the expected values when compared to the ones obtained from the training of a RC neural network.

Analysing Figure 3, it is possible to observe that, even if the average normalized mean absolute error is low and considered a better result when compared to other techniques, the curve of the calculated values do not approach the one with the real values. When it is desired to predict the maximum power (peaks) or the minimum (the valleys), these values are not well forecast and it can jeopardize the planning and decision making of a wind farm.

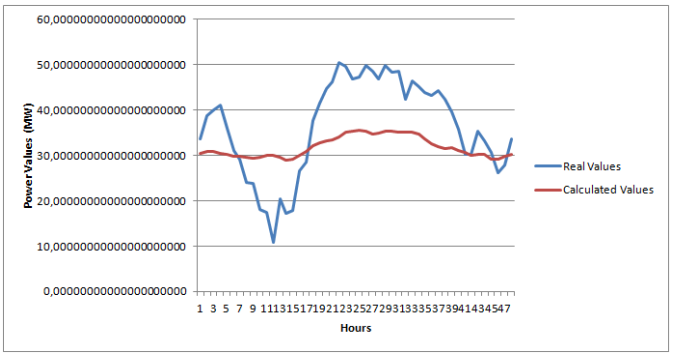

Fig. 3: Graphic comparing the curves of the calculated values with the real ones

Finally, for each set of 30 simulations, we performed statistical tests and the process began with Shapiro-Wilk test. The R software was used [14] and it defines the value for the significance level as 0.05. It was observed that the sample belonging to MLP network does not come from a normal population, i.e., that is not normally distributed, since the p-value calculated during the test was 0.005 for the MLP, thus less than the level of significance.

From this result, it became unnecessary to perform the Student t test, whose pre-condition for its use is that the samples were normal. For this reason, the next step was the application of Wilcoxon Rank-Sum test.

This test is non-parametric, that is, it is assumed that the data distribution is not regular. The result of this test showed that the p-value has a value much smaller than the significance level, hence, the null hypothesis is refuted, which states that the performance of neural networks with the RC and MLP architectures are considered statistically equal and concludes that the use of the proposed technique RC has a better performance.

V. CONCLUSION AND FUTURE WORK

This work aimed to predict the power generated by a wind farm for 1 day ahead using the technique of Reservoir Computing and compare it with the results provided by other

 ISBN: 978-1-61208-340-7

existing prediction models. Since the MLP neural network is the most widely used in this type of application, it was the model chosen and its results were compared with the results of the RC technique.

In order to achieve this objective, a neural network with the RC topology was implemented and a database provided by the brazilian Operador Nacional de Sistema Elétrico (ONS) or National Operator of Electrical System was used. Several simulations were performed for both topologies and the results were compared.

Through statistical tests, it was proven that the performance with the RC is better than the one obtained by the MLP. This result opens a field of research for the study of dynamic neural networks, such as the RC for time-series forecasting.

As future work, further studies of the parameters of the RC will be conducted in order to find the best way to define them. Good and more accurate values can positively impact the RC's performance.

In addition to that, it is necessary to work with databases from across the country and the world. With different databases, it is possible to observe if the RC technique can still be considered the best solution.

Finally, since the graphic showed discrepancy between the calculated values and the real ones, a correction technique will be employed to ensure a more realistic representation of the real power curve.

REFERENCES

[1] W. de Cerqueira e Francisco. (2008) Energy sources [retrieved: August, 2012] [Online]. Available: http://www.mundoeducacao.com.br/geografia/fontes-energia.htm

[2] R. Albadó, *Wind Energy*, 1st ed. ArtLiber, 2002.

[3] B. Schrauwen, D. Verstraeten, and J. V. Campenhout, "An overview of reservoir computing: theory, applications and implementations," *Proceedings of the 15th European Symposium on Artificial Neural Networks*, 2007, pp. 471–482.

[4] M. Lukosevicius and H. Jaeger, "Reservoir computing approaches to recurrent neural network trainning," *Computer Science Review*, vol. 3, 2009, pp. 127–149.

[5] A. F. Araújo, "A method for design and training of reservoir computing applied to time-series forecasting," Ph.D. dissertation, Federal University of Pernambuco, 2011.

[6] W. Mass, T. Natschläger, and H. Markram, "Real-time computing without stable states: A new framework for neural computation based on perturbations," *Neural Comput.*, vol. 14, 2002, pp. 2531–2560.

[7] H. Jaeger, "The ''echo state'' approach to analysing and training recurrent neural networks," 2001.

[8] D. Verstraeten, "Reservoir computing: computation with dynamical systems," Ph.D. dissertation, Ghent University, 2009.

[9] J. A. Fill and D. E. Fishkind, "The moore-penrose generalized inverse for sums of matrice," *SIAM Journal on Matrix Analysis and Applications*, vol. 21, 1999, pp. 629–635.

[10] ONS. (2012) Operador nacional do sistema elétrico (national operator of electrical system) [retrieved: October, 2012] [Online]. Available: http://www.ons.org.br/home/

[11] M. J. S. Valença, *Fundamentals of Neural Networks*, T. Pereira, Ed. Livro Rápido, 2011.

[12] S. C. O. M. dos Santos, "A hybrid system based on neural network and ant colony," Master's thesis, Universidade of Pernambuco, 2010.

[13] N. Juristo and A. M. Moreno, *Basics of Software Engineering Experimentation*. Kluwer Academic Publisher, 2001.

[14] W. N. Venables, D. M. Smith, and the R Core Team, *An Introduction to R*, 2008.

 ISBN: 978-1-61208-340-7

Training a Cognitive Agent to Acquire and Represent Knowledge from RSS feeds onto Conceptual Graphs

Alexandros Gkiokas * Alexandra I. Cristea †
University of Warwick
Department of Computer Science
Coventry, CV4 7AL, UK
*e-mail: a.gkiokas@warwick.ac.uk †e-mail: a.i.cristea@warwick.ac.uk

***Abstract*—Imitative processes, such as knowledge transference, have been long pursued goals of Artificial Intelligence (AI). The significance of Knowledge Acquisition (KA) in animals and humans has been studied by scientists from the beginning of the 20th century. Our research focuses on observational imitation through agent-user interaction, for acquisition of symbolic knowledge. The cognitive agent (CA) emulates an imitative learning system, trained for the purpose of learning to represent knowledge, acquired from Rich Site Summary (RSS) feeds. It learns to autonomously represent that knowledge in a manner that is both logically sound, and computationally tractable, through the fusion of Conceptual Graphs (CG) and Reinforcement Learning (RL). The novel algorithm enabling this agent extends Reinforcement Learning, by approximating decisions via exploitation of distributional and relational semantics governing the knowledge domain.**

Keywords–Cognitive Agent; Reinforcement Learning; Conceptual Graphs; Expert Systems; Imitation Learning.

I. Introduction

Similar to recent research projects, which try to acquire knowledge from the Internet, such as KnowRob [1] or Never Ending Image Learner [2], this paper focuses on the acquisition of knowledge found on the Internet, a large source of ever growing data. We examine RSS feeds [3] as the source of knowledge, due to their parsimony and quality of information. RSS has been around for more than a decade, and is used to display and update in real time information from various news agencies, websites and social media, and represent an important and stable, widely used means of information distribution of the modern world.

The CA emulates, but does not simulate, a perceptive process and learning system, based upon psychological studies in humans [4] and animals [5]. The CA purpose is to acquire knowledge; for that we train the agent using RL, instead of heuristics, which is the norm. Doing so, we hypothesise makes the agent adaptive, and enables it to, domain-independently, augment its acquisition capabilities (KA) and thus, expand its knowledge in an autonomous or semi-supervised manner. The CA described in the paper, employes a symbolic-based imitation learning process (observational imitation) as defined by previous research [5][6]. The actual algorithm emulating the imitational process, is performed through the fusion of AI technologies as well as a new approximation algorithm we've developed for RL, in order to enable the CA to keep learning indefinitely, after training. Machine Learning (ML) literature treats an increased state space as a problem rather than an aid [7], something usually dealt with state or action approximation. In contradiction to this belief, we attempt to show that by re-using existing reinforced episodic experience, through semantic approximation, learning can benefit from an expanding state space. CA learning to acquire information, cannot afford to perform random actions (e.g., Monte-Carlo search) as part of the Markov Decision Process (MDP) used by RL, as this leads to poor performance or slow convergence [8]. Modelled after imitation [5] and Programming By Example (PBE) [6], we hypothesise that the rate at which prior experience is exploited can alter the decision making process of RL, through the fusion of approximation methods. By employing semantics and reasoning on underlying semiotics governing the symbolic particles found in the knowledge domain, we attempt to restrict the amount of random decisions, and replace them with known actions, assumed to be correct. The purpose of the RL algorithm is to obtain RSS feeds, and then learn how to isomorphically project the feed onto a CG [9].

Section II visits related research, describing the context in which the current proposal has been created. Section III describes the main problems we are attempting to solve in this paper in greater detail. Section IV describes the learning architecture of the CA. In Section V, we describe the algorithm that implements semantic approximation, and thereby extends RL. This is followed by a discussion in section VI and conclusions in Section VII.

II. Related Research

Existing research on automated KA has focused on heuristics [10][11] or statistical and probabilistic analysis, either via Natural Language Processing (NLP) or as part of the Knowledge Representation (KR) generation [12] of CG. Other researchers have used CG [13] for mining, yet others used semantics and morphosyntactics [14] in order to extract concepts (not CG). Older research has seen combination of concept maps and neural networks, such as the KBMiner [15] for KA or mining. Direct comparison

 ISBN: 978-1-61208-340-7

with all the aforementioned research won't do justice to either the work described, or ours, as it would partially compare one side of our work (KA) to research that was not focusing on CA or imitation learning. As such, the only comparison possible, would be the performance of our fully trained CA, against the performance of the algorithms described above.

AI research in imitation has historically [5] attracted attention from roboticians, as it stands to be the field that would mostly benefit from knowledge transference. Whilst research on knowledge transference in software agents [6] has focused on inference and pattern prediction for Web interfaces, programming automated tasks, etc., we address bridging CA and RL, for acquiring knowledge (KA), as part of an imitation process. Lieberman set the foundations for PBE [6] on which a great deal of our research relies on. However, most of the research by Lieberman (or his associates) does not deal with agents (much less CA), nor does it deal with KR. The only research by Lieberman on agents [16], was for Web browsing and text mining, which has fundamental differences from KA. Other researchers using PBE have done quite similar research (with respect to intentions and processes) [17], but still the comparison is incomplete as different technologies were used, and for a different purpose.

In comparison to both PBE and KA research, we employ RL, in order to train the agent. The algorithm described in this paper here can be said to belong to the family of stochastic semi-supervised learning algorithms. The agent does not attempt to detect patterns, mine information, or summarize text, but instead focuses only on projecting information into a formal representation (KR structure), such that it can be manipulated for other knowledge management operations (which are outside the scope of this paper). *Knowledge is making sense of information*, and for *learning to make sense of RSS*, we use RL, which has been widely used for a variety of AI tasks, ranging from robotics [18], to games, to intelligent agents [7]. RL research has, however, been conscious about approximating and regressing state-actions since its inception [8][7], and there exists a plethora of methods on how to effectively regress and approximate, in order to infer correct policies. However, our approach using semantically-driven approximation in combination with distributional semantic similarity calculations, should provide grounds to support episodic experience re-usability in CA learning via RL.

III. Problem Setting and Objectives

The primary objective of the described CA is to obtain feeds and construct the correct Conceptual Graph (CG) from each feed. We assume each feed to contain knowledge that can produce one or more CG [9]. Traditionally, CG creation has been assigned to knowledge engineers, human users acting as experts who construct the correct CG. The second, more practical objective, is to enable the CA to learn how to acquire knowledge by reusing its own experience, thereby aspiring to enable the CA to self-augment its capabilities. By creating a trainable agent to acquire knowledge, we aim to enable the CA with certain advantages over conventional approaches:

- The agent should be able to process any domain of symbolic information.
- The agent should be adaptive, thus be able to learn training indefinitely and adapt to non-monotonic knowledge (through the use of RL).
- The agent after being trained, should be able to autonomously acquire knowledge without the need of a knowledge engineer.
- The (trained) agent should be able to deal with unknown domain particles (via Semantic approximation) and uncertainty.

IV. Cognitive Agent Architecture

According to the criteria set by Lawniczak and Di Stefano [19], the described agent could be partially called a CA. It satisfies four of the five criteria:

- Perceives Information (RSS) in its environment (Web) and provided by other agents (through textual queries)
- Reasons about that information using existing knowledge (through ML, RL and Semantics)
- Responds to other agents, human (via Web interface) or artificial (via textual responses)
- Learns and changes the existing knowledge if the newly acquired information allows it

In fact, the only criteria not satisfied, is the ability to judge obtained information using existing knowledge [19]. The novelty in the design of the cognitive agent is not merely the fusion of different A.I. technologies, but finding a novel usable expression of the notion that a cognitive agent can be trained to learn how to acquire knowledge, by reusing its own accumulating experience. It is however important to note that this agent is designed to deal only with symbolic knowledge, and not with continuous, metric or numeric information. As the source of information, RSS feeds are used. RSS offer certain distinct advantages over other sources of information. Thelwall, Prabowo and Fairclough [3] mention that RSS feeds are one of the very few sources on the internet, which may be able to offer quality information relevant to specific subjects. The Knowledge Representation (KR) meta-structure used is Sowa's CG [9], which are formal structures, based upon philosophical principles, that offer logically sound reasoning operations [20]. They also offer a few advantages over other KR structures, such as Web Ontology Language (OWL) or the Resource Description Framework (RDF). They do not use a subject-predicate-object format, but are relation centric. Their greatest advantage is that they are visually simple to understand, even by (human) users who are not knowledge engineers or computer scientists. They also offer a computationally affordable [13] and tractable way, in order to perform various logic and reasoning operations [20], which are important and desirable for the future of this project. The agent's main task is to parse feeds,

 ISBN: 978-1-61208-340-7

and construct the correct Conceptual Graph (CG) g such that g correctly represents the knowledge encapsulated in the feed r. What this implies, is that the agent learns how to read text found on the internet and represent it internally. The actual manipulation and management of the acquired knowledge is outside of our scope, we only focus on enabling such a process so as to emulate imitation and observation learning. We model this, as shown in (1), indicating that the imitating function f is a mapping or projecting function.

$$f : r \mapsto g. \tag{1}$$

The function f is composed of a parsing f_p and an isomorphic projection f_m so that $r \cong g$, as shown in (2).

$$f_p(r) = t_r, f_m(t_r) = g_r \therefore (f_m \circ f_p) = f_m(f_p(r)). \tag{2}$$

Those two functions compose the actual operation of the CA: first the feed r is parsed as a set of tokens t_r , and then that set is isomorphically projected onto graph g. If parsing f_p does not produce the correct output, then projection f_m may have undefined behaviour. Function f_m is the subject of RL, and by using f_m as a policy for projecting $r \cong g$ (1), we may replace f_m with Q, as shown in (3).

$$f_m : r \cong g \Leftrightarrow Q(s_t, a_t). \tag{3}$$

where (3) Q is the Markov decision, calculated as a policy for a given state s_t when taking action a_t, at step t. Function f_p parses the feed r, into the set of tokens t_r:$\{t_1,..,t_n\}$ by tokenizing it. Parsing and tokenizing is a NLP task, which we do not include within the projection, or the learning material for the agent; instead we rely on simple white-space tokenizing, using a grammatical rule-based approach [21]. We chose to do so, in order to simplify the decomposition operation, into a minimal algorithm with small complexity, and thus, focus on the projection algorithm. Using heuristic parsing [21], amongst others, this process concatenates words that are encapsulated by quotes (single or double) into a single token. Using morphosyntactic (part-of-speech) tagging [22], the parsing algorithm also finds tokens, which denote a person, and concatenates them into a single token. Trailing "'s" found after a word, are removed, and replaced by the token "owns". Free particles, such as "the", "a", "an" are also removed. All implied tokens, not found in the actual feed r, should be discoverable by the CA, as it has no other way of inferring those tokens. The tokenizing should capture the ontology of the feed, in the resulting token set t_r.

Following the tokenizing, the projection starts, and is done in two stages, and represented as a MDP in the form of an episode of RL:

- In function f_n tokens have to be converted to a vertex (Concept or Relation) [9].
- In function f_c relations have to connect to concepts with an edge [9].

The state is always represented by the same CG (see figure 1), which is being constructed by the RL algorithm, and is only finished when a terminal state is reached [7]. The construction of the CG, is what that the CA learns to perform, described by the MDP used by RL. In a temporal sense, each time-step in the MDP is describing the algorithm constructing a piece of the CG. As the graph

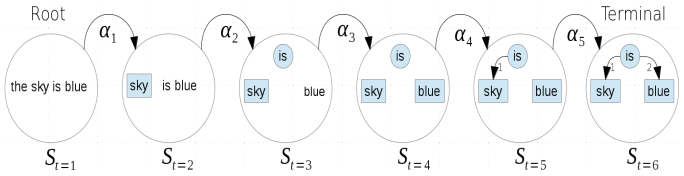

Figure 1. MDP as a RL State-Path

is constructed by the feed tokens, the graph vertices are eventually connected, in order to form the final graph. We employ states and actions as per the RL literature [7], and the human trainer provides a reinforcement at the end of each episode, rewarding that CG. The CA uses that reward to reinforce correct CGs. We chose to use RL over other methodologies, because it deals best with partially observed MDP [7]. The *Q-Policy* value is calculated by the SARSA algorithm [7], as shown in (4).

$$Q(s_t, a_t) = Q(s_t, a_t) + \alpha[R_{(t+1)} + \gamma Q(s_{t+1}, a_{t+1}) - Q(s_t, a_t)]. \tag{4}$$

The algorithm back-propagates that reward R_{t+1} for terminal states, when re-iterating previous states, using a discount factor γ and learning rate α. We chose SARSA over Q-learning, as it is assumed to be more greedy with respect to immediate rewards [7]. The actual action a_t in (4), has the binary nature described by (figure 1) and, can logically be represented, as shown in (5).

$$a_t \leftarrow f_n(t_r) \vee f_c(g). \tag{5}$$

The disjunction signifies the two-staged construction as a temporal process: either vertices, or edges, are created. The action search space can vary, and is denoted by $S_p a_t$, as shown in (6), where n is the number of all vertices in g.

$$S_p a_t(f_n) = 2^n. \tag{6}$$

A correct decision, could be expressed as a search in that action space, where the algorithm has to find the correct vertex types for graph g, or establish the correct edges between them. The action space is also proportional to the number of tokens in the feed, and is dynamically parametrised by the decided relations r and concepts c of g where x_r is the available edges for a relation, as shown in (7).

$$S_p a_t(f_c) = \int_1^c (r * x_r). \tag{7}$$

Each relation vertex r can have minimum one edge to a concept, and maximum an edge for each concept. Only relations can establish edges to concepts [9].

The CA is complemented by a semantic graph, represented internally by a Word-Net instance [23]. Contrary to CG literature [20], we do not employ two distinct maps for relations and concepts, as Word-Net has its own classification and categorization. All semantic operations are delegated to Word-Net, which acts as a semantic authority. Using an action a_t which has been reinforced, implies that this action has been performed at least once. Normally, this action would be randomly chosen from the space of possible actions $S_p a_t$ and only after being reinforced, could

 ISBN: 978-1-61208-340-7

it become a policy. Whilst this may not be a problem for other AI-related areas, it is of the utmost importance for the CA to decide the right actions the first time, and not wait for a policy. In reality, the same, identical states would rarely be revisited, in order for a policy to become of much use.

V. Semantic Approximation

A vast search space is a problem in RL when computing or searching for policies [7]. Conventionally, RL is a semi-random MDP, often employing a Monte-Carlo search. However, due to the importance of semantics in symbolic domains [23], the described algorithm for selecting an action for a state, assuming s_t has never been experienced before, attempts to avoid random selections, and instead relies on semantic distance and word similarity, in order to reason, as to why an action should be performed. The premise upon which this notion is based, is that of reusing prior positive experience. Furthermore, the operation is to approximate state similarity, and then approximate action similarity through semantics. Assuming enough reinforced experience exists, the algorithm should have enough sources to reason as to why an approximation *could* or *should* work. The semantic similarity between the particles that describe a state is inherited from the lexicon of the domain, for which knowledge is acquired. Those semantic relations are exploited in a logic fashion, so as to reason about re-using, known to-be-correct (via reinforcement) actions. Each episode in memory, can be positively or negatively rewarded by the trainer. The first operation is to approximate similarity to all positively rewarded graphs in memory, as shown in (8), by using a Vector Space Model (VSM) [24].

$$S_r = \frac{M * V_r}{\|M\| * \|V_r\|}. \tag{8}$$

Sparse matrix M (8) contains token-frequencies, and is created by indexing each unique CG as a column, and each token used as a vertex in a CG, as a row. V_r is the (respective to matrix M) row vector of tokens representing the feed r. The VSM discovers similarity based upon distributional semantics, and returns a column vector S_r of degrees of similarity, as shown in (9), representing how similar each CG in memory, is to the input vector V_r.

$$S_r = [cos(\Theta_1), ..., cos(\Theta_n)]\,. \tag{9}$$

For each identical particle in graph *g'* (the graph already in memory) that is similar to g (e.g., the one currently being created), we perform the same action. For example, if a_t converted t to concept c, we assume the same decision to be valid. Thereby by approximating the state s_t we can obtain policy $Q(s_t,a_t)$. However, for non-identical particles, assuming that graph $g' \in S_r(cos(g_n))$, has tokens g':$\{t_1,..,t_n\}$, we subtract the identical particles of *g'* from g, with result set X:$\{g_{particle} - g'_{particle}\}$. Each particle in X should exist in g but not in *g'*, as shown in (10).

$$(p \in X) \wedge (p \notin g'). \tag{10}$$

The next phase of the action-decision algorithm, iterates for each particle p ∈ X, and tries to establish, if ∃ *[n,n']*, a semantic relation as a graph path, for $n \in X$ and $n' \in g'$. Please note that *n and n'* are the semantic vertices within a semantic graph, with the respective symbolic value of token t, concept c, or relation r. The semantic relation describes an "IS A" relation. Semantic relations in the semantic graph are hierarchically ordered. This semantic graph should in fact be a *Hasse diagram* where super-ordinates are sorted near the root and sub-ordinates are sorted near the bottom, similar to the conceptual graph literature [20]. However, that depends on the semantic authority, in this case, Word-Net [23], which does indeed sort hierarchically the vertices, as hypernyms and hyponyms.

Finding a path in the semantic graph, between n and *n'*, denotes that there exists some form of semantic similarity. In case a semantic relation is discovered as a path, then the action-decision mechanism in RL will use the same action that was used in state s_t when constructing the graph *g'*. The theoretical basis for this decision, is the principle of reusing positively rewarded experience; something known to be correct, will be re-used and assumed correct, until reinforced otherwise. However, the direction of that semantic similarity is important [23]. Super-ordinates denote a super-type, from which sub-ordinates are assumed to inherit all or some of its properties, a form of *inductive* hypothesis. The exact opposite, a path connecting super-ordinate n to subordinate *n'*, implies a *deductive* hypothesis (e.g., a specialization of n to *n'*). As such, n may not inherit properties or attributes of *n'*. The actual search which tries to establish if there exists a path between n and *n'* is simply a *breadth-first search* (BFS).

Semantic distance $d_{[n,n']}$ also plays an important role [23]; the further apart the semantic relation discovered, the weaker it is assumed to be. The algorithm will sort the resulting set of semantic paths discovered between n and n', based upon the semantic distance, biased towards smaller, over longer distances (measured in steps t). Semantic direction d_t, is described by the upwards movement towards a super-ordinate or towards the downwards movement towards a sub-ordinate. Direction towards super-ordinates is preferred over sub-ordinate direction, and is perceived to be more important [9]. Direction is accumulated, as *+1* for sub-ordinates and *-1* for super-ordinates for each step t until the search terminates. The accumulated sum, as shown in (11), is discounted by factor γ.

$$v[n, n'] = w_s(d_{[n,n']} + \gamma * \sum d_t). \tag{11}$$

However, Word-Net also uses a sense classification [23], related to the frequency at which a semantically hierarchical tree appears. We chose to weight the sense by using w_s, thereby further biasing the computed value $v_{[n,n']}$, to prefer the most frequent sense. The sense weight w_s is *min-max* normalised in the event that many senses are discovered. Therefore, the resulting path values are described by three attributes: frequency of path, distance and direction. By using those attributes, and computing a $v_{[n,n']}$ value, we approximate the best action a_t, for the most similar state obtained by the VSM earlier. The algorithm will use an action a_t with the smallest $v_{[n,n']}$, as shown in (12).

$$\exists : ([n, n']) \therefore a_t \leftarrow a_t(min(v_{[n,n']})). \tag{12}$$

Below is the pseudo-code describing Semantic approximation. Selecting a vertex of *Concept* or *Relation* type, as shown in (5), is algorithmically implementable, as shown in (Algorithm 1). More specifically, operation *Sim* (Algorithm 1, line 2) is the VSM vector output from formula (8), whereas *Sort* (Algorithm 1, line 4) is simply a descending ordering based upon *cosine*, as shown in equation (9). Please note that the BFS is not shown in (Algorithm 1). The algorithm may terminate when:

- A path between n and n' is found.
- The search is exhausted (e.g., there exists no path)

The CA commences (Algorithm 1) whilst there exist tokens not converted to vertices in the CG. As such, this is a linear operation, proportional to the tokens found in the feed r. Complexity is $O(n^2)$, and the algorithm describes the function $f_n(t_r)$, as shown in (5).

The second part of the action space, function $f_c(g)$, as shown in (5), is depicted in (Algorithm 2) which has to decide what *edges* to create for *Relations*. In (Algorithm 2), the complexity is at least $O(n^3)$, and depending on the output of the similarity function, there is no guarantee that a decision may be possible to be approximated. The minimum $min(v_{[n,n']})$ calculation has been omitted, albeit it should be at (Algorithm 2, line 15). Deciding for relations r, is a bit different: the algorithm not only has to establish if there exists a similarity between relations r and r', but also discover if r' is usable by establishing if the concepts, to which r' is known to connect to, exist in our graph g. Failing to establish such a condition, the algorithm will try to find if for any of the concepts c' connected by r', there exists a semantic relation (Algorithm 2, line 14). Therefore, the action approximation will not be based solely on the similarity between relations but is further based upon the similarity of concepts. Only in the event that the algorithm cannot provide an appropriate action a_t, a random action will be selected. In such an event, the algorithm falls back to being a semi-random MDP, where $f_n(t_r)$ randomly selects a vertex type, and f_c(g) randomly connects relations to concepts.

Algorithm 1. Token Action Decision

```
1: function DECIDE(M,V_r, t)                    ▷ t is a token
2:     S_r = SIM(M, V_r)                        ▷ set of similar graphs
3:     if S_r¬∅ then
4:         S_r = SORT(S_r)
5:         for g' ∈ S_r(cos(g_n)) do
6:             if (x = s_g–g')¬∅ then
7:                 for t' ∈ x do
8:                     if t ≡ t' then return g' : (a_t)
9:                     else if ∃v_[n,n'] then
10:                        a_t : min(v_[n,n']) return g' : (a_t)
11:                    else return Null
12:                    end if
13:                end for
14:            end if
15:        end for
16:    end if
17: end function
```

Algorithm 2. Edge Action Decision

```
1: function DECIDE(M,V_r, r)                    ▷ r is a relation
2:     S_r = SIM(M, V_r)
3:     if S_r¬∅ then
4:         S_r = SORT(S_r)
5:         for g' ∈ S_r(cos(g_n)) do
6:             if (x = s_g–g')¬∅ then
7:                 for r' ∈ x do
8:                     if (r' ≡ r) ∨ (∃v_[r,r']) then
9:                         edges_r' : {[r', c'_1], .., [r', c'_n]}
10:                        for c' ∈ edges_r' do
11:                            for c ∈ g do
12:                                if c' ≡ g_c then
13:                                    return g' : (a_t)
14:                                else if ∃[c, c'] then
15:                                    return g' : (a_t)
16:                                end if
17:                            end for
18:                        end for
19:                    else return Null
20:                    end if
21:                end for
22:            end if
23:        end for
24:    end if
25: end function
```

VI. Discussion and Further Work

Reusing known positively rewarded experience is a characteristic of the human psyche known as crystallized intelligence [4]. By extending RL in such a way, which is also modelled upon psychological processes [7], we hope to enable a form of RL algorithm, which can avoid random selections as often as possible, whilst emulating a cognitive function in a somewhat realistic manner. Furthermore, an expansion in experience should actually aid the action-decision, as more experience implies that there will exist a plethora of episodes and their respective graphs, upon which the algorithm may reason why an action should be taken. The proposed action-decision algorithm is an on-policy approximation, based upon logic and semantics, as shown in (13).

$$Q(s_t, a_t) \leftarrow Q(s_t(max(cos(\Theta_g))), a_t(min(v_{[n,n']}))). \quad (13)$$

Entirely avoiding random selections is not possible, as a cold-start issue may always ensure that at some point, a random choice will have to be made. Furthermore, semantic relations are obtained by a semantic authority, such as Word-Net [23]. Semantic relations may not be discoverable, due to being non existent in Word-Net, as may be the case with highly specialized terms or words, in which case, the algorithm will fall back to random selections. This relates to whether the MDP is fully observable; it is assumed not to be due to the limitations of discovering semantic relations. In addition to the above, the actual size of reinforced experiences (as episodes or conceptual graphs) would not benefit from a high ratio of negative experiences, albeit those could be used to avoid negative actions when randomly deciding. We have empirically optimised the RL

 ISBN: 978-1-61208-340-7

algorithm in our preliminary experiments, by adjusting for a low α learning rate and high γ discount factor. During non-RSS trial runs, convergence occurred with a thousand iterations whilst using an exploration-greedy policy. Early tests of the algorithm indicate that it appears to approximate *states* and *actions*, with an accuracy that could be related to the VSM model and Word-Net accuracy, but that remains to be evaluated. Future work will see the comparison of a plain RL (Markov e-greedy) algorithm, a probabilistic (Morphosyntactic) RL algorithm, and the Semantic-driven RL algorithm described in this paper. A double-blind experiment where human users have to project RSS feeds to CG, may also provide further psychological insight and information on the modelled process and algorithm.

VII. Conclusions

The need for such an algorithm was discovered after early anecdotal experiments indicated that frequent random actions occurred due to infrequent Q policy revisitation, and thus had a dramatic effect on the learning ability of the agent. The novelty is in implementing approximation methods on a purely symbolic basis. As most approximation and regression methods are based on numeric foundations [8][7], semeiotic relations governed by distributional and relational semantics, were the most important factor in dictating the design of this algorithm.

Whereas a lot of effort has been put into approximation, regression, knowledge mining, acquisition and management, it is our belief that trying to tackle such a task using a trainable and adaptive cognitive agent, presents some very interesting dilemmas and hence, can provoke interesting solutions. However, the algorithm is still rudimentary, as it does not rely on exploiting knowledge acquired by conceptual graphs, but only episodic experience. The absence of domain knowledge re-usability should not be a limiting factor for learning, but it could be a limiting factor for discovering new knowledge, or other logic operations based upon that domain knowledge. Will prior knowledge and experience aid learning? Could the agent successfully reason after the solution? It is widely accepted that an increase in the number of propositions has a dramatic impact on learning algorithms [8]. More importantly, as the state space grows, will the propositional logic deteriorate or augment? The algorithm and framework is based upon the principality that relations discovered will not drastically change over time, but even if they do, the agent should be able to adapt to those changes through learning.

References

[1] M. Tenorth and M. Beetz, "KnowRob - A Knowledge Processing Infrastructure for Cognition-enabled Robots. Part 1: The KnowRob System", International Journal of Robotics Research (IJRR), vol. 32, no. 5, April 2013, pp. 566-590.

[2] X. Chen, A. Shrivastava, and A. Gupta, (retrieved:May,2014), "NEIL: Extracting Visual Knowledge from Web Data", Available (URL): `http://www.neil-kb.com`

[3] M. Thelwall, R. Prabowo, and R. Fairclough, "Are Raw RSS Feeds Suitable for Broad Issue Scanning? A Science Concern Case Study", Journal of the American Society for Information Sciences and Technology, vol. 57, Issue 12, 2006, pp. 1644-1654.

[4] R. B. Cattell, "Abilities: Their structure, growth, and action", New York, Houghton Mifflin, 1971, ISBN-10: 0395042755

[5] C. L. Nehaniv and K. Dautenhahn, "Imitation in Animals and Artifacts", Bradford, Complex Adaptive Systems, 2002, ISBN: 9780262042031

[6] H. Lieberman, "Your wish is my command: Programming by example", Interactive Technologies, Kaufmann, 2001, ISBN-10: 1558606882

[7] R. S. Sutton and A. G. Barto, "Reinforcement Learning: An Introduction", MIT press, 1998, ISBN-10: 9780262193986

[8] P. Tadapalli, R. Givan, and K. Driessens, "Relational Reinforcement Learning: An Overview", Proceedings of the ICML'04, Workshop on Relational Reinforcement Learning, Ban, Canada, July 2004, pp. 1-9.

[9] J. F. Sowa, "Knowledge Representation: Logical, Philosophical and Computational Foundations", Brooks Press, 1999, ISBN-10: 0534949657

[10] A. Karalopoulos, M. Kokla, and M. Kavouras, "Comparing Representations of Geographic Knowledge Expressed as Conceptual Graphs", First International Conference, GeoS 2005, Mexico City, Mexico, Nov. 2005, pp. 1-14.

[11] A. Strupchanska, M. Yankova, and S. Boytcheva, "Conceptual Graphs Self-tutoring System", Proceedings of the 11th International Conference on Conceptual Structures (ICCS), Dresden, Germany, July 2003, pp. 323-336.

[12] D. T. Wijaya, P. P. Talukdar, and T. M. Mitchell, "PIDGIN: Ontology Alignment using Web Text as Interlingua", Proceedings of the Conference on Information and Knowledge Management (CIKM), ACM, 2013, pp. 589-598.

[13] M. Monstes-y-Gomez, A. Gelbukh, and A. Lopez-Lopez, "Text Mining at Detail Level Using Conceptual Graphs", 10th International Conference on Conceptual Structures (ICCS), Borovets, Bulgaria, July 2002, pp. 122-136.

[14] D. Rajagopal, E. Cambria, and D. Olsher, "A Graph-Based Approach to Commonsense Concept Extraction and Semantic Similarity Detection", WWW 2013 Companion, Rio de Janeiro, Brazil, May 2013, pp. 565-570.

[15] T. Hong and I. Han, "Knowledge-based data mining of news information on the Internet using cognitive maps and neural networks", Expert Systems with Applications, vol. 23, Issue 1, July 2002, pp. 1-8.

[16] H. Lieberman, B. A. Nardi, and D. J. Wright, "Training Agents to Recognize Text by Example", Autonomous Agents and Multi-Agent Systems, vol. 4, Issue 1-2, March 2001, pp. 79-92.

[17] M. S. Pandit and S. Kalbag, "The Selection Recognition Agent: instant access to relevant information and operations", Knowledge-Based Systems, vol. 10, Issue 5, March 1998, pp. 305-310.

[18] J. Kober, J. A. Bagnell, and J. Peters, "Reinforcement learning in robotics: A survey", The international journal of Robotics Research, vol. 32, no. 11, Sep. 2013, pp. 1238-1274.

[19] A. T. Lawniczaka and B. N. Di Stefano, "Computational intelligence based architecture for cognitive agents", International Conference on Computational Science (ICCS), 2010, pp. 2227-2235.

[20] M. Chein and M. Mugnier, "Graph-based Knowledge Representation", Springer, 2009, ISBN: 978-1-84800-285-2

[21] D. Jurafsky and J. H. Martin, "Speech and Language Processing", 2nd Edition, Prentice Hall, 2008, ISBN-10: 0131873210

[22] H. Van Halteren, J. Zavrel, and W. Daelemans, "Improving Accuracy in Word Class Tagging through the combination of Machine Learning Systems", Association for computational Linguistics, 2001, pp. 200-229.

[23] C. Fellbaum, "WordNet: An Electronic Lexical Database (Language, Speech, and Communication)", MIT press, 1998, ISBN-10: 026206197X

[24] P. Turney and P. Pantel, "From Frequency to Meaning: Vector Space Models of Semantics", Journal of Artificial Intelligence Research, vol. 37, 2010, pp. 141-188.

 ISBN: 978-1-61208-340-7

Cognitive Social Simulation and Collective Sensemaking: An Approach Using the ACT-R Cognitive Architecture

Paul R. Smart

Electronics & Computer Science
University of Southampton
Southampton, UK
Email: ps02v@ecs.soton.ac.uk

Katia Sycara

School of Computer Science
Carnegie Mellon University
Pittsburgh, PA, USA
Email: katia@cs.cmu.edu

***Abstract*—Cognitive social simulation is a computer simulation technique that aims to improve our understanding of the dynamics of socially-situated and socially-distributed cognition. Cognitive architectures are typically used to support cognitive social simulation; however, the most widely used cognitive architecture – ACT-R – has, to date, been the focus of relatively few cognitive social simulation studies. The current paper reports on the results of an ongoing effort to develop an experimental simulation capability that can be used to undertake studies into socially-distributed cognition using the ACT-R cognitive architecture. An ACT-R cognitive model is first presented that demonstrates one approach to solving a task previously used to investigate sensemaking performance within teams of human subjects. An approach to the implementation of an ACT-R cognitive social simulation capability is then described. The approach relies on the use of a variety of custom ACT-R modules and memory-resident Lisp databases. The custom modules enable ACT-R agents to exchange information with each other during the course of their sensemaking activities. The Lisp databases, in contrast, are used to store information about communicative transactions, the experimental setup and the structure of the communication network. The proposed solution provides the basic elements required to run cognitive social simulation experiments into collective sensemaking using the ACT-R architecture; however, further work needs to be undertaken in order to address a number of limitations associated with agent communication capabilities and the ability of agents to interact with the task environment.**

Keywords–collective cognition; sensemaking; distributed cognition; team sensemaking; cognitive architecture.

I. INTRODUCTION

In recent years, there has been a growing interest in the socially-distributed or socially-situated nature of human cognition across a number of scientific disciplines [1][2][3][4][5]. Cognitive processes that were typically studied at the level of individual agents, such as memory, are now being re-examined within a more social context [6], and increasing attention is being paid to the factors that enable groups to function as the processors of information [7]. This interest in the social dimension of cognition is, in part, a reflection of the growing popularity of embodied, extended and situated approaches within the sciences of the mind [8][9][10]. However, the research is also motivated by an attempt to engineer systems that harness the collective cognitive potential of groups of individuals. The advent of global information and communication networks, such as the World Wide Web, has clearly been one of the drivers in such research; however, systems that support socially-distributed cognition are also important in more restricted organizational contexts. This is particularly so as advances in sensor technology lead to a significant expansion in the scale and scope of available data assets. As organizations move into this 'Big Data' era, so they are under increasing pressure to distribute cognitive effort and harness the collective cognitive potential of their workforces.

In order to improve our understanding of the factors that affect the performance of teams of individuals, researchers have relied on the use of both human experimental studies and multi-agent simulation techniques. Multi-agent simulation techniques are of particular interest given the efficiency with which experimental studies can be undertaken and the control that can be exerted over experimental factors of interest. However, while such techniques have proven useful in investigating a number of social psychological phenomena, most notably social influence [11], they have sometimes been criticized in terms of their cognitive sophistication and fidelity. Recently, Sun [12] has advocated the use of cognitive architectures in multi-agent simulation as a means of improving the cognitive sophistication of agent implementations and enhancing the fidelity of computational models of human social behavior. Cognitive architectures are frameworks that make particular commitments about the kind of mental representations and computational procedures that are sufficient to explain important aspects of human cognition, such as problem solving, memory and learning [13]. Although a cognitive architecture can be implemented using connectionist schemes, some of the most influential cognitive architectures, such as ACT-R (Adaptive Control of Thought-Rational) [14][15] and SOAR (State, Operator and Result) [16][17] rely on rule and symbol forms of processing. Of particular note is ACT-R, which has been the focus of a sustained research and development effort for more than 30 years and which has been used to model cognitive performance in a wide variety of experimental settings. The integration of cognitive architectures into social simulation results in what Sun [12] refers to as *cognitive social simulation*.

By incorporating cognitive architectures into multi-agent simulations, we are provided with the opportunity to study the interaction between social and cognitive factors; for example,

 ISBN: 978-1-61208-340-7

we can study the effect that different cognitive factors (such as memory decay rates, learning rates, attention, and so on) have on aspects of collective performance. Cognitive architectures thus enrich the range of experimental opportunities that are open to investigators. In addition, because cognitive architectures provide a framework for detailed cognitive modeling, cognitive social simulations may yield results of greater predictive validity compared to multi-agent simulations that assume only rudimentary cognition on the part of agents.

This paper describes an ongoing effort to use ACT-R as a platform for cognitive social simulation in respect of a particular form of socially-distributed cognition, namely collective sensemaking. Following a brief overview of ACT-R in Section II, a specific sensemaking task is described in Section III. This sensemaking task has been the focus of previous experimental work (involving both human and synthetic agents), and it has been used to advance our understanding of the factors that affect performance in team-based situations. These features make the task particularly attractive as a starting point for the current modeling and software development effort. Section IV describes the implementation of an ACT-R agent that can perform the aforementioned sensemaking task, and Section V outlines the approach taken with respect to the implementation of a multi-agent simulation capability in ACT-R. This multi-agent simulation capability serves as the basis for performing cognitive social simulations in ACT-R. In particular, it establishes the basis for future experimental work that can systematically vary factors at the cognitive, social, technological, and informational levels in order to observe the effect of these factors on collective cognitive performance. Section VI outlines areas of further work that are needed to support these experimental efforts.

The main aims of the current paper are to 1) present an ACT-R cognitive model that be used to perform a sensemaking task, and 2) illustrate how the ACT-R model can be exploited in the context of cognitive social simulations via the use of extensions to the core ACT-R architecture. The paper also describes one means by which sensemaking capabilities can be implemented in ACT-R by adopting conventional knowledge engineering techniques. The main contributions of this work are to advance our understanding of how to model distributed cognitive processes using a popular pre-existing cognitive architecture, namely ACT-R. Such models serve as an important focus for experimental work that seeks to predict and explain the impact of social, technological and psychological factors on team-level performance.

II. ACT-R

Sun [12, p. 33] defines a cognitive architecture as "a domain-generic computational cognitive model that captures essential structures and processes of the individual mind for the purpose of a broad (multiple domain) analysis of cognition and behaviour". A cognitive architecture is thus a framework that captures some of the relatively invariant features of the human cognitive system – those features that are deemed to be more-or-less constant across domains, tasks and individuals. One example here would be the mechanisms that support the storage and retrieval of information from long-term memory. Although a number of features of the task environment may affect the ability of subjects to recall information, the mechanisms that actually realize the recall process are unlikely to change from one task to another.

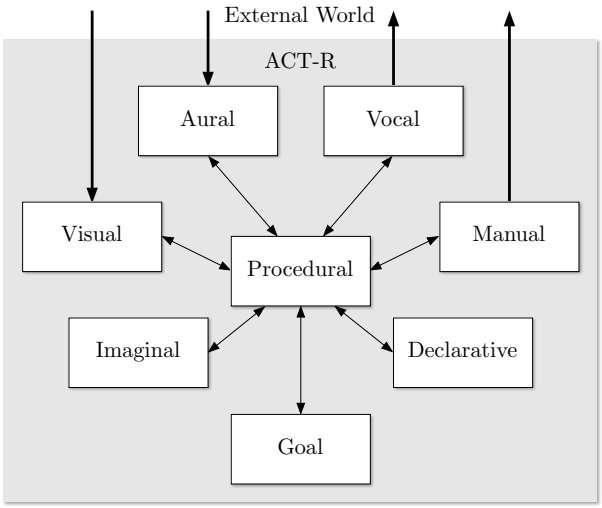

Figure 1: The core modules of the ACT-R v.6 cognitive architecture.

ACT-R is one of a number of cognitive architectures that have been used for cognitive modeling [14][15]. It is primarily a symbolic cognitive architecture in that it features the use of symbolic representations and explicit production rules; however, it also makes use of a number of subsymbolic processes that contribute to aspects of performance [15].

ACT-R consists of a number of modules (see Figure 1), each of which is devoted to processing a particular kind of information. Each module is associated with a capacity-constrained buffer that can contain a single item of information, called a chunk. The modules are assumed to access and deposit information in the buffers, and coordination between the modules is achieved by a centralized production system module – the procedural module – that can respond to the contents of the buffers and change buffer contents (via the execution of production rules). Importantly, the procedural module can only respond to the contents of the buffers; it cannot participate in the internal encapsulated activity of modules, although it can influence such processes. As shown in Figure 1, there are eight core modules in the latest version of ACT-R:

- **Input and Output Modules.** There are four input/output modules (Visual, Aural, Vocal and Manual). These provide support for modeling agent-world interactions.
- **Goal Module.** Actions within ACT-R are often dependant upon the current goal being pursued. The goal module is a specialized form of memory, with its own buffer, and it stores the current state of these goals.
- **Imaginal Module.** The imaginal module is responsible for manipulating intermediate representations of a problem when working towards a goal. For example, when calculating x in $x - 4 = 7$, the intermediate stage $x = 7 + 4$ can be stored in the imaginal module before being evaluated.

 ISBN: 978-1-61208-340-7

- **Declarative Module.** This module implements the memory system of the agent. It stores information in the form of chunks, each of which is associated with activation levels.
- **Procedural Module.** The procedural module is responsible for coordinating between the other modules. It contains rules that fire in response to the contents of the module buffers. The contents of the various modules are typically changed as a result of rule execution.

These modules (and their associated buffers) tend to form the basis of most ACT-R models. Cognitive modelers are not, however, restricted to the use of these modules, and new modules can be added to implement additional functionality. As an example of this kind of extension of the default ACT-R architecture, Rodgers et al. [18] added a total of nine buffers to the ACT-R architecture as part of their effort to implement a situation model (corresponding to a "mental model of the objects, events, actions, and relationships encountered in a complex task simulation" [18, p. 313]).

The ACT-R architecture has been used to model human cognitive performance in a wide variety of experimental contexts. It has generated findings of predictive and explanatory relevance to hundreds of phenomena encountered in the cognitive psychology and human factors literature, and this has earned it a reputation as the cognitive architecture that is probably the "best grounded in the experimental research literature" [19, p. 24]. ACT-R has also been used to model performance in a range of complex task settings. For example, ACT-R has been used to model driver behavior [20], including the effects of concurrent activities (such as cell phone usage) [21] and sleep deprivation on driver performance [22]. These features make ACT-R a compelling target for cognitive social simulation. To date, however, very few studies have sought to apply ACT-R to situations involving socially-distributed information processing (recently, however, Reitter and Lebiere [23] have demonstrated the use of ACT-R in a social information foraging task). The aim of the current work is to develop a generic framework for using ACT-R in cognitive social simulation experiments, and to then apply this framework to a particular kind of socially-distributed cognitive processing, namely collective sensemaking.

III. Collective Sensemaking and the ELICIT Framework

Sensemaking has been the focus of sustained research attention over the past 10-20 years [24][25][26][27]. It has been defined as a "motivated, continuous effort to understand connections (which can be among people, places, and events) in order to anticipate their trajectories and act effectively" [24]. Sensemaking is clearly something that individuals engage in as part of their attempt to explain and predict the features of some object, event or situation. This does not mean, however, that sensemaking is *only* something that individuals engage in. There is, in fact, a growing appreciation of the prevalence and importance of what might be called 'collective sensemaking' [3] or 'team sensemaking' [28], namely, the activities that are performed by groups of individuals in order to develop understanding at both the individual and collective levels. Collective sensemaking is a phenomenon of considerable importance in a number of different task contexts, such as intelligence analysis [25][29], military planning [30] and healthcare provision [31], and it is deemed to be of generic relevance to the problem-solving capabilities of military coalition organizations [3]. This highlights the importance of collective sensemaking as a focus area for cognitive social simulation experiments.

In order to support the effort to develop an ACT-R framework to study issues in collective sensemaking, it helps to have a concrete example of a sensemaking task on which to focus. For the purposes of this exercise, a particular sensemaking task was selected called the ELICIT sensemaking task. ELICIT, in this case, is an acronym that stands for the Experimental Laboratory for Investigating Collaboration, Information Sharing and Trust. It denotes an ongoing effort to provide a common experimental framework to investigate issues in group-level problem-solving [32]. The ELICIT sensemaking task is a particular activity that is performed by subjects within the context of the ELICIT framework. In essence, the task involves the selective presentation of information items – called factoids – to experimental subjects. Each factoid provides a limited amount of information about a situation, and the aim of the subject is to assimilate enough information in order to make a decision regarding the features of an impending terrorist attack (these features are typically referred to as the dimensions of the sensemaking task). The particular features the subject needs to resolve are as follows:

- **who:** the group that will attempt to perform the attack
- **where:** the country in which the attack will take place
- **what:** the kind of target the attack will be against (e.g., an army base)
- **when:** the date and time of the attack

A number of studies have been undertaken with different factoid sets (i.e., collections of factoids) in order to investigate the factors that affect performance in this task (e.g., [33]). A synthetic agent has also been developed to support multi-agent simulations involving the ELICIT sensemaking task [34]. This agent is, however, not based on a cognitive architecture, and it does not therefore provide access to the kinds of cognitive parameters that ACT-R makes available (e.g., the ability to run simulations in which agents use different cognitive strategies or possess different mnemonic capabilities).

One of the main advantages of the ELICIT sensemaking task is that it provides access to collections of factoids that have been used in a variety of experimental studies. This supports the attempt to develop a cognitive model in ACT-R because the factoids provide insight into the kind of knowledge structures that an agent needs in order to solve the designated problem. In addition, the availability of empirical results from previous studies (particularly those with human subjects) enables us to compare the performance of the model and assess how the results differ from those obtained with human subjects.

The first 10 factoids from one particular ELICIT factoid set (namely 'factoidset4aGMU') are shown in Table I (there are 68 factoids in the full factoid set). As can be seen from this subset of factoids, each factoid provides information about the entities and relationships associated with the situation, and

 ISBN: 978-1-61208-340-7

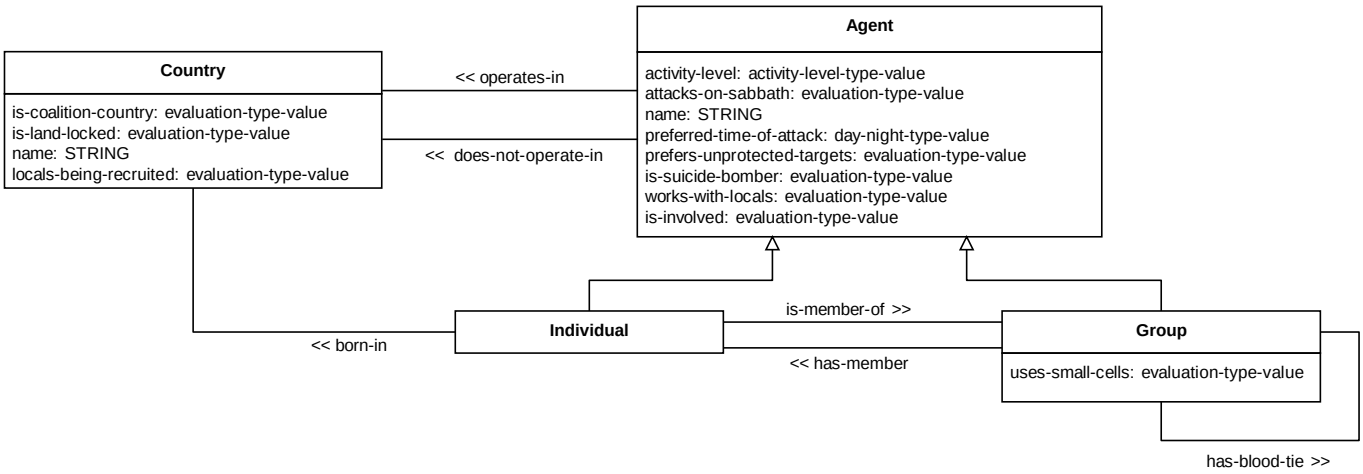

Figure 2: Part of the domain schema for the ELICIT 'factoidset4aGMU' factoidset, focusing on the Country and Agent concepts.

TABLE I: Subset of factoids from one of the factoid sets (namely 'factoidset4aGMU') used in ELICIT experiments. The characters in the 'Type' column specify the type of the factoid: E = Essential, K = Key, S = Supportive and N = Noise.

#	Type	Factoid
1	E	The Gray and Teal groups do not employ suicide bombers
2	E	There will be a suicide bomber attack at a school
3	E	The Silver group does not work in Pi
4	E	The Silver group only attacks during the day
5	N	The Rose group may be involved
6	K	The Sienna and Rose groups only target the military
7	S	Reports from the Teal group indicate standard levels of activity
8	N	There is a lot of activity involving the Rose group
9	N	The Gray group is recruiting locals – intentions unknown
10	K	The Turquoise group focuses on destroying energy infrastructure

at least some of these factoids support inferences that enable particular kinds of suspect entities (e.g., groups, countries and targets) to be eliminated. An example is provided by factoids 1 and 2 from Table I. Factoid 2 states that the impending attack will be a suicide bombing attack, and we learn from factoid 1 that Gray and Teal groups do not employ suicide bombing tactics. As a result of being presented with these two pieces of information, we can infer that neither the Gray nor the Teal group can be involved in the attack, and they can thus be eliminated from our list of suspect groups. We can also see from Table I that factoids come in four basic types: essential, key, supportive and noise [32] (these are indicated by the letters 'E', 'K', 'S', and 'N' in Table I). Expert and key factoids provide important information that is relevant to the process of resolving the who, what, when and where aspects of the task; supportive factoids provide information that tends to support the information contained in the key and essential factoids; and noise factoids contribute nothing to an agent's ability to solve the problem – the problem can be solved even if these factoids are ignored. In a typical ELICIT experiment, subsets of factoids are distributed to the members of an analysis team, and the profile of factoid sharing is controlled to mimic the features of different organizational environments. For example, the communication network can be configured so as to investigate the impact of hierarchically structured versus decentralized military command structures [33].

In order to support the development of a simulation capability in which ACT-R agents can process the ELICIT factoids and solve the sensemaking problem, a knowledge analysis of the ELICIT factoid set 'factoidset4aGMU' was undertaken. This analysis was performed in order to better understand the conceptual structures that were required by an agent tasked with processing the ELICIT factoids and to also enumerate the various inferences that were supported by each of the factoids. This analysis yielded a knowledge model that was represented using the modeling formalisms associated with the CommonKADS methodology [35]. Part of the domain schema associated with the knowledge model is illustrated in Figure 2 using UML (Unified Modeling Language) notation [36]. It highlights some of the properties and relationships that exist between two of the main components of the situation model, namely 'Agent' (a supertype of 'Group') and 'Country'. The knowledge analysis also yielded a knowledge base that contained all of the rules necessary to support factoid-related reasoning. In particular, the rules captured the essential inferences that were necessary to progressively eliminate suspect entities and identify the who (group), where (country) what (target) and when (month, day, hour) of the terrorist attack. One of these rules is shown in Figure 3. The rule, in this case, implements the inference that groups using suicide bombing tactics cannot be involved in an attack that is known to be a suicide bombing attack.

It is important to note that although the nature of the inferences associated with the processing of ELICIT factoids can seem straightforward, as is exemplified by the rule in Figure 3, the problem-solving process itself is by no means simple from the perspective of a human subject. The number of factoids to be processed ($N = 68$) imposes a heavy cognitive burden on the subjects. In addition, the subjects have no way of knowing at the outset of the process which factoids are relevant (key and essential factoids) as opposed to those that are not (i.e., the noise factoids). The number of suspect entities in each dimension of the problem also creates difficulties.

 ISBN: 978-1-61208-340-7

```
attack.is-suicide-bombing-attack = yes AND
group.is-suicide-bomber = no
     IMPLIES
group.is-involved = no
```

Figure 3: An example of a rule that resulted from a knowledge analysis of the ELICIT factoidset.

In total there are 7 groups, 5 countries, and 8 target types mentioned in the factoids, any of which could be involved in the attack. The result is that even when supportive cognitive artefacts are used (e.g., paper and paper) the challenge of identifying the correct suspect entities can seem formidable, and not all human subjects are able to solve the problem. Partly as a result of this complexity, it was difficult to validate the integrity of the aforementioned knowledge model in terms of its scope and accuracy. In fact, it is by no means clear simply by looking at all the rules in the knowledge base whether a reasoning system that implemented all the rules would be able to derive the correct solution to the problem. In order to evaluate this, a reasoning system was developed using the CLIPS (C Language Integrated Production System) expert system shell [37] (the CommonKADS knowledge model, in this case, served as a specification for the CLIPS-based implementation). This implementation effort served to identify a number of shortcomings in the original knowledge model specification. One particular shortcoming relates to factoid 51, which reads 'Sigma has closed all its schools'. This factoid is actually intended to rule out Sigma (a country) as a suspect entity. Given that we know an attack will be against a school (factoid 2), we know that a country must contain schools in order for it to be a suspect. The problem with factoid 51, in this case, is that the closure of schools is intended to mean that there are no schools in Sigma that are *viable* targets. The original (CommonKADS) knowledge model assumed that a country was a suspect entity irrespective of whether the targets located within that country were 'open' or 'closed'. This error perhaps serves to highlight one of the shortcomings of the current ELICIT factoid sets: they require subjects to make particular kinds of interpretations; however, not all of these interpretations are enforced by the semantics of the statements themselves. Obviously, further work is required to investigate this issue. Ideally, one would like the ACT-R agent to interpret factoids in the same way as human subjects, and thus one strategy could be to modify the text of the factoid statements in order to reduce semantic ambiguity. A second strategy could involve an effort to record the kinds of interpretational errors humans make when reading the sentences and then ensure that ACT-R agents make the same sort of errors with similar frequency. In both cases, one can imagine collecting the required data with questionnaires that present each of the factoids and solicit input from respondents in the form of (for example) multiple choices.

IV. Instantiation of an ACT-R Agent for Individual Sensemaking

In order to develop an ACT-R system to investigate collective sensemaking, it is necessary to develop an ACT-R cognitive model that implements the sensemaking process itself. In the present case, it is necessary to develop a cognitive model that can process each of the factoids in the aforementioned factoid set, build a mental model of the prospective situation, and then engage in reasoning processes that progressively eliminate suspect entities. In fact, this is just a *minimum* requirement. ACT-R is intended to model human cognitive processes in a way that is cognitively realistic. This means that an ACT-R sensemaking agent should not just be able to reason over the ELICIT factoids, it should also do so in a way that mimics the strategies adopted by human agents: this is what enables us to gain an explanatory and predictive toehold over human performance in particular experimental contexts. For the purposes of the current modeling and development effort, this constraint was relaxed, and the aim of simply developing a cognitive model that could solve the ELICIT sensemaking task was adopted. The motivation for this departure from standard cognitive modeling practice was based on a number of factors. Firstly, a cursory analysis of a small sample of human individuals ($N = 3$) engaged in the sensemaking task revealed a variety of different strategies. A notable difference was the way in which subjects made use of external resources, particularly pencil and paper. These enabled subjects to create paper-based lists and tables that were modified as each sentence was encountered. These bio-external representations appeared to function as cognitive aids in the problem-solving process, serving as a durable trace of task-relevant information (e.g., reminders as to which groups were not involved in the attack). This suggests that there may not be a uniform way to solve the ELICIT problem, and multiple kinds of model may be required depending on the nature of the task environment that subjects are confronted with (e.g., the kinds of representations and visualizations that are made available by a computer interface). Practical issues also governed the decision not to engage in detailed cognitive modeling for the purposes of this initial development effort. The primary goal of the current activity is to develop an experimental simulation capability that can accommodate multiple cognitive agents (i.e., agents that incorporate at least some of the constraints, characteristics and limitations associated with the human cognitive system). The details of the actual cognitive processing performed by the agents is largely irrelevant to this development effort, although it is clearly an important focus of attention when simulation experiments are being performed.

As with all ACT-R models, the implementation of the ELICIT sensemaking process in ACT-R draws on the use of production rules that match against the contents of the buffers associated with each of the ACT-R modules (see Figure 1). For the purposes of testing the cognitive model, chunks encoding the information content of each of the factoid statements were pre-loaded into declarative memory using the ACT-R `(add-dm)` command. This meant that agents were not required to engage in low-level perceptual processing of the factoid statements, neither were they required to engage in the linguistic analysis of those statements. Instead, the agents began the simulation having effectively 'memorized' all the facts implied by the factoids. Although this is clearly unrealistic relative to the kind of experimental contexts in which the ELICIT task has been investigated, it constituted an important simplifying assumption in the context of the early stages of the modeling effort. In particular, it was important to avoid a situation where assumptions were being made about the specific nature of the task environment (e.g., computer interfaces and communication equipment) that would then influence the modeling effort. In addition, the implementation

 ISBN: 978-1-61208-340-7

```
(P evaluate-group-suicide-bombing-tactics-3
=goal>
    isa                 sensemaking-goal
    selected-dimension  who
    status              evaluate-property
    selected-object     =object
    target-attribute    is-suicide-bomber
=imaginal>
    isa                 statement
    object              =object
    attribute           is-suicide-bomber
    value               no
=retrieval>
    isa                 statement
    object              attack
    attribute           is-suicide-bombing
    value               yes
==>
+imaginal>
    isa                 statement
    object              =object
    attribute           is-suspect
    value               no
    source              self
=goal>
    status              check-suspect-status
)
```

Figure 4: One of 124 productions that enables an ACT-R agent to solve the ELICIT sensemaking task.

of simulated perceptual processing and agent-world interaction mechanisms would have served to complicate what was already a challenging modeling activity.

The result of the modeling effort was an ACT-R cognitive model capable of solving the ELICIT sensemaking task. As with all ACT-R models, the key components of the model are the various chunk-types, chunks and production rules used as part of the solution. A chunk-type, in this case, specifies the structure of a chunk in terms of the slots that it can contain (a chunk-type essentially provides a template for a chunk, in the same way that a class in object-oriented programming provides a template for the data structure of an object). The main chunk-type for the model is the `statement` chunk-type:

```
(chunk-type statement
   object
   attribute
   value
   (is-true yes)
   (source self)
   (confidence 100))
```

The `statement` chunk-type represents a basic fact about the sensemaking situation, which is captured as an <`object`, `attribute`, `value`> triple, similar to the triples seen in the Resource Description Framework [38]. The chunk type contains a number of slots, the most of important of which are the `object`, `attribute` and `value` slots. The function of these and other slots is described in Table II.

Aside from chunk-types, the model contained a total of 124 production rules, one of which is shown in Figure 4. Rule execution was controlled by task state information that was stored in the ACT-R goal buffer. In particular, the process of evaluating and eliminating suspect entities was decomposed

TABLE II: Description of the slots associated with the `statement` chunk-type.

Slot	Description
object	Contains the name of an object that features as part of a situation model.
attribute	Contains the name of an attribute associated with the object named in the 'object' slot.
value	Contains the value of the attribute named in the 'attribute' slot.
is-true	Indicates whether the statement made about the object in question is true (yes) or false (no) (default is yes).
source	Specifies the source of the statement. This could be the name of a particular agent, the name of a physical information source, such as a sensor, or the name of an information repository. In cases where the statement exists as the result of an inference made by the agent, the value of the slot will be `self` (this is the default value).
confidence	Indicates the level of confidence the agent has in the truth or falsity of the statement. A value of 100 (default) indicates maximum confidence, whereas a value of 0 indicates no confidence. At present, this slot is not used as part of the reasoning process; however, it could be used in experiments that aim to study the influence of uncertainty on processes at both the individual and collective (team) levels.

into a number of inference steps, which are illustrated in Figure 5 and described in Table III. These inference steps correspond to particular stages in the larger reasoning process, and each one is associated with a particular subset of rules. By recording which inference step is 'active' at any given time, an agent can track its progress and limit the number of rules that can apply. The rule depicted in Figure 4 exemplifies this: the rule features a conditional element that matches to the `status` slot of a `sensemaking-goal` chunk that is contained in the goal buffer. This rule can only be selected for execution when the value of the `attribute` slot corresponds to 'evaluate-property', and this identifies one of the inference steps associated with the larger reasoning process (see Figure 5).

Together, the productions work to enable an ACT-R agent to eliminate suspects and yield the correct answer to the ELICIT sensemaking puzzle. Using a PC with an Intel Quad Core 2.93 GHz processor, 3 GB of RAM and running a 64-bit version of Windows 7, the entire process runs in a simulated time of 16.25 seconds. This, of course, in no way resembles the performance of human subjects in actual experimental contexts – the human subjects take much longer to find the solution to the problem. This serves to highlight the fact that the assumptions made by the current model (e.g., perfect initial memory of all facts, adoption of a robust suspect elimination strategy, and knowledge about what evaluative criteria to apply to each kind of suspect entity) do not apply to the situation seen in many of the experimental studies performed in the context of the ELICIT framework. An additional concern relates to the use of a variety of Lisp functions in order to realize the reasoning process. Although not shown in Figure 4, some of the rules rely on the use of '!bind!' and '!eval!' evaluations in order to invoke Lisp functions. As is noted by the ACT-R 6.0 reference manual [39, p. 165], the use of '!bind!' and '!eval!' in these situations may cause the model to depart from ACT-R theory, and it also creates potential problems for ACT-R's production compilation or rule learning mechanism. In spite of these shortcomings, the ACT-R model presented here does provide a working example

 ISBN: 978-1-61208-340-7

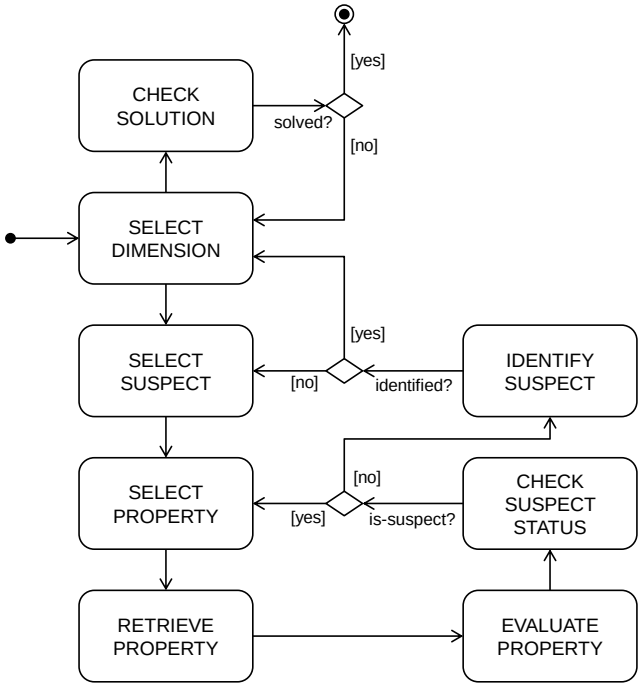

Figure 5: Activity diagram showing the inference steps implemented by an ACT-R agent engaged in the ELICIT sensemaking task.

TABLE III: Stages of the reasoning process that are implemented by the ACT-R cognitive model designed to solve the ELICIT sensemaking task.

Name	Description
CHECK-SOLUTION	Determines whether the sensemaking problem has been solved, i.e., whether the who, what, when and where dimensions of the sensemaking task have been resolved.
SELECT-DIMENSION	Selects one of the dimensions (who, what, when or where) of the sensemaking task to focus on.
SELECT-SUSPECT	Selects a particular suspect entity (e.g., a particular group) to focus on.
SELECT-PROPERTY	Selects a particular property (e.g., 'is-suicide-bomber') of the selected suspect entity to evaluate.
RETRIEVE-PROPERTY	Retrieves information about the selected property from declarative memory.
EVALUATE-PROPERTY	Evaluates the information retrieved from memory and assesses whether the suspect status of the selected entity should be modified.
CHECK-SUSPECT-STATUS	Determines whether the selected suspect entity is still a suspect following evaluation of the property retrieved in the 'RETRIEVE-PROPERTY' inference step.
IDENTIFY-SUSPECT	Assesses whether a particular suspect entity (e.g., a particular group) for a particular dimension (e.g., who dimension) can be identified. If so, the agent will proceed to select a different dimension to focus on. If not, another suspect entity will be selected until all suspect entities of a particular type have been evaluated. At this time, control passes back to the 'SELECT-DIMENSION' inference step.

of how a process previously glossed as sensemaking [34] can be implemented in a cognitive architecture that incorporates the kinds of constraints and characteristics presumed to apply in the case of human cognition.

V. An ACT-R Framework for Cognitive Social Simulation

In order to use ACT-R as a platform for cognitive social simulation, a number of extensions were made to the core ACT-R architecture. The most important extension, from the perspective of cognitive social simulation, relates to the creation of a specialized 'messaging' module that enables agents to exchange text messages with other agents. The messaging module features two buffers: 'send-message' and 'receive-message'. The send-message buffer enables agents to post a message to other agents in the simulation, while the receive-message buffer enables agents to check for unread messages and retrieve any messages that are available. A memory-resident Lisp database – the 'message database' – is used to store all the messages sent by agents, and the messaging module interfaces with this database to both create new messages and retrieve existing ones. Together, the messaging module and the message database implement the capability for agents to communicate with one another as part of a socially-distributed, collaborative problem-solving process.

The messages that get communicated by agents are represented by particular kinds of chunks, called `message` chunks. These chunks contain the following slots:

- **source:** Specifies the name of the agent that posted the message.
- **target:** Specifies the intended target of the message. If the value of this slot is 'any', the message will be posted to any agent that the originating agent can communicate with based on the structure of the communication network (see below).
- **text:** Specifies the text of the message to be communicated.

Whenever a `message` chunk is asserted in the send-message buffer as a result of rule execution, the messaging module first determines whether the target agent is a peer of the originating agent (this information is stored in another memory-resident Lisp database, called the 'connection database'). If this is the case, the messaging module will create a new record in the message database that reflects the information content of the `message` chunk. All such records are initially marked as 'unread', reflecting the fact that they have not been processed by the intended recipient.

Whenever an agent wants to retrieve new messages from the database, they can make a request to the receive-message buffer. This will cause the messaging module to check the message database for any unread messages that have been posted to the agent. If any such messages are available, one of the messages will be retrieved and a new `message` chunk will be created in the receive-message buffer. The manner in which unread messages are selected from the database can be controlled by a particular parameter, called the 'message-selection-mode' parameter, which is associated with the messaging module (for example, the most recently posted messages can be selected by setting the message-selection-mode parameter to 'newest'.). Figure 6 presents two production rules that exemplify the process of sending and receiving messages via the buffers of the messaging module.

Once a message is available in the receive-message buffer, the agent needs to interpret the message and translate the contents of the message into one or more of the `statement`

```
(p retrieve-unread-messages
=goal>
    isa       sensemaking-goal
    task      process-messages
?receive-message>
    unread    true
    buffer    empty
==>
+receive-message>
    isa       message
)

(p interpret-and-send-received-message
=goal>
    isa       sensemaking-goal
    task      process-messages
=receive-message>
    isa       message
    text      =text
?send-message>
    state     free
    buffer    empty
==>
+parse-message> =receive-message
+send-message>
    isa       message
    text      =text
    target    any
)
```

Figure 6: Two production rules that exemplify the use of the messaging module to send and receive messages via the send-message and receive-message buffers. The request to the parse-message buffer in the 'interpret-and-send-received-message' rule causes the language module to interpret the received message and create `statement` chunks in the agent's declarative memory module (see main text for details).

chunks that were described in Section IV. In order to accomplish this, the agent makes use of a second module, called the 'language' module. Like the messaging module, this module is a new custom module that does not form part of the core ACT-R architecture (see Figure 1). The language module exposes a single buffer, called 'parse-message' that can receive `message` chunks, 'interpret' the text content of the chunks (i.e., the text contained in the `text` slot of the `message` chunk), and create `statement` chunks reflecting the information content of the message. At the present time, the interpretation process is a simple one involving a string-based pattern matching mechanism. The language module makes the results of the interpretation process available to the agent by using the `(add-dm)` command to assert the `statement` chunks directly into the agent's declarative memory module. This means that the information content of any messages passed to the language module can be accessed by the agent by making retrieval requests to its declarative memory module. The use of the `(add-dm)` command, in this context, allows for situations in which multiple `statement` chunks must be asserted to reflect the factual content of a message – unfortunately, there is not always a one-to-one mapping between the messages that represent a factoid and the `statement` chunks that represent the semantic content of the factoid.

Aside from the message database, the current framework incorporates a number of additional databases. One of these is the connection database, which is used to define the structure of the communication network that exists between agents. This database contains records that specify the direct channels of communication that exist between agents. The database is queried by the messaging module to determine whether an originating agent can post a message to a particular target agent. Another database is the 'triple database'. This is used to store general information about the experimental simulation. For example, the triple database can be used to store information about the number of agents to create, the properties of agents, the particular factoid set to use, the time allowed for agents to complete the sensemaking task, and so on.

VI. LIMITATIONS

The approach described in Section V yields a system in which multiple ACT-R agents, each associated with a distinct cognitive model can engage in the sort of reasoning process described in Section IV. Each agent can thus engage in sensemaking in parallel with other agents. In contrast with the situation in Section IV, there is no need to represent all of the factoid-related information in an agent's memory at the outset of the simulation. Instead, agents can be provided with an initial subset of factoids (by creating messages in the message database), and then additional factoids can be made available as the simulation progresses (either as a result of a centralized information distribution mechanism, or, more interestingly, as a result of agents posting messages to each other via their respective messaging modules). As such, this system implements the basic requirements of a system designed to support the execution of cognitive social simulation experiments: each of the agents engages in a sensemaking process and is also able to communicate task-relevant information to other agents at specific junctures in the problem-solving process. As it stands, however, the current system possesses a number of limitations, and these are the focus of future research and development efforts. These limitations are described below.

A. Question/Answering Capabilities

At present, ACT-R agents can only communicate factual information to each other; they cannot pose questions for their peers to answer. In order to support question/answering capabilities in the context of the current approach, agents need to be able to 1) recognize the conditions under which a question should be asked, 2) formulate the question in a way that other agents can understand, 3) post the question to other agents and 4) recognize what information is being sought in a question posed by another agent. Of these, only points 1, 2 and 4 are significant challenges – the posting of information to other agents is already addressed by the solution presented in Section V. The challenge related to recognizing the conditions under which a question should be asked could perhaps be addressed by the possibility of what are known as retrieval failures in ACT-R. These are essentially situations in which a request to the retrieval buffer fails to retrieve information from declarative memory. A solution to the fourth challenge could rest on the structure of the `statement` chunk used for knowledge representation (see Section IV). In particular, a question could be encoded as a specialized form of the `statement` chunk in which the `value` slot is either empty or absent. The values of the `object` and `attribute` slots would then signal what information was being requested, and this could be used by a recipient to implement a retrieval request against their own declarative memory module.

 ISBN: 978-1-61208-340-7

B. Communication Strategy

In addition to question/answering capabilities, agents will need to make decisions about what to communicate, when to communicate and who to communicate with. A number of different strategies are possible here. For example, agents could adopt a somewhat passive strategy and only communicate facts when requested to do so, perhaps in response to a particular question. Alternatively, they could adopt an active strategy in which all information is readily communicated. Agents also need to make decisions about who to communicate with. They can thus adopt strategies that might be described as directed or undirected in nature. Directed strategies, in this case, are strategies where agents send messages to particular individuals within their social network; undirected strategies, on the other hand, are ones in which a message is broadcast to all connected agents. A final decision that agents need to make concerns the nature of what should be communicated. Should agents, for example, limit to their communication to information that has been received from external sources (e.g., other agents), or should they include information that has been inferred as a result of their own sensemaking activity? A number of previous studies using cognitive architectures (including ACT-R) have begun to explore these issues in some detail [23][40], and a closer examination of the solutions used in those particular studies is likely to be helpful in the present context.

C. Cognitive Strategy

As discussed in Section IV, the particular strategy adopted by agents to solve the ELICIT sensemaking task is unlikely to be the same as that used as human subjects. In order to better understand the effect of specific manipulations on the performance of human subjects in the task it will thus be necessary to pay closer attention to the kinds of strategies adopted by human subjects. In all likelihood, this will require studies involving the use of protocol analysis techniques [41].

D. Task Environment

Related to the previous point is the need to consider the role that material elements of the task environment play in shaping and influencing cognitive processes at both the individual and collective levels. In cases where humans are tasked with the ELICIT sensemaking problem, they typically resort to using bio-external artefacts, such as pen and paper (see Section IV). The external resources, in these cases, appear to be functioning as a form of environmentally-extended working memory that potentially enhances the cognitive capabilities of the human subject [42]. Inasmuch as ACT-R attempts to duplicate the cognitive constraints and limitations of the human brain, then ACT-R sensemaking agents may need to rely on the same sort of cognitive scaffolding as is seen in the case of their environmentally-situated human counterparts. In particular, it may be that a successful model of complex task performance in naturalistic situations will need to avail itself of computational analogues of the specific aspects of the physical problem-solving environment that are exploited by human subjects. In situations where human subjects are attempting to solve the ELICIT sensemaking problem via computer interfaces, it may thus be necessary to represent elements of the computer interface within the ACT-R simulation. For example, in situations where human subjects are able to view a list of messages that have been posted by other agents, it may be necessary to equip ACT-R agents with an ability to 'see' such messages in order to replicate the kind of mnemonic support that is provided by the real-world list. Recent versions of ACT-R provide support for modeling agent-world interactions through the use of what is called a 'device' object. The use of this object to represent features of the task environment within which agents are situated constitutes an important focus area for future research efforts.

E. Task Features

In addition to these issues, it should be noted that all the factoids in the ELICIT sensemaking task are assumed to be true. This is clearly unlike the situation in real-world sensemaking contexts where agents have to deal with conflicting, uncertain and dynamic information from a constantly evolving situation. Therefore, in addition to the aforementioned issues, future work will need to consider modifications to the ELICIT sensemaking task in order to establish a closer alignment with the kinds of situations faced by real-world sensemakers.

VII. Conclusion and Future Work

The aim of cognitive social simulation is to improve our understanding of the complex inter-play between factors that are spread across the psychological, social and technological domains. This makes cognitive social simulation techniques particularly appealing as a means to undertake experiments into socially-distributed cognition. Cognitive social simulation studies typically rely on the use of cognitive architectures; however, to date, the most widely used cognitive architecture – ACT-R – has seen only limited use in computational studies exploring group-level cognitive dynamics. The current paper reports on the results of an ongoing effort to develop an experimental simulation capability that can be used to undertake studies into socially-distributed cognition using the ACT-R architecture. Using an existing experimental task as a starting point, a cognitive model was developed to show how sensemaking processes could be accommodated within ACT-R. A cognitive social simulation capability was then implemented in ACT-R by relying on the use of a combination of custom modules and memory-resident databases in order to enable agents to exchange information during the course of their sensemaking activities. This solution provides the basic ingredients required to undertake cognitive social simulation experiments into collective sensemaking; however, further research needs to be undertaken in order to improve the communicative capabilities of agents, as well as the task environment in which they are situated (see Section VI). Our future work in this area will aim to improve the sophistication of the ACT-R cognitive model so that agents are able to adopt a variety of communication strategies concerning what information (i.e., factoids) to share and who to share the information with. We will also seek to enable better forms of agent-environment interaction by implementing a custom ACT-R device object. These extensions will support cognitive social simulations that aim to replicate and extend previous results obtained with human subjects in the context of the ELICIT sensemaking task [33].

 ISBN: 978-1-61208-340-7

ACKNOWLEDGMENT

Research was sponsored by US Army Research laboratory and the UK Ministry of Defence and was accomplished under Agreement Number W911NF-06-3-0001. The views and conclusions contained in this document are those of the authors and should not be interpreted as representing the official policies, either expressed or implied, of the US Army Research Laboratory, the U.S. Government, the UK Ministry of Defence, or the UK Government. The US and UK Governments are authorized to reproduce and distribute reprints for Government purposes notwithstanding any copyright notation hereon.

REFERENCES

[1] N. J. Cooke, J. C. Gorman, C. W. Myers, and J. L. Duran, "Interactive team cognition," Cognitive Science, vol. 37, no. 2, 2013, pp. 255–285.

[2] G. R. Semin and E. R. Smith, "Socially situated cognition in perspective," Social Cognition, vol. 31, no. 2, 2013, pp. 125–146.

[3] P. R. Smart and K. Sycara, "Collective sensemaking and military coalitions," Intelligent Systems, vol. 28, no. 1, 2013, pp. 50–56.

[4] G. Theiner, C. Allen, and R. L. Goldstone, "Recognizing group cognition," Cognitive Systems Research, vol. 11, 2010, pp. 378–395.

[5] M. Kearns, "Experiments in social computation," Communications of the ACM, vol. 55, no. 10, 2012, pp. 56–67.

[6] J. Sutton, C. Harris, P. Keil, and A. Barnier, "The psychology of memory, extended cognition, and socially distributed remembering," Phenomenology and the Cognitive Sciences, vol. 9, no. 4, 2010, pp. 521–560.

[7] V. Hinsz, R. Tindale, and D. Vollrath, "The emerging conceptualization of groups as information processors," Psychological Bulletin, vol. 121, 1997, pp. 43–64.

[8] R. Menary, The Extended Mind. Cambridge, Massachusetts, USA: MIT Press, 2010.

[9] P. Robbins and M. Aydede, The Cambridge Handbook of Situated Cognition. New York, USA: Cambridge University Press, 2009.

[10] L. A. Shapiro, Embodied Cognition. Abingdon, Oxfordshire, UK: Routledge, 2011.

[11] W. Mason, F. Conrey, and E. Smith, "Situating social influence processes: Dynamic, multidirectional flows of influence within social networks," Personality and Social Psychology Review, vol. 11, no. 3, 2007, pp. 279–300.

[12] R. Sun, "Cognitive social simulation incorporating cognitive architectures," Intelligent Systems, vol. 22, no. 5, 2007, pp. 33–39.

[13] P. Thagard, "Cognitive architectures," in The Cambridge Handbook of Cognitive Science, K. Frankish and W. M. Ramsey, Eds. Cambridge, UK: Cambridge University Press, 2012, pp. 50–70.

[14] J. R. Anderson, How Can the Human Mind Occur in the Physical Universe? Oxford, UK: Oxford University Press, 2007.

[15] J. R. Anderson, D. Bothell, M. D. Byrne, S. Douglass, C. Lebiere, and Y. Qin, "An integrated theory of the mind," Psychological Review, vol. 111, no. 4, 2004, pp. 1036–1060.

[16] J. E. Laird, A. Newell, and P. S. Rosenbloom, "SOAR: An architecture for general intelligence," Artificial Intelligence, vol. 33, no. 1, 1987, pp. 1–64.

[17] J. E. Laird, The SOAR Cognitive Architecture. Boston, Massachusetts, USA: MIT Press, 2012.

[18] S. M. Rodgers, C. W. Myers, J. Ball, and M. D. Freiman, "Toward a situation model in a cognitive architecture," Computational and Mathematical Organization Theory, vol. 19, no. 3, 2013, pp. 313–345.

[19] J. E. Morrison, "A review of computer-based human behavior representations and their relation to military simulations," Institute for Defense Analyses, Tech. Rep. IDA Paper P-3845, 2003.

[20] D. D. Salvucci, "Modeling driver behavior in a cognitive architecture," Human Factors, vol. 48, no. 2, 2006, pp. 362–380.

[21] D. D. Salvucci and K. L. Macuga, "Predicting the effects of cellular-phone dialing on driver performance," Cognitive Systems Research, vol. 3, no. 1, 2002, pp. 95–102.

[22] G. Gunzelmann, R. L. Moore, D. D. Salvucci, and K. A. Gluck, "Sleep loss and driver performance: Quantitative predictions with zero free parameters," Cognitive Systems Research, vol. 12, no. 2, 2011, pp. 154–163.

[23] D. Reitter and C. Lebiere, "Social cognition: Memory decay and adaptive information filtering for robust information maintenance," in 26th AAAI Conference on Artificial Intelligence, Toronto, Canada, 2012.

[24] G. Klein, B. Moon, and R. R. Hoffman, "Making sense of sensemaking 1: Alternative perspectives," Intelligent Systems, vol. 21, no. 4, 2006, pp. 70–73.

[25] D. T. Moore, "Sensemaking: A structure for an intelligence revolution," National Defense Intelligence College, Tech. Rep., 2011.

[26] P. Pirolli and D. M. Russell, "Introduction to this special issue on sensemaking," Human-Computer Interaction, vol. 26, no. 1-2, 2011, pp. 1–8.

[27] K. E. Weick, Sensemaking in Organizations. Thousand Oaks, Califfornia, USA: Sage Publications, 1995.

[28] G. Klein, S. Wiggins, and C. O. Dominguez, "Team sensemaking," Theoretical Issues in Ergonomics Science, vol. 11, no. 4, 2010, pp. 304–320.

[29] P. Pirolli and S. Card, "The sensemaking process and leverage points for analyst technology as identified through cognitive task analysis," in International Conference on Intelligence Analysis, vol. 5, McLean, Virginia, USA, 2005.

[30] E. Jensen, "Sensemaking in military planning: A methodological study of command teams," Cognition, Technology & Work, vol. 11, no. 2, 2009, pp. 103–118.

[31] S. A. Paul and M. C. Reddy, "Understanding together: Sensemaking in collaborative information seeking," in ACM Conference on Computer-Supported Cooperative Work. Savannah, Georgia, USA: ACM, 2010, pp. 321–330.

[32] M. Ruddy, "ELICIT – the experimental laboratory for investigating collaboration, information sharing and trust," in 12th International Command and Control Research and Technology Symposium (ICCRTS), Newport, Rhode Island, USA, 2007.

[33] M. Manso and M. Ruddy, "Comparison between human and agent runs in the ELICIT N2C2M2 validation experiments," in 18th International Command and Control Research and Technology Symposium (ICCRTS), Alexandria, Virginia, USA, 2013.

[34] M. Ruddy, D. M. Wynn, and J. McEver, "Instantiation of a sensemaking agent for use with ELICIT experimentation," in 14th International Command and Control Research and Technology Symposium, Washington D.C., USA, 2009.

[35] G. Schreiber, H. Akkermans, A. Anjewierden, R. de Hoog, N. R. Shadbolt, W. Van de Velde, and B. Weilinga, Knowledge Engineering and Management: The CommonKADS Methodology. Cambridge, Massachusetts, USA: MIT Press, 2000.

[36] "Unified Modeling Language (UML)," URL: http://www.uml.org/ [accessed: 2014-04-17].

[37] "CLIPS: A Tool for Building Expert Systems," URL: http://clipsrules.sourceforge.net/ [accessed: 2014-04-14].

[38] "RDF – Semantic Web Standards," URL: http://www.w3.org/RDF/ [accessed: 2014-04-14].

[39] "ACT-R 6.0 Reference Manual," URL: http://act-r.psy.cmu.edu/actr6/reference-manual.pdf [accessed: 2014-04-15].

[40] M. Kang, "The effects of agent activeness and cooperativeness on team decision efficiency: A computational simulation study using TeamSoar," International Journal of Human-Computer Studies, vol. 65, no. 6, 2007, pp. 497–510.

[41] N. R. Shadbolt and P. R. Smart, "Knowledge elicitation: Methods, tools and techniques," in Evaluation of Human Work, 4th ed., J. R. Wilson and S. Sharples, Eds. Boca Raton, Florida, USA: CRC Press, in press.

[42] A. Clark, Supersizing the Mind: Embodiment, Action, and Cognitive Extension. New York, New York, USA: Oxford University Press, 2008.

 ISBN: 978-1-61208-340-7

Handling Seasonality using Metacognition

Kenneth M'Balé, Darsana Josyula
Department of Computer Science
Bowie State University
Bowie, MD USA
kmbale@cs.umd.edu and darsana@cs.umd.edu

***Abstract*— This paper summarizes a work in progress in the area of the metacognitive loop (MCL). The objective of MCL is to provide a design approach supported by software to extend an intelligent system's ability to cope with perturbations. A perturbation is any deviation from optimal performance for the system. Many MCL implementations exist, each increasing in sophistication. This paper describes an approach to produce the next implementation of MCL, which we call the General Purpose Metacognition Engine (GPME). The GPME evolves the functionality of the current implementation developed at the University of Maryland, MCL2, in particular, to handle seasonality. Seasonality is a periodic or cyclic variation in conditions that causes agents to re-learn when the length of the seasonal cycle exceeds their ability to detect the cycle.**

Keywords-Metacognition;Learning;Reasoning;Situated Agents;Autonomous Agents.

I. INTRODUCTION

One of the objectives of Artificial Intelligence is to impart upon systems the ability humans have for overcoming the "brittleness problem." The "brittleness problem" is the characteristic of systems to fail when operating circumstances exceed the designer's expectations. The Metacognitive Loop is a proposed solution for addressing this problem [1].

Metacognition is cognition about cognition; reasoning about one's own reasoning. Conceptually, the solution consists of one system, referred to as the host, which is integrated with another system referred to as MCL. The host supplies information to MCL about its actions and about the expectations of the results of these actions. MCL monitors the success of the host's actions by comparing expectations and outcomes. When an outcome does not match an expectation, MCL notes the anomaly. It assesses the anomaly using its internal knowledge such as significance, priority, similarity to other anomalies and possible responses. Finally, MCL guides the host by providing a suggestion to address the anomaly. MCL applies a basic algorithm composed of these steps; note, assess, guide, repeat [2].

Consider a robot trained to perform a certain function. Its initial training occurs on a dry surface. After some time in operation, it arrives at a wet surface. It needs to learn how to function efficiently on this new surface. A slightly wet surface might require minor adjustments such as tolerating wheel slippage. A very wet surface requires major adjustments that amount to relearning how to function. Learning is a time-consuming and expensive operation. After some time operating on the wet surface, the robot moves again onto a dry surface. Ideally, it is not necessary for the robot to once again invest the same level of effort for learning how to function on a dry surface. A better option is for the robot to note the change in the environment it is situated in, to assess which of its learned procedures have the best chance to work and to proceed efficiently. While this example used a robot, MCL and GPME are intended to integrate with cognitive robots or cognitive software agents. We use the terms host, agent and robot interchangeably to mean a cognitive host.

Several approaches have been researched to address seasonality. For example, Zhang and Qi describe the inability of artificial neural networks to handle seasonality [3]. Using simulated and real trend time series data, their research concludes that neural networks are not well suited to forecast without substantial prior data processing. In another paper, Taskaya-Temizel and Casey conclude that neural networks model seasonality provided their architecture is properly configured [4]. To address seasonality, the input layer size should be equal to the longest cycle information. In this paper, we discuss how seasonality, changes that repeat periodically, can be handled using expectation violations.

In Section II, we describe the initial MCL implemented using different strategies. In section III, we describe the current implementation of MCL (MCL2). In Section IV, we describe the design of the GPME, the successor to MCL2. In Section V, we describe our testing approach. Finally, we conclude.

II. MCL-ENHANCED Q-LEARNERS

Agents equipped with MCL have the ability to recover from unanticipated failures. Several applications of MCL exist that improve the performance of the underlying cognitive agent. The earliest MCL implementations utilized simple strategies to improve a host system that consisted of a Q-Learner as the baseline [5]. The baseline Q-Learner enhanced with MCL was capable of increasingly complex responses to expectation violations (anomalies).

The Q-Learner was deployed in a basic 8x8 grid where two grid locations contained rewards. After a set number of cycles, the reward locations, magnitude and type were changed to force an anomaly. The performance of the Q-Learner to relearn the location of the rewards, by abandoning the policy it had previously learned and restarting the learning when needed, is the key measure used to compare performance between several variations of MCL, as reported in Table I.

In response to the anomaly, simple MCL purges the policy that the Q-Learner has learned and restarts learning. The simple MCL acted after the occurrence of three

 ISBN: 978-1-61208-340-7

anomalies. The sensitive MCL considered reward values, time to reward and the expected reward per cycle. In addition, it expanded the definition of anomalies to include an unexpected reward, delays in finding rewards and the actual value of the reward compared to the expectation. The next two MCL added an effect on exploration by introducing an exploration factor called ε. A Q-learner will take the action recommended by its policy (the so-called ‘‘greedy action’’) with probability (1 – ε), and will take a random action with probability ε. This helps ensure that the agent comprehensively and continuously explores its world, learning the effect of all the actions it can take from all possible states, rather than sticking to what it already knows will bring rewards. In addition to purging, the ε value is changed to encourage the Q-Learner to explore the grid. In the steady case, the ε value is set to a fixed amount for a fixed number of cycles and then returned to the baseline value. In the decaying case, the ε value is set to the same fixed amount but it decays linearly back to the baseline value over the same number of cycles.

TABLE I. Q-LEARNER PERFORMANCE SUMMARY.

MCL type	Performance
Baseline Q-Learner	0.530
Simple MCL	0.545
Sensitive MCL	0.546
Steady ε	0.510
Decaying ε	0.526
Sophisticated MCL	0.567

Finally, the sophisticated MCL carried out an analysis of the anomaly and incorporated the results in its suggestion. It measured the magnitude of the anomaly and used this calculation to affect ε, and beyond a certain threshold, to purge. It used a decision tree to classify the degree of perturbation of the anomaly, to moderate its response.

In all these approaches, when the world has changed considerably, MCL throws out the current policy and restarts learning. Tsumori and Ozawa showed that in cyclical environments, reinforcement learning performance could be enhanced with a long-term memory and a ‘‘change detector’’, which would recall stored policies when a given known environment reappeared [6]. The different “throw-out current policy and explore” MCLs discussed above act as change detectors but they do not have a memory to store policies associated with a given environment and to recall policies when a known environment reappears (seasonality).

MCL has been applied to other systems to improve their responses to anomalies. In the Air Traffic Controller (ATC) [7] and the Natural Language Processor (Alfred) [8] implementations, MCL is implemented as a component within the host agent. In the Mars Rover [9] implementation, MCL is an external component that controls the behavior of the host agent.

An important consideration from the implementation of MCL across these several domains is that a general purpose, domain independent MCL could be possible and useful.

III. MCL2

MCL2 applies the note-assess-guide cycle for metacognition using three ontologies organized as a Bayes net shown in Figure 1. Indications nodes are connected to fringe nodes associated with domain specific expectation violations. Response nodes are connected to fringe nodes associated with domain specific actions. Failure nodes connect indications to responses. MCL2 tracks the success of suggestions against anomalies classified by indications and probable causes. The responses are statically defined at initialization to ensure that the host can process them appropriately.

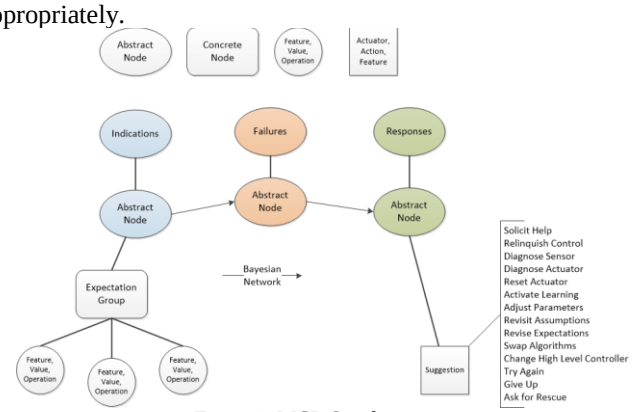

Figure 1. MCL Ontology

MCL2 succeeds in separating the MCL function from the host, as an independent process performing a general purpose function. However, MCL2 cannot handle seasonal changes efficiently since it does not have an episodic memory. Without an episodic memory, the Bayes net evolves continually without any note of time.

IV. GPME

The GPME squarely aims to remove brittleness from MCL itself and to facilitate integration with applications [10]. The communication between the host and the GPME is fully asynchronous (Figure 2).

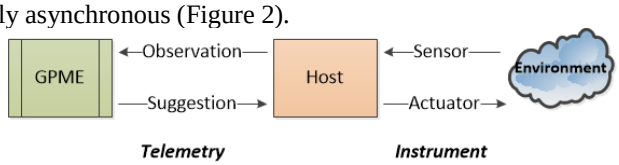

Figure 2. GPME and Host Integration

As a result, the burden is fully upon the GPME to detect anomalies from the telemetry. Therefore, some of the cognitive burden is alleviated from the host. Furthermore, the GPME defines anomalies dynamically by learning expectations from the telemetry. Consequently, the GPME uses an episodic memory to store, process and analyze its experiences.

A. *Episodic Memory*

The host supplies the GPME with a continuous telemetry stream. For the purpose of analyzing and detecting patterns in the telemetry, the GPME needs to break the telemetry into parts. We can consider each part as its own stream.

 ISBN: 978-1-61208-340-7

*1) **Segments***

Each distinct observation and suggestion is captured in an object we call a Segment (Figure 3).

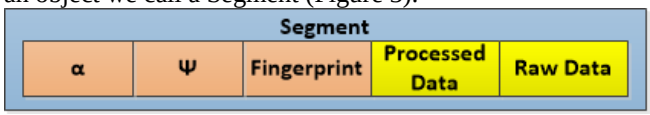

Figure 3. GPME Segment

The Processed Data and Raw Data originate from the host. Raw Data is actual sample data from the instrument. Processed Data is produced by the host using the Raw Data. For example, if the Raw Data contains a photograph, the Processed Data might contain a list of recognized faces or objects in the photograph. The α attribute is the A-distance; the probability of occurrence of this segment and its values within its own segment stream. To create the Fingerprint, the GPME samples 256 words (2 bytes) at fixed positions in the Raw Data. The fingerprint is an abbreviation of the Raw Data created from a fixed positional filter. To create the ψ attribute, the GPME measures the Hamming distance between the fingerprint and a constant fingerprint called the Prime Fingerprint. The Prime Fingerprint is randomly generated at initialization and it never changes throughout the life of the GPME.

2) Frames

We define a Frame (Figure 4) as the set of all segments received during a given GPME moment.

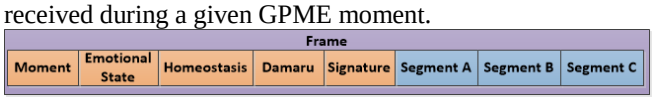

Figure 4. GPME Frame

The GPME adds a unique moment identifier to the frame. It then initializes the Damaru metric (decay value) to a special constant value called β and records the GPME's current homeostasis and emotional state (described later). The Damaru metric is a measure of the utility of the frame. It is a function of the number of times the frame is referenced in the episodic memory. The GPME generates the signature of the frame. The signature of the frame is a vector that identifies which instruments contributed segments to the frame and the number of segments each instrument contributed.

3) Links

Frames are interconnected using links. A link has a direction. The types of links are temporal, causative, attributive, spatial, order and composition. Temporal, causative and attributive links are established between adjacent frames when the frame is created. Causative and attributive links decay while temporal links do not decay. The temporal link reflects the order in which the frame arrived over time. This ordering is immutable. The causative link denotes that conditions in the successor frame are the result of preconditions in the predecessor frame. The attributive link denotes the inverse. Over time, incorrect causative and attributive links decay and disappear from the knowledge base. Spatial, order and composition links are created in response to certain anomalies. Temporal links connect successor and predecessor frames in order of arrival. There can be one of each type of link between two frames.

4) Clusters

The GPME stores each frame internally and generates additional data structures using sets of related frames. We call such a structure a Cluster. The GPME has a hierarchical knowledge base built using clusters (Figure 5). A cluster has a fixed maximum number of member frames (a prime number such as 13 or 17). The GMPE derives an artificial or abstract member called a Centroid. The centroid member contains the most significant information from each member, where significance is a function of the segment's α attributes. The centroid inherits all the links of its members. We refer to the abstract frame of a centroid as a Fragment because it is a partial or incomplete frame. A mature cluster exhibits a very tight grouping; the centroid is essentially equivalent to the members. Recall that a frame consists of several segments. The GPME uses the segments' ψ attributes to place the parent frame in a ψ cluster. The GPME uses the frame signature to place the frame in a signature cluster. A cluster can be understood as a super frame, where the member frames are treated as equivalent to each other and all of their links are available for traversal.

5) Decay and Moments

In order to keep the internal knowledge base manageable, every object carries the Damaru decay attribute. When the Damaru value reaches zero, the object is deleted. A GPME moment is defined as the time required to decrement the Damaru metric of every object by one. Therefore, each moment results in one frame, and in each moment every object decays.

6) Episodes

The GPME creates an episode in response to an anomaly. An episode begins with the content of short-term memory and includes all future frames, until the anomaly is no longer detected or decays. Therefore, an episode is a set of sequential frames. Episodes can overlap by sharing frames. The anomaly is identified by its signature. The anomaly signature consists of the attributes that caused the anomaly.

7) Cases

Episodes with similar anomaly signatures and similar data patterns are clustered into a Case. A case is equivalent to a cluster, but its members are episodes (sets of sequential frames). Therefore, the case centroid is an artificial or abstract episode that contains the most significant information from each member, where significance is a function of the anomaly signature**.**

Case-based reasoning is closely related to episodic memory. A case describes a problem the system encountered and the solution to the problem [11]. The system needs to match a new problem to an existing case to arrive at a previously successful solution.

The GPME uses a variant of case-based reasoning. Traditionally, the cases result in well-known solutions. However, the GPME creates its own cases from episodes and refines them over time. As a result, each case provides several overlapping solutions to the same problem. The cases form an abstraction hierarchy above the detailed episodes.

 ISBN: 978-1-61208-340-7

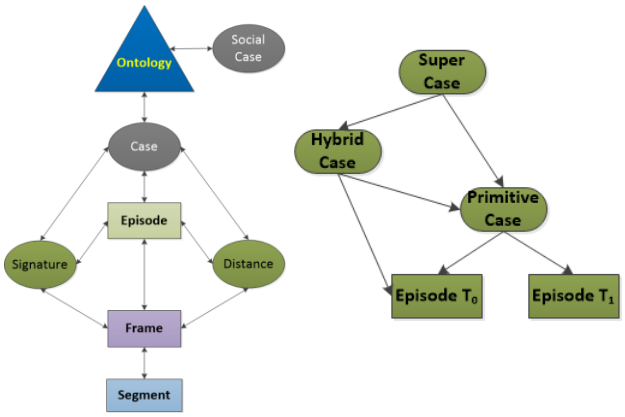

Figure 5. GPME Knowledge Base

The GPME uses cases to determine when to adjust the knowledge base by looking for cases that resemble the current anomaly circumstances.

8) Homeostasis

The GPME is an intrinsic reinforcement learner. It uses an internal reward that is a function of the number and types of anomalies that currently exist and the projection of the reward in the future. We refer to the result of this function as the homeostasis. As a result, the GPME can react to an anomaly caused by future unexpected homeostasis values.

9) Selective Imitation

In addition to being an intrinsic reinforcement learner, the GPME learns by imitation. The formalization of the knowledge base makes it possible for the GPME to share parts of its knowledge base with other instances. The recipient GPME can then select the portions of the model's knowledge base that it wants to incorporate within its own. The GPME is able to learn new cases and reasoning mechanisms from other GPME instances without needing to experience the environment first hand.

B. Episodic Memory-Driven Projections

The GPME uses its episodic memory in two ways. First, it matches the current frame to its experiences in order to project the future. Second, it matches the current anomaly to its experience to select a suggestion and project the future. Refer to Figure 6 during the description of the projection procedure.

1) Expectation Generation

The projection contains fragments and homeostasis. The GPME matches the current frame to the projection to determine whether anomalies are occurring. This approach allows the GPME to define anomalies and expectations dynamically.

2) Anomalies

The GPME creates an episode when it detects an anomaly. There are four types of anomalies; reflex, rational, context and emotional. The episode ends when the anomaly is no longer detected or it has fully decayed. A rational anomaly occurs when the projected homeostasis value is not achieved when expected, either because the actual homeostasis is over or under the projected homeostasis.

The other types of anomaly detection use the concept of Bandwidth. A bandwidth is the projected range of a certain value. The projection is based on historical value contained in the short-term memory. The value is projected to occur within an upper and lower bound. An anomaly occurs whenever the value falls outside the band. The anomaly is resolved when the value returns to its original projection. Since the short-term memory changes over time, the bandwidth also changes. Therefore, it is possible for the bandwidth to catch up to the projected value. When this situation occurs, the anomaly is aborted.

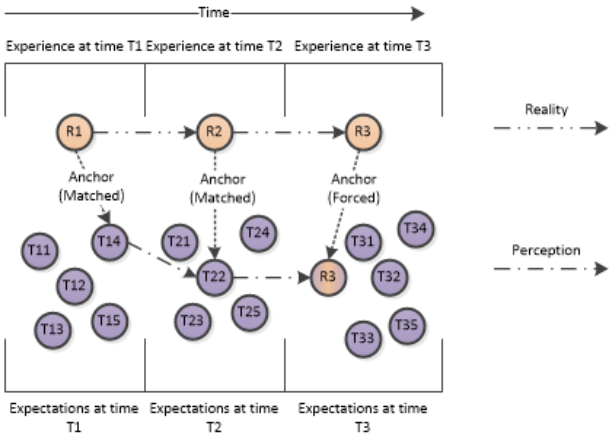

Figure 6. Projections

The reflex method projects an arrival rate of frames for each instrument stream. This projection is called the instrument arrival rate bandwidth. For example, the GPME expects the camera to provide an image every five seconds. After six seconds, if an image has not arrived, the GPME detects a reflex anomaly. The same anomaly would also be detected if the image arrived three seconds after the previous one. Since instruments are unlikely to be as regular as the example indicates, the GPME uses a range based on its experiences.

The context method detects an anomaly in two different ways. The first way relies on segment significance. The anomaly occurs when a segment that should be significant is not, or, when a segment that should not be significant is found to be. When the significance of a segment does not match its projected significance, the GPME detects the anomaly and creates an episode. The second way projects the accuracy of the projection. This expectation is called the projection accuracy bandwidth.

The emotional method relies on the homeostasis value. The GPME projects the homeostasis value to be within a certain range, called the homeostasis bandwidth. If the homeostasis value is outside the band, the GPME detects the anomaly and creates an episode. The bandwidth is the range between the highest and lowest homeostasis value in short-term memory, however, it is further adjusted by the emotional state.

3) Deadlines

When the GPME provides a suggestion, it also projects the effect the suggestion will have in the future, based on its

 ISBN: 978-1-61208-340-7

experience. As a result, the GPME also establishes deadlines by which results are expected. Deadlines allow the GPME to respond to anomalies of absence.

4) Reasoning Mechanisms

While responding to anomalies, the links allow the GPME to traverse the knowledge base in search of experiences that link current conditions to goal conditions. The algorithm the GPME uses to search the knowledge base is called a Reasoning Mechanism. The reasoning mechanism is specified in an internal language called Amri. The GPME is deployed with a number of reasoning mechanisms; deductive, qualitative, probabilistic, inductive, abductive, analogical, reactive, look-ahead and creative. The GPME can create new reasoning mechanisms by applying a Programming Method. The methods are random, mutation, interleaving and grafting.

For example, the deductive reasoning mechanism looks for the highest homeostasis value in linked cases, following the causal type links only. The abductive reasoning mechanism uses the causative or order link between super cases only. The look-ahead reasoning mechanism uses the temporal link through the clusters to find co-occurring centroids to build projections. The creative reasoning mechanism generates a result using its internal representation of the environment. The interleaving programming method blends two reasoning mechanisms into a new one.

5) Bayes Ontology

The GPME retains the Bayes ontology from MCL2. However, it is used to manage the success of reasoning mechanisms in producing a successful suggestion. In MCL2, it was used to track the success of specific suggestions.

C. GPME Processes

In principle, the GPME is similar to the Ouroboros model [12] at a high level. Comparisons between the models will be possible once there is an Ouroboros implementation. At the core of the Ouroboros model lays a self-referential recursive process with alternating phases of data acquisition and evaluation. In comparison, the GPME is a highly parallel system with several distinct processes operating concurrently on the episodic memory and the projection. There are eight distinct GPME processes named after Hindu mythology based on their function. Figure 7 depicts the GPME processes and their high-level data flows.

The **Vishnu** process assembles the current frame from the telemetry and supplies it to the Brahma and the Shiva processes. Vishnu sources the knowledge base to create projections based on the current frame. These projections are not related to anomalies; they are expectations of what normally happens in the future based on current conditions. The projections and their links are referred as the Vishnu Web.

The **Shiva** process identifies fragments (projections) that match the current frame. Such a fragment is referred to as an Anchor. Anchors are placed in short-term memory. Shiva reverses the decay of useful cases (and their underlying frames) and generates anomalies related to matching.

The **Kali** process decays every object in the knowledge base by one unit. It calculates the current homeostasis value and emotional state. It publishes a new moment unique identifier. It also triggers homeostasis anomalies.

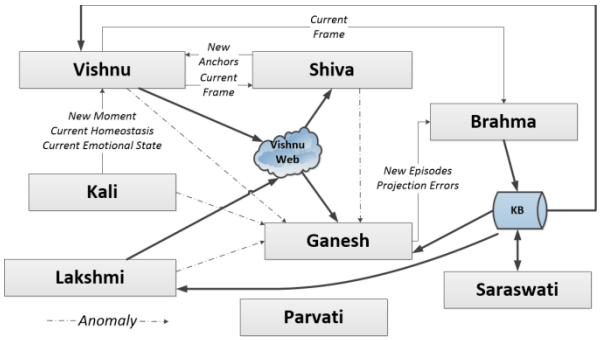

Figure 7. GPME Processes

The **Ganesh** process is responsible for responding to anomalies by doing nothing, waiting or using a reasoning mechanism to identify a suggestion. It creates an episode in the presence of an anomaly. If a suggestion is identified, it projects the expected results in the Vishnu Web.

The **Brahma** process manages the knowledge base and continually revises and optimizes clusters and cases. It also maintains the ontology.

The **Saraswati** process is responsible for communicating with other GPME instances.

The **Lakshmi** process is responsible for handling special requests from the host and for monitoring the accuracy of the Vishnu Web.

The **Parvati** process provides an instrumentation and management interface.

V. ONGOING AND FUTURE WORK

Since the GPME improves on MCL2, the testing strategy revolves around comparing the performance of systems placed in the same circumstances and scenarios. We intend to compare the system's performance when integrated with MCL2 in comparison to integrated with GPME. If possible, we will also compare performances with an established metacognitive framework such as SOAR-RL [13].

While several metrics will be collected, the principal metric is homeostasis. As we described earlier, homeostasis is the number of anomalies weighed by type. During the sampling interval, we will calculate the homeostasis of the system and examine the curve over time.

The core test involves a maze the system must navigate to obtain rewards. Periodically, the location and nature of the rewards will change in a non-random manner, cycling back through known states. The test emulates seasonality. We can envision that the system is an animal and the reward is food. Depending on the season, the animal finds the food in different locations and in different quantity. However, the location and quantity of the food is consistent with the season.

We expect that each time the season changes, the system experiences a surge in anomalies as rewards become scarce. In response, the metacognitive component helps the system find new rewards. Once a new source is found, the number

 ISBN: 978-1-61208-340-7

of anomalies should trend back towards a norm. We can measure cleverness based on the norm. The system with the lower norm is cleverer at finding rewards. We can measure adaptability based on how quickly the system responds to the change in seasons. The system that recognizes the change faster is more adaptable. Finally, we expect that as the cycle of seasons repeats itself, the GPME will outperform MCL2 and the RL in terms of total homeostasis over time.

Plotting the weighted anomalies over time, we calculate the slope of the curve from the change of season to the peak number of anomalies, to measure the efficiency of the metacognitive component's ability to recognize the change of season. The slope of the curve between the peak and the normal number of anomalies measures the efficiency of adaptation. The actual value of the normal number measures cleverness.

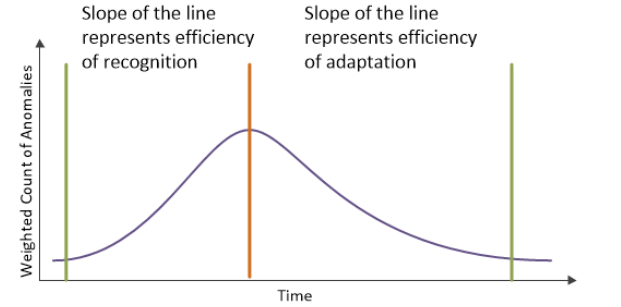

Figure 8. Projected Performance Curve over a Season

The test will execute several thousand seasonal cycles. Analyzing the performance curves of all cycles, we expect that the GPME will outperform MCL2 and RL by substantially minimizing the slopes over time.

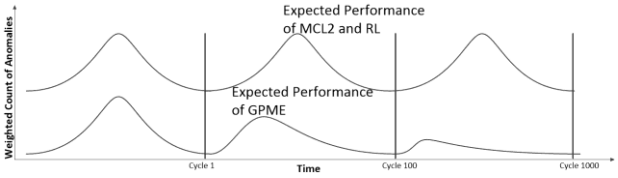

Figure 9: Projected Aggregate Performance Comparison

VI. CONCLUSION

The domain-generality of the GPME and its open and flexible interface will allow designers to build robust systems more rapidly, accelerating the application of metacognition enabled solutions in a larger number of domains.

The GPME builds on MCL2 by introducing the ability to deal with seasonality. To support this ability, the GPME develops its own expectations to supplement those the designer specifies. As a result, the foresight of the designer is no longer a limiting factor and it is free to discover and handle anomalies the designer did not anticipate. The GPME uses its episodic memory to match attributes of anomalies to cases it generates. This approach substantially lowers the need to relearn when dealing with seasonal changes. The introduction of decay means that experiences and cases that are not valuable eventually exit the episodic memory in order to keep its performance constraints manageable.

ACKNOWLEDGMENTS

This research is supported in part by the Office of Naval Research grant ONR #N00014-12-1-0430.

REFERENCES

[1] [1] M. T. Cox, "Metacognition in computation: A selected research review," *Artif. Intell.*, vol. 169, no. 2, pp. 104–141, Dec. 2005.

[2] [2] M. D. Schmill, M. L. Anderson, S. Fults, D. P. Josyula, T. Oates, D. Perlis, H. Shahri, S. Wilson, and D. Wright, "The Metacognitive Loop and Reasoning about Anomalies." p. 17, 2011.

[3] [3] G. P. Zhang and M. Qi, "Neural network forecasting for seasonal and trend time series," *Eur. J. Oper. Res.*, vol. 160, no. 2, pp. 501–514, 2005.

[4] [4] T. Taskaya-Temizel and M. C. Casey, "A comparative study of autoregressive neural network hybrids.," *Neural Netw.*, vol. 18, no. 5–6, pp. 781–9, 2005.

[5] [5] M. L. Anderson, T. Oates, W. Chong, and D. Perlis, "The metacognitive loop I: Enhancing reinforcement learning with metacognitive monitoring and control for improved perturbation tolerance," *J. Exp. Theor. Artif. Intell.*, vol. 18, no. 3, pp. 387–411, Sep. 2006.

[6] [6] K. Tsumori and S. Ozawa, "Incremental learning in dynamic environments using neural network with long-term memory," *Proc. Int. Jt. Conf. Neural Networks, 2003.*, vol. 4, pp. 2583–2588, 2003.

[7] [7] D. P. Josyula, H. Vadali, B. J. Donahue, and F. C. Hughes, "Modeling metacognition for learning in artificial systems," *2009 World Congr. Nat. Biol. Inspired Comput.*, pp. 1419–1424, 2009.

[8] [8] D. P. Josyula, S. Fults, M. L. Anderson, S. Wilson, and D. Perlis, "Application of MCL in a Dialog Agent," in *Third Language and Technology Conference*, 2007.

[9] [9] D. Wright, "Finding a Temporal Comparison Function for the Metacognitive Loop," Doctoral Dissertation. University of Maryland, College Park. 2011.

[10] [10] K. M. M'Balé and D. P. Josyula, "Integrating Metacognition into Artificial Agents," in *AAAI 2013 Fall Symposium Series*, 2013, pp. 55–62.

[11] [11] R. C. Schank, *Dynamic Memory Revisited*, 2nd ed. New York, NY: Cambridge Press, 1999, p. 302.

[12] [12] K. Thomsen, "The Cerebellum in the Ouroboros Model, the ' Interpolator Hypothesis ,'" in *COGNITIVE 2013*, 2013, pp. 37–41.

[13] [13] R. P. Marinier and J. E. Laird, "Emotion-Driven Reinforcement Learning," *Cogn. Sci.*, pp. 115–120, 2008.

 ISBN: 978-1-61208-340-7

Toward Modeling Task Difficulty: The Case of Chess

Dayana Hristova, Matej Guid, Ivan Bratko
Faculty of Computer and Information Science
University of Ljubljana
Ljubljana, Slovenia
a0902496@unet.univie.ac.at, matej.guid@fri.uni–lj.si, bratko@fri.uni–lj.si

Abstract— **We investigate the question of experts' ability to estimate task difficulty through a case study that asks players to rate tactical chess positions. In an eye tracking experiment, experts' estimations are compared to the statistic–based difficulty ratings of the chesstempo.com website. The subjects' solutions of chess problems and their considered chess variations are analyzed in connection to ChessTempo's solutions. In addition, eye tracking and performance data (time and accuracy) are used as physiological indicators of subjectively perceived difficulty. In the course of our research, we also aim to identify the attributes of tactical positions that induce difficulty. Understanding the connection between players' estimation of difficulty and the properties of the search trees of variations considered is essential for modeling the difficulty of tactical positions.**

Keywords– Task Difficulty, Problem Solving, Search Trees, Chess, Chess Tactical Problems, Eye Tracking, Chesstempo.com

I. INTRODUCTION

Modeling the difficulty of problems is a topic becoming increasingly salient in the context of the development of tutoring systems and dynamic difficulty adjustment (DDA) for gaming [1]. Since, in chess, as in other domains, there is no developed methodology to reliably predict difficulty for each person solving a problem, we are attempting to understand different ways of assessing difficulty. The starting point of our investigation is scrutinizing the relationship between a player's chess expertise and their ability to assess the difficulty of a tactical problem.

We are primarily concerned with "task difficulty" that mediates between the "subjective experience of difficulty" (that cannot be objectified) and the "task complexity" – as an inherent quality of a task (e.g. the properties of its space state). In order to approach task difficulty we are using psychophysiological measures (eye tracking), performance measures (accuracy of solution, time, variations considered, ranking positions), as well as qualitative retrospective reports (on perceived difficulty and on variations considered). We define the difficulty of a problem as the probability of a person succeeding in solving the problem. Hence we have adopted the difficulty ratings of chesstempo.com – an online chess platform – as a reference. These ratings are based on two principles: 1) the success rate for the particular position; 2) the ChessTempo score of the user, who has attempted to solve it. These ratings provide a basis to analyse the ability of human experts to estimate the difficulty of a problem, and in our case – to predict the statistically accumulated measure of difficulty.

In the case of chess, the difficulty for humans is induced by exceeding the limitations of player's cognitive abilities: to detect relevant motifs, to think strategically, to calculate a variation, and find a solution. The perception of difficulty is also influenced by psychological aspects, e.g. when the player is not able to calculate a variation all the way through to a checkmate, they have to deal with uncertainty (stemming from the incompleteness of the information set [2]). To our knowledge, in chess no work has been conducted that explicitly focuses on modeling the difficulty of chess tactical problems. Also, current research on expertise in chess has been mostly focused on the perceptual advantages of experts over novices [3]. Our study aims to explore the connection between task difficulty and expertise, as well as the variability among individuals.

The paper is organized as follows. In Section II, we state our hypothesis and explain why modeling the difficulty of chess tactical positions is problematic. Section III describes our methodology. We present our preliminary results of data analysis in Section IV, which is followed by a thorough discussion of an illustrative example from the eye-tracking experiment. The final section of the paper is reserved for concluding remarks and directions for future work.

II. TOWARD MODELING DIFFICULTY

A. Hypothesis

Our hypothesis is that the players' ability to estimate the difficulty of a position is positively correlated with the players' chess strength measured by World chess federation (FIDE) Elo rating. However, we conceive of chess strength as only one among multiple factors influencing the ability to make good predictions. E.g. in the case of teaching, one should develop skills related to estimating difficulty in order

 ISBN: 978-1-61208-340-7

to select appropriate tasks for the students. Being a greater expert in a domain (e.g., being a stronger chess player) should (in principle) increase the chances of making better predictions – due to the better overview over the mass of possibilities. However, for a group of people of similar expertise, the problem's difficulty may vary due to their specific knowledge and individual style. Hence, we do not expect a high linear correlation between player's Elo rating and their success in ranking the positions.

B. *Modeling the difficulty of tactical positions*

We observed that the algorithm for estimating difficulty of chess positions in ordinary chess games proposed by Guid and Bratko [4] fails to perform well on chess tactical problems for the following reason: the programs tend to solve the problems very quickly, usually at the shallowest depths of search. Since the algorithm takes into account the differences in computer evaluations when changes in decisions take place with increasing search depth, the computer simply recognizes most of the chess tactical problems to be rather easy, and does not distinguish between positions of different difficulties (perceived by humans). Estimating difficulty of chess tactical problems therefore requires a different approach, and different algorithms. We ought to gain an insight into the way the players of different strength solve the tactical problems, and to better understand what may be the properties of such algorithm. Hence, we use physiological measures that gauge performance in chess players' ability to assess the difficulty of tactical problems, and qualitative reports.

III. METHODOLOGY

In the experiment, so far conducted with 11 strong chess players, eye tracking is used in order to gather perceptual data about performance and difficulty. In our experiment, chess experts are solving and then ranking according to their difficulty a selection of ChessTempo problems with established difficulty ratings (each solved by minimum 600 people). The participants who have completed the experiment are 10 male and 1 female (avg. age= 48 years) chess experts. Their FIDE Elo ratings vary between 1900 and 2300. The chess problems were displayed as ChessBase 9.0 generated images, 70 cm from the players' eyes. The players' eye movements were recorded by an EyeLink 1000 eye tracking device (SR Research), sampling at 500 Hz. Nine–point calibration was carried out before (each part of) the experiment session.

Participants were presented with 12 positions randomly selected from ChessTempo according to their difficulty ratings: 6 hard; 4 medium; 2 easy. The estimation of the difficulty level is relative to the level of skills of the participants, who, as already mentioned, are strong chess players. Each of the three difficulty classes is separated from the other by 350 points. The problems within each class have very similar difficulty rating. The 12 positions were presented in 3 blocks of four positions: randomized within the blocks and between blocks to avoid a sequence effect. The experiment with each player lasted between 20 and 45 minutes.

The subjects were instructed to input their solution (their suggested best move) as soon as they have found a variation that occurs to be winning. For each position, they were not allowed to exceed the time limit of three minutes. Retrospective reports were obtained after the completion of the experiment. These reports serve as a key to understanding the way experts approached the presented position, and to the variations they considered. Chess experts are able to remember variations and are capable of reconstructing even full chess games. Hence, the retrospective reports obtained have high validity. After the experiment, participants were asked to rate the problems (from 1 to 12) in ascending order of their difficulty.

DataViewer is used to generate reports about the participants' eye activity: saccades, fixations, interest areas, and trial report. The data analysis will be further discussed in the next section.

IV. DATA ANALYSIS

A. *Kendall's τ rank correlation coefficient*

We computed the correlation between various difficulty rankings of our set of chess positions. The rankings come from individual players that took part in the experiment, and from the ChessTempo database. The ChessTempo ranking order was derived from the ChessTempo difficulty ratings of individual positions. The players did not estimate difficulty ratings, but produced their ranking orders directly. We used Kendall's τ rank correlation coefficient which we applied to our data as follows. Given two rankings, Kendall's τ is defined by:

$$\tau = \frac{n_c - n_d}{n * \frac{(n-1)}{2}} = \frac{n_c - n_d}{n_c + n_d}$$

Here n is the number of all chess positions in the rankings, and n_c and n_d are the numbers of concordant pairs and discordant pairs, respectively. A pair of chess positions is concordant if their relative rankings are the same in both ranking orders. That is, if the same position precedes the other one in both rankings. Otherwise the pair is discordant. In our data, some of the positions were, according to ChessTempo, of very similar difficulty. Such positions belong to the same difficulty class. To account for this, the formula above was modified. In the nominator and denominator, we only counted the pairs of position that belong to different classes.

Fig. 1 shows for the 11 players the relation between the player's Kendall rank correlation coefficient with ChessTempo ranking, and the player's FIDE Elo rating.

 ISBN: 978-1-61208-340-7

Pearson product–moment correlation coefficient (Pearson's *r*) was computed in order to determine the relationship between Kendall's τ and the chess strength of the participants (reflected by their rating). There was a medium correlation that is statistically not significant between Kendall's τ and FIDE Elo ratings (r = .436, n = 11, p = 0.174). While a higher number of participants in this experiment is required, these initial results suggest that stronger players indeed tend to produce more correct rankings of chess tactical problems with respect to their difficulty.

In our experiment the strongest player was actually the best predictor of difficulty, by high margin. Furthermore, when ranking the extremes: 1 – easiest and 12 – hardest position; most players' estimations were close to the respective end of the difficulty spectrum (± 2 positions). However, participants showed high variability in their estimation. There were even cases of positions that were at the same time rated as a 1 and a 12 by the different players.

Until we finish data collection and are able to calculate the final results, and check whether there is a statistically significant correlation between Elo ratings and Kendall's coefficient for each participant, it is crucial to take positions of the experiment as case studies. This will allow us to identify aspects that have so far influenced participants' problem solving and estimation of the task difficulty.

B. Eye tracking data

A crucial part of the eye tracking data processing is the analysis of fixations and saccades in relation to the squares of the chessboard, defined as interest areas (IAs). We analyzed what percentage of the fixations fall on a particular interest area for both cases: 1) for each individual; 2) for all fixations of all participants. For the purpose of the analysis, we focus on the following phases: 1) the first 10 seconds after presentation; 2) the last 5 seconds preceding the input of a solution; 3) overall duration of the trial. The first two time phases are important for the data analysis as the first is conceptualized by Bilalić *et al.* [5] as a perceptual phase, and the second- as a conclusive decision making phase [5].

In the sequel, we analyze position N4 (Fig. 2) – one of the positions that was systematically estimated as more difficult than its ChessTempo rating (1861) indicates. Only 33% of the participants in our experiment inputted the correct solution, as opposed to a 50% Standard success rate in ChessTempo. According to both ChessTempo and to chess program Houdini the problem has only one good solution – Nc2-a1.

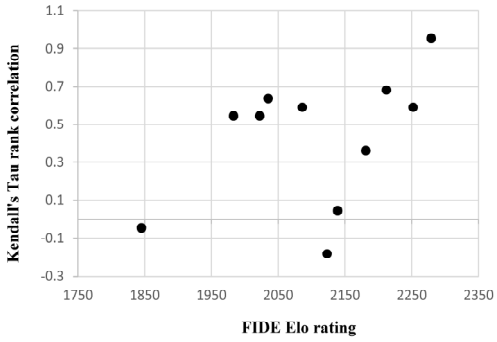

Figure 1. Correlation between Kendall's τ and FIDE Elo rating

The retrospective accounts of the variations the players considered indicate the presence of two main motifs that all participants attended to: 1) weakness of Black King on e8; 2) trapping Black Queen on b3. The diagrams from the perceptual phase and the retrospection data confirm that all participants spotted the first motif. The players considered different variations aiming at exploiting this motif (Fig. 2, solid arrows): attacking with Re4xe7 or strengthening their attack through playing Qc1-e3. During the perception phase and for the overall duration of the trial, the e7 square is the most attended IA – accounting for respectively 9.5%, and 9.3% of the fixations. Another main piece in this motif – Re4 – is the third most visited area, accounting for 7.3% of the fixations in the perception phase.

The other salient motif – trapping the Black Queen on b3 – has also been reported in the retrospections by all participants. As shown on Fig. 2 (with dashed arrows) three moves were considered by participants: Re4-b4, Nc2-d4 or Nc2-a1. The percentage of fixations recorded on a1 is low – 0.3% of the whole trial. However, this may also be influenced by the fact that a1 is a corner square. Once the potentially winning move Nc2-a1 is spotted, the calculations should be focusing on the squares surrounding the Qb3 – to verify whether this move leads to a success in trapping the Queen. During the perceptual phase only the Knights on c2 (2.9%) and c3 (8.9%), of all squares surrounding the Qb3 were among the fixations with highest attendance. However, during the decision phase, in addition to the knights (c3 –

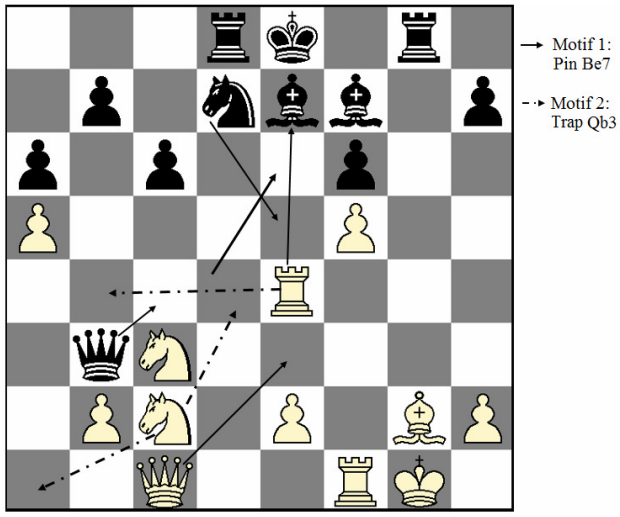

Figure 2. Position N4. The two main motifs: 1) pinned Bishop on e7; 2) trapped Queen on b3.

 ISBN: 978-1-61208-340-7

11.7%; c2 – 7.4%), players were also fixating more on other squares relevant to the second motif, such as: b3 (4.9%), a2 (4.3%) and b2 (3.7%).

C. Discussion of prelimiary results

Our data shows that despite of the differences in strength, participants' line of thought focused on the above two motifs. This position has only one good solution (Nc2-a1), but two salient motifs (two families of branches of the search tree). The first motif triggers variations that do not contain the right solution. It is evident and invites for violent moves in the center of the board and along the e-file. This motif is even more appealing as White has two Knights at her disposal– pieces that are strong precisely in the center of the chessboard. The candidate moves are: Re4xe7 - direct attack; Qc1-e3 – strengthening White's attack. The second motif's candidate moves appear less intuitive. Choosing to move a Knight to the edge, or even to the corner (a1), is a rather counter intuitive move since Knights are considered to be strongest in the middle of the chessboard. Ultimately, the aforementioned characteristics of the problem create predisposition for increased difficulty even for skilled chess players. Hence, the success rate for this position was 33%.

66% of the participants identified the Knight on c2 as the piece that should be used in the first move of the winning variation in this tactical position. However, half of these players were simply unable to see the move Nc2-a1 because all chess players are taught not to move a night into a corner. For a good player, a move like Nc2-a1 is almost "unethical". For the same reason, the incorrect alternative Nc2-d4, putting the night in the center, is so natural that it makes the correct Nc2-a1 practically invisible to many players. This is an example of a mistake made due to negative transfer [6] when the player oversees the solution of the problem as a result of their training. In other words, seemingly good moves can increase the difficulty of the chess position due to simple (but misleading) heuristics that people may use in order to solve the problem.

The number of feasible options for the player, as well as for her opponent, defines the number of nodes that are searched by the player. Then, more importantly, the chess player, according to his ability, can distinguish between relevant and not relevant moves. A player's search tree, i.e. a set of moves and variations the player might consider as reasonable candidate moves, depends on cutting off branches that do not seem promising. Often violent moves, such as capturing or mating, are favored as they lead to immediate improvement in one's situation. However, as in the case of position N4, the moves that seem to be the most promising are distracting the player from the correct solution.

V. CONCLUDING REMARKS

The preliminary data does not offer statistically significant results supporting or disproving our hypothesis that the ability to predict the ChessTempo ratings correlates with the player's Elo rating. More conclusive results are expected upon completion of the data gathering. However, the mismatches between ChessTempo ratings and experts' ranking of problems according to their difficulty shed light on aspects of tactical chess positions that influence the estimation of difficulty. One of them is the properties of player's search tree. Furthermore, our case study in one of the problems also highlighted the impact of negative transfer [6] on problem solving and hence on the perception of difficulty.

Taking into account the limitations and the specificities of human problem solving, is a challenge for attempts to model the difficulty of chess problems. However, using performance and psychophysiology measures can provide the basis for modeling difficulty. This will enable the automatic detection of difficulty [2] of tactical positions that will be instrumental in the development of tutoring systems for chess. Since chess has proven itself in cognitive science research as a domain with high external validity, we hope that our work will be beneficial for modeling the difficulty of problems in other domains.

ACKNOWLEDGMENT

Sincere thanks to Grega Repovš, Anka Slana, Christian Armeni and Gregor Geršak for their support during the preparation of experiment this study is based on.

REFERENCES

[1] R. Hunicke and V. Chapman, "AI for dynamic difficulty adjustment in games," in Challenges in game artificial intelligence, D. Fu, S. Henke and J. Orkin. Eds. Paper from the 2004 AAAI workshop, Technical report Wj–04–04, Menlo Park, CA: AAAI Press, July 2004, pp. 91–96.

[2] G. Dosi and M. Egidi, "Substantive and procedural uncertainty: An Exploration of Economic Behaviours in Changing Environments" Journal of Evolutionary Economics Volume 1 (2), June 1991 , pp. 145–168, doi:10.1007/ BF01224917

[3] E. Reingold and N. Charness, "Perception in chess: Evidence from eye movements," in Cognitive processes in eye guidance, G. Underwood, Ed. New York: Oxford university press, pp. 325– 354, 2005

[4] M. Guid and I. Bratko, "Search–Based Estimation of Problem Difficulty for Humans". Artificial Intelligence in Education. Lecture Notes in Computer Science (AIED 2013), Memphis, USA, vol. 7926, July 2013, pp. 860–863, doi: 10.1007/978–3–642–39112–5_131

[5] M. Bilalić, P. McLeod and F. Gobet, "Why good thoughts block better ones: the mechanism of the pernicious Einstellung (set) effect" Cognition.;108(3), September 2008, pp. 652–661. doi: 10.1016/j.cognition.2008.05.005

[6] R. J. Sternberg and K. Sternberg, "Cognitive psychology" Wadsworth: Cengage Learning, 2012

 ISBN: 978-1-61208-340-7

The GATM Computer Assisted Reasoning Framework in a Security Policy Reasoning Context

Johan Garcia
Department of Mathematics and Computer Science
Karlstad University
Karlstad, Sweden
Email: johan.garcia@kau.se

***Abstract*—Humans are often faced with the need to make decisions regarding complex issues where multiple interests need to be balanced, and where there are a number of complex arguments weighing in opposite directions. The ability of humans to understand and internalize the underlying argumentation structure resulting from reasoning about complex issues is limited by the human cognitive ability. The cognitive limit can manifest itself both in relation to an inappropriate level and amount of detail in the presentation of information, as well as in the structuring of the information and the representation of the interrelationships between constituting arguments. The GATM model provides a structured way to represent reasoning, and can be useful both in the decision-making process as well as when communicating a decision. In this work a component-based overview of the GATM model is provided in the context of security policy reasoning, where previous work has shown that decision-making transparency and improved understanding of the reasoning behind a security policy may lead to a beneficial impact on policy compliance.**

Keywords–Security policies; GATM; Reasoning; Argumentation.

I. INTRODUCTION

This paper presents the General Argumentation, Type, and Modifier (GATM) model as a way to structure reasoning of complex issues in scalable way. The objective is to provide a foundation for reasoning representation and visualization in a manner that can make the most of the human cognitive abilities. The GATM model aims to provide a framework for representing, storing, and presenting reasoning involving a complex set of argumentative statements, where the statements in turn can have multiple levels of statements that are either supportive or dismissive. One defining aspect of the GATM model is that it, unlike the well-known Toulmin approach, does not have multiple argument statement classes. Classes such as grounds, warrant, and backing as found in the Toulmin approach means that the exact same statement can belong to different classes, depending on the context in which a statement is used when reasoning about a particular claim. By avoiding the class approach, GATM simplifies the use of statements as well as the construction of joint repositories of reusable statements. Instead of classes, the GATM model uses a statement typology in which type represent an inherent characteristic of an argument statement. The type is invariant regardless of which issue is reasoned about, or where in the hierarchy a statement occurs. Further, the GATM model uses the concept of modifiers to capture the instance-specific aspects of the use of a particular statement in relation to a specific issue.

While the sketched framework can be applied across many domains, in this particular paper, we consider it in the context of security policy creation and effective dissemination. In the context of computer security policies, previous work have identified that information security awareness positively affects both attitude and outcome with regards to policy compliance [5], and concluded that security awareness should be the principal focus of a systematic approach to policy management [13]. It is presumed that an improved ability to communicate the reasoning behind security policy measures can increase security awareness and policy acceptance. This ties in to the well-known tradeoff between the strictness of computer security measures on one side and the willingness and capability of the end-users to successfully follow the measures while providing appropriate effectiveness in their regular activities. Consider, as an example, the case of forced password change. From a strictly security related point of view, it is of benefit to force the users to change passwords frequently, for example once every month, and require long passwords that fulfill criteria such as having characters from multiple groups (a-z, A-Z, 0-9, etc.). Here, there exists a tradeoff between an ideal level of security, and usability and user acceptance.

Furthermore, it is not a straightforward matter to decide what is an appropriate security level and furthermore the appropriate security level might vary between the different domains in one company which potentially leads to further complications. Security policies are typically elaborated and decided upon at the upper management level. Conflicting interests between different areas represented by the individual managers may lead to differences in views on the need for security, the potential criticality of security breaches, the monetary value of security incidents, and other associated factors. Also in this context, a security policy reasoning framework and an associated visualization tool may prove beneficial. Further discussion of the visualization aspects are left for future work, and the focus of this paper is on structural aspects of the GATM model.

The paper is structured as follows. The next section discusses related work, followed by a section that outlines the GATM model. Finally, conclusions are provided.

 ISBN: 978-1-61208-340-7

II. Related work

There are several approaches for reasoning support in the general context and a comprehensive overview and taxonomy is provided by Benathar et al. [3]. The conceptual model of argumentation proposed by Toulmin [15] is one early example of a reasoning model that has been used to guide computer reasoning efforts. An overview of the Toulmin argument structure is provided in Figure 1, where the relationship of the different classes are shown.

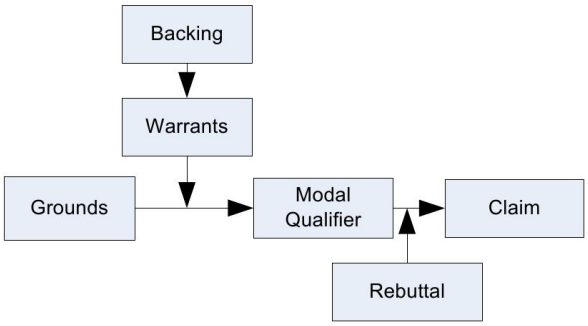

Figure 1. Generic Toulmin-form argument, from [9]

The Toulmin model has also resulted in several extensions such as the one proposed by Bench-Capon [2], which added a presupposition component which adds the ability to add statements which are not under dispute and not core to the claim made, but do represent assumptions that are necessary for the argument. In the GATM model, the same underlying information as in the presupposition component is provided by the recursive statement approach coupled with the statement typology as discussed in the next section. Also related to GATM is the work by Freeman [7], which identifies four central argument structures. The information provided by these argument structures are similar to what is represented in the GATM model, although the GATM model does not consider them in the same explicit manner.

Specifically with regards to security policies, previous research by Bulgurucu et al. [5] has investigated the rationality-based factors that drive an employee to comply with requirements of an Information Security Policy (ISP). The results show that an employee's intention to comply with the ISP is significantly influenced by attitude, normative beliefs, and self-efficacy to comply. A similar result is reported is reported by Knapp and Ferrante [13], where 297 information security professionals were surveyed, and the conclusions stress the importance of awareness. An improved ability to convey the reasoning for particular security policy measures, such as provided the proposed GATM model and associated visualization front-ends, is posited to contribute to improved Information Security Awareness (ISA). An improved ISA is is coupled to positive effects on attitude and outcome of policy compliance [5]. Other aspects of security policy design, such as firewall configuration has been elaborated in the context of reasoning and argumentation by Applebaum et al. [1]. A more formal logic for reasoning about security and security policies is discussed by Glasgow et al. [8]. In other work, Haley et al. [9] aims to to validate security requirements by using propositional logic to construct outer arguments, and informal reasoning is then used to support those with a basis in the Toulmin model of reasoning.

In this paper, password policy is used as an example for GATM. The issue of finding an appropriate tradeoff between security and convenience in a password policy is discussed by Florêncio and Herley [6], where the need for transparency is also highlighted:

> While most of us understand and accept that there is a tradeoff between security and convenience, how and by whom is this tradeoff decided? Few would argue with getting a lot more security for a little inconvenience. But, if the decision-making process is obscure how can we be sure we're not getting lots of inconvenience for little improvement in security?

Along similar lines, Myyry et al. [14], in an empirical study with 163 persons reports findings suggesting that information security policies should be better rationalized, so that the importance of these policies to the organization and the work community is clarified. The GATM model provides one approach to make the decision-making process more transparent and make explicit the consideration that have, or have not, been taken into consideration when arriving at a particular security versus convenience tradeoff.

III. Sketching the GATM model

One novelty of this work is the statement typology approach, which is based on the realization that the Toulmin basic model is cumbersome when considering complex issues with long chains of statements. Whereas the Toulmin classes differentiates between how statements relate to each other using categories such as data, warrant, and backing, the typology approach instead focuses on the basic content of the statement itself and not its relation to the claim. As has been observed by Haley et al. [9], a backing argument can itself be considered a goal which is then supported by additional supportive data, warrants and backing. Given that this recursiveness often occurs when building more elaborate reasoning hierarchies an argumentation model that assigns the argument statements to different classes depending of the vantage point might be problematic. Instead of focusing on the interrelationship between the different arguments the GATM model use an alternative typology abstraction which focuses not on the relative position of the statement to some other claim or statement, but rather on the intrinsic nature of the statement in itself. This intrinsic nature will not change if the statement is viewed as a support for a claim or if it is viewed as a claim for which there are other supporting statements.

A. A password policy GATM example

Figure 2 illustrates the structure of the GATM model using a simplified argumentation for a password policy. The figure shows the claim, which regards the mandated use of a password policy that requires users to change passwords every 60 days, as well as selecting passwords with a minimum length and composition requirements. In addition to the claim, the figure also contains a number of statements. Statements that work in support of the claim have arrows pointing right out from them, while statements that work in contradiction to

 ISBN: 978-1-61208-340-7

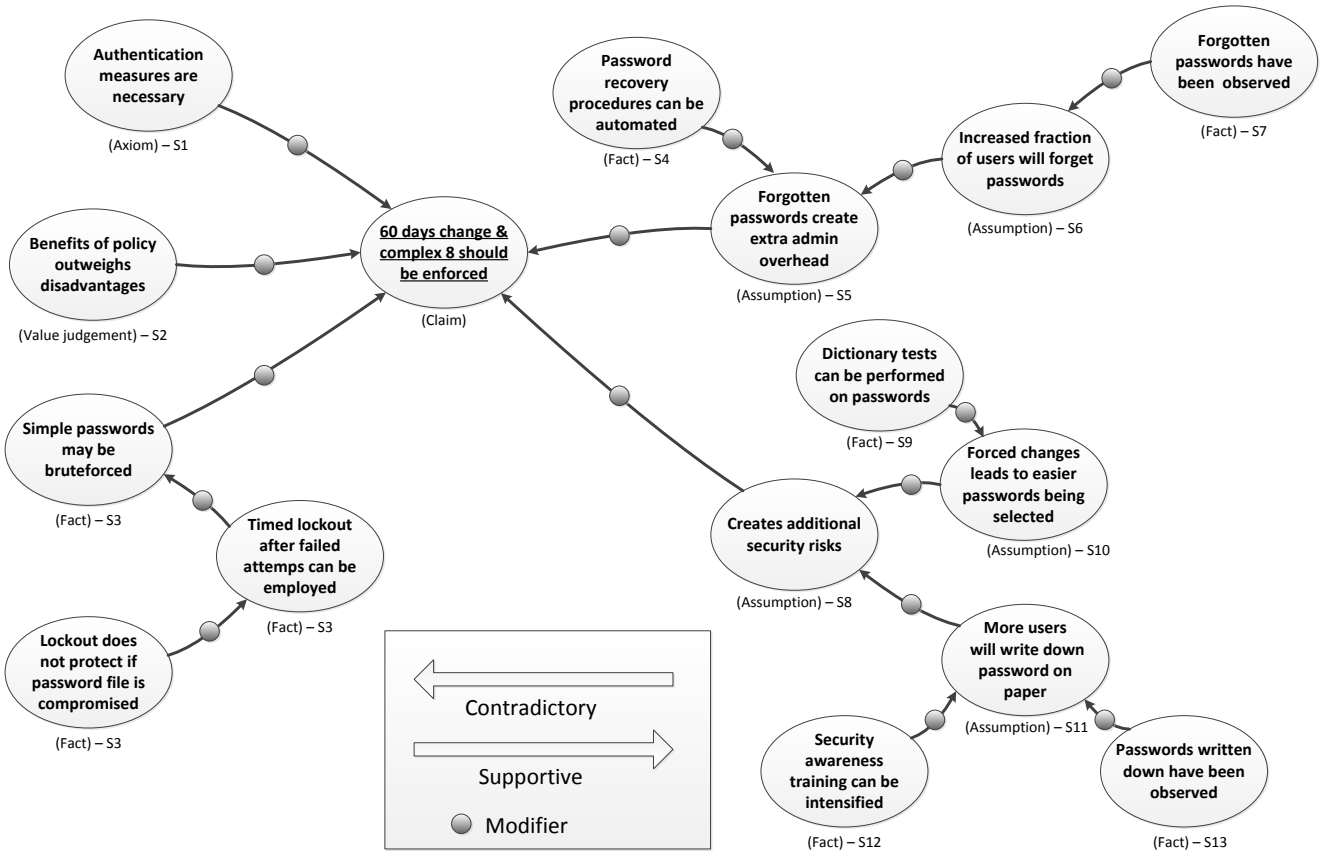

Figure 2. An simplified GATM reasoning graph example for a password policy

the claim have arrows pointing to the left. As an example, statement S5 works in contradiction to the claim, thus having an arrow pointing left. Statement S4 works in contradiction in relation to S5, but in the supportive direction in relation to the claim, and thus have a right pointing arrow. For every statement, the relative effect of the support or contradiction for that statement is captured by a modifier. The modifiers contains attributes such as statement applicability and strength. The properties of the modifier varies between each occurrence of a statement, i.e., the modifier is specific to the instance of a statement that occurs in a particular graph. Statements on the other hand, are in many cases general in the sense that the exact same statements can be used in a several unrelated reasoning graphs. So, while statements often have general applicability also outside a particular reasoning graph, modifiers are coupled to a particular graph. Different reasoning graphs have different claims, thus affecting the contextual aspects of the attributes in the modifier, such as applicability.

Although not discussed here, a feature of the GATM model is that it supports a hierarchical representation and presentation of information. Shown in Figure 2 are only information at the highest abstraction layer, which is the short statement description. In addition to this, there is also a long statement text, and and multi-part slideset that can be used to provide relevant additional information for a particular node. This allows a user to first at a glance get a view of the statements involved with regards to a particular claim. The user can then differentiate between statements which are familiar or new. Statements that are new to the user, or which the user does not agree with, can be examined closer by requesting the additional information contained in the long statement text and/or slide set. This approach lessens the cognitive load, as compared to if all statement information would have been presented at the same level of detail.

As it can be seen in Figure 2, there are several different statement types in the reasoning graph. In the idealized representation used in the figure, the types of the statement is explicitly written below each node. Also provided is a node identifier used in the discussion. In the initial prototype visualization frontend, statement types are instead represented by different geometric shapes of the nodes. A further discussion of the types used in this example are provided in the next subsection.

Considering the password policy reasoning in the figure, it can be seen that the representation allows for an overview representation of the considerations that have been taken into account with regards to this particular claim. As have been discussed in Section 2, transparency and rationalization of policy decisions have a positive impact of security policy compliance. Thus, the communicative properties is one potential benefit of using the GATM model. The GATM approach might also be useful during the policy elaboration and decision phase. Representing the advantages and disadvantages in a structured manner can simplify communication and enhance

 ISBN: 978-1-61208-340-7

TABLE I. GATM TYPOLOGY FOR TYPES USED IN THE EXAMPLE

Type	Statement Prefix	Terminal	Temporally Stable
Axiom	"Unless it is accepted that ..."	Yes	Yes
Fact	"There is a (scientific) consensus that ..."	No	Yes, mostly
Current assumption	"The best current (scientific) understanding is that ..."	No	No
Value judgment	"My personal belief is that ..."	Yes	Yes, mostly

understanding during a decision process involving multiple individuals. Although not discussed here, the versioning control integrated in the GATM model supports dialectic evolution of reasoning which might be useful during policy elaboration. While the reasoning graph in Figure 2 works as an illustrative, albeit simplified, example of the GATM model, it can also be extended with further reasoning around additional aspects that influence the design and decision making for password policies.

By allowing the reasoning to become more explicit, GATM can also be helpful in avoiding fallacious reasoning results with regards to policies. The effects of such reasoning fallacies are observed by Florêncio and Herley [6], which based on an examination of 75 websites somewhat surprisingly report that a more stringent password policy is not coupled to a site having greater security concerns. Rather, more stringent policies are found when the site provides functionality which has little sensitivity to the added user inconvenience of a stricter policy, for example when the use of a particular site is mandated by an employer. Other research useful when elaborating the reasoning around password policies include work by Zhang et al. [16] which questions the continued use of password expiration based on the observed predictability of the new passwords chosen after password expiration. The unsuitability of many password policies are also discussed by Inglesant and Sasse [11], which studied password use in two organizations and states that the focus need to be on using Human-Computer Interaction principles to set an appropriately strong password policy, and not strictly focusing on password length and expiration frequency. In fact, they report that for one of the studied organizations the password policy greatly increases the threat from passwords left written down, an observation that is illustrated by the S13-S11-S8 reasoning chain in the example. Herley [10] uses cost-benefit analysis of security advice with regards to passwords and note that much of the current policies do not fully take user costs into account.

B. GATM statement types

This subsection provides a first brief sketch of the statement types in the GATM model. Due to space constraints, this presentation focuses on the statement types present in the example in Figure 2, and does not cover all statement types of the GATM model.

"Axiom"

Axiomatic statements are the base on which the reasoning chain in many cases will end if the links of statements and supporting statements are recursively followed until the end. However, it is expected to often be uncalled for to follow the reasoning links all the way to the axioms. The axioms can be universally accepted statements regarding physical entities or statements expected to be universally accepted. When an statement is classified as an axiom it is apparent that if another party is not accepting a statement as an axiom it is not meaningful to have a further discussion in relation to the claim at hand. In relation to security policy, an axiomatic statement could be: "Organizations may deny its employees access to parts of the information within the company". Such axioms work as a basic security policy foundation for most companies, and if a party does not accept that axiom it is not meaningful to reason about security policies.

"Fact"

As the GATM model is a general model, the fact statement type eludes a simple definition. When GATM is applied where scientifically based reasoning is appropriate, fact can be seen as meaning "statements that are verifiable by repeatable experiments". However, in contexts where such a definition is not appropriate fact can be considered as "the state of affairs". This correspond to definitional facts such as "Stockholm is the capital of Sweden", which is a fact resulting from social convention. It is important to not mistakenly consider non-definitional phenomena as definitional as illustrated by the observation that although a large fraction of people 600 years ago believed the earth to be flat, the earth still, in fact, was not flat.

"Current assumption"

Current assumption is something that explicitly signals that there is a degree of uncertainty related to the statement. The uncertainty can be related to different causes. In an engineering context, it may be an effect of imprecise measurements, where the tools used to measure a metric of interest have inherent imprecision. Another case is where the underlying values vary considerably due to random factors that cannot be controlled. With regards to what can be done to reduce uncertainty, there is a difference between uncertainty dependent on inherent variability (also called aleatory uncertainty) and uncertainty due to lack of appropriate information (also called epistemic uncertainty) [12]. Whereas the epistemic uncertainty can be reduced by spending resources to gather more information, aleatory uncertainty is inherent and cannot be readily reduced.

"Value judgment"

In this context, a value judgment is a statement that reflects an individual persons inner beliefs which is considered to be largely outside the realm of rational deliberation, and as such being statements for which there exists no obvious way to objectively ascertain a "true or false" or "better or worse". A trivial example of a value judgment is the favorite color of an individual. It is not possible to say that one individual's choice of color is better than another individuals in any objective sense. Neither is it meaningful to argue about an individual's choice of color. On a higher level, value judgments tend to be individualistic and reflect the belief systems and moral

 ISBN: 978-1-61208-340-7

conditioning of individuals. In regards to computer security policy, value judgments can come into play for example with regards to tradeoffs involving privacy, as discussed by Brey [4].

An overview presentation of the discussed types are shown in Table I. The table contains a statement prefix that can function as a guide in deciding what type a given statement should belong to. It should be noted it is unlikely that there exists a single set of generally applicable guidelines on how to classify statements into types. There is no general and clear-cut boundary between axiom and fact, or between fact and current assumption. Also provided in the table is a column indicating whether the type is terminal or not. Terminal types form a definitive end in the statement chain and will not have any underlying supporting or contradicting statements. The final column in the table relates to temporal stability, which signifies the tendency of statements of a particular type to change in the validity as time passes.

Although not elaborated in this paper, the software framework for storing, representing, and presenting GATM reasoning graphs allows multiple individual representations of the same underlying reasoning graph. This makes it possible for multiple users to change the type of the particular statement in case they consider another type to be more appropriate, while the system still maintains relational links between the two individual representations. The proposed system enhances an individual's ability to represent his or hers individual reasoning which regards to a particular claim, and put his reasoning in relation to other people's reasoning on the same subject matter. From the basic observation that reasonable individuals reach multiple divergent standpoints on a given nontrivial matter, it follows that there also exists a multitude of reasoning chains that have been explicitly or implicitly followed to arrive at each individual's particular standpoint.

C. Modifiers

There are two types of modifiers in the GATM model, unipolar modifiers and multipolar modifiers. Unipolar modifiers are related to a single statement and can convey attributes relating to a particular instantiation of an statement, i.e., the use of an statement in reasoning about a specific claim. Similarly, a multipolar modifier conveys attributes but also ties together statements which are functionally dependent. For example, a statement S23 might only work as a support for a statement S18 if a statement S22 is also valid. Such dependencies are captured by the multipolar modifier.

IV. Conclusion

In this paper, we have provided an alternative model to the classical Toulmin model which can be challenging to use with hierarchical reasoning given the relative relations of data, warrant, and backing. The GATM model considers a typology of statements where the type of statement is inherent to the statement itself and not relative to its position in a reasoning hierarchy. We have used the domain of security policies to provide an example for the new model, noting that the model is primarily intended for computer supported human reasoning. While illustrating the GATM concepts with a password policy reasoning graph, the possibility to provide more transparent decision-making is also discussed. In the particular domain of security policy reasoning, it is hypothesized that the use of the GATM framework along with a visualization front-end will be beneficial to information security awareness and security policy compliance. Greater decision-making transparency and improved understanding of the underlying rationale can be important factors in influencing attitudes and normative beliefs of the users so that they strive for increased security awareness and policy compliance.

Although the focus of the GATM model is to provide support for human-centered reasoning, since the data used to represented the reasoning graph is formally structured with typology classes, statement links, etc., GATM data can also be useful for building up more formalized knowledge management systems as well as agent-based reasoning approaches.

References

[1] A. Applebaum, K. N. Levitt, J. Rowe, and S. Parsons, "Arguing about firewall policy." in *COMMA*, 2012, pp. 91–102.

[2] T. J. M. Bench-Capon, "Deep models, normative reasoning and legal expert systems," in *Proceedings of the 2nd International Conference on Artificial Intelligence and Law*, ser. ICAIL '89, 1989, pp. 37–45.

[3] J. Bentahar, B. Moulin, and M. Bélanger, "A taxonomy of argumentation models used for knowledge representation," *Artificial Intelligence Review*, vol. 33, no. 3, pp. 211–259, 2010.

[4] P. Brey, "Ethical aspects of information security and privacy," in *Security, Privacy, and Trust in Modern Data Management*, ser. Data-Centric Systems and Applications, M. Petković and W. Jonker, Eds., 2007, pp. 21–36.

[5] B. Bulgurcu, H. Cavusoglu, and I. Benbasat, "Information security policy compliance: An empirical study of rationality-based beliefs and information security awareness," *Management Information Systems Quarterly*, vol. 34, no. 3, pp. 523–548, Sep. 2010.

[6] D. Florêncio and C. Herley, "Where do security policies come from?" in *Proceedings of the Sixth Symposium on Usable Privacy and Security*. ACM, 2010, pp. 10:1–10:14.

[7] J. B. Freeman, *Dialectics and the macrostructure of arguments: A theory of argument structure*. Walter de Gruyter, 1991, vol. 10.

[8] J. Glasgow, G. MacEwen, and P. Panangaden, "A logic for reasoning about security," *ACM Transactions on Computer Systems (TOCS)*, vol. 10, no. 3, pp. 226–264, 1992.

[9] C. B. Haley, J. D. Moffett, R. Laney, and B. Nuseibeh, "Arguing security: Validating security requirements using structured argumentation," in *in Proceedings of the Third Symposium on Requirements Engineering for Information Security (SREIS'05)*, 2005.

[10] C. Herley, "So long, and no thanks for the externalities: the rational rejection of security advice by users," in *Proceedings of the 2009 workshop on New security paradigms workshop*. ACM, 2009, pp. 133–144.

[11] P. G. Inglesant and M. A. Sasse, "The true cost of unusable password policies: password use in the wild," in *Proceedings of the SIGCHI Conference on Human Factors in Computing Systems*. ACM, 2010, pp. 383–392.

[12] A. D. Kiureghian and O. Ditlevsen, "Aleatory or epistemic? does it matter?" *Structural Safety*, vol. 31, no. 2, pp. 105–112, 2009.

[13] K. J. Knapp and C. J. Ferrante, "Policy awareness, enforcement and maintenance: Critical to information security effectiveness in organizations." *Journal of Management Policy & Practice*, vol. 13, no. 5, pp. 66–80, 2012.

[14] L. Myyry, M. Siponen, S. Pahnila, T. Vartiainen, and A. Vance, "What levels of moral reasoning and values explain adherence to information security rules? An empirical study," *European Journal of Information Systems*, vol. 18, no. 2, pp. 126–139, 2009.

[15] S. E. Toulmin, *The uses of argument*. Cambridge University Press, 1958.

[16] Y. Zhang, F. Monrose, and M. K. Reiter, "The security of modern password expiration: an algorithmic framework and empirical analysis," in *Proceedings of the 17th ACM conference on Computer and communications security*. ACM, 2010, pp. 176–186.

 ISBN: 978-1-61208-340-7

Towards a Cloud-Based Architecture for 3D Object Comprehension in Cognitive Robotics

Charlotte Sennersten, Ahsan Morshed, Martin Lochner, and Craig Lindley
CSIRO Computational Informatics (CCI) Autonomous Systems (AS)
Commonwealth Scientific and Industrial Research Organization (CSIRO)
Hobart, Australia
{charlotte.sennersten, ahsan.morshed, martin.lochner, craig.lindley}@csiro.au

***Abstract*—Cognitive robotics can take advantage of distributed, web-based information as a foundation for comprehending 3D objects in a 3D scanned world. The proposed CogOnto model makes possible grounding a cognitive computing system with sensor data gathered from diverse and heterogeneous sources, associated with humanly crafted symbolic descriptors. The system supports cognitive embodiment within the totality of an information ecology, and not just within the physical world where an individual robot, essentially a mobile peripheral device, is located. The informed system uses 3D objects as common denominators for shared world comprehension.**

Keywords-Cognitive Modelling; Eye Tracking/Steering; Human Robot Interaction; Knowledge base; Ontology.

I. INTRODUCTION

Field robotics technology has matured to the point where commercial robotics platforms are available for diverse applications, such as surveillance, sample and data collection, analysis and return, construction, agriculture and mining operations. Communications links with robots now have high data capacities. A consequence of these advances, however, is that human operators receive increasing amounts of data streamed from robots that they must perceptually and cognitively process, often in real time, in order to perform real-time tele-robotic tasks. This data input is often of an overwhelming volume and complexity. One approach to dealing with this task performance demand is to offload some or all of the required cognitive processing onto the robot platform itself. Hence *cognitive robotics* aims to develop intelligent software capable of performing highly automated cognitive task performance by robots in order to optimize their use and take best advantage of the latest hardware developments. Artificial Intelligence (AI) has long sought solutions for making robots more intelligent, with rather limited success.

The formation and use of representations, and the possibility of making representations meaningful, is a key attribute of intelligence, and is one of the areas where AI has met challenges due to the human authorship of representations in traditional AI systems; the representations are too abstract to be grounded for the technical artifact, do not change with their contexts, require human interpretation to provide their meaning, and have arbitrary bounds [1].

Grounding the formation of symbolic representations in dynamic and embedded processes as biological systems do provides one approach to trying to avoid these issues in knowledge representation. However, the increasing availability of extensive broadband communications networks, high capacity computer memory and processing services, and extensive on-line data, suggests an alternative approach to symbol grounding and embedded cognition. This is by the use of repositories of previously captured sensor data together with real-time sensor data that have labels and semantic annotations supporting their discovery and reuse in AI systems. A cognitive robotics system realized on this basis can have the following features:

- Agency can be nested, where *a robot* consists minimally of a hardware platform.
- The on-board processing ability of a robot can scale, from low level interfaces for sensor transmission and command reception, through increasing levels of on-board autonomy, to full autonomous operation [2].
- Intelligence in the system does not need to be physically encapsulated or localized.
- Intelligent agency can be mapped across one or more robot platforms and hardware processing networks, with cognitive processing that is partially or wholly cloud-based.
- An intelligent agent can use the cloud-based memory of past perceptions of other robotic and human sensory data as a technical analog of human episodic memory.
- All ongoing and past sensor streams, decision processes and generated actions (i.e. the 'experiences') of agents can be stored for analysis and application in ongoing and future task performance.
- The scope of an agent can be scaled in proportion to the task that it is performing and the environment in which the task is performed.

 ISBN: 978-1-61208-340-7

Robotics research is beginning to explore ideas like these in a number of scenarios [3]. In this paper, we focus on the use of robotic 3D object perception and propose the use of a cloud-based infrastructure to implement a machine vision paradigm inspired by Marr's theory [4] of visual cognition. We also propose a method of using 3D simulation integrated with this perceptual approach. The derivation of 3D model data from perception provides world state information as input to an ongoing world simulation. The simulation provides predictions about future states. Those predictions facilitate rapid processing in future perception. The comparison of predicted states with perceived states also provides foundations for tuning the simulation and its parameters, that can also be represented declaratively to support higher level reasoning. The proposed *CogOnto model* described below stores the process and object(s) information in a knowledge system that can guide the robot in physical collaboration, manipulation and navigation.

The structure of the paper brings you as a reader from a 'high level architecture' to '3D visual processing' and thereafter to 'intelligent action in a structured world'. The actual contribution of this paper is presented in the section 'proposed model', followed by 'integrating semantic web concepts, resources, and technologies to the final summary.

II. HIGH LEVEL ARCHITECTURE

When the robot is operating in the physical world it may be controlled by a cognitive agent residing off-board, see Fig. 1.

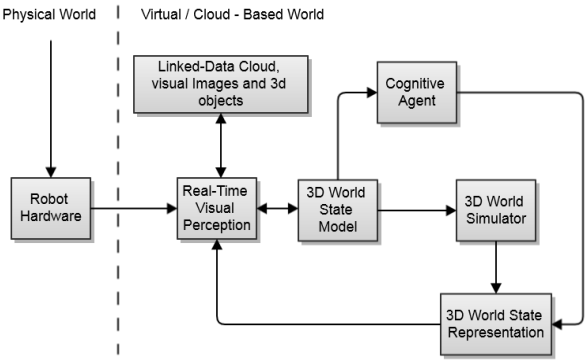

Figure 1. Robot hardware assisted by the cognitive agent where real time 3D object perception and recognition are supported by the 3D virtual world and knowledge cloud.

If the robot shall observe and manipulate a 3D object, it must have real time perception, comprehension and memory recall so that the robot knows how to execute the manipulation task(s) via motor action. The linked data cloud is operatively called to match already stored 3D object information parallel to real time 3D object extraction from the scanned physical world: this is the recognition phase. The 3D world state model constitutes a virtual world derived from a scanned *volume of view* where objects and object motions are captured, digitized and recorded. The recorded information is fed into memory and can be used for simulation scenarios and prediction of scenario events. Notice in relation to 'first order predicate calculus' [5] that 3D objects here are both subjects and objects, while adjectives and verbs are predicates.

III. 3D VISUAL PROCESSING

The ability to scan a real world environment makes it possible to extract digital information about the physical world and how it functions. Three dimensional perception is a key technology for robotics applications where obstacle detection, mapping and localization are core capabilities for operating in unstructured environments. Laser scanning creates a surface point cloud of a 3D physical environment [6] making it possible to map any environment in a rather short time (the Leaning Tower of Pisa was scanned in 20 minutes). This technology can be used in a robotic intelligence system for Simultaneous Localization Mapping (SLAM) and higher level reasoning regarding location and position. However, object recognition and manipulation requires deriving 3D object information from the overall point cloud and building cognitive models with task reasoning for using object and scene data in real time.

Object extraction [7][8][9] makes it possible to know what a robot is looking at, supporting manipulation or collection actions. This can be achieved by an Environmental Scanning-Object Extraction (ES-OE) engine. For human-robot collaboration, a robot can be enabled to use deictic visual references from human gaze by integrating an eye tracker with the ES-OE engine.

A. Background

In a previous work [10], a 3D simulation engine was integrated with an eye tracker. The integrated system allows the human point of gaze on 3D objects within a 3D digital world projected onto a computer screen to be tracked automatically. This development made it possible to log gaze in various task-related environments in a simulated world. From a Human Factor's perspective, the simulation and human observation can be investigated, including collaborative actions performed by groups with various workloads, stressors and decisions. There have been several studies made using the technological framework with different stimuli [11][12][13], but no substantial theoretical framework has been developed in relation to this object-based approach *per se*. A bottleneck in relation to this visual approach has been that 2D image, film and visual stimuli have not met the requirements for incorporating a knowledge-based approach for dynamic 3D worlds, whether the real physical world or a digitized 3D world. The object approach needs to address how both modeled and real world objects can be perceived and manipulated [14] by a robot, allowing the system to sense, think and act in real time: the computer needs to understand how to define an object and how to ontologically and semantically make sense out of such an object in a dynamic spatial world.

1) 3D objects in a 3D world

In [10], a simulation engine integrated with an eye tracker took a gaze fixation (x and y screen coordinates) and ray

 ISBN: 978-1-61208-340-7

casted/traced from that position onto the underlying 3D virtual object's collision box, a volume corresponding with the shape of a virtual object as recognized and processed by a physics engine that is also used to designate objects by interface devices, like a mouse. This made it possible to track gazed objects in real time every 17 ms (using a 60Hz eye tracker). The same principle can be used in a physical world context where an ES-OE engine could be integrated with eye tracking glasses to allow a computational system to know what object a person wearing the glasses is looking at.

2) Structuring a noisy world

The 3D world scenario, simulated or physically real, constitutes an event or scene. A scenario includes objects that are instances of their classes. A class could be something like a *CarClass*, *HumanClass*, *FlowerClass*, etc.

In a constrained world, we can name all objects beforehand so when they are logged we know what they are and what position (x, y, z, θ_1, θ_2, θ_3) they are in. In an unconstrained environment that is scanned and has extracted objects, we must also have a capability to know what the objects are and to be able to classify them. A cloud-based approach of the kind proposed in this paper presents a middle ground, being more open than a highly constrained environment, but still being limited to objects of types that are represented and labeled within the cloud.

IV. INTELLIGENT ACTION IN A STRUCTURED WORLD

Knowledge by definition is "1. Facts, information, and skills acquired through experience or education; the theoretical or practical understanding of a subject and 2. Awareness or familiarity gained by experience of a fact or situation." [15]. To gain an understanding of how robots might learn and operate on knowledge, we have looked at several established models that can fit within an initial architecture that enhances these established models by the ingestion of information from the web. Our overall aim is to build a computational comprehension system for 3D object information, assisted by a hybrid computational ontology (i.e., combining several existing and new ontologies).

A. Existing Models

Extensive effort has been put into the task of understanding and attempting to re-create/simulate the processes by which a human being thinks. Using the underlying assumption that intelligence is wholly "the simple accrual and tuning of many small units of knowledge" [16], production-based models of cognition have had success in displaying human-like performance on a number of tasks (e.g., visual search [17] and natural language processing [18]). While there are debates regarding the similarity of what humans actually do to what we have achieved using the above assumption [19], there is little doubt that such systems can produce intelligent-seeming behavior, that can facilitate the development of vitally useful control structures in the field of robotics and computational intelligence [18].

One of the most influential models of human cognition is the ACT-R, or "Adaptive Character of Thought – Rational" model [16], developed over many years by John Anderson, who was a student of the seminal Cognitive Scientist Alan Newell (1927-1992). Anderson's model is a hybrid symbolic/sub-symbolic system that incorporates various "modules" that are deemed necessary for rational behavior, and are thought to have biological correlates. These include the modules *Declarative* (manages creation, storage and activation of memory "chunks"), *Procedural* (stores and executes productions based on expected utility), *Intentional/Imaginal* (goal formulation for directed behavior), and *Visual (2D)/Audio* (theoretically plausible implementation of visual and auditory perception), see Fig. 2. An internal pattern-matching function searches for a production that matches the current state of the buffers.

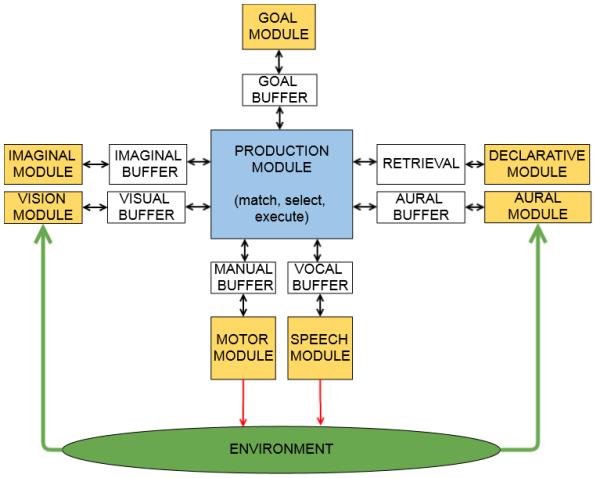

Figure 2. A schematic representation of the canonical ACT-R cognitive model.

ACT-R is formed as a knowledge model where the "chunks" are the elements of declarative knowledge in the ACT-R theory and are used to communicate information between modules through the buffers. A chunk is defined by its chunk type, that is described by its slots (here compared with properties), see table 1. Chunk types can be organized as a hierarchy of parent (SuperType)-child (SubType) relationships. The subtype will inherit all of the slots (properties) of the parent node(s).

Other models that take a similar symbolic approach to model human cognition include Soar [20], EPIC [21], CLARION [22], and others (for a detailed review see [23]). While these have been successful to varying degrees at modeling specific human cognitive task(s) performance, it is becoming evident that such models are intrinsically limited by their disconnections from the real world in which humans (or robots) operate. A production based system is only as adaptive as its rule set allows given the inputs provided to it, that have generally been limited to "screen as eye" and "keyboard/mouse as hands" mappings. A new wave of thought surrounding the development of cognitive models is embracing the need for "embodied" cognition, improving the ability of the system to sense and act. One example of this is the ACT-R/E framework, used as an operating system for

 ISBN: 978-1-61208-340-7

mobile robotics developed by the American Naval Research Lab [24], depicted in Fig. 3.

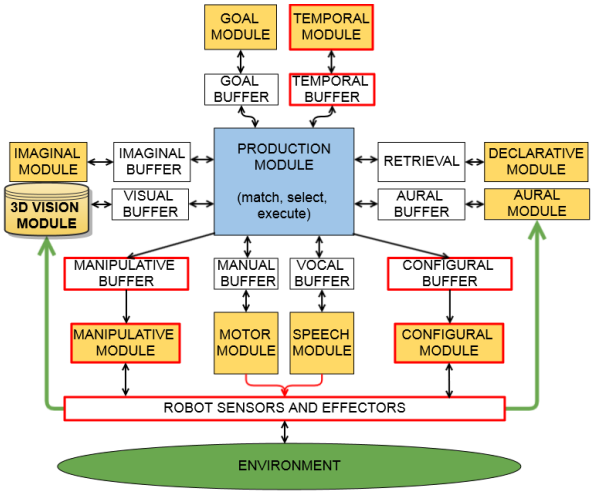

Figure 3. The "embodied" (Visual 3D) modifications introduced by Trafton et al. 2012. Additions in the ACT-R/E are highlighted in red.

The Object-Attribute-Relation (OAR) model of Wang, 2007 [25], specifies the elements of a cognitive model in the fashion of an ontology, the logical model of memory. In an attempt to formally describe the mechanism of human Long Term Memory (LTM), which he states is the "foundation of all forms of natural intelligence" (p. 66), Wang decomposes the construct into three elemental components – Objects, Attributes and Relations. This OAR model allows the computational specification of the human LTM formation and storage process, and is put forth as having sufficient explanatory power as to describe the "mental process and cognitive mechanisms of learning and knowledge representation" (p.72). This model has a strong parallel with the specification of knowledge in information processing Ontologies. This parallel is direct, as described by the relations given in Table I.

TABLE I. COMPARISON OF MODEL TYPE CONSTRUCTS

OAR Model	Ontology Components	ACT-R ACT-R/E
Object(s) Attribute(s) Relation(s)	Class(es) Propert(ies) Relationship(s)	Chunk Type(s) Chunk Slot(s) Function(s)

A critical issue for any of these kinds of models is the relationship of their constructs to the environments in which they are expected to provide foundations for action. The core notion of *embodiment* is to provide the heretofore functionally "disembodied" computational model with sensors and effectors that allow its direct interaction with the physical world. In such a way, the inherent limitation of human-defined input may be overcome. In addition to physical sensory perception and manipulative ability, a human may have access to a detailed semantic understanding of the surrounding world. In the quest to produce a non-human intelligent actor within a physical space, we must provide the actor with an understanding of underlying structures, i.e. specific denotations in the physical world.

V. PROPOSED MODEL

In the CogOnto model, we propose a further augmentation of the cognitive models discussed above, providing the robot with detailed 3D schematic representations of objects that it encounters in real time, supported via task models, knowledge models and ontologies.

The CogOnto model is composed of five parts $<S_i,C_i,A_i,O_i,R_i>$, where $i = 1..N$, and where S_i is a finite set of situations, C_i is a finite set of classes, A_i is a finite set of attributes for characterizing a class, O_i is a finite set of objects in a class, and R_i is a finite set of relationships among the objects. In the CogOnto model (Fig. 4), we consider the following features [26][27]:

- Situation: represents an interactive (i.e. dynamic) real world scenario.
- ConceptNet: is a network of class-to-class relationships applicable in a given situation.
- ObjectNet: an object is an instance of a class. ObjectNet is a network of object-to-object relationships.
- AttributeNet: is a network between properties of classes and objects.
- Relation: is a function associating concepts, classes, objects and attributes; e.g. a *robot* is *part-of* an *Intelligent Agent (IA)*, were the "part-of" relation connects two concepts. The relations (associations) may be modeled or created by an autonomous learning process.

These constructs are not defined in detail here, but unlike the other models are not limited to textual/linguistic meanings. The CogOnto model illustrated in Fig. 4 has four major functional elements that share information: 1) the ES-OE engine, 2) the eye tracking system interconnected with the ES-OE engine, 3) the OAR model functioning as the basis of the Cognitive System, and 4) the knowledge cloud, including external resources such as WordNet or Cyc. The latter is also called the Linked Open Data and may be used to illustrate the intelligent process for sharing and exposing information in machine readable form by using uniform resource identifiers based on Berners-Lee's [27][29] principles. These principles enable data communication guiding perception from procedural memory.

The knowledge system of the CogOnto model can be perceived as a storage system that accesses real world object information and external semantic resource information via the existing knowledge cloud [29].

 ISBN: 978-1-61208-340-7

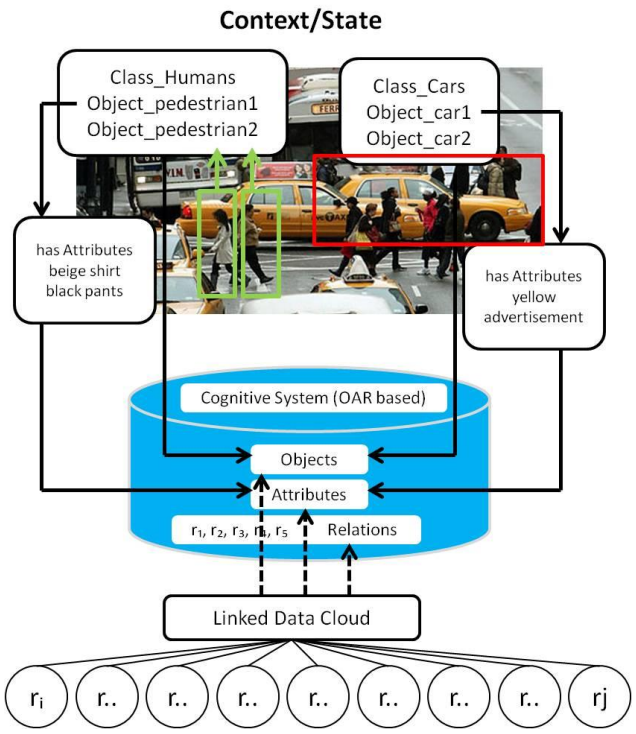

Figure 4. An illustration of the CogOnto model and its operative states.

The knowledge system represents the integration of formal symbolic and free text descriptors of an object.

VI. INTEGRATING SEMANTIC WEB CONCEPTS, TECHNOLOGIES AND RESOURCES

CogOnto integrates its own knowledge resources with external resources accessible via the web. For example, WordNet is a lexical database where nouns, verbs, adjectives and adverbs are grouped into sets of cognitive synonyms (synsets). To recall an object, the 'synsets (WordNet 2.1)' [30] and the W3C [31] standard can be used at a text level, to describe what an object is when it is text-labeled. Ontologies can be expressed by using Semantic Web tools, e.g. Web Ontology Language (OWL) [32] and the Resource description framework Schema (RDFS) [33].

The OAR model, with its Object, Attribute and Relation parts, and the ontological framework, containing Class/Instance, Relationship and Properties, can be inter-mapped so the object world can be comprehended using existing resources and using the 3D information represented internally within an object model. The 3D object's internal structure and shape can either be structured as Free Form Geometry (FFG) with surfaces and curves, or as Polygonal Geometry (PG) with points, lines and faces. The objects can be extracted and exported into different file formats, such as e.g. .obj files, .stl files. The .stl file format is a triangular representation of a 3D object, where each triangle is uniquely defined by its normal and three points representing its vertices. The format is native to the stereolithography Computer Aided Design (CAD) software created by 3D Systems (in this kind of format it is also possible to print the object out from a 3D printing machine).

The 3D object file contains different layers cognitively (form, volume, size, other descriptive attributes, etc.), supporting our senses and perception operating in parallel when performing allocated manipulation tasks. A human looking at an object can relate to the object both on a denotative- and on a connotative level. The denotative level is understood as a pure noun level without any cultural associations, nor any emotional or associative signifiers to the object, it is purely instrumental. The connotative layer is, on the other hand, the level of cultural and personal associations attached to an object with experience over time. Geometrical information within the 3D object can be represented using the X3D XML-based file format, an ISO standard for representing 3D computer graphics.

VII. CONCLUSION AND FUTURE WORK

The CogOnto model with support from the technological implementation of the eye tracker system with the ES-OE engine can represent cognitive relations that can be processed by a robot operating in a spatial world [34].

Formal knowledge structures within CogOnto face similar challenges to other knowledge representation formalisms, and this paper has shown isomorphism with a number of examples. However, the primary advance proposed is to use cloud-based resources that are not limited to formal representations to enhance the robustness of knowledge processing by the integration of similarity-based search. Those cloud-based resources may use text and images. But more interesting extensions for future work include new forms of cloud content, such as multi-spectral images, point clouds and behavior tracks. The main ongoing research challenge is to provide suitable similarity metrics for these data forms, integrating search results with formal structures, and developing methods for integrating them in unified search, or meta-search, results.

REFERENCES

[1] C. A. Lindley, "Synthetic Intelligence: Beyond A.I. and Robotics," in Integral Biomathics: Tracing the Road to Reality, Simeonov, Plamen L.; Smith, Leslie S.; Ehresmann, Andrée C. (Eds.), 2012, Springer.

[2] T. B. Sheridan, "Humans and Automation: System Design and Research Issues," A John Wiley and Sons, Inc., 2002.

[3] J. J. Kuffner, "Cloud-Enabled Robots," IEEE-RAS International Conference on Humanoid Robotics, Nashville, TN, USA, 6-8 Dec, 2010.

[4] D. Marr, "Vision: A Computational Investigation into the Human Representation and Processing of Visual Information," MIT Press, 1982.

[5] J. Barwise, Jon (1977); "An Introduction to First-Order Logic", in Barwise, Jon, ed.. *Handbook of Mathematical Logic*. Studies in Logic and the Foundations of Mathematics. Amsterdam, NL: North-Holland. ISBN 978-0-444-86388-1, 1982.

[6] M. Bosse, R. Zlot, and P. Flick, "Zebedee: Design of a Spring-Mounted 3-D Range Sensor with Application to Mobile Mapping," IEEE Transactions on Robotics, vol. 28, no. 5, 2012.

 ISBN: 978-1-61208-340-7

[7] R. Zeibak and S. Filin, "Object extraction from Terrestrial Laser Scanning Data", TS 8E –Terrestrial Laser Scanning, Visualization and LIDAR, FIG Working Week 2009, Surveyors Key Role in Accelerated Development, Eilat, Israel.

[8] S. Westerberg and A. Shiriaev, "Virtual Environment-Based Teleoperation of Forestry Machines: Designing Future Interaction Methods", Journal of Human-Robot Interaction, vol. 2, no. 3, 2013.

[9] A. El Daher and S. Park, "Object Recognition and Classification from 3D Point Cloud", student project, 2006, http://cs229.stanford.edu/proj2006/ElDaherPark-ObjectRecognitionAndClassificationFrom3DPointClouds.pdf [retrieved: March 2013], Stanford Education at Stanford University, USA.

[10] C. Sennersten and C. Lindley, "Evaluation of Real-time Eye Gaze Logging by a 3D Game Engine", 12th IMEKO TC1 & TC7 Joint Symposium on Man Science and Measurement, Annecy, France, 2008.

[11] C. Sennersten, M. Castor, R. Gustavsson, and C.A. Lindley, "Decision Processes in Simulation-Based Training for ISAF Vehicle Patrols," NATO-OTAN, MP-HFM-202-17, 2010.

[12] P. Jerčić, et al., "A Serious Game Using Physiological Interfaces for Emotion Regulation Training In The Context of Financial Decision Making," ECIS 2012 Proceedings. AIS Electronic Library (AISeL), 2012.

[13] H. Cederholm, O. Hillborn, C. Lindley, C. Sennersten, and J. Eriksson, "The Aiming Game: Using a Game with Biofeedback for Training in Emotion Regulation", 5th Digital Games Research Association (DIGRA) Conference THINK DESIGN PLAY 2011, Utrecht, Netherlands.

[14] J. R. Flanagan, G. Rotman, A. F. Reichelt, and R. S. Johansson, "The role of observers' gaze behavior when watching object manipulation tasks: predicting and evaluating the consequences of action," Philosophical Transactions of the Royal Society –B: Biological Sciences, 2013, UK.

[15] http://www.oxforddictionaries.com/definition/english/knowledge, [retrieved: March 2013].

[16] J. R. Anderson, "ACT," American Psychological Association, Vol. 51, No.4, 1995, p. 355-365.

[17] D. Kieras and D. Meyer, "An overview of the EPIC Architecture for Cognition and Performance with Application to Human-Computer Interaction", University of Michigan, EPIC report No. 5 (TR-95/ONR-EPIC-5), 1995, DTIC Document 1995, 43 pages.

[18] D. P. Benjamin, D. Lonsdale, D. Lyons, and S. Patel, "Using Cognitive Semantics to Integrate Perception and Motion in a Behavior-Based Robot," In Learning and Adaptive Behaviors for Robotic Systems, 2008, LAB-RS'08. ECSIS Symposium on, pp. 77–82. http://ieeexplore.ieee.org/xpls/abs_all.jsp?arnumber=4599431[retrieved: March 2013].

[19] E. Hutchins, Cognition in the Wild (book). Chapter 9 – Cultural Cognition, 1996, pp. 353-374.

[20] J. Laird, A. Newell, and P. Rosenbloom, "SOAR: An Architecture for General Intelligence," Technical report AIP-9, University of Michigan, Carnegie-Mellon University, Stanford University, Artificial Intelligence 33, 1987, pp. 1–63, DTIC Document 1988, 63 pages.

[21] D. Kieras and D. Meyer, "The EPIC architecture for modeling human information-processing and performance: A brief introduction," EPIC Report No.1 (TR-94/ONR-EPIC-1), University of Michigan, 1994, DTIC Document 1994, 43 pages.

[22] R. Sun, "The CLARION Cognitive Architecture: Extending Cognitive Modeling to Social Simulation," Cognition and Multi-Agent Interaction, Oct. 2004, Cambridge University Press, New York, 2006.

[23] D. Vernon, G. Metta, and G. Sandini, "A Survey of Artificial Cognitive Systems: Implications for the Autonomous Development of Mental Capabilities in Computational Agents," IEEE Transactions on Evolutionary Computation 11 (2), April 2007, pp. 151–180, doi:10.1109/TEVC.2006.890274.

[24] G. Trafton, et al., "ACT-R/E: An Embodied Cognitive Architecture for Human-Robot Interaction," Journal of Human-Robot Interaction, vol.2, No.1, 2013, pp. 30-55.

[25] Y. Wang, "The OAR model for knowledge representation," Proc. The 2006 IEEE Canadian Conference on Electrical and Computer Engineering (CCECE'06), Ottawa, Canada, pp.1692-1699.

[26] A. Oltramari and C. Lebiere, "Extending Cognitive Architechtures with Semantic Resources," Department of Psychology, Artificial General Intelligence Lecture Notes in Computer Science, Vol. 6830, 2011, pp. 222-231.

[27] T. Berners-Lee, "Linked data-the story so far," International Journal on Semantic Web and Information Systems, 5(3), 2009, pp. 1-22.

[28] Linked_Data_Design_Issue. http://www.w3.org/DesignIssues/LinkedData.html [retrieved: March 2013].

[29] C. D'este et al., "Sustainability, Scalability, and Sensor Activity with Cloud Robotics", Proceedings of Australasian Conference on Robotics and Automation, 2-3 Dec 2013, University of New South Wales, Sydney, Australia.

[30] WordNet: http://wordnetweb.princeton.edu/perl/webwn[retrieved: March 2013].

[31] World Wide Web Consortium is the main international standards organisation for the World Wide Web

[32] OWL W3C: http://www.w3.org/TR/owl-features/[retrieved: March 2013].

[33] RDFS W3C: http://www.w3.org/TR/rdf-schema/[retrieved: March 2013].

[34] M. Lochner, C. Sennersten, A. Morshed, and C. Lindley, " Modelling Spatial Understanding: Using knowledge representation to enable spatial awareness in a robotics platform", The 6th International Conference on Advanced Cognitive Technologies and Applications, 25-29th of May 2014, Venice, Italy.

 ISBN: 978-1-61208-340-7

The Behavioural Motivation Model in Open Distance Learning

Oleg Zaikin
Warsaw School of Computer Science
WWSI
Warsaw, Poland
e-mail: ozaikin@poczta.wwsi.edu.pl

Magdalena Malinowska
Faculty of Management and Economics of Services,
University of Szczecin,
Szczecin, Poland,
e-mail: magdalena.malinowska@wzieu.pl

Lise Busk Kofoed
Department of Architecture, Design & Media Technology,
Aalborg University,
Aalborg, Denmark
e-mail: lk@create.aau.dk

Ryszard Tadeusiewicz
Department of Automatics and Biomedical Engineering
AGH – University of Science and Technology,
Cracow, Poland,
e-mail: rtad@agh.edu.pl

Andrzej Żyławski
Warsaw School of Computer Science,
WWSI,
Warsaw, Poland
e-mail: andrzej.zylawski@wwsi.edu.pl

***Abstract*—The article contains the concept of developing a motivation model aimed at supporting activity of both students and teachers in the process of implementing and using an open and distance learning system. Proposed motivation model is focused on the task of filling the knowledge repository with high quality didactic material. Open and distance learning system assures a computer space for the teaching/learning process in open environment. The structure of the motivation model and formal assumptions are described. Additionally, there is presented a structure of the linguistic database, helping the teacher to assess the student's motivation and the basic simulation model to analysis the teaching/learning process constrains. The proposed approach is based on the games theory and simulation approach.**

Keywords-motivation model; computer learning platform; knowledge repository; non-cooperative game.

I. INTRODUCTION

Open and Distance Learning Systems can be considered as a new stage of information system evolution in the distance learning domain [1]. Basic concept comes from Open and Distance Learning (ODL), which is an idea of the learning/teaching process organization in higher education institutions [2]. The "distance" aspect describes an educational situation, where the student is situated in a different place than the source of knowledge and the other participants of the teaching/learning process. All the communication and socialization is maintained by the information system. The "open" aspect of ODL is visible at many levels: social, technical, computer and organizational [3].

Implementation of Open and Distance Learning Systems [4] will most probably introduce changes to the entire organization of the education process at higher education institutions, and consequently – changes in the role and relationship between all participants of the learning process while still maintaining status-quo regarding the traditional mission of a university: preparing highly-qualified staff.

In traditional education, the level of competence a student obtained at a university depended on various factors [5], the main of which are: education process organization at all levels (starting from the curriculum, syllabuses, up to the classes themselves), equipment, ergonomic conditions, and most importantly – the staff qualification. The position of each university among others is decided on the basis of a ranking [6] that considers basic activities of each teacher and the university as a whole: didactic, research, and educational.

ODL can be considered as a new teaching technology, it is as good as well it expands everyone's possibilities to learn in every life-situation, practically without constraints, however, the teachers charisma [7], one of very important motivation factors, becomes lost. Open learning joined with the distance learning mode requires students to become active, almost equal to teachers participants of the education process. It is cause by two factors:

1. In ODL conditions students' preferences highly influence the market position of a university.
2. Lack of direct contact with the teacher calls for an conscious student, creating his or her cognitive process independently.

 ISBN: 978-1-61208-340-7

Under the influence of these factors, the education organization management system should consider the new position of the student and reflect it in the frames of a proper motivation model. Source of the research behaviour/attitude:

- Teacher and students should elaborate a new product – the didactic materials repository.
- There is the opportunity to direct collaboration between students and the teacher.
- Student has opportunity to consciously choose a task in accordance with his/her own criteria (e.g. level of task's complexity).

The final result of the student's learning process depends on his/her involvement in the repository development.

The problem of motivation is one of the more important research subjects of psychology and pedagogy. There are many definitions of this concept [8][9], according to which motivation as a phenomenon can be seen as:

a) A system of factors (needs, motives, goals, plans, etc.) determining human actions.
b) A process that supports human activity at a certain level.

When developing a motivation model as a part of an information system aimed at managing an education organization in ODL conditions, one has to define the place of this model in the system, its criteria function and solution method.

In the article, we present a model of a system, in which students and teachers are focus on a new goal - creating the repository with the high quality didactic materials. To achieve this goal, the motivation factors of the learning process participants should be considered, and the analytical mechanism for the assessment of the learning process constrains should be proposed. Our model covers the formalization of the learning process environment based on the motivation and offers a simulation as a mechanism supporting the teacher to influence on his/her and students motivation taking into account the typical learning process constrains (eg., work time).

II. MODEL OF THE DIDACTIC MATERIALS REPRESENTATION

In the conditions of no direct contact between the teacher and students, the scope and way of performing the knowledge-based actions (didactic, research, educational) changes significantly [10]. It occurs due to the various reasons. In the traditional learning, the didactic materials play the complement role to the teacher's charisma and their improvement requires a long time because of the source of knowledge (books, journals, scripts etc.). However, such accumulating and improving of knowledge resources often does not fulfil its purpose due to rapidly changing situation on the technology market. It especially can be seen in a such domains as: computer science (continuously incoming new software frameworks), printing (new pdf-based workflow), banking (new banking products), etc. [24].

Moreover, in traditional learning the motivation occurs through assessing knowledge (tests, exams, etc.). The teacher acts a middle-man between the knowledge source and the student's cognitive process and is responsible for its control [11]. As a management object, the student's cognitive process is characterized by high level of entropy, but through direct contact, through exchanging information, the teacher, on the basis of his/her own competence, continuously lowers the entropy level, meaning that the teacher controls the student's cognitive process in certain boundaries. The effectiveness of this control depends highly on the intensity of interaction and on the interpersonal skills of the teacher.

Kushtina [4] showed that the role of didactic materials in the ODL conditions is greatly increased because of the new expectation - to substitute direct contact and exchange the information between teacher and student. This imposes new requirements to display in the didactic materials not only the information, but also knowledge in the learned subject or topic. Moreover, the role of didactic materials in ODL conditions comes from the assumption that knowledge is a visual and textual information structured according to the goal and level of education.

Processing information received by a human into the form of knowledge takes place with the help of internal cognitive operations like [12]: structuring, coding and clustering as well as creating a kind of internal semantic network, which we can consider subjective ontologies [13].

In order for the didactic material to be in any way capable of playing the role of a broker between the source of information and the cognitive process of a student, it should contain the ontology of the taught subject, developed by the teacher. Currently, the ontology is a widely used method for knowledge representation. There are ontology description languages and programs to operate them. Advantages of using the ontological approach to learning are discussed in [29]. As it was there presented, this method is recognized as a crucial in the development of the student's analytical skills and elaboration the system vision of wide field of knowledge objects and their applications.

A more detailed description of constructing didactic materials on the basis of an ontological model was described by Kushtina et al. [23].

Preparing and making available the ODL didactic material through appropriate computer environment (repository) requires great efforts regarding intelligence and working time of the teacher. The computer aspects of the repository were already discussed by Mayer [14] and the proper repository development involves substantial money capital and consumes a lot of time. Resulting from previous researches shows the need to motivate the teacher to supplement his/her duties with developing and monitoring the state of the repository.

The second difficulty is the necessity to motivate the student to get highly involved in working independently during the education process, what guarantees obtaining a

 ISBN: 978-1-61208-340-7

level of competence comparable to traditional education. Assessing knowledge on the basis of traditional tests in the distance learning mode loses its meaning as an instrument of motivation, as it deprived of all the consequences of direct contact with the teacher and other students (cognitive ones, emotional ones, etc.). A substitution way of rising the activity of the person learning something is a "game", understood as an active cooperation, the result of which will be an object of interest for both the teacher and students (players). In the management sense, it means that the interests of each participant of the cooperation should be described as individual motivation functions that make up one goal function.

The repository is the result of this cooperation, from the didactic point of view it is an open for everyone storage of didactic materials, including ontologies, tasks, example solutions, etc.; from the scientific point of view it is a copyrighted knowledge resource of a university; from the software-technical point of view it is an information system based on an appropriate network platform.

III. MOTIVATION MODEL INTERPRETATION IN THE CONTEXT OF AN EDUCATION SITUATION

A motif (the reason of action) is a consciously understood need for a certain object, position, situation, etc., therefore we can state that the motif comes from a requirement, becomes its current state and leads to certain actions [15]. During the realization of the mentioned chain "need – motif – action", at each step we deal with a decision-situation, meaning: many motifs can lead to a certain action, many needs can make up one motif, many motifs come out of one need. Making a choice is a cognitive process that cannot be observed directly [16]. This means that it is only possible to define the quantitative relationships between the choice parameters through exterior registration of the choice results.

The motivation model can be developed in the form of a certain game scenario, where the activity of a teacher and a student will be supported by their own interests [17]. Developing the motivation model in a specific education situation (subject, goal and education level) is possible with the following assumptions:

- The set of elements of the mentioned chain is defined and contains alternatives.
- The choice is made in a specific education situation.
- The result of a multiple choice made according to the chain is the obtained competence.
- The result can be registered.
- There is a system of assessing the choice results.
- Students and teachers have access to observations and evaluations of the choices, which they made.
- The result of a choice has to be evaluated by the student as a needed and wanted one (usability of the result).
- The student has to be certain that the wanted result can be achieved in a given education situation, with probability higher than zero (subjective probability of achieving the result).

Research's discussion about motivation model can be addressed to different area of education system. The conducted analysis of information-processing in judgmental tasks allows to prepare cognitive-motivational model of decision's satisfaction [18]. In proposed model, confidence serves a role of a major contributing factor of the learning motivation. However, more details investigation proves that the motivation is a set of several components. The ARCS Motivation Model [19] is based on four-factor theory. The student's motivation is hooked up with student's attention, relevance, confidence and satisfaction. The ARCS model also contains strategies that can help an instructor stimulate or maintain each motivational element. Other researchers show that personally valued future goals are core for motivation [20]. Moreover the cultural discontinuities and limited opportunities in students' learning environment may weak the motivational force in the future [21].

The form and content of motivation model is also strong depended on object to be motivated and environment, where motivational action takes place. On the one hand motivation model can be designed for artificial or human object. DeVoe and Iyengar [22] proposed a motivation model for virtual humans such as non-player characters. The motivation model based on overlapping hierarchical classified systems works to generate the coherent behavioural plans. On the another hand, different environment creates individual needs for motivation model. Such situation is caused mainly by multicultural differences [23].

IV. STATING THE MOTIVATION PROBLEM IN A SPECIFIC ODL EDUCATION SITUATION

In ODL conditions, as a motivation model we consider scenario of a game (interaction, interplay) between the teacher and the students, conducted in a specific education situation and oriented on performing the actions which allow to raise the level of student's involvement in subject-specified task realization and extend the repository with new student's solutions (new tasks).

The education process in every education situation includes the didactic, research and education aspects and takes place at the following levels: cognitive, information and computer-based. At each of these levels the teacher and the students have their own roles and involvement intensity. At the cognitive level assumptions are made and tasks are solved. At the information level the information is exchanged between the participants of the teaching/learning process. The computer-based level is characterized by repository organization and ability to use it. The role of the teacher is to develop an ontological model reflecting the subject of the education situation, showing the source of information, formulating tasks and presenting methods and

 ISBN: 978-1-61208-340-7

examples of their solutions. All ontological models are stored in the repository.

In the discussed approach tasks are created on the basis of the ontology and differ in their complexity level [14]. The proposed scenario assumes that the role of the student is to choose a task and solve it. The final grade depends on the correctness of the solution and the complexity level of the task. A task solved by a student and highly graded by the teacher is placed in the repository and will serve as an example solution for other students. All materials stored in the repository are copyrighted. This way the student participates in the didactic activity and we assume that it will raise his/her self-esteem, what has a positive influence on learning, meaning that it will be a part of the *student's motivation function*. At the same time filling the repository with a wide spectrum of high quality solved tasks gives satisfaction to the teacher, for his/her laborious, requiring intelligent efforts of preparing the repository. And this will make up the *teacher's motivation function.*

Teacher's and student's interaction with the repository can have a research character. We assume that thematically the content of the repository is in concordance with the teacher's scientific-research interests, what causes appearance and extension the repository with the tasks differing from the complexity level. For helping to solve tasks stored in the repository, the teacher will pay more attention and spend more time with the students. We can assume that for a certain part of students participation in common research is a challenge and the obtained results are an extra added value.

The educational aspect is reflected in the repository development as a common success of all participants of the education process. Making the material copyrighted shows and visualizes the contribution and involvement of each participant. Feeling the synergy effect motivates to develop cooperation skills and tolerance. Cooperation in distance conditions requires a more logical formulation of questions and answers. All this reflects the interests of both the teacher and the students.

Let us consider the basic components of the motivation model.

Input data

G^D - ontology graph of the domain area *D*,

$G^D = \{W^D, L^D\}$, where

W^D, L^D - set of vertices/arcs of the graph,

$G^C = \{W^C, L^C\}$ - graph of the course *C*, part of the $G^{D,}$ where $W^C \subseteq W^D, L^C \supseteq L^D$,

$R = \{r_i^k\}$ - set of the tasks, where

*i=1,2,..i**- index of task,

*k=1,2,..k**- index of acquired competence,

$S = \{s_j\}$ - set of students/project team, where *j=1,2,...*

*j**- index of student,

$[t_0, T_c]$ - interval /cycle of competence acquiring,

X – repository assigned by the teacher for saving the projects of knowledge,

$G_X(t) = \{W_X(t), L_X(t)\}$ -state of the repository X at the time *t*, where $t \in [t_0, T_c]$.

Decision functions

$y(r_i^k, s_j)$ -student decision's function of the task choice,

$$y(r_i^k, s_j) = \begin{cases} 1, if\ student\ s_j\ chooses task\ r_i^k \\ 0, otherwise \end{cases} \quad (1)$$

$\delta^N(p_i^k)$ - teacher decision's function of assignment the task/project to the repository,

$$\delta^N(p_i^k) = \begin{cases} 1, if\ \ project/task\ p_i^k\ is seleceted\ for\ repository \\ 0, otherwise \end{cases} \quad (2)$$

Criterion

$G(p_i^k)$ - ontology graph of the task/project,

$G(p_i^k) = \{W(p_i^k), L(p_i^k)\}$, where

$W(p_i^k), L(p_i^k)$ - set of the vertices/arcs of the graph

$$W(p_i^k) \subseteq W^c, L(p_i^k) \subseteq L^c \quad (3)$$

$\Delta G_X(p_i^k)$ -knowledge increment caused by the development of the repository *X* by the project p_i^k

$$\Delta G_X(p_i^k) = G_X(t) \cap G(p_i^k) = \{W_X(t) \cap W(p_i^k), L_X(t) \cap L(p_i^k)\} \quad (4)$$

$\left|\Delta G_X(p_i^k)\right|$ -numerical characteristic of knowledge growth in the repository,

$$\left|\Delta G_X(p_i^k)\right| = \delta^N(p_i^k)\left|W^C \cap W(p_i^k)\right|, \text{ where} \quad (5)$$

$\left|W^C \cap W(p_i^k)\right|$ - number of common vertices in the ontology graphs G^C i $G(p_i^k)$,

$Z_N(p_i^k)$ - expenditures(expenses) of the teacher's resources: consultation time in task/project p_i^k,

$$Z^N(p_i^k) = \alpha_N\left|G(p_i^k)\right| \text{ , where} \quad (6)$$

α_N - waging coefficient for teacher's expenditures.

Teacher Goal Function

$\Delta G_X^{\Sigma}(0, T_0)$ - summary increase of the repository *X* in the competence acquiring interval $[t_0, T_c]$,

$$\Delta G_X^{\Sigma}(0, T_0) = \sum_{i=1}^{i^*} \sum_{k=1}^{k^*} \sum_{j=1}^{j^*} \delta^N(p_i^k)\, y(r_i^k, s_j)\, G_X(t) \cap G(p_i^k), \text{where} \quad (7)$$

$\left|\Delta G_X^{\Sigma}(0, T_0)\right|$ - characteristic of the summary knowledge growth in the repository,

$$\left|\Delta G_X^{\Sigma}(p_i^k)\right| = \sum_{i=1}^{i^*} \sum_{k=1}^{k^*} \sum_{j=1}^{j^*} \delta^N(p_i^k)\, y(r_i^k, s_j)\left|W^C \cap W(p_i^k)\right|, \text{ where} \quad (8)$$

$\left|W^C \cap W(p_i^k)\right|$ - number of common vertices in ontology graphs G^C i $G(p_i^k)$,

Z_N^{Σ} - summary expenses/expenditures of the teacher's resources: consultation time, etc., in the competence acquiring interval $[t_0, T_c]$.

$$Z_N^{\Sigma} = \sum_{i=1}^{i^*} \sum_{k=1}^{k^*} \sum_{j=1}^{j^*} \alpha_N \, y(r_i^k, s_j) \left|W(p_i^k)\right|, \text{ where} \quad (9)$$

α_N - waged coefficient of the teacher's expenses/ expenditures,

$\left|W(p_i^k)\right|$ - number of vertices in the task/project

$G(p_i^k)$ - ontology graph,

Φ^N - teacher's goal function: summary increase of the repository X in the competence acquiring interval $[t_0, T_c]$ accounting teacher's expenses

$$\Phi^N = \left|\Delta G_X^{\Sigma}(0, T_0)\right| - Z_N^{\Sigma} =$$
$$\sum_{i=1}^{i^*} \sum_{k=1}^{k^*} \sum_{j=1}^{j^*} y(r_i^k, s_j)\{\delta^N(p_i^k) \left|W^C \cap W(p_i^k)\right| - \alpha_N \left|W(p_i^k)\right|\} \quad (10)$$

Student's goal function

$\Phi(s_j)$ - goal function of student s_j : number of ECTS (European Credit Transfer System) points accounting student's expenses for execution the task/project p_i^k

$$\Phi(s_j) = \sum_{i=1}^{i^*} \sum_{k=1}^{k^*} y(r_i^k, s_j) \gamma^N(p_i^k) \left|W^C \cap W(p_i^k)\right| - \beta^S \left|W(p_i^k)\right|, \text{ where (11)}$$

$\gamma^N(p_i^k)$ - number of ECTS points assigned by the teacher for execution the task/ project p_i^k,

$\left|W^C \cap W(p_i^k)\right|$ - numerical characteristic of growth of the repository as result of task/project p_i^k execution,

$\left|W(p_i^k)\right|$ - numerical characteristic the time-consuming of the task/project p_i^k

β^S - weight coefficient of student's expenses for execution the task/project.

V. MOTIVATION MODEL IDENTIFICATION IN THE GAMES THEORY TERMINOLOGY

Interpretation and solution of the developed model can be conducted on the basis of the games theory, which allows to study the activity of a system depending on the players' behaviour.

The way to involve students in active learning is to create a game situation, which is as follows. A distinctive feature of the ontology developed for educational purposes is that the ontology graph contains different types of subject knowledge: theoretical (what's this?) and the procedural (how to do this?). Theoretical vertices describe the semantics of the concepts and their relationships, and procedural ones - test tasks associated with the corresponding path in the graph. The project task to develop the domain ontology with both types of vertices can be represented as a game with total win and distribution points depending on the student's participation.

Overall gain is considered as the number of both types vertices, added to the domain ontology graph, stored in the repository as a new didactic material. Teacher plays the role of the head of the game, students are combined into sub-groups or can play individually. Motive of the teacher is to extend and update the repository by the independent work of students. Motive of the student is to study the subject under teacher's supervision using live chat, competition recognition, stress reduction compared to traditional testing, increase the choice possibility, etc. The game can be carried out remotely [24]. Some students may choose the simplest tasks and the traditional way of its solution. Final assessment depends on the task complexity, participation in the project, the number of ECTS points.

The proposed model refers to the class of non-cooperative games with a defined number of steps and full information about participants activities in real-time. The game has an arbitrary sum of participants' *wins*: the *win* of the teacher is accrual of knowledge in the repository, the *win* of the student depends on his/her strategy: maximal number of points for a task solved or minimal time loss. The equilibrium is obtained as a result of a dominant strategy, what compared to other strategies gives the game participants the possibility to obtain their maximal *win* regardless of actions of the other participants.

Using game theory terminology the motivation model can be seen as a stimulation task, where motivation management signifies direct rewarding an agent (student) for his actions. The formulated model is consistent to a multi-agent two-layer stimulation system which consists of one centre (teacher) and *n* agents (students). The strategy of each agent is to choose an activity, the centre's strategy – to choose a stimulation function, i.e., relationship between the win of each agent and his actions.

Participants' preferences are reflected by goal functions. The centre's (teacher's) goal function is the difference between his/her reward (ΔW) and the summary reward paid to the agents (sharing one's own resources ($\overline{X}$)). By goal function of each agent, we understand the difference between the reward obtained from the centre and the losses connected to solving the task. At the moment of making the decision (stimulation function for the centre and choice function for the agent) the goal functions and acceptable actions of all participants are known. The centre has the right of the first move, when it chooses a stimulation function, before the agents, with known stimulation functions, choose activities that optimize their goal functions. The centre's choice of a stimulation function takes place on the basis of a simulation meant to serve in foreseeing random characteristics of the basic students knowledge and parameters of the process of their arrival Agents choose their strategies independently and do not exchange information or wins, this signifies that we are dealing with a relational dominant strategy.

 ISBN: 978-1-61208-340-7

Let us denote: M - a set of acceptable stimulation methods, $Y(\sigma)$ - a set of game solutions (strategy of agents having balance in their stimulation method σ). Management (stimulation) effectiveness means obtaining maximum value of the goal function $U(\sigma)$ on an appropriate set of game solutions.

$$U(\sigma) = \max_{y \in Y(\sigma)} f(\sigma, y), \quad (12)$$

where σ is a simulation function of the centre, y is a binary argument of agent's choice. The task of optimization stimulation function synthesis is about searching for an acceptable stimulation function with maximum effectiveness:

$$\sigma^* \in Arg \max_{\sigma \in M} U(\sigma). \quad (13)$$

When solving the model, algorithms proposed by Shubik [24] and Gubko and Novikov [25] can be used.

VI. Simulation Model of the Teacher and the Student Co-operation in the Competence Acquiring Process

Transferring of represented ontological/mathematical model to a simulation platform requires a set of actions. Key factor is defined as an elementary event at the input of the system. Moreover it's necessary to define a kind of arrival pattern: deterministic or stochastic one and the rate of arrival.

The goal of the simulation model and experiment is realization and analysis the didactical process oriented on acquiring competence. Simulation experiment deals with virtual reality and transforms the real learning/teaching process. Using the charge of the resources and other output parameters it is possible to change model of co-operation between teacher and student and plan the competence development. General scheme of simulation model is shown on figure 1. Elements (events) of simulated process are incoming students' tasks and time of teacher's consultation. Students arrive independently, sequentially and each event has to be served.

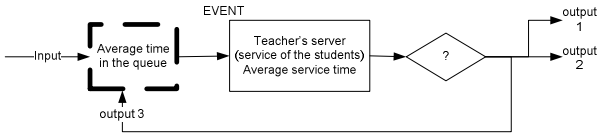

Figure 1. General scheme of simulation model.

On the base of outcome data teacher can change strategy of work with the students and modify motivation function, what means changing the complexity of the tasks setting up background of competence, e.g., to give more simple tasks, that in turn reduces the charge of the teacher and level of acquired competence. Simulation model provides also the estimation of various variants of teacher's work in different constraints of the education situation (time, kind of students group, etc.).

In conditions of the simulation experiment, the process of teacher and student co-operation can be interpreted as a queuing system with the following characteristics:

- Teacher's work relies on examination the students' task while the content and learning objects are known.
- For a given course and a group of students teacher's workplace can be defined as a server with known input, output and average time of service.
- Average time of service depends on the teacher's experience (specific character of course, task complexity, kind of student group, time of studies, etc.) and the results received from the linguistic database; its value is used in the motivation mechanism.
- Workflow of students arrival is stochastic: it's unknown number of arriving students, time of task evaluation, etc..
- Incoming tasks are served with 1 server, characterized by time and discipline of servicing.

Interpreting the given problem in terms of queuing system provides possibility to use well known analytical result for certain class of QS (Queuing Systems) (e.g., M/M/1 for Kendall notation) [30].

Implementation the simulation approach can be realized in the Arena software, which in flexible way gives possibility to research parameters of the education situation: waiting queue, predictable time of servicing of all students, charge of the teacher in specified distribution law of the students' arrival, etc.

Interpretation of the teaching/learning process oriented on acquiring competence in the terms of simulation modelling requires to define the components of this process, which impact its run (Figure 2). These components permit to consider the teaching/learning process as a production one. It results in growth of competence represented by the new repository resources.

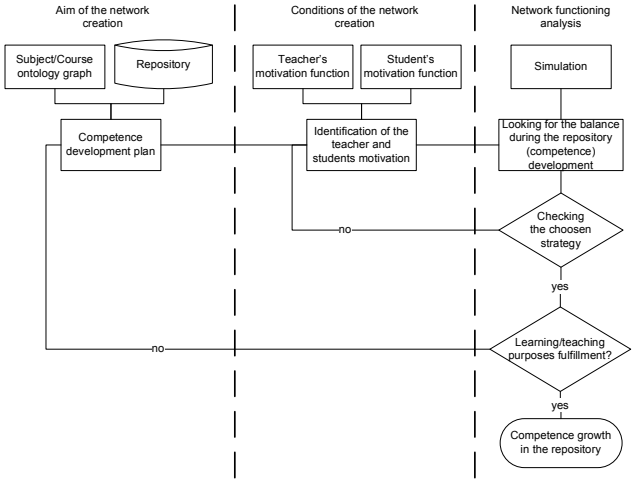

Figure 2. The components of the learning process oriented on acquiring competence [27].

First component of the teaching/learning process is competence development plan directly involved with the repository's ontology and the gathered resources. It permits to specify the tasks assigned for the repository - number of these tasks and theirs complexity level. The determining of the motivation function follows the setting of numerical parameters value. Teacher's motivation function depends on time of tasks control, number of task assigned for the repository and discipline of students' servicing. Meantime, determining the student's motivation function which essentially impacts on the competence development plan is difficult problem. To solve this problem some probabilistic approach based on linguistic database can be proposed. It allows to define the cognitive potential of the group of student. Such database requires to specify and aggregate the features defining the student's motivation function.

A set of features that allow for identification the student's motivation function is the following:

1. Self-estimating (self-assessment) of knowledge perception capability.
2. Estimating (assessment) of the teacher's requirements.
3. Quality of delivered didactic materials.
4. Interest of the subject content.
5. Didactic material capacity and its curriculum.

According to Goodhew [11], every feature sets numerical scale for linguistic quantifier. Distribution law of the linguistic quantifier for the feature 'Quality of the didactic materials' is represented in Figure 3.

Realising at the next steps, partial aggregation of the features in accordance with the linguistic database model enables to define expected level of student motivation in the teaching/learning process (Figure 4).

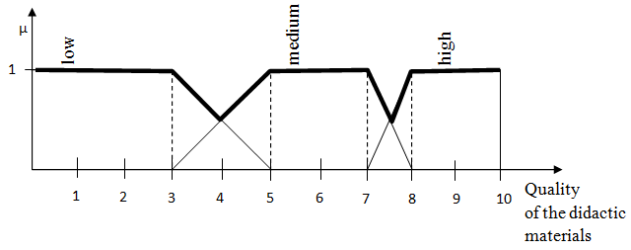

Figure 3. Distribution of the linguistic quantifier for the feature 'Quality of the didactic materials'.

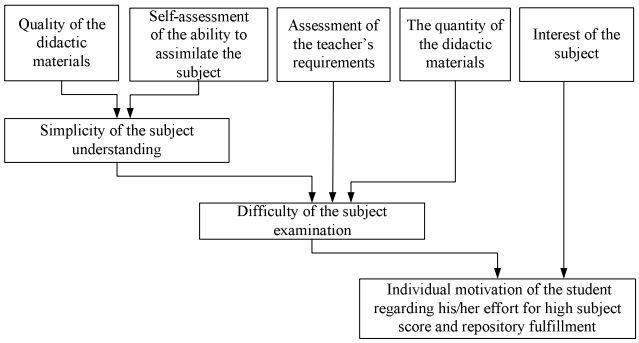

Figure 4. Model of linguistic database for student's motivation estimation [27].

Analysis of student's motivation on the base of the linguistic data/knowledge base defines cognitive potential of the students' group and their interest in the repository development. The results of analysis can be used for evaluation the simulation model parameters: number of students with high, middle and low motivation, interests in the repository development, number of tasks for correction .

The simulation model, represented in Figure 5, allows to verify parameters of the teaching/learning process and to make some changes in teacher's strategy with the group of students. It is based on assumption that "arriving" students must be served by the teacher. The result of this service is a new competence (with or without new resources in the repository) or (in otherwise) student must be declined for correction [12]. This approach allows to interpret the teacher's work with students as queuing system, where:

- For a given content of the didactic materials teacher's work refers to checking the executed students' tasks.
- For a given subject and students' group teacher's workplace can be examined as a server with a given input, output and average service time.
- Students arrival in the queuing system with the known parameters of stochastic workflow.
- Average service time depends on teacher's experience and results from the linguistic knowledge base analysis.

Simulation experiment was realised in Arena software. Co-operation between the teacher and the students was analyzed taking into account the time the teacher has spent with the students in the certain level of the repository development.

 ISBN: 978-1-61208-340-7

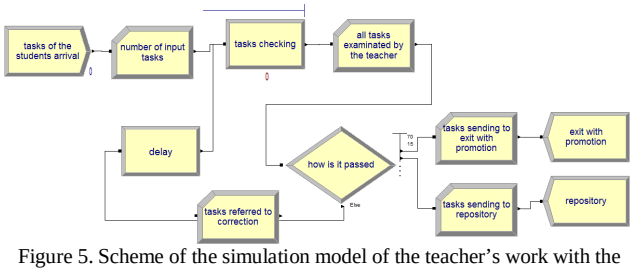

Figure 5. Scheme of the simulation model of the teacher's work with the students' tasks in Arena software [26].

Some parameters which can be analysed on the base of the simulation model are the following:

- Waiting queue on the teacher's workplace.
- Average waiting time of a student.
- Number of tasks completing the teaching/learning cycle with the repository development.
- Number of tasks allowing to pass the subject without fulfilment the repository.
- Number of tasks referred to correction.
- Total time required for the teaching/learning process realisation.

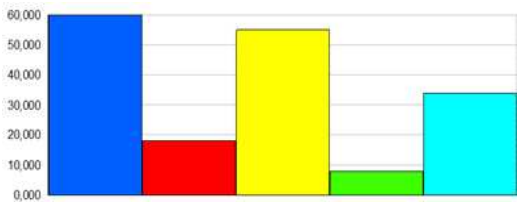

COLOUR	CRITERION	ACHIEVED VALUE
	number of input tasks	55
	tasks sent to exit with promotion	34
	tasks sent to repository	8
	tasks referred for correction	18
	all tasks examined by the teacher	60

Figure 6. Results of the simulation experiment used for estimation the teacher's strategy in collaboration with the group of students [27].

The results of simulation modelling represented in the Figure 6 can be used for analysis the behaviour or strategy of the teacher. The simulation model can be multiply modified and used for balancing the parameters of service the group of students.

VII. CONCLUDING REMARKS

The motivation model has to be an obligatory element of an open and distance learning system. The proposed model constitutes the theoretical formalization of the new situation, when a teacher and the students are obligated to elaborate a didactic materials repository in accordance with the competence requirements. It covers two motivation functions: teacher's and student's, which describe their interests in the knowledge repository development. The proposed approach to the motivation provides not only the efficiency of teacher's work in ODL condition, but also the high quality didactic materials oriented on competence achievement. The measure of success in cooperation between the teacher and the students, according to the presented scenario, is the level of the repository content development in a given time.

To analyze the constrains of this cooperation, it is proposed the simulation approach. The possibility of assessing the various variants of teacher's work in different education situation by using the simulation models and simulation software lets to change this cooperation on the basis of empirical results.

The interpretation the cooperation between the teacher and the students in a game theory causes, that the proposed motivation model can be solved on the basis of one of the known algorithms realizing a non-cooperative game with dominant strategy (RDS) [30].

REFERENCES

[1] E. Kushtina, O. Zaikine, P. Różewski, and R. Tadeusiewicz, "Competency framework in Open and Distance Learning," Proceedings of the 12th Conference of European University Information Systems EUNIS'06, Tartu, Estonia, June 2006, pp. 186-193.

[2] A. Tait, "Open and Distance Learning Policy in the European Union 1985-1995," Higher Education Policy, vol. 9(3), 1996, pp. 221-238.

[3] R. Tadeusiewicz, "Selected problems resulting from the use of internet for teaching purposes," Bulletin of PAS - Tech. Sc. Vol. 56(4), 2009, pp. 403-409.

[4] E. Kushtina, Concept of open and distance information system, (in polish), Szczecin: Publisher house of Szczecin University of Technology, 2006.

[5] E. Aimeur and C. Frasson, "Analyzing a new learning strategy according to different knowledge levels," Computers & Education, vol. 27(2), 1996, pp. 115-127.

[6] M. Rocki, "Statistical and Mathematical Aspects of Ranking: Lessons from Poland," Higher Education in Europe, vol.30(2), 2005, pp. 173 – 181.

[7] D. Solow, S. Piderit, A. Burnetas, and C. Leenawong, "Mathematical Models for Studying the Value of Motivational Leadership in Teams," Computational and Mathematical Organization Theory, vol. 11(1), 2005, pp. 5-36.

[8] B. F. Skinner, Science and Human Behavior, New York: Free Press, 1953.

[9] S. Barker, Psychology, 2nd ed., Boston: Pearson Education, 2004.

[10] e-Quality: Quality implementation in open and distance learning in a multicultural European environment, Socrates/Minerva European Union Project (2003–2006), [Online] Available at: http://www15.uta.fi/projects/e-quality/project.html, [retrieved: April, 2014].

[11] P. J. Goodhew, T. J. Bullough, and D. Taktak, "Materials education: now and in the future," Bulletin of PAS - Tech. Sc. Vol. 58(2), 2010, pp. 295-302.

[12] F. Barthelme, J. L. Ermine, and C. Rosenthal, "Sabroux An architecture for knowledge evolution in organisations," European Journal of Operational Research, vol. 109(2), 1998, pp. 414-427.

[13] O. Zaikine, E. Kushtina, and P. Różewski, "Model and algorithm of the conceptual scheme formation for knowledge

 ISBN: 978-1-61208-340-7

domain in distance learning", European Journal of Operational Research, vol. 175(3), 2006, pp. 1379-1399.

[14] R. E. Mayer, "Cognitive, metacognitive, and motivational aspects of problem solving," Instructional Science, vol. 26(1-2), 1998, pp. 49-63.

[15] J. R. Anderson, Cognitive Psychology and Its Implications, 5th edition, New York: Worth Publishing, 2000.

[16] B. W. Tuckman, "The effect of motivational scaffolding on procrastinators' distance learning outcomes," Computers & Education, vol. 49(2), 2007, pp. 414-422.

[17] R. V. Small and M. Venkatesh, "A cognitive-motivational model of decision satisfaction," Instructional Science, vol. 28(1), 2000, pp. 1-22.

[18] J. M. Keller, "Using the ARCS Motivational Process in Computer-Based Instruction and Distance Education," New Directions for Teaching and Learning, vol. 78, 1999, pp. 37-47.

[19] R. B. Miller and S. J. Brickman, "A Model of Future-Oriented Motivation and Self-Regulation," Educational Psychology Review, vol.16(1), 2004, pp. 9-33.

[20] K. Phalet, I. Andriessen, and W. Lens, "How Future Goals Enhance Motivation and Learning in Multicultural Classrooms," Educational Psychology Review, vol. 16(1), 2004, pp. 59-89.

[21] D. de Sevin and D. Thalmann, "A motivational Model of Action Selection for Virtual Humans," in Computer Graphics International (CGI'2005), New York: IEEE Computer Society Press, 2005, pp. 213- 220.

[22] S. E. DeVoe and S. S. Iyengar, "Managers' theories of subordinates: A cross-cultural examination of manager perceptions of motivation and appraisal of performance," Organizational Behavior and Human Decision Processes, vol. 93(1), 2004, pp. 47-61.

[23] E. Kushtina, O. Zaikin, and P. Różewski, "On the knowledge repository design and management in E-Learning," in Lu, Jie, Ruan, Da, Zhang, Guangquan (Eds.) E-Service Intelligence: Methodologies, Technologies and applications, Series: Studies in Computational Intelligence, vol. 37, Springer-Verlag Book, 2007, pp. 497-517.

[24] M. Shubik, Game theory in the social sciences: concepts and solutions, Massachusetts: MIT Press, 1991.

[25] M. V. Gubko and D. A. Novikov, Game Theory in Control of Organizational Systems, (in Russian), Moscow, Sinteg, 2002.

[26] P. Różewski and M. Ciszczyk, "Model of a collaboration environment for knowledge management in competence based learning," in Kowalczyk, R. (Ed.) Computational Collective Intelligence: Semantic Web, Social Networks and Multiagent Systems, LNAI 5796, Heidelberg: Springer-Verlag, 2009, pp. 333-344.

[27] M. Malinowska, E. Kusztina, and O. Zaikin, "Model of the production network for the knowledge management tasks", EduAkcja - magazyn edukacji elektronicznej, vol. 2(4), pp. 80-88, 2012. [Online] Available at: http://www.eduakcja.eu/, [retrieved: April, 2014].

[28] M. Ciszczyk, "The isue of the competence mangement process," (in polish), Roczniki Informatyki Stosowanej PS nr 10: Metody informatyki stosowanej, Szczecin: Informa, 2006, pp. 173-179.

[29] C. H. Coombs, M. Dawes, and A.Twersky, Mathematical psychology, New York: Englewood Cliffs, 1970.

[30] O. Zaikin, Queuing Modelling Of Supply Chain In Intelligent Production, Szczecin: Wydawnictwo Informa Wydziału Informatyki Politechniki Szczecińskiej, 2002.

 ISBN: 978-1-61208-340-7

The Virtual Patient Simulator of Deep Brain Stimulation in the Obsessive Compulsive Disorder Based on Connectome and 7 Tesla MRI Data

The Virtual Patient Simulator of Deep Brain Stimulation in the Obsessive Compulsive Disorder

Giorgio Bonmassar and Nikos Makris
A. A. Martinos Center for Biomedical Imaging, MGH, Harvard Medical School Boston, USA
e-mails: {gbonmassar, nmakris}@partners.org@partners.org

Abstract— **We present work in progress on the virtual patient model for patients with Deep Brain Stimulation (DBS) implants based on Connectome and 7 Tesla Magnetic Resonance Imaging (MRI) data. Virtual patients are realistic computerized models of patients that allow medical-device companies to test new products earlier, helping the devices get to market more quickly and cheaply according to the Food and Drug Administration. We envision that the proposed new virtual patient simulator will enable radio frequency power dosimetry on patients with the DBS implant undergoing MRI. Future patients with DBS implants may profit from the proposed virtual patient by allowing for a MRI investigation instead of more invasive Computed Tomography (CT) scans. The virtual patient will be flexible and morphable to relate to neurological and psychiatric conditions such as Obsessive Compulsive Disorder (OCD), which benefit from DBS.**

Keywords-virtual patient simulator; VPS; deep brain brain stimulation; DBS; obsessive compulsive disorder; OCD; MRI; CT; MRI safety; specific absorption rate; SAR; connectome; 7 Tesla MRI

I. INTRODUCTION

A. MRI safety in Deep Brain Stimulation (DBS)

Many DBS patients will require regular MRI examinations throughout the course of their lives since MRI is often the diagnostic tool of choice for monitoring structural changes in the brain. Because of safety concerns to the patients approximately 300,000 people per year are denied MRI and the associated health implants such as Implantable Cardioverter Defibrillator (ICD) and DBS leads as well as guide wires and catheters. One of the main concerns of use of MRI for DBS implants is related to potential RF – heating [1]. The Radiofrequency (RF) waves used in MRI to elicit signal from the brain tissue interact with the conductive leads generating potentially high induced currents ("antenna effect") and related increased RF power deposition at the tip of the leads [2]. Several cases of permanent neurological injury were recently reported [3]. The conditions in which currently DBS are indicated for MRI are extremely restrictive. In these patients it is only possible to image with head coils, so that any other part of the body is contraindicated. Also, only transmit-receive heads coil are indicated and the current state-of-the-art MRI receive coils multichannel coils are completely contraindicated. In the near future, the use of MR imaging in these patients will become more and more problematic following the manufacturer guidelines. This is of the upmost importance for the 300,000 people who are denied MRI.

B. Lack of a gold standard DBS Virtual Patient Simulator (VPS)

The state-of-the-art numerical DBS modeling is based on a wire or set of wires, which represents the virtual DBS implant, superimposed to healthy human brains [4]. Several numerical models for electromagnetic analysis of DBS have been proposed [5-9]; however they are incomplete since they do not take in consideration an accurate anatomical modeling of the structures involved in the stimulation, anisotropic dielectric constants, information about head perfusion and the tissue scar from the surgery. Therefore, we need knowledge about the i) anatomy, ii) conductivity and permittivity along x, y, z, iii) blood vessels and iv) encapsulating tissue around the electrodes.

C. Importance of structural MRI-based modeling

The Ventral Capsule/Ventral Striatum (VC/VS) in the Anterior Limb of the Internal Capsule (ALIC, which is approximately 20 mm long in its dorsoventral extension and 2-5 mm wide mediolaterally at the coronal sections where the nucleus accumbens is present) is currently a target for DBS in Obsessive-Compulsive Disorder (OCD) (Medtronic, Minneapolis, MN) (Fig.1). Importantly, a small structure within this large territory, namely the ventromedial Prefrontal-Basal Ganglia (vmPFC-BG) tract is thought to be a more specific target for this procedure in OCD. The latter is a relatively small fiber bundle, of about 2 mm diameter, which courses approximately 4-5 mm above the nucleus accumbens interconnecting ventral prefrontal cortex with basal ganglia [10].

D. Importance of Connectome-based modeling

Anisotropy of electrical properties of tissue arises in nerve and muscle fibers which consist of bundles of long, parallel myelinated elements. Diffusion Tensor Imaging

 ISBN: 978-1-61208-340-7

(DTI) data will be used to model tissue anisotropic conductivity. In general, we will convert the acquired diffusion tensor **D** into a complex relative permittivity tensor ε* using a simple linear transform $\boldsymbol{\varepsilon}^* = \frac{\varepsilon^*}{d} \cdot \mathbf{D}$ where ε* is the tissue complex relative permittivity [11] and d is the diffusivity. Our preliminary data (Fig. 1B) show that Connectome MRI data (voxel size: 2 × 2 × 2 mm^3) could be reliable in identifying the fiber tracks connecting vmPFC and BG. The gradient strength determines the sensitivity, accuracy, and resolution of diffusion imaging. The connectome MRI is a new scanner purpose-built for diffusion MRI with ultra-high gradients of 300 mT m^{-1}, more than three times stronger than any previously achieved in human subjects. The new Connectome scanner at the A. A. Martinos Center has reduced read out time , increased time-efficiency, and improved structural resolution with reduced diffusion time. Recent data show that this technology allows for enhanced sensitivity and resolution of white matter imaging and MRI tractography of 5-10 fold over any other human DTI or High-Angular Resolution Diffusion Imaging (HARDI) such as the Diffusion Spectrum Imaging (DSI) technology. We will be generating fiber tracks by using spatial information derived from high spatial resolution ex-vivo diffusion imaging (voxel size: 100 μm isotropic). Finally, VPS with DBS have been proposed for real time MRI surgical guidance, we propose to develop a post-operative VPS tool for safe MRI.

E. Importance of Computed Tomography Angiography (CTA)-based modeling

Heat transport in biological tissues, which is usually expressed by the Pennes bio-heat equation, is a complicated process since it involves thermal conduction in tissues, convection and perfusion of blood (delivery of the arterial blood to a capillary bed in tissues). We propose to model the heat transfer from the blood to the tissue (q_p) in the Pennes bio-heat equation as a term proportional to the temperature difference between the arterial blood entering the tissue and the venous blood leaving the tissue. A total of continuous 15 minutes exposure to heating may result reversible thermal lesions occur at 42–44°C, and irreversible lesions occur at temperatures greater than 45°C. At higher temperatures, the thermal damage depends on both the temperature levels and the time of exposure. Since ex-vivo CTA is a standard tool in micro vasculature modeling, we will use CTA with contrast agents containing large barium or iodine particles to elucidate vascular tissues in 3D.

F. Importance of Tissue Scaring around the DBS Electrode

Chronically implanted recording electrodes provoke an immune reaction against them. The histopathological finding is that of gliosis and spongiosis around the electrode track, which forms an encapsulation layer referred to as the "glial scar". This reactive glial tissue which surrounds the implanted electrodes is approximately 200 μm thick and progressively isolated the electrode from surrounding neurons modifying the electric field and acts as a natural neuro protector against heating of the electrode tips. We will model the conductivity and permittivity of the scar tissue at the frequency of interest (124 MHz). The scar tissue will affect the bio-heat modeling behaving as a thermal insulating shield, thus improving the accuracy of the model.

G. Impact of the new RF pulse

The issue of heating of implants during MRI has been studied [12] and analytical solutions (Green's function) to the problem have been proposed for simple geometries. Modifications of the implant leads and wires for reducing the RF-induced heating have been proposed introducing chokes or special geometrical paths of the wire. However, all of these leads design modifications may be not appropriate for patients who already have DBS implants, since replacing the original leads with these modified safer leads requires major brain surgery. Since the heating due to conductive wires depends on the phase distribution of the MRI transmit field, the modification of the transmit field to minimize the electric field in and around the implant to minimize the RF pickup of the DBS wire is critical.

II. METHODS

A. Overview of study design

The study is based on *ex-vivo* analysis of collected 7 Tesla (7T) T2* and Connectome diffusion MRI data.

(a) <u>*Structural T2* 7 Tesla MRI*</u> The model is generated by segmenting 21 different brain structural entities on the *ex-vivo* structural MRI, as well as 28 non-brain structural entities following the approach described in Makris and colleagues [13]. This *ex-vivo* brain consisted of MRI data of a hemisphere fixed in Periodate-Lysine-Paraformaldehyde (PLP) using the following parameters: T2*-W, 100 μm^3 isotropic resolution, TR/TE/flip=40ms/20ms/20°, 1600×1100×896 matrix. Segmentation of OCD-DBS target-related cerebral structures, specifically the putamen, caudate nucleus, nucleus accumbens and anterior limb of the internal capsule were manually outlined (on a re-sampled dataset at 1 mm isotropic spatial resolution of the original *ex-vivo* high-resolution (100 μm^3 isotropic resolution) dataset acquired at 7 Tesa) using the segmentation methods by Filipek [14] and Makris [15], which have been developed and validated at the MGH Center for Morphometric Analysis, and have been implemented in several clinical studies (Fig. 1A). The VC/VS in the ALIC is currently a target for DBS in OCD (Medtronic). Importantly, a structure within this large territory, namely the vmPFC-BG tract is thought to be a more specific target for this procedure in OCD. This is a relatively small fiber bundle, however, by reaping the benefits of the high-resolution dataset, we will segment the ALIC/VS as follows. The anterior limb of the internal capsule is delimited medially by the head of the caudate nucleus, laterally by the putamen and ventrally by

the nucleus accumbens. These structures were delineated by direct visualization using intensity-based contours in the Cardviews software system). *(b) Connectome DSI data* are transformed into DTI data to estimate complex relative permittivity tensor $\hat{\varepsilon}^* = \frac{\varepsilon^*}{d} \cdot \mathbf{D}$, introduced above. The vmPFC-BG tract is delineated using diffusion Connectome data as shown in Fig. 1B. DTI/DSI data are visually validated by comparing the computed fiber tracks with since the VPS is meant to be used for 3T scanners with head transmit birdcage coil, where the quasi-static approximation applies. Finally, the simulations are tested by following the same procedure for the published CHEMA model [4] and running the FDTD simulations described in this paragraph. This data are then resampled at 1mm^3 and compared with our published results and [4] only if the error of the 10g - averaged SAR data is within 20% the test is considered passed.

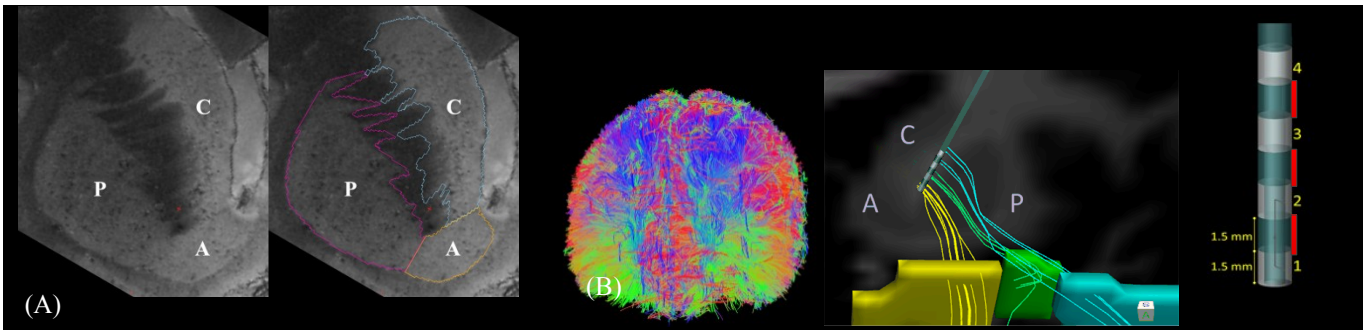

Fig. 1. (A) *Coronal section at the C.A.P. (Caudate-Accumbens-Putamen) level of a 7T high-resolution (100 µm3 isotropic) ex-vivo human dataset showing detailed anatomy of the VC/VS target area (cross-hair in red) within the anterior limb of the internal capsule.* ***(B) :*** *(left) DSI connectome data set, (middle) electrode placement in the VC/VS target area traversed by fibers (yellow fibers) of the ventromedial prefrontal-basal ganglia tract at the C.A.P. coronal slice. The latter fibers stem from the ventromedial prefrontal area (yellow block). (A=nucleus accumbens, C=caudate nucleus, P=putamen), and (right) electrode geometry with the proposed embedded thin solid state temperature sensor film (red).*

anatomical atlases with particular emphasis to the basal ganglia region as shown in Fig. 1A. Finally, DTI/DSI data provide detailed information on the fiber tract connectivity between the ventromedial prefrontal cortex and basal ganglia that is useful for DBS programming [16] and basic neuroscience research.

B. Numerical Model of Deep Brain Stimulation implant

One or two bilateral implants, as shown by the post-operative MRI, are modeled as insulated wire(s) connected to the left and/or right targets in the head [3]. The wires are modeled as a Perfect Electrical Conductor (PEC) and the dielectric is modeled as Teflon. A four-electrode connection [16] and the scar tissue are modeled in full detail reaping the benefits of the proposed 100 µm^3 isotropic resolution based on the actual Medtronic electrode set that will be used. The four electrodes are modeled as PEC and the scar tissue is modeled with the known dielectric properties. We model only the head without the shoulders,

III. RESULTS

Our preliminary results are principally in identification and segmentation of the OCD target structures for DBS using high-resolution T2*-W and diffusion spectrum MRI data and electromagnetic simulations for MRI safety. Given that this is work in progress our pilot data provide a basis for validation and completion of the VPS database.

In Fig. 1 (A and B), we show data from a manual segmentation procedure to outline the different anatomical structures related to the VC/VS target area derived from a high-resolution 7 Tesla dataset and DSI-based tractography. In Fig. 2, we present a geometrical model of the coil array and the VPS model [13] with examples of different parallel transmit excitation phases and the resulting B_1 maps (nT/ampere) [18].

IV. DISCUSSION

Clinical work in obsessive-compulsive disorder (OCD) indicates that several compulsive behaviors in this disorder

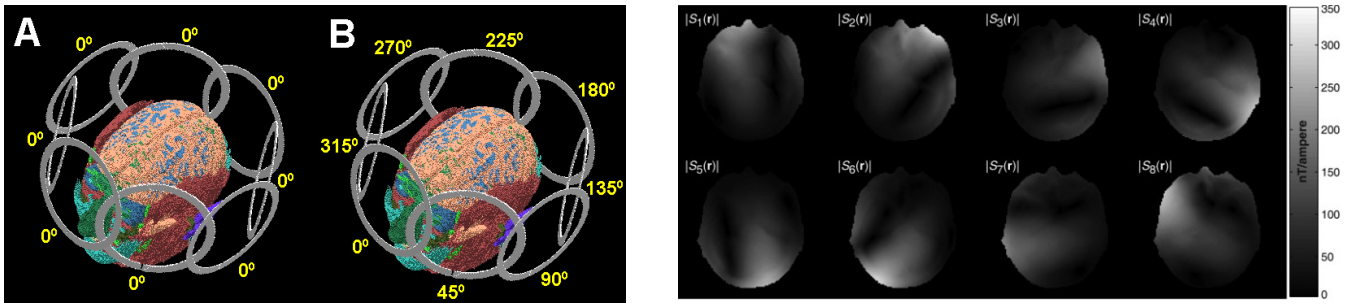

Fig. 2 (Left) Geometrical model of the coil array and our model [13] with examples of null (A) and uniform (B) $\vec{\varphi}$ vectors [17]. (Right) 8-channel transmit phase array FDTD B_1 maps (nT/ampere) of the center transverse slice of our model when each channel is driven with a 1-ampere peak-to-peak 300-MHz sinusoid [18].

 ISBN: 978-1-61208-340-7

are related to avoidance of putative dangerous situations. The neural system that mediates avoidance is the same one that also underlies reward-seeking and comprises (anterior cingulate/orbital)-Basal-Ganglia (BG) connections. DBS is a therapeutic procedure aiming to change activity in fronto-basal ganglia circuits by injecting electrical stimulation in the Ventral Anterior Internal Capsule (VA-ALIC) and adjacent Ventral Striatum (VS), i.e., nucleus accumbens septi. In many OCD patients the benefits of DBS as a therapy outweighs the risks of surgery. However, there have been reports of serious accidents associated with magnetic resonance imaging (MRI)-related heating [3]. OCD patients with DBS would benefit from regular MRI examinations, as MRI is often the diagnostic tool of choice to diagnose injury due to trauma or evaluate comorbidities (e.g., stroke, cancer, etc.). The Food and Drug Administration (FDA) has approved the use of DBS leads by restricting the use to transmit head only coils and fields up to 1.5 Tesla. However, excluding the use of 3 Tesla systems severely limits MRI as a diagnostic tool. There are over 75,000 patients with DBS implants worldwide and only approximately one patient in twenty is assessed with (FDA restricted) MRI. In this pilot study investigating the VPS application in patients with DBS implants we gathered preliminary results on the anatomical characterization of the OCD target structures for DBS using high-resolution 7 Tesla and Connectome MRI data and performed electromagnetic simulations for MRI safety. VPS are realistic computerized human models that allow medical-device companies to test new products earlier, helping the devices get to market more quickly and cheaply according to the FDA. We envision that the proposed new OCD VPS will enable radio frequency (RF) power dosimetry on patients with DBS implants undergoing MRI. Based on VPS dosimetry, we will be able to modify ad hoc the MRI parameters to allow for MRI acquisition on patients with DBS implants in situ. Future OCD patients with DBS implants may profit from the proposed VPS by allowing for a MRI investigation instead of more invasive computerized tomography (CT) scans.

ACKNOWLEDGMENT

National Institute of Health, National Institute of Biomedical Imaging and Bioengineering 1R21EB016449-01A1.

REFERENCES

[1] C. K. Chou, J. A. McDougall, and K. W. Chan, "RF heating of implanted spinal fusion stimulator during magnetic resonance imaging," *IEEE Trans Biomed Eng,* vol. 44, pp. 367-73, May 1997.

[2] L. M. Angelone, A. Potthast, F. Segonne, S. Iwaki, J. W. Belliveau, and G. Bonmassar, "Metallic electrodes and leads in simultaneous EEG-MRI: specific absorption rate (SAR) simulation studies," *Bioelectromagnetics,* vol. 25, pp. 285-95, May 2004.

[3] J. M. Henderson, J. Tkach, M. Phillips, K. Baker, F. G. Shellock, and A. R. Rezai, "Permanent neurological deficit related to magnetic resonance imaging in a patient with implanted deep brain stimulation electrodes for Parkinson's disease: case report," *Neurosurgery,* vol. 57, p. E1063; discussion E1063, Nov 2005.

[4] L. Angelone, J. Ahveninen, J. Belliveau, and G. Bonmassar, "Analysis of the Role of Lead Resistivity in Specific Absorption Rate for Deep Brain Stimulator Leads at 3 T MRI," *IEEE Trans Med Imaging,* vol. 29, pp. 1029-38, Mar 22 2010.

[5] M. Oliveri, G. Koch, S. Torriero, and C. Caltagirone, "Increased facilitation of the primary motor cortex following 1 Hz repetitive transcranial magnetic stimulation of the contralateral cerebellum in normal humans," *Neurosci Lett,* vol. 376, pp. 188-93, Mar 16 2005.

[6] C. R. Merritt, H. T. Nagle, and E. Grant, "Fabric-Based Active Electrode Design and Fabrication for Health Monitoring Clothing," *Information Technology in Biomedicine, IEEE Transactions on,* vol. 13, pp. 274-280, 2009.

[7] C. R. Butson, S. E. Cooper, J. M. Henderson, and C. C. McIntyre, "Patient-specific analysis of the volume of tissue activated during deep brain stimulation," *Neuroimage,* vol. 34, pp. 661-70, Jan 15 2007.

[8] M. Seyal, A. J. Shatzel, and S. P. Richardson, "Crossed inhibition of sensory cortex by 0.3 Hz transcranial magnetic stimulation of motor cortex," *J Clin Neurophysiol,* vol. 22, pp. 418-21, Dec 2005.

[9] F. Tyc, A. Boyadjian, and H. Devanne, "Motor cortex plasticity induced by extensive training revealed by transcranial magnetic stimulation in human," *Eur J Neurosci,* vol. 21, pp. 259-66, Jan 2005.

[10] J. F. Lehman, B. D. Greenberg, C. C. McIntyre, S. A. Rasmussen, and S. N. Haber, "Rules ventral prefrontal cortical axons use to reach their targets: implications for diffusion tensor imaging tractography and deep brain stimulation for psychiatric illness," *J Neurosci,* vol. 31, pp. 10392-402, Jul 13 2011.

[11] C. Gabriel, S. Gabriel, and E. Corthout, "The dielectric properties of biological tissues: III. Parametric models for the dielectric spectrum of tissues," *Phys. Med. Biol.,* vol. 41, pp. 2271–2293, 1996.

[12] C. K. Chou, H. Bassen, J. Osepchuk, Q. Balzano, R. Petersen, M. Meltz, R. Cleveland, J. C. Lin, and L. Heynick, "Radio frequency electromagnetic exposure: tutorial review on experimental dosimetry," *Bioelectromagnetics,* vol. 17, pp. 195-208, 1996.

[13] N. Makris, L. Angelone, S. Tulloch, S. Sorg, D. Kennedy, and G. Bonmassar, "MRI-based anatomical model of the human head for specific absorption rate (SAR) mapping," *Med Biol Eng Comput,* vol. 46, pp. 1239-51, 2008.

[14] P. A. Filipek, C. Richelme, D. N. Kennedy, and V. S. Caviness, Jr., "The young adult human brain: an MRI-based morphometric analysis," *Cereb Cortex,* vol. 4, pp. 344-60, Jul-Aug 1994.

[15] N. Makris, J. W. Meyer, J. F. Bates, E. H. Yeterian, D. N. Kennedy, and V. S. Caviness, "MRI-Based topographic parcellation of human cerebral white matter and nuclei II. Rationale and applications with systematics of cerebral connectivity," *Neuroimage,* vol. 9, pp. 18-45, 1999.

[16] T. Eichele, S. Debener, V. D. Calhoun, K. Specht, A. K. Engel, K. Hugdahl, D. Y. von Cramon, and M. Ullsperger, "Prediction of human errors by maladaptive changes in event-related brain networks," *Proc Natl Acad Sci U S A,* vol. 105, pp. 6173-8, Apr 22 2008.

[17] L. M. Angelone, N. Makris, C. E. Vasios, L. Wald, and G. Bonmassar, "Effect of transmit array phase relationship on local Specific Absorption Rate (SAR)." in *ISMRM Fourteenth Scientific Meeting*, Seattle, USA, 2006.

[18] A. C. Zelinski, L. M. Angelone, V. K. Goyal, G. Bonmassar, E. Adalsteinsson, and L. L. Wald, "Specific absorption rate studies of the parallel transmission of inner-volume excitations at 7T," *J Magn Reson Imaging,* vol. 28, pp. 1005-18, Oct 2008.

 ISBN: 978-1-61208-340-7

System for Evaluation of Cognitive Performance under the Emotional Stressors

Kresimir Cosic, Siniša Popović, Bernard Kovač, Davor Kukolja
University of Zagreb Faculty of Electrical Engineering and Computing
Zagreb, Croatia
kresimir.cosic@fer.hr, sinisa.popovic@fer.hr, bernard.kovac@fer.hr, davor.kukolja@fer.hr

Dragutin Ivanec
University of Zagreb Faculty of Humanities and Social Sciences
Zagreb, Croatia
divanec@ffzg.hr

Tanja Jovanovic
Emory University School of Medicine
Atlanta, GA, USA
tjovano@emory.edu

***Abstract*—It is well known that emotional stressors may have adverse effects on cognitive-motor performance. The system for evaluation of cognitive-emotional interactions, described in this paper, is based on real-time interplay between a selected cognitive task and selected emotional stressors, and may facilitate insight into an individual's variation of cognitive and emotional parameters and variables. To illustrate the effects of emotional distraction on cognitive-motor performance, specific cognitive-motor test has been designed and combined with aversive highly arousing emotional distractions, including pictures, sounds, acoustic startle impulses and air blasts, while measuring multimodal physiological, vocal, facial, and electroencephalography (EEG) responses. Preliminary two-phase experimental paradigm has been conducted: Phase 1 – cognitive-motor performance testing with neutral distractions, and Phase 2 – cognitive-motor performance testing under aversive highly arousing emotional distractions. Aversive emotional distractions delivered in Phase 2 transiently reduced cognitive-motor performance and produced stronger skin conductance changes in comparison to Phase 1 neutral distractions.**

Keywords-cognitive-emotional interactions; cognitive performance; emotional distractions; cognitive-motor test; multimodal physiological, vocal, facial, and EEG responses.

I. INTRODUCTION

It is well known that emotional stressors may have harmful and damaging effects on cognitive-motor performance. While some individuals are resilient, others are extremely vulnerable to such emotional disturbances. Cognitive-emotional interactions are mediated by functional connectivity between the PreFrontal Cortex (PFC) and limbic dynamic neural networks, which shape behavior [1][2][3][4]. The amygdala as the emotional hub is extensively interconnected with the PFC, especially the posterior OrbitoFrontal Cortex (OFC), and the Anterior Cingulate Cortex (ACC). The influence of emotional distractors and stressors on cognitive capacities is challenging to study due to the complexity of interconnection and interaction PFC and limbic neural networks that mediate cognitive-emotional interactions. Protective higher-order cognitive performance within an emotionally stressful environment is extremely important for individual judgment, reasoning, decision making and maintaining cognitive abilities in psychologically demanding environments. Therefore, this paper presents the design and implementation of a synthetic experimental environment for assessment of individual cognitive-motor performance under stressful emotional distractions. Real-time monitoring of individual cognitive-motor performance based on appropriate cognitive metrics, real-time generation of emotional distractions and measurements of the individual's multimodal physiological, EEG, vocal and facial responses enable real-time tracking of individual cognitive-emotional interaction. Such real-time tracking of cognitive and emotional performance over time can be used as a predictor of individual cognitive deficits prior to a negative impact of hard emotional stressors on strategic decision-making failures. Identification and recognition of individuals with a low level of emotional stability and robustness is very important to avoid the negative impact of reduced higher-order cognitive capacities, such as judgment, planning, and attention on effective decision-making. Therefore, the prediction of individual cognitive performance within stressful environments, which may significantly reduce their cognitive performance, is of foremost importance.

Section 2 describes the technical aspect of the system used for evaluation of cognitive-emotional interactions. The proposed novel computerized testing of subject's cognitive-motor performance, as well as the corresponding cognitive-motor performance metrics is introduced in Section 3. The process of generation of emotional distractions and measurement of their impact on subject's physiological, acoustic, facial and EEG reaction is shown in Section 4. Section 5 describes the experimental paradigm and preliminary results conducted using the proposed system. The last section gives a brief overview of experimental results.

 ISBN: 978-1-61208-340-7

II. SYSTEM FOR EVALUATION OF COGNITIVE-EMOTIONAL INTERACTIONS

The system for evaluation of cognitive-emotional interactions is shown in Figure 1, which is based on real-time interplay between a selected cognitive task and selected emotional stressor, and enables better and deeper real-time insight into an individual's variation of cognitive and emotional parameters and variables.

As shown in Figure 1, it can be divided into three subsystems:

1. Cognitive-motor subsystem for generation and delivering of a variety of cognitive tasks and evaluation of cognitive-motor performance such as motor reaction time, tracking accuracy, latency, inhibition of distractions, recovery time, etc.
2. Emotional subsystem for generating of emotional distractors like images, sounds, narratives, stories, video clips, acoustic startle, air blast, etc.
3. Multimodal acquisition subsystem for monitoring subject's physiological, acoustic, linguistic, facial and EEG features, etc.

Multimodal acquisition subsystem include: Biopac MP150 unit with ECG100C, RSP100C, EMG100C, GSR100C and SKT100C modules for physiology acquisition; voice acquisition system headset Sennheiser PC 360; video acquisition system Logitech C920 webcam; and EEG acquisition system NeuroSky ThinkGear AM. The air blast delivery module [5][6] includes Messer air tank, solenoid valve, camelback with nozzle attached to hose and solenoid controller. The 140 p.s.i. air blast is triggered by Measurement Computing DIO24 PCI Card, which is also used for synchronization of cognitive-motor, emotional and multimodal acquisition subsystem. The acoustic startle module generates 108 dB (A) Sound Pressure Level (SPL) 40-msec white noise bursts with 0-msec rise and fall times, which are delivered by a Samson headphone amplifier and Sennheiser PC 360 professional audio headphones. Aggregated longitudinal real-time analysis of cognitive-motor and emotional performance offers considerable potential in deeper and better understanding of a specific individual's cognitive-emotional strengths or weaknesses and enables comprehensive training and selection.

III. COMPUTERIZED COGNITIVE TESTING

Cognitive-motor performance in a complex, dynamically changing environment in which emotional and cognitive processes continuously influence each other depends on an individual's perception, reasoning, feeling, and action tendencies. The system shown in Figure 1 can facilitate a variety of cognitive, motor and neuropsychological tests that have their own metrics for evaluation of specific aspects of an individual's higher cognitive-motor competencies and functions in stressful environments. The human abilities of reasoning, thinking, analyzing and problem solving as valid measures of individual performance are widely recognized as excellent predictors of job performance. But, such approach could not capture and predict cognitive competencies and cognitive-motor performance within stressful emotional environments. Therefore, this paper describes the design and testing of an experimental testbed where subjects are faced with a complex set of cognitive tasks and conditions as well as a variety of environmental emotional distractors.

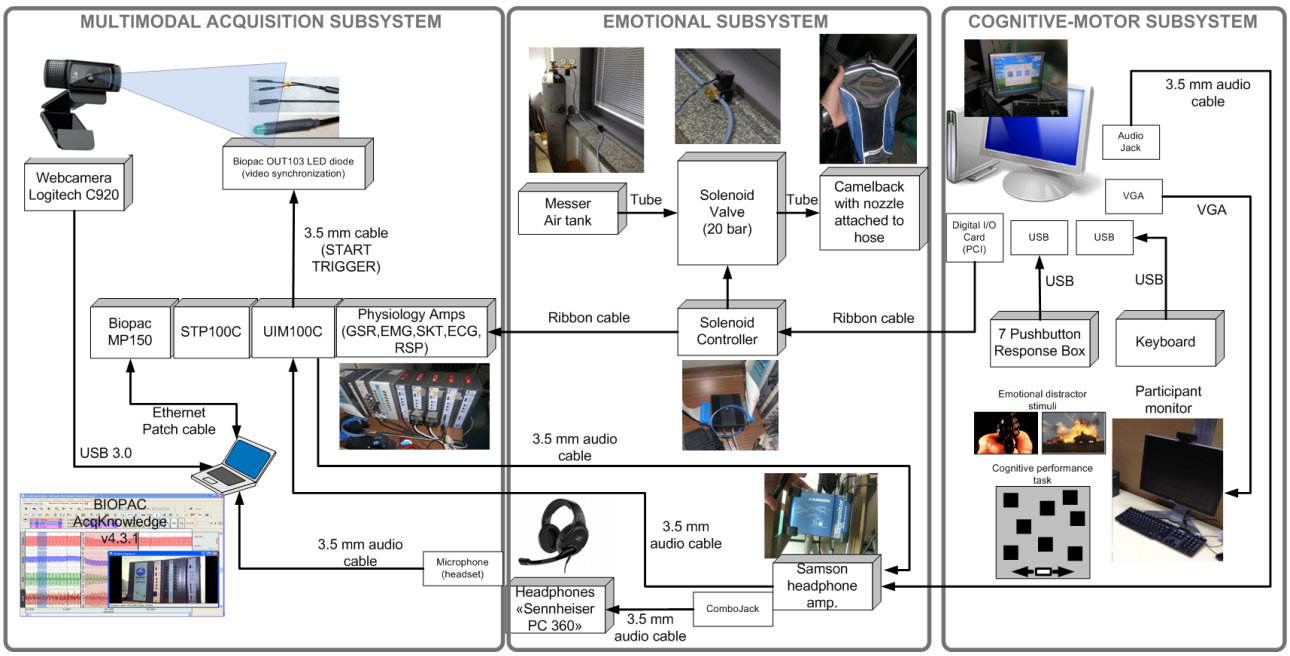

Figure 1. Block diagram of the system for evaluation of cognitive-emotional interactions

Cognitive performance might be related to: fluid reasoning as mental operations for solving novel problems; spatial ability as the ability to generate, retain, retrieve and transform visual images, including spatial visualization and spatial orientation; situation awareness as a mental process of knowing what is going on around you and is closely related to the accuracy and completeness of situation awareness, which imposes a heavy demand on working memory; executive function related to planning and organization, initiation and inhibition of behavior, strategizing, problem solving, flexible thought processes, behavior monitoring, self-awareness, and judgment [7]. Real-time measurements of all these individual's cognitive-motor abilities in a rapidly changing complex and stressful environment deserve more attention.

To illustrate the effects of emotional distraction on cognitive-motor performance the following cognitive-motor test has been designed as a computer game displayed on the computer screen, in which the subject's task is to avoid collisions with falling objects. The subject uses two buttons on the response pad to evade the falling objects by moving left or right. In this example the cognitive effectiveness of the individual could be studied and measured by correctly headings cursor surface to effectively engage joystick pads through dynamically moving obstacle surfaces. The cognitive-motor test is used in two phases of experimental paradigm: in Phase 1 the test is delivered to the subjects mixed with emotionally neutral distractions, while in Phase 2 the test is mixed with fear-related emotional distractions and stressors, which are described in the next section. Before Phase 1, there is practice session to stabilize the subject's performance on this test when no distractions occur at all. During the game, collision area with falling objects is calculated in real-time, from which cognitive-motor performance can be computed. Development and evaluation of relevant quantitative measures of joystick manipulations enable appraisal of the individual's current skill levels. During the execution of cognitive-motor test, the collision area with falling objects is computed in real-time, as the basis of cognitive-motor performance metric. Configurations of falling objects are randomized, in order to avoid learning effects. However, in order to maintain maximum comparability between subjects, they are exposed to the same order and the same configurations of falling objects.

Cognitive-motor performance in time interval $[t_i, t_i+1]$, which is large enough to smooth the stochastic relationship between cursor surface $CS(t_j)$ and dynamically moving obstacle surfaces $OS(t_j)$, can be defined based on intersection areas:

$$CP(t_i, t_{i+1}) = 1 - \frac{\sum_{t_i \le t_j < t_{i+1}} \text{area}(CS(t_j) \cap OS(t_j))}{\sum_{t_i \le t_j < t_{i+1}} \min[\max_{o \in OS(t_j)}(\text{area}(o \cap CSZone)), \text{area}(CS(t_j))]} \quad (1)$$

which measures the ratio of the subject's cumulative intersection area with falling objects versus the worst possible cumulative intersection area. The worst cumulative intersection area would be achieved if, at each moment t_j, the subject was always in the spot of the falling object, which had the largest intersection with the subject's zone of motion. This computerized cognitive-motor test can be configured flexibly with different levels of difficulty, in order to avoid floor or ceiling effects on performance.

IV. EMOTIONAL DISTRACTIONS GENERATION AND MEASUREMENT

Multimodal emotional elicitation [8] includes a variety of audio and visual stimuli like images, video clips, multimedia picture databases with universal facial expressions like NimStim Face Stimulus Set [9], International Affective Picture System (IAPS) [10], natural and manmade sounds, International Affective Digitized Sounds (IADS) [11], recorded speech, written text messages, virtual reality synthetic environments, spoken narratives, stories, face-to-face conversation, acoustic startle, air blast, fear conditioning/fear extinction paradigm, etc. Sounds and suitable narratives can be played and read along the visual stimuli enhancing the effects of the pictures and thereby taking full advantage of the multimodal emotion elicitation paradigm. As specific multimodal composite stimuli to enhance arousal level during emotion distraction we include highly arousing aversive IAPS video images and IADS sounds, in combination with 40 ms acoustic impulses of 108 dB (A) SPL broadband noise and 250 ms 140 p.s.i. air blasts startle delivered to the subject's larynx. Additional aversive stimuli include a 500-ms electric shock ranging from 0.5 to 5.0 mA, delivered through electrodes attached to the fourth finger of the non-dominant hand, which can be selected to be highly irritating but not painful. The goal of multimodal emotion elicitation is to provide a variety of stimuli, which are capable of eliciting broadband emotional distractions to analyze the subject's vulnerabilities related to the decline of specific cognitive performance due to deficits in attention, anticipation, speed of motor reactions, etc. Cognitive-emotional interactions can be measured by cognitive task performance and multimodal bodily physiological and motor reactions, as well as subjective feelings.

Estimation of elicited emotion is based on data fusion of *Physiological-Features(t)*, *Vocal-Features(t)*, *Facial-Features(t)* and *EEG-Features(t)* extracted from individual's physiological, facial, speech, and EEG signals [12] (Figure 2). *Physiological-Features(t)* include: $F_{HR,mean}$ heart rate mean value, $F_{HR,std}$ heart rate standard deviation, $F_{SC,mean}$ skin conductance mean value, $F_{SC,std}$ skin conductance standard deviation, LF/HF low frequency/high frequency ratio (heart rate variability measure), $F_{SCR,freq}$ frequency of SCRs and $F_{SCR,mag}$ mean magnitude of SCRs, etc. Altogether, over three hundred physiological features can be computed from the acquired signals [13]. *Vocal-Features(t)* include: F_{T,kw_vec} keyword vector, $F_{E,std}$ standard deviation of a speech signal energy, $F_{P,jitt}$ jitter of a pitch frequency contour, $F_{S,F1\_bw\_mean}$ mean value of a first formant bandwidth and $F_{ZCR,mean}$ mean value of a zero cross rate, etc. More than four hundred vocal

features can be computed [14]. *Facial-Features(t)* include: F_{MW} mouth width, F_{MH} mouth height, F_{REW} right eye width, F_{REH} right eye height, F_{LEW} left eye width, F_{LEH} left eye height of the current facial expression, etc. *EEG-Features(t)* include: *alphaPSD* power spectral density of frequency band alpha (8-12 Hz), *betaPSD* power spectral density of frequency band beta (12-30 Hz), *gammaPSD* power spectral density of frequency band gamma (30-100 Hz), etc., *sig_avg* average EEG signal value, *sig_max* maximal value of EEG signal, etc. [15].

Based on this set of multimodal features it is also possible to estimate the individual's discrete emotions, e.g., fear intensity, happiness, sadness, disgust, or intensity of valence and/or arousal [16] and current level of perceived stress (e.g., see [9][17]).

For illustration, acoustic startle, which induces muscle contractions can be detected by orbicularis oculi electromyography (EMG) response and can be computed by

$$F_{EMG,mean} = \frac{1}{N}\sum_{i=0}^{N} EMG(t_{noise\_onset} + 20ms + i\cdot\Delta T),\ \text{where } N\cdot\Delta T = 180ms \quad (2)$$

Equation (2) represents the mean level of the orbicularis oculi EMG response in the period of 20–200 ms after the onset of the white noise burst, during any high-threat aversive time interval in Phase 2. The obtained EMG signal is acquired at 1 kHz, and rectified and smoothed by a moving average of 10 data points.

Skin conductance features during each high-threat aversive time interval $[t_i, t_i+k\Delta T]$ of Phase 2 are computed by

$$F_{SC,diff\_mm} = \max(\overline{SC}(t_i, t_i + k\Delta T)) - \min(\overline{SC}(t_i, t_i + k\Delta T)) \quad (3)$$

where $\overline{SC}$ represents normalized skin conductance signal and $k\Delta T$ is the duration of any high-threat aversive time interval.

Heart rate features during each high-threat aversive time interval $[t_i, t_i+k\Delta T]$ of Phase 2 are computed by

$$F_{HR,max\_offset} = \max(HR(t_i, t_i + k\Delta T)) - \text{mean}(HR(t_i - k\Delta T, t_i)) \quad (4)$$

where HR represents the values acquired by measurement during high-threat aversive time intervals of Phase 2. The features like $F_{EMG,mean}$, $F_{SC,diff\_mm}$, and F_{HR,max_offset} can be appropriately combined and integrated as a single physiological measure. Aggregated fluctuations in emotional distraction multimodal metrics are computed by:

$$EMR(t_i, t_{i+1}) = f(F_{EMG,mean}, F_{SC,diff\_mm}, F_{HR,max\_offset}, ...) \quad (5)$$

where f is some function that aggregates all emotional multimodal response features.

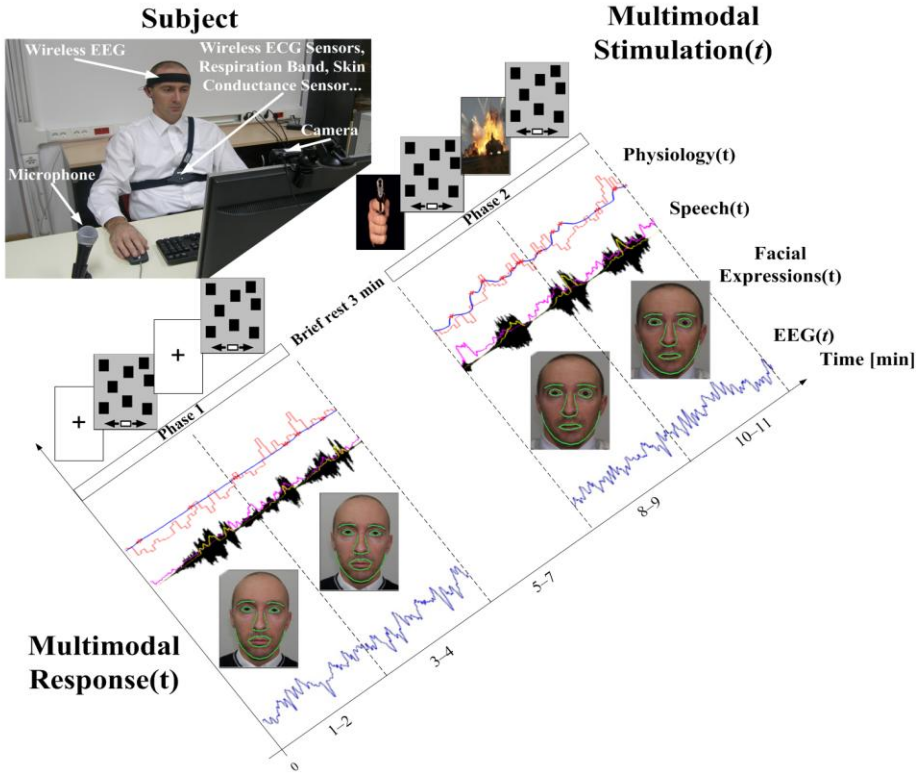

Figure 2. Illustration of multimodal measurements of subject's response based on physiology, speech, facial and EEG signals.

 ISBN: 978-1-61208-340-7

V. EXPERIMENTAL PARADIGM AND RESULTS

To develop cognitive performance predictive models as specific indicators of individual effective performance we need quantifiable variables and metrics to systematically evaluate cognitive performance within environments characterized with a variety of specific emotional distractors. A methodology for evaluation of the degradation of cognitive-motor performance will be presented, including metrics of cognitive-motor tasks, metrics of emotional response, as well as metrics of combined cognitive-motor-emotional interaction. Evaluation of cognitive-motor metrics under emotional distraction might be used as a measure of individual cognitive resilience within stressful environment, like high individual situational awareness, cognitive orientation, focused attention and situational assessment, etc. under the influence of environmental emotional noise. Such an approach enables evaluation and better understanding of complex higher-order cognitive processes and emotional vulnerability as well as better prediction of individual behavioral performance.

For evaluation and selection of resilient or vulnerable subjects in the presented cognitive-motor-emotional game the following metric is introduced:

$$CP_{Phase1} = \sum_{i=-m}^{-m+k} CP(t_i, t_{i+1}) \tag{6}$$

where CP_{Phase1} is cumulative cognitive-motor performance on selected time interval of $k\Delta T$ in Phase 1, and represents aggregated baseline cognitive-motor performance on selected time interval;

$$CP_{Phase2}(t_n) = \sum_{i=n}^{n+k} CP(t_i, t_{i+1}) \tag{7}$$

where CP_{Phase2} is cumulative cognitive-motor performance on selected time interval of $k\Delta T$ in late period of Phase 2;

$$e(t_n) = \left| CP_{Phase1} - CP_{Phase2}(t_n) \right| < \varepsilon_1 \tag{8}$$

where $e(t_n)$ describes cognitive-motor performance difference between baseline value in Phase 1, CP_{Phase1}, and cognitive-motor performance $CP_{Phase2}(t_n)$ in Phase 2. The optimal solution is to fulfill condition (8) in the minimum amount of time $t_n = t_{\min}$, and represents cognitive recovery time $t_{\min}$ in which the subject converges to baseline cognitive-motor performance within ε range.

The cognitive-emotional game can be additionally enhanced by the following condition:

$$EMR_{Phase1} = \sum_{i=-m}^{-m+k} EMR(t_i, t_{i+1})_{Phase1}$$
$$\left| EMR_{Phase1} - \sum_{i=n}^{n+k} EMR(t_i, t_{i+1})_{Phase2} \right| < \varepsilon_2 \tag{9}$$

which represents the mean difference between emotional multimodal response EMR along time interval $k\Delta T$ in Phase 1 and emotional multimodal response along time interval $k\Delta T$ in Phase 2.

The optimal solution of the presented cognitive-emotional game for special tasks or jobs can be given by the Index of Performance (*IP*)

$$IP = t_{\min}, \text{ which satisfies conditions below:}$$
$$\Delta CP = \left| CP_{Phase1} - CP_{Phase2}(t_{\min}) \right| < \varepsilon_1,$$
$$\Delta EMR = \left| EMR_{Phase1} - \sum_{i=n}^{n+k} EMR(t_i, t_{i+1})_{Phase2} \right| < \varepsilon_2 \tag{10}$$

Monitoring cognitive-motor performance variations under stressful stimuli is important for evaluating how each individual copes with different emotional distractors and might be used to assess individual differences to inhibit fearful stimuli and retain higher levels of cognitive function. Prediction of how people will behave in emergency situations and how they perceive and anticipate stressful stimuli may have enormous practical values. Such experimental laboratory infrastructure enables prediction of the individual's cognitive-motor performance in stressful environments and can be used in progress monitoring during mental readiness training and selection of individuals with robust cognitive-motor performance under the stress. Evaluation of cognitive-motor performance degradation due to emotional distractors might be also used to develop predictive models of individual cognitive-motor performance in correlation with intensity of emotional distractors. The supervisor may select specific cognitive tasks and a variety of audio-visual stimuli distractors using the relevant user friendly interface.

The sensitivity analysis concerning the influence of emotional stressors on cognitive-motor performance under the impact of aversive IAPS images, IADS sounds, acoustic startle and air blast in the high-threat period of Phase 2, is shown in Figure 3. The purpose of this experiment is to investigate how emotional distraction affects performance of a cognitive-motor task described in Section 2. For illustration of the discrimination potential of the system, two-phase experimental paradigm has been conducted, as described previously: Phase 1 – cognitive-motor performance testing with neutral distractions, and Phase 2 – cognitive-motor performance testing under high-threat arousing emotional distractions. In Phase 2, aversive IAPS images and IADS sounds enhanced by an acoustic startle and air blast are delivered to the subject.

 ISBN: 978-1-61208-340-7

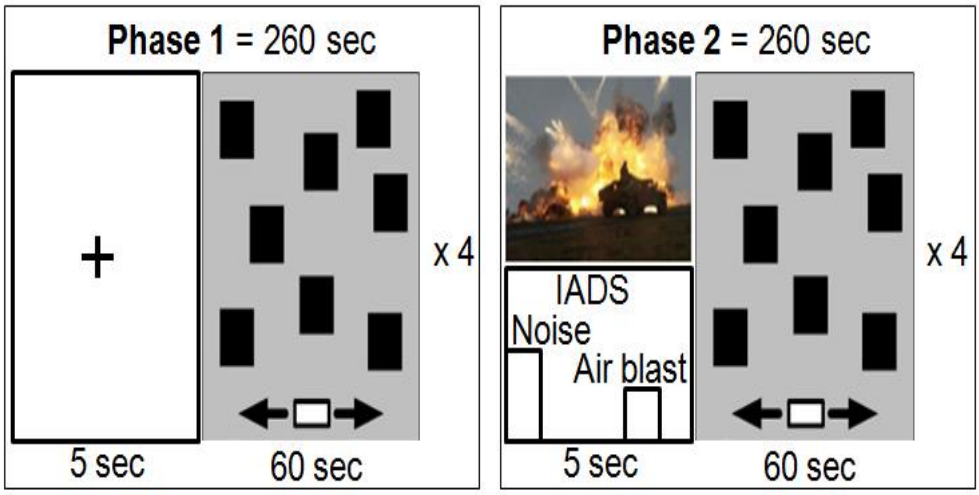

Figure 3. Experimental protocol for evaluation of cognitive-emotional interactions.

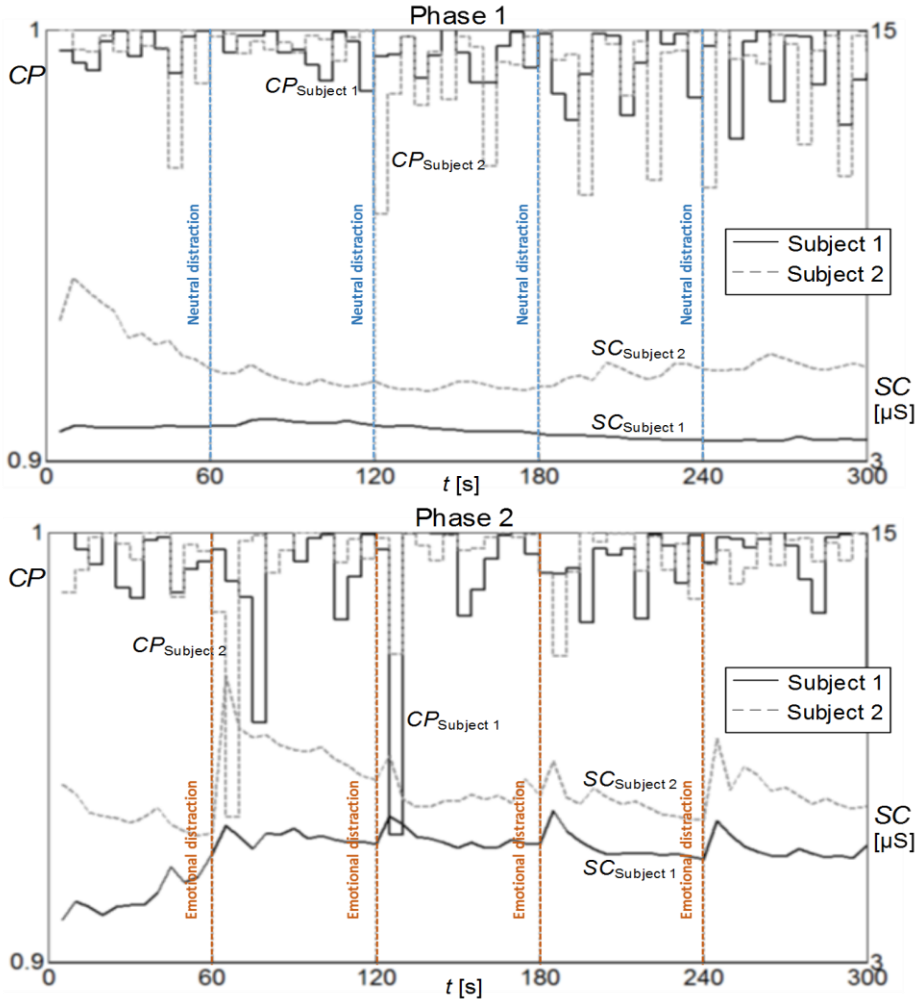

Figure 4. Illustration of experimental results for two subjects, showing their cognitive-motor performance (CP) and corresponding average skin conductance (SC) values in 5-second time intervals, with onsets of Phase 1 neutral distractions and Phase 2 aversive emotional distractions at 60, 120, 180 and 240 seconds.

 ISBN: 978-1-61208-340-7

Figure 4 illustrates that aversive emotional distractions delivered in Phase 2 can transiently reduce cognitive-motor performance relative to neutral distractions, since performance of both subjects decreased after first two emotional stressors at 60 and 120 seconds. Cognitive-motor performance was computed on 5-second intervals according to equation (1). Furthermore, aversive emotional distractions in Phase 2 produced stronger skin conductance changes for both subjects, in comparison with neutral distractions in Phase 1, and these changes were visible after all four emotional distractors. Despite this presence of emotions, the subjects seem to have habituated their cognitive-motor performance on the third and fourth emotional distractor.

Preliminary proof-of-concept testing with two subjects precludes broader statistical analyses, but the results illustrate that designed emotional distractors were able to produce reliable physiological changes, which may also transiently lead to decreased performance on this specific game.

VI. CONCLUSION

In this paper, we presented a computerized system for real-time monitoring of cognitive-emotional interactions. This paper also illustrates an approach to objective measurement of cognitive-motor performance simultaneously with measurements of subject's multimodal physiological, acoustic, facial and EEG response. Preliminary testing on two participants was conducted, which showed transient decrease in cognitive-motor performance induced by various emotional distractors in comparison to neutral distractors. Physiological response measurements also indicated apparent difference in subject's bodily response to emotional distractors in comparison with neutral distractors. The cognitive-emotional interaction in the experimental paradigm was illustrated by inverse relationship between the subject's cognitive-motor performance and physiological, i.e., skin conductance response.

REFERENCES

[1] E. R. Kandel, J. H. Schwartz, T. M. Jessell, S. A. Siegelbaum, and A. J. Hudspeth, Principles of Neural Science, 5th ed., New York: McGraw-Hill Professional, 2012, pp. 982-997.

[2] M. D. Lewis, "Bridging emotion theory and neurobiology through dynamic systems modeling," Behavioral and Brain Sciences, vol. 28, Apr. 2005, pp. 169-194; discussion pp. 194-245.

[3] C. D. Salzman and S. Fusi, "Emotion, cognition, and mental state representation in amygdala and prefrontal cortex," Annual Review of Neuroscience, vol. 33, 2010, pp. 173-202.

[4] D. M. Amodio and C. D. Frith, "Meeting of minds: the medial frontal cortex and social cognition," Nature Reviews Neuroscience, vol. 7, Apr. 2006, pp. 268-277.

[5] T. Jovanovic et al., "Impaired fear inhibition is a biomarker of PTSD but not depression," Depression and Anxiety vol. 27, 2010, pp. 244-251.

[6] S. D. Norrholm et al., "Timing of extinction relative to acquisition: a parametric analysis of fear extinction in humans," Behavioral Neuroscience, vol. 122, Oct. 2008, pp. 1016-1030.

[7] NATO Research and Technology Organisation, "Psychological and physiological selection of military special operations forces personnel," Final Report of Task Group HFM-171.

[8] M. Horvat, "Generation of multimedia stimuli based on ontological affective and semantic annotation," Ph.D. thesis [Croatian], Zagreb: University of Zagreb Faculty of Electrical Engineering and Computing, 2013.

[9] G. A. van Wingen, E. Geuze, E. Vermetten, and G, Fernández, "Perceived threat predicts the neural sequelae of combat stress," Molecular Psychiatry, vol 16, 2011, pp. 664-671.

[10] P. J. Lang, M. M. Bradley, and B. N. Cuthbert, "International Affective Picture System (IAPS): affective ratings of pictures and instruction manual," technical report A-6, Gainesville, FL: University of Florida, 2005.

[11] M. M. Bradley and P. J. Lang, "The International Affective Digitized Sounds (2nd Edition; IADS-2): affective ratings of sounds and instruction manual," technical report B-3, Gainesville, FL: University of Florida, 2007.

[12] K. Ćosić et al., "Computer-aided psychotherapy based on multimodal elicitation, estimation and regulation of emotion," Psychiatria Danubina, vol. 25, Sep. 2013, pp. 340-346.

[13] D. Kukolja, "Real-time estimation of emotional states based on physiological signals," Ph.D. thesis [Croatian], Zagreb: University of Zagreb Faculty of Electrical Engineering and Computing, 2012.

[14] B. Dropuljić, S. Popović, D. Petrinović, and K. Ćosić, "Estimation of emotional states enhanced by a priori knowledge," Proc. 4th IEEE International Conference on Cognitive Infocommunications, Dec. 2013, pp. 481-486.

[15] K. Ćosić et al., "The concept for assessment of pilot mental readiness training," Proc. 54th Conference of the International Military Testing Association (IMTA), Nov. 2012, pp. 55-66.

[16] D. Kukolja, S. Popović, B. Dropuljić, M. Horvat, and K. Ćosić, "Real-time emotional state estimator for adaptive virtual reality stimulation," Lecture Notes in Computer Science / Lecture Notes in Artificial Intelligence, vol. 5638, 2009, pp. 175-184.

[17] A. Anticevic, D. M. Barch, and G. Repovs, "Resisting emotional interference: brain regions facilitating working memory performance during negative distraction," Cognitive, Affective, & Behavioral Neuroscience, vol. 10, Jun. 2010, pp. 159-173.

 ISBN: 978-1-61208-340-7

Altered Resting-State Functional Connectivity in Internet Addicts

Jin-Hun Sohn
Department of Psychology
Chungnam National University
Daejeon, S. Korea
jhsohn@cnu.ac.kr

Ji-Woo Seok
Department of Psychology
Chungnam National University
Daejeon, S. Korea
suk6124@naver.com

Suk-Hee Kim
Department of Professional Counseling & Psychotherapy
Wonkwang University
Iksan, S. Korea.
sookheekim22@gmail.com

Sunju Sohn
Department of Social Welfare
Cheongju University
Cheongju, S. Korea
sunjusohn124@gmail.com

***Abstract*—The purpose of this study was to examine functional disconnectivity in Internet addicts using resting-state functional Magnetic Resonance Imaging (rs fMRI). Internet addicts and demographically similar non-addicts were scanned using rs fMRI. For the connectivity analysis, Regions Of Interests (ROIs) were defined based on previous studies of addictions. The functional connectivity assessment for each subject was obtained by correlating time-series across the ROIs, resulting in 8x8 matrix for each subject. Within-group functional connectivity patterns were observed by entering the z maps of the ROIs of each subject into second-level one sample *t* test. Two sample *t* test was also performed to examine differences between two groups. A significant increase was observed in positive functional connectivity between the Orbito Frontal Cortex (OFC) and several brain regions in the non-addicted group. However, no significant correlations in these structural connectivities were found in the Internet addiction group. The Internet addiction group presented significant negative connectivity between the OFC and insula. Our findings provide the evidence that Internet addicts have aberrant functional connectivity in the corticostriatal circuit at resting state. Particularly, we suggest that the OFC, which is associated with processing negative affect and behavioral inhibition, may play a crucial role in the pathophysiology of the Internet addiction.**

Keywords-Resting-state fMRI; Internet addicts; Functional connectivity; Orbitofrontal cortex

I. INTRODUCTION

Internet addiction disorder is marked by an inability to control one's Internet use, which eventually leads to psychological, social or work difficulties [1]. Internet addiction is defined as an Internet gaming disorder in DSM-V [2], but the nosology and optimal diagnostic criteria for an Internet gaming disorder remain controversial. The reason is that Internet addiction shares features in common with impulse control, behavioral addiction, and obsessive-compulsive disorders [3].

Regardless of whether Internet addiction is best conceptualized as a behavioral addiction or an impulse control disorder, Internet addiction has been speculated to be related to impaired inhibitory control. While impulsivity has always been recognized as central to Internet addiction, it is increasingly acknowledged to impact upon risk for and maintenance of addictive disorders.

Clinical evidence suggests that Internet addicts have a high level of impulsivity as measured by behavioral task of response inhibition (Go-No go task) and a self report questionnaire (BIS-2 scale) [4]. An Event-Related Potential (ERP) study of executive control ability (Go-No go task) found Internet addicts represented less efficient information processing and lower impulse control than controls [5]. In a functional Magnetic Resonance Imaging (fMRI) study using color-word stroop paradigm, Internet addicts also showed diminished efficiency of response inhibition processes relative to controls [6]. While numerous studies have focused on task-based ERP and fMRI related to Internet addiction and impulsivity, few studies have explored resting-state brain activity in relation to Internet addiction and impulsivity.

The purpose of this study was to examine functional disconnectivity in Internet addicts using resting-state fMRI.

II. METHODS

A. Participants

Fifteen individuals from the Internet addicts (15 men; mean = 22.20, SD = 3.07) and 15 from the normal group (15 males; mean = 22.47, SD = 2.53), both university students, participated in the current fMRI experiment. To sample the final participants of the experiment, the Korean translated/modified version of the Internet Addiction Scale (IAS) [1] and the K-scale [7] were used. The original IAS is a self-reported scale of the pathological use of the Internet (i.e., preoccupation, compulsive use, behavioral problems, emotional changes, impact on life related to Internet usage), consisting of 20 questions. Each question is based on a 5-point scale (1: Never to 5: Very). Individuals scoring 70 points or higher compose the Internet addiction group, for whom the Internet use can cause a serious problem in daily

 ISBN: 978-1-61208-340-7

life; people by 40–69 points are categorized as a mild Internet addiction group, and those with 39 points and less are considered normal users. The Korean version of the IAS showed desirable internal consistency (Cronbach's α=. 9) [8].

The K-scale is a Korean adults' Internet addiction self-diagnosis scale developed based on a survey of 146 university students. The scale consists of 20 questions and includes 4 subscales: disability to distinguish daily life and reality; the positive expectation of the Internet; tolerance and withdrawal; and self-awareness of the Internet. Each question is asked on a Likert-type 4-point scale (1: Never to 4: Very), with 53 points or below indicating that the individual should be classified as part of the general user group, whereas individuals with a score of 54 points or above are included in the Internet addiction group.

To obtain more accurate behavioral and neuroimaging data on Internet addicts, all subjects included in the Internet addiction group and the normal controls did not simultaneously experience other addictive diseases such as alcoholism or gambling addiction. The average IAS score of participants selected as the final Internet addicts was 70.80 (SD = 10.31), and the average K-scale score was 60.00 (SD = 4.47); the average IAS score of the control group was 28.60 (SD = 7.35), and their average K-scale score was 32.60 (SD = 7.70) (p < 0.001). All participants of the experiment provided their signed consent to voluntarily participate in the experiment after being thoroughly informed of the details of the experiment.

To determine whether Internet addicts were more impulsive than controls, Barrett's Impulsiveness Scale II (BIS-II), as adapted by Lee [9], was used. BIS-II consists of 35 questions with dichotomized "yes" (1) or "no" (0) answers. The total score ranges between 0 and 35, with higher scores indicating greater levels of impulsiveness. The scale was reported to be reliable (Cronbach's α=. 85) [10].

B. *Regions of Interest for Network Analysis*

On the basis of previous studies on the functional neuroimaging of addiction [11], the following regions, including the reward network, were considered a priori to be of particular interest: the Inferior Parietal Cortex (IPC), Anterior Cingulate Cortex (ACC), caudate nucleus, Putamen, Orbital Frontal Cortex (OFC), Dorso Lateral PreFrontal Cortex (DLPFC), amygdala, and insua. Thus, 8 seed regions were defined.

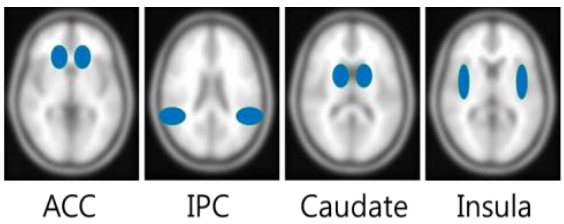

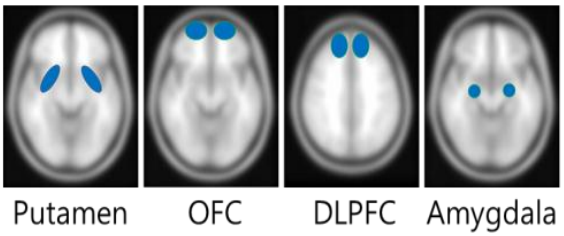

Figure 1. Selected ROIs for connectivity
(ACC, Anterior Cingulate Cortex; IPC, Inferior Parietal Cortex; OFC, Orbito Frontal Cortex; DLPFC, DorsoLateral PreFrontal Cortex)

Figure 1 shows selected Regions Of Interest (ROIs) for connectivity analysis. These ROIs masks were built by using the WFU pick atlas 2.4 toolbox [12].

C. *Functional MRI Image Acquisition*

Imaging was conducted using a 3.0 T whole-body ISOL Technology FORTE scanner (ISOL Technology, Korea) equipped with whole-body gradients and a quadrature head coil. Single-shot echo-planar fMRI scans were acquired in 35 continuous slices, parallel to the anterior commissure–posterior commissure line. The parameters for fMRI included the following: the Repetition Time/Echo Time (TR/TE) were 3000/40 ms, respectively, flip angle was 80, field of view was 240 mm, matrix was 64 × 64, slice thickness was 4 mm, and the in-plane resolution was 3.75 mm. Three dummy scans from the beginning of the run were excluded to decrease the effect of non-steady state longitudinal magnetization. T1-weighted anatomic images were obtained using a 3-D FLAIR sequence (TR/TE = 280/14 ms, flip angle = 60, FOV = 240 mm, matrix = 256 × 256, slice thickness = 4 mm).

D. *Analysis- Functional MRI Preprocessing*

The first 4 time points of the resting-state were discarded to avoid the instability of the initial MRI signal. After that, preprocessing steps, carried out with the SPM 8 toolbox, consist of slice-timing correction for interleaved acquisition, motion correction, and spatial normalization into a standard template provided by the Montreal Neurological Institute (MNI). The normalized images were smoothed with 8-mm Gaussian kernel. For the resting-state data, linear detrending and band-pass filtering (0.01-0.08 Hz) were performed by using conn toolbox. In addition, the head motion parameters, averaged signals from white matter, cerebrospinal fluid, and global brain signal were regressed out to remove the possible spurious variances derived from cardiac and respiratory fluctuations [13][14].

 ISBN: 978-1-61208-340-7

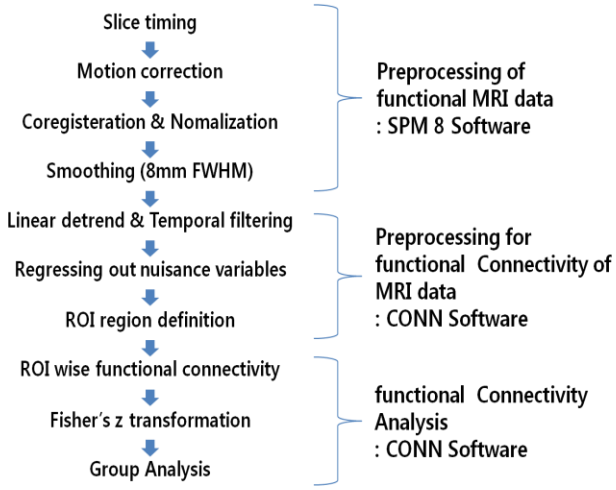

Figure 2. The flow chart of resting-state functional connectivity analysis

E. Analysis- Functional Connectivity: ROI-Wise Manners

After extracting the 8 ROIs for each subjects, we computed the functional connectivity between each pair of the 8 ROIs.

Functional connectivity analysis were conducted in ROI-wise manners. For ROI-wise functional connectivity computing the correlations between ROIs, network functional connectivity was conducted at one to one basis.

The ROI-to-ROI functional connectivity analysis was performed by averaging the time series in the two seed regions, respectively, and then, computing the Pearson's R correlation coefficient between the two averaged time series. Therefore, we obtained an 8*8 matrix for each subject in resting-state, with each element representing the strength of the functional connectivity between the corresponding two brain regions within the reward network. Specifically, the diagonal element was self-correlated to the corresponding region. Finally, the resulting correlation coefficients then were normalized to z-scores with Fisher's r-to-z transformation.

F. Analysis - Statistical Analysis

To determine whether the correlations between regions were significantly nonzero across subjects, we performed one-sample t test for each group. To examine the differences in the strength of connectivity between the two groups in resting-state, we performed two sampled t tests on the elements with significant nonzero connections of either control or Internet addicts. The significance threshold between group differences was set at $p < 0.05$, and the False Discovery Rate (FDR) [15] procedure was used to find a threshold that would restrict the expected proportion of type I errors to $q = 0.05$.

To investigate the relationship between resting state connectivity strength and degree of Internet addiction and degree of impulsivity, the correlation between functional connectivity of ROIs and scores of Internet addiction were assessed.

III. RESULTS

Table 1 provides functional networks showing significant connectivity of each ROI between controls and Internet addicts.

TABLE 1. CORRELATION COEFFICIENT BETWEEN ROIs
BLACK: NON-ADDICTION, RED: INTERNET ADDICTION

	ACC	IPC	Insula	Caudate Nucleus	Putamen	OFC	DLPFC	Amygdala
ACC			0.13**	0.17** 0.17**	0.16** 0.15**	0.21**		
IPC						0.16**	0.65** 0.65**	
Insula					0.33** 0.19**	-0.12**	-0.19** -0.20**	0.22**
Caudate Nucleus					0.17** 0.23**			
Putamen						0.17**		0.34** 0.31**
OFC							0.19** 0.12**	
DLPFC								
Amygdala								

(* $p < 0.05$, ** $p < 0.01$, *** $p < 0.001$, FDR)

In resting state, controls showed increased connectivity in several pair regions, including connectivity between the caudate nucleus and the anterior cingulate cortex, between the putamen and the insula, between the putamen and the caudate nucleus, between the dorso lateral prefrontal cortex and the inferior parietal cortex, between the dorso lateral prefrontal cortex and the orbito frontal cotrex, and between the amygdala and the putamen, while showed decreased connectivity between the dorso lateral prefrontal cortex and the insula ($p < 0.05$, FDR).

In Internet addicts, a significant increase was observed in functional connectivity between the caudate nucleus and the anterior cingulate cortex, between the putamen and the anterior cingulate cortex, between the putamen and insula, between the caudate nucleus and the putamen, between the dorso lateral prefrontal cortex and the inferior parietal cortex, between the dorso lateral prefrontal cortex and the orbito frontal cotrex, between the amygdala and the putamen, and a significant decrease was observed in functional connectivity between the orbito frontal cortex and the insula, between the dorso lateral prefrontal cortex and the insula ($p < 0.05$, FDR).

Between group analysis revealed that the connectivity in between the orbito frontal cortex and inferior parietal cortex, between orbito frontal cortex and putamen, between the orbito frontal cortex and anterior cingulate cortex, between the insula and anterior cingulate cortex, and between amydgala and insula were significantly stronger in control group than in the Internet addicts (Figure 3a), while the

 ISBN: 978-1-61208-340-7

connectivity in between the orbito frontal cortex and insula showed stronger negative correlation in the Internet addicts relative to control group (Figure 3b) ($p < 0.001$, uncorrected).

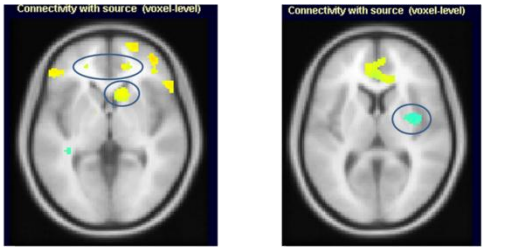

a) OFC-ACC correlation map in non-addiction group

b) OFC-insula correlation map in internet addiction group

Figure 3. Significant differences in resting state functional network connectivity between groups. Yellow: positive correlation, Blue: negative correlation

No significant relationship between functional connectivity strength and current degree of Internet addiction and degree of impulsitivy was seen.

IV. CONCLUSIONS

This study found that Internet addicts had declined connectivity strength in the Orbito Frontal Cortex (OFC) and other regions (e.g., ACC, IPC, and insula) during resting-state. It may reflect deficits in the OFC function to process information from different area in the corticostriatal reward network. Evidence indicates that the OFC participates in the executive control of information processing and behavioral expression by inhibiting neural activity associated with irrelevant, unwanted, or uncomfortable information, or actions [16]. The role of the OFC in inhibition has gained increasing prominence in the literature due to the dramatic rise in research investigating the neural correlates of social and emotional processing [16][17] .

Our findings provide the evidence that Internet addicts have aberrant functional connectivity in the corticostriatal circuit at resting state. Particularly, we suggest that the OFC, which is associated with processing negative affect and behavioral inhibition, may play a crucial role in the pathophysiology of the Internet addiction.

ACKNOWLEDGEMENTS

This research has been supported by the Converging Research Center Program funded by the Ministry of Education, Science and Technology (2013K000332) and the Korea Science and Engineering Foundation (No.20120006577).

REFERENCES

[1] K. S. Young, “Internet addiction: The emergence of a new clinical disorder,” Cyberpsychology & Behavior, vol. 1, 1998, pp. 237-44.

[2] A. P. Association, Diagnostic and statistical manual of mental disorders: DSM-V, text revision, Washington, DC: American Psychiatric Association, 2013.

[3] E. Aboujaoude, L. M. Koran, and N. Gamel, “Prevalence underestimated in Problematic Internet Use Study (response to Dr. Jerald J. Block.),” CNS Spectrums, vol. 12, 2006, pp.14-15.

[4] F. Cao and L. Su, “Internet addiction among Chinese adolescents: prevalence and psychological features,” Child: Care, Health, and Development, vol. 33, 2007, pp. 275-281.

[5] G. Dong, Q. Lu, H. Zhou, and X. Zhao, “Impulse inhibition in people with Internet addiction disorder: Electrophysiological evidence from a Go/NoGo study,” Neuroscience Letter, vol. 485, 2010, pp. 138–142.

[6] G. Dong, E. DeVito, X. Du, and Z. Cui, “Impaired inhibitory control in Internet addiction disorder: A functional magnetic resonance imaging study,” Psychiatry Research: Neuroimaging, vol. 203, 2012, pp. 503-508.

[7] K.A.D.O Promotion. The development study of Internet addiction to prevent program and K-scale, Seoul: Korea Agency for Digital Opportunity and Promotion press, 2002.

[8] M. S. Lee, E. Y. Oh, S. M. Cho, M. J. Hong, and J. S. Moon, “An assessment of adolescent Internet addiction problems related to depression, social anxiety and peer relationship,” Journal of the Korean Neuropsychiatry Association. vol. 40 2001, pp. 616-626.

[9] H. S. Lee, Impulsivity test. Seoul: Korea Guidance. 2002.

[10] H. J. Jang, The psychological characteristics of adolescent addictive using cellular phone. Unpublished master's thesis, Seoul: Sungshin Women's University, 2002

[11] D. J. Kuss, and M. D. Griffiths, “Internet gaming addiction: A systematic review of empirical research,” International Journal of Mental Health and Addiction, vol. 10, 2012, pp. 278-296.

[12] J. A. Maldjian, P. J. Laurienti, R. A. Kraft, and J. H. Burdette, “An automated method for neuroanatomic and cytoarchitect onic atlas-based interrogation of fMRI data sets,” Neuroimag e, vol. 19, 2003, pp. 1233-1239.

[13] M. D. Fox, A.Z. Snyder, D.M. Barch, D. A. Gusnard, and M. E. Raichle, “Transient BOLD responses at block transitions,” Neuroimage, vol. 28, 2005, pp. 956–966.

[14] M. D. Fox, D. Zhang, A. Z. Snyder, and M. E. Raichle, “The golbal signal and observed anticorrelated resting state brain n etworks,” Journal of Neurophysiology, vol. 101, 2009, pp. 32 70-3283.

[15] C. Genovese, N. Larzar, and T. Nichols, “Thresholding of sta tistical maps in functional neuroimaging using the false disco very rate,” Neuroimage, vol. 15, 2002, pp. 870-878.

[16] A. P. Shimamura, “The role of the prefrontal cortex in dynam ic filtering,” Psychobiology, vol. 28, 2000, pp. 207-218.

[17] R. R. Rule, A. P. Shimamura, and R. T. Knight, “Orbitofron t al cortex and dynamic filtering of emotional stimul,” Cogniti ve, Affective, & Behavioral Neuroscience. vol. 2, 2005, pp. 2 64-270.

 ISBN: 978-1-61208-340-7

Evaluating Data Storytelling Strategies: A Case Study on Urban Changes

Flavia De Simone
Scienza Nuova Research Centre
Suor Orsola Benincasa University
Naples, Italy
Email: flavia.desimone@centroscienzanuova.it

Roberta Presta
Scienza Nuova Research Centre
Suor Orsola Benincasa University
Naples, Italy
Email: roberta.presta@centroscienzanuova.it

Federica Protti
Scienza Nuova Research Centre
Suor Orsola Benincasa University
Naples, Italy
Email: federica.protti@centroscienzanuova.it

***Abstract*—Understanding urban changes is important for both citizens and administrations from several perspectives, ranging from the monitoring of the territorial development in the long run, to the support to business decision making, and to the people involvement in the administration policy. Data storytelling plays a big role in explaining both the factors involved in this complex phenomena and the effects that administration choices have on the territory. This work aims to compare the communication power of different data storytelling strategies using "semantic" language (newspaper articles) and "perceptive" language (maps) in the context of urban changes. The study focuses on the cognitive strategies that human beings apply to process perceptive and semantic information. In particular, we compare the ability of two groups of users to understand and to recall information about the metamorphosis of the Italian city of Turin after the XX Olympic Winter Games competition in 2006. The same information about the city has been provided through infographics to the first group and through newspaper articles to the second one. Both users' groups have been observing the information support for the same interval of time. The fruition strategies of the users have been observed by means of an eye tracker device, while the comprehension of the information has been verified using a questionnaire. The experiments show that, within fixed time constraints, the users provided with infographics gain a deeper understanding and a better ability of recall the represented phenomenon then the others. Further results about the comparison of the view patterns on the different types of information support are documented.**

Keywords–Human Reasoning; Data Storytelling; Eye Tracking.

I. INTRODUCTION

In a global scenario, cities have become nodes in a world-wide network and this connection context has increased the attention they need to receive. Preserving and increasing the competitiveness and the attractiveness of cities is a challenge not only for local administrations but also for central governments [1]. Indeed, at the time of writing, we find in the first point of the USA President's agenda the creation of a White House Office on Urban Policy focused on the development of a strategy for the American metropolis for ensuring that all the resources allocated to urban areas are effectively spent on the highest-impact programs [2]. This is a measure to contrast poverty, to facilitate the economic integration of families and communities. However, to strike the goal, people need to know they are part of the project: they need to be updated about the progress of the strategy in action and how it affects the urban environment in a way they can easily understand. The territorial development can be observed by citizens through different information supports: reading newspaper articles, for examples, or exploring narrative visualizations such as interactive maps.

Data storytelling can play a big role in explaining the factors involved in this kind of complex phenomena, such as the metamorphosis of a city as the effect that administration choices have on the territory. Indeed, human beings have always used stories to convey information, because structuring facts into a narrative schema is an effective way to present their main features and to recall them, by making a point. In this context, information visualizations can be used to communicate in a story-like fashion, providing the readers with a narrative experience and, when properly arranged, piloting their attention and keeping them oriented across scene transitions [3] [4].

This work studies how human beings process the information conveyed by different data storytelling media. We compare strategies using respectively semantic language (newspaper articles) and perceptive language (maps) in the context of urban changes. In particular, we consider the regeneration process of the Italian city of Turin triggered by the XX Olympic Winter Games. That competition, indeed, has played the role of catalyst of an urban, social and economic renewal [5]. In this paper, we evaluate the ability of two groups of users to understand and to recall information about Turin's metamorphosis. The same information about the city has been provided through information visualizations to the first group and through two newspaper articles to the second one.

Subjects have been asked to answer to a questionnaire about the message they have extracted by the different supports. Moreover, in order to gain further insights about the information processing, their ocular movements and other statistics about their visual patterns [6] have been studied and compared thanks to an eye tracking device.

In the following, we present related work needed to place our research and experimental efforts in Section II. We delve into the details of our comparison procedure in Section III. Results analysis is provided in Section IV. Finally, we conclude and introduce future work in Section V.

II. RELATED WORK

Storytelling is one of the main players within the Information Visualization field, especially when considering

 ISBN: 978-1-61208-340-7

information comprehension and recall issues [7]. Narrative visualizations help to turn information into knowledge that people use to understand phenomena and to make decisions. In particular, Data Storytelling exploits visualization features and structures belonging to traditional storytelling for conveying the information associated with digital data. By exploiting perception and visual sense it is then possible to improve the understanding and the recall of stories based on data representing complex phenomena. Indeed, stories provide the connecting fabric between facts to make them memorable [8]. A well-told story conveys great quantities of information in a format that is easy to assimilate.

Storytelling effectiveness has been exploited, analyzed and evaluated especially in the context of learning strategies. In particular, the cognitive results have been typically verified by supplying to the students a questionnaire or by interviewing them after the visualization of the information support [9] [10].

Eye tracking is an outstanding tool for studies related to visual search and visual perception. It allows for the recording of eye movements during the visualization of information supports and for the analysis of view patterns. It has been widely exploited for this kind of analysis on supports such as websites [11], videos [12], newspapers [13], maps [14] [15], and others. Furthermore, it is currently widely adopted in human-machine interface usability tests [16].

In this work, within the context of the evaluation of urban changes communication strategies, we couple the traditional methods for the informative power evaluation with the eye tracking analysis in order to gain deep insights, both qualitative and quantitative, about the cognitive features related to the fruition of two different kind of information supports in time-constrained conditions.

III. EXPERIMENT

In the following, we describe the experiment we run.

A. Participants

Twenty-eight participants have volunteered in the experiment. They are students at the University of Naples "Suor Orsola Benincasa" (16 girls and 12 boys). None of them have received money or course credit for their participation. Their age range is 20-23. All of them come from Naples and its surroundings and have normal or corrected to normal vision. Participants have been divided into two groups, Group 1 and Group 2, each of 14 subjects.

B. Materials

The two groups have been provided with information displayed in two different ways:

- Prototype 1: Infographic maps (*perceptive* information supports)
- Prototype 2: Articles (*semantic* information supports)

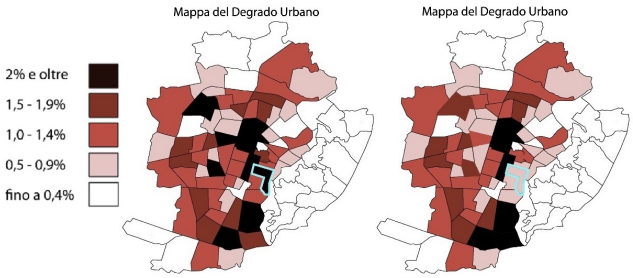

Figure 1. Prototype 1 supports

Figure 2. Prototype 2 supports

1) Prototype 1: Group 1 has been provided with two maps of the city of Turin showing different states of urban decay for each district by using colors (Figure 1). The level of urban decay is in the legend of the infographic with increasingly darker shades of color, starting from low urban decay (*white*) up to a high level of urban decay (*black*). One district among the others, the San Salvario one, has been highlighted in both the first and the second map, in order to make the viewer focus on the decay trend of that area in particular.

2) Prototype 2: The second group of participants (Group 2) has been provided with two articles from an Italian newspaper (web edition) about urban decay in the San Salvario district in 2002 and in 2010 (Figure 2). Article 1 describes the umpteenth fact of crime in a neighborhood characterized by degradation and drug smuggling. In particular, it refers to the fact that citizens are forced to fend for themselves, since the police is not able to stem the flow. Article 2 states that, according to the collected data, the quality of life in San Salvario district, known as a symbol of the drug dealing and crime, has improved a lot. Reports of citizens now concern normal maintenance of the roads. In both articles, two words have been highlighted: "urban decay", ("degrado" in Italian), because we wanted the participants to focus on the topic, and "San Salvario", which is the name of the district where the facts are set.

C. Procedure

Participants have been instructed to simply observe the pictures passing on the screen. The images have been showed for 15 seconds each and have been presented in different succession to avoid fatigue or list effects. After watching the slide show, participants have been asked to answer a short

 ISBN: 978-1-61208-340-7

questionnaire about what they had seen. In both cases, the questionnaire was made by four open questions.
The questionnaire in the case of Prototype 1 was:

- Question 1: Which city is represented in maps?
- Question 2: What phenomenon is described in the maps you've seen?
- Question 3: Is the observed phenomenon increased or decreased from the beginning to the end?
- Question 4: With respect to the area highlighted in light blue in the map, is the phenomenon increased or decreased?

The questionnaire in the case of Prototype 2 was:

- Question 1: In which city the facts described in the articles take place?
- Question 2: What kind of phenomenon is described in the articles?
- Question 3: Is the phenomenon increased or decreased from the first to the last article?
- Question 4: According to the articles, which area of the city is particularly struck by the phenomenon?

Answers to questions 2 and 3 are fundamental to compare the subjects' comprehension of the represented urban change. Question 1 and question 4 are exploratory questions that have been provided to the students in order to let the authors gain further knowledge. In particular, question 1 allows for the evaluation of the subjects' ability to geographically contextualize the phenomenon while question 4 concerns the cognitive impact of the selective highlighting used in both supports. The selective highlighting is a strategy adopted by the experiment designers for driving the viewer's attention on some specific parts of the supports in order to help him in the information extraction process. As already mentioned when describing the supports, the highlighted parts were the topic name and the district name in the articles and the San Salvario area in the maps.

During the experiment, eye tracking data have been collected. The Facelab 5.0 desktop eye tracking system [17] has been exploited to observe, record and objectively measure subjects' behavior in presence of both the information supports. Such system, developed by TEA Seeing Machines, consists of two cameras mounted on a stereo head and of an infrared (IR) pod. The IR pod emits infrared light, which is reflected off users' eyes; the reflection is recorded by the two cameras to track the eye movements. Unlike wearable eye trackers, the Facelab system is non-invasive, so that the subjects' behavior has not been affected by the presence of the tracking device. A software suite called Eyeworks from Eyetracking Inc. [18] has been used for data collection and analysis. In particular, we have exploited such tool to perform Area-of-Interest (AOI) analysis and to build useful data representations such as heat maps, gaze cluster visualizations, gaze fixation maps, and statistical charts.

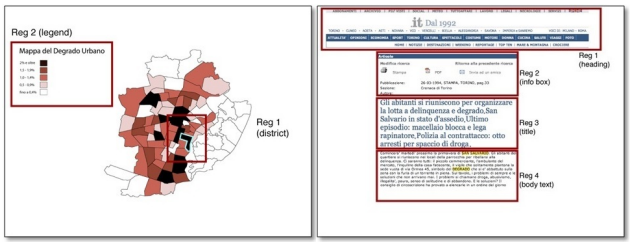

Figure 3. Areas of interest in Prototype 1 and Prototype 2

IV. RESULTS

In order to generate statistics, it has been necessary to identify the AOIs, i.e., the relevant target regions to analyze. The heat map is a convenient method to aggregate results and gives an immediate impression of the AOIs watched by subjects. A color scale, moving from blue to red, indicates the duration of gazes. In Prototype 1, the AOIs are the legend and the district; in Prototype 2 the AOIs are the heading, the info box, the title and the body text (Figure 3).

A series of metrics have been selected to evaluate the participants' ocular behavior we have captured by means of the eye tracker. Particularly, we have focused on two aspects: fixations (FX) and gazes (GZ) [19] [6]. The more frequent the gaze, the more important the area: if a particular region on the screen attracts the user's attention, the number of gaze directed to that particular region is greater than that of any other region on the screen [20]. It is assumed that a big number of fixations on a particular region indicates a significant area of interest. Fixation duration (FD) is considered a measure of the visual complexity of an AOI: longer fixations indicate the difficulty of participants to extract information by a display area. Time to first Fixation (TF) is the time occurring between the start of the task and the first fixation on an AOI. This measure is informative about the scanning strategies adopted by participants [20].

We have analyzed and herein provide the Means (M) and the Standard Deviation (SD) for the measurements of the aforementioned metrics in the experiment results shown in Table I and Table III. Parametric tests (t-tests and F-tests) on dependent means were realized for each of the measures to compare the performances of participants in the different AOIs.

A. Results for Prototype 1 (perceptive support)

1) Heat map: Figure 4 represents a sample heat map we have obtained from the eye tracking analysis of the testers visualizing the Prototype 1 support. In the bottom-left part, the support is represented without the overlapping heat map in order to show that the most viewed region is exactly the one with the bold cyan borders, corresponding to the San Salvario district. Indeed, the red spots, over the legend and the highlighted district, indicate that the group of subjects have moved to these regions of interest for a significant period of time.

2) Gaze Observations in Each Region : Data on the number of gazes in each region in Table I reveal that all subjects have looked both regions ($t(13) = 1.44$, $p = .17$) and that the

 ISBN: 978-1-61208-340-7

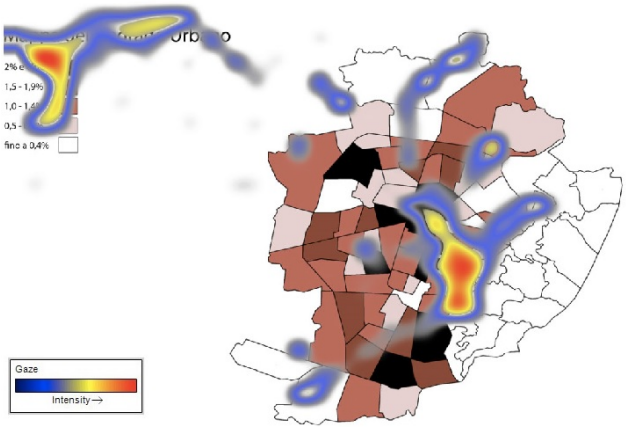

Figure 4. Heat map for Prototype 1

TABLE I. Eye tracking data for Prototype 1.

Prototype 1	GZ		FX	
AOIS	M	SD	M	SD
Map	309.08	130.46	11.43	5.00
Legend	221.43	125.77	7.07	2.81

Prototype 1	FD (sec)		TF (sec)	
AOIS	M	SD	M	SD
Map	0.31	0.15	1.54	1.01
Legend	0.32	0.23	3.59	1.01

subjects have shifted the gaze more times on the map than to the legend.

3) Fixations and Fixation Duration in Each Region: The data collected confirm that all subjects have watched both regions. Most of subjects have focused their attention more times on the map, in particular on the highlighted district, rather than on the legend ($t(13) = 2.35$, $p = .03$). Moreover, each fixation has lasted almost the same time on the legend and on the map, ($t(13) = .08, p = .94$).

4) Time to First Fixation in Each Region: During the scanning phase, participants have started by looking at the map and then they have switched to the legend ($t(13) = 3.81, p = .002$). This is what we expected: it is a supporting evidence that the task has been performed correctly because from the legend the subjects have extracted the information to interpret the map.

5) Answers to the Questionnaire: According to the results represented in Table II, no subject has recognized the city map represented in Prototype 1 (question 1). This is reasonable since the considered sample of subjects (made by students all living far from Turin) presumably is not familiar with the Turin city map. Of the 14 people who have seen Prototype 1, only one has not been able to recognize the urban decay phenomenon described by the maps (question 2). 8 subjects have responded correctly to question 3, by then understanding when the general trend of the urban decay (incremented or decremented, according to the order the pictures have been presented). Finally, most of subjects (11 of 14) have been able to correctly determine the trend of the decay level in the highlighted district (question 4).

TABLE II. Questionnaire results for Prototype 1.

Prototype 1	Qst1	Qst2	Qst3	Qst4
Right answers	0	13	8	11
Wrong answers	14	1	6	3

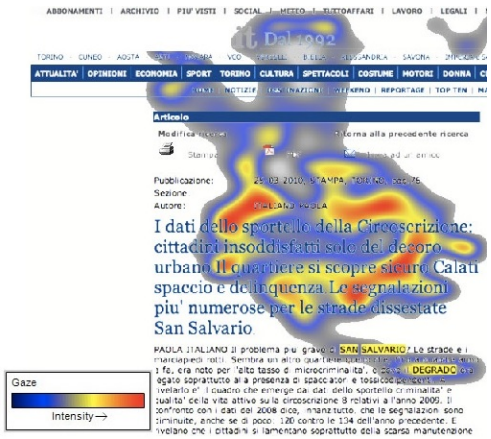

Figure 5. Heat map for Prototype 2

B. Results for Prototype 2 (semantic support)

1) Heat map: Figure 5 represents the heat map we have obtained from the eye tracking analysis of the testers visualizing the Prototype 2 support (Article 1). Red spots, over the info box and the title, indicate that the group of subjects have moved to these regions of interest for a significant period of time. Moreover, we can notice that the highlighted words in the text have also captured the subjects' gaze.

2) Gaze Observations in Each Region: Considering the gaze results in Table III, the majority of subjects have mainly looked the information box of the article and the title ($t(13) = .26$, $p = .79$), as it can be noticed by the comparison with the newspaper heading measurements. The text of the article has been watched by only 8 of 14 subjects, probably because of the time constraints ($F(3.39) = 18.8, p = .000$).

3) Fixations and Fixation Duration in Each Region: The data provided in Table III confirm that all subjects have watched much more the info box and the title rather than to the newspaper heading and the text ($F(3.39) = 17.6, p = .000$). The fixations have lasted almost the same time in each AOI ($F(3.39) = 2.12, p = .11$), indicating a comparable visual complexity between each AOI.

4) Time to First Fixation: As it emerges from the recordings, the subjects have adopted similar strategies to scan the image, starting from the top of the page, i.e., from the newspaper heading , to the bottom, i.e., the text of the article, passing trough the info box. The participants have ended the scanning phase on the title where they have spent most of the time in order to get information ($F(3.39) = 2.96, p = .04$).

5) Answers to the Questionnaire: As Table IV shows, only two subjects have realized that the phenomenon took place in Turin. 8 of 14 have been able to recognize the phenomenon described in the articles and have answered correctly to the

 ISBN: 978-1-61208-340-7

TABLE III. Eye tracking data for Prototype 2.

Prototype 2	GZ		FX	
AOIS	M	SD	M	SD
Heading	259.86	94.20	35.48	21.13
Title	245.67	116.66	83.57	40.51
Info box	118.66	67.28	89.04	37.77
Text	20.95	38.49	6.67	14.65
Prototype 2	FD (sec)		TF (sec)	
AOIS	M	SD	M	SD
Heading	0.25	0.05	2.24	1.13
Title	0.23	0.07	5.21	2.97
Info box	0.15	0.26	2.31	1.56
Text	0.29	0.12	3.01	3.86

TABLE IV. Questionnaire results for Prototype 2.

Prototype 2	Qst1	Qst2	Qst3	Qst4
Right answers	2	8	7	2
Wrong answers	12	6	7	12

question 2. The other 6 subjects have not remembered exactly what kind of issues was the article about, even if the topic was extensively described in the news and the word "decay" was highlighted in yellow. Of 14 subjects, half of the subjects have answered correctly to question about the decrease or increase of the phenomenon and the other half in the wrong way (question 3). Finally, 12 subjects have not been able to remember the name of the San Salvario district, despite of the layout emphasis it has been given within the text.

The answers reflect the effects of a natural reading approach performed by young students in 15 sec. While they known in advance they would have had only that limited time interval to observe the support, they have not been instructed to read as much as they can from the articles, nor to apply, if known by them, any strategy of rapid reading (that is, however, a quite rare skill). By relaxing the time constraints, the subjects would have had, of course, the possibility of acquiring all the needed information to answer the questions correctly. Even without considering the application of fast reading methodology, the ability of extracting information by text should be considered quite high, since university students are acquainted with the task, presumably more than other categories of subjects involved with more practical and manual activities or with a minor level of education.

C. Comparison

After the separate analysis of the behavior of the groups in relation to Prototype 1 and Prototype 2, a between-groups-analysis has been performed for comparing the heuristic strategies adopted by the participants. Newspaper heading and text of Prototype 2 have been excluded by the comparison since they have been considered only by a minority of the subjects for an irrelevant time, as it emerges by previous analysis. The times of gaze observation on the legend and district regions belonging to Prototype 1 and the ones on the info box and title regions in Prototype 2 are nearly similar ($F(1.26) = 1.56, p = 0.22$).

The frequency of fixations in the legend and district regions belonging to Prototype 1 and the one in the info box and title regions in Prototype 2 are nearly similar ($F(1.26) = 3.28, p = 0.08$). The fixation durations in the legend and district regions belonging to Prototype 1 and the ones in the info box and title regions in Prototype 2 are nearly similar ($F(1.26) = 0.156, p = 0.69$). In time constrained contexts, the totality of the subjects has adopted comparable heuristics, within the regions considered most significant.

In order to evaluate the informative power of the two supports, a comparison has been also made between the correct and the wrong answers to the questionnaires.

As the answers to question 1 show, almost all the participants have not been able to geographically contextualize the represented phenomenon, either by looking at the city map nor by scanning the text articles. This is probably due to the fact that the represented urban change involves an area which is not the one the participants live in, so they are not familiar with the cartographic representation of the city and with the local peculiar urban and social problems.

Questions 2 and 3 focus on the topic and on the trend comprehension, regardless the understanding of the involved physical area. Performances in terms of correct answers seems to show there is a better understanding of both the arguments for participants looking at the perceptual support.

Questions 4 have been designed to explore the effectiveness of the selective highlighting in the supports. Due to the diversity between the kind of the support, questions 4 are formulated differently but they both focus on the same purpose, i.e., they check for the effects of higlights: in the first case, what is highlighted in the perceptual supports is an area and the minimum effort the subject can do is observing the change in the color; in the case of the semantic supports, words are highlighted and the minimum effort the subject can do is reading them. While the eye tracking has demonstrated that the highlighted keywords in Prototype 2 have attracted the subjects' attention, almost nobody has been able to recall the name of the district interested by the urban change. The highlighted region of the map also captured the viewers' gaze, as showed by the eye tracker. Participants have focused on the changes on such area and correctly interpreted the time evolution of the phenomenon represented by the infographics.

Question 2 and 4 registered a significant difference of correct and wrong answers between Prototype 1 and 2. A chi-square test has been performed by considering the answers to questions 2 and 4. Such a test has showed that, despite the semantic information is clearly and extensively described through a textual description, synthetic perceptual information is more effective for informational purposes ($X_2(1) = 12.65$, $p = .000$).

V. Conclusion and Future Work

Cities are living systems and urban changes are complex phenomena that involve time and space. Understanding cities metamorphosis is important for citizens and administrations for several reasons: for example, to empower the weakest areas by means of the presence of public services, to keep under control the urban decay, to monitor the effects of administrations' choices in the long run, to support business decision making on the territory and to directly involve citizens in the administration policy.

 ISBN: 978-1-61208-340-7

The aim of this study was to test the communicative effectiveness of different data storytelling strategies in the field of urban changes. To this purpose, we have provided two groups of 14 young students each with respectively an infographic support and a textual support for a time interval of 15 sec. All the subjects have no a priori hints about the represented phenomena.

We have compared the informative power of the two strategies on the basis of eye tracking data and answers to ad-hoc designed questionnaires.

While questionnaires are a typical way to check the information processing and comprehension in real experiments, by the eye tracking we gain deeper insights with respect to the classical path between the questions and the answers.

Thanks to the eye tracker device, we have observed the fruition strategies of the subjects. We have found that they have applied a similar scanning strategy for the understanding of the infographics and of the news reports, i.e., within each support, they focus on a single area that better synthesizes the main information (the legend area for the map and the title for the article).

On the other hand, by considering the answers to the questionnaires, we have discovered that, in a time constrained situation, the subjects better understand the phenomena when they are depicted in the synthetic infographics rather than when they are extensively described by narrative texts.

These data let us conclude that, for young people with a medium-high level of education, the informative power of infographics is stronger than the newspaper articles' one in time-constrained scenarios, where the users apply a scanning strategy of the information support, rather than a careful reading.

To generalize the statement, we first need to enlarge and differentiate the sample of participants in future experiments. We can exploit such analysis in a future comparison with people having a prior knowledge about the urban problems, in order to assess how the understanding of the represented phenomena changes when the recipient of the communication strategy is already aware of (and directly touched by) the topics.

Finally, we are going to apply the presented methodology of evaluation of different data storytelling supports in more complex urban changes evolution scenarios, as well as in application domains with other communication goals.

REFERENCES

[1] L. Kamal-Chaoui and J. Sanchez-Reaza, "Urban Trends and Policies in OECD Countries," OECD Regional Development Working Papers, 2012, ISSN: 2073-7009.

[2] "The agenda of the Obama Administration about Urban Policy," 2014, URL: http://change.gov/agenda/urbanpolicy_agenda/.

[3] R. Kosara and J. Mackinlay, "Storytelling: The Next Step for Visualization," Computer, vol. 46, no. 5, 2013, pp. 44–50.

[4] E. Segel and J. Heer, "Narrative visualization: Telling stories with data," Visualization and Computer Graphics, IEEE Transactions on, vol. 16, no. 6, 2010, pp. 1139–1148.

[5] P. Bondonio and C. Guala, "Gran Torino? The 2006 Olympic Winter Games and the tourism revival of an ancient city," Journal of Sport and Tourism, vol. 16, no. 4, 2011, pp. 303–321.

[6] K. Holmqvist, M. Nyström, R. Andersson, R. Dewhurst, H. Jarodzka, and J. Van de Weijer, Eye tracking: A comprehensive guide to methods and measures. Oxford University Press, 2011.

[7] S. Bateman, R. Mandryk, C. Gutwin, A. Genest, D. McDine, and C. Brooks, "Useful Junk? The Effects of Visual Embellishment on Comprehension and Memorability of Charts," in ACM Conference on Human Factors in Computing Systems (CHI 2010), Atlanta, GA, USA, 2010, pp. 2573–2582.

[8] M. Austin, Useful fictions: evolution, anxiety, and the origins of literature. University of Nebraska Press, 2011.

[9] M. Jenkins and J. Lonsdale, "Evaluating the effectiveness of digital storytelling for student reflection," in ICT: Providing choices for learners and learning. Proceedings ASCILITE Singapore 2007, 2007.

[10] M. R. Davidson, "A phenomenological evaluation: using storytelling as a primary teaching method," Nurse Education in practice, vol. 4, no. 3, 2004, pp. 184–189.

[11] E. H. Chi, P. Pirolli, K. Chen, and J. Pitkow, "Using information scent to model user information needs and actions and the Web," in Proceedings of the SIGCHI conference on Human factors in computing systems. ACM, 2001, pp. 490–497.

[12] V. Lavrusik, "Local Online News Video Design and Usability: What's working, what's not," Online Journalism Blog, 2009.

[13] H. Bucher and P. Schumacher, "The relevance of attention for selecting news content. an eye-tracking study on attention patterns in the reception of print and online media," Communication, vol. 31, no. 3, 2006, pp. 347–368.

[14] V. Krassanakis, V. Filippakopoulou, and B. Nakos, "An application of eye tracking methodology in cartographic research," Proceedings of the EyeTrackBehavior (Tobii), Frankfurt, 2011.

[15] T. Opach and A. Nossum, "Evaluating the usability of cartographic animations with eye-movement analysis," in 25th International Cartographic Conference, 2011, p. 11.

[16] W. Gibbs and R. Bernas, "Visual Attention in Newspaper versus TV-Oriented News Websites," Journal of Usability Studies, vol. 4, no. 4, 2009, pp. 146–165.

[17] URL: http://www.seeingmachines.com/product/facelab/.

[18] URL: http://www.eyetracking.com/Software/EyeWorks.

[19] A. Poole and L. J. Ball, "Eye Tracking in Human-Computer Interaction and Usability Research: Current Status and Future," in Prospects, Chapter in C. Ghaoui (Ed.): Encyclopedia of Human-Computer Interaction. Pennsylvania: Idea Group, Inc, 2005.

[20] R. J. Jacob and K. S. Karn, "Eye tracking in human-computer interaction and usability research: Ready to deliver the promises," Mind, vol. 2, no. 3, 2003, p. 4.

 ISBN: 978-1-61208-340-7

A Brain–Computer Interface Speller with a Reduced Matrix: A Case Study in a Patient with Amyotrophic Lateral Sclerosis

Ricardo Ron-Angevin,
Sergio Varona-Moya
and Leandro da Silva-Sauer
Departamento de Tecnología Electrónica
E.T.S.I. Telecomunicación, University of Málaga
Málaga, Spain
Email: rra@dte.uma.es
{sergio.varona, sauer}@uma.es

Trinidad Carrión-Robles
Departamento de Enfermeríaa
Escuela de Enfermería, University of Málaga
Málaga, Spain
Email: trinicar@uma.es

***Abstract*—Visual P300-based Brain–Computer Interface (BCI) paradigms for spelling are aimed at offering a non-muscular communication channel for those people with severe motor impairment, such as locked-in patients. To be as effective as other assistive technologies, these systems have to achieve a greater communication rate. One way to do so is to develop better interfaces. In this regard, we thought of using a 4 x 3 symbol matrix based on the T9 interface developed for mobile phones. Due to presenting a reduced matrix and relying on an adaptation of the T9 predictive text system, we expected that this speller would provide a higher communication rate than usual 6 x 6 matrix spellers that are based on Farwell and Donchin's classic proposal. As a proof of concept, a locked-in patient with amyotrophic lateral sclerosis tested our T9-like visual BCI speller along with two different 7 x 6 conventional matrix spellers. The comparison of her performance results with those of a sample of three healthy participants suggested that it was possible for this locked-in patient to control the T9-like speller as well as they did, and thus, write a target sentence considerably faster than when she used the alternative spellers.**

Keywords-Brain-Computer Interface; P300; Speller; T9 interface, Amyotrophic Lateral Sclerosis.

I. INTRODUCTION

Patients who have suffered a brainstem stroke, a cerebral palsy or that have been diagnosed with a neurological disease such as the Amyotrophic Lateral Sclerosis (ALS) face severe motor impairments. In some cases, they may even enter in a locked-in state [1], in which they lose control of practically all muscular activity. These patients are believed to retain their cognitive abilities intact, although some authors disagree with this assumption (cf. [2][3]).

Brain–Computer Interface (BCI) systems [4] have been developed during the last 40 years to offer a non-muscular channel to these patients, so that they can communicate or control external devices [5][6]. These systems transform the user's brain activity into commands that are interpreted by a machine through which they can control the environment or express needs and feelings.

Regarding the type of brain activity required from the user, BCIs can be roughly divided into those based on spontaneous brain activity, such as Slow Cortical Potentials (SCP, [7]) and SensoriMotor Rhythms (SMR, [8]) and those based on brain responses to external events, mainly the P300 Event-Related Potential (ERP) [9].

To be used efficiently, SCP- or SMR-based BCIs demand from the user an adequate control of his/her brain activity, which is usually acquired after a training period that might take even months. By contrast, P300 is a naturally elicited, positive deflection of the electroencephalogram (EEG) typically appearing about 300 ms after the presentation of an unexpected stimulus. Thus, P300-based BCIs do not demand such an intensive training. Users have simply to attend to the stimulus that is associated to a certain option as it is displayed among other non-relevant stimuli. This elicits a brain activity that is systematic enough so as to be classified with usually perfect accuracy, so that the desired option can be identified.

The first P300-based BCI paradigm for communication purpose was the visual speller developed by Farwell and Donchin [10]. In this speller, a 6 x 6 matrix of symbols was shown to the user. Its rows and columns were randomly intensified for a certain time, during which he/she counted the number of times that the row/column containing the desired symbol was intensified. Those intensifications or flashes constituted the infrequent stimuli, which elicited the P300. Once a sequence of flashes was over, the symbol belonging to the row and column that had produced the largest P300 was regarded as the attended matrix element and displayed to the user.

The effectiveness of this visual speller is supported by several studies that have tested it not only with healthy participants [11]–[15], but also with users affected by some motor disability [16]–[21]. However, the communication rate of these systems is still lower than that of alternative assistive technologies such as the eye tracker.

Aimed at improving the usability of BCI spellers, some authors have examined the impact of user-centred factors on performance. In this regard the mental fatigue induced by a long use [22]–[24], the sustained attention at a symbol that

 ISBN: 978-1-61208-340-7

it demands [25][26], the resting heart rate variability [27] or the user's motivation [22][28][29] can influence or be related with performance (see [30], for a review) At the same time, other authors have explored the extent to which performance can be improved by providing BCI spellers with predictive text techniques [31]–[34], or by modifying the temporal of spatial aspects of their interface [35]–[40].

Following these latter research lines, we hypothesized that restricted BCI end-users could benefit from using a visual P300-based BCI paradigm for spelling that shows a reduced 4 x 3 symbol matrix, resembling the T9 interface developed for mobile phones [41]. Specifically, we expected that locked-in patients would benefit from needing less time to select a symbol—due to using a matrix with fewer rows and columns than usual—as they frequently cannot stare at the desired symbol for a long time.

Although a reduced matrix interface has already been proposed with an auditory [42] and a visual P300-based speller [43], it has never been tested, to our knowledge, with BCI end-users. Such a test is necessary because the performance results from a sample of healthy participants do not necessarily apply to end-users in the locked-in state [44]. For example, the higher frequency with which the attended row/column would be intensified together with the complexity of typing through a T9-like interface could overload the cognitive resources of a BCI end-user, which may not be fully available [2][3].

In order to obtain a proof of concept of its actual usability, a locked-in patient diagnosed with ALS performed a copy spelling task using the proposed T9-like speller and also two adaptations of the classic Farwell and Donchin speller. Her performance results were compared with those of a sample of three healthy subjects that had participated in a previous experiment [45]. In the following sections, we will provide a detailed account of the experimental procedure and of the results, and finally discuss their implications.

II. METHODS

A. The case

We visited a 62-year-old woman on two separate days with a time interval of two days between them. She was diagnosed with amyotrophic lateral sclerosis in 2008 and is currently in the locked-in state. Without any independent means of communication, she relies on a partner-scanning approach based on eye blinks to communicate with her relatives and caregivers and on assistive technology (i.e., an eye-tracker system connected to her personal laptop) in order to browse the Internet and interact with friends in social networks.

B. Experimental setup

We carried out only morning testing sessions. The patient sat comfortably in an armchair. A laptop was placed before her over a tray attached to the armchair (see Figure 1). The viewing distance was about 75 cm.

On our first visit to the patient's home, we conducted two sessions to test two BCI paradigms: first, an adaptation of Farwell and Donchin's 6 x 6 matrix speller (hereafter termed *Spellermod*), and then, a Spellermod that included a word predictor (hereafter termed *SpellermodPred*). The proposed

Figure 1. Experimental setup at the patient's home.

T9-like 4 x 3 matrix speller (hereafter termed *SpellerT9*) was tested on a third session on our second and last visit. These three BCI paradigms are described next.

C. Tested BCI spellers

To make a proper comparison of the three mentioned BCI spellers in terms of typing speed, the values of all the temporal parameters related to the selection of a symbol were equal across them. These values were based on those used by [12]. Specifically, each row and column was randomly flashed 10 times. Therefore, each character was randomly intensified 20 times. The duration of each flash was 125 ms and the InterStimulus Interval (ISI) between flashes was also 125 ms. There was a pause of 2 s after each sequence of flashes (i.e., after a character had been selected) and also in the beginning of each trial. It is important to notice that the duration of a sequence of flashes depended on the size matrix, so that bigger matrices entailed longer sequences.

1) SpellerT9: The SpellerT9 presented the user a 4 x 3 virtual keyboard (see Figure 2a), in which only eight keys - the ones corresponding to the numbers 2 to 9 - were used for spelling. Each of those keys corresponded to three to four letters. To disambiguate key sequences, we implemented a modified version of the T9 predictive text system, which worked as follows. Given a certain sequence, the system computed the corresponding *textonyms*, that is, all the possible combinations of letters with lexical meaning that could be formed with those contained on the selected keys. These textonyms were then ordered according to their lexical frequency in the Spanish language [46]. The system regarded the most frequently used one as the word the user was trying to type and accordingly displayed it in the text box below the keyboard (see Figure 2a). If that was indeed the desired word, the user accepted it by selecting the key 0 (i.e., selecting the command *espacio*), which simply added a blank space afterwards. Otherwise, he/she could personally disambiguate the key sequence by selecting the key C (i.e., select the command *cambiar*) to switch to a new keyboard that displayed the four most frequently used textonyms in row-major order. For example, given the key sequence 2272, the word *casa* would be displayed in the text box below the keyboard. If the user selected the key C, then the textonyms *casa*, *cara*,

 ISBN: 978-1-61208-340-7

capa, and *basa* would be displayed on the new keyboard (see Figure 2b). The user could then select one of those textonyms, in which case the word plus an additional blank space were displayed in the mentioned text box. Alternatively, he/she could go back to the previous keyboard by selecting the left arrow key (i.e., selecting the command *volver*).

In order to further increase typing speed, we decided to provide the SpellerT9 with a word predictor. In this case, given a certain key sequence, the predictor computed the lexical frequency of all the words starting with any of all the possible combinations of letters contained on the selected keys, that is, not only textonyms—as in the implemented T9 predictive text system—but also combinations with no lexical meaning. The predictor then regarded the most frequently used one as the word the user was trying to type and displayed it in a text box to the left of the keyboard (see Figure 2a). If that was indeed the desired word, the user could validate it by selecting the key 1 (i.e., selecting the command *validar*). As a consequence, the word plus an addition blank space were written in the text box below the keyboard. In the previous example, the predicted word would have been *barcelona*. Therefore, whereas the word predictor could suggest the user words of more letters than the number of keys selected, the T9 predictive text system only computed words of as many letters as selected keys.

To delete characters the user had to select the key X (i.e., select the command *borrar*). To write digits, he/she had to select the key C just after a blank space had been introduced, either to validate a textonym or because of having accepted the word retrieved by the word predictor. The user could then type the digits from 0 to 9 just by selecting the corresponding keys. Once the desired sequence digits was written, the user had to select the key C again to continue writing words. This selection automatically added a blank space to the numeric sequence.

As the SpellerT9 displayed a 4 x 3 keyboard, the time needed to select a key was 19.5 s, that is, the initial 2 second pause plus the time needed to flash four rows and three columns 10 times each.

2) Spellermod: The Spellermod presented the user a 7 x 6 virtual keyboard, shown in Figure 3a. The last row contained only two command keys - BORRAR and ESPACIO - for deleting the last inserted character and introducing a blank space, respectively. The characters typed by the user were displayed inside a text box below the keyboard.

According to the aforementioned temporal parameters, the time needed to select a key of the Spellermod interface was 34.5 s - the initial 2 second pause plus the time needed to flash seven rows and six columns 10 times each - , that is, almost twice the time needed to select a key from the SpellerT9.

3) SpellermodPred: As we had implemented a word predictor in the SpellerT9 to make typing faster, we decided to add that feature to the Spellermod to control its influence on user performance. Thus, we developed the SpellermodPred, which presented a 7 x 6 virtual keyboard that included the command key VALIDAR (see Figure 3b). The time needed to select a key using the SpellermodPred was 34.5 s, like in the Spellermod.

The typed characters were displayed in a text box below the keyboard and fed into the word predictor. The suggested word was displayed in an additional text box to the left of the former (see Figure 3b). In case that word was the one the user wanted to write, he/she could do it by selecting the command key VALIDAR. As in the SpellerT9, that selection implied writing the suggested word and adding a blank space afterwards.

D. Testing sessions

Prior to all testing sessions, we verbally informed the patient in detail about the procedure and obtained her consent to participate in the study and proceed with the different sessions through partner scanning. The experiment was conducted in accordance with standard ethical guidelines as defined by the Declaration of Helsinki [47].

Each testing session was divided into two phases: a first one for calibration purpose and a second one to evaluate user performance. At the beginning of each session, the researchers explained the patient how to spell words with the corresponding speller. They told her to silently count how many times the symbol she wanted to select was intensified (i.e., flashed) during a sequence of flashes. They informed her that during calibration she would not be receiving any feedback (i.e., the attended symbol). As for the SpellermodPred and the SpellerT9, they also explained her how the word predictor and the T9 predictive text system worked.

In the calibration phase, the patient was asked to copy spell five sequences of three to four characters, specifically “hoy”, “sin”, “casa”, “remo”, and “tus” for the Spellermod and “159”, “357”, “1xc3”, “4796”, and “258” for the SpellerT9. The classification weights from the Spellermod were also used for the SpellermodPred. In the evaluation phase, she was asked to write the sentence “experiencia bci en la universidad de malaga” (i.e., bci experience at the university of malaga).

Two days after our second visit, we contacted the patient through e-mail to gather her experience as user of the three spellers. We asked her to complete a test consisting of nine questions to be answered with a 5-point Likert scale and also to reply to six open-answer questions, e.g., whether she had any suggestions concerning the interfaces she had interacted with. Her answers were recorded by her relatives and e-mailed back to us six days later.

E. Data acquisition and analysis

Scalp EEG signals were recorded from eight positions according to the 10-20 standard (FPz, Cz, Pz, Oz, P3, P4, PO7, and PO8) using active electrodes (actiCAP, Brain Products Gmbh, Germany). All channels were referenced to the left earlobe and grounded to FPz. The EEG signals were amplified with an actiCHamp amplifier (Brain Vision LLC, USA), and recorded at 200 Hz using BCI2000 [48].

The stimulation paradigms of the three spellers were implemented using BCI2000. The T9 predictive text system as well as the word predictor used both by the SpellerT9 and the SpellermodPred were implemented as MATLAB R2007a (The MathWorks Inc., USA) routines that were called from the BCI2000 framework. The P300 component was classified using stepwise linear discriminant analysis like in [10].

 ISBN: 978-1-61208-340-7

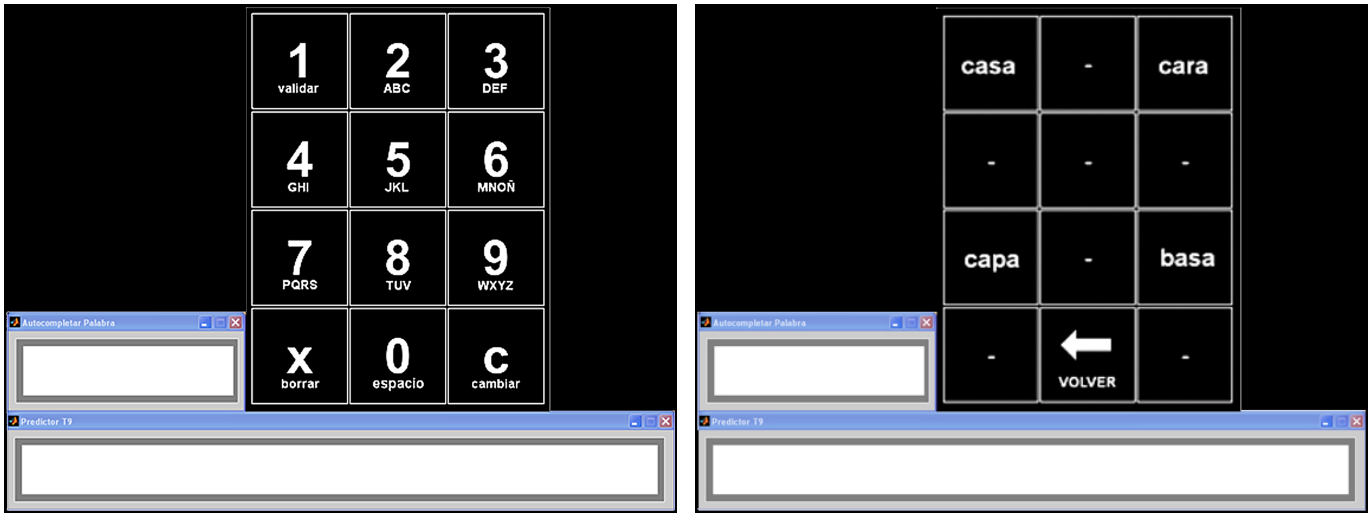

(a) (b)

Figure 2. The two different interfaces of the SpellerT9. (a) The 4 x 3 virtual keyboard for typing. The text box below the keyboard showed the user's message interpreted by the predictive text system, while the text box to the left displayed the outcome of the word predictor. (b) In case the textonym selected was not the word desired by the user, he/she could disambiguate the key selection by choosing among the four most frequently used textonyms. In the figure, the selected keys would have been 2272. See text for details.

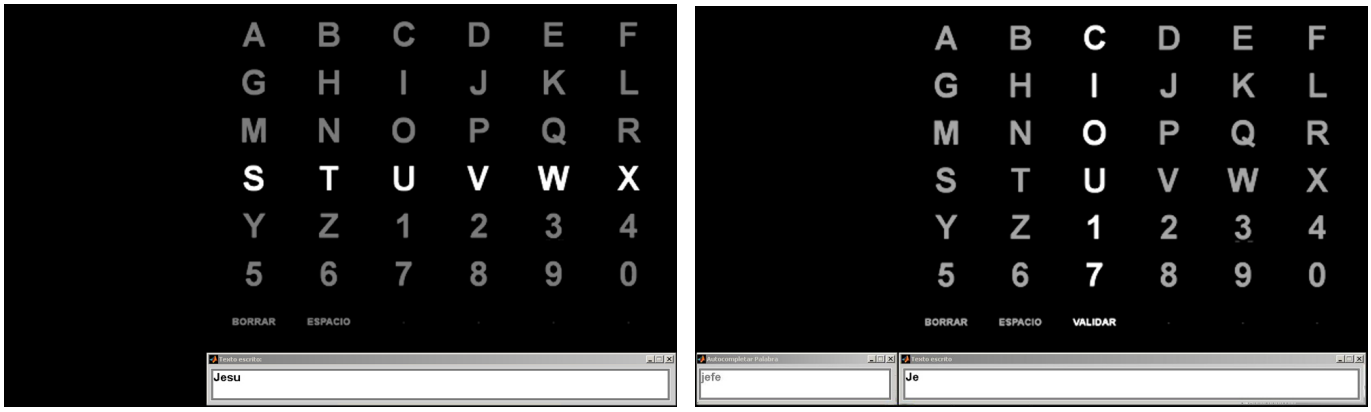

(a) (b)

Figure 3. The interfaces of the two 7 x 6 matrix spellers that were tested: the Spellermod (a) and the SpellermodPred (b). The Spellermod presented a 7 x 6 virtual keyboard and a text box for displaying the user's message, whereas the SpellermodPred showed an additional text box for displaying the word suggested by the word predictor.

III. RESULTS AND DISCUSSION

The time needed by the locked-in patient and by the three healthy participants to spell each word of the target sentence (i.e., "experiencia bci en la universidad de malaga") using the three compared spellers are shown in Table I. Unfortunately, most of the data corresponding to the first testing session (i.e., the one corresponding to the Spellermod) at the patient's home were lost due to a software failure.

Table I also shows the minimum required times, that is, the time that a user that made no mistake nor slip would need to write each word. As can be seen, the total spelling times of the locked-in patient were similar to those of the healthy participants when using the same speller, that is, the SpellermodPred and the SpellerT9.

The data from healthy participants suggest that the word predictor included in the SpellermodPred contributed to reducing the overall time needed to write the target sentence with respect to the Spellermod. Comparing the results of the SpellermodPred and the SpellerT9, it also seems likely that using a matrix with fewer rows and columns increased the communication rate further than the word predictor did. In fact, the locked-in patient wrote the target sentence over 1.5 times faster with the SpellerT9 than with the SpellermodPred. It is also remarkable that the patient made no mistake nor slip using the SpellerT9 when writing four of the seven words of the target sentence (i.e., "experiencia", "en", "la", and "de").

As for her personal assessment of the spellers, she regarded the SpellerT9 as the fastest of all three and did not find it too difficult to use. She also indicated that all the spellers were equally exhausting to use. Despite her good performance, she found the SpellerT9 more confusing to use than both the

 ISBN: 978-1-61208-340-7

TABLE I. TIME NEEDED BY THE LOCKED-IN PATIENT AND BY THE THREE HEALTHY PARTICIPANTS TO WRITE EACH WORD OF THE TARGET SENTENCE AS A FUNCTION OF THE SPELLER THEY USED.

	Time for each word (s)							
Speller	"Experiencia"	"BCI"	"en"	"la"	"Universidad"	"de"	"Málaga"	Total time (s)
Locked-in patient								
Spellermod	586.5							
SpellermodPred	172.5	138	103.5	103.5	207	103.5	207	1035
SpellerT9	78	97.5	58.5	39	136.5	39	214.5	663
Healthy participant 1								
Spellermod	414	138	103.5	103.5	621	103.5	276	1759.5
SpellermodPred	172.5	138	103.5	69	207	103.5	207	1000.5
SpellerT9	78	78	58.5	39	97.5	39	117	507
Healthy participant 2								
Spellermod	483	345	310.5	172.5	483	103.5	276	2173.5
SpellermodPred	138	103.5	103.5	172.5	517.5	69	345	1449
SpellerT9	78	156	58.5	78	214.5	78	177	840
Healthy participant 3								
Spellermod	414	138	103.5	103.5	414	172.5	270	1615.5
SpellermodPred	138	138	103.5	69	172.5	69	207	897
SpellerT9	78	117	78	39	97.5	39	156	604.5
A user that made no mistake								
Spellermod	414	138	103.5	103.5	414	103.5	270	1546.5
SpellermodPred	138	103.5	103.5	69	172.5	69	207	862.5
SpellerT9	78	78	58.5	39	97.5	39	117	507

Spellermod and the SpellermodPred, particularly due to not knowing which letter was going to be chosen after a key selection. Nevertheless, she also found it more entertaining than those two. Importantly, she thought she needed more training with all the spellers.

IV. CONCLUSION AND FUTURE WORKS

The main goal of this study was to obtain a proof of concept that a locked-in patient diagnosed with amyotrophic lateral sclerosis could efficiently control a visual P300-based speller with a T9-like interface consisting of 4 x 3 virtual keyboard and an adaptation of the T9 text predictive system of mobile phones.

Our data suggest that the locked-in end-user that participated in the study was able to control the proposed speller as well as a sample of healthy participants did. Importantly, the communication rate the patient achieved with this new speller was higher than the one achieved when using a 7 x 6 matrix speller, even when this also included a word predictor.

However, it should be kept in mind that this particular locked-in patient uses her laptop almost daily to browse the Internet or interact in social networks. Besides, she is always greatly motivated to participate in research studies and has a very supportive circle of relatives and friends around her. Therefore, her good performance results and her assessment of the proposed speller cannot be fully generalized to other locked-in patients. More studies involving other locked-in end-users should be done to account for individual differences.

ACKNOWLEDGMENT

This work was partially supported by the University of Málaga, by the Innovation, Science and Enterprise Council of the Junta de Andalucía (Spain)—project P07-TIC-03310—, by the Spanish Ministry of Science and Innovation—project TEC 2011-26395—and by the European fund ERDF.

REFERENCES

[1] F. Plum and J. B. Posner, The Diagnosis of Stupor and Coma. Philadelphia: F. A. Davis, 1966.

[2] J. Lakerveld, B. Kotchoubey, and A. Kübler, "Cognitive function in patients with late stage amyotrophic lateral sclerosis," J. Neurol. Neurosurg. Psychiatry, vol. 79, Jan. 2008, pp. 25–29, doi:10.1136/jnnp.2007.116178.

[3] M. Rousseaux, E. Castelnot, P. Rigaux, O. Kozlowski, and F. Danze, "Evidence of persisting cognitive impairment in a case series of patients with locked-in syndrome," J. Neurol. Neurosurg. Psychiatry, vol. 80, Feb. 2009, pp. 166–170, doi:10.1136/jnnp.2007.128686.

[4] J. J. Vidal, "Toward direct brain–computer communication," Annu. Rev. of Biophys. and Bioeng., vol. 2, Jun. 1973, pp. 157–180, doi:10.1146/annurev.bb.02.060173.001105.

[5] N. Birbaumer, "Breaking the silence: Brain–computer interfaces (BCI) for communication and motor control," Psychophysiology, vol. 43, Nov. 2006, pp. 517–532, doi:10.1111/j.1469-8986.2006.00456.x.

[6] J. R. Wolpaw, N. Birbaumer, D. J. McFarland, G. Pfurtscheller, and T. M. Vaughan, "Brain-computer interfaces for communication and control," Clin. Neurophysiol., vol. 113, Jun. 2002, pp. 767–791, doi:10.1016/S1388-2457(02)00057-3.

[7] N. Birbaumer, "Slow cortical potentials: Plasticity, operant control, and behavioral effects," Neuroscientist, vol. 5, Mar. 1999, pp. 74–78, doi:10.1177/107385849900500211.

[8] G. Pfurtscheller, "Event-related EEG desynchronization," Electroencephalogr. Clin. Neurophysiol., vol. 75, Supplement, Jan. 1990, pp. S117–S118, doi:10.1016/0013-4694(90)92147-O.

[9] J. Polich, "Updating P300: An integrative theory of P3a and P3b," Clin. Neurophysiol., vol. 118, Oct. 2007, pp. 2128–2148, doi:10.1016/j.clinph.2007.04.019.

[10] L. A. Farwell and E. Donchin, "Talking off the top of your head: Toward a mental prosthesis utilizing event-related brain potentials," Electroencephalogr. Clin. Neurophysiol, vol. 70, Dec. 1988, pp. 510–523, doi:10.1016/0013-4694(88)90149-6.

[11] L. Bianchi et al., "Which physiological components are more suitable for visual ERP based brain–computer interface? A preliminary MEG/EEG study," Brain Topogr., vol. 23, Jun. 2010, pp. 180–185, doi:10.1007/s10548-010-0143-0.

[12] E. Donchin, K. M. Spencer, and R. Wijesinghe, "The mental prosthesis: Assessing the speed of a P300-based brain–computer interface," IEEE Trans. Rehabil. Eng., vol. 8, Jun. 2000, pp. 174–179, doi:10.1109/86.847808.

[13] C. Guger et al., "How many people are able to control a P300-based

brain–computer interface (BCI)?," Neurosci. Lett., vol. 462, Sep. 2009, pp. 94–98, doi:10.1016/j.neulet.2009.06.045.

[14] D. J. Krusienski, E. W. Sellers, D. J. McFarland, T. M. Vaughan, and J. R. Wolpaw, "Toward enhanced P300 speller performance," J. Neurosci. Methods, vol. 167, Jan. 2008, pp. 15–21, doi:10.1016/j.jneumeth.2007.07.017.

[15] E. W. Sellers, D. J. Krusienski, D. J. McFarland, T. M. Vaughan, and J. R. Wolpaw, "A P300 event-related potential brain–computer interface (BCI): The effects of matrix size and inter stimulus interval on performance," Biol. Psychol., vol. 73, Oct. 2006, pp. 242–252, doi:10.1016/j.biopsycho.2006.04.007.

[16] P. Cipresso et al., "The use of P300-based BCIs in amyotrophic lateral sclerosis: From augmentative and alternative communication to cognitive assessment," Brain Behav., vol. 2, Jul. 2012, pp. 479–498, doi:10.1002/brb3.57.

[17] J. N. Mak et al., "EEG correlates of P300-based brain–computer interface (BCI) performance in people with amyotrophic lateral sclerosis," J. Neural Eng., vol. 9, Apr. 2012, p. 026014, doi:10.1088/1741-2560/9/2/026014.

[18] F. Nijboer et al., "A P300-based brain–computer interface for people with amyotrophic lateral sclerosis," Clin. Neurophysiol., vol. 119, Aug. 2008, pp. 1909–1916, doi:10.1016/j.clinph.2008.03.034.

[19] R. Ortner et al., "Accuracy of a P300 speller for people with motor impairments," Clin. EEG Neurosci., vol. 42, Oct. 2011, pp. 214–218, doi:10.1177/155005941104200405.

[20] F. Piccione et al., "P300-based brain computer interface: Reliability and performance in healthy and paralysed participants," Clin. Neurophysiol., vol. 117, Mar. 2006, pp. 531–537, doi:10.1016/j.clinph.2005.07.024.

[21] E. W. Sellers and E. Donchin, "A P300-based brain–computer interface: Initial tests by ALS patients," Clin. Neurophysiol., vol. 117, Mar. 2006, pp. 538–548, doi:10.1016/j.clinph.2005.06.027.

[22] H. Kececi, Y. Degirmenci, and S. Atakay, "Habituation and dishabituation of P300," Cognitive and Behavioural Neurology, vol. 19, no. 3, Sep 2006, pp. 130–134, doi:10.1097/01.wnn.0000213911.80019.c1.

[23] A. Murata and A. Uetake, "Evaluation of Mental Fatigue in Human-Computer Interaction - Analysis using Feature Parameters Extracted from Event-Related Potential," in Proceedings of the 10th IEEE International Workshop on Robot and Human Interactive Communication, 2001, Sep 2001, pp. 630–635, doi:10.1109/ROMAN.2001.981975.

[24] A. Riccio et al., "Workload measurement in a communication application operated through a P300-based brain–computer interface," Journal of Neural Engineering, vol. 8, no. 2, Apr 2011, p. 025028, doi:10.1088/1741-2560/8/2/025028.

[25] G. R. Mangun and L. A. Buck, "Sustained visual–spatial attention produces costs and benefits in response time and evoked neural activity," Neuropsychologia, vol. 36, no. 3, Mar 1998, pp. 189–200, doi:10.1016/S0028-3932(97)00123-1.

[26] A. Riccio et al., "Attention and P300-based BCI performance in people with amyotrophic lateral sclerosis," Frontiers in Human Neuroscience, vol. 7, Nov 2013, pp. 1–9, doi:10.3389/fnhum.2013.00732.

[27] T. Kaufmann, C. Vögele, S. Sütterlin, S. Lukito, and A. Kübler, "Effects of resting heart rate variability on performance in the P300 brain–computer interface," International Journal of Psychophysiology, vol. 83, no. 3, Mar 2012, pp. 336–341, doi:10.1016/j.ijpsycho.2011.11.018.

[28] S. C. Kleih, F. Nijboer, S. Halder, and A. Kübler, "Motivation modulates the P300 amplitude during brain–computer interface use," Clin. Neurophysiol., vol. 121, Jul. 2010, pp. 1023–1031, doi:10.1016/j.clinph.2010.01.034.

[29] S. A. Sprague, D. B. Ryan, and E. W. Sellers, "The Effects of Motivation on Task Performance Using a Brain-Computer Interface," in Proceedings of the Fifth International BCI Meeting. Technischen Universität Graz, Jun 2013, p. 085, doi:10.3217/978-4-83452-381-5/085.

[30] J. Polich and A. Kok, "Cognitive and biological determinants of P300: An integrative review," Biological Psychology, vol. 41, no. 2, 1995, pp. 103–146, doi:10.1016/0301-0511(95)05130-9.

[31] T. Kaufmann, S. Völker, L. Gunesch, and A. Kübler, "Spelling is just a click away — A user-centered brain–computer interface including auto-calibration and predictive text entry," Front. Neurosci., vol. 6, May. 2012, p. 00072, doi:10.3389/fnins.2012.00072.

[32] D. B. Ryan et al., "Predictive spelling with a P300-based brain–computer interface: Increasing the rate of communication," Int. J. Hum.-Comput. Interact., vol. 27, Dec. 2010, pp. 69–84, doi:10.1080/10447318.2011.535754.

[33] W. Speier, I. Fried, and N. Pouratian, "Improved P300 speller performance using electrocorticography, spectral features, and natural language processing," Clin. Neurophysiol., vol. 124, Jul. 2013, pp. 1321–1328, doi:10.1016/j.clinph.2013.02.002.

[34] Ç. Ulaş and M. Çetin, "Incorporation of a Language Model into a Brain–Computer Interface-based Speller through HMMs," in Proc. 38th IEEE Int. Conf. Acoustics, Speech, and Signal Processing (ICASSP 2013), IEEE Press, May 2013, pp. 1138–1142, doi:10.1109/ICASSP.2013.6637828.

[35] J. Lu, W. Speier, X. Hu, and N. Pouratian, "The effects of stimulus timing features on P300 speller performance," Clin. Neurophysiol., vol. 124, Feb. 2013, pp. 306–314, doi:10.1016/j.clinph.2012.08.002.

[36] J. N. Mak et al., "Optimizing the P300-based brain–computer interface: Current status, limitations and future directions," J. Neural Eng., vol. 8, Mar. 2011, p. 025003, doi:10.1088/1741-2560/8/2/025003.

[37] D. J. McFarland, W. A. Sarnacki, G. Townsend, T. M. Vaughan, and J. R. Wolpaw, "The P300-based brain–computer interface (BCI): Effects of stimulus rate," Clin. Neurophysiol., vol. 122, Apr. 2011, pp. 731–737, doi:10.1016/j.clinph.2010.10.029.

[38] M. Salvaris and F. Sepulveda, "Visual modifications on the P300 speller BCI paradigm," J. Neural Eng, vol. 6, no. 4, Aug. 2009, p. 046011, doi:10.1088/1741-2560/6/4/046011.

[39] H. Serby, E. Yom-Tov, and G. Inbar, "An improved P300-based brain–computer interface," IEEE Trans. Neural Syst. Rehabil. Eng., vol. 13, Mar. 2005, pp. 89–98, doi:10.1109/TNSRE.2004.841878.

[40] J. J. Shih et al., "Comparison of Checkerboard P300 Speller vs. Row-Column Speller in Normal Elderly and Aphasic Stroke Population," in Proc. Fifth Int. BCI Meeting, Verlag der Technischen Universität Graz, Jun. 2013, p. 020, doi:10.3217/978-3-85125-260-6-20.

[41] D. L. Grover, M. T. King, and C. A. Kushler, "Reduced keyboard disambiguating computer," Patent US 5 818 437, 10 06, 1998.

[42] J. Höhne, M. Schreuder, B. Blankertz, and M. Tangermann, "A novel 9-class auditory ERP paradigm driving a predictive text entry system," Front. Neurosci., vol. 5, Aug. 2011, p. 00099, doi:10.3389/fnins.2011.00099.

[43] J. Jin et al., "P300 chinese input system based on Bayesian LDA," Biomed. Eng.-Biomed. Tech., vol. 55, Feb. 2010, pp. 5–18, doi:10.1515/BMT.2010.003.

[44] T. Kaufmann, E. M. Holz, and A. Kübler, "Comparison of tactile, auditory and visual modality for brain-computer interface use: A case study with a patient in the locked-in state," Front. Neurosci., vol. 7, Jul. 2013, p. 00129, doi:10.3389/fnins.2013.00129.

[45] R. Ron-Angevin and L. da Silva-Sauer, "Proposal of a P300-based BCI Speller Using a Predictive Text System," in Proc. Int. Cong. Neurotechnology, Electronics and Informatics (NEUROTECHNIX 2013), SCITEPRESS Digital Library, Sep. 2013, pp. 35–40.

[46] "Corpus de referencia del español actual (CREA) - Listado de frecuencias [Current Spanish Reference Corpus (CREA) - Frequency list]," http://corpus.rae.es/lfrecuencias.html [Retrieved January, 30, 2014].

[47] "World Medical Association Declaration of Helsinki: Ethical Principles for Medical Research Involving Human Subjects,". JAMA-J. Am. Med. Assoc., vol. 284, Dec. 2000, pp. 3043–3045, doi:10.1001/jama.284.23.3043.

[48] G. Schalk, D. J. McFarland, T. Hinterberger, N. Birbaumer, and J. R. Wolpaw, "BCI2000: A general-purpose brain–computer interface (BCI) system," IEEE Trans. Biomed. Eng., vol. 51, Jun. 2004, pp. 1034–1043, doi:10.1109/TBME.2004.827072.

 ISBN: 978-1-61208-340-7

Visual Awareness in Mind Model CAM

Zhongzhi Shi[1], Jinpeng Yue[1,2], Gang Ma[1,2]
[1]Key Laboratory of Intelligent Information Processing, Institute of Computing Technology
Chinese Academy of Sciences, Beijing, China
[2]University of Chinese Academy of Sciences, Beijing, China
e-mail: { shizz, yuejp, mag}@ics.ict.ac.cn

***Abstract*—Visual awareness is an important function in mind model CAM (Consciousness And Memory). In this paper，we construct a visual awareness component from two respects, namely, objective processing and spatial processing. The Conditional Random fields based Feature Binding computational model (CRFB) is applied to visual objective processing. For visual spatial processing, we explore three important kinds of relationships between objects that can be queried: topology, distance, and direction. The details of object processing and spatial processing are presented.**

Keywords-visual awareness; CAM; visual objective processing; visual spatial processing

I. INTRODUCTION

The visual system is characterized by functional specialization, and each different visual attribute is processed by a different specialized system. Psychophysical experiments have demonstrated that different visual attributes are perceived at different times and independently from each other. Most scientists have the common understanding that primary visual cortex (V1) perceives any visual feature, while higher brain areas may perceive particular visual features. A ventral pathway leading from V1 to the temporal lobe is for representing 'what' objects are. A dorsal pathway leading from V1 to the parietal lobe is for representing 'where' objects are located. The Middle-Temporal (MT) area is for motion perception.

Mental imagery resembles perceptual experience, but occurs in the absence of the appropriate external stimuli. Visual mental imagery is the thought to be caused by the presence of picture-like representations in the mind, soul, or brain. Kosslyn [1] proposed the processing system of visual mental imagery mainly consists of visual buffer, object properties processing, spatial properties processing, associative memories, information shunting and attention shifting.

Inspired by Kosslyn's visual mental imagery, Laird et al. [2] have added memory and processing structures to directly support perception-based representation. The Spatial-Visual Imagery (SVI) focused on modeling the characteristics of human mental imagery [3]. A Spatial Visual System (SVS) combines the concrete spatial representations and abstract symbolic representations [4]. All of these expanded Soar's capabilities [2] with human reasoning.

Object properties processing and spatial properties processing are two important processing issues in visual awareness. The paper will present the main principles for handling visual awareness in CAM (Consciousness And Memory) [5].

In this paper, Section II will outline the architecture of CAM. Object properties processing is discussed in Section III. Sections IV will explore the spatial properties processing. Finally, the conclusions of this paper are drawn and future works are pointed out.

II. CAM ARCHITECTURE

A mind model entitled CAM is proposed by Intelligence Science Laboratory of Institute of Computing Technology, Chinese Academy of Sciences [5]. Comparing with other mind models CAM has several important distinct characteristics, such as unique and sophisticated computational models for perception and cognition; complete memory system including working memory, short-term memory, and long-term memory which has semantic memory, episodic memory and procedural memory; the global workspace and motivation-model based consciousness. The architecture of CAM is illustrated in Figure 1 and organized into ten modules.

A. Visual Module

Visual module is the part of the central nervous system, which gives organisms the ability to process visual detail, as well as enabling the formation of several non-image photo response functions. It detects and interprets information from visible light to build a representation of the surrounding environment. The visual system carries out a number of complex tasks, including the reception of light and the formation of monocular representations; the buildup of a binocular perception from a pair of two dimensional projections; the identification and categorization of visual objects; assessing distances to and between objects; and guiding body movements in relation to visual objects. From Lateral Geniculate Nucleus (LGN) neuron send their signals to the primary visual cortex V1. About 90% of the outputs from the retina project to the LGN and then onward to V1. In the ventral pathway, many signals from V1 travel to ventral extra striate area V2, V3 and V4 and onward to many areas of the temporal lobe.

B. Aural Module

The auditory module is comprised of many stages and pathways that range from ear, to the brainstem, to subcortical nuclei, and to cortex. The advent of neuroimaging techniques has provided a wealth of new data for understanding the cortical auditory system.

 ISBN: 978-1-61208-340-7

C. Sensory Buffers

Each of the classical senses is believed to have a brief storage ability called a sensory buffer.

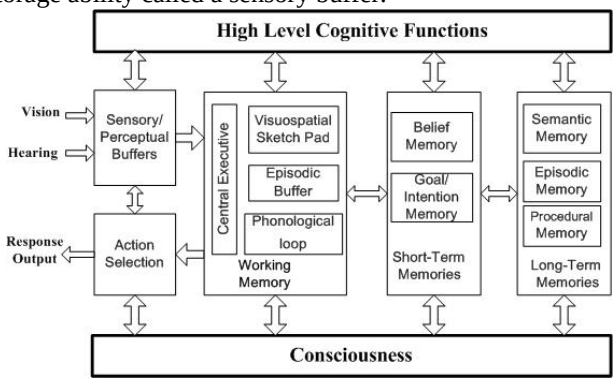

Figure 1. CAM architecture [6]

D. Working Memory

Baddeley [8] presented that working memory includes the central executive, visuo-spatial sketch pad, phonological loop and episodic buffer as illustrated in Figure 1 [7, 8]. The central executive is future directed and goal oriented in effective, flexible and adaptive. At the basic level the working memory is located in the prefrontal cortex. Working memory provides temporary storage and manipulation for language comprehension, reasoning, problem solving, reading, planning, learning and abstraction.

The ability to mentally maintain information in an active and readily accessible state, while concurrently and selectively process new information is one of the greatest accomplishments of the human mind. Working memory provides temporary storage and manipulation for language comprehension, reasoning, problem solving, reading, planning, learning and abstraction.

In working memory, the central executive is the core component. It drives and coordinates other subcomponents in working memory to accomplish cognitive tasks. The visuo-spatial sketch pad holds the visual information about what the cognitive system had seen. The phonological loop deals with the sound or phonological information. The episodic buffer stores the linking information across domains to form integrated units of visual, spatial and verbal information with time sequencing (or chronological ordering), such as the memory of a story or a movie scene. The episodic buffer is also assumed to have links to long-term memory and semantic meaning.

E. Short-Term Memory

Short-term memory stores agent's beliefs, goals and intention contents, which are change rapidly in response to environmental conditions and agent's agenda. Perceptual short-term memory stores the pre-knowledge of objects coded in relational coding scheme and empirical expectations of correlated objects.

F. Long-Term Memory

Long-term memory contains semantic, episodic and procedural knowledge which change gradually or not at all.

1) Semantic memory stores general facts which are represented as ontology. In philosophy, ontology is a theory about the nature of existence. In information science, ontology is a document or file that formally defines the relations among terms. The most typical kind of ontology for the semantic Web has a taxonomy and a set of inference rules. In CAM, ontology specifies a conceptualization of a domain in terms of concepts, attributes, and relations in the domain. Dynamic Description Logic (DDL) is used to define ontology [9].

2) Episodic memory is one part of long-term memory that involves the recollection of specific events, situations and experiences which are snapshots of working memory. Nuxoll and Laird demonstrated that an episodic memory can support an intelligent agent to own a multitude of cognitive capabilities [10].

In CAM, the episode is an elementary unit that stores previous scene in episodic memory where an episode is divided into two levels: one is an abstract level in terms of logic, another is a primitive level which includes perception information correlated to abstract level of the described object.

3) Procedural memory is a type of long-term memory for the performance of particular types of action. Procedural memory stores knowledge about what to do and when to do it. In ACT-R, 4CAPS, SOAR [2], etc., procedure knowledge is encoded as situation-action rules which provide an efficient and scalable representation. In CAM, procedural knowledge is represented in DDL logic.

G. Action Selection

Action selection is the process of constructing a complex composite action from atomic actions to achieve a specific task. Action selection can be divided into two steps, first is atomic action selection, i.e., select related atomic action from action library. Then, selected atomic actions are composed together using a planning strategy. One of action selection mechanism is based on a spiking basal ganglia model.

H. Response Output

The motor hierarchy begins with general goals, influenced by emotional and motivational input from limbic regions. The primary cortical motor region directly generates muscle based control signals that realize a given internal movement command.

I. Consciousness

The primary focus is on global workspace theory, motivation model, attention, and the executive control system of the mind in CAM. Baars [11] proposed the global workspace theory which all the elements have reasonable brain interpretations, allowing us to generate a set of specific, testable brain hypotheses about consciousness and its many roles in the brain. We presented a new motivation model which is 3-tuples {N, G, I}, where N means needs, G is goal, I means the motivation intensity [12].

 ISBN: 978-1-61208-340-7

J. High Level Cognitive Functions

It includes a class of high level cognitive functions, such as reasoning, planning, learning, etc., which perform cognitive activities based on the basic cognitive functions supported by the memory and consciousness components of CAM.

K. High Level Cognitive Functions

It includes a class of high level cognitive functions, such as reasoning, planning, learning, and etc., which perform cognitive activities based on the basic cognitive functions supported by the memory and consciousness components of CAM.

III. VISUAL OBJECTIVE PROCESSING

Many findings have shown that the ventral pathway acts as an object-properties processing subsystem, whereas the dorsal pathway acts as a spatial-properties processing subsystem. By "object properties" means shape, color, and texture; by "spatial properties" means relative positions in space of two or more objects or parts. Objective processing is to understand what the object is and spatial processing is to know where the object locates. Visual object processing is discussed in this section, whereas next section will explore visual spatial processing.

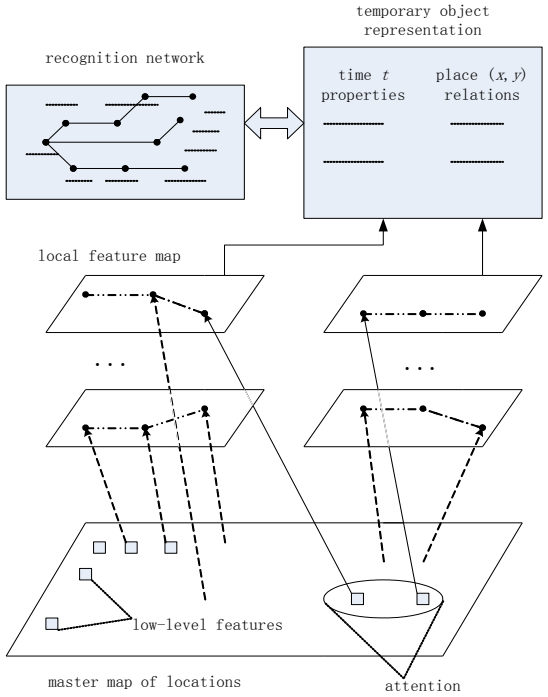

Figure 2. The framework of visual objective processing

We have proposed CRFB in 2010 [13]. Now we apply CRFB for visual object processing. Figure 2 shows the framework of CRFB model. We regard a whole image as a master map of locations [14]. With respect to the precise position tags on the master map, low-level image features are extracted. According to the relational coding schemes, the position tags and low-level image features are locally combined into feature maps [14]. When attentional window [15] scans the master map, the being scanned locations stimulate their corresponding feature maps, forming a temporary object representation, which describe the object in relational coding scheme with no object name. Then, we search the recognition network in perceptual short-term memory, which stores the pre-knowledge of objects coded in relational coding scheme and empirical expectations of correlated objects. When serial scan [15] (for a 2-D image, horizontal and vertical scans are sufficient) of the master map finished, we accomplish the binding process. In the whole process, the fundamental concepts and principles of random fields enlighten us a lot to model the binding problem.

Following the framework, we detail the image features extraction in subsection A. Next, we stipulate the relational coding schemes in subsection B. In subsection C, we learn the recognition network according to the maximum entropy principle. At last, we clarify visual conjunction search process in subsection D.

A. Low-level Feature Extraction

Feature extraction constructs combinations of the variables to get around these problems while still describing the data with sufficient accuracy. Low-level image features are cornerstones for feature binding process. It is desired that we could extract the feature of single object one by one, but to our disappointment, up till now, there are no methods could perfectly sketch the contour of single object among interacted ones. So, we synthesize the latest effective methods to extract image features to represent the low-level visual information to our best.

We present a Coding and Combing Feature framework (CCF) in multi-scale space. We first partition an image into square grids with the same size. For each grid, we compute complement features, i.e., the gradient texture histogram, color histogram and normalized intensity histogram. After various features are extracted, we compact them into efficient and effective codes. The coding process preserves as much information as possible and repesents features with effecive codes. The codes generated in the compact coding step are then combined by multi-kernel hashing to make a more discriminative feature representation. The final representation is effective in different situations. Then, we enlarge the size of the grid and obtain the features for the larger grid as the former procedure and we regard the feature of the larger grid as regional feature. At last, we normalize the local features for an image into a vector. For many images, vectors are clustered and each image is assigned an index of cluster center. We call the index global feature of an image.

The coding and combining framework is evaluated on the UKbench image retrieval dataset [16]. From Figure 3, we can see that the combined feature achieves a higher recall than the color histogram and the texture feature. The combined feature utilizes complementary features and benefit from compact coding; thus, the features generated by our CCF framework is more discriminative and robust.

 ISBN: 978-1-61208-340-7

The multi-scale feature is proposed for the following two reasons: a) It is intractable to represent the feature of an object for difficult outlining objects. Features from different scales could compensate the above problem on some extent; b) Multi-scale feature enrich our association function in relational coding scheme, which we will see in subsection B.

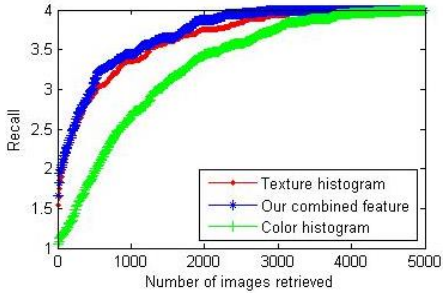

Figure 3. Combined feature evaluation

B. Relational Coding Scheme

We stipulate the relational coding scheme for three functions. First, we lock the low-level features to the locations of the master map. Secondly, correlations between low-level features and high-level knowledge are coded. Thirdly, transfer relations among knowledge are coded. These functions also construct the local feature map. For the first function, we build a 2-D coordinates for the image, then, assign each local grid a precise position (x, y), so we can map the location to the corresponding low-level feature.

We implement the second function under the following considerations: *a*) a longer coding scheme is expected to manage the unstructured image information; *b*) the coding length is restricted by the attentional window. So, we make a compromise to design a reasonable length of the coding scheme. We introduce the association function, inspired by the state feature function [17], to encode the correlations. Let o be an observed low-level local feature, s_t be a state s at time t and l be a name of some object. Association function is defined as follows,

$$f_i(o, s_t) = \delta\left(x_i(o,t)\right)\delta(s_t = l) \quad (1)$$

where s_t=l means that current state s_t is associate with the object name l. $x_i(o,t)$ is a logical function to judge whether or not a specific serial of low-level features. $\delta(e)$ is equal to 1 if the logical expression e is true, and 0 otherwise. We design the logical function $x_i(o,t)$ within the attentional window. Figure 2 shows the procedure.

In Figure 4, the attentional window size is $2n$ +1, so the maximum length of our logical function is n+1. The arrow indicates the current state. o represents the low-level local feature, r represents the combination of low-level regional and global feature and l represents the high-level knowledge. For a current state, there are some fixed schemes to construct $x_i(o,t)$, such as o_0, $o_{-1}o_0$, $r_{-1}r_0$, $r_{-1}r_0o_0$ and so on. We can see that multi-scale low-level features are engaged to construct $x_i(o,t)$, which gives more feature combination schemes for logical function than with the low-level local features only. For a 2-D image, adjacent low-level features are correlated by the logical function. We associate the current observed low-level feature with its horizontal and vertical neighbors within length n to construct $x_i(o, t)$. The 2-D structural correlation coding scheme could better reflect the image semantics.

We introduce the interaction function, similar to the edge feature function [16], to realize the third function. Interaction function is defined as follows,

$$g_j(s_{t-1}, s_t) = \delta(s_{t-1} = l')\delta(s_t = l) \quad (2)$$

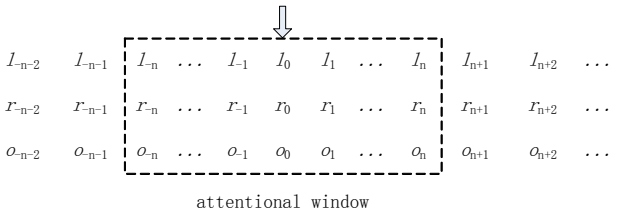

Figure 4. Designing the logical function $x_i(o,t)$.

We introduce the interaction function, similar to the edge feature function [17], to realize the third function. Interaction function is defined as follows,

$$g_j(s_{t-1}, s_t) = \delta(s_{t-1} = l')\delta(s_t = l) \quad (2)$$

This formula suggests that the interaction function presents the object name transfers from previous state to current state, which indeed indicates the transfer scheme of high-level knowledge. Similar to the association function, the knowledge transfer scheme also employed a 2-D structure, coding the relational knowledge horizontally and vertically.

We assemble the association and interaction functions as relation functions, which construct the local feature map. With the ensemble of local feature maps, we can represent the relationships among low-level features and high-level knowledge.

C. Learning the Recognition Network

Relational Coding associate the local feature maps with the master map of locations. At the same time, abundant chaotic correlations between low-level feature and high-level knowledge are supplied. How do we organize the association functions and the interaction functions to gain maximal empirical pre-knowledge for recognizing object?

We need to build a probability distribution p as general as possible to give a maximum entropy of the relation functions which contains the maximal quantity of information [18]. We apply certain expectation constraints with respect to feature functions:

$$E\left(f_i(o, s_t)\right) = \alpha_i \quad (3)$$

$$E\left(g_j(s_{t-1}, s_t)\right) = \beta_j \quad (4)$$

For the association function $f_i(o,s_t)$, if certain serial of observed low-level features associate with some object name, it equals 1, otherwise 0; for the interaction function $g_j(s_{t-1},s_t)$,if the previous object transfers to the current one, it equals 1, otherwise 0. In enormous observing samples, we may set the expectation value $\alpha_i = \propto, \beta_j = \propto$. We assume p_x an element of finite length vector P. Now we may formalize our

target as a convex optimization problem subject to linear constraints:

$$\max_{p} \quad -\sum_{x} p_x \log p_x \tag{5}$$

subject to

$$\sum_{x} p_x f_i(o, s_t) = \alpha_i \tag{6}$$

$$\sum_{x} p_x g_j(s_{t-1}, s_t) = \beta_j \tag{7}$$

$$\sum_{x} p_x = 1 \tag{8}$$

We write the Lagrangian as

$$J = -\sum_{x} p_x \log p_x + \sum_{i} \lambda_i \left(\sum_{x} p_x f_i(o, s_t) - \alpha_i \right) + \sum_{j} \mu_j \left(\sum_{x} p_x (s_{t-1}, s_t) - \beta_j \right) + \theta \left(\sum_{x} p_x - 1 \right) \tag{9}$$

Taking derivatives with respect to a specific element p_x

$$\frac{\partial J}{\partial p_x} = -1 - \log p_x + \sum_{i} \lambda_i f_i(o, s_t) + \sum_{j} \mu_j g_j(s_{t-1}, s_t) + \theta = 0 \tag{10}$$

Hence

$$p_x = \frac{1}{Z} \exp\left(\sum_{i} \lambda_i f_i(o, s_t) + \sum_{j} \mu_j g_j(s_{t-1}, s_t) \right) \tag{11}$$

That is the distribution we are pursuing. In learning process, we estimate the weight parameters of the relation functions through the *K* training image samples by maximum the log-likelihood of the objective function [18]:

$$L(\lambda, \mu) = \sum_{k} \log p_x(\mathbf{s_k}, \mathbf{o_k}) \tag{12}$$

We define

$$F(\mathbf{s_k}, \mathbf{o_k}) = \sum_{i} \lambda_i f_i(o, s_t) + \sum_{j} \mu_j g_j(s_{t-1}, s_t) \tag{13}$$

Then, we seek the zero of gradient

$$\nabla L(\lambda, \mu) = \sum_{k} \left[F(\mathbf{s_k}, \mathbf{o_k}) - E_{p_x(\mathbf{S}|\mathbf{o_k})} F(\mathbf{S}, \mathbf{o_k}) \right] \tag{14}$$

The expectation $E_{p_x(\mathbf{S}|\mathbf{o_k})} F(\mathbf{S}, \mathbf{o_k})$ can be efficiently computed with the forward-backward algorithm in [17]. For the 2-D structural of our relation functions, the transition matrix differs [17] in the following formula

$$M_t(l', l) = \exp\left(\sum_{m} \lambda_m f_m(s_t, o) + \sum_{n} \mu_n g_n(s_{t-1}, s_t) \right) \tag{15}$$

which means that the current matrix $M_t(l', l)$ sums up all the association functions and interaction functions of current state s_t in both horizontal and vertical direction. We penalize the likelihood with a spherical Gaussian weight prior to avoid overfitting [20]. We input the gradient of the log-likelihood to the L-BFGS [21] algorithm for an iteration process which gives the values of parameters $(\lambda_1, \lambda_2, \cdots \mu_1, \mu_2, \cdots)$. With the weighed relation functions, we build the recognition network. Suppose we have learnt $|L|$ categories of object, we can build a $|L| \times |L|$ knowledge transfer matrix by summing up the weighted interaction functions across the overall learning samples where $g_j(s_{t-1}, s_t)$ satisfies $s_{t-1} = l'$ and $s_t = l$.

$$M_i(l', l) = \exp\left(\sum_{j} \mu_j g_j(s_{t-1}, s_t) \right) \tag{16}$$

The transfer matrix implies the empirical knowledge that on what extent object *B* co-occurs with the object *A*. The association functions with weights, which indicate how much low-level features relate to a specific object, are stored in the recognition network, ready for retrieval.

D. Conjunction Search

The binding process is driven by both attention and particular expectations. Attention works through the attentional window scanning the image and expectations mean predicting the presence of a particular object by contextual constraints, which can be represented by the knowledge transfer matrix. With the preparations in the former sections, we clarify the conjunction search below.

When a new image comes, low-level features are first extracted in a set $S = \{o_1, o_2, \cdots r_1, r_2 \cdots\}$. Then, local feature maps are generated in relational coding scheme. Here, our local feature maps only code the location information and the related serial of low-level features. Location information is coded in a map where each local feature o_i in *S* corresponds to an only precise position coordinate (x_i, y_i), formulated as $o_i \leftrightarrow (x_i, y_i)$. Positional adjacent features are coded in the form: $\mathbf{c} = o_1 \cdots o_s r_1 \cdots r_k (s, k \le n+1)$. Next, at time *t*, the attentional window whose maximum size is $2n+1$, scans the master map of locations with respect to both horizontal and vertical directions. Low-level features within attentional window are cared, and the outside features are temporarily neglected. The relevant feature maps are activated by the window to form a temporary object representation, which contains the location of low-level features and the low-level features combination schemes set $C = \{c_1, c_2, \cdots\}$,of the current state s_t. Now, we search the recognition network to find the association functions which contain the element of set ***C***. Related weighted association functions containing the same object name *l* are added up. Looking up to the transfer matrix, we obtain the transfer probability from every other object *l'* to *l*. We pick the maximal exponential sum of the two factors to be the object *l* associated with state s_t as formula (17).

$$\max \left\{ \underbrace{\exp\left(\sum_{i} \lambda_i f_i(s_t, o) + \sum_{j} u_j g_j(s_{t-1}, s_t) \right), \ldots}_{\text{total number } |L|} \right\} \tag{17}$$

As the attentional window moving forward step by step, the procedure we discussed above is repeated. With regards to the previous states, we get a recursive expression as follows

$$\varphi_{t+1}(s_i) = \max_{s_j} \left(\varphi_t(s_j) \exp F(\mathbf{s}, \mathbf{o}, t+1) \right) \tag{18}$$

where $\varphi_t(s_i)$ denotes the probability that state s_i associate with a particular object *l*. When attentional window scans over the whole image, we obtain the conjunction search result as follows

$$\mathbf{s}^* = \arg\max_{\mathbf{s}} \exp\left(\sum_{t} F(\mathbf{s}, \mathbf{o}, t) \right) \tag{19}$$

 ISBN: 978-1-61208-340-7

We apply Viterbi algorithm to the above process to perform an efficient computing. When conjunction search finished, we bind the features to get an integrated understanding of the image.

Conjunction search procedure can be accelerated by the hint of feature inhibition [15], which means that the active features suppress the non-target features. In the low-level local features, adjacent features share similar characteristics causing identical local feature maps. We define the highly similar local features as non-target features. In the conjunction search process, when we come across non-target features, we ignore them and move the attentional window to the next target features. By doing so, we obtain the same binding result but compute less.

Conjunction search associates the every element of low-level local feature set *S* with object name *l*. Looking up to the map of relational coding scheme, using $o_i \leftrightarrow (x_i, y_i)$, we can locate the objects in one image. Up till now, the recognition task is accomplished.

IV. VISUAL SPATIAL PROCESSING

Visuo-spatial sketch pad holds the information it gathers during the initial processing and often in normal thought processes with visualization and conscious effort. Logie has proposed that the visuo-spatial sketch pad can be subdivided into two components [22]: a) The visual cache, which stores information about form and color. b) The inner scribe deals with spatial and movement information.

In order to do visual spatial processing, we follow SVS idea which is proposed by Wintermute [4]. CAM adds a quantitative spatial representation in the spatial scene short-term memory and a visual depictive presentation in the visual buffer short-term memory. In addition to the two short-term memories, there is a long-term memory in CAM for visual, spatial, and motion data and it is called Perceptual LTM. Visual imagery is cognitively useful and can be implemented without true perception. Predicate extraction provides symbolic processing with qualitative properties of the contents of the spatial scene and visual buffer.

For the spatial system, there are three important kinds of relationships between objects that can be queried: topology, distance and direction. Topological relationships describe how the surfaces of objects relate to one another. Distance queries are similarly simple. Currently, the system can query for the distance between any two objects in the scene along the closest line connecting them. Direction queries are implemented as in the approach of Hernández [23].

V. CONCLUSIONS AND FUTURE WORKS

Visual awareness is an important function in mind model CAM. This paper has presented to apply the conditional random fields based feature binding computational model (CRFB) for visual objective processing. We have also shown the main idea for visual spatial processing in the paper.

Visual spatial processing is more difficult and we will continue to look for good representation and algorithm to solve the problem.

ACKNOWLEDGMENT

This work is supported by the National Program on Key Basic Research Project (973) (No. 2013CB329502), National Natural Science Foundation of China (No. 61035003, 61202212, 61072085), National High-tech R&D Program of China (863 Program) (No.2012AA011003), National Science and Technology Support Program(2012BA107B02).

REFERENCES

[1] S. M. Kosslyn, “Mental Images and the Brain.”, Cognitive Neuropsychology, 2005, 22 (3/4): pp. 333–347.

[2] J. E. Laird, “The Soar Cognitive Architecture.” MIT Press, 2012.

[3] S. D. Lathrop, “Extending Cognitive Architectures with Spatial and Visual Imagery Mechanisms.” Ph.D. dissertation, University of Michigan, 2008.

[4] S. Wintermute, “An Architecture for General Spatial Reasoning.” Ph.D. Dissertation. University of Michigan, 2009.

[5] Z. Shi, “On Intelligence Science and Recent Progress.” Invited Speaker, ICCI2006, Beijing, 2006.

[6] Z. Shi, J. Yue, J. Zhang, “Mind Modeling In Intelligence Science.” IJCAI WIS-2013, 30-35, 2013.

[7] A. D. Baddeley, “Working Memory.” Oxford: Oxford University Press, 1986.

[8] A. D. Baddeley, “The episodic buffer: a new component of working memory?” Trends Cogn. Sci. (Regul. Ed.), 2000, 4 (11): pp. 417–423.

[9] L. Chang, Z. Shi, T. Gu, and L. Zhao, “A Family of Dynamic Description Logics for Representing and Reasoning About Actions”, J. Autom. Reasoning, 2012, 49(1): pp. 1-52.

[10] A. Nuxoll and J. E. Larid, “Extending Cognitive Architecture with Episodic Memory”, In Proceedings of the 22nd AAAI Conference on Artificial Intelligence, 2007, pp. 1560-1564.

[11] B. J. Baars, “In the Theatre of Consciousness: Global Workspace Theory, A Rigorous Scientific Theory of Consciousness”. Journal of Consciousness Studies 4, 1997, 4: pp. 292-309.

[12] Z. Shi, J. Zhang, J. Yue, and B. Qi, “A Motivational System For Mind Model CAM”, AAAI Symposium on Integrated Cognition, pp. 79-86, Virginia, USA, 2013.

[13] X. Wang, X. Liu, Z. Shi, and H. Sui, “A feature binding computational model for multi-class object categorization and recognition.” Neural Computing and Applications, 2012, 21(6): pp. 1297-1306.

[14] A. Treisman and G. Gelede, “A feature-integration theory of attention”. Cognit Psychol, 1980, 12: pp. 97-136.

[15] A. Treisman, “Feature binding, attention and object perception” Phil. Trans. R. Soc. Lond. B, 1998, 353, pp. 1295-1306.

[16] D. Nister and H. Stewenius, “Scalable Recognition with a Vocabulary Tree”. In CVPR, 2006, pp. 2161-2168.

[17] J. Lafferty, A. McCallum, and F. Pereira. “Conditional random fields: Probabilistic models for segmenting and labelling sequence data”, In Proceedings of the Eighteenth International Conference on Machine Learning (ICML), 2001, pp. 282–289.

[18] H. Wallach, “Efficient Training of Conditional Random Fields”, M.Sc. thesis, Division of Informatics, University of Edinburgh, 2002.

[19] F. Sha and F. Pereira. “Shallow Parsing with Conditional Random Fields”. Proceedings of HLT- NAACL 2003 213-220N.

 ISBN: 978-1-61208-340-7

[20] S. F. Chen and R. Rosenfeld. “A Gaussian prior for smoothing maximum entropy models”. Technical Report CMU-CS-99-108, Carnegie Mellon University, 1999.

[21] R. H. Byrd, J. Nocedal, and R.B. Schnabel. “Representations of quasi-newton matrices and their use in limited memory methods”, Mathematical Programming, 1994, 63:129–156.

[22] R. H. Logie, “Visuo-Spatial Working Memory.” Lawrence Brlbaum Associates Ltd., Publishers, East Sussex, UK, 1995.

[23] D. Hernández, "Qualitative Representation of Spatial Knowledge ." Springer-Verlag, 1994 .

 ISBN: 978-1-61208-340-7

How the Relationship Between Information Theory and Thermodynamics Can Contribute to Explaining Brain and Cognitive Activity: An Integrative Approach

Guillem Collell
Research Unit in Cognitive Neuroscience, Dptm. Psychiatry & Forensic Medicine
Universitat Autònoma de Barcelona
Bellaterra (Cerdanyola del Vallès), Spain
g.collell@student.maastrichtuniversity.nl

Jordi Fauquet
Dptm. Psychobiology & Methodology of Health Sciences
Universitat Autònoma de Barcelona
Bellaterra (Cerdanyola del Vallès), Spain
Jordi.Fauquet@uab.cat

***Abstract*— The brain is both a thermodynamic system and an information processor. Cognition is described well in terms of information-based models and brain activity as a physical process, is accurately addressed via a thermodynamic approach. A connection between information theory and thermodynamics in neuroscience is currently lacking in the literature. The aim of this paper is to propose an integrative approach regarding information and energy as two related magnitudes in the brain, and to discuss the main connections between information theory and thermodynamics that may be helpful for understanding brain activity. In this sense, the link between both approaches is based on the concepts of entropy and negentropy, the Boltzmann formula, the Landauer's Principle and the energetic cost for the observation of information proved by Szilard. This set of connections enables us to show that information and energy are two strongly related and interchangeable magnitudes in the brain with the possibility of making this relationship explicit, as well as the possibility of translating the quantities from one to the other. This view also contributes to a better understanding of the fundamental relationship between cognition and physical brain activity. Finally, we propose new conjectures and future lines to work concerning the study of spontaneity of the brain activity from this integrative perspective.**

Keywords-entropy; negentropy; brain thermodynamics; cognitive models; information theory.

I. INTRODUCTION

The brain is both a thermodynamic system and an information processor. Hence, it is indeed subjected to the main constraints of both theories, i.e., the second law of thermodynamics as well as Shannon's source coding theorem, which states that a message cannot be compressed below its entropy bound [1]. It is well known that there exists a set of connections between information theory and thermodynamics. These are essentially its respective entropies and negentropies, as well as the Boltzmann formula, the Landauer's Principle [1][11] and the energetic cost for the observation of information proved by Szilard [2].

Several attempts have been made to find a tenable explanation for brain activity from the framework of thermodynamics, as well as from the information theory perspective [3]. The first perspective describes well the physical brain activity, and the second is able to explain several cognitive aspects (perception, learning, action, active inference, etc.) [4][5]. On the one hand, we consider the contribution of Prigogine [6] to the field of the thermodynamics of the open dissipative systems, in which the brain fits well. In this sense, the concept of *negentropy* is essential [7], and its flow can be expressed by an ordinary differential equation that describes the energetic income/outcome of the brain [8]. Following the thermodynamic stream, La Cerra [9] proposed a physically-principled model of the mind, embedded in an energetic framework. It regards the brain as the machine in charge of ensuring by means of adaptive behavioral responses the optimal ratio of costs/benefits in energetic terms for the entire system. From this perspective, the second law of thermodynamics is considered the main principle that rules human brain activity. On the other hand, Friston [4] presents an information-based brain model embedded in Bayesian variational analysis and hierarchical generative dynamics. This model describes well the learning, perception and inference cognitive processes. From this viewpoint, it is legitimate to expect that if there exists a set of connections between thermodynamics and information theory, these must preserve the validity of the statements and principles that underlie each of the above models, and will show, indeed, a high degree of consistency when we transform the quantities and magnitudes from one model to the other by using such links. That is to say, if a certain model predicts the change of the system in one direction basing its prediction on energetic measures, we expect to find the same outcome in an information-based model if we translate these energetic quantities into its equivalent information magnitudes.

In Section II, we expose the main connections between thermodynamics and information theory that may be useful for understanding the exchange between energy and information in the brain. In Section III, we introduce, analyze and connect some of the most relevant brain and cognitive models formulated from the scope of thermodynamics as well as from the information theory viewpoint. Thereafter, we give insight for a new integrative approach to the brain activity considering the points commented before. Finally, we make some conjectures referred to the possibility of using this new view of brain modeling in order to study the spontaneity of the cognitive and brain processes.

 ISBN: 978-1-61208-340-7

II. CONNECTIONS BETWEEN INFORMATION THEORY AND THERMODYNAMICS

A selection of the connections between information theory and thermodynamics that may be helpful for understanding brain activity is presented in this section.

A. The thermodynamic and Shannon's entropies and negentropies

A core concept appears in both theories, the so-called *entropy*. The meaning of the thermodynamic entropy and Shannon's entropy -from information theory- is not exactly the same, but the intuitive ideas behind both are very similar, as Boltzmann formula evidences.

The meaning of the *physical entropy* S is essentially the degree of disorder of the system, namely the energy dissipated in the form of molecular vibration that cannot be used to produce work. Its difference ΔS between two states a_1 and a_2 can be computed as follows [10]

$$\Delta S = S_1 - S_2 = \int_{a_2}^{a_1} \frac{\delta Q}{T} \quad (1)$$

where Q is the heat function and T the absolute temperature of the system.

From entropy, its complementary concept appears naturally, namely *negentropy* or *free energy* [7]. It corresponds to the amount of energy that can be used to produce work. For instance, there is negentropy present in a system that has an electrical or a pressure gradient, like a neuron before spiking. In the physical sense, it can be described as the Helmholtz free energy F_H [6]

$$F_H = U - TS \quad (2)$$

where U is the internal energy of the system.

Before describing Shannon's entropy, we must first define the *information I* contained in one character x_i [11]:

$$I(x_i) = -\log_2 p(x_i) \quad (3)$$

where $p(x_i)$ is the probability of the occurrence of the character x_i.

The information expected in one message X composed of one character from the set of all possible $\{x_i\}$, i=1,...,n is known as *Shannon's entropy H:*

$$H(X) = -\sum p(x_i) \log_2 p(x_i) \quad (4)$$

B. The Boltzmann formula

The first statistical formulation of thermodynamic entropy was provided by Boltzmann in 1877, giving an absolute interpretation of this quantity (no longer as a measure of the entropy difference between two states). Historically, this work was done about 70 years before Shannon's entropy was introduced. In particular, the latter was thought of an abstraction of the former.

The physical entropy S of a system can be computed as follows [10]

$$S = k \cdot \ln(W) \quad (5)$$

where W is the number of possible microstates of the system (assuming that all are equiprobable) and *k* is the Boltzmann constant (approximately $1.38 \cdot 10^{-23}$).

C. Landauer's principle and the information observation

Szilard [2] proved that there is a minimum energetic cost of $T \cdot k \cdot ln(2)$ J (or equivalently, an increase of physical entropy of $k \cdot ln(2)$ J/K) that every system must pay in order to observe one bit of information, namely if we want to know whether it is a "0" or a "1". Here, *k* is the Boltzmann constant. Brillouin generalized this principle stating that negentropy can always be transformed into information and vice versa [12].

Likewise, Laundauer's principle states that the same minimal quantities are to be paid for encoding (or erasing) the same bit of information [1]. This energetic cost for both procedures is due to the very nature of them, which are, in turn, the most optimal possible.

III. THE THERMODYNAMIC AND THE INFORMATION-BASED MODELS OF THE BRAIN AND COGNITION

A selection of thermodynamic models is considered for our work. These can be regarded together as a simple set of equations and principles that describes brain activity in energetic terms. Thereafter, we briefly illustrate the main ideas of Friston's model [4], which describes cognition in terms of information theory. Since it is not the aim of this paper, we will leave out the mathematical details of this theory and will focus on the intuitive concepts behind it. Nevertheless, we want to stress that the mathematical treatment of this model is fundamental in order to connect the two theories. Moreover, an important part our current work is based on the mathematical definitions of the respective entropies and free energies present in both theories.

A. Thermodynamic models of the brain activity

A fundamental constraint to which all thermodynamic systems are subject is the *second law of thermodynamics*. It states that the entropy for every isolated system can only increase (except for small random fluctuations, according to its probabilistic formulation). Thus, this principle restricts the *spontaneous processes* (i.e., those that occur without external help) to only one possible direction, namely the one which implies a gain of entropy, or, equivalently $dS/dt \geq 0$. By using the above links, the second law of thermodynamics can be reformulated into informational terms as: "our information about an isolated system can never increase (only by measurement can new information be obtained). Reversible processes conserve, irreversible ones (mostly spontaneous) loose information." [13]

The brain is a thermodynamic device characterized by being an open dissipative system, isothermal, isobaric and with a constant flow of negentropy [8]. In order to study the entropy exchange between the inside and outside of the

brain (and the same can be applied to a single neuron or every biological system), we must split the dS into two terms, making the distinction between the entropy produced within the system $d_i S$, and the transfer of entropy across its boundaries $d_e S$ [6]. Therefore, since the second law of thermodynamics must hold, after every cognitive task $d_i S > 0$ is always obtained. This initial increase of entropy within the system is always followed by a removal of entropy through its frontiers in order to preserve the structure and functionality [3][9]. Moreover, so as to recover the capacity of producing work (e.g., to transmit an electric impulse) there must be an inflow of negentropy (adenosine triphosphate (ATP), for instance). Hence, this energy/entropy flow for the brain can be expressed by the following ordinary differential equation [8] obtained by differentiating (2).

$$\frac{dF_H}{dt} + T\frac{d_i S}{dt} = J_{i1} + J_{c1} - J_{i2} - J_{c2} \quad (6)$$

Here, J_i and J_c denote the radiation and chemical energy flows respectively, and the subscripts 1 and 2 refer to the incoming and out coming flows [8].

From this perspective, the brain activity is driven by the quest to consume free energy in the least possible time [14]. That is to say, the flows of energy (i.e., electric activity) themselves will search for the paths of transduction, selecting those that consume free energy in the least time. The transduction paths are established when an experience, encoded in some sort of energy, is recorded. These paths for energy dispersal within the neuronal network constitute memory, i.e., the register of remembrance that can be consolidated or reorganized when a certain path is activated again by an energy flow.

B. Information-based model of cognition

Friston's model is embedded in machine learning framework and regards the brain as an inference machine ruled by the "free energy minimization principle". Here the so-called free energy is defined as an upper bound for what Friston defines as "surprise", i.e., how unlikely it is for the system to receive a certain input. In short and skipping mathematical content, the free energy function F can be expressed conceptually as:

(i) F = Cross Entropy + Surprise

At the moment, we just notice that the "cross entropy" is a positive term (the so-called Kullback-Liebler divergence). Equivalently, by algebraic rearrangement of its mathematical formulation the following equation is obtained

(ii) F = Expected Energy – Entropy

where "expected energy" corresponds to the surprise of observing an input jointly with its cause, and "entropy" is equivalent to the Shannon's entropy of the variable causes (i.e., what caused input). Interestingly, notice that (ii) resembles the Helmholtz free energy in the physical sense.

Via free energy minimization, neuronal networks [4] always tend to optimize the probabilistic representations of what caused its sensory input, and therefore the prediction error is minimized. This free energy minimization in the system can be performed by changing its configuration to change the way it samples the environment, or by modifying its expectations [4]. Therefore, hypothetically the system must encode in its structure a probabilistic model of the environment, and the brain uses hierarchical models in order to construct its prior expectations in a dynamic context. In this sense, this model is capable of explaining a wide variety of cognitive processes.

C. Connections between the two approaches

A close look at Friston's and La Cerra's models yielded a finding of the following functional similarities:
(1) The system (brain) must avoid phase transitions, i.e., drastic changes in its structure and properties, and (2) the system encodes a probabilistic relationship between: the internal state of the organism, specific sensory inputs, behavioral responses, and the registered adaptive value of the outcomes of these behaviors.

Interestingly, we notice that the principles that underlie both the thermodynamic model of the brain and the information-based model of cognition are consistent in the sense that they steer the system in the same direction. Let us consider the case where both the Friston's and the thermodynamic free energies are large within a certain neuronal population. In the Friston's case, this indicates that the input received is highly "surprising" (e.g., facing a novel or dangerous situation). According to this model, the system will react by taking some action as well as by updating its perception, yielding to free energy minimization ($\Delta F < 0$). The same will occur under the same situation if we think in terms of thermodynamics models. The physical free energy is also large due to the initial blood and energetic inflow that accompanies a novel situation, but this amount will be rapidly reduced by the activation of neuronal paths that consume free energy in the least possible time ($\Delta F_H < 0$). By doing so, the brain is carrying out a codification task in the sense that a smaller amount of free energy will be necessary to activate the same neuronal path on subsequent occasions. Analogously, Friston's model prescribes a subsequent prediction error reduction (i.e., a better encoding of the causes of the input) following this free energy minimization.

In order to provide some insight into how the information must be encoded, let us suppose that we are set the task of memorizing a random number between 0 and 256. It is obvious that we have to encode it somewhere in our neuronal network. Due to Shannon's source coding theorem, we cannot codify it using fewer bits than the information contained in it. Thus, at least 8 bits ($I = \log_2(256) = 8$ bits), namely 8 "places" in our brain circuitry with 2 possible combinations in each one. Of course, we must consider that some numbers can be compressed by using some heuristics.

 ISBN: 978-1-61208-340-7

The former statement can be generalized to every behavior or cognitive task, considering that these are nothing but an "algorithm" that our brain has to encode in our neuronal network, even if it is not a permanent, but rather, a temporal encoding in our working memory.

Clearly, the Szilard and Landauer principles shed some light on the theoretical bounds for the exchange between information and energy present in the brain activity. Nevertheless, these are not realistic quantities in this context, since the encoding mechanisms in the brain are far from being entirely efficient. Moreover, there are also important noise and redundancy factors [15]. Laughlin has shown that considering a consumption of 10^6 ATP molecules for each neuronal spike and the fact that a sensory spike carries between 1 and 10 bits of information, then, the metabolic cost for processing 1 bit of information is about to 10^5 ATP molecules [16], or equivalently $5 \cdot 10^{-14}$ Joules. This means that the human brain is operating about 10^7 times above the thermodynamic limit of $k \cdot T \cdot ln(2)$ J per each bit encoded, which is still more efficient than the modern computers. We want to highlight the fact that these quantities refer to the energetic cost of visual perceptive processing, and therefore, these cannot be extrapolated neither to all the brain areas nor to all cognitive processes, since the redundancy and noise factors are topographic and population-size dependent [15]. In general, the larger the neuronal ensembles, the greater the number of redundant interactions between neurons. We hypothesize that the exchange between energy and information in the brain is performed at a constant rate, similar to Landauer's limit, but this constant depends on the redundancy factor of a particular neuronal ensemble as well as on the type of neurons it contains. This limit would be given by the very nature of the neuronal encoding procedures. Besides, it is clear that higher level visual areas like for instance the MT (responsible of motion perception) are processing, at most, the whole amount of bits received from the sensory neurons plus some extra information that is already stored in our neuronal network (i.e., our pre-knowledge or expectations about the world) which is necessary to integrate the new input. For our conscious and deliberate thinking (e.g., solving a problem that affects our life), there is no external sensory information to integrate, and therefore all the information processed comes from the internal representations stored in our neuronal network. From this, we can conclude that a measure of the energetic expense during a certain cognitive task obtained by means of electroencephalography (EEG) or functional magnetic resonance (fMRI) (ideally a combination of both) would provide a reliable measure of the processing complexity of this task, as well as about its information content. For the conversion from observed energy into its information content we must have previous knowledge about the redundancy factor of the involved brain areas, as well as its energetic cost of processing (as Laughlin computed for the visual sensory coding). Conversely, the model could also be checked the other way around, that is estimating first the necessary information to compute a certain cognitive operation (e.g., a mathematical mental computation) and then comparing the energy expense seen in fMRI and/or EEG during the task with the predicted quantity. From machine learning and computational approaches, the prediction of the information content of a certain cognitive operation could be obtained by computing an equivalent algorithm which carries out the same process in a computer. Indeed, an integrative model must incorporate the referred energetic-informational correspondence so as to allow making predictions by using both magnitudes. We suggest that the empirical validation of the model should be done in the direction described in the above lines.

We consider that a challenging aspect of the neuronal activity to explore is the concept of spontaneity. Namely the direction in which the transformations of the system occur, and which necessary (but not sufficient, due to the non-deterministic inherent character of brain activity) conditions are to be held for the occurrence of these changes. Currently, the Gibbs free energy function G describes this well in terms of thermodynamics, being the spontaneity possible only if $\Delta G < 0$ [10], where $\Delta G = \Delta H - T\Delta S$ and H is the enthalpy. However, with the previous considerations of the interrelationship between information and energy magnitudes, we consider the possibility of enhancing the characterization given by Gibbs into spontaneous processes in the brain by adding information quantities.

IV. CONCLUSIONS AND FUTURE WORK

A first sketch of an integrative approach to studying brain activity was presented here. We provided a set of useful tools, namely the links between information theory and thermodynamics that can be used to connect the cognition described in informational terms with the physical activity of the brain modeled by thermodynamics. Nevertheless, from a theoretical point of view, there are still several points to be connected between the two main models, such as, for instance, the free energy present in Friston's model with the thermodynamic measure equally termed. Our main current work is focused on further elaborating the connections between the thermodynamic and information-based models of the brain, aiming to present the explicit form of the equations that permit us to relate and unify both theoretical approaches in the near future. The possibility of validating the model empirically in the future in the way we indicated above is suggested. We also aim to inspire more researchers to contribute further to this new integrative approach, as well as to empirically studying its consequences.

REFERENCES

[1] L. del Rio, "The thermodynamic meaning of negative entropy," Nature 476, August 2011, pp. 61–63.

[2] L. Szilard, "On the decrease of entropy in a thermodynamic system by the intervention of intelligent beings," Z. Phys., vol. 53, 1929, pp. 840.

[3] L.F. del Castillo, "Thermodynamic Formulation of Living Systems and Their Evolution" JMP, vol.2, 2011, pp. 379-391.

 ISBN: 978-1-61208-340-7

[4] K. Friston, "The free energy principle: a unified brain theory?," Nature Neuroscience, vol. 11, 2010, pp. 227–138.

[5] M. Lee, "How cognitive modeling can benefit from hierarchical Bayesian models," Journal of Mathematical Psychology vol. 55, 2011, pp. 1–7.

[6] I. Prigogine, "Time, Structure and Fluctuations," Science, vol. 201, Issue 4358, September 1978, pp. 777–785.

[7] E. Schrödinger, What is life?, Trinity College, Dublin, February 1943.

[8] J. Kirkaldy, "Thermodynamics of the human brain," Biophys. J. 1965.

[9] P. La Cerra, "The First Law of Psychology is the Second Law of Thermodynamics: The Energetic Evolutionary Model of the Mind and the Generation of Human Psychological Phenomena," Human Nature Rev. vol. 3, 2003, pp.440-447.

[10] R. Feynman, The Feynman Lectures on Physics . 3 vol. 1964.

[11] R. Feynman, Feynman Lectures on Computation, Addison-Wesley Longman Publishing Co., Inc. Boston, US, 1998.

[12] L. Brillouin, "The Negentropy Principle of Information," Journal of Applied Physics, vol. 24, Sep.1953, pp. 338–343.

[13] J. Rothstein "Information, "Measurement, and Quantum Mechanics," Science, vol. 114, 1951, pp. 171–175.

[14] S. Varpula, "Thoughts about Thinking: Cognition According to the Second Law of Thermodynamics," Advanced Studies in Biology, vol. 5, no. 3, 2013, pp. 135 – 149.

[15] S. Nandakumar, "Redundancy and Synergy of Neuronal Ensembles in Motor Cortex," The Journal of Neuroscience, 25, April 2005, pp. 4207–4216.

[16] S. Laughlin, R. d. Ruyter van Steveninck, and J. Anderson, "The metabolic cost of neural computation," Nature Neuroscience, vol. 1, no. 1, 1998, pp. 36–41.

 ISBN: 978-1-61208-340-7

Is Word Generalization for Novel Concepts Modelled by Similarity or by Formal Concepts?

Sujith Thomas
Department of Computer Science and Engineering
Indian Institute of Technology Kanpur
Kanpur, India
Email: sujith@cse.iitk.ac.in

Harish Karnick
Department of Computer Science and Engineering
Indian Institute of Technology Kanpur
Kanpur, India
Email: hk@cse.iitk.ac.in

***Abstract*—In this paper, we conduct two word learning experiments to study the human word learning and generalization behaviour. The participants are shown abstract figures that form the positive examples of a word concept. All the positive examples have a common defining feature. The participants are then asked whether the word applies to various test examples. We vary several independent variables across our two word learning experiments. Our results show that the word generalization behaviour is based on the similarity of a test example with the positive examples of a word. The generalization behaviour is not based on the defining features. This is true even when enough examples exist from which the defining features can be inferred.**

***Keywords*—Human Word Learning; Hypothesis Space; Word Generalization; Formal Concepts; Object Similarity.**

I. INTRODUCTION

Humans have the ability to learn a new word after seeing a few examples of the word. Carey [1] named this phenomenon as *fast mapping*. Xu and Tenenbaum [2][3] demonstrate that fast mapping can be accurately modelled using a similarity-based generalization. In similarity-based generalization, the probability of generalization becomes higher for the test examples that are more similar to the positive examples of a word. Xu and Tenenbaum use a hierarchical clustering tree as their hypothesis space. Each node in the tree forms a hypothesis for a word concept.

Abbott, Austerweil and Griffiths [4] describe an approach for constructing a hypothesis space for word learning. The hypothesis space they use is also similarity based where the similarity is derived from the relationship between images and words in ImageNet [5] and WordNet [6] respectively. Abbott, Austerweil and Griffiths show that their similarity based generalization matches the empirical data.

The word categories used in the above papers [2][3][4] do not have a well-defined set of necessary and sufficient conditions. If the word categories have a set of necessary and sufficient conditions, will the generalization still be similarity based? Our hypothesis is that the generalization behaviour will be similarity based even when the word categories are well-defined. By well-defined, we mean that the necessary and sufficient conditions for the word category can be easily deduced from the positive examples.

We use artificial word concept categories defined using boolean features. Each word concept can be represented as a formal concept. We study the generalization behaviour of the human participants after showing them a few examples of a word concept.

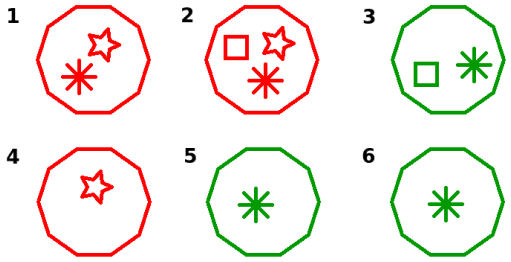

Fig. 1. The figure shows six objects that occur in a boolean world. Each figure can be represented using a set of boolean features.

TABLE I. THE TABLE LISTS THE OBJECTS SHOWN IN FIGURE 1. THE 'X' MARK DENOTES THAT AN OBJECT HAS A BOOLEAN FEATURE.

	star	red	spike-wheel	square	green
1	X	X	X		
2	X	X	X	X	
3			X	X	X
4	X	X			
5			X		X
6			X		X

In Section II, we describe our definition based hypothesis space. Section III explains how we construct our similarity based hypothesis space. The details of the two word learning experiments are given in Section IV and Section V. In Section VI, we discuss how our work relates to other works. Finally, we list our conclusions and point to future directions of our work in Section VII.

II. DEFINITION BASED HYPOTHESIS SPACE

Formal concepts form our hypothesis space of definition based concepts, i.e., the concepts that have a set of necessary and sufficient conditions. Here we follow the intuition that the set of boolean features that always occur together provide information about the categories present in the boolean world. For example, consider the six objects depicted in Figure 1. Table I lists these six objects along with the boolean features present in them. The 'X' mark denotes that an object 'has a' boolean feature.

 ISBN: 978-1-61208-340-7

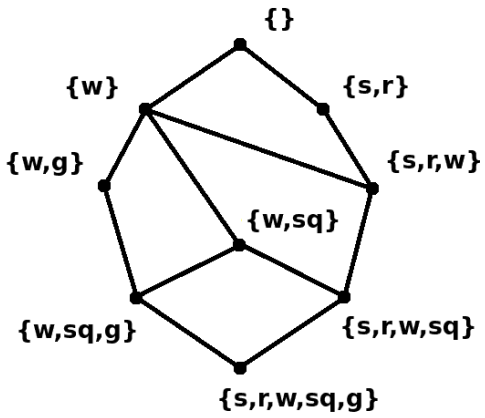

Fig. 2. The figure shows the complete lattice constructed from all the closed sets in Table I. Each node forms a hypothesis in the definition based hypothesis space.

We use the abbreviations s, r, w, sq and g to denote the presence of boolean features 'has a star', 'is red', 'has a spike wheel', 'has a square' and 'is green', respectively. All the objects also have one feature in common, namely, the decagon shape of the figures. But this feature is omitted here for the sake of brevity. In Table I, we notice that the sets of features $\{s, r, w\}$, $\{w, g\}$ etc., occur together in the world. These sets of features should provide information about the concept categories present in the boolean world.

We call a set of features A, a *closed set* if there does not exist a feature f such that the set of features $A \cup \{f\}$ have the same frequency of occurrence. In other words, if A is a closed set then for any feature f the set of features $A \cup \{f\}$ occurs with a frequency strictly less than that of set A. By this definition the set of features $\{r, w\}$ is not a closed set because $\{r, w\}$ occurs with frequency two and so does the set $\{s, r, w\}$. On the other hand, $\{w, g\}$ is a closed set with frequency three. This is because we cannot add a boolean feature to $\{w, g\}$ such that its frequency of occurrence remains the same. Every closed set of features has an extension that contains the set of objects that have those features. The extension of closed set $\{w, g\}$ is the set $\{3, 5, 6\}$ because w and g is present in all the three objects. Every closed set of boolean features along with its extension form a *formal concept*.

The notion of a closed set of features is useful because they carry all the information about the features that co-occur. Considering only the closed sets in a boolean world is advantageous because the closed sets of features are usually much lesser in number compared to all possible subsets of boolean features.

The formal concepts in Table I are the following—$\{\}$:6, $\{w\}$:5, $\{s, r\}$:3, $\{w, g\}$:3, $\{w, sq\}$:2, $\{s, r, w\}$:2, $\{w, sq, g\}$:1, $\{s, r, w, sq\}$:1 and $\{s, r, w, sq, g\}$:0. The number after the colon represents the frequency of occurrence of each formal concept. Note that $\{\}$ (null set) and $\{s, r, w, sq, g\}$ (set of all features) are also closed sets in the boolean world shown in Table I. The formal concepts satisfy a partial order relation $\supset$ (superset of), and therefore, can be arranged in the form of a complete lattice [7]. The complete lattice in Figure 2 depicts all the formal concepts in Table I. Each node in Figure 2 forms a hypothesis in the definition based hypothesis space of word concepts.

Ganter and Wille [7] explain the theoretical aspects of formal concept analysis in great detail. For a brief introduction to formal concept analysis refer Krötzsch and B Ganter [8]. Formal concept analysis has been successful in a wide area of applications ranging from linguistics and software engineering to artificial intelligence [9].

The lattice of formal concepts discussed in this section forms our hypothesis space of definition based word concepts.

III. Similarity Based Hypothesis Space

In order to construct a similarity-based hypothesis space, we need a notion of similarity. Xu and Tenenbaum [2][3] construct a hierarchical clustering tree using the average similarity ratings between the various images. These ratings were provided by the human participants. Abbott, Austerweil and Griffiths also use a tree structured hypothesis space where the notion of similarity between the hypothesis is derived from WordNet and ImageNet [4].

Tversky [10] discusses the similarity measures that can be used to emulatex human similarity judgments. Tversky introduces a similarity measure called Ratio model which is as follows:

$$S(X, Y) = \frac{f(X \cap Y)}{f(X \cap Y) + \alpha f(X \setminus Y) + \beta f(Y \setminus X)} \quad (1)$$

where X,Y are the sets of boolean features for the two objects to be compared and $\alpha, \beta \geq 0$. The α and β values determine the weights given to the features in X and Y while computing the similarity.

We use a simplified form of Tversky's Ratio model, where $\alpha = 1$, $\beta = 1$ and $f(Z) = |Z|$, where Z is a set. We let $\alpha = \beta = 1$ so that the features present in both the objects get equal weights while computing the similarity. The simplified form of Tversky's Ratio model becomes :

$$S(X, Y) = \frac{|X \cap Y|}{|X \cap Y| + |X \setminus Y| + |Y \setminus X|} \quad (2)$$

This simplified form is just another way of writing the Jaccard similarity coefficient [10]:

$$J(X, Y) = \frac{|X \cap Y|}{|X \cup Y|} \quad (3)$$

where X and Y are the sets of boolean features corresponding to the two objects to be compared.

Figure 3 shows the hierarchical clustering tree constructed from all the objects in Figure 1 using the Jaccard similarity coefficient (3). Each node in the tree forms a hypothesis in the similarity based hypothesis space. The hypothesis that are present in Figure 2 need not be present in Figure 3, and vice versa. This is because objects that satisfy a definition in Figure 2 need not be very similar to form a cluster, and the objects that form a cluster in Figure 3 need not have a set of defining features.

Which hypothesis space do humans use for the learning and generalization of word concepts? We try to answer this question in the following two sections.

 ISBN: 978-1-61208-340-7

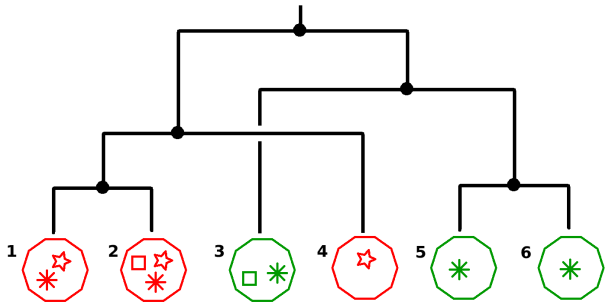

Fig. 3. The figure shows the hierarchical clustering tree constructed from all the objects in Figure 1 using the Jaccard similarity coefficient (3). Each node forms a hypothesis in the similarity based hypothesis space.

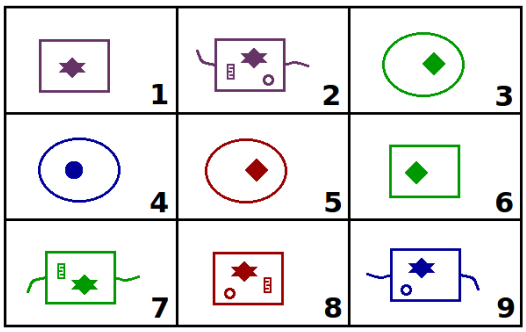

Fig. 4. A sample stimulus for the word learning experiment. Objects 7, 8 and 9 form the positive examples, and the objects 1, 2 and 3 form the test examples.

IV. First Word Learning Experiment

In this experiment, 23 participants were shown 3 positive examples of a word and asked whether the word generalizes to a test example. We used a random four letter word in our experiment having consonants and vowels in alternating positions. The positive examples in our experiment always correspond to a formal concept.

Figure 4 shows a sample stimulus. The participants were told that a novel word applies to objects 7, 8 and 9 in Figure 4. They were then asked whether the word applies to objects 1, 2 and 3. The rectangular bounding box and the star are the features that are common to objects 7, 8 and 9. If the generalization behaviour is based on a formal concept, then we would expect the participants to generalize a word to both objects 1 and 2. This is because both the objects 1 and 2 have a rectangular bounding box and a star. On the other hand, if the generalization behaviour is based on similarity, then we would expect the participants to generalize the word more often to object 2 compared to object 1. This is because object 2 is more similar to objects 7, 8 and 9.

Figure 5 shows another sample stimulus. The participants were told that a word applies to objects 7, 8 and 9. They were then asked whether the word generalizes to objects 4, 5 and 6. The only feature that is common to objects 7, 8 and 9 is the red colour. If the generalization behaviour is based on necessary and sufficient conditions then we would expect the participants to generalize the word to both objects 5 and 6 equally often.

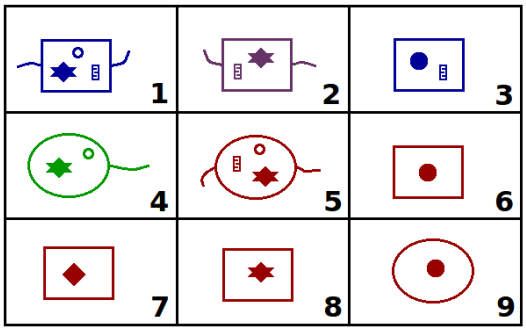

Fig. 5. Another sample stimulus for the word learning experiment. Objects 7, 8 and 9 form the positive examples, and the objects 4, 5 and 6 form the test examples.

> This experiment is designed to study human word learning ability.
> You will be given three examples of a word. Based on this information you need to judge whether the word applies to another example.
> Respond to the questions as quickly and accurately as you can.

Fig. 6. Instruction for the first word learning experiment.

On the other hand, if the generalization behaviour is based on similarity then we would expect that the word is generalized to object 6 more often.

There were six stimuli similar to Figure 4 and Figure 5. Each stimulus had three test questions associated with it. The test questions varied in their degree of similarity—very similar, less similar and not similar—with the positive examples of a word. The first two types of the test examples (i.e., very similar and less similar) also satisfied the formal concept.

Participants were first given five trial questions to familiarize them with the task. The participants were then asked to respond to 18 generalization questions. Figure 6 shows the instructions that were given to the participants.

A. Similarity Measure Used

We use the Jaccard similarity coefficient (3) to find the similarity between any two objects. We did the following experiment to see how well the Jaccard similarity coefficient matches the human similarity judgments. We asked a different set of 24 participants to rate the similarity between 50 pairs of abstract figures similar to those shown in Figure 4 and Figure 5. We found that the Spearman rank correlation coefficient [11] between the Jaccard similarity coefficient and average similarity ratings was significant $(r(48) = .77, p < .001)$.

B. Results

For each participant, if the generalization behaviour is based on formal concepts, then, we would expect that the word gets generalized to the less similar test example as often as it does to the more similar example. This is because both the types of test examples belong to the extension of the same formal concept.

 ISBN: 978-1-61208-340-7

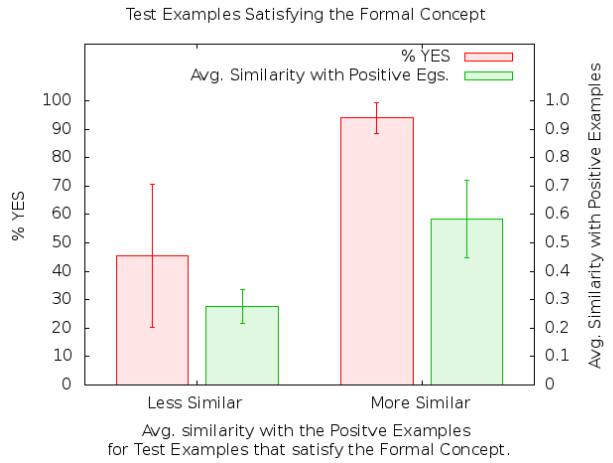

Fig. 7. The test example that satisfy the formal concepts were taken, and divided into two groups—less similar and more similar. More similar group received significantly higher percentage of word generalizations.

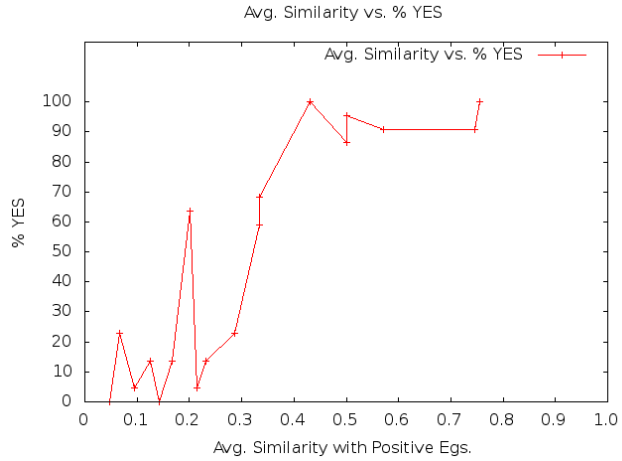

Fig. 8. The figure plots the percentage of participants that generalize a word to a test example against the average similarity of the test example with the positive examples. The correlation was found to be significant ($p < .005$).

We divided the test examples that satisfy the formal concept into two groups—more similar and less similar. The test examples in the more similar group had a higher average similarity with the positive examples. Figure 7 shows the average percentage of trials in which a word was generalized to a test exemplar in each of the two groups. We see that this percentage is much higher for the more similar group. We also found the frequencies with which each participant generalized a word to a very similar and to a less similar test example group. The difference between the two frequencies for each participant was found to be statistically significant using the Wilcoxon signed ranks test [11] ($W(23) = 5.5, p < .001$). This shows that the generalization behaviour was not based on formal concepts. The reason is that both the groups—more similar and less similar—satisfied the formal concept, and yet had a significantly different percentage of generalization.

Figure 8 shows how the percentage of trials in which a word was generalized to a test example varies with the average

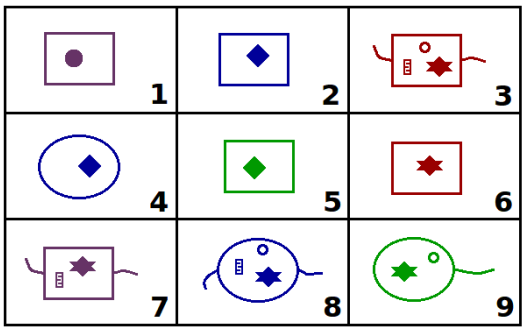

Fig. 9. Figure shows the stimulus corresponding to the anomalous spike in Figure 8 at X=0.2.

Jaccard similarity with the positive examples. The figure shows that the percentage increases with the increase in the average similarity of a test example. The Spearman rank correlation coefficient between the two variables in the figure was found to be statistically significant ($r(16) = .85, p < .005$).

The above two results show that the generalization behaviour for the experiment is better modelled using the similarity based generalization compared to a formal concept based generalization.

C. Discussion: The Anomalous Spike in Figure 8

Figure 8 shows the data for the first word learning experiment. The figure plots the percentage of participants that generalize a word to a test example against the average similarity of the test example with the positive examples. In Figure 8, we see that there is a sudden spike in the graph at the value X=0.2 along the X-axis.

Figure 9 shows the stimulus corresponding to the anomalous spike in Figure 8. In the word learning experiment, participants were told that a word applies to objects 7, 8 and 9 in Figure 9. The formal concept corresponding to the positive examples was the presence of a star shape. After showing the positive examples the participants were asked whether the word applies to object 6 in Figure 9. Sixty-four percent of participants preferred to generalize the word to object 6 even though its average Jaccard similarity coefficient was only 0.2 (See Figure 8).

One reason for this could be the fact that the star shape present in object 6 and in the positive examples is visually more salient. This is because the star feature has more edges and corner points compared to the other boolean features. The Jaccard similarity coefficient in (3) does not take into account the visual saliency of any of the boolean features. The Tversky's ratio model in (1) also does not allow individual boolean attributes to take on different weights depending on its visual saliency. For this reason, we used a different similarity measure for our second word learning experiment in Section V.

V. Second Word Learning Experiment

Our first word learning experiment in Section IV used only a few boolean features. Due to this, we could not have test examples that were very similar to the positive examples,

 ISBN: 978-1-61208-340-7

TABLE II. THE FOUR TYPES OF TEST EXAMPLES FOR EACH STIMULUS

	Similar to positive examples?	Satisfies the formal concept?
Type 1	Yes	Yes
Type 2	Yes	No
Type 3	No	Yes
Type 4	No	No

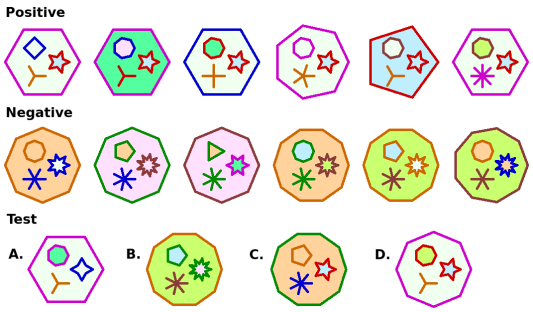

Fig. 10. The figure shows a sample stimulus. The top row, middle row, and the bottom row list the positive, negative, and test examples respectively. All the positive examples have a five pointed blue star with a red border.

and yet did not satisfy the formal concept. In our second word learning experiment we increase the number of boolean features, so that we can have four distinct types of test examples as shown in Table II. We also increase the number of positive examples and introduce negative examples of a word. We wanted to investigate whether increasing the number of positive examples would help the participants infer the defining features, and generalize based on it.

The second word learning experiment was conducted as follows. Each participant was shown six positive and six negative examples of a word. The participant was then asked whether the word generalizes to a test example. We used a random four letter word having consonants and vowels in alternating positions. Just like the previous experiment, the positive examples always corresponded to a formal concept. We had 24 participants in our experiment.

Figure 10 shows a sample stimulus that was used. The top row lists the positive examples of a word. The middle row lists the negative examples. The bottom row contain the test examples for which we want to study the generalization behaviour. The test examples are shown to the participant one at a time.

In Figure 10, all the positive examples contain a five pointed star with a blue background and a red border. This is the only feature that is common across all the positive examples. If the generalization behaviour is based on formal concepts then we would expect that the word will be generalized to both test examples C and D with equal frequency. This is because both C and D have a five pointed star with a blue background and a red border. On the other hand, if the generalization behaviour is based on similarity then we would expect that the word is generalized to A and D more frequently compared to B and C. This is because A and D are more similar to the positive examples of the word.

Figure 11 shows the positive, negative and test examples for another stimulus. The positive examples in Figure 11 contain

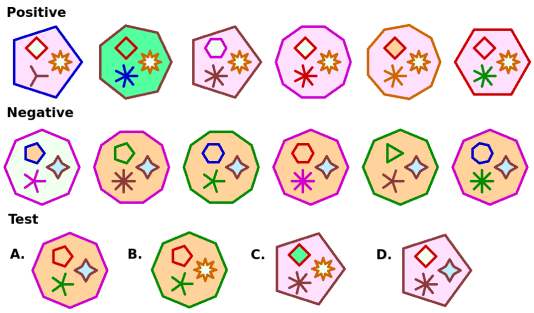

Fig. 11. The figure shows another sample stimulus. The top row, middle row, and the bottom row list the positive, negative, and test examples respectively. All the positive examples have an eight pointed star with a white background and orange border.

> The experiment is designed to study the generalization behaviour in human word learning task. You will be shown three sets of figures on the screen. First set will contain six positive examples of a novel word. The second set will contain six negative examples of the same novel word. The third set will contain a single figure for which you need to decide whether the word applies or not. You will have 12 seconds to answer each question. Please be as fast and as accurate as you can be.

Fig. 12. Instruction for the second word learning experiment.

an eight pointed star with a white background and an orange border. This is the only feature that is common to all the positive examples. If the word generalization is based on formal concepts then we would expect the word to be generalized to examples B and C with the same frequency. On the other hand, if the generalization behaviour is based on similarity then we would expect the word to be generalized to examples C and D more often.

There were six stimuli as shown in Figure 10 and Figure 11. Each stimulus had four test examples, and hence there were 24 test examples in total. Table II shows the four types of test examples that were used in each stimulus. There were 24 test examples in total. The participants were given five trial questions to familiarize them with the task. Figure 12 shows the instruction that was given to the participants.

A. *Similarity Measure Used*

We need a notion of similarity for this experiment also. As discussed in Section IV-C, the Jaccard similarity coefficient does not take into account the visual saliency of any of the boolean features. To solve this problem, we use a linear regression model. A linear regression model can learn the appropriate weights that needs to be assigned to each of the boolean features to account for its visual saliency.

In order to train the linear regression model, we conducted the following experiment. We asked a different set of 20 participants to rate the similarity between two figures that were randomly generated by our Python program. The figures were the same as those used as objects for the second word learning experiment. Each participant was asked to provide similarity

 ISBN: 978-1-61208-340-7

measures for 40 pairs of randomly generated figures. This gave us 800 (20×40) data-points to train our linear regression model.

The Spearman rank correlation coefficient between the user similarity ratings and those predicted by the trained linear regression model was found to be .70. The trained linear regression model was used to obtain the similarity measures for our second word learning experiment.

B. Result

If the similarity based generalization dominates the formal concept based generalization then we would expect a word to generalize to type 2 test examples more often than type 3 test examples (See Table II). The participants generalized a word to a type 2 test example 75% (108 of 144) of the trials but this percentage was only 37% (53 of 144) for the type 3 test examples. The difference between the type 2 and type 3 generalization frequencies for each participant was found to be statistically significant using the Wilcoxon signed ranks test ($W(21) = 24, p < .001$). Here $df = 21$ because for 3 participants the difference between the frequencies was zero. The statistical significance of the difference in frequencies shows that the generalization behaviour is not based on formal concepts.

Figure 13 shows the 24 test examples divided into two groups—those that satisfy the formal concept and those that do not. We find the average percentage of participants who generalize a word to the test examples in each of these two groups. If the generalization behaviour is based on formal concept, then we would expect the average percentage to be closer to 100% for one group and closer to zero for the other. Figure 13 shows the average percentage of participants who generalized a word to the test examples in each group. We see that for both the groups the average percentage is closer to 50%. Spearman rank correlation coefficient between the generalization made by the participants and the generalization based on definition was found not to be statistically significant ($r(574) = .15, ns$). Here $df = 574$ because we have 24 participants and 24 trial questions ($N = 24 \times 24 = 576$).

Figure 14 shows the 24 test examples divided into two groups based on their similarity to the positive examples of a word. If the participant generalization behaviour is based on similarity, then, we would expect this percentage to be closer to 100% for one group and closer to zero for the other. The data in Figure 14 confirms this. Spearman rank correlation coefficient between the generalization made by the participants and the generalization based on similarity was found to be statistically significant $r(574) = .51, p < .001$). Here $df = 574$ because we have 24 participants and 24 trial questions ($N = 24 \times 24 = 576$).

Figure 15 shows how the percentage of participants who generalized a word to a test example varies with the average similarity between the test example and the positive examples. In the figure, we see that the percentage increases with the average similarity. The Spearman rank correlation coefficient between the two variables was found to be significant ($r(22) = .87, p < .005$). Here $df = 22$ because there are 24 test examples.

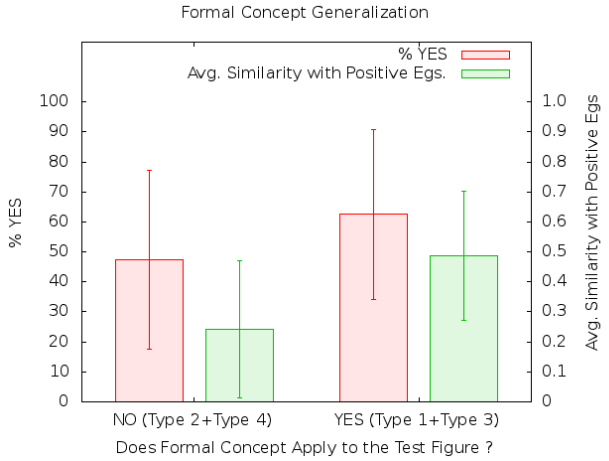

Fig. 13. The 24 test examples are divided into two groups—those that satisfy the formal concept and those that do not. There is no significant difference between the two groups when it comes to the average percentage of participants, who generalized the word to the test example.

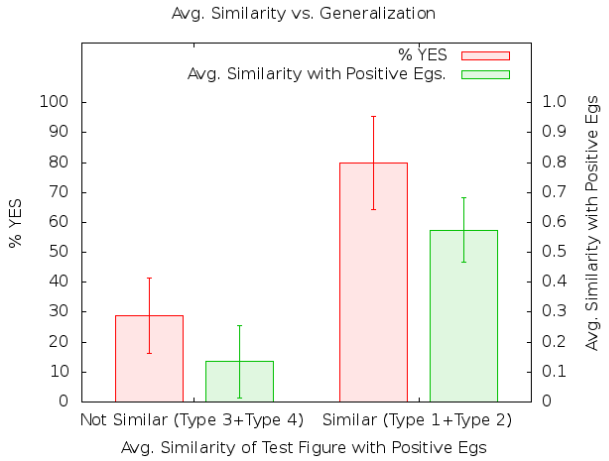

Fig. 14. The 24 test examples are divided into two groups based on their average similarity with the positive examples. The figure shows that the more similar group has a significantly greater percentage of word generalization.

The above results show that the generalization behaviour for the second word learning experiment is better modelled using the similarity based generalization compared to a formal concept based generalization.

VI. Discussion

Our results show that the word generalization behaviour is similarity based even when the word category has a set of defining features. This result is consistent with earlier results [2][3][4] that show that the word generalization in fast-mapping is similarity based. Our word learning experiments are different from previous works because we ensure that a word in our experiment always corresponds to a formal concept.

Tenenbaum et al. [12] discuss the importance of abstract knowledge in helping humans do fast learning. The representation of this abstract knowledge is domain specific, and varies

 ISBN: 978-1-61208-340-7

Fig. 15. The figure shows how the percentage of generalization for at test example varies with its average similarity with the positive examples. The correlation was found to be significant ($p < .005$).

widely from a tree structure to a directed acyclic graph [12]. In our work, we have tried to explore the nature of this knowledge representation for human word learning. Human word learning is usually modelled using Bayesian inferencing on a structured hypothesis space [3][4]. Selecting the right knowledge representation is important because it implies qualitatively different set of hypotheses, for a probabilistic model to choose from [13].

Laurence and Margolis [14] review the various, major theories on concept formation. Formal concepts are more like the classical theory of concepts, while the similarity-based generalization conforms more to the prototype theory [15]. Laurence and Margolis [14] also discuss other theories of concepts that try to combine the classical and prototype theory. M. Freund [16] proposes a formal model that combines the notion of *typicality* from the prototype theory with the formal concept analysis.

We have used abstract figures as examples in our word learning experiments. This ensures that the generalization behaviour is not influenced by the background knowledge that the participants might have about the examples used in our experiments. The features present in the examples can only be visual features; therefore, it becomes easier to ensure that the positive examples correspond to a formal concept.

We have changed several independent variables in our two word learning experiments. These include the stimuli, number of boolean features, number of positive examples, and the presence of negative examples. Despite changing several independent variables, we found that the generalization behaviour (dependent variable) was based on similarity, and not on defining features. We speculate that the reason for this is that abstracting out a definition from a set of positive examples puts a greater cognitive load on the participants, compared to judging the similarity between a test example and the positive examples.

VII. Conclusion and Future Work

We have conducted two word learning experiments that show that the generalization behaviour during fast mapping is based on similarity, and not on a set of defining features. This is true even when enough positive examples exist from which the defining features can be inferred.

The two experiments used different sets of stimuli and had different sets of participants. We increased the number of boolean features, the number of positive examples and introduced negative examples, for our second word learning experiment. Despite changing several independent variables, our results consistently show that the generalization behaviour is not based on formal concepts.

Currently, the knowledge representations used in the literature are domain specific, and not stimuli specific. In our future work, we want to investigate whether the same word concept representation can be used to model word learning across different stimuli conditions.

References

[1] S. Carey, "The child as word learner," in *Linguistic theory and psychological reality*, M. Halle, J. Bresnan, and G. A. Miller, Eds. Cambridge, MA: MIT Press, 1978, pp. 264–293.

[2] J. Tenenbaum and F. Xu, "Word learning as bayesian inference," in *Proceedings of the 22nd annual conference of the cognitive science society*, 2000, pp. 517–522.

[3] F. Xu and J. Tenenbaum, "Word learning as bayesian inference." *Psychological review*, vol. 114, no. 2, pp. 245–272, 2007.

[4] J. Abbott, J. Austerweil, and T. Griffiths, "Constructing a hypothesis space from the web for large-scale bayesian word learning," in *Proceedings of the 33rd Annual Meeting of the Cognitive Science Society*, 2012, pp. 54–59.

[5] J. Deng, W. Dong, R. Socher, L.-J. Li, K. Li, and L. Fei-Fei, "ImageNet: A Large-Scale Hierarchical Image Database," in *CVPR09*, 2009.

[6] G. A. Miller, "Wordnet: a lexical database for english," *Communications of the ACM*, vol. 38, no. 11, pp. 39–41, 1995.

[7] B. Ganter and R. Wille, *Formal concept analysis*. Springer Berlin, 1999.

[8] M. Krötzsch and B. Ganter, *A Brief Introduction to Formal Concept Analysis*. Chapman & Hall/CRC, 2009, vol. Conceptual Structures in Practice, ch. 1, pp. 3–16.

[9] U. Priss, "Formal concept analysis in information science," *Annual Review of Information Science and Technology*, vol. 40, no. 1, pp. 521–543, 2006.

[10] A. Tversky, "Features of similarity," *Psychological review*, vol. 84, no. 4, pp. 327–352, 1977.

[11] J. Greene and M. d'Oliveira, *Learning to use statistical tests in psychology*. McGraw-Hill International, 2005.

[12] J. B. Tenenbaum, C. Kemp, T. L. Griffiths, and N. D. Goodman, "How to grow a mind: Statistics, structure, and abstraction," *science*, vol. 331, no. 6022, pp. 1279–1285, 2011.

[13] T. L. Griffiths, N. Chater, C. Kemp, A. Perfors, and J. B. Tenenbaum, "Probabilistic models of cognition: exploring representations and inductive biases," *Trends in Cognitive Sciences*, vol. 14, no. 8, pp. 357–364, 2010.

[14] S. Laurence and E. Margolis, "Concepts and cognitive science," *Concepts: core readings*, pp. 3–81, 1999.

[15] E. Rosch and C. Mervis, "Family resemblances: Studies in the internal structure of categories* 1," *Cognitive psychology*, vol. 7, no. 4, pp. 573–605, 1975.

[16] M. Freund, "On the notion of concept i," *Artificial Intelligence*, vol. 172, no. 4-5, pp. 570–590, 2008.

 ISBN: 978-1-61208-340-7